ANCHAM

FEBRUARY 1979

analytical chemistry

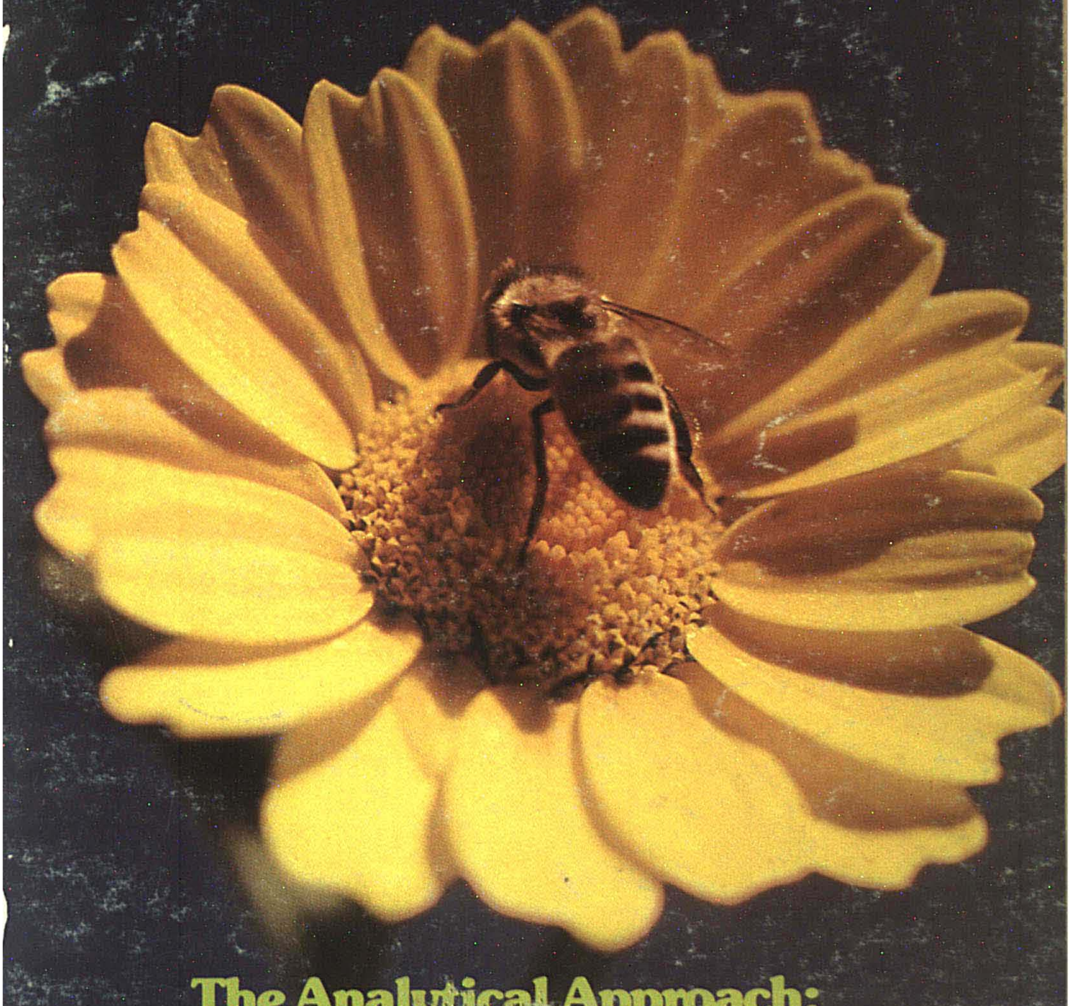

The Analytical Approach: Honey or Syrup?

1979 Pittsburgh Conference

When your applications change, this recorder changes with them

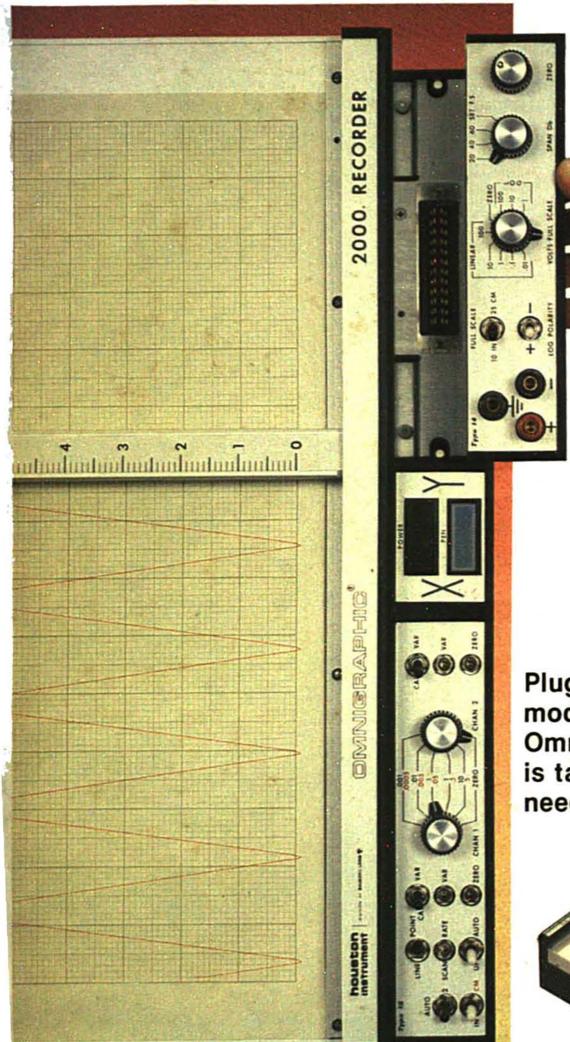
2000. RECORDER
OMNIGRAPHIC®
houston instrument
ZERO
SPAN
VOLTS FULL SCALE
LINEAR
LOG
FULL SCALE
LOG POLARITY
POWER
PEN
X
Y
CHAN 1
CHAN 2
4
3
2
1
0

Plug in your choice of modules and the Omnigraphic® Model 2000 is tailored to your need

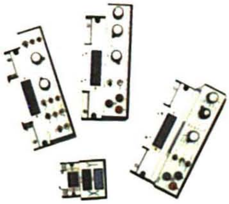

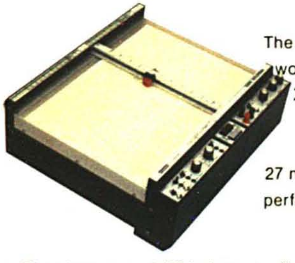

The Omnigraphic Model 2000 is the world's best known most versatile X-Y recorder. The basic building block is a rugged die cast metal mainframe. A choice of 27 modules enables the recorder to perform in virtually any application.

- 30 in./sec. speed (40 in./sec. available)
- ± 0.2% accuracy
- Best common mode rejection
- Same servo response on both axes
- Modules can be changed in minutes
- Amplifiers interchangeable
- Priced from $1200.* OEM discounts available.

® Registered Trademark of Houston Instrument

* U.S. Domestic Price Only

Visit us at the Pittsburgh
Conference booths 217 & 219

CIRCLE 94 ON READER SERVICE CARD

houston instrument
DIVISION OF BAUSCH & LOMB

ONE HOUSTON SQUARE
AUSTIN, TEXAS 78753
(512) 837-2820
TWX 910-874-2022

EUROPEAN OFFICE Rochesterlaan 6 8240 Gistel Belgium
Phone 059/277445 Telex Bausch 81399

"the graphics - recorder company"

For rush literature requests or local sales office information only, persons outside Texas call toll free 1-800-531-5205.

The Dohrmann connection

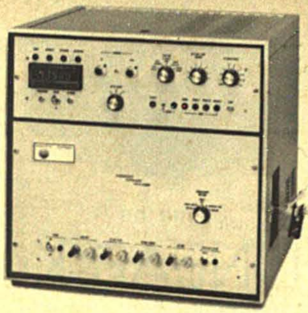

Nitrogen. Basic Dohrmann DN-10 Oxidative Nitrogen Analyzer for ppm nitrogen in liquids, solids and gases.

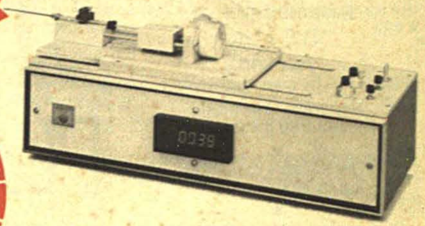

The CRI. The Constant Rate Injector, when connected to the Dohrmann DN-10 or the Dohrmann MCTS, makes ±20 ppb analysis of N and S easy and convenient. The CRI may be used with your existing analyzer.

Sulfur. The Dohrmann MCTS Microcoulometric Titrating System, the standard for ppm sulfur in liquids, solids and gases.

For ±20ppb S or N – automatically!

The new Dohrmann Constant Rate Injector (CRI), when combined with the Dohrmann® analyzers shown here, provides a dramatic improvement in trace level detection of sulfur and nitrogen.

Operation of the CRI couldn't be easier. Simply place your loaded syringe on the carriage of the injector and push it through the septum of the instrument. Injection is then electronically actuated and precisely controlled to provide constant rate sampling.

Results are digitally displayed by the Constant Rate Injector. In addition to permitting far more sensitive analyses, adding the CRI converts earlier Dohrmann analyzers to digital systems.

The CRI is priced under $3,000, an investment you'll soon recover!

See us at the Pittsburgh Conference, Booth 812.

ENVIROTECH | **DOHRMANN**

3240 Scott Boulevard
Santa Clara, CA 95050

CALL TOLL FREE (800) 538-7708

In Alaska, California, Hawaii, Puerto Rico, call collect (408) 249-6000.

See us at Booth #812 at the Pittsburgh Conference

CIRCLE 50 ON READER SERVICE CARD

new dimensions in TLC

With the

KC18

reversed-phase
TLC plate
you can:

- Separate at extreme polarity ranges.
- Get sample capacity up to 10X silica gel.
- Separate at rates of 2 min/cm.
- Use *simple* solvent systems and easily optimize.
- Get high efficiency: HETP ≈ 10 μm.
- Correlate KC18 TLC* with C18 HPLC.

*12% silanized carbon load.

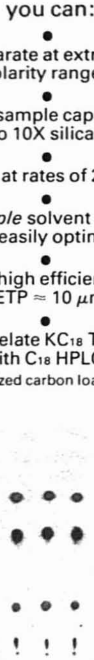

Interested?
FREE SAMPLE KC18 PLATES – WHILE SAMPLE SUPPLIES LAST.

Write now for samples:
Whatman Inc., 9 Bridewell Place,
Clifton, N.J. 07014
or phone: (201) 777-4825.

Whatman

NEW μSLIDE R-P TLC PLATES

(1″ × 3″)

Write for free Samples.

Reversed-phase TLC. Whatman's famous KC18 layers now on micro-slides, packed 100 to the box. An inexpensive way to get extraordinary R-P TLC performance in a new size, ideal for many applications. While samples last, write:

Whatman Inc.
9 Bridewell Place, Clifton, N.J. 07014
Tel.: 201-777-4825

Whatman

new dimensions in TLC

With the

LINEAR-K

preadsorbent area
on silica gel TLC plate
you can:

- Use crude, dilute, organic or aqueous samples *without prepurification.*
- Cut spotting time by 85-90%.
- Use acidic, basic, neutral solvents.
- Get R_f deviation of *only 0.95*%.
- Use 10-60 μl/channel of sample.
- Easily transfer from conventional silica gel.
- Choose 40 or 80Å silica gel.

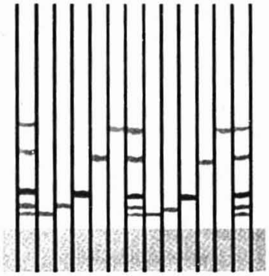

FREE SAMPLES WHILE SAMPLE SUPPLIES LAST.

Write now for samples:
Whatman Inc., 9 Bridewell Place,
Clifton, N.J. 07014
or phone: (201) 777-4825.

Whatman

See us at the Pittsburgh Conference, Booths 1925, 1926 and 1927

CIRCLE 234 ON READER SERVICE CARD

Volume 51, No. 2, February 1979
ANCHAM
51(2) 107A–300A/177–320 (1979)
ISSN 0003-2700

© Copyright 1979
by the American Chemical Society

Permission of the American Chemical Society is granted for libraries and other users to make reprographic copies for use beyond that permitted by Sections 107 or 108 of the U.S. Copyright Law, provided that the copying organization pay the appropriate per-copy fee through the Copyright Clearance Center, Inc. Educational institutions are generally granted permission to copy upon application to Office of the Director, Books and Journals Division, ACS, 1155 16th St., N.W., Washington, D.C. 20036.

Published monthly with review issue added in April and Laboratory Guide in August by the American Chemical Society, from 20th and Northampton Sts., Easton, Pa. 18042. Executive and Editorial headquarters, American Chemical Society, 1155 16th St., N.W., Washington, D.C. 20036 (202) 872-4600. Second class postage paid at Washington, D.C., and at additional mailing offices.

1979 Subscription prices—including surface postage

	1 yr	2 yr	3 yr
MEMBERS:			
Domestic	$12	$22	$30
Canada, Foreign	21	40	57
NONMEMBERS:			
Domestic	16	29	42
Canada	25	47	69
Other Foreign	33	61	89

Airmail and air freight rates are available from Membership & Subscription Services, ACS, P.O. Box 3337, Columbus, Ohio 43210 (614) 421-7230.

New and renewal subscriptions should be sent with payment to the Office of the Controller at the ACS Washington address.

Subscription service inquiries and changes of address (include both old and new addresses with ZIP code and *recent mailing label*) should be directed to the ACS Columbus address noted above. Please allow six weeks for change of address to become effective.

Claims for missing numbers will not be allowed if loss was due to failure of notice of change of address to be received in the time specified; if claim is dated (a) North America: more than 90 days beyond issue date, (b) all other foreign: more than one year beyond issue date; or if the reason given is "missing from files."

Microfilm and microfiche editions are available by single volume or back issue collection. Inquiries and payments to Microforms Program, ACS Washington address.

Single issues, current year, $3.00 except review issue and Labguide, $4.00; **back issues and volumes:** *write or call* Special Issues Sales, ACS Washington address (202) 872-4365.

Advertising Management: Centcom, Ltd., 25 Sylvan Road South, Westport, Conn. 06880 (203) 226-7131

analytical chemistry

CONTENTS

REPORT

The theory plus current and future applications of resonance Raman spectroscopy are reviewed by M. D. Morris and D. J. Wallan of the University of Michigan **182 A**

INSTRUMENTATION

Warren D. Reynolds, NCTR, presents the principles and important analytical applications of field desorption mass spectrometry **283 A**

THE ANALYTICAL APPROACH

Methods developed at USDA for the detection of adulterated honey are described by L. W. Doner, I. Kushnir, and J. W. White, Jr. **224 A**

REGULATIONS

Problems and opportunities for the analytical profession abound in the need to develop, validate, and apply appropriate analytical methodology for the regulation of priority pollutants **223 A**

PITTSBURGH CONFERENCE

The 30th Pittsburgh Conference on Analytical Chemistry and Applied Spectroscopy will be held March 5–9, 1979, in Cleveland, Ohio. The complete technical program is presented **124 A**

NEW PRODUCTS

Products to be featured at the 1979 Pittsburgh Conference Exposition are introduced **234 A**

NEWS

ANALYTICAL CHEMISTRY appoints Tomas Hirschfeld, Carter L. Olson, and Thomas H. Ridgway to its Instrumentation Advisory Panel **195 A**

BOOKS

Books on IR and Raman spectra, and gas chromatography are reviewed by Ira Levin and D. F. Logsdon **263 A**

EDITORS' COLUMN

In 1978 over 60% of ANALYTICAL CHEMISTRY's manuscripts were published within six months of submission. Factors involved in minimizing publication times are discussed **277 A**

EDITORIAL

The analytical research worker should understand the various "black boxes" in his research system, even though the central focus of his research is only on one component in the system **177**

Technical Contents/Briefs **110 A**
Reader Survey Results **122 A**
Call for Papers **200 A**
Meetings **200 A**
Short Courses **204 A**
Manufacturers' Literature **255 A**
Advertising Index **298 A**
Author Index **IBC**
Future Articles **IBC**

Photo by John Gussman/Uniphoto

Our cover illustrates part of the process that produces honey. See THE ANALYTICAL APPROACH*, page 224 A*

ห้องสมุด กรมวิทยาศาสตร์บริการ

Briefs

Determination of Trace-Level Vanadium in Marine Biological Samples by Chemical Neutron Activation Analysis 178

A cation-exchange chromatography procedure using ^{52}V neutron activation analysis is outlined for the determination of V with a limit of detection of 30 ppb.

Alan J. Blotcky, Carl Falcone, Victor A. Medina, and Edward P. Rack,* General Medical Research, Veterans Administration Hospital, Omaha, Neb. 68105, and Department of Chemistry, University of Nebraska, Lincoln, Neb. 68588, and **David W. Hobson,** Department of Biology, Texas A&M University, College Station, Tex. 77840 *Anal. Chem., 51 (1979)*

Viscosity, Calorimetric, and Proton Magnetic Resonance Studies on Coal Liquid Fractions in Solution 182

In coal liquids, asphaltene, and heavy oil fractions, hydrogen bonding involves phenolic hydrogens as proton-donors.

Krishna C. Tewari, Nan-sing Kan, David M. Susco, and Norman C. Li,* Department of Chemistry, Duquesne University, Pittsburgh, Pa. 15219 *Anal. Chem., 51 (1979)*

Determination of Tetraalkyllead Compounds in Water, Sediment, and Fish Samples 186

Hexane is used to extract tetraalkyllead compounds for analysis by GC-AAS. The detection limits for water, sediment, and fish are 0.50 μg/L, 0.01 μg/g, and 0.025 μg/g, respectively.

Y. K. Chau,* P. T. S. Wong, G. A. Bengert, and O. Kramar, Canada Centre for Inland Waters, Burlington, Ontario L7R 4A6, Canada *Anal. Chem., 51 (1979)*

Parametric Neutron Activation Analysis of Samples Generating Complex γ-ray Spectra 189

Using the Fe–Ru method of flux determination, good agreement in accuracy is achieved when compared with the relative measurements using Standard Reference Materials from NBS.

P. F. Schmidt,* Bell Telephone Laboratories, Incorporated, Allentown, Pa. 18103, **J. E. Riley, Jr.,** Bell Telephone Laboratories, Incorporated, Murray Hill, N.J., and **D. J. McMillan,** Northern-Tracor, Inc., Middleton, Wis. *Anal. Chem., 51 (1979)*

Comparison of the Determination of Cobalamins in Ocean Waters by Radioisotope Dilution and Bioassay Techniques 196

The isotopic methods are shown to measure both biologically active and inactive cobalamins indiscriminatively when porcine intrinsic factor is used as the B_{12}-specific binder.

G. M. Sharma,* Henry R. DuBois, Albert T. Pastore, and Stephen F. Bruno, New York Ocean Science Laboratory, Montauk, N.Y. 11954 *Anal. Chem., 51 (1979)*

Enzymatic Determination of Urea in Serum Based on pH Measurement with the Flow Injection Method 199

By maintaining a constant buffering capacity of the carrier stream solution, a linear relationship between the recorded pH signal and the urea content is obtained.

J. Ruzicka,* E. H. Hansen, and Animesh K. Ghose, Chemistry Department A, The Technical University of Denmark, Building 207, DK-2800, Lyngby, Denmark, and **H. A. Mottola,** Department of Chemistry, Oklahoma State University, Stillwater, Okla. 74074 *Anal. Chem., 51 (1979)*

Development and Application of a Thermistor Enzyme Probe in the Urea–Urease System 204

Urea solutions are analyzed in less than 1 min, and the linear response range to urea concentrations is 5–30 mM.

Steven Rich, Hofstra University, 1000 Fulton Avenue, Hempstead, N.Y. 11550, and **Robert M. Ianniello and Neil D. Jespersen*** Chemistry Department, St. John's University, Grand Central and Utopia Parkways, Jamaica, N.Y. 11439 *Anal. Chem., 51 (1979)*

Solvent Extraction Method for Determination of Thorium in Soft Tissues 207

Thorium is extracted in 25% trilaurylamine in xylene, back-extracted with 10 M HCl, electrodeposited on a platinum planchet, and counted alpha spectrometrically. The final total recovery ranges from 24–93%.

Narayani P. Singh.* Shawki Amin Ibrahim, Norman Cohen, and McDonald E. Wrenn, Institute of Environmental Medicine, New York University Medical Center, 550 First Avenue, New York, N.Y. 10016 *Anal. Chem., 51 (1979)*

Determination of Benzidine, Dichlorobenzidine, and Diphenylhydrazine in Aqueous Media by High Performance Liquid Chromatography 210

These compounds can be assayed by direct injection, solvent extraction, or resin adsorption with detection limits of 1 μg/L, 50 ng/L, and 100 ng/L, respectively.

R. M. Riggin* and C. C. Howard, Organic, Analytical, and Environmental Chemistry Section, Battelle's Columbus Laboratories, 505 King Avenue, Columbus, Ohio 43201 *Anal. Chem., 51 (1979)*

Determination of Trace Level Arsenic(III), Arsenic(V), and Total Inorganic Arsenic by Differential Pulse Polarography 215

As(III), As(V), and total inorganic As are speciated at ppb levels in aqueous reference materials with a preliminary HSO_3^- reduction of As(V). Relative errors range from 0–19.2% and a RSD range of 2.4–33.1%.

F. T. Henry, T. O. Kirch, and T. M. Thorpe,* Department of Chemistry, Miami University, Oxford, Ohio 45056 *Anal. Chem., 51 (1979)*

* Corresponding author.

ORION's "no lemon" meters will suit you to a T-shirt.

Model 501: New, low-cost digital pH meter readable to 0.01 pH. Features ATC and digital reading of temperature.

Model 407A: Versatile, top-of-the-line analog meter for pH and specific ion work. Also available in battery-powered field version, with carrying case.

Model 201: A low-cost, hand-held digital that reads to 0.05 pH. Comes with carrying case and line adaptor to permit laboratory use.

Model 701A: Research-grade digital pH/mV meter with 0.001 pH resolution. Features ATC and digital output for interfacing to ORION printer. Comes with swing arm electrode holder.

901 Microprocessor Analyzer: Unique "thinking" meter offers unmatched simplicity of operation, makes electrode analysis faster, easier. Pushbutton standardization and blank correction. No calibration curves to draw.

The famous ORION "no lemon" T-shirt, yours with a demo of any ORION "no lemon" meter.

Ask for a demonstration of any ORION "no lemon" meter and receive a "no lemon" T-shirt, free!

Take your pick of the "no lemon" crop! These are just a few of ORION's pH and specific ion meters, priced from as little as $220. They're so reliable, each one comes with our famous "no lemon" guarantee: if your meter quits for any reason other than abuse within one year of purchase, we'll replace it with a brand new one. Immediately, and without charge. That's why we say, "ORION eats lemons!" Mail the coupon today for your demo and free T-shirt.

Please call me for a demo of (circle):

501 901 407A 201 701A

T-shirt size: ☐medium ☐large ☐extra-large

Name ________________________

Title ____________ Phone ( ) ________

Organization ____________________

Street ________________________

City ____________ State _____ Zip _____

ORION RESEARCH

380 Putnam Ave., Cambridge, MA 02139

Orion® "No lemon"®

CIRCLE 156 ON READER SERVICE CARD

Briefs

Photometric Acid–Base Titrations in the Presence of an Immiscible Solvent
218

In the titration apparatus described, one liquid phase is continuously pumped out of a vigorously stirred two-phase solvent mixture, passed through a spectrophotometer flow cell, and returned to the mixture.

Frederick F. Cantwell* and Hussain Y. Mohammed, Department of Chemistry, University of Alberta, Edmonton, Alberta, Canada T6G 2G2 *Anal. Chem., 51 (1979)*

Measurement of Ions within a Pulsed Electron Capture Detector by Mass Spectrometry
223

Positive ions play a significant role in determining the current observed with a pulsed electron capture detector.

E. P. Grimsrud,* S. H. Kim, and P. L. Gobby, Department of Chemistry, Montana State University, Bozeman, Mont. 59717 *Anal. Chem., 51 (1979)*

Mass Spectrum Dictionary for Library Searching
229

The technique reported requires on the average less than 1% of the spectra to be examined in searching for an unknown.

R. Geoff Dromey, Department of Computing Science, University of Wollongong, P.O. Box 1144, Wollongong, N.S.W. 2500, Australia *Anal. Chem., 51 (1979)*

Optimizing Precision in Standard Addition Measurement
232

Equations are presented and plotted describing the effect of increment size on the precision of a standard addition or standard subtraction measurement.

Kenneth L. Ratzlaff, Department of Chemistry, The Michael Faraday Laboratories, Northern Illinois University, DeKalb, Ill. 60115 *Anal. Chem., 51 (1979)*

Fluorescence and X-Ray Photoelectron Spectroscopy Surface Analysis of Metal Oxide Electrodes Chemically Modified with Dansylated Alkylaminesilanes
236

Fluorometric analysis of the hydrolysate sulfonamide concentration assays its surface concentration at $0.5–2 \times 10^{-10}$ mol/cm^2, and XPES determination of sulfonamide reaction coupling efficiency yields an average alkylaminesilane coverage of 2.6×10^{-10} mol/cm^2.

Henry S. White and Royce W. Murray,* Department of Chemistry, University of North Carolina, Chapel Hill, N.C. 27514 *Anal. Chem., 51 (1979)*

Pulse (Photon) Counting: Determination of Optimum Measurement System Parameters
240

Experimental pulse height distributions and linearity measurements are used to evaluate semiquantitatively the trade-offs among stability, sensitivity, and dynamic range.

E. J. Darland, G. E. Leroi, and C. G. Enke*, Department of Chemistry, Michigan State University, East Lansing, Mich. 48824 *Anal. Chem., 51 (1979)*

Pulse (Photon) Counting: A High-Speed Direct Current-Coupled Pulse Counter
245

The pulse counter has no base-line shift, long-term stability, sensitivity of $130\ \mu V$, speed greater than 90 MHz, and permits remote operation.

E. J. Darland, J. E. Hornshuh, C. G. Enke,* and G. E. Leroi, Department of Chemistry, Michigan State University, East Lansing, Mich. 48824 *Anal. Chem., 51 (1979)*

Micromolar Voltammetric Analysis by Ring Electrode Shielding at a Rotating Ring-Disk Electrode
250

Ring electrode shielding permits the determination of Ag(I), Bi(III), Cu(II), and Fe(III) at concentration ranges of 0.1 to 10×10^{-6} M.

Stanley Bruckenstein* and P. R. Gifford, Chemistry Department, State University of New York at Buffalo, Buffalo, N.Y. 14214 *Anal. Chem., 51 (1979)*

Optimization of Precision in Dual Wavelength Spectrophotometric Measurement
256

Dual wavelength spectrometric measurement is shown to be effective in combatting uncertainty due to optical artifacts produced by samples and cells under non-ideal conditions.

Kenneth L. Ratzlaff* and Hamzah bin Darus, Department of Chemistry, The Michael Faraday Laboratories, Northern Illinois University, DeKalb, Ill. 60115 *Anal. Chem., 51 (1979)*

Reduction of Matrix Interferences for Lead Determination with the L'vov Platform and the Graphite Furnace
261

Using the carbide-coated platform, Pb in matrices which contain chloride, sulfate, and phosphate without resorting to matrix modifications is determined.

Walter Slavin* and D. C. Manning, The Perkin-Elmer Corporation, Main Avenue, Norwalk, Conn. 06856 *Anal. Chem., 51 (1979)*

Molecular Absorption Spectra of Complex Matrices in Premixed Flames
266

Nonatomic absorption in premixed flames by untreated complex matrices is shown to be low in magnitude and due only to molecular spectra of inorganic salts.

R. C. Fry and M. B. Denton,* Department of Chemistry, University of Arizona, Tucson, Ariz. 85721 *Anal. Chem., 51 (1979)*

NEW!

NOW, CALCULATE AND PLOT GPC RESULTS AUTOMATICALLY.

If your work involves polymer characterizations using gel permeation chromatography, here's a new product that can save you time and increase your throughput. It's the Chromatix LDS series, a laboratory data system with turnkey software specifically designed to handle GPC data. Yet, it's so versatile because of the disk based operation, that it's easy to customize for your particular needs or to modify as your requirements change.

With the Chromatix LDS, you run your experiment in the usual way. Then, while the sample is eluting from the column, the LDS automatically calculates and stores the data in real time, and provides a printout and plot of the results. If desired, the program can easily be modified to provide different computations, reports, or plots, as required.

Besides the GPC program, other turnkey application software now available on disk from Chromatix includes: 1) molecular weight distributions (using a GPC and a Chromatix KMX-6 light scattering photometer, 2) absolute molecular weight (using the KMX-6), and 3) diffusion coefficients and molecular size (using the KMX-6 and an autocorrelator such as the Chromatix Model 64).

Basic elements of the LDS series are the Chromatix developed software coupled with a powerful disk-based DIGITAL® LSI-11 Microcomputer (part of the PDP-11 family) operating under DIGITAL's RT-11. The input/output terminal is a high resolution printer/plotter combined into a single unit with a keyboard. For program creation and editing, either of two widely used programming languages are optionally available on system disks, BASIC and FORTRAN. Also, since the LSI-11 is part of the PDP-11 family, the extensive software already developed for this widely used computer can generally be run without modification by simply inserting a new disk.

If you'd like to learn more about this exciting new product, call or write Chromatix today. Or circle No. **37** for *LDS brochure*, No. **38** for *KMX-6 brochure*, No. **39** for *Model 64 brochure*, or No. **40** for a technical representative to call.

chromatix

560 Oakmead Parkway
Sunnyvale, CA 94086
Phone: (408) 736-0300
TWX: 910-339-9291

D6903 Neckargemünd 2
Unterestrasse 45a
West Germany
Phone: (06223) 7061/62
Telex: 461-691

See this new product in Booths 1934/35 at the Pittsburgh Conference

NEW

Tape Recordings on

TOXIC SUBSTANCES CONTROL

☐ **Toxic Substances Control Act**
Implementation of the Toxic Substances Control Act poses many problems and offers some opportunities. The role of Government, industry and universities is discussed.
5 Speakers

☐ **Methods for Risk Assessment**
Risks and hazards posed to society by chemicals, radiation, and other toxic materials are discussed by scientists and Government spokesmen. **5 Speakers**

☐ **Monitoring Toxic Substances**
Dr. Bruce Ames and scientists from ERDA and MIT discuss hazards and detection of carcinogens, mutagens, and other toxic substances found in industrial environments.
4 Speakers

☐ **Biological Effects of Pollutants**
Experts examine the effects of environmental pollutants on health. Long-term/low-level studies, and controlled studies in humans are discussed. **5 Speakers**

☐ **Chemical Carcinogens**
An in-depth look at the problem of hazardous substances in the environment. Experts from N.I.O.S.H., EPA, and the National Cancer Institute discuss the what, why, how, and management of this growing national problem.
5 Speakers

Prices: $19.95 per title (Postpaid)

cassettes only
price includes printed copies of slides used

SPECIAL—$49.95 Any Three Titles (Postpaid)

ORDER FROM:
American Chemical Society
1155 Sixteenth Street, N.W.
Washington, D.C. 20036
Dept. AP

Name ____________________

Address ____________________

City __________ State __________ Zip __________

(Allow 4 to 6 weeks for delivery)

Briefs

Gas Chromatographic–Mass Spectrometric Determination of Etorphine with Stable Isotope Labeled Internal Standard 269

Etorphine, a potent synthetic analgesic, is determined in concentrations as low as 2 ng/mL in urine with errors of about 0.1 ng/mL.

Satya P. Jindal,* Theresa Lutz, and Per Vestergaard, Rockland Research Institute, Orangeburg, N.Y. 10962
Anal. Chem., 51 (1979)

Hydroxyl Ion Negative Chemical Ionization Mass Spectra of Steroids 272

The spectra are simple and might serve as a basis for analysis of steroids.

T. A. Roy and F. H. Field,* The Rockefeller University, New York, N.Y. 10021, and **Yong Yeng Lin and Leland L. Smith,** The University of Texas Medical Branch, Galveston, Tex. 77550
Anal. Chem., 51 (1979)

High Sensitivity, Continuous Flow Thermochemical Analyzer 278

Small (120 μL) samples of HCl, Ca, and nitrite are analyzed by a flow thermal detector at a throughput of 60 samples/h with a precision of 1–3%.

Richard S. Schifreen, Carolyn Sue Miller, and Peter W. Carr,* Department of Chemistry, University of Minnesota, Minneapolis, Minn. 55455 *Anal. Chem., 51 (1979)*

Liquid Chromatographic–Fluorometric System for the Determination of Indoles in Physiological Samples 283

Several important indolic tryptophan metabolites are determined in cerebrospinal fluid, brain, plasma, and urine with absolute detection limits of 5–22 pg.

George M. Anderson* and William C. Purdy, Department of Chemistry, McGill University, Montreal, Quebec, Canada
Anal. Chem., 51 (1979)

Dual Wavelength Spectrophotometric Detector for High Performance Liquid Chromatography 287

Differentiation of structural related compounds in serious overlapping elution peaks is demonstrated.

Kuang-Pang Li* and John Arrington, Department of Chemistry, University of Florida, Gainesville, Fla. 32611
Anal. Chem., 51 (1979)

Analysis of Gasoline for Antiknock Agents with a Hydrogen Atmosphere Flame Ionization Detector 292

Detection limits are calculated to be 7.2×10^{-12} g/s of Pb and 1.7×10^{-14} g/s of Mn in leaded and unleaded gasoline.

M. D. DuPuis and H. H. Hill, Jr.,* Department of Chemistry, Washington State University, Pullman, Wash. 99164
Anal. Chem., 51 (1979)

The Ohaus Brainweigh 1500D.
The electronic balance that thinks twice for you.

What makes our new Ohaus Dual-Range 1500D so smart?

It gives you two ways to profit from one electronic balance:

1) 150g x 0.01g capacity and sensitivity or
2) 1500g x 0.1g capacity and sensitivity

By the touch of a bar you enjoy the advantages of two different balances. In one compact unit. With one low price tag — only $1,595 (a lot less than some electronic balances with a lot less to offer).

The brain behind it all.

The tiny genius that controls the 1500D is our sophisticated microprocessor, which stores operator commands, then responds **only** after the reading is stable.

That means human interaction without human error, in more ways than one.

Consider all the intelligent features Ohaus squeezed into each compact 1500D...

- Die-Cast Construction. Stands up to abuse. Stain resistant. Wipes clean. Protects against dust and spills.
- Microprocessor "Brain". Fewer components for greater reliability.
- Compact Size. Ideal for lab table. Sturdy enough for production line.
- Clearly Labelled Controls. Right up front for quicker and easier operation.
- Large, Stable Platform. Takes variety of objects and unexpected overloads in stride.
- Big, Easy to Read Digits. Seen when seated or standing. If overloaded, "error" shows.
- Span Calibration Adjustment. Recessed above tare bar.
- Rock-Steady Display. "g" lights up for stable reading.
- "Rapidtouch" Tare Bar. Recessed to avoid accidentally taring.

And you can learn to operate one in just a few minutes.

Give the new 1500D the twice over.

Send us this coupon — and we'll send you our full-color catalog about the 1500D and all the new Ohaus Brainweighs. The weigh of the future.

The Ohaus 1500D. Fully guaranteed. And backed by over 70 years of Ohaus quality engineering.

Once you have one, you won't have to think twice about it.

OHAUS

Ohaus Scale Corporation, Dept. 11-029,
29 Hanover Road, Florham Park, N.J. 07932, (212) 377 9000

☐ Yes, show me the weigh of the future. Send me the full color catalog on the Ohaus Brainweighs.

☐ I'm ready to see a demonstration. Please have a dealer sales rep call me.

NAME ____________________
TITLE ____________________
ORGANIZATION ____________________
CITY ____________________
STATE ____________ ZIP ____________
PHONE NUMBER ____________________

CIRCLE 157 ON READER SERVICE CARD

0.00 g
OHAUS
THE OHAUS BRAINWEIGHS™
The weigh of the future.

© [illegible]

LIF-O-GEN®
SPECIALTY GASES

Lif-O-Gen® is a leading specialty gas manufacturing company with total capabilities in processing a broad range of high purity research gases, primary gas calibration standards, and gas mixtures as well as a complete line of gas handling equipment, instrumentation and analytical devices.

For particular gases or equipment to meet your own special requirements, please write or phone Lif-O-Gen®, Specialty Gas Department, P.O. Box 149 Woods Rd., Cambridge, Maryland 21613 (301) 228-6400 TWX: 710-865-9652

LIF-O-GEN® OFFERS

• Pure Gases • Gas Mixtures • Gas Handling Equipment • Gas Chromatographs • Electronic Gases • Pollution Monitoring Gases • Calibration Gases • Complete range of refillable and disposable aluminum and steel cylinders • Lif-O-Gen® Gas Encyclopedia, the most complete and advanced encyclopedia of its kind in the world

LIF-O-GEN®
American Life Support Corp.
P.O. Box 149, Woods Rd.
Cambridge, Maryland 21613

A Subsidiary of Liquid Air Corp. of North America

© Copyright 1979, Lif-O-Gen®

CIRCLE 213 ON READER SERVICE CARD
See us at the Pittsburgh Conference, Booths 1701 and 1703

Briefs

Simultaneous Determination of Americium and Curium in Soil 295

The precision for americium and curium activities between 0.1 pCi/g and 1.0 pCi/g is between 3–8%. The detection limit is 0.002 pCi/g and there is no detectable bias.

Michael H. Hiatt and Paul B. Hahn, U.S. Environmental Protection Agency, Office of Research and Development, Environmental Monitoring and Support Laboratory, P.O. Box 15027, Las Vegas, Nev. 89114 *Anal. Chem., 51 (1979)*

Correspondence

Regression Line That Starts at the Origin 298

Frederick C. Strong III, Faculdade de Engenharia de Alimentos e Agrícola, Universidade Estadual de Campinas, Caixa Postal No. 1170, 13100 Campinas, S.P., Brasil *Anal. Chem., 51 (1979)*

Exchange of Comments: Analytical Methods of Bis(chloromethyl) Ether in Air 299

Charles C. Yao,* Bendix Special Projects Laboratory, Launch Support Division, Cocoa Beach, Fla. 32931, and **Heinrich Zollinger,** Technisch-chemisches Laboratorium, Eidgenössische Technische Hochschnle (ETH), 8092 Zurich, Switzerland, and **G. J. Kallos,* R. A. Solomon, and J. C. Tou,** Analytical Laboratories, Dow Chemical U.S.A., Midland, Mich. 48640 *Anal. Chem., 51 (1979)*

Thin Carbon Foils for the Elimination of Charging Effects in Proton Induced X-Ray Emission Spectrometry 302

H. Oona, Stephen J. Kirchner, Peter L. Kresan, and Quintus Fernando,* Department of Chemistry, University of Arizona, Tucson, Ariz. 85721, and **Harry Zeitlin,** Department of Chemistry, University of Hawaii, Honolulu, Hawaii 96822 *Anal. Chem., 51 (1979)*

Exchange of Comments: Particle Size Effects in the Determination of Respirable α-Quartz by X-ray Diffraction 304

S. Altree-Williams, Division of Occupational Health & Radiation Control, Health Commission of New South Wales, P.O. Box 163, Lidcombe, Australia 2141, and **J. W. Edmonds,** Analytical Laboratories, Bldg. 574, Dow Chemical Co., Midland, Mich. 48640 *Anal. Chem., 51 (1979)*

Aids for Analytical Chemists

Determination of the Natural Abundance of Iron-58 by Neutron Activation Analysis 306

P. F. Schmidt,* Bell Telephone Laboratories, Incorporated, Allentown, Pa. 18103, and **J. E. Riley, Jr.,** Bell Telephone Laboratories, Incorporated, Murray Hill, N.J. 07974 *Anal. Chem., 51 (1979)*

Effective X-Ray Analysis
TN-2000

The TN-2000 is the most powerful system available for quantitative X-Ray spectrum analysis.

With *programmable operation,* a number of data reduction and analysis routines are available (such as ZAF, Bence-Albee, Rasberry Heinrich, thin film corrections and multiple least squares fitting and deconvolution).

And the hardware is strictly "state of the art": The distributed processing design uses the LSI-11/2® (which is capable of a variety of simultaneous operations) for data analysis and system control. For the ultimate in number-crunching quantitative analysis, a PDP-11® type minicomputer can be substituted for the LSI-11/2.

X-Ray spectra are stored in a 24 bit (bipolar) memory, and displayed on a high resolution CRT. Multiple Regions of Interest are standard along with an exclusive peak search routine that displays KLM line markers and up to 20 separate elemental peak labels.

Yet, with all this, the TN-2000 features an economy of operation unmatched by any other analyzer. The *English language commands* that control the system are entered on a pressure sensitive touchpad that is backlighted for use in the darkened lab environment.

Northern
Northern TN 2000

A variety of options are also offered to upgrade the TN-2000, including floppy disk storage, mag tape, printers, plotters, etc. Where column automation is required, the TN-1310 MECCA (*Modular Electron Column Automation*) can be combined with the TN-2000 system for simultaneous EDS and WDS. The TN-1310 has been successfully used to automate a number of different columns and provides outstanding results when used with the TN-2000.

For more information contact Tracor Northern.

Tracor Northern

2551 West Beltline Highway / Middleton, Wisconsin 53562 / (608) 831-6511 / TWX-910-280-2521
Tracor Europa B.V. / Schiphol Airport Amsterdam / Building 106, The Netherlands / Telephone (020) 41 1865 / Telex 13695

® DEC Trademark

CIRCLE 201 ON READER SERVICE CARD

Briefs

Errors in the Atomic Absorption Determination of Calcium by the Standard Addition Method 307

J. W. Hosking,* K. R. Oliver, and B. T. Sturman, Department of Chemistry, Western Australian Institute of Technology, Bentley, W.A. 6102, Australia *Anal. Chem., 51 (1979)*

Analysis of Bis(trimethylsilyl)acetamide for Purity by Proton Magnetic Resonance Spectrometry 311

Gordon Munro,* John H. Hunt, and Leonard R. Rowe, Glaxo-Allenburys Research Ltd., Ware, Herts., England, and **Michael B. Evans,** The Hatfield Polytechnic, Hatfield, Herts., England *Anal. Chem., 51 (1979)*

Pressure-Volume Technique for the Calibration of Ozone Analyzers 313

Ikuo Watanabe and Edgar R. Stephens,* Statewide Air Pollution Research Center, University of California, Riverside, Calif. 92521 *Anal Chem., 51 (1979)*

Wet Digestion Method for the Determination of Mercury in Biological and Environmental Samples 315

J. Ross Knechtel* and J. L. Fraser, Wastewater Technology Centre, Environmental Protection Service, Environment Canada, Burlington, Ontario L7R 4A6, Canada *Anal. Chem., 51 (1979)*

Probe for Direct Exposure of Solid Samples to the Reagent Gas in a Chemical Ionization Mass Spectrometer 317

Robert J. Cotter, Johns Hopkins University School of Medicine, Department of Pharmacology and Experimental Therapeutics, Baltimore, Md. 21205 *Anal. Chem., 51 (1979)*

Spectrophotometric Determination of Secondary Amines 319

Dale H. Karweik* and Carl H. Meyers, Department of Chemistry, Wayne State University, Detroit, Mich. 48202 *Anal. Chem., 51 (1979)*

CONSERVE GAS — SAVE $$$ WITH GAS MISER™

Helium or other carrier gas costs for GC can be reduced considerably with the Gas Miser from Matheson. Gas Miser enables gas chromatographers to maintain a reduced carrier gas flow when their GCs are on standby. The Gas Miser pays for itself in less than a year.

Matheson recommends that gas chromatographs be set on standby when not in use. Until now, this entailed spending valuable time adjusting the pressure regulators and needle valves – only to readjust them when the system was put back into use. Gas Miser does the job of reducing the gas flow with the flick of a switch. Full gas flow is restored just as easily.

Construction is of copper and brass. Gas Miser is sold with a 100 psig gauge. Instructions for set up are included with every instrument. Contact **Matheson, 1275 Valley Brook Ave., P.O. Box E, Lyndhurst, NJ 07071.**

CIRCLE 138 ON READER SERVICE CARD

LAB STAT II® MONITOR

Matheson's LAB-STAT II Model 8222 is a controller that can monitor any laboratory operation involving a changing liquid level.

There are two interconnected components: a sensing probe and an amplifier control chassis. The sensing probe employs a temperature compensated, voltage regulated, solid-state oscillator sensitive to small changes in electrical capacitance to ground. Slight changes in a liquid level alter the electrical capacitance of the probe and its circuitry.

Matheson
Matheson

Clipped to a laboratory thermometer, it can be used as a warning device for accurate, temperature control, to 0.1° C. It can detect slight liquid changes in barometers, manometers, and sight glasses. Outlets on the amplifier accommodate on/off switches and alarm. A Multiple Probe Module (also pictured) is available for attaching up to four probes to a single LAB-STAT II.

For further information, contact **Matheson, 1275 Valley Brook Avenue, P.O. Box E, Lyndhurst, NJ 07071.**

CIRCLE 139 ON READER SERVICE CARD

See us at the Pittsburgh Conference, Booth 108

USE GASES IN YOUR LAB? CHANCES WE CAN HELP YOU ARE 99.9999%.

1. GASES
   We carry more gases and more grades of these gases than any of our competitors.
2. EQUIPMENT
   To deliver the gas safely and correctly to its point of use, we list over 2,000 matched component equipment items including regulators, flowmeters, manifolds, filters, and automated mixing apparatus just to name a few.
3. CALIBRATION GAS STANDARDS
   We always felt we wrote the book on gas mixtures. And we did. Pages 8 through 57 of our new catalog can tell you almost anything you need to know about calibration mixtures and those very special high purity gases which meet the requirements of today's instrumentation.
4. SAFETY
   Job and plant safety? We publish more information on this subject than anyone else where gases and how you should handle them are concerned.

We have two reader service numbers below. The lower one is for our new catalog and the higher one is for our safety information. We have the information to help you.

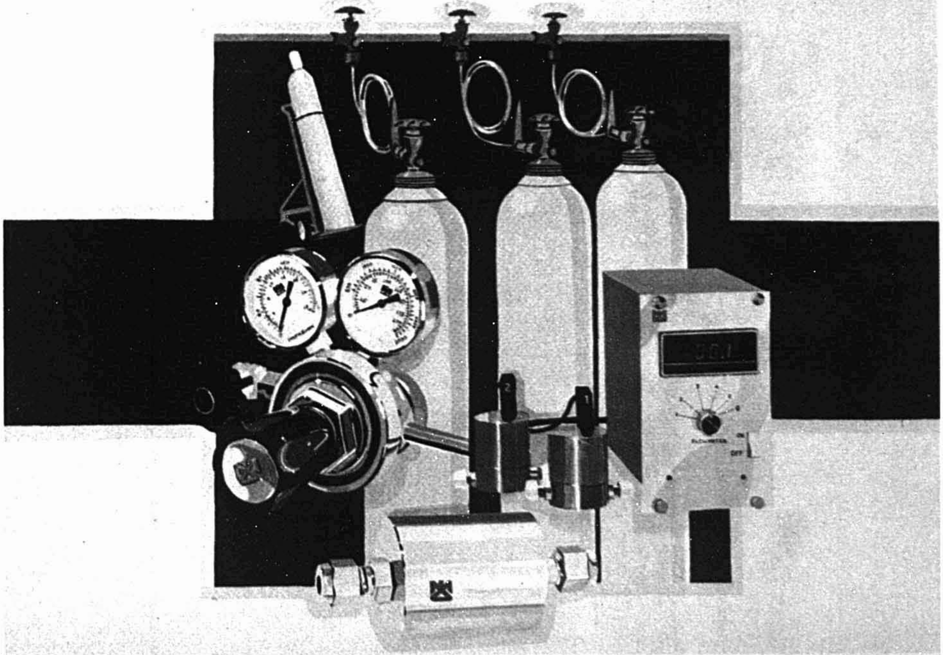

Matheson
Lyndhurst, N.J. 07071

East Rutherford, N.J. 07073/Morrow, Georgia 30260/La Porte, Texas 77571
Gloucester, Massachusetts 01930/Joliet, Illinois 60434/Gonzales, Louisiana 70737
Cucamonga, California 91730/Newark, California 94560/Bridgeport, N.J. 08014
Dorsey, Maryland 21227/Whitby, Ontario, Canada L1N 5R9
Edmonton, Alberta, Canada T5B 4K6/B2431 Oevel, Belgium
6056 Heusenstamm, West Germany

Circle No. 140 for Catalog

See us at the Pittsburgh Conference, Booth 108

Circle No. 141 for Information

The Bausch & Lomb Blue Line of SPECTRONIC® Spectrophotometers.

You're looking at the finest family of single beam spectrophotometers in the world.

The Blue Line.

These four great Bausch & Lomb instruments give you sampling versatility that can't be matched.

They give you longer wavelength ranges, a choice of narrow spectral slit widths, and a variety of sample handling techniques.

They give you speed and accuracy with features such as automatic 0%T, direct concentration readouts, optional flow cells, and automation systems.

They even give you updateability, because they're designed to grow as you grow. The more demanding you are, the more capable they can become.

The Blue Line—the SPECTRONIC 70, 88, 710, and the famous SPECTRONIC 100—is the best, not just because of Bausch & Lomb's proven reputation for the finest performing instrumentation.

And not just because the Blue Line is supported by a nationwide network of product support specialists.

But because you can get research quality from any one of the Blue Line at a routine instrument price.

Call your nearest Bausch & Lomb representative, or one of our dealers—Fisher Scientific or VWR Scientific. Or call us at (716) 385-1000, ext. 325.

THE RIGHT ANSWERS again & again

BAUSCH & LOMB
ANALYTICAL SYSTEMS DIVISION
ROCHESTER, NEW YORK 14625

One very blue-blooded family.

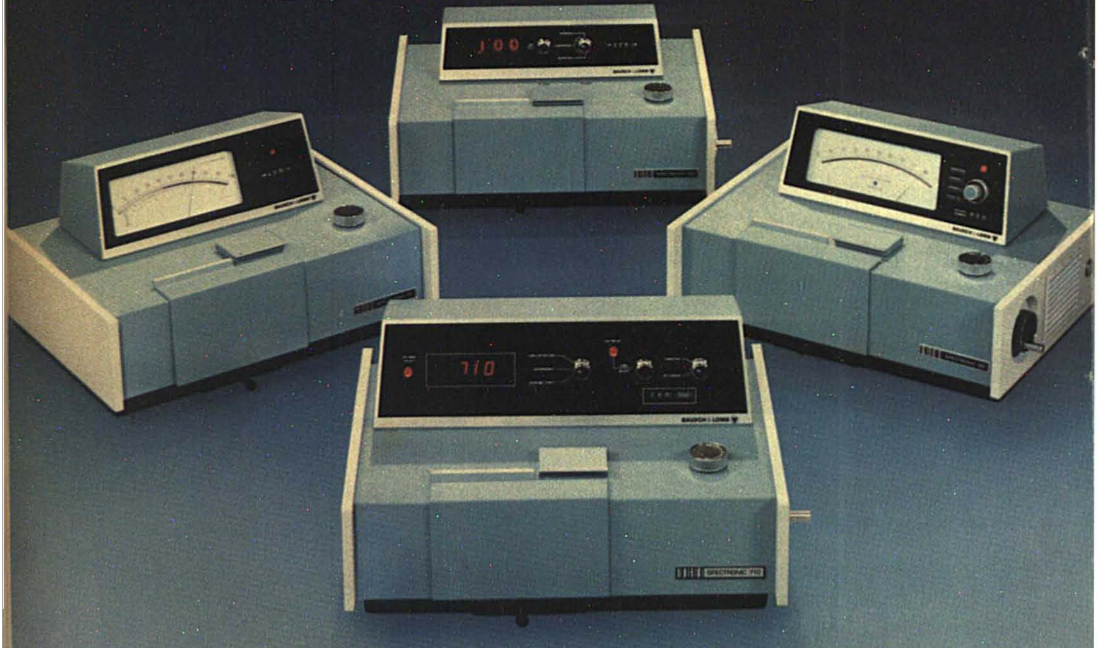

Get more than reliable spectrophotometric hardware. Get unmatched backup to go with it.

Bausch & Lomb Service A Bausch & Lomb SPECTRONIC® Spectrophotometer is the most reliable of its kind to own, for several reasons. First, it's backed by a nationwide network of Bausch & Lomb and dealer sales/service centers. Our people help you before the sale as well as after, showing you the best way to use our instruments. Next, you'll find that our hardware is designed for the utmost uptime. It can be easily checked and calibrated in minutes, and its modular electronic components are quickly replaced in the lab. And all of our spectrophotometers, of course, carry a free one-year warranty covering all parts and labor. So, again and again, our service assures you of getting the right answers when you need them.

Bausch & Lomb Applied Research Our Analytical Products Applications Laboratory is another source of right answers for you. It's staffed with scientists whose job it is to answer the who's, what's, where's, when's and why's concerning spectrophotometric analysis. Whether you own one of our instruments or are evaluating instruments for purchase, you can avail yourself of this valuable service—absolutely free. And if through our equipment we can't help you obtain those all-important right answers, we can tell you who can. What's more, you'll benefit from the information we provide, not only from our own data bank, but from our access to the Corporate Science Library and other information retrieval systems such as NERAC and Lockheed/DIALOG. Bausch & Lomb Applied Research . . . helping you get the right answers again and again.

Bausch & Lomb's Data Bank Again, more right answers. Within our Applications Laboratory, our Data Bank contains more than 14,000 references to methodologies applicable to Bausch & Lomb instruments, many of which were developed in the Laboratory to answer requests like yours. The content of this Data Bank is multidisciplinary. Access is immediate. And access to this information is free to all owners of Bausch & Lomb instruments. The Bausch & Lomb Data Bank—the need for right answers keeps it working for you.

Bausch & Lomb: 716-385-1000, Ext. 325. Call us today at this number and get the right answers about any of our services—our superb line of spectrophotometers, our unmatched service, our Applications Laboratory, or our Data Bank. Find out how all this makes Bausch & Lomb your best choice for what your business needs:

THE RIGHT ANSWERS again & again

BAUSCH & LOMB
ANALYTICAL SYSTEMS DIVISION
ROCHESTER, NEW YORK 14625

Again and again, the right answers come from Bausch & Lomb

See us at the Pittsburgh Conference, Booth 220.

CIRCLE 26 ON READER SERVICE CARD

The Complete Mass Spectrometry Company

GC/MS
Extranuclear Laboratories simplifies organic analysis in the mass range of 3-1200 amu with the spectrEL GC/MS. Versatile design allows the vacuum system to accept a batch inlet or solids probe in addition to the GC. Data systems can be coupled to the instrument.

GC/MS with Simultaneous CI/EI
SIMULSCAN, the latest development in GC/MS, provides simultaneous but separate CI/EI spectra for the same sample combining the structural and fingerprint characteristics of EI with the high sensitivity and simpler molecular ion spectra of CI.

Atmospheric Pressure Ionization
This most efficient ionization technique for MS is capable of detecting ultratrace quantities of drugs, pesticides and hazardous chemicals (for example, 1 part TNT in 10^{12} parts air).

"plus"-SIMS
For surface analysis and depth profiling, "plus"-SIMS offers higher sensitivity, full elemental and isotope coverage and high mass analysis as an add-on instrument to Auger and ESCA systems.

Modulated Beam Mass Spectrometer
An instrument of innovative design that separates sample from background spectrum, preserves sample identity, and examines samples unacceptable to conventional MS.

Quadrupole Mass Spectrometer Components
Extranuclear provides a variety of QMS components with a combination available to solve specific analytical problems.

Special Systems
Special systems for negative ions, phase spectrometry, Knudsen cell studies, isotopic ratios, flame analysis, and molecular beam experiments are available.

Extranuclear Laboratories, Inc.
P.O. Box 11512 / Pittsburgh, Pennsylvania 15238
(412) 782-3884 *Telex: 812-318 Extralab Pgh*

CIRCLE 74 ON READER SERVICE CARD
Visit at the Pgh. Conference.
Booths 1041-46

analytical chemistry

Reader Survey Results

A large majority, 85.2%, of respondents to the November Reader Survey on Federal regulations believe that scientists need new mechanisms to make their views known to Federal authorities. Only 21% believe that the scientific data used as the basis for the formulation of regulations are adequate. However, only a slight majority, 58.8%, feel that the number and kind of Federal regulations that impinge upon the work of chemists are excessive. For complete results to the November Reader Survey, see below.

1. In general, do you feel that the number and kind of Federal regulations that impinge upon the work of chemists are excessive?

Yes 58.8% No 41.2%

2. Are there any facets of your work (research, monitoring, testing, etc.) that are in any way related to Federal regulations or the regulation-setting process?

Yes 81.2% No 18.8%

3. Do the regulations with which you are familiar make sense to you in comparing costs vs. the public good?

Yes 43.2% No 56.8%

4. Are you or any of your colleagues interacting with Federal regulation adoption processes?

Yes 50.1% No 49.9%

5. Do you feel that the scientific data used are adequate for regulations as they are now being formulated?

Yes 21.0% No 79.0%

6. Do you believe that scientists have an effective voice in the regulation-setting processes?

Yes 14.6% No 85.4%

7. Do you believe that scientists need new mechanisms to make their views known to Federal authorities?

Yes 85.2% No 14.8%

8. Do you believe that scientists should become more involved in the political processes?

Yes 78.0% No 22.0%

9. Do you keep up-to-date with Federal moves in regulatory areas by reading the *Federal Register* or another publication devoted to the regulatory area?

Yes 45.6% No 54.4%

10. Did you read the article on REGULATIONS in this issue, page 1229 A?

Yes 87.0% No 13.0%

HPLC Solvents by J.T. Baker

Maximum consi
to-lot, bottle-to-
to-lot, bottle-to-
to-lot, bottle-to-
to-lot, bottle-to-b
to-lot, bottle-to-b
to-lot, bottle-to-bo
to-lot, bottle-to-bo
to-lot, bottle-to-bo
to-lot, bottle-to-bo
to-lot, bottle-to-bott
to-lot, bottle-to-bottl

High performance liquid chromatography problems are frequently related to the *variability* of the reagents used. Specifically: spurious UV absorbance, particulate matter, residues, unknown or uncontrolled water, etc. 17 Baker HPLC solvents, however, now provide maximum reproducibility... new predictability... exceptional consistency.

How is such unusual consistency achieved?

Extremely tight specifications coupled with superior product definition create consistency.

Examples? HPLC Acetonitrile is controlled for low UV absorbance at 210 nm (0.10 max.), 254 nm (0.05 max.), 280 nm (0.02 max.) and at 350 nm (0.01 max.); water 0.02% max.: residue 0.0005% max. Refractive index: controlled, consistent. Plus physical data. And of course, the actual lot analysis *for the specific lot in question* is always on the 'Baker Analyzed'™ container label. You can always verify our claims for reproducibility beforehand.

Consistency? Here are 10 consecutive lots of Baker HPLC Methanol:

Lot	1	2	3	4	5	6	7	8	9	10
Water %	0.03	0.04	0.02	0.03	0.02	0.03	0.02	0.02	0.02	0.03
Residue %	0.0003	0.0001	0.0001	0.0001	0.0001	0.0002	0.0002	0.00005	0.00005	0.00005
Abs. at 254 nm	<0.01	<0.05	<0.04	<0.05	<0.04	<0.03	<0.04	<0.05	<0.05	<0.03

A tested water content of 0.02-0.04% and a residue after evaporation of 0.00005-0.0003%. Our lot-to-lot product consistency provides you with solvents affording the best reproducibility.

Baker HPLC solvents are stocked where you need them. Contact one of the more than 120 Baker distributor locations in the U.S. and Canada to implement a stocking program to suit your needs.

For emergency shipments on HPLC solvents, your distributor can provide special Baker Super Service by calling a Baker Super Service Center for immediate shipment to you.

For more information, please use the coupon below and send to J.T. Baker Chemical Co., Phillipsburg, N.J. 08865, or call 201/859-5411.

J. T. Baker
"use matched" products and...Super Service

J.T.Baker®
CHEMICALS

J. T. Baker Chemical Co.
Phillipsburg, N.J. 08865

☐ I'm interested in learning more about the Baker HPLC solvents that are consistent bottle-to-bottle, lot-to-lot, bottle-to-bottle, lot-to-lot, bottle-to-bottle, lot-to-lot, bottle-to-bottle, lot-to-lot, bottle-to-bottle.

Name ______________________
Title ______________________
Department ______________________
Organization ______________________
Address ______________________
______________________ Zip __________
____

CIRCLE 19 ON READER SERVICE CARD

See us at the Pittsburgh Conference, Booths 405, 407, 409 & 411.

ห้องสมุด กรมวิทยาศาสตร์บริการ

PITTSBURGH CONFERENCE

Cleveland Convention Center
Cleveland, Ohio

March 5-9, 1979

The 30th Pittsburgh Conference on Analytical Chemistry and Applied Spectroscopy will feature a technical program appealing to the wide range of interests of chemists and spectroscopists. The 84 technical sessions scheduled include 15 planned symposia and a total of 739 papers. In addition, the Exposition of Modern Laboratory Equipment, held in conjunction with the meeting, will feature the largest exhibition in conference history with over 370 exhibitors showing the latest analytical instrumentation and related chemicals and supplies.

Preregistration is urged. Registration forms mailed before February 9, 1979, can be processed so that a badge, program, and souvenir will be mailed to attendees. Registration fees are $10 for preregistration, $20 for regular registration, and $3.00 for students and are payable when badges are picked up. A pocket admission tab for the exposition only will be provided free of charge. Registration forms may be obtained by writing to Mrs. Margaret Davison, Convention & Business Bureau of Greater Cleveland, 511 Terminal Tower, Cleveland, Ohio 44113. Housing information may be obtained from Alice Virnak at the same address.

During the Conference several awards will be presented to honor scientists who have made outstanding contributions to analytical chemistry and spectroscopy. The 1979 Pittsburgh Spectroscopy Award will be presented by the Spectroscopy Society of Pittsburgh to John S. Waugh, Noyes Professor of Chemistry at the Massachusetts Institute of Technology. Dr. Waugh will be cited for his many valuable contributions toward the development of NMR instrumentation and the mathematical treatment of nuclear spin systems. His most notable effort was the development of techniques for obtaining high-resolution NMR spectra of solids.

The Society for Analytical Chemists of Pittsburgh will present the 1979 Pittsburgh Applied Analytical Chemistry Award to Malvina Farcasiu of Mobil Research and Development Corp. The award is given for her paper, "Fractionation and Structural Characterization of Coal Liquids" (*Fuel*, **56**, 9, 1977).

John H. Beynon, Royal Society Research Professor of Chemistry at University College of Swansea, Wales, will receive the 1979 Maurice F. Hasler Award for his studies of organic molecules using mass spectrometry. The Williams-Wright Award, recently established by the Coblentz Society for the recognition of industrial spectroscopists who have made contributions to the

1979 CONDENSED PROGRAM

All Sessions Are in the Cleveland Convention Center

March 5

MONDAY MORNING

Gel Permeation Chromatography	Room 205
Mass Spectrometry Applications	Room 239
New Instrumentation I	Room 3A
Liquid Chromatography System Components	Club Room B
Symposium: Application of High-Pressure Liquid Chromatography to Environmental Problems—Practical Applications and Regulatory Considerations I	Room 235A
Environmental Analysis—Water Pollution I	Room 235B
Symposium: Laboratory Data Management	Little Theater
Atomic Absorption Spectroscopy I (Flameless)	Ball Room
Gas Chromatography—Instrumentation	Music Hall

MONDAY AFTERNOON

General Mass Spectroscopy	Room 240
Polymer Analysis	Room 205
UV–Visible Spectrophotometry I	Room 239
New Instrumentation II	Room 3A
Detectors in Liquid Chromatography	Club Room B
Symposium: Application of High-Pressure Liquid Chromatography to Environmental Problems—Practical Applications and Regulatory Considerations II	Room 235A
Environmental Analysis—Water Pollution II	Room 235B
Symposium: Applications of Ion Chromatography	Little Theater
Atomic Absorption Spectroscopy II	Ball Room
Gas Chromatography—Data Processing	Music Hall

March 6

TUESDAY MORNING

UV–Visible Spectrophotometry II	Room 240
General Photoacoustic Spectroscopy	Room 205
ESCA, Auger, and Electron Analysis Techniques	Room 239
Optimization of Liquid Chromatography Operating Parameters	Club Room B
New Instrumentation III	Room 235A
Environmental Analysis—Air Pollution I	Room 235B
Symposium: Fourier Transform/Computer Dispersive Spectroscopy	Little Theater
Atomic Absorption Spectroscopy III	Ball Room
Symposium: Practical Applications of Glass Capillary Columns in Gas Chromatography	Music Hall

TUESDAY AFTERNOON

New Instrumentation and Instrumental Concepts	Room 240
Symposium: Photoacoustic Spectroscopy	Room 205
General Surface Analysis	Room 239
Fourier Transform Infrared Spectroscopy I	Room 3A
Liquid Chromatography Applications I	Club Room B
Ion Chromatography–Thin-Layer Chromatography	Room 235A
Environmental Analysis—Air Pollution II	Room 235B
Symposium: Microprocessors in Action	Little Theater
Atomic Absorption Spectroscopy IV	Ball Room
Symposium: Trace Analysis with Glass Capillary Column in Gas Chromatography	Music Hall

March 7

WEDNESDAY MORNING

Magnetic Resonance Spectrometry	Room 240
Emission Spectrographic Analysis	Room 205
Symposium: New Techniques in Applied Surface Characterization	Room 239
Fourier Transform Infrared Spectroscopy II	Room 3A
Liquid Chromatography Applications II—Biomedical	Club Room B
Symposium: Environmental Organic Analysis of Water and Sediment	Room 235A
Environmental Analysis—Air Pollution III	Room 235B
Gas Chromatography—Detectors	Little Theater
Atomic Absorption Spectroscopy V	Ball Room
Dal Nogare Award Symposium	Music Hall

WEDNESDAY AFTERNOON

Raman Spectroscopy	Room 240
Trace Analysis	Room 205
Symposium: New Instrumentation and Techniques for Surface Analysis (ASTM E-42)	Room 239
Clinical Chemistry	Room 3A
Infrared Spectroscopy I/Liquid Chromatography for Drug and Clinical Analysis	Club Room B
Symposium: Use of ICAP Emission for Environmental Analysis	Room 235A
Environmental Analysis—General	Room 235B
1979 Awards Symposium	Little Theater
Gas Chromatography—Aids	Ball Room
Laboratory Automation	Music Hall

March 8

THURSDAY MORNING

Fluorescence–Luminescence	Room 240
Electroanalytical Chemistry	Room 205
Analysis of Oil and Other Organic Pollutants	Room 239
Infrared Spectroscopy II	Room 3A
Preparative Liquid Chromatography/Sampling Systems: HPLC	Club Room B
Inductively Coupled Plasma Spectroscopy	Room 235A
Symposium: New Techniques on the Horizon	Room 235B
Symposium: Biomedical Aspects	Little Theater
Gas Chromatography—Ancillary Techniques	Ball Room
Computer Applications I: Microprocessors	Music Hall

THURSDAY AFTERNOON

Luminescence Applications	Room 240
General Analysis	Room 205
Biochemical Analysis	Room 239
Emission Spectroscopy—General I	Room 3A
The Column in High-Performance Liquid Chromatography	Club Room B
Symposium: Trace Analysis in Characterization of Materials	Room 235A
Automated Electrochemical and Spectrochemical Methods	Room 235B
Coblentz Society Award Presentations and Symposium	Little Theater
Gas Chromatography—Applications	Ball Room
Computer Applications II: Minicomputers	Music Hall

March 9

FRIDAY MORNING

Thermal Methods of Analysis	Room 240
X-Ray Fluorescence, X-Ray Diffraction	Room 205
Toxicology and Drug Analysis	Room 239
Emission Spectroscopy—General II	Little Theater
Liquid Chromatography Analysis After Detection: Data Handling	Room 235A
Food Analysis	Room 235B

interpretation of vibrational spectra, will be presented to Norman B. Colthup, American Cyanamid Co.

On Wednesday morning the 1979 Stephen Dal Nogare Award will be presented to J. Calvin Giddings of the University of Utah for his contributions to chromatographic theory. On Thursday afternoon the Coblentz Award will be presented to Lionel A. Carreira of the University of Georgia for his work in coherent anti-Stokes Raman spectroscopy.

The social program will begin Sunday evening with "The Common Bond," a Cleveland-based singing group. The performance will be held in the Music Hall at the Convention Center, and admission will be by registration badge. Other planned activities include Americana Night at the Frederick C. Crawford Auto-Aviation Museum, a conference mixer, and a dinner-theater party.

Technical tours have been planned during the week to Gould Laboratories, Union Carbide Corp. Parma Technical Center, NASA Lewis Research Center, and Standard Oil Research Center.

The American Chemical Society will present seven short courses just preceding and following the conference. For titles, fees, and other details, see page 204 A, this issue. During the meeting Kontes will present a seminar on procedures for sample preparation and cleanup, and SAVANT (Sloane Audio-Visuals for Analysis and Training) will offer two audiovisual courses on liquid chromatography and atomic absorption. Further information on these can be found in this issue, page 208 A.

During the course of the week, various committees and subcommittees of the American Society for Testing and Materials will meet. Executive and governing board meetings of other societies are also scheduled, and ANALYTICAL CHEMISTRY's Instrumentation Advisory Panel will meet.

An employment bureau will be operating in Room 216 at the Convention Center. This service is available to all registrants without charge. Advance registration is urged. Job candidate or employer forms are available from Peter M. Castle, Westinghouse R & D Center, 1310 Beulah Road, Pittsburgh, Pa. 15235 (412-256-3566).

Further information on the meeting is available from John A. Queiser, U.S. Dept. of Energy, 4800 Forbes Avenue, Pittsburgh, Pa. 15213 (412-892-2400, ext. 585).

The following pages of ANALYTICAL CHEMISTRY contain the complete technical program and coverage of new products to be shown at the Exposition.

Award Winners

John S. Waugh
Pittsburgh Spectroscopy Award

Malvina Farcasiu
Pittsburgh Applied Analytical Chemistry Award

John H. Beynon
Maurice F. Hasler Award

Norman B. Colthup
Williams-Wright Award

J. Calvin Giddings
Dal Nogare Award

Lionel A. Carreira
Coblentz Award

Conference Officials

1979 Board of Directors

President: Herbert L. Retcofsky, *U.S. Dept. of Energy*

Vice President: Harold A. Sweeney, *Koppers Co., Inc.*

Chairman (Society for Analytical Chemists of Pittsburgh): Robert W. Baudoux, *U.S. Steel Corp.*

Chairman-Elect (Society for Analytical Chemists of Pittsburgh): Richard S. Danchik, *Alcoa Technical Center*

Chairman (Spectroscopy Society of Pittsburgh): Richard Obrycki, *Koppers Co., Inc.*

Chairman-Elect (Spectroscopy Society of Pittsburgh): John E. Graham, *Koppers Co., Inc.*

Past Conference Chairman: Jane H. Judd, *Westinghouse Electric Corp.*

Treasurer: John E. Graham, *Koppers Co., Inc.*

Assistant Treasurer: Robert W. Baudoux, *U.S. Steel Corp.*

Executive Secretary: Charles J. McCafferty, Jr., *PPG Industries, Inc.*

Conference Committees

Activities:

Chairman: J. Kevin Scanlon, *PPG Industries, Inc.*

Assistant Chairman: John P. Auses, *Alcoa Technical Center*

Cleveland Liaison: Norma Bottone, *Union Carbide Corp.*

PERKIN-ELMER

CONFERENCE CLARION

★★★ **Pittsburgh Conference in Cleveland, Ohio, March 5 — March 8** ★★★

PERKIN-ELMER READIES BIG PITT EXHIBIT

Coffee mug crowd *Perkin-Elmer's offer of free coffee mug, personalized with owner's photo, drew big crowds at previous Pittsburgh Conferences. Offer will be repeated this year.*

Universal LC system to be unveiled at show

Possibly the most far-reaching development in LC makes its bow at the exhibit this year. It's a super-versatile system that offers virtually infinite options for tailoring an analysis without regard *(Continued in Cleveland)*

Four rooms for demos augment floor booths

Besides its floor exhibit, Perkin-Elmer will present demonstrations of new instrumentation *(Continued in Cleveland)*

New IR Data Station big“inframation”source

A fast, precise, and low-cost unit for handling data from IR instruments performs practically any function the operator desires, including *(Continued in Cleveland)*

AA instruments crowd agenda of things to see

A unit whose automatic flame and flameless capabilities enable it to deliver two days' work in one day's time will be a feature of the Perkin-Elmer AA exhibit. It's the Model 5000, the top-line instrument that can process 50 samples for six elements in 30 minutes automatically, with every parameter under microcomputer control.

There's also the new HGA-400 Graphite Furnace with microcomputer control and *(Continued in Cleveland)*

More fluorescence, UV units being introduced

A full line of fluorescence spectrophotometers will make their appearance at Perkin-Elmer's show exhibit. They range from the microcomputer-controlled research grade Model MPF-44B, incorporating many advances in technology, to the new Model 3000, which brings the performance advantages of the microcomputer to routine work.

The new UV/Vis Model 320 — the second generation in microcomputer control *(Continued in Cleveland)*

Thirty booths to reveal mammoth array of analytical instrumentation, technology

In an exhibit packed with innovation and variety, Perkin-Elmer again emerges as the "must see" attraction for thousands of Pittsburgh Conference visitors.

The big overall feature, of course, is the extension of microcomputer control to practically every analytical technique served by Perkin-Elmer instrumentation. For example, there's the new AS-100 Automatic Sampler that measures sample volumes and injects them automatically to provide round-the-clock operation for the SIGMA series of gas chromatographs.

(Continued in Cleveland)

All product lines on view

- Atomic Absorption
- Data Handling Systems
- Elemental Analysis
- Fluorescence
- Gas Chromatography
- Head Space Analysis
- Infrared
- Liquid Chromatography
- Microbalances
- Nuclear Magnetic Resonance
- Polarimetry
- Scanning Auger Microprobes
- Thermal Analysis
- Ultraviolet

Stay-at-homes can visit show by mail

Anyone who can't get to the Conference can still learn the details of instruments at the exhibit. Simply write for literature to Perkin-Elmer Corp., MS-12, Main Ave., Norwalk, CT 06856.

PERKIN-ELMER

Expanding the world of analytical chemistry.

CIRCLE 160 ON READER SERVICE CARD

Audiovisuals:

Chairman: Charles D. Gaitanis, *Alcoa Technical Center*

Assistant Chairman: Paul Bauer, *Westinghouse Electric Corp.*

Employment:

Chairman: Peter M. Castle, *Westinghouse R & D Center*

Assistant Chairlady: Marilyn Senneway, *ARCO/Polymers, Inc.*

Exposition:

Chairman: Allen J. Sharkins, *Alcoa Technical Center*

Assistant Chairman: Richard S. Danchik, *Alcoa Technical Center*

Assistant: Joseph Drost, *Alcoa Technical Center*

Housing:

Chairman: Homer J. Birch, *U.S. Steel Corp.*

Assistant Chairman: Ralph M. Raybeck, *Jones & Laughlin Steel Corp.*

Printing:

Chairman: John A. Queiser, *U.S. Dept. of Energy*

Assistant Chairman: Marjorie A. Phillips, *Koppers Co., Inc.*

Program:

Chairman: S. David Cifrulak, *Calgon Corp.*

Assistant Chairman: Hector Silva, *Westinghouse R & D Center*

Publicity:

Chairman: Charles J. Belle, *Ferro Corp. Technical Center*

Assistant Chairman: Dan P. Manka, *Consultant*

Cleveland Liaison: Allen T. Pollock, *Harshaw Chemical Co.*

Registration:

Chairman: Richard Obrycki, *Koppers Co., Inc.*

Assistant Chairman: Frank W. Plankey, *University of Pittsburgh*

Assistant: Rita M. Bastiani, *Pittsburgh Public Schools;* Ernest F. Tretow, *Wheeling Pittsburgh Steel Co.*

Society Meeting Coordination:

Chairman: William D. McAninch, *Alcoa Technical Center*

Assistant Chairlady: Margaret A. McMahon, *Allegheny Ludium Steel Corp.*

Special Projects:

Chairman: William M. Hickam, *Westinghouse R & D Center*

Assistant Chairman: George L. Vassilaros, *Colt Industries*

Assistant: Rita M. Bastiani, *Pittsburgh Public Schools*

Special Assistant to the President:

Edwin S. Hodge, *Retired*

Advisory to the President:

Harry Fracek, *Fisher Scientific Co.*

Spouses' Program:

Chairlady: Irene McCafferty, *Pittsburgh, Pa.*

Assistant Chairlady: Louise Manka, *Pittsburgh, Pa.*

Long-Range Planning Committee:

Chairlady: Jane H. Judd, *Westinghouse Electric Co.;* Robert Mainier, John F. Jackovitz, Joseph A. Feldman, Alex J. Kavoulakis, Robert E. Witkowski

---

SEE ALL THIS AT CLEVELAND—AND MORE!

You'll miss plenty if you don't see our new thermal analysis equipment at the Pittsburgh Conference. **From the leader:** DSC-2 Differential Scanning Calorimeter ■ TGS-2 Thermogravimetric Analyzer ■ TMS-2 Thermomechanical Analyzer ■ Model 240 Automatic Elemental Analyzer ■ and a new microprocessor-controlled temperature programmer. If you can't come—write! Perkin-Elmer Corp., M.S.12, Main Avenue, Norwalk, CT 06856. Or Telephone: (203)762-6915.

PERKIN-ELMER
Expanding the world of analytical chemistry.

CIRCLE 158 ON READER SERVICE CARD

FOR QUALITY INSTRUMENTATION, ENTER PERKIN-ELMER

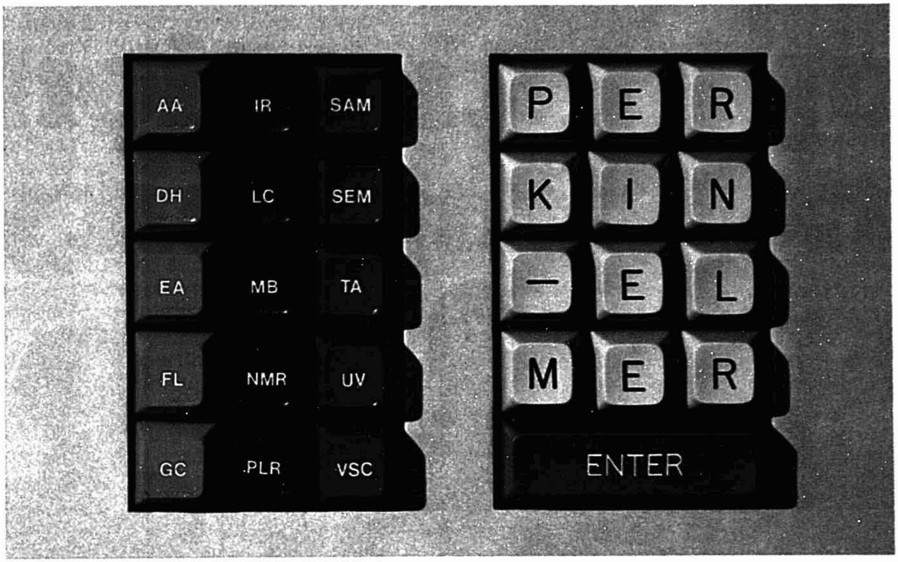

Enter Perkin-Elmer on your purchase order for the widest variety of analytical chemistry instruments available anywhere. We offer instrumentation ranging from sophisticated research units to workhorse models. All have state-of-the-art electronics. Most have microprocessor control. And we've got the accessories you want to broaden their usefulness. We're a single source for nearly all of your analytical instrument needs.

Send for a copy of our analytical instrument sourcebook. It describes our instruments and includes a collection of useful articles. You can get it as easily as pushing a button — just circle the Reader's Service Card number. Or write "Instrument News (IN-591)" and your name on your letterhead and send it to us at one of the addresses listed below.

Perkin-Elmer Corp., MS-12, Main
Avenue, Norwalk, CT 06856.

Coleman Instruments Division,
2000 York Road, Oak Brook,
IL 60521.

Bodenseewerk Perkin-Elmer &
Co. GmbH, 7770 Ueberlingen,
Bundesrepublik Deutschland.

Perkin-Elmer Limited,
Beaconsfield, Buckinghamshire
HP9 1QA, England.

Perkin-Elmer's analytical instrument product lines include:

- Atomic Absorption
- Data Handling
- Elemental Analysis
- Fluorescence
- Gas Chromatography
- Infrared
- Liquid Chromatography
- Microbalances
- Nuclear Magnetic Resonance
- Polarimetry
- Scanning Auger Microprobes
- Scanning Electron Microscopy
- Thermal Analysis
- Ultraviolet
- Vapor Space Chromatography

PERKIN-ELMER

Expanding the world of analytical chemistry.

CIRCLE 161 ON READER SERVICE CARD

หองสมุด กรมวิทยาศาสตรบริการ

A new level in HPLC sophistication and simplicity.

Also available as components. Buy what you need now, and add more as you need it.

Micromeritics proudly introduces its new 7500 microcomputer-based Liquid Chromatograph—a beautiful blend of engineering sophistication and operating simplicity.

We've taken the most advanced features available in HPLC today and packaged them so you can have the exact system to fit your specific application. Both gradient and isocratic integrated systems are available to accommodate rigorous quality control and methods development needs or the complex analysis functions of research and development laboratories.

Simple keyboard entry
All operating commands can be made from a single microcomputer-based control module. An alphanumeric display readout continually informs the operator of entry status for such parameters as flow rate, pressure limits, solvent concentration and column temperature.

Total analysis reporting
Comprehensive analysis reporting is achieved through a printer/plotter which not only gives you the chromatograms, but also a printout of gradient/solvent conditions, flow rate, pressure, temperature and operational status. Sample retention times, peak area and height, percent of concentration, sample and injection numbers can also be printed out.

Total automation
The 7500 system can be totally automated to give you unattended analysis around the clock. It can initiate 192 analyses of up to 64 samples . . . automatically.

Other advanced design features
The new 7500 also has an all new Ternary Solvent Mixer for more accurate and reliable low pressure solvent blending; a precision heated column compartment for faster more stable analysis; a new pulseless solvent delivery system; and a choice of three detectors—variable wavelength, fixed wavelength or refractive index.

Available as components, too
And finally, you have the option of buying as much or as little of the system as you presently need. The 7500 system is also available as individual components. You can buy what you need now and add more later as you need it.

To learn more about the many features that separate the new 7500 from all the other HPLCs on the market, contact Micromeritics Instrument Corporation, 5680 Goshen Springs Road, Norcross, Georgia 30093 USA (404) 448-8282 TELEX: 70-7450.

See it in operation at this year's Pittsburgh Conference Booths 101-106. Seminars in Room 246.

mi® micromeritics®

CIRCLE 134 ON READER SERVICE CARD

Whatever your HPLC needs, count

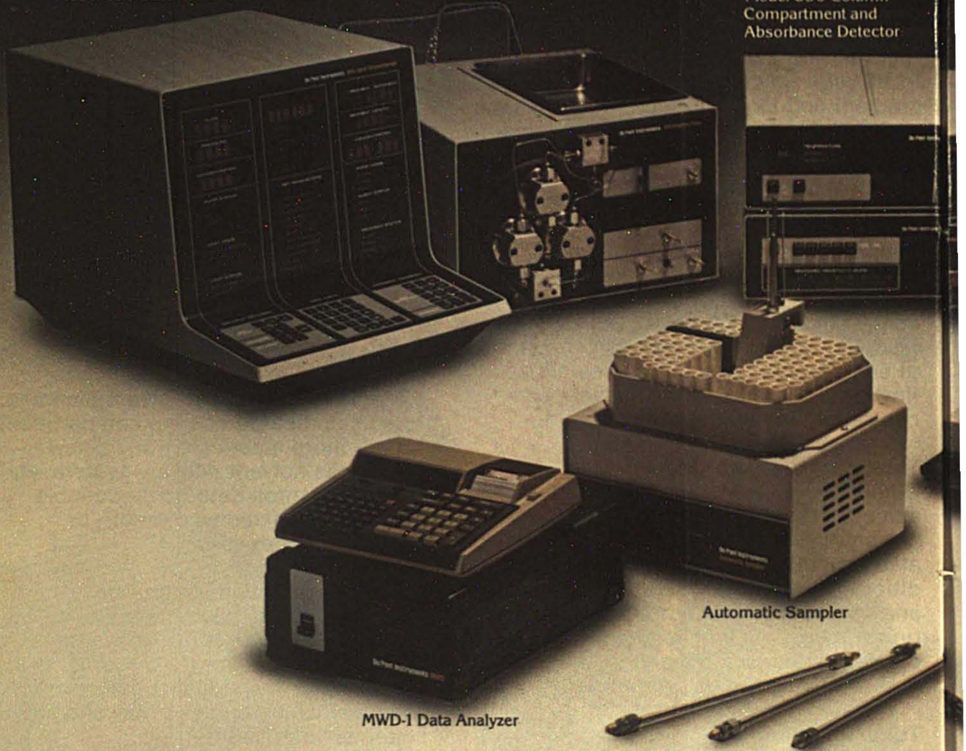
Model 850 LC Controller
Model 850 Gradient Pump
Model 850 Column Compartment and Absorbance Detector
Automatic Sampler
MWD-1 Data Analyzer
ZORBAX Columns

A look at this comprehensive line-up of instruments shows that DuPont offers today's broadest selection of HPLC Systems. And you can rely on this advanced generation of analyzers and accessories to provide precision, ease of use and day-in day-out reproducibility.

Our new Model 850 HPLC system offers flexible yet precise control over major separation variables. Our new high-performance 860 system is priced for repetitive LC functions, yet it gives you research level performance. The new DuPont PREP I Automated Sample Processor reduces sample preparation to a quick, simple process. And we've just introduced a new on-line Size Exclusion Chromatography Analyzer, the DuPont MWD-1 for quantitative molecular weight determination.

But DuPont offers much more than exceptional instruments. *We meet your total HPLC needs in three other ways as well: strong research, advanced column technology, and widespread facilities and services.* DuPont is unsurpassed in this combination.

You will profit continually from the work of our LC research team. It includes scientists recognized worldwide for their chromatographic publications, textbooks and new methodology.

Our LC columns offer the most advanced

on DuPont for the total answer.

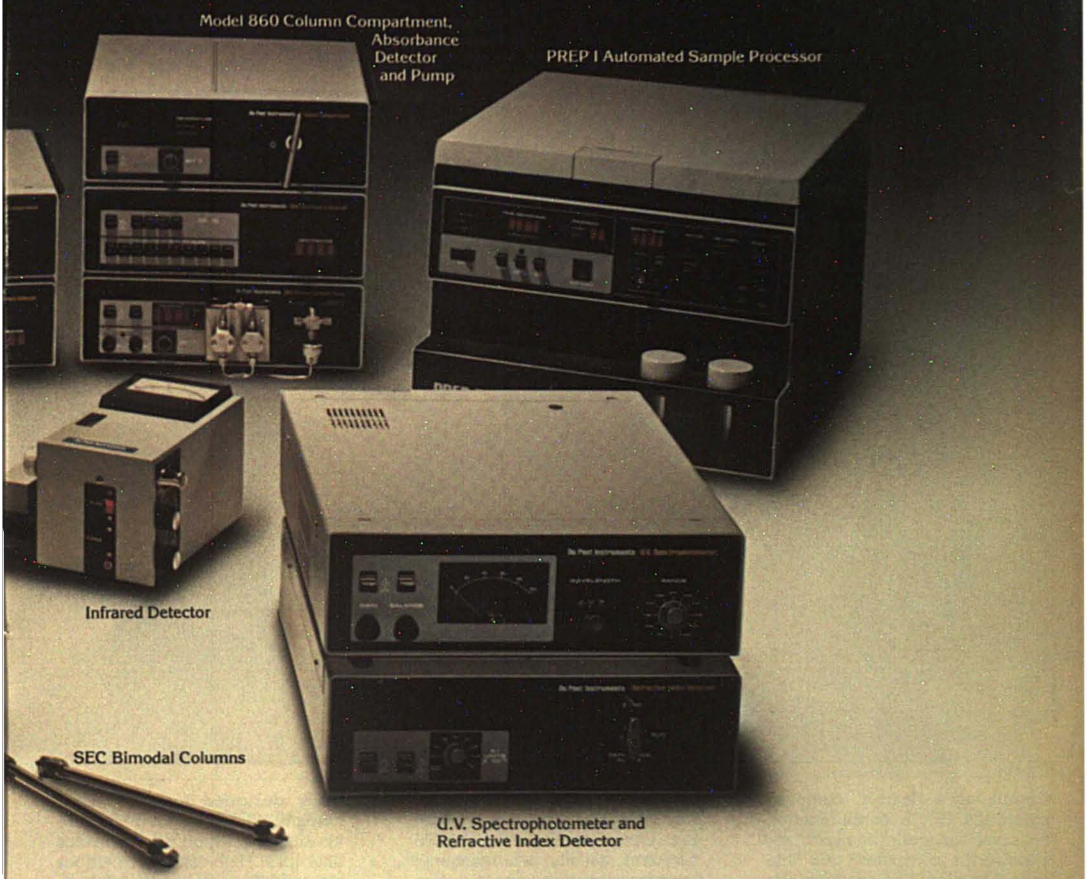
Model 860 Column Compartment, Absorbance Detector and Pump
PREP I Automated Sample Processor
Infrared Detector
SEC Bimodal Columns
U.V. Spectrophotometer and Refractive Index Detector

technology available, with guaranteed performance. One recent DuPont development—our new Bimodal SEC columns—provides an unprecedented linear calibration range of 2000 to 2,000,000. Another recent development —nonaqueous reversed phase chromatography (NARP)—significantly extends the power of reversed chromatography.

DuPont has totally dedicated its LC organization to meet your needs at all times: trained technical representatives to help meet your needs; service engineers to maintain your instruments; experienced chromatographers to help you solve specific separation problems; DuPont training courses to provide new users with an effective start in HPLC.

Call or write for full details.

Get our new LC literature or arrange for a visit by the DuPont Technical Representative in your area. Write to DuPont Instruments, Room 37074, Wilmington, DE 19898. For faster action, phone us toll-free at 800-411-9760. (In Delaware 772-5388.)

Liquid Chromatographs

Scientific & Process Instruments Division

DUPONT

CIRCLE 51 ON READER SERVICE CARD

Nine special features make Mass Spectrometer more

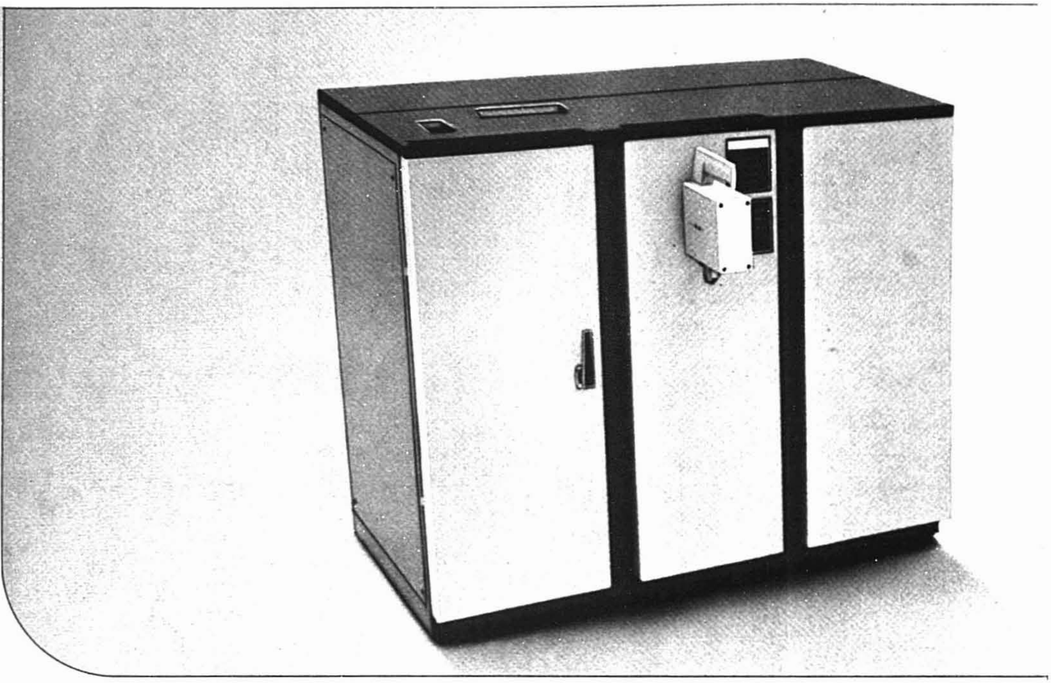

Combining a flexible, computer controlled GC, a contamination-resistant magnetic analyzer, and a powerful computer, this integrated system can produce analytical results on a variety of applications more easily than has ever before been possible.

Highest Available Sensitivity

EI signal-to-noise ratio of 10:1 on 100 pg of methyl stearate is easily attained and maintained in day-to-day use. A single computer-assisted tuning results in maximum sensitivity and resolution in both EI and CI modes.

Magnetic Analyzer with Accelerating Voltage Scan

High scan rates allow fast, continuous scanning over a wide mass range, and selected ion monitoring. Optimum sensitivity, resolution and stability are maintained over the entire mass range.

New Operating Ease and Flexibility

The DP 102 is controlled by the computer from a single software oriented keyboard with many specially designed function keys. Foreground/background capability with acquisition priority avoids data loss. High-capacity methods storage allows easy set-up for different applications and experiments.

Widest Dynamic Range Commercially Available

Data system dynamic range of 10^9 simplifies trace analysis, improves quantitative results, reduces need for repeat runs.

Automated Direct Introduction Probe

The utility of the DP 102 is enhanced by fully automatic sample insertion, vacuum valve operation and temperature control that

Du Pont's new DP 102 useful to more users.

make it easy to achieve excellent analytical results.

Instant EI to CI Switching

Versatility is expanded by a dual EI/CI source and instant selection of reagent gases for CI. Both EI and CI spectra can be generated in the same run, often on the same GC peak.

High-performance Capillary Column Interface

New, highly efficient jet separator and optional capillary column inlet provide optimum sample transmission and resolution with all types of GC columns.

Interpolation and Pattern Correction Software

Spectral abundances are automatically corrected and computed with greater accuracy than ever before in GC/MS.

Automatic Ion Source Rejuvenation

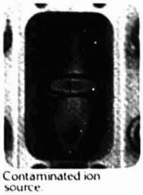

Contaminated ion source.

Ion source after rejuvenation.

Exclusive gold sputtering process restores source performance, without shutdown. Source rejuvenation is shown in these unretouched photographs.

For full details, phone (800) 441-9740 (in Delaware 772-5388), or write Du Pont Mass Spectrometers, Room 36945, Wilmington, DE 19898

See the DP 102 Mass Spectrometer at the Pittsburgh Conference, Booth 121, beginning March 5.

Mass Spectrometers

Scientific & Process Instruments Division

DU PONT

REG. U.S. PAT. & TM OFF.

CIRCLE 52 ON READER SERVICE CARD

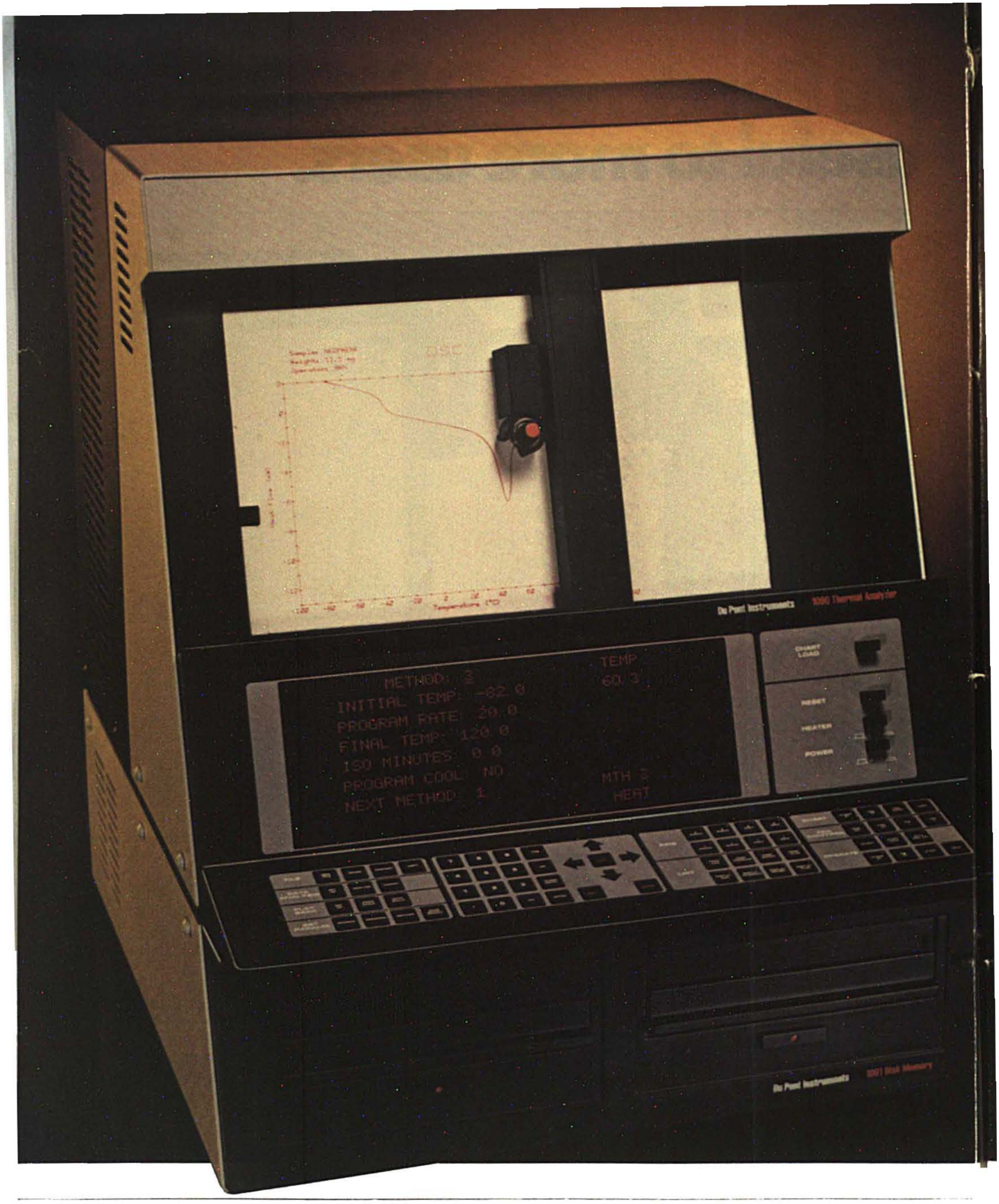

DSC
Temperature (°C)
Du Pont Instruments
1090 Thermal Analyzer
METHOD: 3
INITIAL TEMP: -82.0
PROGRAM RATE: 20.0
FINAL TEMP: 120.0
ISO MINUTES: 0.0
PROGRAM COOL: NO
NEXT METHOD: 1
TEMP
60.3
MTH 3
HEAT
CHART LOAD
RESET
HEATER
POWER
Du Pont Instruments
1091 Disk Memory

Thermal Analyzers

Scientific & Process Instruments Division

Du Pont's new 1090 Thermal Analyzer collects, processes, stores, and reports the data you want, the way you want it.

The 1090 Thermal Analyzer/Data System combines speed and versatility with expanded data manipulation capabilities in a sophisticated new instrument for research and product development.

Microcomputer Data Analysis

The 1090 System microcomputers free personnel from time-consuming data computations and provide more complete reports than ever before. Minor transitions can be expanded and specific portions of the thermogram can be selected for data analysis. You can even analyze data from one scan while a second run is in progress.

Multiple Reporting System

In addition to the thermogram, the 1090 System can provide a printout of test conditions and analytical results. A bright alphanumeric display continuously indicates sample temperature and system status. Other program parameters are instantly displayed on command. All experimental data is stored on disks for recall at any time. You decide what to save or discard.

Expanded and Simplified Programming

Two-way conversational interaction between operator and instrument via the display makes programming easy. Increased versatility provides 12 linkable methods, heating rate selection in 0.1°C increments, and temperature scale expansion capability to 0.2°C/cm. Internal computer diagnostics inform you of errors in programming or circuitry.

Get Our New Literature

For details on the 1090 Thermal Analyzer and other DuPont Thermal Analysis Systems, phone (800) 441-9740 (in Delaware, 772-5488) or write DuPont Thermal Analyzers, Room 37028, Wilmington, DE 19898.

See the 1090 Thermal Analyzer at the Pittsburgh Conference, Booth 121, and Conference Suite M-149, beginning March 5.

DU PONT

REG. U.S. PAT & TM OFF

CIRCLE 53 ON READER SERVICE CARD

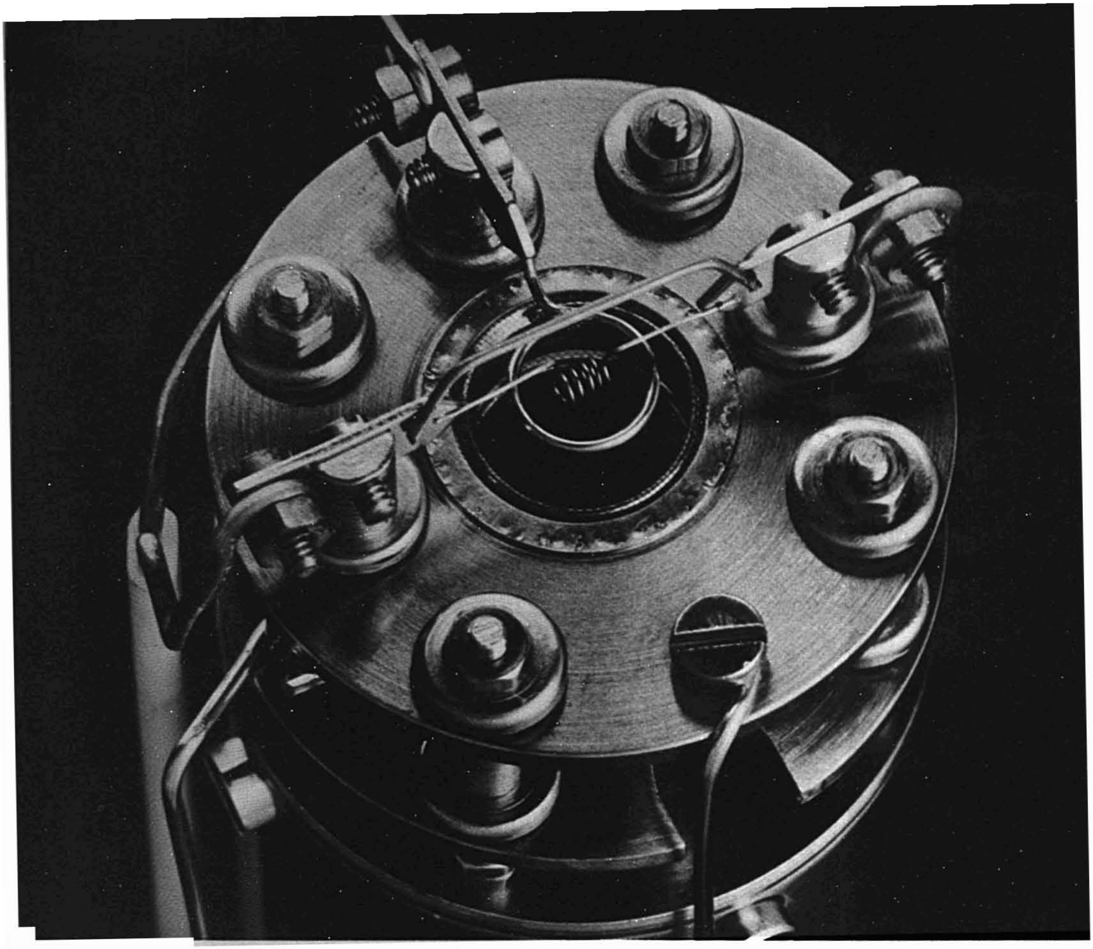

Our attention to detail makes the best quadrupole mass spectrometer

The quality in the ion source for our most powerful quadrupole mass spectrometer, the Model QMG 511, is reflected throughout the system. In the laboratory, you'll discover the QMG 511 has reliability that comes from our process control background, and in manufacturing, you'll see refinements from our experience in research applications.

The QMG 511's digital circuitry provides excellent signal stability; detection limits are at the parts-per-billion level. With mass ranges up to 1023, the system is adapted to problem-solving across many fields, and advanced computer compatibility makes possible control of virtually all operational parameters.

Many of these features are also available in our Model QMG 311, an extendable quadrupole mass spectrometer for research and production, and in the Model QMG 111B, our compact residual gas analyzer. And the quality in all three of these systems is in all of our other high vacuum, thin film, and mass analyzer products.

BALZERS

For literature about the QMG 511, QMG 311, and
QMG 111B mass analyzers, write Balzers Corporation,
8 Sagamore Park Road, Hudson, NH 03051.

CIRCLE 31 ON READER SERVICE CARD

Program

Monday, March 5

Gel Permeation Chromatography

Monday Morning, Room 205

G. P. Cunningham, *Presiding*

8:30 **Two-Detector Method for Concentration and Refractive Index of Solutes in Liquid Chromatography.** R. A. Sanford, Applied Automation, W. H. Dennis, D. D. DeFord

8:50 **Substrate-Solute Interaction in Gel-Permeation Chromatography.** Y. Kato, T. Sato, H. Sasaki, M. Aiura, T. Hashimoto, Toyo Soda Manufacturing Co.

9:10 **High-Speed, High-Temperature GPC.** J. L. Ekmanis, T. C. Huard, Waters Associates

9:30 **Systems Approach to Size Exclusion Chromatography.** S. D. Abbott, G. Dallas, Du Pont

9:50 **Low-Angle Laser Light Scattering Photometer for a Detector in Gel-Permeation Chromatography.** Y. Kato, M. Fukuda, N. Mamba, M. Fukutomi, M. Aiura, T. Hashimoto, Toyo Soda Manufacturing Co.

10:20 **On-Line Data System for HPSEC.** S. D. Abbott, J. M. DiCesare, Du Pont

10:40 **Flexible Dedication: New Data System for GPC Laboratory.** R. C. Jordan, M. L. McConnell, R. W. Wallace, Chromatix

11:00 **New Data Module for LC and GPC.** R. J. Limpert, A. Leung, Waters Associates

11:20 **Low-Cost Automatic SEC/GPC Computing Integrator.** M. Tarter, J. Donoghue, Laboratory Data Control

11:40 **On-Line Process Liquid Exclusion Chromatography Applied to Production of Styrene-Butadiene Copolymers.** E. N. Fuller, G. T. Porter, L. B. Roof, Applied Automation

Mass Spectrometry Applications

Monday Morning, Room 239

E. S. Hodge, *Presiding*

8:30 **Analysis of Organic Materials by Laser Ionization and Secondary Ion Mass Spectrometry.** R. Wechsung, H. J. Heinen, H. Peters, Leybold-Heraeus

8:50 **Instrumental Aspects of Molecular SIMS.** W. E. Baitinger, R. J. Day, S. E. Unger, R. G. Cooks, Purdue U

9:10 **Analytical Applications of Organic SIMS.** S. E. Unger, R. J. Day, R. G. Cooks, Purdue U

9:30 **High-Resolution Field Desorption Mass Spectrometry of Pharmaceutical Compounds.** G. D. Roberts, S. Rottschaefer, L. B. Killmer, Jr., R. J. Warren, J. E. Zarembo, Smith Kline Corp.

9:50 **On-Line Computer Optimization of Instrumental Parameters in High-Resolution Mass Spectroscopy.** S. L. Kaberline, C. L. Wilkins, U of Nebraska

10:20 **Identification of Glycols by Negative Ion Chemical Ionization Mass Spectrometry.** J. W. Russell, Q. V. Thomas, Finnigan Corp.

10:40 **Use of GC-MS in Polymer Degradation.** Y. Al-Sultan, Kuwait Institute for Scientific Research, R. Sedgwick

11:00 **New Fully Integrated GC/MS/DS System.** M. S. Story, D. M. Taylor, T. R. Stevens, Finnigan Corp.

11:20 **Some Applications of LC/CI/MS to Pharmaceutical Research.** S. Rottschaefer, L. B. Killmer, Jr., G. D. Roberts, R. J. Warren, J. E. Zarembo, Smith Kline Corp.

11:40 **Pyrolysis GC/MS as a Technique for Identifying Polymers and Organic Solids.** T. A. Blazer, E. M. Chait, Du Pont

New Instrumentation I

Monday Morning, Room 3A

B. M. LaRue, *Presiding*

8:30 **Introducing a New, Microcomputer Automated Ultraviolet-Visible Spectrophotometer—Answer Oriented and Energy Optimized.** N. Brenner, J. A. Miller, Beckman Instruments

8:50 **Inexpensive UV-Visible Colorimeter for Flow Injection Analysis and Liquid Chromatography.** G. R. Beecher, K. K. Stewart, USDA

9:10 **New Concept in Infrared Spectrophotometry.** C. V. Perkins, R. F. Kydd, Pye Unicam

9:30 **Performance Characteristics of New Microcomputer Infrared Spectrophotometer.** R. J. Obremski, J. W. Mohar, Beckman Instruments

9:50 **Applying Microcomputer to Maximum Benefit Within Automated UV-Visible Spectrophotometer.** J. A. Miller, D. G. Barber, Beckman Instruments

10:20 **Microprocessor-Controlled Near-Infrared Circular Dichroism Spectrophotometer.** M. E. Koehler, Glidden Coatings and Resins, F. L. Urbach

10:40 **Time-Lapse Infrared Spectroscopy.** J. H. Hartshorn, Du Pont

11:00 **A New Accessory for Industrial UV-Visible Spectrophotometric Kinetic System.** J. A. Miller, Beckman Instruments

11:20 **Raman Spectroscopy in Real Time.** R. E. Grayzel, A. Grillo, D. O. Landon, Instruments SA

11:40 **Absorption Measurement Precision and Sensitivity Using a Modern, Automated UV-Visible Spectrophotometer.** J. A. Miller, Beckman Instruments

Liquid Chromatography System Components

Monday Morning, Club Room B

E. W. Albaugh, *Presiding*

8:30 **New Integrated/Component Liquid Chromatography System.** D. Ball, Micromeritics Instrument Corp.

8:50 **Computer-Controlled System Incorporating a Liquid Chromatograph, Scanning UV-VIS Spectrophotometer, and Coherent Anti-Stokes Raman Spectrometer.** R. Von Wandruszka, U of Georgia, G. W. Martin, L. P. Goss, L. A. Carreira, L. B. Rogers

9:10 **True Constant-Temperature Oven for HPLC.** G. Killip, D. Ball, Micromeritics Instrument Corp.

9:30 **Precise Measurement of Flow Rate in Liquid Chromatography: The Electronic Volumeter.** I. Molnar, KG. Dr. Knauer

9:50 **New Solvent Mixer for HPLC.** R. Fincher, D. Ball, R. Camp, Micromeritics Instrument Corp.

10:20 **Unique Solvent Delivery System for Liquid Chromatography with Intrinsic Gradient Formation.** P. Achener, K. Judah, D. Boehme, Varian

10:40 **Compression Feedback: New Concept in HPLC Pump Design.** M. L. McConnell, Chromatix, H. Funke

11:00 **Inexpensive Pulse Dampener for High-Pressure Liquid Chromatography.** J. G. Nikelly, D. A. Ventura, Philadelphia College of Pharmacy and Science

11:20 New Pumping System for HPLC. P. Howard, D. Ball, Micromeritics Instrument Corp.

11:40 New, Unique Solvent Delivery System for Dedicated LC Applications. B. A. Bidlingmeyer, B. Hutchins, L. Abrahams, J. Myers, Waters Associates

Symposium: Application of High-Pressure Liquid Chromatography to Environmental Problems—Practical Applications and Regulatory Considerations

Monday Morning, Room 235A
P. C. Talarico, *Presiding*

8:30 Keynote Address: **Impact of HPLC on the Monitoring Requirements for Trace Organics.** W. May, U.S. Bureau of Standards

9:00 Uses of LC in Analyzing Nonvolatile Organics in Waste Effluent. H. Walton, U of Colorado

9:30 Use of HPLC in Monitoring Trace Level Organics for Chronic Toxicity. G. Wilson, EG&G Bionomics

10:20 Cleanup and Concentration of Environmental Samples for HPLC. C. Creed, LCS Labs, A. Wolkoff

10:40 Determination of Polynuclear Aromatics in Industrial Hygiene Samples by High-Performance Liquid Chromatography. G. Gibson, U.S. Dept. of Labor

11:20 Determination of Selected Carcinogens by HPLC. W. Hendricks, U.S. Dept. of Labor

Environmental Analysis—Water Pollution I

Monday Morning, Room 235B
C. E. Gonter, *Presiding*

8:30 Organic Compound Characterization of Wastewater for Environmental Assessment Study. M. F. Marcus, H. H. Miller, P. H. Cramer, Midwest Research Institute

8:50 Determination of Arsenic in Natural Waters. W. A. Richards, M. A. Thomas, S. R. Goode, U of South Carolina

9:10 Metal Transport: Role of Naturally Occurring Organic Substances in Aqueous Systems. C. A. Crumm, O. T. Zajicek, U of Massachusetts

9:30 Analysis of Trace Water-Soluble Polymers in Wastewater by HPLC. A. C. Hayman, G. Dallas, Du Pont

9:50 Some Improvements in Analysis of Industrial Wastes for Priority Pollutants. W. Averill, J. E. Purcell, Perkin-Elmer

10:20 Analysis of Consent Decree PAH's in Water. K. Ogan, E. Katz, W. Slavin, Perkin-Elmer

10:40 DC Argon Plasma Emission Spectrometry Applied to Environmental Water Samples. M. S. Hendrick, D. Eastwood, U.S. Coast Guard

11:00 ICP-ES Analysis of NURE Surface Waters of Rocky Mountain States and Alaska. C. T. Apel, B. A. Palmer, D. V. Duchane, L. B. Cox, J. V. Pena, A. D. Hues, D. L. Gallimore, Los Alamos Scientific Lab

11:20 Determination of pH in Soils and Specific Conductance in Wastewater Using Automated ISE System. A. Buccafuri, J. Potts, R. B. Roy, Technicon Industrial Systems

11:40 Oxidative Methods for Minimizing Reagent Blank in Determination of Low-Range Oxygen Demand. L. Stookey, B. Klein, Manchester Labs

Symposium: Laboratory Data Management

Monday Morning, Little Theater
G. A. Gibbon, *Presiding*

8:30 Overview

8:40 Laboratory Systems Management—Progress Toward Computerized Laboratory. P. W. Fletcher, G. P. Cunningham, PPG Industries

9:25 Sample Inventory Management. J. A. Cupps, Gulf Oil Chemicals, T. O. Martin

10:30 Paperwork Problem of a Regulatory Agency Laboratory. F. A. Madsen, OSHA

11:15 Laboratory Data Management in the Pharmaceutical Industry. R. A. Johnson, Upjohn Co.

Atomic Absorption Spectroscopy I (Flameless)

Monday Morning, Ball Room
J. Bukowski, *Presiding*

8:30 Direct Determination of Trace Quantities of Antimony, Arsenic, Bismuth, Cadmium, Lead, Selenium, Silver, Tellurium, and Thallium in Refined Nickel by Electrothermal Atomic Absorption Spectrometry. J. E. Forrester, V. Lehecka, J. R. Johnston, W. L. Ott, Falconbridge Nickel Mines

8:50 Determination of Wear Metals in Aircraft Lubricating Oils by Atomic Absorption Spectrophotometry Using a Graphic Furnace Atomizer. C. S. Saba, U of Dayton Research Institute, P. S. Fair, J. R. Brown, W. E. Rhine, K. J. Eisentraut

9:10 Trace Metal Analysis of Scalp Hair by Furnace Atomic Absorption. R. W. Handy, T. R. Hess, Research Triangle Institute

9:30 Determination of Lead in Environmental Water Samples Using Flameless Atomic Absorption Spectrophotometry. R. J. Faust, Calgon Corp.

9:50 Application of Flameless Atomic Absorption Spectrophotometry to Analysis of Metals in Coating Materials. C. E. Cowan, PPG Industries

10:20 Determination of Total Phosphorus in Industrial Process Waters by Flameless Atomic Absorption. E. L. Henn, Calgon Corp.

10:40 Quantitative Determination of Trace Levels of Titanium in Hydrazine. I. M. Citron, Fairleigh Dickinson U, H. Martens

11:00 Background Analysis in Carbon Rod Atomic Absorption Spectrometry. J. L. Maglaty, P. G. Rowley, K. R. O'Keefe, Colorado State U

11:20 Automated Atomic Absorption Analysis with Furnace Atomizer. J. J. Sotera, C. Shapiro, M. Conley, Instrumentation Lab

11:40 New Ways in Automated Furnace AA. B. Welz, T. Tomoff, E. Wiedeking, Bodenseewerk Perkin-Elmer

Gas Chromatography—Instrumentation

Monday Morning, Music Hall
H. Fracek, *Presiding*

8:30 Unijector—A Multifaceted Injection System for Glass Capillary Column Chromatography. E. F. Dawes, G. J. Jordan, Scientific Glass Engineering

8:50 All Glass Capillary Effluent Splitter. F. J. Yang, J. V. Lovie, Varian

9:10 New Microprocessor-Controlled Automatic Sampler for Gas Chromatography. M. J. Hartigan, E. W. March, Perkin-Elmer

9:30 Automatic Head Space Glass Capillary Gas Chromatography. G. Sisti, Carlo Erba Strumentazione, P. Gagliardi, S. Trestianu

9:50 Automated GC Heart Cut Analyses. H. Silverman, E. M. Warren, Hewlett-Packard

10:20 New Column Configurations for Gas Chromatography. D. Rogers, Kontes, J. C. Touchstone

10:40 New Design Concept of Compact Gas Chromatography. K. Sato, Y. Hayashi, Shimadzu Seisakusho

11:00 New Glass Capillary Gas Chromatograph for Analytical Needs of Tomorrow. T. A. Rooney, R. R. Freeman, Hewlett-Packard

11:20 Designing New Chromatograph for Tomorrow's Applica-

Gilson manufactures an extensive line of quality equipment and instrumentation for liquid chromatography. Shown here are three of our most popular and well-accepted instruments. For complete details on these units as well as many other items to make your LC work more precise and productive, call, write, or circle the reader service number below.

CHROMATOGRAPHIC COMPATIBLES FROM GILSON

Micro-Fractionator, Model FC-80. This diminutive, low cost fraction collector is ideal for use with small and medium size LC columns. Can be operated in *cold room.* Model FC-80 weighs only 13 lbs (6 kg) and occupies a bench span of only 11½" X 6" (29 cm X 15 cm). Move it anywhere, or store it in a drawer when you don't use it. A wide range of tube sizes may be used—up to 80 13 X 100 mm or 12 X 75 mm or 10 X 75 mm. It is a combination drop counting or time fractionator.

MICRO FRACTIONATOR
GILSON

CIRCLE 87 ON READER SERVICE CARD

Double-beam UV/VIS Monitor. (Model HM shown.) Gilson has paid painstaking attention to the critical parameters of UV/VIS design. Column resolution is maintained by our unique blown quartz cell with its high bubble-clearing capabilities. High sensitivity is assured by maintaining long light paths and using low noise electronics. Cells are easily interchangeable and include Kel-F 8 μl volume, 10 mm light path cells for HPLC. Internal heater allows cold room operation.

CIRCLE 88 ON READER SERVICE CARD

Peristaltic Pumps. Our MINIPULS line of miniature pumps have long set the performance standard. They are available in 1, 4, 8 and 16 channel models. All feature high torque motors, extremely stable electronic speed control, pump heads with 10 rollers to minimize pulsation, and chemically resistant tubing that can be replaced while the motor is running. Widest flow range: from 1 ml to 1300 ml/hr for all pumps except the HP16 (0.5 to 650 ml/hr). *Multichannel pumps generate gradient for ion exchange chromatography and density gradient centrifugation.* Optional models are available with flow ranges from very slow to very high.

minipuls 2
GILSON

CIRCLE 89 ON READER SERVICE CARD

Demonstration of these fine instruments is available upon request through a network of qualified GME representatives.

GILSON®

Gilson Medical Electronics Inc.
P.O. Box 27 • Middleton, Wisconsin 53562 • Phone (608) 836-1551

Your companion in chromatography

tions. L. Mikkelsen, M. Murphy, Hewlett-Packard

General Mass Spectroscopy

Monday Afternoon, Room 240
E. M. Chait, *Presiding*

1:30 Applications of Angle-Resolved Mass Spectrometry. J. A. Laramee, D. Fedor, R. G. Cooks, Purdue U

1:50 Alternate Scan CI/EI Mass Spectrometry. K. R. Compson, K. T. Taylor, J. R. Chapman, C. J. Wakefield, Kratos, Ltd.

2:10 Recent Applications of DCI (Desorption–CI) Technique. W. A. Wolstenholme, U. Rapp, H. Kaufman, Varian MAT

2:30 Determination of Herbicide Photolysis Products by LC/MS. R. F. Skinner, Q. Thomas, Finnigan Corp.

2:50 Chemical Applications of LC–MS Interface. A. Melera, Hewlett-Packard

3:20 Pyrolysis–Mass Spectrometry for Analysis of Small Samples of Polymeric Material. D. A. Hickman, Metropolitan Police Forensic Science Lab

3:40 Applications of Programmed Temperature Direct Introduction Probe with Fast Scanning Computer-Controlled Mass Spectrometer. E. M. Chait, Du Pont

4:00 Performance of Automated Magnetic Mass Spectrometer Intended for Quantitative and Trace Analysis at Resolving Powers Up to 2500 or More. L. F. Herzog, Nuclide Corp.

4:20 New High-Performance, High-Resolution Mass Spectrometer—MS 80. K. R. Compson, Kratos, Ltd., D. R. Denne, A. Taylor, R. J. Rutherford

4:40 Effects of Automatic Ion Source Rejuvenation on Performance of Sensitive GC/MS. E. M. Chait, C. W. Hull, Du Pont

Polymer Analysis

Monday Afternoon, Room 205
L. Wolfram, *Presiding*

1:30 Characterization of Organic Coatings by Dynamic Mechanical Analysis (DMA). P. S. Gill, R. L. Hassel, Du Pont

1:50 Chromatopyrography Analysis of Rubbers and Other High Polymers. J. C. Hu, Boeing Aerospace

2:10 Thermal History Determination of Textured Polyester Yarn by Thermomechanical Analysis. P. S. Gill, R. L. Blaine, Du Pont

2:30 Polymer Analysis—Quality Control of Plastic Foams by Thermal Analysis. D. W. Breakey, R. B. Cassel, Perkin-Elmer

2:50 Shear Modulus by Dynamic Mechanical Analysis. R. L. Hassel, P. S. Gill, Du Pont

3:20 Microcomputer Techniques for Thermal Analysis of Plastics. R. L. Fyans, R. B. Cassel, W. P. Brennan, Perkin-Elmer

3:40 Thermal Analysis of Composites. R. L. Hassel, R. L. Blaine, Du Pont

4:00 Trace Metal Speciation by Liquid Chromatography with Element Specific Detection. J. A. Koropchak, G. N. Coleman, U of Georgia

4:20 New HPLC Applications on μ-Spherogel and Other Stable Macroporous Polystyrene Resins. V. A. McKay, R. Stevenson, Altex Scientific

UV–Visible Spectrophotometry I

Monday Afternoon, Room 239
C. Burton Clark, *Presiding*

1:30 Gel Scanner Accessory for Model 219 Spectrophotometer. A. H. Sturtevant, Varian

1:50 New Microcomputer-Controlled UV–VIS–NIR Recording Spectrophotometer. M. Takada, O. Akiyama, T. Nishimura, R. Hira, T. Kurita, Shimadzu Seisakusho

2:10 Design of Microcomputer-Controlled UV–VIS Spectrophotometer. W. Kaye, D. Barber, R. Marasco, Beckman Instruments

2:30 Quantitative Effect of Halides on Determination of Aluminum in Various Matrices. B. Klein, L. Stookey, Manchester Labs

2:50 Spectrophotometric Analysis of Aldehydes by Thiadiazoline Formation with 1,5-Diphenyl-3-thiocarbohydrazide. R. H. Hunt, D. A. Pettigrew, Illinois State U

3:20 Kinetic Analysis of Multicomponent Mixtures by Parameter Estimation. R. J. Bell, B. G. Willis, N. Bell, Hewlett-Packard

3:40 Characteristics and Design of High-Performance Parallel Access Spectrophotometer. B. G. Willis, C. E. Bryson III, R. L. Chaney, Hewlett-Packard

4:00 Operations of User-Oriented, Programmable, UV/Visible Spectrophotometer. E. J. Bonelli, B. G. Willis, A. Schleifer, R. Bell, N. Bell, P. Dryden, Hewlett-Packard

4:20 Processor-Controlled UV/VIS Spectrophotometer in Laboratory-Automation Environment. A. Schleifer, B. Willis, G. Steiner, P. Dryden, A. Ben-Dor, Hewlett-Packard

4:40 Direct Quantitation of Linear and Nonlinear Chemical Systems Using Microprocessor-Controlled Spectrophotometer. N. W. Bell, B. G. Willis, P. Dryden, R. Bell, A. Schleifer, A. Stefanski, Hewlett-Packard

New Instrumentation II

Monday Afternoon, Room 3A
N. W. Gordon, *Presiding*

1:30 SAW Devices—New Solid State Detector for Study of Thin-Film Polymeric Material and Process Control Streams. R. Dessy, H. Wohltjen, VPI&SU

1:50 Studies of Spark Solid Sampling with Inductively Coupled Plasma. J. S. Beaty, R. L. Crawford, C. C. Wohlers, Jarrell-Ash

2:10 High-Speed Continuous Stream Flow Injection Analysis. H. O. Ranger, Lachat Chemicals

2:30 Polymerization Kinetics by Precision Densitometry. K. J. Abbey, Glidden

2:50 Coupled HPLC/GC System: Instrumentation and Automation. S. P. Cram, A. C. Brown III, E. Freitas, R. E. Majors, E. L. Johnson, Varian

3:20 Coupled HPLC/GC System: Applications. R. E. Majors, E. L. Johnson, S. P. Cram, A. C. Brown III, E. Freitas, Varian

3:40 Analytical Fourier Mass Spectrometry—Instrumentation. E. B. Ledford, Jr., R. B. Spencer, S. Ghaderi, P. S. Kulkarni, M. L. Gross, C. L. Wilkins, U of Nebraska

4:00 Analytical Fourier Mass Spectrometry – Low-Pressure Chemical Ionization. C. L. Wilkins, S. Ghaderi, P. S. Kulkani, M. L. Gross, R. B. Spencer, E. B. Ledford, Jr., U of Nebraska

4:20 Automated Gravimetric Titrations. L. Luft, Luft Instruments

4:40 New Infrared Spectrophotometer with Self-Contained Data Manipulation Capabilities. R. J. Obremski, J. W. Mohar, G. Solomon, Beckman Instruments

Detectors in Liquid Chromatography

Monday Afternoon, Club Room B
J. D. Guthrie, *Presiding*

1:30 Novel Detection Principle in Modern High-Pressure Liquid Chromatography: Ultraviolet Photometer / Refractometer (UV–RI)-Dualdetektor, an Important Tool for Identification of Unknown Substances. I. Molnar, KG. Dr. Knauer

1:50 Applications of Polarographic Detector to HPLC. L. R. Taylor, EG&G Princeton Applied Research Corp.

2:10 Dielectric Constant Detector for Liquid Chromatography and Its Applications. L. V. Benningfield, Jr., Applied Automation

2:30 New Variable Wavelength HPLC Detector. P. Froehlich, J. Stewart, Spectra-Physics

ARL's ICP is hot!

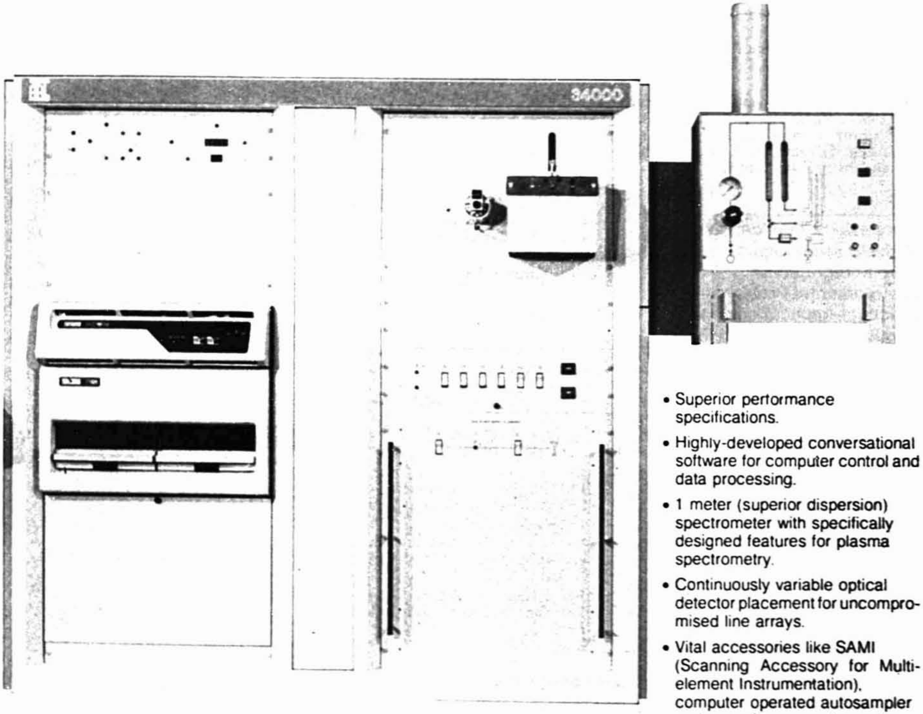

Imagine! Analyzing a sample per minute for up to 48 elements simultaneously. Almost 3000 determinations in an hour! No wonder Inductively Coupled Plasma is news. Matching the sensitivity of atomic absorption with multielement capability, it can't be equaled for high-throughput applications. Wide linear dynamic ranges allow automatic analysis without changing parameters. The ARL 34000 ICP gives you all this!

ARL was the first with a commercial ICP Instrument, and more man-years of applications experience have been invested in ARL instruments than any other. More ARL systems have been sold worldwide, too.

Unquestionably, ARL has more experience. It all shows in the 34000 ICP's features:

- Superior performance specifications.
- Highly-developed conversational software for computer control and data processing.
- 1 meter (superior dispersion) spectrometer with specifically designed features for plasma spectrometry.
- Continuously variable optical detector placement for uncompromised line arrays.
- Vital accessories like SAMI (Scanning Accessory for Multi-element Instrumentation), computer operated autosampler and scanning monochromator.

If you need multielement high-throughput with all the sensitivity of atomic absorption in a convenient-to-operate package, you owe it to yourself to investigate what the 34000 ICP can do for you. Whatever your field is — waters, soils, foods, pharmaceuticals, petroleum, biologicals, or geological samples, ARL's ICP works. Because we have more experience. Write today for information!

ARL Applied Research Laboratories
a division of BAUSCH & LOMB

USA	9545 Wentworth St., Sunland, California 91040
FRANCE	FICA, F 78320 Le Mesnil Saint Denis
AUSTRIA	Rudolfinergasse 2, A 1190 Wien
AUSTRALIA	P.O. Box 426, Brookvale 2100
CANADA	P.O. Box 147 Mississauga, Ontario L4T 3S5
SUISSE	En Vallaire, CH 1024 Ecublens
GB	Wingate Road, Luton, Bedfordshire
BRD	Konigstrasse 5, D 4000 Dusseldorf
SVERIGE	Rasundavagen 101, S 17103 Solna
RSA	P.O. Box 557, Kempton Park

CIRCLE 3 ON READER SERVICE CARD

2:50 New Lamp Intensity Compensated Fluorescence Detector for HPLC. B. Leaver, P. DeLand, D. Janzen, Laboratory Data Control

3:20 LC Detection Using AA and Precolumn Metal Labeling. W. Slavin, G. J. Schmidt, Perkin-Elmer

3:40 High-Resolution Detection Method for HPLC Using Dual Wavelength Spectrophotometry. K. Li, J. Arrington, U of Florida

4:00 New RI Detector for HPLC. M. N. Munk, E. Goodnight, E. Watson, Laboratory Data Control

4:20 FDLC-10—A Unique Fluorescence Spectrometer for HPLC. A. C. Grillo, D. O. Landon, Instruments SA

4:40 The Economics for Low-Cost HPLC Variable UV Detector Without Compromising Performance. D. Janzen, E. Goodnight, Laboratory Data Control

Symposium: Application of High-Pressure Liquid Chromatography to Environmental Problems—Practical Applications and Regulatory Considerations II

Monday Afternoon, Room 235A

C. Creed, *Presiding*

1:30 Monitoring Wastewater for Munitions by HPLC. D. Helton, Midwest Research Institute

2:00 HPLC Determination of Pesticides in Water. T. Steinheimer, U.S. Geological Survey

2:30 Analysis of Industrial Wastewaters by HPLC. R. Hites, MIT

3:50 Use of HPLC to Isolate a Mutagen from a Plant Waste Effluent. K. Carlberg, EPA, R. H. Laidlaw

4:20 Analysis of Pesticides in Fish in HPLC. J. Moore, Gulf Breeze ERL

Environmental Analysis—Water Pollution II

Monday Afternoon, Room 235B

A. Pollock, *Presiding*

1:30 Reduction of Foaming in Analysis of Volatile Organics in Industrial Effluent Waters When Using Purge and Trap GC Techniques. B. N. Colby, M. E. Rose, Systems, Science and Software

1:50 Ultratrace Determination of Thallium in Natural Waters by Differential Pulse Anodic Stripping Voltammetric Techniques. J. E. Bonelli, H. E. Taylor, R. K. Skogerboe, U.S. Geological Survey

2:10 Isolation of Polynuclear Aromatic Hydrocarbons from Water by Adsorption on Membrane Filters. F. Amore, Illinois State Water Survey

2:30 Analytical Problems Encountered During Restoration of Mercury-Contaminated Public Water Supply. J. C. Cooper, C. Hackbarth, C. M. Hellwig, D. L. Venezky, Naval Research Lab

2:50 Automatic Sampler for Trace Organics in Water. J. D. Pope, Jr., A. W. Garrison, EPA

3:20 Statistical Evaluation of DR-EL/4 Portable Wastewater Laboratory vs. Standard Methods. B. Culver, S. Schuler, D. Miller, C. Gibbs, Hach Chemical Co.

3:40 Spectrophotometric Determination of Phenols by Their Oxidation with Sodium Metaperiodate. L. R. Sherman, U of Akron

4:00 High-Pressure Liquid Chromatography of Nitrophenols. A. F. Haeberer, EPA

4:20 Determination of Acrylonitrile in Water at ppb Level. J. Going, K. Thomas, Midwest Research Institute

4:40 Sample Preparation for Environmental Analysis. D. R. Lorenz, H. Rodriguez, Waters Associates

Symposium: Applications of Ion Chromatography

Monday Afternoon, Little Theater

G. L. Carlson, *Presiding*

1:30 Keynote Address: **Conception and Early Development of Ion Chromatography.** H. Small, Dow Chemical USA

2:05 Three Years of Ion Chromatography. C. Anderson, Dionex Corp.

2:35 Process Control Using Ion Chromatography and Related Techniques. T. Stevens, Dow Chemical USA

3:25 Application of Ion Chromatography to Analysis of Atmospheric Pollutants. J. D. Mulik, EPA

3:55 Studies of Anions in Perchlorate Mixtures. R. Holm, Monsanto Research Corp.

4:25 Trace Ion Analysis in Power Production Industry. D. F. Pensenstadler, M. A. Fulmer, Westinghouse

Atomic Absorption Spectroscopy II

Monday Afternoon, Ball Room

H. Silva, *Presiding*

1:30 Direct Determination of Phosphorus in Fertilizers by Atomic Absorption Spectroscopy. R. C. Gurira, D. Hoft, J. Oxman, Grinnell College

1:50 Hydride Generation in Atomic Absorption Spectroscopy—Improvements to Technique and Recent Applications. D. R. Thomerson, R. G. Godden, Baird-Atomic

2:10 Flameless Atomic Absorption Determination of Arsenic in Geological Materials Following Hydride Generation. R. F. Sanzolone, T. T. Chao, E. P. Welsch, U.S. Geological Survey

2:30 Rapid AA Determination with New Hydride/Mercury System. D. E. Shrader, K. G. Brodie, Varian

2:50 Slurry-Injection Atomic Absorption Spectrophotometry. J. E. O'Reilly, U of Kentucky, D. G. Hicks

3:20 Direct Nonflame Atomic Absorption of Trace Elements in Solids. D. D. Siemer, J. M. Baldwin, Allied Chemical Corp.

3:40 Effect of Metal Particle Size on Measurement of Trace Elements Using AA, AE, and OES-ICP. L. P. Giering, Baird Corp.

4:00 AA Techniques in Food Analysis. B. Welz, Z. Grobenski, M. Melcher, D. Weber, Bodenseewerk Perkin-Elmer

4:20 Evaluation of Simultaneous Multielement Atomic Absorption-Electrothermal Atomization Analysis Applied to Natural Water Matrices. P. G. Rowley, P. R. Beaulieu, J. L. Maglaty, K. R. O'Keefe, Colorado State U

4:40 Multielement Atomic Spectroscopy. S. B. Smith, R. G. Schleicher, A. G. Dennison, Instrumentation Lab

Gas Chromatography—Data Processing

Monday Afternoon, Music Hall

S. J. Ondrey, *Presiding*

1:30 Advanced Techniques Using Glass Capillary Columns. R. R. Freeman, T. A. Rooney, L. H. Altmayer, T. M. Przybylski, Hewlett-Packard

1:50 New Generation in Evolution of Single-Channel Integrator. D. G. Gillen, L. Robison, Spectra-Physics

2:10 Industrial Hygiene Air Sample Analysis—Improved Results Through Automation Using Glass Capillary Columns and Multichannel Data System. R. C. Domingo, J. W. Bailly, D. R. Brezinski, DeSoto

2:30 Information from Chromatography. I. Quantitation in Real Time. L. Altmayer, J. DeGood, P. Dryden, Hewlett-Packard

2:50 Information from Chromatography. II. Post Run Processing of Chromatographic Data. P. C. Dryden, L. H. Altmayer, J. S. DeGood, Hewlett-Packard

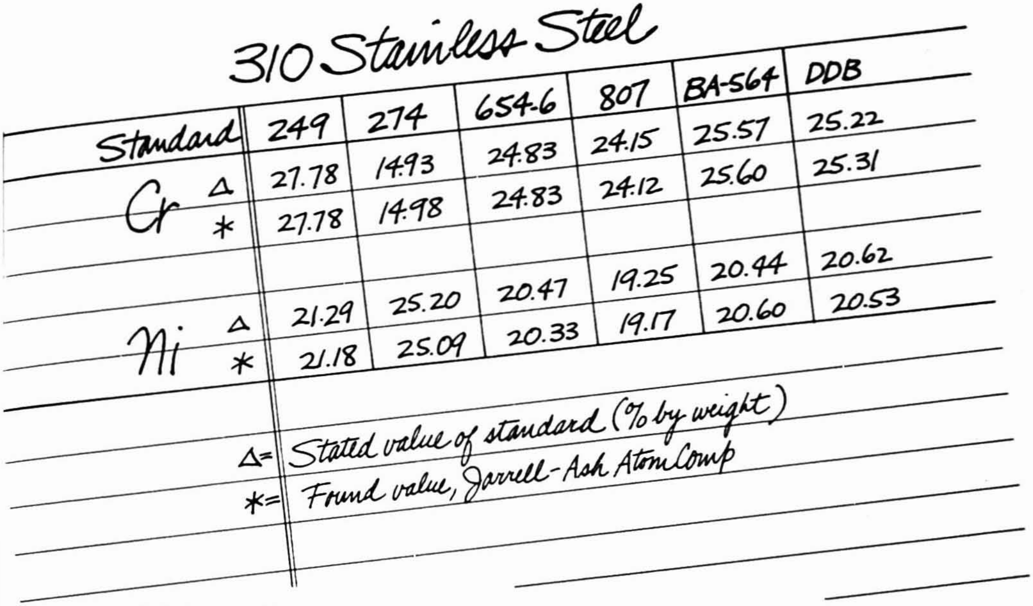

310 Stainless Steel

Standard		249	274	654-6	807	BA-564	DDB
Cr	Δ	27.78	14.93	24.83	24.15	25.57	25.22
	*	27.78	14.98	24.83	24.12	25.60	25.31
Ni	Δ	21.29	25.20	20.47	19.25	20.44	20.62
	*	21.18	25.09	20.33	19.17	20.60	20.53

Δ= Stated value of standard (% by weight)
*= Found value, Jarrell-Ash AtomComp

NOBODY BUT JARRELL-ASH ASSURES HIGH-ALLOY ACCURACY LIKE THIS.

Accuracy is the word for the Jarrell-Ash 750 AtomComp spectrometer with electronically-controlled waveform source (ECWS).

Above is a typical AtomComp analysis of six 310 stainless-steel standards for chromium and nickel. The AtomComp delivers equally remarkable results for Al, C, Cu, Fe, Mn, Mo, P, S, Si, Ti and V. And delivers them **faster** (and at lower cost) than the traditional method for high-alloy steels.

Add to this the remarkable **precision** of the Jarrell-Ash system and you can see why knowledgeable primary metals management is increasingly turning to Jarrell-Ash direct-readers.

Send for our new bulletin "Analysis of 310 Stainless Steels." The facts-&-figures show what the right instrument can do for **your** production and quality-control workloads.

Jarrell-Ash Division
Fisher Scientific Company
590 Lincoln Street
Waltham, Massachusetts 02154
Phone (617) 890-4300

CIRCLE 110 ON READER SERVICE CARD

3:20 **Information from Chromatography. III. Extended Calculation Procedures and Reports.** J. DeGood, L. Altmayer, P. Dryden, T. Przybylski, Hewlett-Packard

3:40 **New, Completely Automatic Peak Integration Algorithm for Chromatography.** B. L. Tomlinson, Spectra-Physics

4:00 **Use of Central Processor Unit (CPU) in Low-Cost Temperature-Programmed Gas Chromatograph.** R. J. Szymansky, Gow-Mac Instrument, F. Gonzales

4:20 **Development of Computer-Controlled Gas Chromatograph, GC–RIA.** T. Sato, S. Takimoto, I. Kohsaka, Y. Nagayanagi, Shimadzu Seisakusho

4:40 **Chromatographic Data Processors with New Functions.** T. Sato, S. Takimoto, I. Kohsaka, Shimadzu Seisakusho

Tuesday, March 6

UV–Visible Spectrophotometry II

Tuesday Morning, Room 240

R. Raybeck, *Presiding*

8:30 **Spectral Data Acquisition and Processing Computer, Model SAPCOM-1, for Recording Spectrophotometer, and Its Applications.** M. Takada, T. Nishimura, T. Ichikawa, H. Yamamoto, T. Kurita, Shimadzu Seisakusho

8:50 **Absorbance Standards for UV/Visible Spectroscopy.** M. R. Sharpe, Pye Unicam

9:10 **Derivative Spectroscopy.** J. E. Cahill, Perkin-Elmer

9:30 **Derivative Spectroscopy with the Varian Cary 219.** D. W. Priesner, M. Kelly, Varian

9:50 **Comparison of Linear and Nonlinear Parameter Estimation Algorithm in the Chemical Laboratory: Multicomponent Analysis in Molecular Spectroscopy.** K. R. O'Keefe, Colorado State U

10:20 **Determination of Saccharin in Plating Solutions by Liquid Chromatography and Derivative UV Spectroscopy.** G. L. Fix, J. D. Pollack, R. K. Wice, Raytheon Co.

10:40 **Photoproduct Identification by Means of Chromatography and Spectrophotometry.** A. Ehrl, Gesellschaft für Strahlen-und Umweltforschung

11:00 **Determination of "Free" Dithiocarbamate Compounds in Rubber Formulations.** R. Raja, T. Clark, G. Palmer, National Can Corp.

11:20 **Determination of Reaction Rates by Laser Intracavity Thermal Lens Spectroscopy.** T. D. Harris, Bell Labs, F. E. Lytle

General Photoacoustic Spectroscopy

Tuesday Morning, Room 205

A. Rosencwaig, *Presiding*

8:30 **Overview of Photoacoustic Spectroscopy with Current Applications Data.** R. E. Blank, T. Wakefield II, Ann Silversmith, D. Polacsek, Gilford Instrument Labs

8:50 **Modern Instrumentation for Photoacoustic Spectroscopy.** H. S. Reichard, J. A. Noonan, EG&G Princeton Applied Research Corp.

9:10 **Theory Verification and Phase Measurements in Photoacoustic Spectroscopy.** A. Silversmith, T. D. Wakefield II, R. E. Blank, Gilford Instrument Labs

9:30 **Determination of Condensed Phase Absorptivities via Photoacoustic Phase Angle Spectroscopy (ΦAS).** R. A. Palmer, J. C. Roark, Paul M. Gross Chemical Lab

9:50 **Sample Preparation in Photoacoustic Spectroscopy.** J. A. Noonan, H. S. Reichard, EG&G Princeton Applied Research Corp.

10:20 **Data Reduction in Photoacoustic Spectroscopy.** J. M. Long, A. Silversmith, Gilford Instrument Labs

10:40 **Some Applications of Photoacoustic Spectroscopy to Examination of Small Solid and Liquid Samples.** G. F. Kirkbright, Imperial College

11:00 **Photoacoustic Spectroscopy Studies of Laser Windows and Coatings.** N. C. Fernelius, U of Dayton Research Institute

11:20 **Laser Optoacoustic Detection of NO_2 in a Flow System.** A. Fried, National Center for Atmospheric Research, D. H. Stedman

11:40 **Laser Optoacoustic Spectrometer for Gas Concentration Measurements.** T. D. Wakefield II, Gilford Instrument Labs

ESCA, Auger, and Electron Analysis Techniques

Tuesday Morning, Room 239

Robert Duss, *Presiding*

8:30 **Surface Studies of Pt-Re/Al_2O_3 Catalysts.** L. Salvati, Jr., D. M. Hercules, U of Pittsburgh

8:50 **Rh(I) Complexes as Supported Homogeneous Catalysts Studied by ESCA and IR.** M. B. Carvahlo, A. Luchetti, D. M. Hercules, U of Pittsburgh

9:10 **ESCA and ISS Studies of Co/Al_2O_3 Catalysts.** R. L. Chin, D. M. Hercules, U of Pittsburgh

9:30 **Surface Studies of Molybdenum Alumina Catalysts.** D. S. Zingg, U of Pittsburgh, D. M. Hercules, L. E. Makovsky, F. R. Brown

9:50 **More Efficient ESCA Profiles with Differential Sputtering System.** M. V. Zeller, Physical Electronics

10:20 **Valence-Band Density of States of Selected Metallic Glasses.** M. A. Steggert, D. M. Hercules, U of Pittsburgh

10:40 **Application of Surface Analytical Techniques to Glass Capillary Gas Chromatography Column Preparation.** L. V. Phillips, U of Pittsburgh, D. M. Hercules, M. L. Lee, G. R. Conner

11:00 **Investigation of Polymer Surface Structure by ESCA, SIMS, and ISS.** J. A. Gardella, Jr., D. M. Hercules, U of Pittsburgh

11:20 **ESCA Thin-Film Analysis of Polymer Surfaces.** M. V. Zeller, Physical Electronics

11:40 **Trace Element Analysis of Altered Deep Sea Drilling Project Basalts by Selected Area X-Ray Fluorescence and Electron Microprobe.** I. B. Ailin-Pyzik, S. E. Sommer, U of Maryland

Optimization of Liquid Chromatography Operating Parameters

Tuesday Morning, Club Room B

J. A. Feldman, *Presiding*

8:30 **Instrumental Sources of Error in High-Precision Quantitative LC Analysis.** A. Poile, H. Major, Perkin-Elmer

8:50 **Comparison of Reversed-Phase Chromatographic Parameters Under Wetting and Nonwetting Conditions.** D. A. Nelson, J. H. Bush, R. Roat, U of Wyoming

9:10 **Effects of Ionic Strength on Sorption of Organic Electrolytes in Reversed-Phase High-Performance Liquid Chromatography.** T. D. Rotsch, D. J. Pietrzyk, U of Iowa

9:30 **Determination of Detector Contributions to Chromatographic Band Broadening.** V. Castro, Instituto Nacional de Energia Nuclear, C. Poitrenaud

9:50 **Solvent Effects in RPLC: Variation with Bonded Phase Loadings.** F. M. Rabel, D. J. Popovich, C. J. Lancaster, G. J. Kusha, Whatman

10:20 **Rapid Determination of HPLC Solvent Systems.** D. M. Kent, R. K. Vitek, V-tech Corp.

10:40 **On the Prediction of the Retention Behavior in Liquid Chromatography.** T. Hanai, M. D'Amboise, U of Montreal

11:00 **Use of High pH Mobile Phases in HPLC Methods Using Silica Guard Column.** G. J. Schmidt, J. G. Atwood, W. Slavin, Perkin-Elmer

11:20 **Chemical Systems for Liquid Chromatography. Precolumn Derivatization and Fluorescence**

Now you can have it both ways!

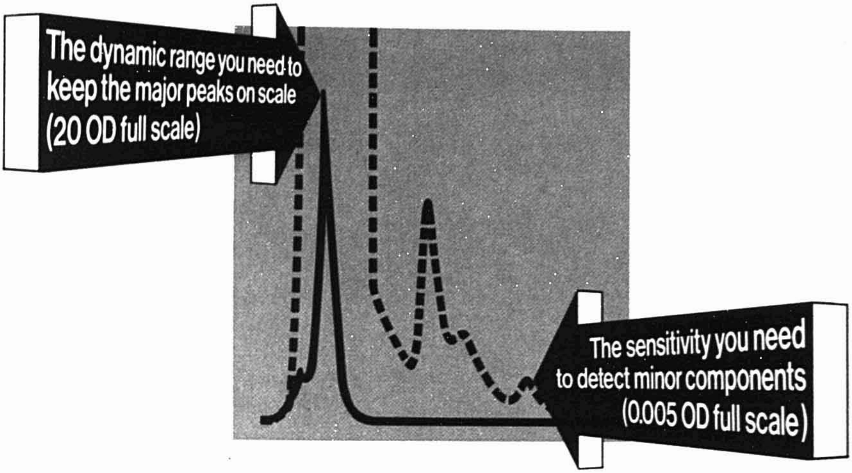
The dynamic range you need to keep the major peaks on scale (20 OD full scale)
The sensitivity you need to detect minor components (0.005 OD full scale)

Pharmacia Dual Path Monitor UV-2

has a unique flow cell with two optical path-lengths for new versatility in UV-monitoring.

- Monitor absorbance quantitatively up to 20 OD units full scale with a sensitivity of 0.005 OD units full scale at the same time, in the same run.
- Monitor at 254 nm and/or 280 nm with two completely independent measuring systems.

The Dual Path Monitor UV-2 has all the other features you expect of a high performance monitor: stability, cold room operation convenience and compact design. For less-demanding applications you can choose the Pharmacia Single Path Monitor UV-1 with a choice of 3 mm or 10 mm flow cell and operation at 254 nm or 280 nm.

Find out more about the practical advantages of column monitoring with the UV-2 and UV-1 Monitors. Ask about the Pharmacia Recorders too.

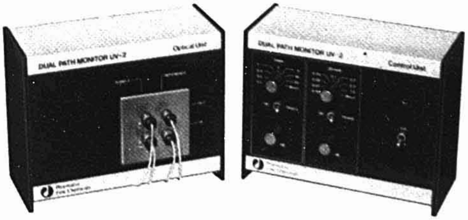
DUAL PATH MONITOR UV-2
Optical Unit
DUAL PATH MONITOR UV-2
Control Unit

Pharmacia Fine Chemicals
Division of Pharmacia, Inc.
Piscataway, New Jersey 08854
Phone (201) 469-1222

Pharmacia
Fine Chemicals

CIRCLE 162 ON READER SERVICE CARD

P-250
500 g
(1.1 lb)
Certified A.C.S.
Potassium Hydroxide
Pellets
FISHER SCIENTIFIC CO
Certified A.C.S.
Potassi
Hydrox
Pellets
S-271
500 g
(1.1 lb)
Certified A.C.S.
Sodium Chloride
For laboratory and manufacturing use only, not for drug, food, or household use.
LOT
FISHER SCIENTIFIC COMPANY
Chemical Manufacturing Division
Fair Lawn, New Jersey 07410
Made in U.S.A.

Reagents don't do you any good until they're on your shelf.

Nobody gets them there faster than Fisher.

Fisher delivers **the goods**. Whether your reagent needs are in routine testing or purest research. Our product range is spectacular. From high-pressure liquid chromatography and ppb pesticide trace analysis . . . to histology, electronics, and in vitro diagnostics. We develop new reagents. We manufacture them. We test them scrupulously. And we deliver them — dependably. Some **20,000** different chemicals and chemical specialties in all. Shipped to you from strategically located warehouses coast to coast. Your order is monitored every step of the way by one of the most sophisticated computers the lab supply industry has ever seen. (It's one reason Fisher will shortly be the first American reagent-maker to be 100% metric.) Thinking reagents? **Reach for the label.**

Fisher Scientific Company

CIRCLE 76 ON READER SERVICE CARD

The 1979 Fisher Chemical Index
will soon be off the press.
For your copy, circle reader-service card.

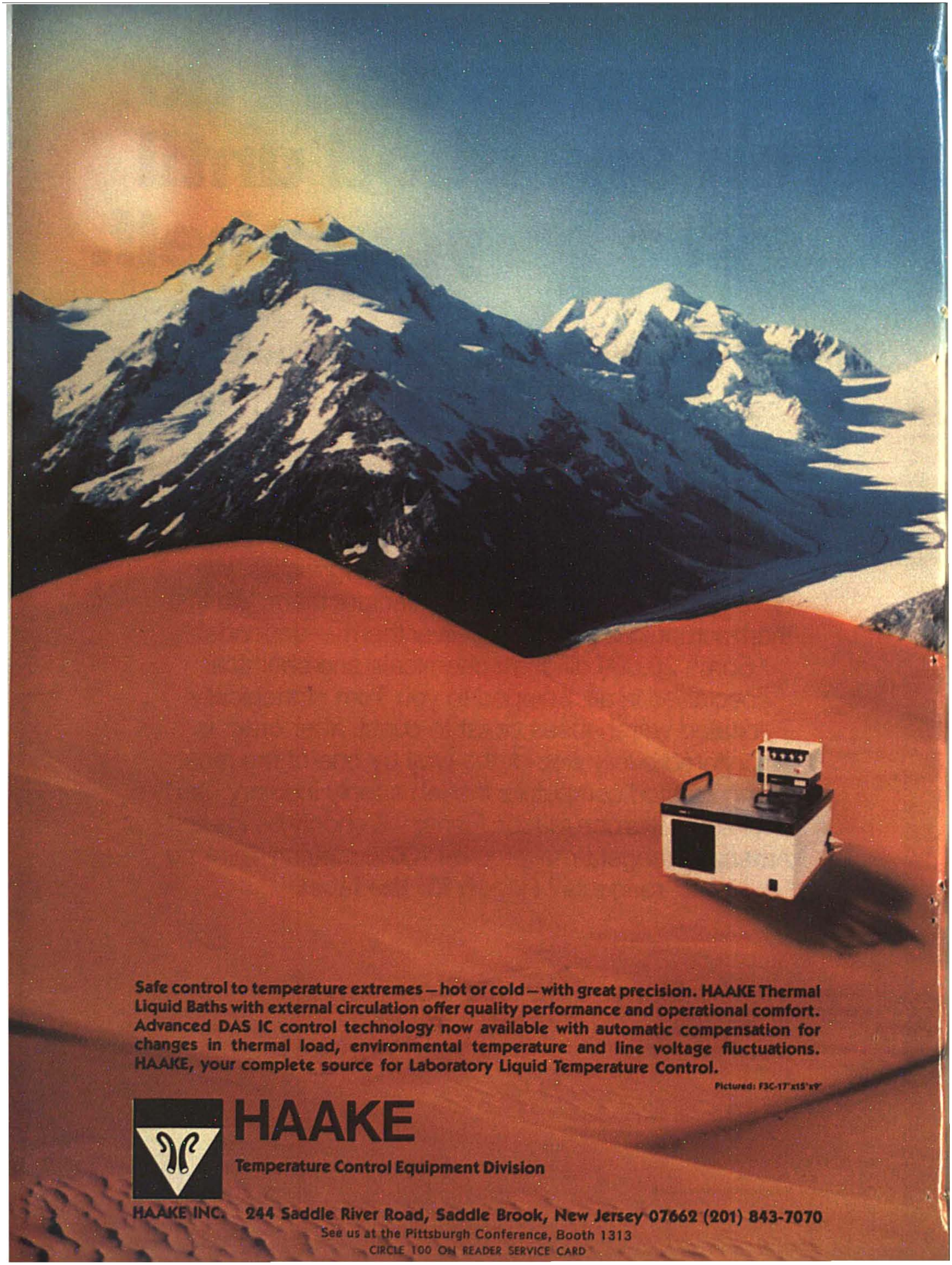

Safe control to temperature extremes — hot or cold — with great precision. HAAKE Thermal Liquid Baths with external circulation offer quality performance and operational comfort. Advanced DAS IC control technology now available with automatic compensation for changes in thermal load, environmental temperature and line voltage fluctuations. HAAKE, your complete source for Laboratory Liquid Temperature Control.

Pictured: F3C-17"x15"x9"

HAAKE

Temperature Control Equipment Division

HAAKE INC. 244 Saddle River Road, Saddle Brook, New Jersey 07662 (201) 843-7070

See us at the Pittsburgh Conference, Booth 1313

CIRCLE 100 ON READER SERVICE CARD

Detection. F. L. Vandemark, G. J. Schmidt, W. Slavin, Perkin-Elmer

11:40 **Effect of Temperature on Precision of Retention Measurements in Liquid Chromatography.** R. K. Gilpin, Kent State U

New Instrumentation III

Tuesday Morning, Room 235A

F. P. Byrne, *Presiding*

8:30 **High-Temperature Solid Electrolyte Electrochemical Cell for Monitoring Oxygen and Combustibles.** W. M. Hickam, C. Y. Lin, Westinghouse

8:50 **Development and Application of Photogoniometer to Coatings Systems.** T. H. Grentzer, R. A. Zander, M. E. Koehler, T. Provder, R. M. Holsworth, Glidden

9:10 **Particle Size Analysis by Automatic Sieving.** C. Orr, R. W. Camp, D. K. Davis, Micromeritics Instrument Corp.

9:30 **Microcomputer-Controlled Titrator.** A. Graneli, L. Andersson, Chalmers U of Technology and U of Gothenburg

9:50 **Applications of Photoconductivity Detector.** J. B. Dixon, D. E. Harris, Tracor Instruments

10:20 **Automatic Numerical Evaluation of Potentiometric Titrations.** E. P. Kujawa, Brinkmann Instruments

10:40 **Photometric Instrument that Provides Extended Linear Range by Automatically Switching Between Photon Counting and Analog-to-Digital Modes.** V. Nau, T. A. Nieman, U of Illinois

11:00 **Direct Monitoring of Airborne Heavy Metal by Air Plasma Spectrometry.** S. Hanamura, National Measurement Lab

11:20 **Du Pont PREP I, a New Automated Sample Processor for Automatic Extraction and Concentration of Selected Sample Components in Fluids.** J. D. Lowry, J. G. Forsythe, R. F. Bree, Du Pont

11:40 **On-Line Ferrography.** E. R. Bowen, R. H. Rotondi, Foxboro Analytical

Environmental Analysis—Air Pollution I

Tuesday Morning, Room 235B

J. Frohliger, *Presiding*

8:30 **Portable Plasma Emission System for Determination of Mercury and Mercury Species in Air.** D. D. Gay, EPA, K. O. Wirtz, L. C. Fortmann, H. L. Kelley, C. W. Frank

8:50 **Statistical Studies of 1975–1977 Air Pollution and Weather Data for the Phoenix, Arizona, Metropolitan Area.** M. L. Parsons, Arizona State U, L. Y. Hara, D. D. Pratt

9:10 **Analysis of Air, Stack Gas, and Solution Particulates by Secondary Target Energy-Dispersive X-Ray Fluorescence.** D. J. Kalnicky, Exxon

9:30 **Determining Trace Quantities of Acrylonitrile in Air.** R. L. Campbell, D. R. Marrs, N. W. Standish, Vistron Chemical Co.

9:50 **Preparation and Evaluation of Silica and Asbestos Reference Materials for Pollution Studies.** J. A. Mackey, NBS, O. Menis, P. D. Garn

10:20 **Polymer Combustion: Analysis of Volatile Smoke Products by GC and GC/MS.** R. O. Gardner, R. F. Browner, Georgia Institute of Technology

10:40 **Experimental Improvements in Chromatographic Analysis of Ambient Level Hydrocarbons.** R. Denyszyn, Scott Specialty Gases, J. M. Harden, D. L. Hardison

11:00 **Quantitative Determination of Sulfur Gases by Gas Chromatography.** E. R. Kebbekus, Matheson

11:20 **Evaluation of ppm Level Sulfur Gases in N_2 and Air Contained in High-Pressure Aluminum Cylinders.** F. J. Kramer, Jr., S. G. Wechter, Airco Industrial Gases

11:40 **New Digitally Controlled API Mass Spectrometer Based System.** N. M. Reid, J. A. Buckley, J. B. French, C. Poon, Sciex

Symposium: Fourier Transform/Computer Dispersive Spectroscopy

Tuesday Morning, Little Theater

C. W. Brown, *Presiding*

8:30 **Chemiluminescence Studies by FTIR Emission Spectroscopy.** J. Sung, W. G. Fateley, Kansas State U

9:00 **Comparison of Real and Calculated Infrared Spectra.** P. F. Lynch, U of Rhode Island

9:30 **Operational Comparison of FT–IR and Computerized Classical Spectrometers.** T. Hirschfeld, Block Engineering

10:20 **Infrared Computerized Interpretive Search System.** R. W. Hannah, M. Ford, H. Carter, J. Coates, A. Savitzky, S. Geary, A. Muir, Perkin-Elmer

10:50 **Factor Group Analysis of FTIR Spectra.** J. L. Koenig, D. Kormos, M. Antoon, Case Western Reserve U

11:20 **Computerized Infrared Spectroscopy—Accomplishments and Limitations.** R. J. Obremski, J. W. Mohar, Beckman Instruments

Atomic Absorption Spectroscopy III

Tuesday Morning, Ball Room

J. H. Judd, *Presiding*

8:30 **Nongraphite Constant-Temperature Electrothermal Atomizers.** R. Woodriff, J. Boyer, Montana State U

8:50 **Thermal Environment of Furnaces of Massmann Design.** S. Myers, D. C. Manning, F. J. Fernandez, Perkin-Elmer

9:10 **Fast Automated Microsampler System for Flame Atomic Absorption.** J. A. Steensrud, Varian, T. N. McKenzie

9:30 **Signal Enhancements in Flameless AA: An Explanation Based on Gas-Phase Reactions.** J. A. Holcombe, R. H. Eklund, U of Texas

9:50 **Optimization of Performance of Atomic Absorption Spectrophotometers by Design of Gas Flow Control Systems.** C. G. Fisher III, F. J. Fernandez, S. Slavin, Perkin-Elmer

10:20 **Comparison of Proton-Induced X-Ray Emission (PIXE) with AAS for Determination of Acid Leachable Trace Metals in Marine Sediments.** G. C. Grant, R. K. Jolly, D. C. Buckle, College of William and Mary

10:40 **Techniques for Studying Graphite Furnace Peaks.** W. B. Barnett, M. M. Cooksey, L. P. Morgenthaler, Perkin-Elmer

11:00 **Slurry Atomization: New System for "Preparation-Free" Atomic Spectrochemical Analysis.** R. C. Fry, N. Mohammed, S. Hughes, Kansas State U

11:20 **Computerized Zeeman Atomic Absorption.** J. D. Miller, Nissei Sangyo Instruments

11:40 **Use of Inductively Coupled Plasma Emission for Traditional Atomic Absorption Applications.** R. D. Ediger, Perkin-Elmer

Symposium: Practical Applications of Glass Capillary Columns in Gas Chromatography

Tuesday Morning, Music Hall

J. Q. Walker, *Presiding*

8:30 **Overview of Glass Capillary Application Trials and Tribulations.** R. E. Kasier, Institut für Chromatographie Bad Dur Kheim

9:15 **Biochemical Analyses with Glass Capillary Columns.** M. Novotny, Indiana U

10:15 **Environmental Analysis with Glass Capillary Columns.** W. Bertsch, U of Alabama

Total lab automation: Only Digital can help you every step of the way.

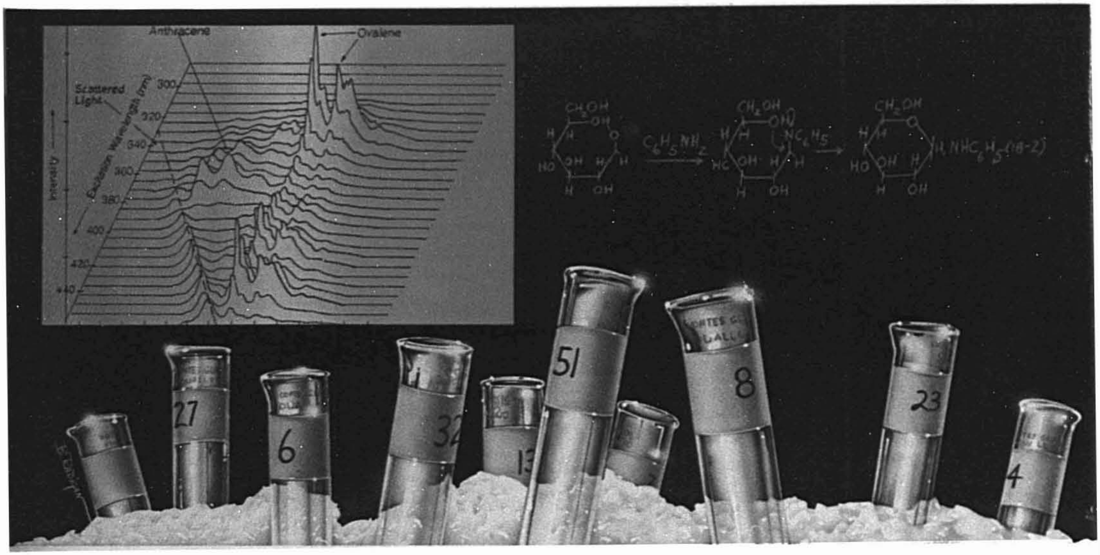
Anthracene
Ovalene
Scattered Light
Excitation Wavelength (nm)
Intensity
300
320
340
360
380
400
420
440
C6H5NH2
27
6
32
13
51
8
23
4

Big chemical labs have big computer requirements. And small requirements, and everything in between. Which is precisely why so many of them count on Digital as they plan their automation.

Digital is the only computer company with a complete line of compatible systems that spans the range from small interactive MINC-11's, which can be literally rolled from bench to bench, right up to powerful PDP-11/70's and VAX-11/780's for large scale computation and data base management.

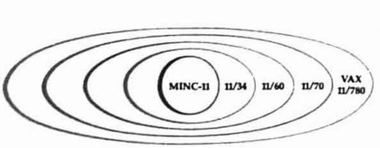
MINC-11
11/34
11/60
11/70
VAX 11/780

The DECLAB Family
Computers For The Laboratory.

You can choose Digital systems for the little jobs like data acquisition, and the big jobs like simulation and analysis. And with Digital's uniquely compatible software and advanced networking capability, these systems can be hooked to each other and even to the control systems in your processing plants to make your computer dollars work harder at every step.

Call your local Digital sales office and find out why the largest chemical companies in the world choose Digital. Or write Digital Equipment Corporation, Laboratory Data Products, MR2-4/M16, One Iron Way, Marlborough, Massachusetts 01752. European headquarters: 12, av. des Morgines, 1213 Petit-Lancy/Geneva. In Canada: Digital Equipment of Canada, Ltd.

See us at booth 1017-1020 at the Pittsburgh Conference, March 5 through March 8.

digital

CIRCLE 47 ON READER SERVICE CARD

11:00 **Food and Essential Oil Analyses with Glass Capillary Columns.** W. G. Jennings, U of California

New Instrumentation and Instrumental Concepts

Tuesday Afternoon, Room 240

T. C. O'Haver, *Presiding*

1:30 **Spectroscopic Solutions to LC Separations Problems.** R. Conlon, A. Poile, Perkin-Elmer

1:50 **Tunable Infrared Diode Lasers for Industrial Analytical Application: RTV Laser Analyzer.** A. W. Mantz, Laser Analytics, R. Moore, L. R. Sherinski, L. Wall

2:10 **Determination of Diffusible Hydrogen in Steel.** T. Otsubo, S. Goto, M. Amano, H. Sato, Nippon Steel Corp.

2:30 **Criteria for Low-Pressure HPLC Gradient Instrument.** R. W. Stout, J. A. Scott, G. Dallas, Du Pont

2:50 **Millionfold Dynamic Range on Electron Capture Detector.** J. J. Sullivan, Hewlett-Packard

3:20 **Sensitive Detector for Hydrocarbons Suitable for Gas Chromatography.** J. E. Melzer, D. G. Sutton, K. Westberg, Aerospace Corp.

3:40 **Low-Level Nitrogen Analysis with New Elemental Analyzer.** R. F. Culmo, Perkin-Elmer

4:00 **Photometric Capabilities of New UV-VIS Spectrophotometer.** M. J. Kelley, D. Priesner, Varian

4:20 **New Automated UV Spectrophotometer for Fast, Accurate Analyses.** J. P. Salsgiver, United Technical Corp.

Symposium: Photoacoustic Spectroscopy

Tuesday Afternoon, Room 205

P. M. Castle, *Presiding*

1:30 **Photoacoustic Spectroscopy—An Overview.** A. Rosencwaig, U of California

2:10 **Optoacoustic Spectroscopy: High-Resolution Study of Weak Transitions and Excited States.** C.K.N. Patel, Bell Labs

2:50 **Photoacoustic and Piezo Electric Detector Studies of Solid-Gas and Solid-Liquid Interface.** A. J. Bard, U of Texas

3:40 **Characterization of Metal Cluster Catalysts Using Photoacoustic Spectroscopy.** R. B. Somoano, S. K. Khanna, A. Gupta, Jet Propulsion Lab

4:20 **Dermatological Applications of Photoacoustic Spectroscopy.** E. Pines, T. Cunningham, Johnson and Johnson

General Surface Analysis

Tuesday Afternoon, Room 239

J. Amy, *Presiding*

1:30 **Spectroscopy of Surfaces by Transmission Fourier Transform Infrared Spectroscopy.** R. J. Jakobsen, C. J. Riggle, E. Drauglis, Battelle Columbus

1:50 **EPMA Measurement of SiO_2 Film Thickness on IC Devices.** T. Edamura, M. Watanabe, Y. Hiratsuka, Hitachi, Ltd.

2:10 **Electrochemical and Surface Analytical Characterization of Electrochemically Reformed Silver Surfaces.** J. F. Evans, D. M. Ullevig, R. M. Hexter, M. G. Albrecht, U of Minnesota

2:30 **ESCA-ISS Analysis of Al-Ni Alloy.** S. Storp, Bayer AG, K. Berrescheim, M. Wilmers

2:50 **Surface Analysis of Particulates.** C. J. Powell, T. Jach, NBS

3:20 **Elemental Mapping with Automated Auger Microprobe.** K. S. Majumder, T. A. Pandolfi, Varian

3:40 **Low-Voltage Scanning Electron Microscopy and Its Applications.** Y. Sakitani, H. Todokoro, T. Komoda, Hitachi, Ltd.

4:00 **In-Situ High-Pressure Sample Preparation for Surface Analysis.** H. D. Polaschegg, M. Jungel, E. Schirk, K. Berrescheim, M. Wilmers, Leybold-Heraeus

4:20 **Effect of Argon Pressure on Auger Spectra of Lightly Oxidized Metal Specimens.** H. L. Yeh, D. J. Hunt, International Nickel Co.

4:40 **Ellipsometric Study of Thin Films Formed on Copper by Aqueous Benzotriazole and Benzimidazole.** N. D. Hobbins, R. F. Roberts, Bell Labs

Fourier Transform Infrared Spectroscopy I

Tuesday Afternoon, Room 3A

W. Fateley, *Presiding*

1:30 **New High-Resolution Infrared Evaluated Quantitative Reference Spectra Compendium.** M. Flanagan, Sadtler Research Labs

1:50 **Ionic Behavior of Chemically Modified Enzyme, Chymotrypsin, as Studied by Fourier Transform Spectroscopy.** K. Krishnan, Digilab, J. A. Stewart

2:10 **Automated Infrared Pharmaceutical Analysis.** W. A. McAllister, G. W. Martin, F. Sancilio, Burroughs Wellcome Co.

2:30 **Criteria for and Implementation of Design for Evacuable High-Resolution FT-IR Spectrometer.** J. P. Covey, D. W. Vidrine, Nicolet Instrument Corp.

2:50 **Choice of Optimum Resolution, Aperture, Apodization, and Transform Size in Fourier Transform Spectroscopy.** T. Hirschfeld, Block Engineering

3:20 **Accurate Phase Correction of Fourier Transform Infrared Measurements.** D. R. Mattson, Nicolet Instrument Corp.

3:40 **TLC-IR Using Ready-Made Commercial Coated Plates.** T. Hirschfeld, Block Engineering

4:00 **Characterization of Polymer Deformation and Orientation by Rapid-Scanning FTIR Spectroscopy.** H. W. Siesler, Bayer AG

4:20 **Time-Dependent Infrared Spectroscopy.** C. R. Anderson, D. W. Vidrine, Nicolet Instrument Corp.

4:40 **Factors Determining Ultimate Signal-to-Noise Ratio in Practical FT-IR Measurements.** D. A. Huppler, D. R. Mattson, Nicolet Instrument Corp.

Liquid Chromatography Applications I

Tuesday Afternoon, Club Room B

M. A. Phillips, *Presiding*

1:30 **Separation of Methyl Polycyclic Aromatic Carboxylates by HPLC and GPC.** R. E. Winans, R. L. McBeth, R. Hayatsu, M. H. Studier, Argonne National Lab

1:50 **Carbohydrate Separation by HPLC: Selected Packings.** L. Cummings, Bio-Rad Labs

2:10 **Rapid and High-Resolution Method to Determine Composition of Corn Syrups by Liquid Chromatography.** L. E. Fitt, W. Hassler, D. E. Just, CPC International

2:30 **Hydrodynamic Chromatography of Coatings and Resins Utilizing a Differential Refractometer Detector.** G. P. Cunningham, C. A. Higginbotham, PPG Industries

2:50 **Use of Liquid Chromatography Apparatus to Study Solubility of Sodium Chloride in Dry Steam.** J. Galobardes, G. Oweimreen, L. B. Rogers, U of Georgia

3:20 **Rapid SARA Separation by HPLC.** L. G. Galya, J. C. Suatoni, Gulf Science and Technology Co.

3:40 **Analysis of Some Waste Lubricating and Residual Fuel Oils by High-Performance Liquid Chromatography.** J. M. Brown, W. E. May, NBS

4:00 **Analysis of Surfactants by HPLC.** A. C. Hayman, G. Dallas, Du Pont

4:20 **Hydrophobic Chromatography of Imidazole Derivatives on Variety of Reverse-Phase Columns.** E. R. White, J. E. Zarembo, Smith Kline Corp.

4:40 **HPLC Analysis of Divalent Metals as Dithizone Complexes.** D. E. Henderson, R. Chaffee, Trinity College

A GaAs PMT doesn't have to be fragile to be sensitive.

Pinbased for simple retrofitting.

Now it's easier than ever to replace that outdated and fragile glass PMT with a sensitive and rugged Varian photomultiplier tube. Varian utilizes ceramic-to-metal seal body construction, surrounds the photocathode and dynode stages with a silicone rubber material, encloses it all in a fiberglass housing and adds a pinbase for simple plug-in.

Compare Varian GaAs PMT's against glass tubes, specification for specification, and you'll choose a VPM-192 MB to upgrade your system. Add Varian's one year warranty and there's no comparison.

Throughout its long life the Varian PMT will dramatically increase the sensitivity and peak quantum efficiency of your analytical instruments.

Performance you can count on... with a full year warranty.

The outstanding performance of Varian end-window PMT's is achieved through a semitransparent III-V Gallium Arsenide photocathode, six times the size of most others, which allows light collection between 300 and 900 nm. Optimum signal-to-noise performance results from advanced electron optics, solid first and second dynodes and −78°C coolability.

Varian PMT's detailed in FREE brochure.

For more information on the family of Varian Photomultiplier products write for the color brochure, *Excellence in Photodetection.* Contact Varian, LSE Division, 601 California Avenue, Palo Alto, California 94303. Telephone (415) 493-4000, ext. 3094/3608, or call any of the Varian PMT sales representatives throughout the world.

varian

CIRCLE 218 ON READER SERVICE CARD

Ion Chromatography–Thin-Layer Chromatography

Tuesday Afternoon, Room 235A

D. Pensenstadler, *Presiding*

1:30 **Ion Chromatography Coupled with Ion Exclusion (IC/IE): Instrumentation and Applications.** W. Rich, F. C. Smith, Jr., L. McNeill, Dionex Corp.

1:50 **Determination of Anionic Species in Sodium Aluminate Liquors by Ion Chromatography.** N. J. Hornung, Aluminum Co. of America

2:10 **Application of Ion Chromatography to Analysis of Industrial Process Waters.** J. A. Rawa, Calgon Corp.

2:30 **Analysis of Metals by Ion Chromatography.** A. Schoffman, R. Posner, U.S. Testing Co.

2:50 **Anion Analysis by HPLC.** K. Harrison, The Separations Group, D. Burge

3:20 **Determination of Chloroacetate, Glycolate and Chloride in Surfactant Reaction Mixtures via Ion Chromatography.** J. J. Robinson, Ciba-Geigy, E. W. Ciurczak

3:40 **Simple Automated Ion Chromatography System.** K. F. Kahnke, Phillips Petroleum

4:00 **Rapid Selection of Optimum Separation Parameters in TLC.** R. K. Vitek, D. M. Kent, V-tech Corp.

4:20 **Thin-Layer Chromatography: Simple Approaches to Complex Separation Problems.** H. J. Issaq, N. H. Risser, NCI Frederick Cancer Research Center

4:40 **Selectivity Enhancement with SB/CD Chamber, New Form for TLC.** L. G. Glunz, J. A. Perry, Regis Chemical Co.

5:00 **Scolecite as an Adsorbant for Thin-Layer Chromatography.** K. Srinivasulu, A. K. Sonakia, Vikram U

Environmental Analysis—Air Pollution II

Tuesday Afternoon, Room 235B

H. Ryba, *Presiding*

1:30 **Determination of Ammonia in the Atmosphere of Multiple Wavelength Absorption Spectrometry.** J. M. Shekiro, Jr., K. R. O'Keefe, Colorado State U

1:50 **Application of Trapping Concentrator/GC System to Trace Analysis of Volatile Organics in Polymers and Air.** E. J. Levy, Chemical Data Systems

2:10 **Simple Tenax Collector/Injector for Atmospheric Sampling.** F. H. Jarke, IIT, S. Cotton, A. Dravnieks

2:30 **Laboratory Environment—Air Pollution Control.** J. Librizzi, Heat Systems-Ultrasonics

2:50 **Surface Analysis Techniques as Probes of Metal Speciation in Environmental Samples.** R. W. Linton, M. Bednar, M. E. Farmer, U of North Carolina

3:20 **Microcomputer-Controlled Infrared Spectrometer for Ambient Air Analysis.** J. G. Kocak, D. K. Wilks, Foxboro Analytical

3:40 **Standards for Quantitative Gas Analysis.** E. R. Kebbekus, D. D. Murray, Matheson

4:00 **Computerized Display of Chromatographic Data for Environmental Analyses.** R. E. Clement, F. W. Karasek, U of Waterloo

4:20 **Microprocessor-Controlled Process Gas Chromatographic System for Area Monitoring.** J. M. Clemons, E. Leaseburge, Bendix

4:40 **Photoacoustic Spectra of Organic Compounds on Coal Fly Ash.** T. Mauney, D.F.S. Natusch, Colorado State U

Symposium: Microprocessors in Action

Tuesday Afternoon, Little Theater

F. W. Plankey, *Presiding*

1:30 **Introduction and Overview**

1:40 **Microcomputers in Support of Chemistry.** E. R. Fisher, U of California

2:25 **Utilizing a Microprocessor in a Dedicated Analytical Instrument.** C. J. Sitek, R. B. Edwards, LECO Corp.

3:30 **Applying a Microprocessor to Multicomponent Infrared Analysis.** P. Wilks, Wilks-Foxboro Analytical

4:15 **Application of the KIM-1 Microcomputer.** J. D. Ingle, Oregon State U

Atomic Absorption Spectroscopy IV

Tuesday Afternoon, Ball Room

P. E. Bauer, *Presiding*

1:30 **Simultaneous Multielement Atomic Absorption Spectroscopy Using Electrothermal Atomization.** P. G. Rowley, P. R. Beaulieu, J. L. Maglaty, K. R. O'Keefe, Colorado State U

1:50 **Application of Multielement Atomic Absorption Spectrometer for Simultaneous Determination of Elements in a Flame.** P. R. Beaulieu, K. R. O'Keefe, Colorado State U

2:10 **Analytical Versatility in Atomic Spectroscopy.** R. G. Schleicher, J. J. Sotera, H. L. Kahn, Instrumentation Lab

2:20 **High-Speed, Background Corrected, Simultaneous Multielement Atomic Absorption Spectrometer.** J. M. Harnly, U of Maryland, T. C. O'Haver, W. R. Wolf

2:50 **Instrumental Parameters in Atomic Absorption.** H. L. Kahn, P. M. Moran, J. D. Miller, Instrumentation Lab

3:20 **Sampling System for Direct Atomic Absorption Analysis of Chelated Trace Elements Using Constant-Temperature Furnace.** J. Nichols, R. Woodriff, Montana State U

3:40 **Applications of Vitreous Carbon Components to Electrothermal Atomizers.** M. Verwolf, R. Woodriff, L. Hageman, Montana State U

4:00 **Comparison of Lead Interferences in Pulse Type vs. Constant-Temperature Electrothermal Atomizers.** L. Hageman, R. Woodriff, Montana State U

4:20 **Interferences in Graphite Furnace Atomic Absorption Spectroscopy.** J. P. Erspamer, T. M. Niemczyk, U of New Mexico

4:40 **L'vov Platform Provides More Constant Thermal Conditions for Furnace AA Analyses.** D. C. Manning, W. Slavin, Perkin-Elmer

Symposium: Trace Analysis with Glass Capillary Column in Gas Chromatography

Tuesday Afternoon, Music Hall

W. Suits, *Presiding*

1:30 **Practical Capillary Chromatography—A Systematic Approach.** K. Grob, Swiss Federal Institute for Water Resources and Water Pollution Control

2:30 **Use of Selective Detectors to Simplify Interpretation of Complex Capillary GC/MS Environmental Analyses.** M. Marcus, Midwest Research Institute

3:15 **Screening for Priority Pollutants in Industrial Wastewaters.** T. Sabatino, Rutgers U

3:40 **Cost Saving Through Time Optimization of Trace Drug Analysis.** L. F. Hanneman, Dow Corning

4:10 **Analysis of Chlorinated Anisols, Chlorinated Dibenzofurans, and Brominated Biphenyls.** T. Farrell, FDA

4:35 **Column Selection for Pesticide and PCB Analyses in Water—Advantages and Pitfalls.** F. Onuska, Canadian National Water Research Institute

Tracor

if you don't have Tracor chromatographs in your lab...

Gas Chromatography

A Tracor 560 gas chromatograph equipped with the New HALL® 700A Electrolytic Conductivity Detector and the Tracor 702 Nitrogen-Phosphorous Detector can do specific analysis of almost any class of compounds.

700A HALL® Electrolytic Conductivity Detector

The new HALL® 700A is more compact and up to 10 times more sensitive than its predecessors. It incorporates such new features as

- An automatic solvent venting valve and a differential conductivity cell for improved long term stability
- A new microreactor platinum resistance heater/sensor which allows for faster and more accurate temperature control of the reaction zone
- A combustion tube of small I.D. nickel tube which gives more efficient conversion of the combusted compounds

The 700A also incorporates a bipolar-pulsed excitation signal across the cell electrodes which eliminates the non-linearity, cell heating and capacitive noise problems previously associated with other conductivity measurements.

702 Nitrogen-Phosphorous Detector

The Tracor 702 Nitrogen and Phosphorous Detector has several outstanding features over other available nitrogen phosphorous detectors. *First*, the source desensitizer allows the user to inject *chlorinated solvent derivatizing agents* and ordinary solvents without degenerating or destroying the source. Second, the source is electrically heated/precision temperature controlled for better source life even in the event of column flow loss . Next, source alignment is quick and easy with alignment tool provided. What can you do with the Tracor 560/700A/702 element selective chromatograph?

- Specific detection of halogen, nitrogen or sulfur compounds over a 10^4 linear range with the HALL® 700A Electrolytic Conductivity Detector.
- Specific detection of nitrogen and phosphorous compounds with easy detector operation using the 702 Nitrogen-Phosphorous Detector.

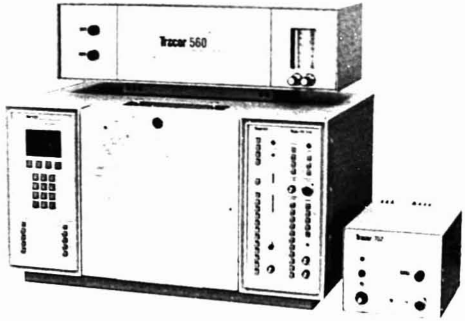

702 NPD
Phosphorous

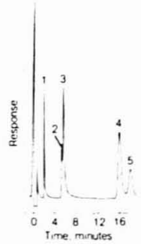

Instrument Tracor 560/702 NPD

Peak	Identity
1	Thimet—1.8 ng ea
2	Malathion—3.6 ng ea
3	Parathion—3.6 ng ea
4	Ethion—3.6 ng ea
5	Trithion—3.6 ng ea

700A HECD
Specific Sulfur Mode

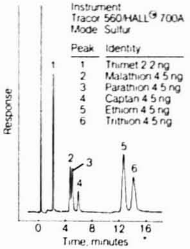

Instrument
Tracor 560/HALL® 700A
Mode Sulfur

Peak	Identity
1	Thimet 2.2 ng
2	Malathion 4.5 ng
3	Parathion 4.5 ng
4	Captan 4.5 ng
5	Ethiorn 4.5 ng
6	Trithion 4.5 ng

The 700A detector provides improved linearity and selectivity for sulfur over the FPD

Specific Nitrogen Mode
Nitrosamines

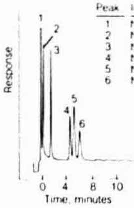

Instrument
Tracor 560/HALL® 700A
Mode Nitrogen

Peak	Identity
1	N-Nitrosodimethylamine
2	N-Nitrosodiethylamine
3	N-Nitrosodipropylamine
4	N-Nitrosodibutylamine
5	N-Nitrosopiperidine
6	N-Nitrosopyrrolidine

Chromatogram of 1 ng each of nitrosamines listed. 250 *picograms* of the same compounds are clearly measurable

Contact Tracor for Chromatrographic Conditions.

Tracor Instruments Tracor, Inc. 6500 Tracor Lane Austin, Texas TELEX 77-6414

CIRCLE 208 ON READER SERVICE CARD

Chromatography

look at the chromatography capability you are missing!

Liquid Chromatography

Tracor's 900 Series Liquid Chromatograph provides selective detection of halogen, nitrogen and sulfur compounds in liquid chromatography using the Tracor 965 Photo-conductivity detector. This detector, like the 700A for gas chromatography, uses a bipolar pulsed signal across the differential cell electrodes to give increased linearity and sensitivity. Chromatograms below illustrate its operation.

Another Tracor designed product, the Model 970A Variable Wavelength Absorbance Detector, includes both deuterium and quartz iodide sources for absorbance measurements over the entire UV-visible spectral range—190nm-650nm. This type of detector has become the most generally used detector in the field of high pressure liquid chromatography. The 970A features fiber transfer optics, a holographically ruled grating for low noise, high energy operation even in the far UV. This modern optical technology has produced a simple design resulting in maximum energy with no cell alignment requirements. A low cost wavelength scanning option is offered to provide spectral information.

The Models 965 and 970A combine two powerful detectors in a single LC system.

Tracor's new Model 950 pumping system features a unique quickly removable micro liquid head assembly, interchangeable with a high flow liquid head. Also an improved electronic flow compensation circuit is used which eliminates pulsing resulting from piston movement—thus providing longer column life and higher sensitivity detector compatibility.

This pump is complemented by the 980A solvent programmer for gradient elution operation.

Nitrogen

Nitrosamines

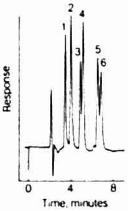

Instrument Tracor 950/965
Separation Normal Phase

Peak	Identity
1	N-Nitrosodimethylamine
2	N-Nitrosodiethylamine
3	N-Nitrosodipropylamine
4	N-Nitrosodibutylamine
5	N-Nitrosopiperidine
6	N-Nitrosopyrrolidine

8 ng each

Halogen

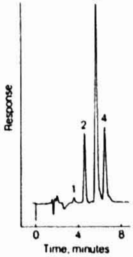

Instrument Tracor 950/965
Separation Reverse Phase

Peak	Identity
1	Fluorobenzene 550 ng
2	Chlorobenzene 550 ng
3	Iodobenzene 400 ng
4	4 Bromotoluene 300 ng

Relative response to halogenated benzenes. All halogens are detected with fluorine being the least sensitive in this case.

Sulfur and Nitrogen

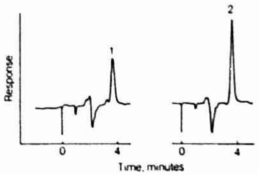

Instrument Tracor 950/965
Separation Reverse Phase

Peak	Identity
1	5 µg Spectracide
2	1 µg Diazinon

On the left, a direct injection of spectracide run on the Tracor 950/965 after a simple 1/100x1/100 dilution with methanol. The component of interest diazinon is selectively detected with the Photo-conductivity Detector—here at a level of 0.5 ug. On the right, a 1.0 µg standard of diazinon.

Telephones 512:926 2800 512:926 9161 504:272 1421 312:595 2420 201:534 4081 415:938 5490

CIRCLE 209 ON READER SERVICE CARD

Wednesday, March 7

Magnetic Resonance Spectrometry

Wednesday Morning, Room 240

R. Mooney, *Presiding*

8:30 **Moisture Determination in Solids by Pulsed NMR.** A. Attalla, B. Craft, Monsanto

8:50 **Applications of Proton and Carbon-13 NMR to Coatings.** J. H. Smith, PPG Industries

9:10 **Magnetic Resonance and Infrared Spectral Studies of Structural Changes During Coal Liquefaction.** M. R. Hough, H. L. Retcofsky, T. A. Link, D. H. Finseth, U.S. Dept. of Energy

9:30 **Deuteron Quadrupole Coupling Constants of Intramolecular Hydrogen-Bonded Compounds.** J. C. Trewella, L. M. Jackman, Pennsylvania State U

9:50 **Tetraarylborates as NMR Shift Reagents for Onium Compounds.** G. E. Pacey, C. E. Moore, Loyola U

10:20 **Toward an Optimal Paramagnetic Relaxation Agent for ^{31}P Nuclear Magnetic Resonance.** T. M. Carr, W. M. Ritchey, Case Western Reserve U

10:40 **Relaxation Agents for Improved Sensitivity of ^{29}Si NMR.** D. Cory, A. Wong, W. M. Ritchey, Case Western Reserve U

Emission Spectrographic Analysis

Wednesday Morning, Room 205

J. E. Paterson, *Presiding*

8:30 **Utility of ICP Spectroscopy for Routine Multielement Analysis of Nutritional Products.** W. B. Tucker, J. O. Rasmuson, Mead Johnson & Co.

8:50 **Inductively Coupled Argon Plasmas: Introduction of Organic Species.** A. W. Boorn, R. F. Browner, Georgia Institute of Technology

9:10 **Application of Inductively Coupled Plasma/Direct Reading Polychromator to Multielement Analysis of Stream Sediment Extracts.** G. F. Larson, R. W. Morrow, L. E. White, Union Carbide

9:30 **Sequential Determination of 60 Elements in Geochemical and Environmental Matrices by Inductively Coupled Plasma-Atomic Emission Spectrometry.** M. A. Floyd, A. P. D'Silva, V. A. Fassel, M. Tschetter, Iowa State U

9:50 **Improved Potassium Determination in Direct Reading Spectrometer with Inductively Coupled Plasma Source.** B. A. Hudgens, U of Missouri, D. A. Yates, S. R. Koirtyohann

10:20 **Elemental Trace Analysis of Human Blood Using ICAP Spectroscopy.** C. H. Annett, U of Kansas Medical Center, R. C. Bearse

10:40 **Determination of Sulfur via Hydride Evolution Using Vacuum Ultraviolet Plasma Atomic Emission Spectrometry.** S. R. Ellebracht, P. D. Swaim, Dow Chemical

11:00 **Determination of Carboxyl and Phenolic Content of Coal and Lignite Residues by Sodium Flame Emission Spectroscopy.** R. C. Duty, J. Austin, J. J. Dumais, Illinois State U

11:20 **Spectrochemical Determination of Beryllium and Lithium in Stream Sediments.** D. L. Gallimore, A. D. Hues, B. A. Palmer, O. R. Simi, U of California

11:40 **Analyses of Aircraft Engine Oils for Wear Metal Particulates by Plasma Source, Rotating Disc Atomic Emission and Atomic Absorption Spectroscopy.** P. S. Fair, U of Dayton Research Institute, J. R. Brown, W. E. Rhine, K. J. Eisentraut

Symposium: New Techniques in Applied Surface Characterization

Wednesday Morning, Room 239

D. M. Hercules, *Presiding*

8:30 **Introductory Remarks.** D. M. Hercules

8:40 **EXAFS Applied to Catalysts.** F. W. Lytle, Boeing Co.

9:15 **EXAFS Studies of Surfaces Using Electron Yield Spectroscopy.** J. Stohr, Stanford Synchrotron Radiation Lab

10:10 **Electron Energy Loss Spectroscopy.** H. Ibach, Institute for Grenzflachenforschung und Vacuum physik der Kernforschungsanlage

10:50 **Inelastic Electron Tunneling Spectroscopy Applied to Modified Surfaces.** A. Diaz, IBM

11:25 **Simultaneous Work Function and Surface Composition Measurements.** G. A. Haas, Naval Research Lab

Fourier Transform Infrared Spectroscopy II

Wednesday Morning, Room 3A

P. R. Griffiths, *Presiding*

8:30 **Quantitative Methods in FT-IR.** D. W. Vidrine, Nicolet Instrument Corp.

8:50 **Molecular-Level Approach to Blood-Surface Interactions.** R. M. Gendreau, R. J. Jakobsen, Battelle Columbus

9:10 **Automated Interface Between a Liquid Chromatograph and a Fourier Transform Infrared Spectrometer.** D. Kuehl, P. R. Griffiths, Ohio U

9:30 **Identification and Determination of Minerals in Whole Coal by Diffuse Reflectance Infrared Spectrometry.** M. P. Fuller, P. R. Griffiths, Ohio U

9:50 **Environmental Chamber for Complete Characterization of Polymer Aging via Infrared Spectroscopy.** B. J. Bulkin, E. Pearce, J. Y. Huang, Polytechnic Institute of New York

10:20 **GC/IR Analysis of Commercial Divinyl Benzene.** J. D. Witt, Allied Chemical Corp., R. L. Julian, M. Gabriel

10:40 **Functional Group Analysis of GCIR Data Using Correlation Interferometry.** R. C. Wieboldt, B. A. Hohne, D. A. Hanna, T. L. Isenhour, U of North Carolina

11:00 **Infrared Search System Based on Direct Comparison of Interferograms.** G. W. Small, G. T. Rasmussen, T. L. Isenhour, U of North Carolina

11:20 **High-Sensitivity Fourier Transform Infrared Spectra of Pyrolysis-Gas Chromatographic Peaks.** K. Krishnan, R. C. Noonan, Digilab

11:40 **Fourier and Transform Infrared Spectroscopic Study of Phase Transition in Some Liquid Crystals.** R. C. Noonan, K. Krishnan, S. H. Hill, Digilab

Liquid Chromatography Applications II—Biomedical

Wednesday Morning, Club Room B

N. Kotsko, *Presiding*

8:30 **Realistic Approach to Optimizing Chromatographic Systems. Application to Reverse-Phase HPLC Separation of Several PTH-Amino Acids.** M. W. Watson, P. W. Carr, U of Minnesota

8:50 **Use of Reverse-Phase HPLC in Isolation and Separation of Peptides.** M. Savage, G. Hewett, G. McKay, Altex Scientific

9:10 **Vitamins A, D, and E via Fast LC.** A. L. Pietrantonio, J. I. Fernandez, J. R. Gant, Technicon Industrial Systems

9:30 **Rapid Liquid Chromatographic Determination of Amino Acids in Picomole Range.** D. W. Hill, U of Connecticut, J. D. Stuart, T. D. Wilson, F. H. Walters

9:50 **Separation of Nucleic Acid Components on New Bonded-Phase Anion Exchanger.** C. T. Wehr, S. R. Abbott, Varian

10:20 **Analysis of Methylated Nucleosides in Biological Fluids by HPLC.** D. J. Popovich, C. J. Lancaster, G. J. Kusha, Whatman, Inc.

10:40 **Liquid Chromatographic Separation and Fluorescence Measurement of Taurine—A Key Amino Acid.** J. D. Stuart, U of Connecticut, D. W. Hill, T. D. Wilson, F. H. Walters, S. Y. Feng

FLUOROMETRY MADE EASY

Analysis is simple, quick, and accurate with this sophisticated, ratio recording Spectrofluorometer from BAIRD...

Providing sensitivities in the low parts-per-trillion, Baird's Model SFR-100 is a versatile, state-of-the-art instrument that can speed routine work and simplify the most complex analysis.

A double-beam ratio system for corrected spectra, together with excellent long-term stability, provides outstanding accuracy. A high signal-to-noise ratio assures clear, unambiguous results. Readout of reference, emission and ratio signals can be selected on an integral panel display and separate XY recorder. An analog panel meter facilitates set-up, and BCD output is available for simple computer interfacing. Many other advanced operating features are included.

Send today for complete SFR-100 specifications and operating details, together with data on a broad range of accessory equipment and devices.

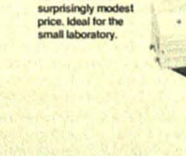

FLUORICORD — Exceptional versatility for research and difficult routine analysis. Easy to operate, with excellent resolution and accuracy . . . high repeatability and sensitivity.

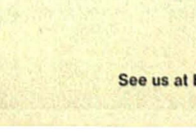

FLUORIPOINT — A high-quality, automatic scanning, spectrofluorometer at a surprisingly modest price. Ideal for the small laboratory.

Let us demonstrate the SFR-100 in your own laboratory. We will leave you a free copy of "Practical Fluorescence Theory, Methods, and Techniques," by G. G. Guilbault, for giving us a chance to show what this unique instrument can do.

BA BAIRD-ATOMIC

Home Office: Baird-Atomic, Inc.
125 Middlesex Tpk., Bedford, MA 01730
Tel. (617) 276-6000 — Telex: 923491 —
Cable: BAIRDCOBFRD

CIRCLE 22 ON READER SERVICE CARD

See us at Booth 801-808 at the Pittsburgh Conference

11:00 **Characterization of Bonded NH_2 Packing and High-Sensitivity Determination of Saccharides.** M. D'Amboise, D. Noel, T. Hanai, U of Montreal

11:20 **Applications of Anionic Surfactants as Mobile Phase Modifiers in High-Performance Liquid Chromatography of Pharmaceutical Compounds.** J. M. Jushchyshyn, L. G. Meehan, C. D. Muller, Smith Kline & French

Symposium: Environmental Organic Analysis of Water and Sediment

Wednesday Morning, Room 235A

D. H. Freeman, *Presiding*

8:30 **Introduction to Symposium.** D. H. Freeman

8:35 **Organics in the Environment: Statistical Sampling and Instrumental Analysis.** H. S. Hertz, NBS

9:20 **Implications of Transport and Transformation for Environmental Pollutant Analysis.** G. L. Baughman, Environmental Research Lab

10:20 **Strategies for Ultratrace Analysis of Prevalent Environmental Organic Contaminants.** C. S. Giam, Texas A&M U

10:45 **Methodless Methodology—Strategy for Alkyl Phthalate Measurement in Marine Sediments.** D. H. Freeman, J. C. Peterson, U of Maryland

11:10 **Nonvolatile Organic Impurities in Wastewater by Liquid Chromatography.** H. F. Walton, U of Colorado

11:35 **Aromatic Hydrocarbon Biogeochemistry in Model Eco-System.** N. M. Frew, A. C. Davis, K. Tjessem, J. W. Farrington, Woods Hole Oceanographic Institution

Environmental Analysis—Air Pollution III

Wednesday Morning, Room 235B

A. J. Kavoulakis, *Presiding*

8:30 **Analysis for Selected Toxic and Carcinogenic Organic Vapors in Ambient Air.** J. W. Bozzelli, J. Kemp, J. LaRegina, B. Kebbekus, New Jersey Institute of Technology

8:50 **Evaluation of Sorbents for Trapping of Organic Vapors from the Ambient Atmosphere.** B. Kebbekus, R. Vaccaro, J. W. Bozzelli, New Jersey Institute of Technology

9:10 **Chemical Characterization of Trace Elements in Ashes from Refuse Fueled Processes.** G. M. Trischan, Midwest Research Institute

9:30 **Analysis of Coal Liquefaction Products by MIKES.** D. Zakett, V. M. Shaddock, R. G. Cooks, Purdue U

9:50 **Sampling and Analyzing Techniques of Air Bag Inflator Effluents.** B. M. Joshi, E. L. Stokes, Ford Motor Co.

10:20 **Determination of Vinyl Chloride Monomer in the Ambient Air Near Point Source Emissions.** J. L. Lindgren, G. Speller, Texas Air Control Board

10:40 **Analysis of Ambient Particulate Matter Using Fourier Transform Infrared Spectroscopic Technique.** K. H. Shafer, Battelle Columbus, W. M. Henry, R. J. Jakobsen, R. Burton

11:00 **Sample Preparation in Determination of Free Crystalline Silica in Respirable Dust from Steel-Making Environments.** O. P. Bhargava, A. S. Alexiou, H. Meilach, W. G. Hines, Steel Co. of Canada

11:20 **Development of Purging Technique for Determination of Volatile Organic Pollutants in Biological Matrices.** M. D. Erickson, L. C. Michael, S. P. Parks, J. L. Barclay, E. D. Pellizzari, Research Triangle Institute

11:40 **Application of Proton-Induced X-Ray Analysis for Aerosols in the Atmosphere.** S. Tanaka, Keio U, R. Chiba, H. Kutsuna, Y. Osada, Y. Hashimoto

Gas Chromatography—Detectors

Wednesday Morning, Little Theater

J. Sember, *Presiding*

8:30 **Organotin Detection with Hydrogen Atmosphere Flame Ionization Detector (HAFID).** J. E. Roberts, T. Kumar, H. H. Hill, Jr., Washington State U

8:50 **Response of Thermionic Specific Detector to Various Nitrogen Compounds.** Z. Penton, Varian

9:10 **Group Specific Infrared Detector for Gas Chromatography.** H. H. Hausdorff, Foxboro Analytical

9:30 **Evaluation of Nitrogen Specific Mode of New Version of Hall Electrolytic Conductivity Detector (HECD).** R. J. Anderson, R. C. Hall, Tracor Instruments

9:50 **Capillary Column Gas Chromatography of Inorganic Compounds with Specific Element Detection.** P. C. Uden, T. P. Tetu, C. A. Poirier, B. D. Quimby, R. M. Barnes, U of Massachusetts

10:20 **Use of Photoionization Detector for Determination of Trace Contaminants in Pharmaceutical Compounds and in the Environment.** W. E. Moeckel, E. R. White, J. E. Zarembo, Smith Kline Corp.

10:40 **Glass Capillary GC Columns with Photoionization Detector.** J. Driscoll, L. Jaramillo, HNU Systems

11:00 **Photoionization Detector: Selective or Nearly Universal Detector for Gas Chromatography.** L. Jaramillo, J. Driscoll, HNU Systems

11:20 **Multicolumn Multidetection Capabilities of Capillary Column Dedicated Gas Chromatograph.** G. Sisti, Carlo Erba Strumentazione, G. R. Verga, S. Trestianu

11:40 **Fresh Design for Thermal Conductivity Detectors.** J. Craven, D. Clouser, Hewlett-Packard

Atomic Absorption Spectroscopy V

Wednesday Morning, Ball Room

P. Walters, *Presiding*

8:30 **Interfacing Inexpensive Home Computers to Analytical Instruments and Laboratory Minicomputers.** T. S. Wasco, M. E. Hughes, J. L. Fasching, U of Rhode Island

8:50 **Evaluation of Reliability of Results Using New AA Spectrophotometer.** M. W. Routh, P. A. Bennett, Varian

9:10 **Fritted Disk Pneumatic Nebulizer—A Nebulous Phenomenon.** C. T. Apel, D. V. Duchane, Los Alamos Scientific Lab

9:30 **Evaluation of Utility of New Nebulizer System in Water Analysis.** M. W. Routh, T. McKenzie, Varian

9:50 **Use of Organic Acids for Improved Signal Stability and Sensitivity for Determination of Metals in High Salt Solutions by Atomic Absorption Spectroscopy.** E. G. Gooch, P. R. Roupe, Dow Corning

10:20 **Fundamental Studies of Continuum Source Atomic Fluorescence to Determination of Arsenic, Antimony, and Selenium.** E. M. Heithmar, U of New Orleans, F. W. Plankey

10:40 **Determination of Arsenic, Selenium, and Antimony by Nondispersive Continuum Source Atomic Fluorescence Spectrometry.** F. Lipari, F. W. Plankey, U of Pittsburgh

11:00 **CW Laser-Enhanced Ionization and Atomic Fluorescence Spectroscopy.** S. J. Weeks, NBS, J. C. Travis, G. C. Turk, J. R. DeVoe, P. K. Schenck

11:20 **Ionization Interferences in Laser-Enhanced Ionization Spectrometry.** T. O. Trask, G. J. Havrilla, R. B. Green, West Virginia U

11:40 **Fate of Trace Metals in Batch-Type Coal Gasification Unit.** P. M. Grohse, S. K. Gangwal, D. E. Wagoner, Research Triangle Institute

SIEMENS

When choosing an X-ray analytical system…

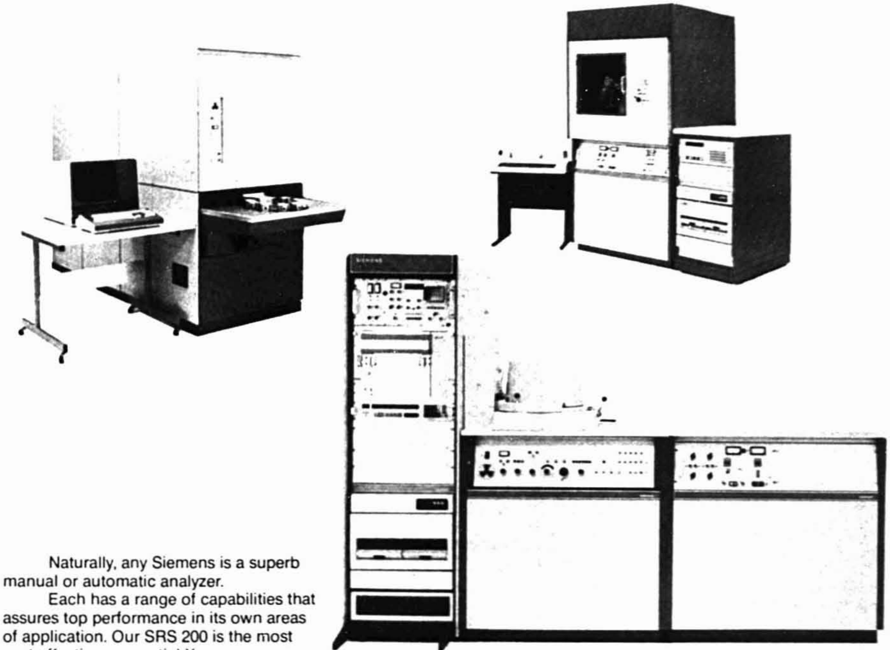

Naturally, any Siemens is a superb manual or automatic analyzer.

Each has a range of capabilities that assures top performance in its own areas of application. Our SRS 200 is the most cost-effective sequential X-ray spectrometer on the market today. Our new MRS 400 high-performance, multichannel spectrometer delivers 28 simultaneous X-ray evaluations in as little as 40 seconds. And our D 500 diffractometer… with 1-, 40-, or 80-specimen magazine, all with sample-rotation capabilities; integrally mounted X-ray tube; and independent θ, 2θ, motion… is absolutely unexcelled in the industry.

They're all tangible, hard-working, highly productive hardware. But when the chips are down, the Siemens intangibles can be equally essential:

People. Thoroughly competent people who give you hard, unbiased information … not product puffery. Cooperative people who *listen* and *deliver*. Permanent people who'll be there when you want them, year after year.

Service. A widespread, mobile service organization. Fast, fast response. Unexcelled facilities. Top-notch engineers and technicians.

Attitude. Siemens is a world leader in X-ray technology and equipment. We got that way through state-of-the-art thinking, absolute product quality, and a simple corporate policy: The fastest way to get ahead, is to put your customers' interests first.

For more information on our full range of X-ray analyzers, use the reader-response card. For complete information, plus a free 30 x 43-inch, four-color wall chart of the X-ray periodic table of the chemical elements, contact Mr. Pedro Arredondo, **Siemens Corporation,** 2 Pin Oak Lane, Cherry Hill, New Jersey 08034. (609) 424-9210.

even the intangibles are tangible reasons to buy Siemens.

CIRCLE 191 ON READER SERVICE CARD

Dal Nogare Award Symposium

9:00—Wednesday Morning, Music Hall
R. A. Barford, *Presiding*
Presentation of
Dal Nogare Award
by
Lyle H. Phifer
for
The Chromatography Forum of
Delaware Valley
to
J. Calvin Giddings
University of Utah
Award Address

10:00 **Recycle Chromatography.** L. B. Rodgers, U of Georgia

10:45 **Extended Capabilities in Gas Chromatography Through High-Resolution Techniques.** S. P. Cram, Varian

11:10 (To be announced). B. L. Karger, Northeastern U

11:35 **Factors Affecting Selectivity in Reverse Phase Chromatography with Hydrocarbonaceous Bonded Phases.** C. Horvath, Yale U

Raman Spectroscopy

Wednesday Afternoon, Room 240
W. F. Edgell, *Presiding*

1:30 **Seizing the Advantage—Multiplex Laser Raman Spectroscopy.** C. J. Vear, Anaspec, Ltd.

1:50 **Raman Spectrometer System Free of Chromatic Aberrations.** J. F. Rendina, Spex Industries

2:10 **Raman Spectrum of Dilute Tetrahydrofuran Solutions of $NaCo(Co)_4$ Structure at Ion Sites. Selection Rules.** W. Edgell, Purdue U, K. T. Joseph

2:30 **CARS Study of Combustion-Related Species.** M. E. McIlwain, J. C. Hindman, Argonne National Lab

2:50 **Associational Effects of Tetraalkylammonium Salts on Raman Spectrum of Acetonitrile.** H. S. Gold, U of Delaware, J. E. Pemberton, R. P. Buck

3:20 **Resonance Raman Method for Rapid Detection and Identification of Bacteria in Water.** W. F. Howard, W. H. Nelson, J. Sperry, U of Rhode Island

3:40 **Rejection of Fluorescence from Ultraviolet Resonance Raman Spectra.** T. H. Bushaw, T. L. Gustafson, F. E. Lytle, R. S. Tobias, Purdue U

4:00 **AC-Coupled Inverse Raman Spectroscopy: Improved Experimental Design and Resonance Enhancement.** G. P. Ritz, J. P. Haushalter, D. J. Wallan, M. D. Morris, U of Michigan

4:20 **Radiometric Correction of Raman Spectra.** F. Purcell, R. Kaminski, Spex Industries

4:40 **Use of Molecular Microprobe for Analysis of Sulfur Compounds in Coal and for Monitoring of P-N Junctions.** F. Adar, R. Grayzel, D. Landon, Instruments SA

Trace Analysis

Wednesday Afternoon, Room 205
R. Nadalin, *Presiding*

1:30 **Ultramicro-Ultratrace Element Analyzer Based on Laser Ablation and Selectively Excited Radiation.** H. W. Kwong, R. M. Measures, U of Toronto

1:50 **Role of Sample Containers in Gas Analysis.** A. Pebler, Westinghouse

2:10 **Total Sulfur in Hydrocarbons by Oxidative Microcoulometry: 10 ppb to 10%.** R. T. Moore, Envirotech, P. Clinton, V. Barger

2:30 **Acid Bomb Decomposition Method for Isotope Dilution Spark Source Mass Spectrometric Analysis.** D. W. Koppenaal, R. G. Lett, F. R. Brown, U.S. Dept. of Energy

2:50 **Trace and Minor Element Analyses of Liquefaction Products from West Virginia Coal.** R. G. Lett, R. R. DeSantis, J. W. Adkins, R. A. Hahn, U.S. Dept. of Energy

3:20 **Analysis of Metal Particulates in Lubricating Oils by Plasma Emission, Spark Emission, and Atomic Absorption.** W. E. Rhine, U of Dayton Research Institute, P. S. Fair, C. S. Saba, J. R. Brown, K. J. Eisentraut

3:40 **Determination of Total Organic Carbon (TOC) in Seawater by UV-Promoted Persulfate Oxidation.** Y. Takahashi, Envirotech

4:00 **Microwave-Plasma Chemical-Ionization Source for Gas Impurity Analysis by Mass Spectrometry.** M. W. Siegel, Extranuclear Labs

4:20 **Total Nitrogen in Hydrocarbons by Automated Chemiluminescence Detection System: 20 ppb to 1%.** J. M. Castro, R. T. Moore, Envirotech

4:40 **Ppb Sulfate Determination by MECA-VAP.** S. L. Bogdanski, A. Townshend, I.S.A. Shakir, U of Birmingham

Symposium: New Instrumentation and Techniques for Surface Analysis (ASTM E-42)

Wednesday Afternoon, Room 239
T. L. Barr, *Presiding*

1:30 **Noise Removal and Deconvolution Techniques in X-Ray Photoelectron Spectroscopy.** F. J. Grunthaner, Jet Propulsion Labs

2:00 **New Developments in SIMS Instrumentation.** C. A. McGee, RCA/David Sarnoff Research Center

2:30 **Computer System for a Multi-instrument Surface Analysis Laboratory.** S. H. McFarlane, RCA/David Sarnoff Research Center

3:30 **Improvements in ISS Instrumentation.** T. Rush, 3M Co.

4:00 **Sample Transfer Techniques for Electrode Surface Analysis by Auger Electron Spectroscopy.** E. Yaeger, Case-Western Reserve U

4:30 **Position-Sensitive Detector for Photoelectron Spectroscopy.** W. B. Dress, ORNL

Clinical Chemistry

Wednesday Afternoon, Room 3A
C. Coleman, *Presiding*

1:30 **Determination of Urinary Catecholamines by On-Column Concentration Method.** H. Nakamura, T. Sugimoto, K. Matsumoto, N. Baba, Toyo Soda Manufacturing Co.

1:50 **Development of Radioimmunoassay Procedure for Procainamide: Production and Characterization of a Specific Antibody.** P. Mojaverian, G. D. Chase, Philadelphia College of Pharmacy and Science

2:10 **Analysis of Therapeutic Drugs and Metabolites in Physiological Fluids and HPLC and a New Centrifugally Based Extractor/Concentrator.** R. C. Williams, J. L. Viola, D. K. Igou, Du Pont

2:30 **Determination of Lactate and Lactic Dehydrogenase by Biamperometric Monitoring of Hexacyanoferrate (II) in a Flowing Stream.** A. S. Attiyat, G. D. Christian, U of Washington

2:50 **Multilevel Analysis of Variance Used to Determine Centrifugal Analyzer System Precision.** D. M. Fast, E. J. Sampson, C. A. Burtis, Center for Disease Control

3:20 **Simultaneous Spectrophotometric Estimation of Lactate Dehydrogenase Isoenzymes.** G. R. Robinson, K. R. O'Keefe, Colorado State U

3:40 **Analysis of Neuroendocrine Peptides by Reversed-Phase High-Performance Liquid Chromatography (HPLC).** J. A. Feldman, Duquesne U, M. I. Cohn, D. Blair

4:00 **Ionic Strength Effects of Sodium Chloride on Michaelis Constants of Soluble and Immobilized Isoenzymes of Lactate Dehydrogenase.** N. D. Danielson, Miami U, C. Potter, V. O. Brandt, F. G. Gerberich, D. W. Lowman, L. B. Rogers

4:20 **Separation and Quantitation of Acetaminophen and Its Metabolites in Bile of Mice.** L. T. Wong, L. W. Whitehouse, G. Solomonraj, C. J. Paul, Drug Research Labs

NEW!

LECO® CS-144 SIMULTANEOUS CARBON/SULFUR DETERMINATOR

More Automatic

Simplified Operation

Easy Maintenance

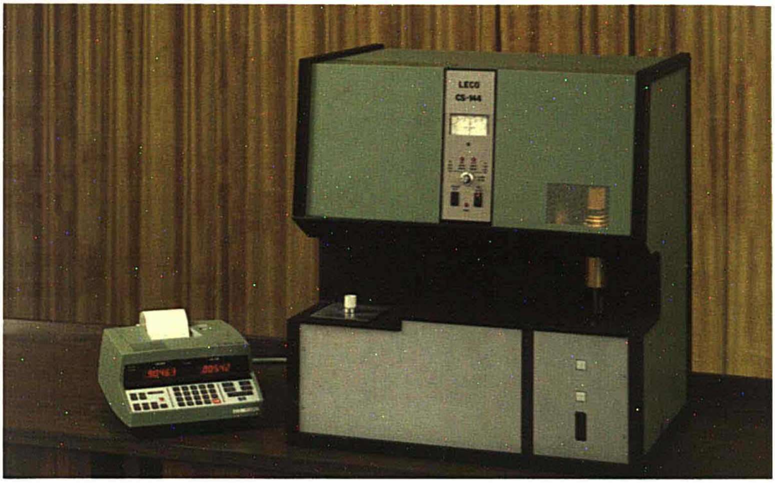

The LECO® CS-144, a new concept in automatic instrumentation, determines carbon and sulfur in iron, steel, ferrous alloys and other metals.

.90463
.00542

Control Console

- Automatic calibration
- Automatic weight compensation
- Automatic crucible loading
- Integral electronic balance & printer
- Integral diagnostic program

CONTACT LECO TODAY!

LECO®

LECO CORPORATION 3000 Lakeview Ave. St. Joseph, MI 49085, U.S.A. Phone: (616) 983-5531
Offices: California (714) 957-8227 • Texas (713) 931-0000 • Pittsburgh (412) 776-4891 • Canada (416) 270-6610

FIRST CLASS
PERMIT NO. 391
ST. JOSEPH, MI.

BUSINESS REPLY MAIL
No Postage Stamp Necessary if Mailed in the United States

POSTAGE WILL BE PAID BY

LECO CORPORATION
3000 LAKEVIEW AVENUE
ST. JOSEPH MI 49085

LECO®

Products for demonstration include:

(Check area of interest)

☐ **ANALYTICAL INSTRUMENTS FOR THE DETERMINATION OF:**

Carbon Hydrogen in Metals
Sulfur Silicon and many
Oxygen Phosphorous Inorganic
Nitrogen Manganese Materials

☐ **SC-32 SULFUR DETERMINATOR FOR COAL & COKE**

☐ **PROTEIN IN CEREALS, GRAINS, ANIMAL FEED, PET FOOD, AND FOOD STUFFS**

☐ **NITROGEN, CARBON AND SULFUR IN SOILS**

☐ **SAMPLE PREPARATION EQUIPMENT FOR SPECTROSCOPIC ANALYSIS**

☐ **THERMOCOUPLES**
Instrumentation, Small & Large Diameter Units

☐ **EXPENDABLES**
Diskpins, Accelerators, and other items

☐ **CERAMICS**
Shrouds, Nozzles and Melting Crucibles

☐ **MICROSCOPES**
Olympus: PME, Vanox, AHM, MG, BHM, SZIII, PM-10, SZIII-Tr

Jenoptics: Neophot 21

☐ **METALLOGRAPHIC**
Cut-Off's, Grinders, Polishers and Mounting Presses, Micro Hardness Tester

☐ **SPECTROSCOPIC SAMPLE PREPARATION**
Melting Furnace, Fusion Furnace

NAME ____________
TITLE ____________
FIRM ____________
ADDRESS ____________
CITY ____________ STATE ____________
ZIP ____________ PHONE ____________
☐ My title and/or address has changed as indicated above.

AC 2-79
50 M.

LECO

SULFUR IN PETROLEUM PRODUCTS* IN 2 MINUTES...

*Applicable only to samples with a boiling point above 177 C (350 F) and containing not less than 0.05 percent sulfur

with the LECO SC-32

- Accuracy ±2 percent of Sulfur content
- Microprocessor Technology
- Large Sample (up to 1 gram)
- Integral Diagnostic Program (lab technician can easily perform service)
- Solid State IR Detection (no standard solutions)
- Integral Electronic Balance

CONTACT LECO TODAY!

LECO CORPORATION **3000 Lakeview Ave. St. Joseph, MI 49085, U.S.A. Phone: (616) 983-5531**
Offices California (714) 957-8227 • Texas (713) 931-0000 • Pittsburgh (412) 776-4891 • Canada (416) 270-6610

LECO

4:40 HPLC Nucleotide Analysis of Mammalian Blood. M. McKeag, P. R. Brown, U of Rhode Island

Infrared Spectroscopy I

Wednesday Afternoon, Club Room B
J. Katon, *Presiding*

1:30 Microprocessor Control and Data Transfer in New Infrared Spectrophotometer. R. F. Kydd, C. V. Perkins, Pye Unicam

1:50 Oil Analysis—Further Applications of Computerized Infrared Spectroscopy. J. P. Coates, Perkin-Elmer

2:10 Infrared Studies in Solution with Aid of Computer Processing Techniques. J. P. Coates, Perkin-Elmer

2:30 Semiautomatic Multicomponent Quantitative Analysis with Infrared Flow Cell. J. Bernard, J. W. Mohar, R. J. Obremski, Beckman Instruments

2:50 Semiautomatic Standard Addition Method for Analysis of Pesticide Formulations. R. J. Obremski, J. Bernard, J. W. Mohar, Beckman Instruments

Liquid Chromatography for Drug and Clinical Analysis

Wednesday Afternoon, Club Room B

3:20 Rapid Method for Determination of Selected Hallucinogenic Drugs via Positive/Negative Ion LC/MS. P. E. Kelley, R. F. Skinner, Finnigan Corp.

3:40 Fluorometric Determination of Octopamine in Tissue Homogenates by High-Performance Liquid Chromatography. L. D. Mell, Jr., Naval Medical Research Institute

4:00 Analysis of Proprietary Products by High-Performance Liquid Chromatography. M. A. Carroll, J. E. Zarembo, M. A. Wagner, J. W. Horodniak, Smith Kline & French Labs

4:20 Pre- and Postcolumn Reactions with FAST LC Analyzer. D. A. Burns, J. I. Fernandez, J. R. Gant, A. L. Pietrantonio, Technicon Industrial Systems

4:40 214-nm Fixed Wavelength Detector—A New Aid for the Clinical and Industrial Chemist. B. America, P. Deland, L. Leazenbee, Laboratory Data Control

Symposium: Use of ICAP Emission for Environmental Analysis

Wednesday Afternoon, Room 235A
R. W. Freedman, *Presiding*

1:30 ICAP Analysis of Environmental Samples—Successes and Failures. F. N. Abercombie, D. J. Koop, R. B. Cruz, Barringer Research

2:15 Inductively Coupled Plasma Atomic Emission Spectroscopy—Questions Often Asked and Their Answers. V. A. Fassel, Iowa State U

3:20 Practical Application of ICAP to Environmental Analysis. C. D. Carr, Applied Research Labs

4:10 Analytical Aspects of ICAP in Water Quality Control. A. F. Ward, Jarrell-Ash

Environmental Analysis—General

Wednesday Afternoon, Room 235B
J. P. McKaveney, *Presiding*

1:30 Determination of Tracer Compounds by Liquid Scintillation Counting After Preparation of Samples by Oxidation of Host Matrix. J. E. Caton, ORNL, M. P. Maskarinec, G. M. Henderson, R. W. Harvey, M. R. Guerin, Z. K. Barnes

1:50 Some Limitations in Determination of Labile Species by Anodic Stripping Voltammetry. P. M. Figura, B. McDuffie, State U of New York at Binghamton

2:10 Time-Resolved Solvent Leaching for Surface Characterization of Particles. M.D.M. Tucker, U of Illinois, D.F.S. Natusch

2:30 GC-MS Analysis of Volatile Organics from Atmospheres Impacted by Amoco Cadiz Oil Spill. B. J. Dowty, J. W. Brown, F. N. Stone, J. Lake, J. L. Laseter, U of New Orleans

2:50 Determination of Several Polyaromatic Hydrocarbons at Selected Sites in Texas. J. L. Lindgren, Texas Air Control Board, H. J. Krauss, M. A. Fox

3:20 Determination of Polyaromatic Hydrocarbons Not Collected by Particulate Filter Media. J. L. Lindgren, Texas Air Control Board, H. J. Krauss, M. A. Fox

3:40 Partial Chemical Speciation Techniques for Aquatic Humic Metal Complexes. D. S. Chase, J. D. Ingle, Jr., Oregon State U

4:00 Determination of Fly Ash in Biological Tissue from Animals Exposed to Coal Combustion Fly Ash. S. H. Weissman, L. C. Griffis, R. F. Henderson, Lovelace Biomedical and Environmental Research Institute

4:20 Determination of Total N-Nitrosamines in Cutting Oils. R. D. Cox, C. W. Frank, U of Iowa

4:40 Determination of Nitrate and Nitrite at the Parts per Billion Level. R. D. Cox, U of Iowa

1979 Awards Symposium

Wednesday Afternoon, Little Theater
Herbert L. Retcofsky, 1979 Conference President, *Presiding*

1:30—Presentation of
1979 Pittsburgh Spectroscopy Award
by
Richard Obrycki
Chairman, Spectroscopy Society of Pittsburgh
to
John S. Waugh
Massachusetts Institute of Technology
Award Address
Nonlinear NMR: The Spectroscopist as Alchemist

2:30—Presentation of the
1979 Pittsburgh Applied Analytical Chemistry Award
by
Robert W. Baudoux
Chairman, Society for Analytical Chemists of Pittsburgh
to
Malvina Farcasiu
Mobil Research and Development Corp.
Award Adress
Fractionation and Structural Characterization of Coal Liquids

3:30—Presentation of the
1979 Maurice F. Hasler Award
by
Herbert L. Retcofsky
President, 1979 Pittsburgh Conference
to
John H. Beynon
University College of Swansea, Wales
Award Address
Thirty Years of Mass Spectrometry

Gas Chromatography—Aids

Wednesday Afternoon, Ball Room
A. Bartoli, *Presiding*

1:30 Advances in Measurement and Control of Carrier Gas. R. Nalepa, Hewlett-Packard

1:50 New Compact Hydrogen Storage Source for Gas Chromatography. E. J. Serfass, Sercon Corp.

2:10 Nickel Tubing for Gas Chromatography. S. L. McKinley, S. Ramachandran, R. S. Henly, Applied Science Labs

2:30 Use of Precolumns for Analyzing Surfactant Mixtures via Gas Chromatography. E. W. Ciurczak, Henkel, Inc., J. J. Robinson

2:50 The (r, Q) Matrix—A Tool for Manipulation of Chromatographic Patterns, Parts 1 and 2. S. M. McCown, Environmental Science and Engineering, H. H. Land III, D. R. Pitzer, C. M. Ernest

3:20 Chiral Stationary Phase for GC Capillary Work. S. Ramachandran, R. S. Henly, W. C. Kossa, S. L. McKinley, Applied Science Labs

3:40 **New Synthetic Support for Gas Chromatography—Volaspher.** M. Gurkin, R. Fischer, MC/B

4:00 **Deactivation of Glass Capillary Columns by Acid Leaching.** M. L. Lee, Brigham Young U, R. W. Wright, L. V. Phillips, D. M. Hercules, G. R. Conner

4:20 **New, Low-Cost, Interchangeable Injector for Use with Packed and Capillary Columns.** F. J. Yang, R. L. Howe, E. Freitas, S. P. Cram, Varian

4:40 **New Retention Index for PAH in Temperature-Programmed Glass Capillary Gas Chromatography.** D. L. Vassilaros, Brigham Young U, M. L. Lee, C. M. White, M. V. Novotny

Laboratory Automation

Wednesday Afternoon, Music Hall
J. J. McGovern, *Presiding*

1:30 **Discontinuous Feedback Control in Laboratory Automation.** L. Luft, Luft Instruments

1:50 **Thermometric Titration System Using Automatic Digital Endpoint Indicator.** P. Sadtler, Sanda, T. Sadtler, V. Davar, D. Stutts

2:10 **Applications of Thermometric Titrimetry to Study of Catalysts.** P. Sadtler, Sanda, T. Sadtler, D. Stutts

2:30 **Automation of Percent Nonvolatiles Analysis.** P. W. Fletcher, PPG Industries

2:50 **Results of Interlaboratory Cooperative Test on Total Sulfur in Liquid Hydrocarbons.** C. L. Kimbell, L. J. Drobnitch, Houston Atlas

3:20 **Microprocessor-Controlled Laboratory Octane Analyzer.** L. J. Rogers, Foxboro/Arcas

3:40 **Automated Solid-Liquid Extraction.** R. W. Arndt, Mettler Instrumente

4:00 **SASDRA: Dissolution Tool of the Future.** J. I. Fernandez, M. Sahn, Technicon Industrial Systems

4:20 **Inexpensive System for Rapid Precise Slurry Sampling.** J. F. Brown, H. T. Slover, USDA

4:40 **Application of Two Mechanized Methods for Decomposition of Organic Materials to Trace Analysis.** G. Knapp, Technical U Graz, H. Gstrein, W. Wegscheider, B. Schreiber

Thursday, March 8

Fluorescence–Luminescence

Thursday Morning, Room 240
L. J. Cline Love, *Presiding*

8:30 **The Model 650-40—A New Microprocessor-Controlled Fluorescence Spectrophotometer.** J. L. DiCesare, Perkin-Elmer

8:50 **Analysis of Synfuel Wastewater by Second-Derivative Synchronous Luminescence Spectroscopy.** T. Vo-Dinh, R. B. Gammage, A. R. Hawthorne, ORNL

9:10 **Derivative Techniques Used with Fluorescence Applications.** D. A. Terhaar, J. L. DiCesare, Perkin-Elmer

9:30 **Several Techniques for Sensitivity Enhancement in Fluorescence Spectrophotometry.** T. Nogami, G. Baba, K. Fukuda, T. Harada, Hitachi, Ltd.

9:50 **New Routine, Quantum-Corrected Fluorescence Spectrometer.** A.T.R. Williams, Perkin-Elmer

10:20 **Design and Application of Intensified Diode Array System to Luminescence Measurements.** M. A. Ryan, J. D. Ingle, Jr., Oregon State U

10:40 **Fluorescence Background Discrimination by Prebleaching.** T. Hirschfeld, Block Engineering

11:00 **Measurement of Phosphorescence by Fluorescence Echoes.** T. Hirschfeld, Block Engineering

11:20 **Time-Resolved Spectroscopy.** F. Purcell, R. Kaminski, Spex Industries

11:40 **Measurement of Instrument Sensitivity of a Fluorescence Spectrophotometer.** T. J. Porro, D. A. Terhaar, Perkin-Elmer

Electroanalytical Chemistry

Thursday Morning, Room 205
R. T. Oliver, *Presiding*

8:30 **Analysis of Cyanide Plating Baths by Differential Pulse Polarography.** W. M. Peterson, F. J. Muscolino, EG&G Princeton Applied Research Corp.

8:50 **Speciation of Arsenic(III), Arsenic(V), Monomethylarsonic Acid, and Dimethylarsinic Acid by Differential Pulse Polarography.** F. T. Henry, T. M. Thorpe, Miami U

9:10 **Recent Advances in the Voltammetry of Thiophenes.** A. Robbat, J. Jordan, Pennsylvania State U

9:30 **Electrochemical Detection of Mercury.** D. D. Nygaard, Bates College

9:50 **Potentiometric Stripping Analysis—New Method for Determination of Some Heavy Metals.** D. Jagner, Chalmers U of Technology and U of Gothenburg

10:20 **Cumulative Coulographic Titrimetry.** S. B. Pierce, S. T. Hirozawa, BASF Wyandotte Corp.

10:40 **Advances in Ion-Selective Electrode Technology.** J. Driscoll, E. Atwood, J. Fowler, HNU Systems

11:00 **Extension of Ion-Selective Electrode Methodology by Optimization of the Solvent.** J. F. Coetzee, W. K. Istone, M. W. Martin, U of Pittsburgh

11:20 **Novel Microcomputer-Based Potentiometric Analysis System.** C. R. Martin, H. Freiser, U of Arizona

11:40 **New Liquid Membrane Electrode Sensitive and Selective for Strychnine.** S.S.M. Hassan, M. B. Elsayes, Ain Shams U

Analysis of Oil and Other Organic Pollutants

Thursday Morning, Room 239
A. P. Bentz, *Presiding*

8:30 **Artificial Oil Weathering Techniques.** C. P. Anderson, U of Connecticut, T. J. Killeen, J. B. Taft, A. P. Bentz

8:50 **Interlaboratory Comparison of Environmental Analyses Associated with Increased Energy Production.** F. R. Guenther, H. S. Hertz, L. R. Hilpert, W. E. May, S. A. Wise, J. M. Brown, S. N. Chesler, NBS

9:10 **Laser-Excited Matrix-Isolation Molecular Fluorescence Spectrometry of Polycyclic Organic Compounds.** E. L. Wehry, R. B. Dickinson, Jr., R. R. Gore, U of Tennessee

9:30 **Investigation of Use of Molecular Fluorescence for Identification of Hazardous Materials.** L. P. Giering, J. T. Brownrigg, Baird Corp.

10:00 **GPC Enrichment and Carbon Chromatographic Fractionation of Hydrocarbons and Other Environmental Contaminants.** J. D. Petty, D. L. Stalling, L. M. Smith, Columbia National Fisheries Research Lab

10:20 **Problems with Chemical Analysis of Marine Sediments.** F. E. Franklin, J. Borges, V. Dunning, C. W. Brown, U of Rhode Island

10:40 **Facile Method for Determination of Trace (sub-ppm) Hexamethylenediamine in Water.** J. Hanrahan, Allied Chemical

11:00 **Detection and Determination of Acetohydroxamic Acid in Industrial Wastewater.** D. Richton, Allied Chemical

11:20 **Infrared Spectrophotometric Determination of Neopentylester Lubricating Oils in Water.** G. J. Gottfried, Biospherics, T. S. Yu, D. G. Shaheen

Infrared Spectroscopy II

Thursday Morning, Room 3A
J. F. Jackovitz, *Presiding*

EVERYBODY LAUGHED WHEN HE INVENTED THE SPECTRA-SEAL ALUMINUM CYLINDER.

Back in 1973, Steve Wechter had a problem at Airco's Riverton plant. It seems his gases were reacting with the steel walls of the cylinders they were stored in, and were changing in composition and purity.

Steve decided to solve the problem. With a lot of time and effort, he eventually came up with a better cylinder—an aluminum cylinder that eliminated reactions between gas mixtures and cylinder walls. And weighed less to ship. He called it the Airco Spectra-Seal™ aluminum cylinder.

When Airco introduced Spectra-Seal cylinders in 1974, our competitors all laughed. They said there was nothing wrong with the good old standard steel cylinders.

But they're not laughing any more. The superior performance of the Spectra-Seal aluminum cylinder has been tested and proved with time. And now others have started offering imitations of our Spectra-Seal aluminum cylinders.

Now Steve is laughing because they haven't been able to duplicate his invention. The aluminum surface inside our cylinders is enhanced by an anodizing process. Then, a second proprietary process further improves the inside surface, eliminates pinhole coating porosity and shields the wall from reactive gases.

Which is why, when you use Airco Spectra-Seal aluminum cylinders, the gas inside is exactly what we certify it to be. And it stays that way for years. (More than five years now, and we have the data to prove it.) Looks like Steve got the last laugh.

So if you have problems with gas standards that aren't standard, or pure gases that aren't so pure, give us a call. We're happy to share our knowledge, experience, facilities—and even Steve Wechter—with you any time you like.

Call any of our offices listed below. Or write Airco Industrial Gases, Specialty Gases and Equipment Department, 575 Mountain Ave., Murray Hill, New Jersey 07974.

AIRCO
Industrial Gases

WE HAVE THE SOLUTIONS BEFORE YOU HAVE THE PROBLEMS.

CIRCLE 7 ON READER SERVICE CARD

Albion, MI (517) 629-9161
outside MI (800) 248-3806
Baton Rouge, LA (504) 383-1436
Chicago, IL (312) 468-4200
City of Industry, CA (213) 960-2871
Houston, TX (713) 225-6027
Phoenix, AZ (602) 273-1255
Pittsburgh, PA (412) 562-3723
Raleigh-Durham, NC (919) 549-0633
Riverton, NJ (609) 829-7878
Santa Clara, CA (408) 247-5470
South Acton, MA (617) 263-7767
Vancouver, WA (206) 695-1255

Take three giant steps to finer results.

Fisher is showing all three at the Pittsburgh Conference — and more.

1

More accurate titrations. Greater automation than ever, too. It's our unique new titration "supercontrol." Shown below in the multi-sample Fisher Titralyzer® II. Its official name is Titrate Demand Module and it automatically varies titrant delivery rate for optimal results. The big news is that it's based entirely on the chemistry of each sample. Totally independent of all other experimental variables, this endpoint-seeking module (patent pending) actually determines your endpoint for you — whatever the sample. Ideal for automating your difficult tests.

CIRCLE 241 ON READER SERVICE CARD

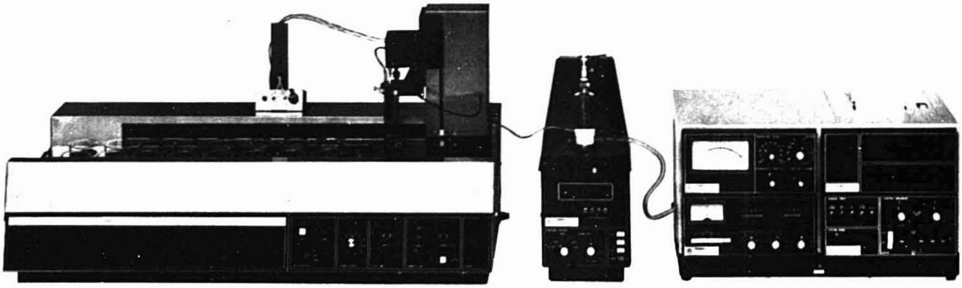

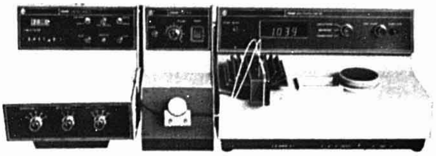

Speedier spectrophotometry. You have to see it to believe it. New Fisher Spectromatic™ discrete analyzer reduces routine operation to the simplest procedure to date — without impairing the flexibility needed for research. Note the special concentration controls for faster setups and pushbutton QC. Compact system includes microprocessor, advanced peristaltic pump, Peltier thermoelectric microflow-cell (most precise temperature control available), and versatile spectrophotometer equally at home in industrial, biochemical and clinical labs. Surprisingly low priced.

CIRCLE 242 ON READER SERVICE CARD

More automated specific-ions. Dramatically new Accumet® 750 pH/ion meter makes pH and specific-ion determinations easier than ever. Just enter data on convenient keyboard. Microprocessor does all calculations for you. There's high-speed, totally automatic standardization. And no temperature restrictions. Read pH, mV, concentration (ppm, moles/liter, mg/liter, whatever) on big bold 5-digit LED display. Temperature too — either continuously or (via pushbutton) in the midst of any other operation.

CIRCLE 243 ON READER SERVICE CARD

Plus...

More reproducible sulfurs. Patented amperometric titration technique — specific for sulfur, unaffected by nitrogen oxides and chlorides — keeps Fisher Sulfur Analyzer outstanding in its field. Results in % and ppm, with ±3% accuracy, ±2% reproducibility and repeatability — without need for skilled personnel. Now with high-speed solid-state resistance furnace.

CIRCLE 244 ON READER SERVICE CARD

Higher-capacity clean-ups. Three Fisher Chemical Clean-Up Kits efficiently, economically control acid, caustic, and flammable solvent spills. Each a scientifically formulated package with up to five times more absorptive capacity than other preparations.

CIRCLE 245 ON READER SERVICE CARD

More consistent HPLC. When you adopt Fisher Certified HPLC-grade solvents. Bottle to bottle, lot to lot, they assure consistent results. Produced in one of the industry's most modern facilities devoted exclusively to reagents, and submicron-filtered to protect your columns and pumps. (Watch for a forthcoming addition: our HPLC-grade water with lowest residual organics ever!)

CIRCLE 246 ON READER SERVICE CARD

More economical weighings. Now there are eight Fisher/Ainsworth electronic toploaders to serve you. Each a budget-priced product of American design and technology — providing the most balance per dollar. Models for 50, 200, 300, 1000, 2000g, including advanced microprocessor versions. Plus a compact BCD-coupled printing/balance. And our unique battery-pack portable for field use.

CIRCLE 247 ON READER SERVICE CARD

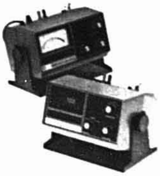

For a brighter lab. Only Fisher brings you full-performance pH in such morale-boosting packages. The bright new Accumet® 600 family of pH/mV meters. Incomparable precision, accuracy and dependability. And what a pleasure to look at! Five clean crisp colors: red, orange, yellow, blue, green.

CIRCLE 248 ON READER SERVICE CARD

Fisher Scientific Company
711 Forbes Avenue
Pittsburgh PA 15219
412/562-8543

We Know Laboratories.

8:30 Fourier Transform Infrared Spectroscopy Applied to Inorganic Compound Determination. R. M. Gendreau, Battelle Columbus, W. M. Henry, R. J. Jakobsen, K. Knapp

8:50 Predicting Performance of Medium and Low-Resolution Infrared Spectrometers and Analyzers. C. W. Brown, U of Rhode Island, P. F. Lynch, M. A. Maris, D. S. Lavery

9:10 Dealing with Effects of Low Resolution on Multicomponent Infrared Analysis. D. S. Lavery, Consultant in Analytical Chemistry, C. W. Brown, P. F. Lynch

9:30 Spectroscopic Investigation with Rotating Cryostat. J. A. Dehaseth, G. Mamantov, U of Tennessee

9:50 On an Interactive, Computer-Dispersive Spectrometer System for Infrared Spectroscopy. Application to Dilute Solution Studies. M. Balk. W. Edgell, Purdue U

10:20 Spectroscopic Investigations of Monosubstituted Acetic Acids. W. J. Ray, Miami U, J. E. Katon, P. S. Crause

10:40 Methyl Rotations in Solid Nitromethane. S. F. Trevino, NBS

11:00 Computerized Dispersive Infrared Spectroscopic Studies of Solute–Solvent Interactions in Paint Systems. A. Muller, PPG Industries

11:20 Analysis of Polymer Additives by Infrared Spectroscopy with Computerized Techniques. E. G. Bartick, R. W. Hannah, Perkin-Elmer

11:40 Applications of New Infrared Spectrophotometer with Microprocessor Control. I. A. Steer, R.C.J. Osland, Pye Unicam

Preparative Liquid Chromatography

Thursday Morning, Club Room B

S. Schmidt, *Presiding*

8:30 Preparation, Optimization, and Application of Reversed Phases in Preparative HPLC. How to Optimize a Chemical Synthesis Process. J. Montastier, Jobin Yvon, S. Cacchi, F. Gasparrini, D. Misiti, L. Charles, J. Giglio, L. Caglioti

8:50 High-Performance Preparative Liquid Chromatography. G. Dallas, A. C. Hayman, Du Pont

9:10 Super Prep Separations—Prep LC of Samples in 85–400-g Range on ISA Chromatospac Prep 100. M. Woodman, G. D. Searle, J. M. Giglio

9:30 Concentration, Purification, and Analysis Using High-Efficiency Semipreparative HPLC. F. M. Rabel, D. J. Popovich, C. J. Lancaster, G. J. Kusha, Whatman, Inc.

9:50 New UV Detector for Preparative LC. J. M. Miller, Drew U, R. Strusz

Sampling Systems: HPLC

Thursday Morning, Club Room B

10:20 New Sample Injection Valve for HPLC. G. Hewett, N.H.C. Cooke, C. Shackleford, Altex Scientific

10:40 Modified Sample Injector for Improved Efficiency in High-Performance Liquid Chromatography. T. Norris, G. J. Jordon, S.G.E. Scientific Pty. Ltd.

11:00 Individual Sample Programmer for Liquid Chromatography. R. W. Camp, Micromeritics Instrument Corp.

11:20 Sampling System for Analysis of Samples in Supercritical Gases by High-Performance Liquid Chromatography. T. Norris, G. J. Jordon, S.G.E. Scientific Pty. Ltd.

Inductively Coupled Plasma Spectroscopy

Thursday Morning, Room 235A

A. W. Varnes, *Presiding*

8:30 Use of Inductively Coupled Plasma (ICP) Emission Spectrometry for Routine Multielement Analyses on Variety of Sample Matrices. B. Winch, G. Wabst, J. Giegerich, Raltech Scientific Services

8:50 Excitation Temperatures and Ion/Atom Line Intensities in the ICP. A. Weiss, G. M. Hieftje, Indiana U

9:10 Modular Analytical Data Management and Acquisition System for Use with ICAP Direct Reader. R. B. Myers, A. F. Ward, Jarrell-Ash

9:30 Sample Introduction into ICAP—Comparison of Available Methods. A. F. Ward, C. C. Wohlers, Jarrell-Ash

9:50 Evaluation Study of a Babington-Type Nebulizer with Induction Coupled Plasma Spectrometer. H. E. Taylor, J. R. Garbarino, U.S. Geological Survey

10:20 Simple Nebulizer for Inductively Coupled Plasma Source. J. F. Wolcott, Sandia Labs, C. S. Butler

10:40 Nebulizers for ICPOES and AAS: Aerosol Characterization. J. W. Novak, R. F. Browner, Georgia Institute of Technology

11:00 Laser Vaporization Sampling System for Inductively Coupled Plasma Emission Spectroscopy. J. Carr, E. D. Salin, G. Horlick, U of Alberta

11:20 Direct Sample Insertion Torch for Inductively Coupled Plasma Emission Spectroscopy. E. D. Salin, G. Horlick, U of Alberta

11:40 Effect of Concomitant Species upon Analyte Signal Observed from Modern ICAP Direct Reading Spectrometer. A. F. Ward, R. B. Myers, Jarrell-Ash

Symposium: New Techniques on the Horizon

Thursday Morning, Room 235B

A. G. Sharkey, Jr., *Presiding*

8:30 Recent Advances in Field Desorption Mass Spectrometry. H. R. Schulten, U of Bonn

9:15 Advances in Capillary GC. M. Novotny, Indiana U

10:20 New Development in Solid State NMR. A. Pines, U of California

11:05 Electron Impact Excitation of Ions from Organics (EIEIO). B. S. Freiser, Purdue, U

11:30 Development of Instrument for Continuous, Automated, and Low-Cost Monitoring of Organic Loading in Water. W. J. Cooper, U.S. Army

Symposium: Biomedical Aspects

Thursday Morning, Little Theater

J. A. Feldman and R. M. Windisch, *Presiding*

8:30 Analysis of Nostrums and Quack Remedies. D. Banes, U.S. Pharmacopeia

9:15 Impact of HPLC on Biomedical Research and Clinical Chemistry. P. R. Brown, U of Rhode Island

10:20 HDL Cholesterol and Risk of Coronary Heart Disease. W. P. Castelli, Framingham Heart Study and Harvard Medical School

11:00 Developments in Forensic Analysis of Drugs. R. L. Williams, Metropolitan Police (Scotland Yard) Forensic Science Lab

Gas Chromatography—Ancillary Techniques

Thursday Morning, Ball Room

D. P. Manka, *Presiding*

8:30 Capillary Column GC/MS—Instrumentation and Applications. W. A. Wolstenholme, U. Rapp, G. Dielmann, H. Kaufmann, Varian

8:50 Data Reduction for GC/MS Analyses of Water and Water Extracts for EPA's Priority Pollutants. J. M. Rombough, NUS Corp.

9:10 Detection of Neurotransmitter Metabolites in Human CSF by Negative Ion GC/MS. Q. V. Thomas, J. W. Russell, Finnigan Corp.

Model 3010
Trace Metals Analyzer.
Measures up to 200 micro or macro samples daily at 90 seconds or less per sample using a rapid exchange reagent. Cost per sample: about one-third that of conventional methods. Excellent accuracy and precision at the nanogram level. **Circle No.** 65

Model 4000
ZnP Hematofluorometer.
Determines the amount of zinc protoporphrin in whole blood without sample preparation. Principle approved by the Center for Disease Control of HEW for lead intoxication and or iron deficiency anemia. Technique OSHA approved and required. **Circle No.** 66

Model 3040
Programmable
Potential Coulometer.
For electro-chemical analyses, measuring chemical levels or changes in solutions, selection and detection of complex compounds, process control, and similar applications. Pushbutton programmable. Available with flow cells, trap cells, and other sensors. **Circle No.** 67

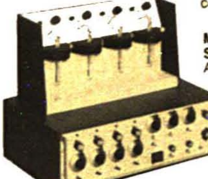

Model 2014 Multiple Anodic Stripping Analyzer.
A laboratory instrument that will perform quantitative or qualitative analyses on trace metals in numerous matrices without destroying the sample. Available with extender units to handle up to 12 discrete samples simultaneously, and with a variety of equipment options for routine analysis or basic research. **Circle No.** 68

ANALYTICAL INSTRUMENTS

ANALYTICAL INSTRUMENTS

Look at this trace metals complex

ANALYTICAL INSTRUMENTS

Model 2011 Single Cell Anodic Stripping Voltammeter.
A portable, single cell version of the Model 2014 that will operate on line power or from a 12-volt storage battery and inverter.
Circle No. 69

...and for halides, chemicals, and other substances and solutions, too.

ESA is a multi-faceted company with capabilities in such diverse areas as industrial hygiene, clinical laboratories and health care centers, industrial processes, environmental technology, and quality control. We operate one of the largest private blood lead screening laboratories in the world, provide the food industry with instruments for measuring and monitoring trace metals in food products and containers, test air filters, and analyze water and soil for lead, tin, cadmium, copper, arsenic, mercury, bismuth, thallium and other heavy, precious, or toxic metals in a variety of matrices. Look us over—then tell us your requirements.

RESEARCH AND DEVELOPMENT

The R&D Laboratory consists of both in-house and consulting groups for development of hardware, and for analytical projects ranging from emission surveys from power plants and smelters to the effectiveness of existing techniques for controlling the environment.
Telephone or letterhead request only, please.

SERVICE LABORATORIES

SYSTEM ACCESSORIES

Screening Laboratories for screening of children and industrial personnel for blood and urine lead, erythrocyte protoporphrin, and hematology testing.... determining the presence and amount of lead, cadmium, copper, mercury, arsenic, tin, bismuth, and thallium in various matrices....or for intermediate or massive repetitive analyses of other trace elements in solids and aqueous solutions. **Circle No.** 70

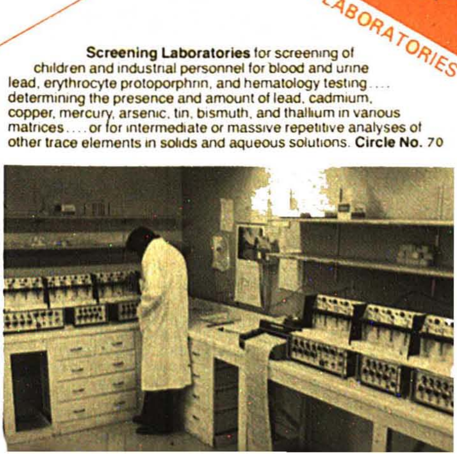

Sampling Kits for obtaining, handling, shipping, and storing blood or other biologicals. **Circle No.** 71

Fast Exchange Reagents that obsolete preparative chemistry for lead in food, water, blood, urine....and other trace substances in different matrices. **Circle No.** 72

Flow Cells and Sensors for continuous or batch measurement and monitoring of chemical and industrial processes, capturing and eliminating undesirable ingredients, and other uses. **Circle No.** 73

See us at the
Pittsburgh Conference
Booth #702-704.

esa

ENVIRONMENTAL SCIENCES ASSOCIATES, INC
45 Wiggins Avenue, Bedford, MA 01730
Telex: 923344 Tel: (617) 275-0100

9:30 Gas Chromatographic Fractionation of Isotope Species in Carbon Monoxide. J. C. Fetzer, P. A. Bloxham, L. B. Rogers, U of Georgia

9:50 Evaluation of Analytical Parameters for High-Sensitivity Selected Ion Monitoring (SIM) in GC/MS. E. M. Chait, Du Pont

10:20 Application of Capillary Column GC/MS to Water Pollutant Analysis. E. M. Chait, T. A. Blazer, Du Pont

10:40 Gunpowder Analysis by Gas Chromatography/Chemical Ionization Mass Spectrometry. J. J. Chera, D. R. Hardy, FBI

11:00 Use of Glass Capillary Columns in Pyrolysis Gas Chromatography. C. A. Jacques, S. L. Morgan, U of South Carolina

11:20 New Developments and Extended Performance of CIRA 101 GC/IR Analyzer. A. Varano, R. H. Shaps, Sadtler Research Labs

11:40 Countercurrent Distribution as Purification Method Prior to Glass Capillary Chromatography in Organic Residue Analysis. L. Vollner, Institut fur Okologische Chemie

Computer Applications I: Microprocessors

Thursday Morning, Music Hall

H. Schultz, *Presiding*

8:30 Microprocessor-Controlled Readout System for Photomultiplier Tubes. G. Horlick, M. L. Blades, U of Alberta

8:50 The Microcomputer as an Intelligent Interface Between Laboratory Instruments and Data Systems: Automating Data Collection from a Grain Analyzer. R. D. Plattner, R. O. Butterfield, T. D. Simpson, USDA

9:10 Microcomputer System for Automation of Industrial R&D Laboratory Instrumentation. M. E. Koehler, T. F. Niemann, T. Provder, Glidden

9:30 Minicomputer-Microcomputer System for Laboratory Automation. T. F. Niemann, M. E. Koehler, T. Provder, Glidden

9:50 Microcomputer Data Acquisition and Analysis System for X-Ray Diffraction and Fluorescence. T. L. Starr, General Electric

10:20 Dual 6502 Microprocessor System for Interactive Data Acquisition. M. E. Hughes, T. S. Wasco, J. L. Fasching, U of Rhode Island

10:40 Standard Interface Card Lines Implementing Standardized Microcomputer Cards Can Save Your Facility. M. D. Maples, M&E Associates

11:00 Comparison of 8080, 8085, and 6502 Single-Board Microprocessor System for Laboratory Data Acquisition. G. Horlick, E. D. Salin, M. L. Blades, U of Alberta

11:20 LAB-PET. G. Horlick, E. D. Salin, U of Alberta

11:40 Integrated Microcomputer System for Rapid Scanning Spectrophotometer. A. O. Wist, F. W. Hawkridge, Virginia Commonwealth U

Luminescence Applications

Thursday Afternoon, Room 240

F. E. Lytle, *Presiding*

1:30 Evaluation of Emit Homogeneous Enzyme Immunoassays on Pye Unicam SP6 Spectrophotometer. G. W. Moody, Pye Unicam

1:50 Fluorescence of Methoxy-Substituted Benzoic Acids. G. H. Schenk, I. Khasawneh, Wayne State U

2:10 Trace Cobalt Determination via Pyrogallol and Lophine Chemiluminescence. J. D. Ingle, Jr., R. Miller, D. Marino, Oregon State U

2:30 Fluorometric Reaction Rate Method for Determination of Thiamine. M. A. Ryan, J. D. Ingle, Jr., Oregon State U

2:50 Fluorometric and Photometric Determination of Titanium. J. J. Topping, Towson State U

3:20 Characterization of Weak Emission from Aromatic Carbonyl Compounds. T. G. Matthews, F. E. Lytle, Purdue U

3:40 Analytical Applications of Micellar Systems in Luminescence Spectrometry. J. Habarta, L. J. Cline Love, Seton Hall U

4:00 Analytical Aspects of Two-Photon Excitation Spectra. M. J. Wirth, U of Wisconsin

General Analysis

Thursday Afternoon, Room 205

J. P. Auses, *Presiding*

1:30 Quality Control/Quality Assurance in the Analytical Laboratory. W. F. Gutknecht, Research Triangle Institute

1:50 Potential Error in Single-Point Ratio Calculations Based on Linear Calibration Curves with a Significant Intercept. M. J. Cardone, Norwich-Eaton Pharmaceuticals, P. J. Palermo, L. B. Sybrandt

2:10 Particle Size Independent Analyses of Wear Metals in Synthetic Lubricating Oils. J. Brown, U of Dayton Research Institute, W. Rhine, C. Saba, K. J. Eisentraut

2:30 SKF High-Precision Standard Samples for Determination of Oxygen, Nitrogen, Carbon, and Sulfur in Steel. G. Johansson, Analytica AB

2:50 On the Use of Minimal Spanning Trees in Oil Classification. J. C. MacDonald, E. Breuel, Fairfield U

3:20 Particle Size Analysis of Engine Oils. J. A. Bierlein, K. J. Eisentraut, Air Force Materials Lab

3:40 Multidimensional Pourbaix Diagrams: New Thermodynamic Guide to Analytical Resource Development. D. Stutts, J. Jordan, Pennsylvania State U

4:00 Examination of Spectrometric Analyzability of Suspended Metal Particulates. K. Scheller, J. A. Bierlein, Air Force Materials Lab

4:20 Amperometric Determination of Polyols Utilizing Flow Injection Methodology. K. G. Schick, C. O. Huber, U of Wisconsin

4:40 New Reagent for Methylation Barbiturates. S. Ramachandran, D. K. McCreary, W. C. Kossa, R. R. Kurtz, R. S. Henly, Applied Science Labs

Biochemical Analysis

Thursday Afternoon, Room 239

A. Liotta, *Presiding*

1:30 Quantitation of Substrate Using Immobilized Coenzyme-Dependent Oxidoreductase Enzymes. A. K. Chen, U of Pittsburgh, N. J. Szuminsky, C. C. Liu, J. G. Schiller

1:50 New Support for Extraction of Lipophilic Substances—Extrelut. M. Gurkin, R. Fischer, MC/B

2:10 Comparison of Serum Nucleoside and Base Profiles of Humans and Dogs Using High-Pressure Liquid Chromatography. S. P. Assenza, P. R. Brown U of Rhode Island

2:30 Determination of Amino Acids by Glass Capillary Column Chromatography. T. Norris, S.G.E. Scientific Pty. Ltd., M. K. Dewar

2:50 Thin-Layer Chromatography of Stinging Insect Venoms. W. B. Elliott, R. Steger, State U of New York at Buffalo

3:20 Reversed-Phase High-Performance Liquid Chromatography of Adenosine 3′,5′-Monophosphate (Cyclic Amp) and Its Metabolites. M.I.J. Chitas, U of Lisbon, M. L. Cohn, J. A. Feldman, E. L. Light

3:40 Separation of Amino Acid Enantiomers as Dipeptide Diastereomers Using Reverse-Phase High-Performance Liquid Chromatography. E. P. Kroeff, W. R. Cahill, Jr., D. J. Pietrzyk, U of Iowa

4:00 Rapid Reversed-Phase High-Performance Liquid Chromatographic Analysis of 3′,5′-Cyclic Adenosine Monophosphate in Rat Brain Extracts. M. Zakaria, U of Rhode Island, A. M. Krstulovic, P. R. Brown

Analabs
Chromatography
Supplies

Wilks
Infrared
Accessories

Analabs
Analabs
Analabs
Analabs

Wilks
Wilks
Wilks
Wilks

TOGETHER
at the
Foxboro Analytical Exhibit
BOOTHS 822-929
1979 Pittsburgh Conference
Cleveland, Ohio, March 5-9

New FT Liquid Cells!
New Prep L.C. Columns!
New Capillary Columns!
New Long Path Gas Cells!

Analabs, Inc.
A Unit of Foxboro Analytical
80 Republic Dr., North Haven, CT 06473
Tel. (203) 288-8463

FOXBORO

Analabs and Wilks are Trademarks of The Foxboro Company

CIRCLE 81 ON READER SERVICE CARD

4:20 High-Pressure Liquid Chromatography: Its Use for Monitoring Enzymatic Assays and Purification of Enzymes. J. L. Hodge, U of Connecticut Health Center, E. F. Rossomando, W. M. Skea

4:40 Separation of Precolumn *o*-Phthalaldehyde Derivatized Amino Acids by HPLC. J. C. Hodgin, Micromeritics Instrument Corp.

Emission Spectroscopy—General I

Thursday Afternoon, Room 3A
C. L. Page, *Presiding*

1:30 Computer-Assisted Calibration System for Direct Reading Spectrometers. R. L. Crawford, Jarrell-Ash

1:50 Study of Noises in Atomic Spectrometer Systems. B. D. Pollard, A. H. Ullman, J. D. Winefordner, U of Florida

2:10 Characteristics of Improved Direct Current Plasma Jet. A. M. Allen, G. N. Coleman, W. P. Braun, U of Georgia

2:30 Experimental Results from Automated System for Characterization of DC Plasma Emission. J. V. Petersen, Colorado State U, K. R. O'Keefe

2:50 Confined Plasma in Graphite Tube for Emission Spectroscopy. S. Lawson, R. Woodriff, Montana State U

3:20 Effect of Fill Gas Type upon Fundamental Nature of Hollow Cathode Discharge. D. M. Mehs, Fort Lewis College, T. M. Niemczyk

3:40 Diagnostic Measurement of High-Power Microwave-Induced Helium Plasma at Atmospheric Pressure. A. T. Zander, Cleveland State U, G. M. Hieftje

4:00 Application of Atmospheric Pressure Helium Microwave Plasma GC Detector to Halogen Specific Detection of Aqueous Organics. P. C. Uden, M. F. Delaney, B. D. Quimby, R. M. Barnes, U of Massachusetts

4:20 Miniature Spark Emission Source for Analysis of Solution and Gaseous Samples. G. T. Seng, NASA, S. M. Koeplin, S. R. Crouch

4:40 New Current Generator for Quarter-Wave Stable Spark Source. T. Araki, J. P. Walters, U of Wisconsin

The Column in High-Performance Liquid Chromatography

Thursday Afternoon, Club Room B
J. Biber, *Presiding*

1:30 The HPLC Super-Column: Fact or Myth? P. Deland, W. America, Laboratory Data Control

1:50 New HPLC Column Technology—Revolution in Resolution. G. J. Fallick, C. W. Rausch, Waters Associates

2:10 New HPLC Column Technology—Comparison with Traditional Forms. G. J. Fallick, C. W. Rausch, Waters Associates

2:30 High-Performance Liquid Chromatography Column Evaluation. J. W. Higgins, Bio-Rad Labs

2:50 HPLC Column Evaluation: Part II. Application and Results. R. G. Brownlee, Brownlee Labs

3:20 How to Get the Best Results from Your HPLC Column. N. A. Parris, Du Pont

3:40 New High-Performance Maximum Coverage Reversed-Phase Columns. N.H.C. Cooke, M. Doyle, Altex Scientific

4:00 Considerations in Column Selection for Reverse-Phase Liquid Chromatography: Influence of Bonded-Phase Chain Length. J. R. Gant, Technicon Industrial Systems

4:20 Guide for Selection of Optimum Bonded Phase Column Packings in Reversed-Phase HPLC. N. A. Parris, Du Pont

4:40 How to Slurry Pack and Test Liquid Chromatography Columns. R. A. Henry, Chemtest

Symposium: Trace Analysis in Characterization of Materials

Thursday Afternoon, Room 235A
H. Freiser, *Presiding*

1:30 Introductory Remarks. H. Freiser, U of Arizona

1:35 Trace Metal Analysis by ESR Using Stable Free Radical Chelating Agent. Y. A. Zolotov, Vernadskii Institute of Geochemistry and Analytical Chemistry

2:10 Trace Analysis in Characterization of Materials. G. H. Morrison, Cornell U

3:05 New Mass Spectrometric Methods for Trace Analysis. R. G. Cooks, Purdue U

3:40 Trace Metal Analysis by Surface Analytical Techniques. L. V. Phillips, U of Pittsburgh, D. M. Hercules, G. R. Conner

4:15 Analysis of Trace Materials in Rapid Reactions. W. G. Fateley, J. Sung, Kansas State U

Automated Electrochemical and Spectrochemical Methods

Thursday Afternoon, Room 235B
W. Straub, *Presiding*

1:30 On-Stream Analysis of $SiCl_4$ During Production of Solar Grade Silicon. G. C. Burrow, R. E. Witkowski, D. H. Lemmon, Westinghouse

1:50 Automated Scanning Polarograph for Solution Labile Compounds. R. E. Cooley, C. E. Stevenson, Eli Lilli and Co.

2:10 Hydrodynamic Voltammetry—Theory and Application to Chemical Analysis. S. das Gupta, B. Fleet, HSA Reactors

2:30 Evaluation of Continuous Monitoring Procedures for Cyanide. B. Fleet, S. das Gupta, HSA Reactors

2:50 Use of Microprocessors in ISE Techniques. C. Westcott, V. Kohler, Beckman Instruments

3:20 CFA-200, New Automated Continuous Flow Instrument. R. Ghadimi, Peerless Electronics Research Corp., C. Schmid, J. Salpeter

3:40 New On-Line Colorimetric Analyzer for Water and Wastewater. R. Clemens, J. Chisholm, C. Hach, P. Larson, D. Schoonover, Hach Chemical Co.

4:00 Automated Titrations: Use of Automated Flow Injection Analysis for Titration of Discrete Samples. K. K. Stewart, A. G. Rosenfeld, USDA

4:20 Versatile Syringe Drive Module for Rapid Mixing Methods. F. J. Holler, U of Kentucky

4:40 Determination of Trace Amount of Chlorine in Petroleum Products by Combustion and Microcoulometric Method. A. Matsuzaki, K. Koyano, Nippon Oil Co.

Coblentz Society Award Presentations and Symposium

Thursday Afternoon, Little Theater
I. W. Levin, *Presiding*

1:30—Presentation of the 1979
Coblentz Award
by
Ira W. Levin
President of the Coblentz Society
to
Lionel A. Carreira
University of Georgia
Award Address
Development and Application of Computer-Controlled CARS Spectrometer

2:50—Presentation of the 1979
Williams-Wright
Industrial Spectroscopist Award
by
Ira W. Levin
President of the Coblentz Society
to
Norman B. Colthup
American Cyanamid Co.
Award Address
Molecular Orbitals and Group Frequencies

We want to clear the air about filters for high-volume air sampling: there's no substitute for S&S No. 1HV.

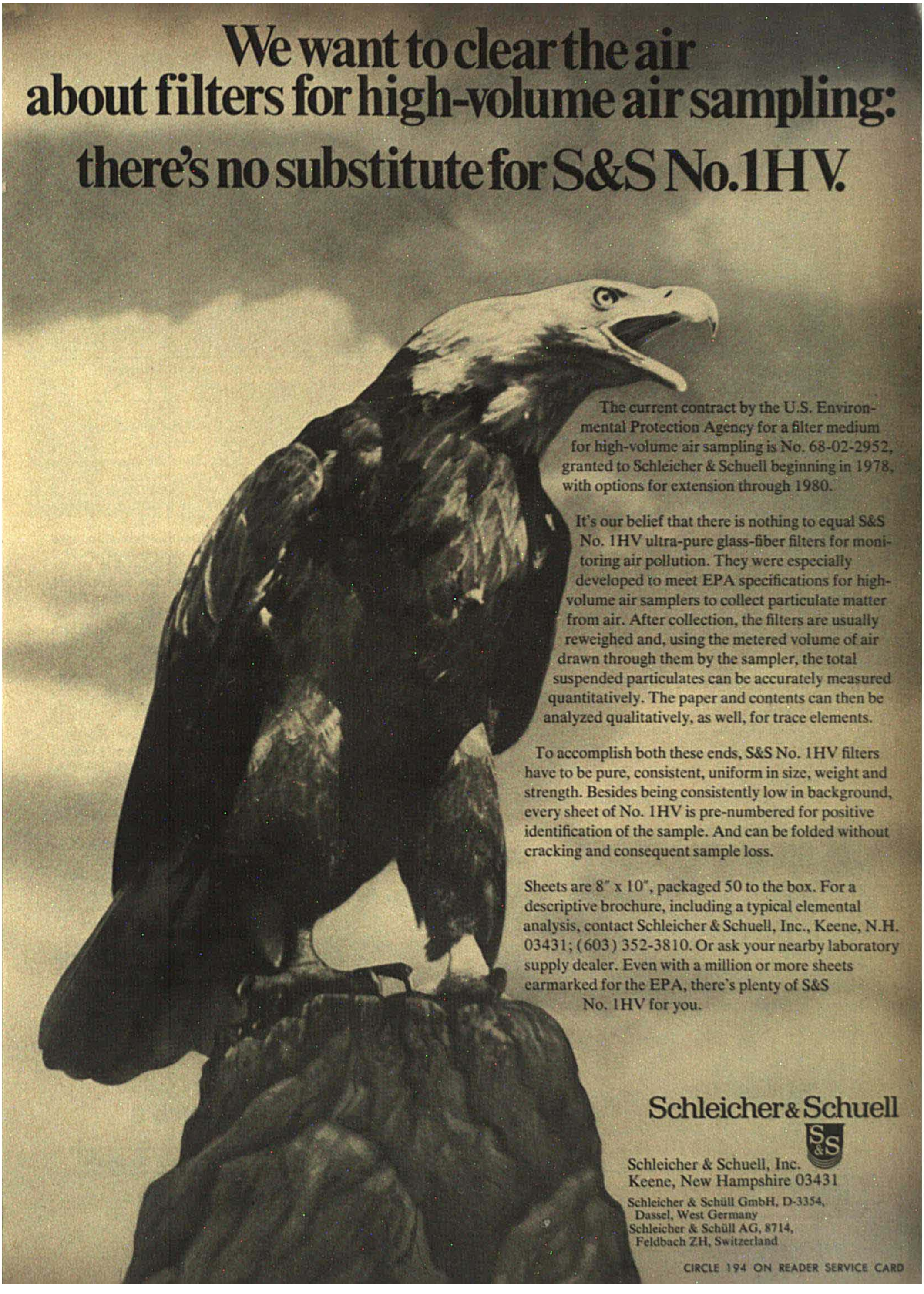

The current contract by the U.S. Environmental Protection Agency for a filter medium for high-volume air sampling is No. 68-02-2952, granted to Schleicher & Schuell beginning in 1978, with options for extension through 1980.

It's our belief that there is nothing to equal S&S No. 1HV ultra-pure glass-fiber filters for monitoring air pollution. They were especially developed to meet EPA specifications for high-volume air samplers to collect particulate matter from air. After collection, the filters are usually reweighed and, using the metered volume of air drawn through them by the sampler, the total suspended particulates can be accurately measured quantitatively. The paper and contents can then be analyzed qualitatively, as well, for trace elements.

To accomplish both these ends, S&S No. 1HV filters have to be pure, consistent, uniform in size, weight and strength. Besides being consistently low in background, every sheet of No. 1HV is pre-numbered for positive identification of the sample. And can be folded without cracking and consequent sample loss.

Sheets are 8" x 10", packaged 50 to the box. For a descriptive brochure, including a typical elemental analysis, contact Schleicher & Schuell, Inc., Keene, N.H. 03431; (603) 352-3810. Or ask your nearby laboratory supply dealer. Even with a million or more sheets earmarked for the EPA, there's plenty of S&S No. 1HV for you.

Schleicher & Schuell

S&S

Schleicher & Schuell, Inc.
Keene, New Hampshire 03431

Schleicher & Schüll GmbH, D-3354,
Dassel, West Germany
Schleicher & Schüll AG, 8714,
Feldbach ZH, Switzerland

CIRCLE 194 ON READER SERVICE CARD

Gas Chromatography—Applications

Thursday Afternoon, Ball Room
W. L. Zielinski, Jr., *Presiding*

1:30 **Fatty Acid Analysis by Short Glass Capillary Column Gas Chromatography.** E. Lanza, J. Zyren, H. Slover, USDA

1:50 **Gas-Liquid Chromatographic Separation of Polycyclic Aromatic Hydrocarbons on Liquid Crystal Capillary Columns.** W. L. Zielinski, Jr., NCI Frederick Cancer Research Center, R. A. Scanlan, M. M. Miller

2:10 **Comparison of Nickel and Stainless Steel Plot Columns for GC of Metal Complexes.** D. E. Henderson, Trinity College

2:30 **Chemical Compound Glass Separation in Shale Oil Analysis.** P. C. Uden, F. P. DiSanzo, S. Siggia, U of Massachusetts

2:50 **Applications of High-Resolution Glass Capillary Gas Chromatography in Analysis of Synthetic Fuels from Coal.** C. M. White, U.S. Dept. of Energy, D. L. Vassilaros, M. L. Lee

3:20 **Utility of Capillary GC in Coatings Analyses.** J. D. Buchner, PPG Industries

3:40 **Quantitative Analysis of PCB Using Glass Capillary Columns.** J. Snow, B. Bush, New York State Dept. of Health

4:00 **Performances and Applications of Modified On-Column Injection System for Glass Capillary Gas Chromatography.** G. Sisti, Carlo Erba Strumentazione, M. Galli, S. Trestianu

4:20 **Applications of Headspace Gas Chromatography.** J. R. Widomski, E. W. March, Perkin-Elmer

Computer Applications II: Minicomputers

Thursday Afternoon, Music Hall
J. Rombough, *Presiding*

1:30 **Mass Spec Automation with LSI-11 Microprocessor: Part I—Hardware.** V. Barton, R. Downey, C. Pomernacki, R. Bedford, R. Crawford, Lawrence Livermore Lab

1:50 **Mass Spec Automation with LSI-11 Microprocessor: Part II—Software.** R. G. Bedford, R. W. Crawford, H. R. Brand, V. Barton, R. Downey, Lawrence Livermore Lab

2:10 **Interactive Microprocessor System for Mass Spectral Data Acquisition and Instrument Control.** R. M. Lum, Bell Labs

2:30 **Executing ARTHUR on DG ECLIPSE Minicomputer.** D. A. Heitke, J. L. Fasching, U of Rhode Island

2:50 **Automated System for Determination of Faradaic Efficiency of Metal/Air Fuel Cells.** T. L. Clark, Lawrence Livermore Lab

3:20 **Intercomputer Communications Using Microprocessors.** J. M. Teuschler, EPA

3:40 **Laboratory Computer System Designed for the Chemist.** R. Washburne, AMP, Inc., L. R. Hoover

4:00 **Laboratory Cost Control Through Computers.** T. Scott, J. Vasily, Villanova U

4:20 **System for Acquisition and Dissemination of Laboratory Data.** R. E. Enrione, H. C. Jackson, U.S. Army

4:40 **Innovative Development of Two-Channel Computing Integrator.** M. Tarter, J. Power, Laboratory Data Control

Friday, March 9

Thermal Methods of Analysis

Friday Morning, Room 240
G. Palmgren, *Presiding*

FREE 24 PAGE CONSTANT TEMPERATURE BATH BROCHURE Attach this ad to your letterhead or business card

If you've got a constant temperature problem, we've got four constant temperature solutions

WATER BATHS • OIL BATHS • DRY HEAT BATHS • FLUIDIZED BATHS

☐ IMMERSION CIRCULATORS—Convert any container into a precise constant temperature bath. Control to ±0.005°C, all solid state with temperature preset and built-in safety features.

☐ SOLID STATE CIRCULATOR—Circulates liquid to maintain cuvettes and external apparatus at set or preset temperatures, stable to ±0.02°C. Has integral safety features.

☐ CIRCULATING BATHS—Seamless stainless steel for water or oil. Solid state controls, stability to ±0.05°C. Various racks, covers, trays and cooling coils available.

☐ POLYPROPYLENE BATH—Low cost, 3½ gallon capacity for educational and clinical applications. Convective circulation maintains temperature within ±0.5°C. Includes tray and thermometer.

☐ DRY HEAT BATHS—Maintain test tube samples to within ±0.1°C accuracy. Silent and solid state. UL listed for safety.

☐ FLUIDIZED BATHS—Dry, inert, clean and non-toxic fluidized aluminum oxide provides safe, isothermal environment from ambient to 1100°C. Superior to heating mantles, oil baths, or air ovens.

✓ Check the appropriate box or write or call for more information, technical details or applications assistance.

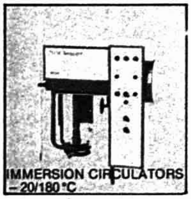
IMMERSION CIRCULATORS −20/180°C

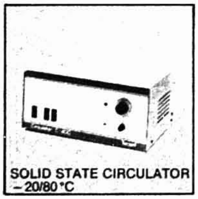
SOLID STATE CIRCULATOR −20/80°C

CIRCULATING BATHS −20/200°C

POLYPROPYLENE BATH 30/100°C

DRY HEAT BATH 30/450°C

FLUIDIZED BATHS 50/1100°C

Techne

Techne Incorporated • 3700 Brunswick Pike • Princeton, NJ 08540
Telephone (609) 452-9275 • Telex 84 3319

CIRCLE 202 ON READER SERVICE CARD

A new name from an old company:

Instrumentation Specialties Co. presents ChemResearch instruments

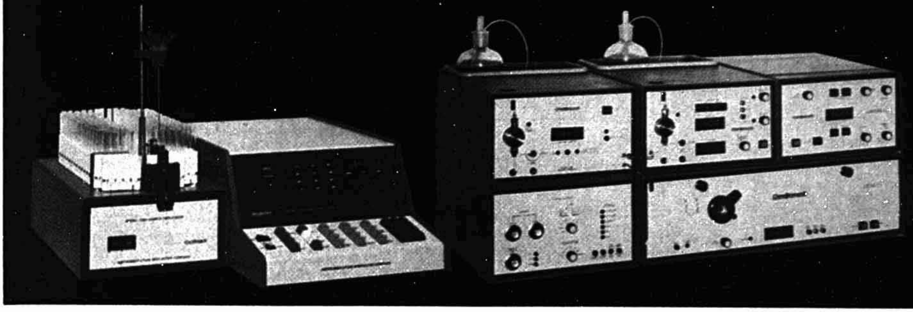

Automate your wet lab.

You can completely automate even the most complex lab procedures with a ChemResearch Sample Processor—it will do virtually everything you can do manually, and often with better precision and reproducibility. If you are a researcher, you can greatly expand your output; if you are in process monitoring or quality control, your procedures can be automated for non-technical personnel.

In addition to ordinary chemical analyses, the Model 1560 is suitable for such diverse purposes as tissue culture growth; automatic control of complex process reactors such as peptide synthesizers; biochemical processing; and the fundamental characterization of reactions by automatically varying experimental parameters. Up to 210 samples can each be processed through thousands of steps involving reagent addition, agitation, incubation, and various measuring procedures. You enter the program by simple keystrokes without having to know a computer language.

Let your HPLC grow.

Start your modular ChemResearch Series 2000 with a choice of two high-sensitivity, UV/visible detectors and an isocratic solvent delivery system. Upgrade it to a gradient system at any time, or add an oven for ion exchange columns.

The ChemResearch single-piston pump is electronically compensated for valve action, system compressibility, and other variables to produce a flow as smooth as multi-piston designs but without their cost and maintenance problems. LED readouts monitor 15 operating parameters. All valve and column plumbing projects from the oven when the door is opened; injections are automatically marked; and a valve quickly relieves airlocks during solvent changes.

The Series 2000 can be interfaced with the Model 1560 Sample Processor to provide your research or quality control lab with a totally automated analytical system.

See us at the Pittsburgh Conference, Booths 926 and 928

ChemResearch

For more information on ChemResearch instruments and applications,

Phone toll free [800] 228-4250

(continental U.S.A. except Nebraska). Or write
Instrumentation Specialties Company, P.O. Box 5347,
Lincoln, Nebraska 68505.

CIRCLE 106 ON READER SERVICE CARD

This is our
Vortex Evaporator

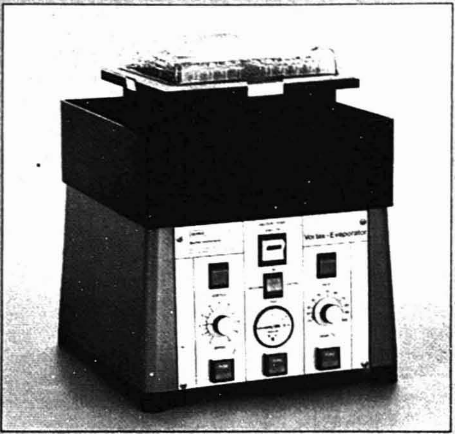

This is the competition

(NONE)

Now you can get evaporation, incubation and vortexing in *one* reliable instrument—and only Buchler makes it. The new Vortex Evaporator is a complete sample preparation station for RIA/CPB, drug abuse screening, electrophoresis, TLC, gas chromatography and quality control. Features include: variable vortexing speed; controlled heating constant within 1°C; optional cooling plate; special vacuum control system guards against bumping. Suitable vacuum source is available as an optional extra. Write today for complete information.

Buchler Instruments, Inc.
1327 16th Street, Fort Lee, N.J. 07024
(201) 224-3333 (212) 563-7844

CIRCLE 25 ON READER SERVICE CARD

8:30 **Design of Isothermal Calorimeter for Measurement of Heats of Water Removal from Tobacco.** C. E. Thomas, W. S. Ryan, Jr., T. S. Laszlo, Philip Morris

8:50 **Dynamic Mechanical Analysis of Engineering Materials.** K. L. Lawson, Bendix Corp.

9:10 **Recent Dynamic Mechanical Analysis (DMA) Applications.** R. L. Hassel, P. S. Gill, Du Pont

9:30 **New Instrumentation: High-Temperature DTA Module.** W. P. Brennan, R. B. Cassel, R. L. Fyans, Perkin-Elmer

9:50 **Thermal Dehydration of Magnesium Sulfite Hexahydrate ($MgSO_3 \cdot 6H_2O$) and Magnesium Sulfite Trihydrate ($MgSO_3 \cdot 3H_2O$).** R. Malek, Reichhold Chemicals, L. Dauerman

10:20 **Kinetic Analysis by New Photopolymerization Calorimeter.** M. Ikeda, Fuji Photo Film Co.

10:40 **ASTM Method of Testing for Determining Arrhenius Kinetic Constants for Screening of Potentially Hazardous Materials.** R. B. Cassel, W. P. Brennan, R. L. Fyans, A. P. Gray, Perkin-Elmer

11:00 **Measurement of Critical Thermal Stability Parameters for Potentially Hazardous Materials.** R. L. Blaine, P. S. Gill, Du Pont

11:20 **Microprocessor-Based Programmer for Thermal Analysis.** R. L. Blaine, P. S. Gill, Du Pont

X-Ray Fluorescence, X-Ray Diffraction

Friday Morning, Room 205
C. J. McCafferty, Jr., *Presiding*

8:30 **X-Ray Spectroscopy Analysis of PVC Compounds.** W. O. Butler, Diamond Shamrock Corp.

8:50 **X-Ray Fluorescence Technique for Quality Control of TiO_2 Content in Paint.** G. P. Cunningham, C. E. Cowan, R. G. Weinbrenner, PPG Industries

9:10 **Determination of Effective Sample Thickness from Scatter Peaks in Energy-Dispersive X-Ray Fluorescence.** R. Van Grieken, F. Adams, P. Van Espen, L. Van't dack, U of Antwerp

9:30 **Analysis of Coal and Coal Ash by Energy-Dispersive X-Ray Fluorescence.** B. D. Wheeler, N. Jacobus, EG&G ORTEC

9:50 **Interelement Corrections for Nickel Base Alloys Using Fundamental Parameters.** T. Arai, Rigaku Industrial Corp.

10:20 **Predicting Quantitative Matrix Effects in X-Ray Fluorescence Analysis.** H. E. Clark, ES Industries

Hitachi Scientific Instruments

Centrifugal Preparative Liquid Chromatograph

A liquid chromatograph uses centrifugal force rather than gravity, capillary action or high solvent pressure to effect separation. The CLC-5 system may be used with almost any type column packing material normally used for TLC or HPLC to provide high performance separation, detection and fraction collection on relatively large sample volumes in a tenth of the time required in conventional preparative systems. This new technique offers many advantages which will make it an important tool in the field of liquid chromatography, not only as a preparative system but as a qualitative and quantitative system as well.

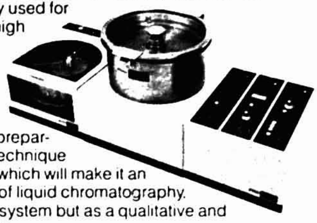

CIRCLE 13

Polarized Zeeman Effect Atomic Absorption System

The new automated system provides not only the great sensitivity, precision, accuracy and background correction ability which only the Zeeman technique can give, but now a completely automatic sampling and data processing system. The data system provides automatic sampling, automatic calibration curve development using a choice of calibration curve algorithms, goodness-of-fit analysis, deviation from linearity and, of course, accurate and precise answers in direct concentration units.

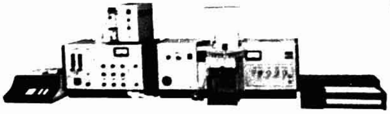

CIRCLE 15

Computerized UV-Visible Recording Spectrophotometer

A Great Advance in Spectrophotometric Instrumentation

A completely computerized low-cost double-beam spectrophotometer system achieves a level of automation, data acquisition, data processing, data presentation, and operating functions never before available at any price.

The Model 80 provides the analyst with the utmost flexibility in wavelength scanning while greatly expanding the capability to collect, process and report quantitative data.

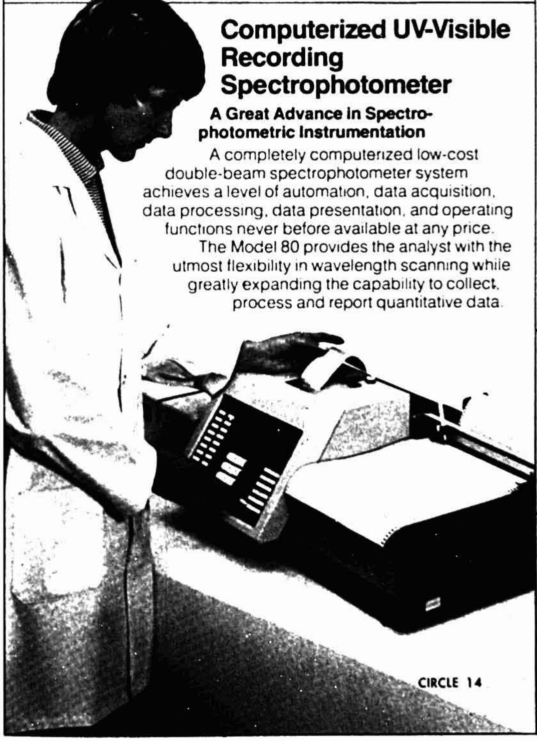

CIRCLE 14

UV Detector Dual-Beam Dual-Channel

A unique detector permits simultaneous monitoring in the UV Region, at two different and selectable wavelengths. Each wavelength is in the double beam mode and is presented as individual recorder traces on a two-pen recorder. A true monochromatic instrument which provides eight push button wavelength selections across the 210-280 nm UV Region with scale expansions of up to 0.005A with less than ±1% noise. The ability to simultaneously monitor at two different wavelengths greatly increases both quantitative and qualitative accuracy and precision by providing adsorption ratios of the two wavelengths.

CIRCLE 101

Low Cost Recorders

A single and dual-pen recorder series is low in cost but retains quality where quality counts. This new series has specifications and features which are normally found on recorders costing many times more.

CIRCLE 102

100 Series Spectrophotometers Double/Single Beam

A complete line of UV/Vis spectrophotometers features advanced concave grating optics.

A complete line of accessories including temperature controlled sampler, high pressure HPLC cell and recorder.

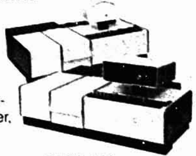

CIRCLE 103

See these new instruments demonstrated at Booths 1602-1608, Pittsburgh Conference
March 5-9, 1979 • Cleveland, Ohio

Sold and Serviced
in the U.S. for
Over 20 Years

NSA HITACHI
SCIENTIFIC INSTRUMENTS

15 Sales and Service
Locations in the
U.S. and Canada

450 E. Middlefield Road • Mountain View, CA 94043 • (415) 969-1100

10:40 Standardless Determination of Some Heavy Metals in Airborne Particulate Matters by X-Ray Fluorescence Spectrometry. K. Ohno, National Research Institute for Metals

11:00 Pigment Analysis of Paint Films by X-Ray Diffraction. P. Kamarchik, PPG Industries

11:20 Large-Scale Automation of LLL Analytical X-Ray Facilities. F. Y. Shimamoto, Lawrence Livermore Lab

Toxicology and Drug Analysis

Friday Morning, Room 239

D. Fretthold, *Presiding*

8:30 Determination of Manganese in Biological Samples. P. A. Pleban, Cleveland State U, K. H. Pearson, D. A. Leto

8:50 Automated Analysis of Lead and Cadmium in Biological Samples. S. E. Bowman, Cleveland Clinic Foundation, P. A. Pleban, K. H. Pearson

9:10 Combined Use of Infrared and Derivative UV-VIS Spectroscopies in Automated Identification System. R. J. Obremski, J. W. Mohar, J. Bernard, J. Miller, Beckman Instruments

9:30 Analysis of Barbiturates in Biological Fluids by Gas Chromatography Using Photoionization Detector. L. Jaramillo, J. Driscoll, HNU Systems

9:50 Routine GC/IR Identification of Drugs for the Forensic Laboratory. R. Saferstein, New Jersey State Police, J. J. Manura, T. A. Brettell, A. Varano

10:20 Determination of Crystalline and Chemical Changes in Drug Substances Through Computerized Infrared Subtractive and Synthetic Techniques. J. E. Zarembo, R. J. Warren, A. Post, Smith Kline Corp.

10:40 Carbon-13 and Proton Fourier Transform Nuclear Magnetic Resonance Spectral Analysis of S-Oxides and N-Oxides of Phenothiazine and Related Analogs. D. B. Staiger, R. J. Warren, J. E. Zarembo, A. Post, Smith Kline Corp.

11:00 Solvent Selectivity Effects in Reversed-Phase Ion Pair Chromatography of Some Amine Drugs. N.H.C. Cooke, M. Doyle, Altex Scientific

11:20 Determination of Meperidine and Normeperidine in the Obstetrical Patient. E. L. Todd, D. T. Stafford, U of Tennessee

11:40 Rapid Quantitative Analysis of Pharmaceuticals via Microcomputer-Controlled IR. R. J. Citerin, W. L. Truett, Foxboro/Wilks

Emission Spectroscopy—General II

Friday Morning, Little Theater

C. J. Belle, *Presiding*

8:30 Comparison of Ruled and Holographic Gratings for Inductively Coupled Plasma. C. C. Wohlers, Jarrell-Ash

8:50 Evaluation of Low-Cost Computerized ICAP Direct Reading Spectrometer for Routine Analysis of Ecological Samples. J. P. Maney, V. J. Luciano, L. F. Marciello, A. F. Ward, Jarrell-Ash

9:10 Background Correction Systems in Multichannel Direct Reading Spectrometer. D. A. Yates, U of Missouri, E. H. Hinderberger, S. R. Koirtyohann

9:30 Evaluation of Axially Viewed (End-on) ICP Source for Atomic Emission Spectroscopy. D. R. Demers, Baird Corp.

9:50 Use of Flow Injection Methods in Conjunction with Plasma Emission Spectrometry for Assay of Elements in Microsamples of Biological Origin. C. B. Baddiel, N. A. Skerten, Unilever Research

10:20 Precision of Flame Emission Measurements. S. G. Metcalf, K. G. Braithwaite, J. D. Ingle, Jr., Oregon State U

10:40 Flame Emission Spectroscopy Using Uniform Sized Sample Droplets. B. M. Joshi, Ford Motor Co., R. D. Sacks

Liquid Chromatography Analysis After Detection: Data Handling

Friday Morning, Room 235A

T. J. Williamson, *Presiding*

8:30 Du Pont "Prep 1"—Rapid Automatic Sample Processor for LC/GC Analysis. A. P. Goldberg, G. Dallas, Du Pont

8:50 New Chromatographic Data Handling System. R. M. King, R. J. Limpert, Waters Associates

9:10 New Microprocessor-Based Gradient Liquid Chromatograph Utilizing CRT Display. S. J. Luchetti, Varian

9:30 Versatile Information Processor and System Controller for LC. K. E. Nelson, R. J. Limpert, Waters Associates

9:50 Automated Method Development in HPLC Utilizing Interactive Communications Between Microprocessor-Based LC and Turn Key Lab Automation System. H. Knosel, R. Schuster, Hewlett-Packard

10:20 Unique Advantages of Ternary Solvent Programming. A. Henshall, Spectra-Physics

10:40 LC System Control by Basic Program. F. E. Eckstein, W. E. Shumaker, Perkin-Elmer

11:00 Useful Programming and Floppy Disc Technique Using a Microprocessor-Based HPLC System. A. Henshall, C. Flarity, R. Honganen, Spectra-Physics

11:20 Methods Development by Automated HPLC. A. P. Goldberg, R. W. Stout, K. P. Golden, Du Pont

11:40 LC Data Processing in Basic Language. F. E. Eckstein, Perkin-Elmer

Food Analysis

Friday Morning, Room 235B

A. Diorio, *Presiding*

8:30 Application and Characteristics of Polymer Adsorption Method Used to Analyze Flavor Volatiles from Peanuts. L. L. Buckholz, Jr., Rutgers, The State U

8:50 HPLC Analysis of Carotenes in Tomatoes. M. Zakaria, K. L. Simpson, P. R. Brown, U of Rhode Island

9:10 Determination of Residual Solvent Vapors in Food and Beverage Containers. G. Hewitt, J. Driscoll, J. Becker, HNU Systems

9:30 Storage of Canned Foods in Original Containers After Opening: Part II. Multielement Analysis of Food Product. S. G. Capar, K. W. Boyer, FDA

9:50 Direct Quantitative Determination of Fat in Food by Infrared Analysis Without Extraction Procedures. P. A. Wilks, Jr., M. Bayliss, Foxboro/Wilks

10:20 Improved Methodology for Analysis of Aflatoxins. A. C. Hayman, G. Dallas, Du Pont

10:40 Quantitative Analysis of Aflatoxins in Natural Products by Reversed-Phase HPLC. G. J. Kusha, D. J. Popovich, C. J. Lancaster, Whatman, Inc.

11:00 Determination of Biogenic Amines in Chocolate by HPLC. W. J. Hurst, P. Toomey, Hershey Foods Corp.

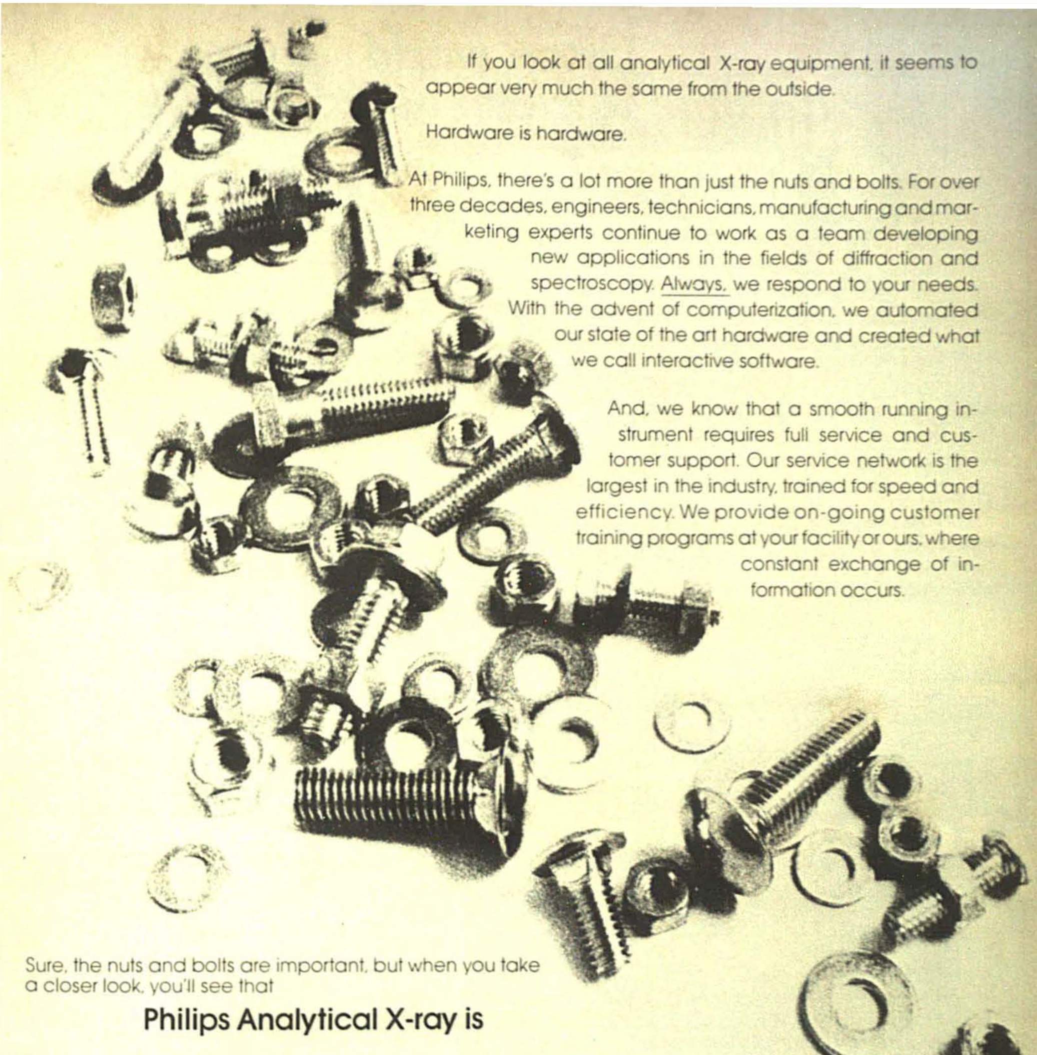

If you look at all analytical X-ray equipment, it seems to appear very much the same from the outside.

Hardware is hardware.

At Philips, there's a lot more than just the nuts and bolts. For over three decades, engineers, technicians, manufacturing and marketing experts continue to work as a team developing new applications in the fields of diffraction and spectroscopy. Always, we respond to your needs. With the advent of computerization, we automated our state of the art hardware and created what we call interactive software.

And, we know that a smooth running instrument requires full service and customer support. Our service network is the largest in the industry, trained for speed and efficiency. We provide on-going customer training programs at your facility or ours, where constant exchange of information occurs.

Sure, the nuts and bolts are important, but when you take a closer look, you'll see that

Philips Analytical X-ray is

More than just Hardware.

Visit us at Pittsburgh Conference. Philips' booth numbers 601-610.

Philips Electronic Instruments, Inc.
85 McKee Drive
Mahwah, New Jersey 07430
201-529-3800
A North American Philips Company

PHILIPS

CIRCLE 147 ON READER SERVICE CARD

Listen world . . .
it's time to clean up your act

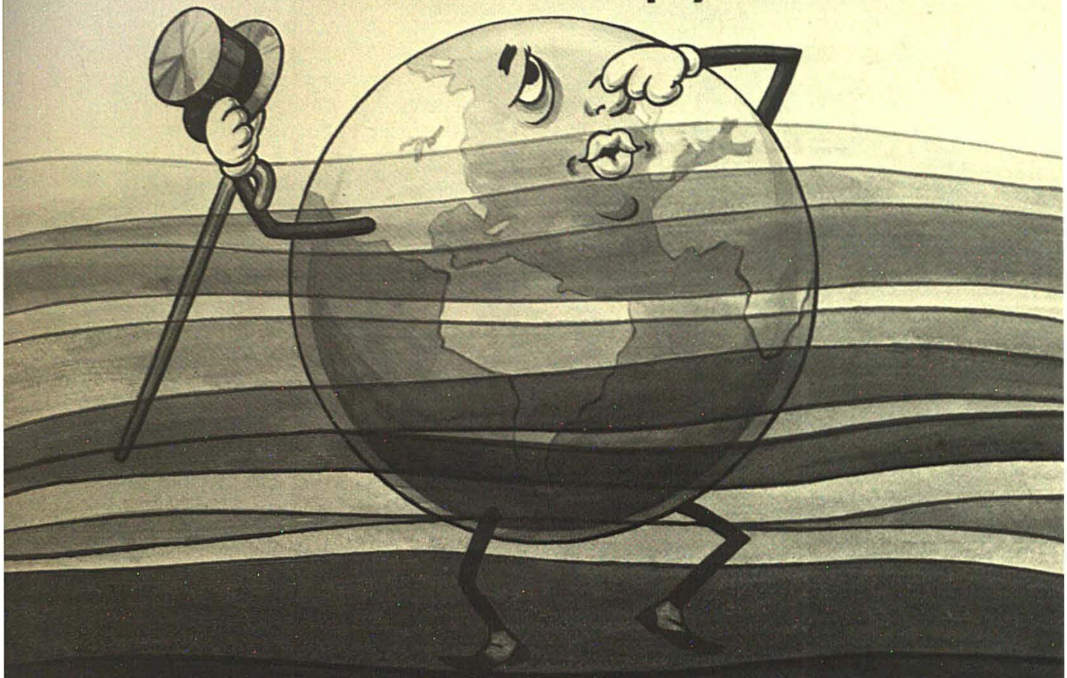

Environmental Science & Technology

SHOWS WHAT *CAN* BE DONE, WHAT *MUST* BE DONE, AND *HOW* TO DO IT!

Environmental clean-up is not only a good idea — it is the law! And ENVIRONMENTAL SCIENCE & TECHNOLOGY gives you the practical, hard facts you need on pollution and control, covers techniques, feasibility, research, equipment (including products, services and supplies) as well as case histories.

Essential reading for businessmen, scientists, legislators, governmental executives, builders, manufacturers and the academic world, ENVIRONMENTAL SCIENCE & TECHNOLOGY covers a broad range of information from what is going on in research labs to how-to-put-it-to-work in the real world. Also included is up-to-date news of current and pending governmental regulations, industry trends, meeting guide, technology reports and much more!

Your Guarantee:
You may cancel your subscription any time you are not pleased and you will receive a refund, in full, for copies still due.

Environmental Science & Technology, American Chemical Society **1979**
1155 Sixteenth Street, N.W., Washington, D.C. 20036

YES, I want to keep up-to-date on the hard facts of environmental clean-up. Please enter my subscription to ENVIRONMENTAL SCIENCE & TECHNOLOGY as follows:

	U.S.	*Foreign*
*ACS Member subscription, 1-year	☐ $16.00	☐ $22.00
Non-member subscription, 1-year	☐ $24.00	☐ $30.00
Institution, Company or Library subscription, 1-year	☐ $64.00	☐ $70.00

Please specify: ☐ Hard copy, or ☐ Microfiche
☐ Payment enclosed. ☐ Bill me. ☐ Bill company.

Toll Free: New Orders: 800—638-2000
Md. only 301—949-1551

Name ____________________ Title ____________________

Organization ____________________

☐ Home
Address ☐ Business ____________________

City, State, Zip ____________________

Allow 60 days for your first copy to be put in the mail.

*ACS Member rates are for personal use only.

0034L

4

. . . the fourth report of the series on the people who make up the chemical profession.

Professionals in Chemistry

Professionals in Chemistry 1977 contains a wealth of employment and educational data of particular interest to academic administrators, faculty members, industrial managers, personnel specialists, individual chemists and chemical engineers, career counselors, and the young men and women contemplating — or preparing for — careers in chemistry.

A Comprehensive Report on:

- Characteristics
- Remuneration
- Employment Projections
- Employers
- Minority Chemists
- Postdoctoral Fellows
- Supply

American Chemical Society
Special Issue Sales
1155 16th Street, N.W.
Washington, D.C. 20036

Please send me ______ copies of *Professionals in Chemistry 1977*. Price: $20.00 Member Price: $10.00

Please send me ______ complete sets of *Professionals in Chemistry*. (1974 through 1977). Price: $40.00 Member Price: $20.00

Payment of $________ is enclosed.

Name ____________________

Address ____________________

____

How to QUICK FREEZE TRANSIENTS DIGITALLY..

then thaw them on any kind of answer machine.

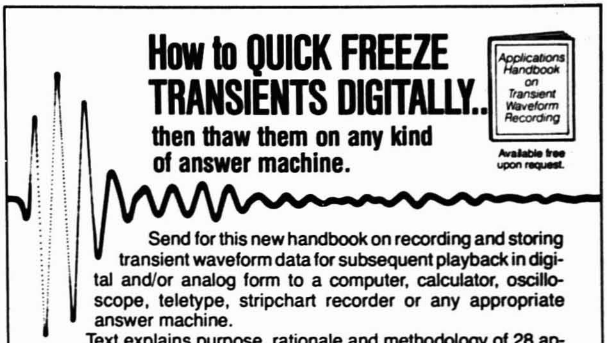
Applications Handbook on Transient Waveform Recording

Available free upon request.

Send for this new handbook on recording and storing transient waveform data for subsequent playback in digital and/or analog form to a computer, calculator, oscilloscope, teletype, stripchart recorder or any appropriate answer machine.

Text explains purpose, rationale and methodology of 28 applications — making efficient use of features such as simultaneous multi-channel recording, pre- and post-trigger recording, interfacing options, variable playback rates and dual timebase facilities. Diagrams illustrate components, interfacing and layout.

PHYSICAL DATA, Inc.
8220 S.W. Nimbus Ave.
Beaverton, OR 97005
Phone: 503 644-9014

Specific applications are from these fields:

- Materials testing • Chemical analysis
- Engine monitoring • Explosives/ballistics
- Electrical testing • Medical research
- Propulsion • Turbine jets • Safety tests
- Nuclear physics • Environment
- And more.

See Demos and get the Handbook at The PITTSBURGH CONFERENCE Booth 1503-5

CIRCLE 155 ON READER SERVICE CARD

QUALITY! SELECTION! FAST DELIVERY!

All Yours From TCI—The Organic Reagent Specialist.

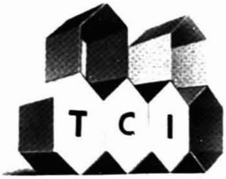

Organic Reagents
Fine Organic Chemicals
Rare Organic Chemicals
Custom Synthesis

Since 1922, TCI (Tokyo Kasei) has supplied leading chemical laboratories and industries worldwide with a broad selection of fine chemicals. Our current catalog includes over 10,000 different chemicals for every type of use. Virtually all orders are shipped within 12 hours of receipt. Five-gallon, 55-gallon and ton lots are available. Be sure of getting quality, selection and fast delivery. Buy TCI!

Write today for your free copy of the 750-page TCI Organic Chemicals Price List.

東京化成

TCI **TOKYO KASEI KOGYO CO., LTD.**
(Tokyo Chemical Industry Co., Ltd.)
9-4, Nihonbashi-Honcho 3-chome, Chuo-ku, Tokyo, 103 Japan
Telex: 222-4719 ASACMN J Cable: ASACHEMCO TOKYO Tel: 241-0861

CIRCLE 206 ON READER SERVICE CARD

NEW!
UPDATED!
EXPANDED!

A totally revised edition of the best selling single publication ever produced by ACS

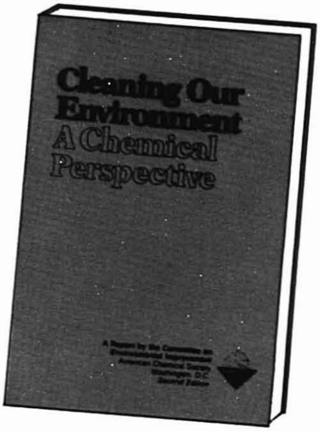

Cleaning Our Environment
A Chemical Perspective

NEW!
- **Analysis & Monitoring**
- **Toxicology**
- **Radiation**

UPDATED!
- **Air**
- **Water**
- **Solid Wastes**
- **Pesticides**

The first edition of CLEANING OUR ENVIRONMENT, published in 1969, quickly became the ACS all-time best-selling book. But, because this is a changing world—*especially* in the environmental field—ACS has completely revised and expanded this important work. The four original topics (air, water, solid wastes, and pesticides) have been updated, and **coverage has been added in three new areas—analysis and monitoring, toxicology, and radiation!**

If you are interested as a professional or as a layman, CLEANING OUR ENVIRONMENT will bring you up to date on what *is* being done, what *can* be done, and what *will* be done!

Even if you already have the earlier edition—you will want this important and *expanded* revision! 457 pages. $9.50 paperbound.

Essential reading for:
- educators
- researchers
- legislators
- administrators
- and a great refresher for environmentalists

Special Issues Sales
American Chemical Society
1155 Sixteenth Street, N.W.
Washington, D.C. 20036

PRICES

1-9 copies	$9.50 each
10-49 copies	$8.50 each
50 or more	$7.50 each

Enclose $1.50 per order for handling and postage.

California residents add 6% state use tax.

Please send me _____ copies of CLEANING OUR ENVIRONMENT—A CHEMICAL PERSPECTIVE

☐ My payment is enclosed ☐ Bill me

Name ______________________

Address ______________________

City ______________________

State ______________ Zip code ______________

We can't really show off Inficon's versatile surface analysis system.

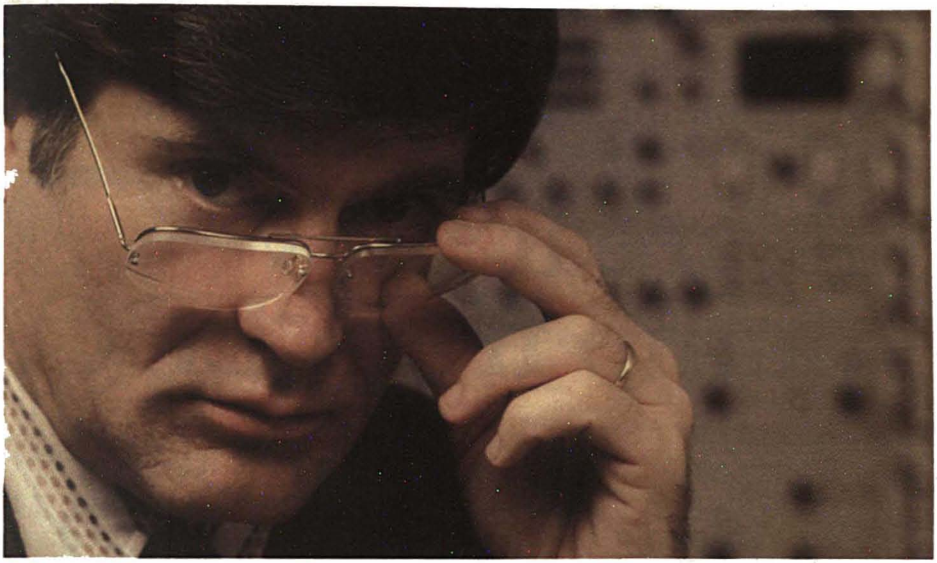

Until you show up with a sample for comparative analysis.

The best way to demonstrate Inficon's LHS-10 surface analysis system is by direct application. So bring in any vacuum compatible sample—give us two weeks' notice, please—and we'll analyze it.

And we'll prove ours is the simplest, most cost-effective system for your surface analyses.

Whatever your analytical problem, the LHS-10 will help you obtain more complete surface characterizations, correlate data faster, and reach firmer experimental conclusions.

LHS-10's universal analysis chamber allows customizing to your exact needs—whether it's catalyst efficiency testing, elemental or quantitative analysis, trace detection, depth profiling, or chemical fingerprinting.

You can have ESCA (XPS), UPS, AES, SAM, SIMS, ISS modules now, or add any later at minimal cost. Even add a computer system for simultaneous instrument operation and data manipulation.

No matter what techniques you select for present or future use, all can be employed on the same sample area—without specimen manipulation—for rapid sample analysis.

For now, let the other surface analysis companies first demonstrate their capabilities—then let Inficon give you proof positive of the LHS-10's superior performance, versatility and simplicity.

Write or call today. We'd like to see you and your sample soon.

We also offer contract surface analysis and assistance with special problems.

The plexiglas model of our universal chamber clearly shows our versatile analysis techniques.

See us at the Pittsburgh Conference.

INFICON
LEYBOLD-HERAEUS
6500 Fly Road, East Syracuse, New York 13057
315/437-0377 ■ TWX 710 541-0594

CIRCLE 105 ON READER SERVICE CARD

HPLC announcement:

A significant advance in solvent delivery…

A great new pump from LDC

The new ConstaMetric III metering pump is a single modular unit designed specifically for HPLC use, not merely adapted from a general purpose pump. Naturally it's from LDC, with their preeminent Milton Roy pump engineering expertise.

LIMITS
HIGH
LOW
POWER
PSI X1000
0 1 2 3 4 5 6
CONSTAMETRIC III
FLOW RATE
ml/min
2 0 0

See us at booths 1337-38-39-40
Pittsburgh Conference

Note these special advantages of the ConstaMetric III:

Dual piston reciprocating pump

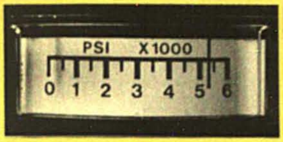

6,000 psi capability

Gradient programmable

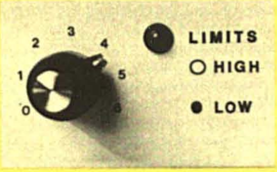

Hi-low limit shutdown

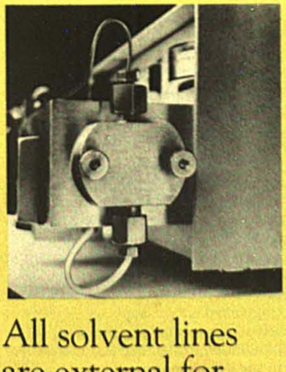

All solvent lines are external for quick servicing or leak detection

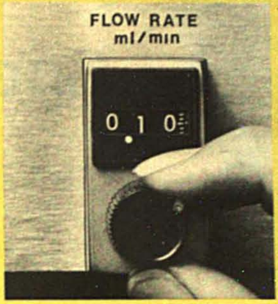

Adjustable flow rate 0.10 to 9.99 mL/min

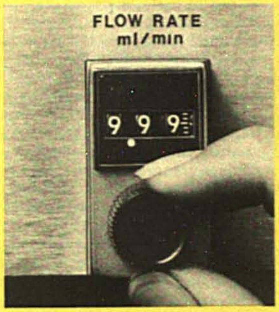

LDC liquid chromatography

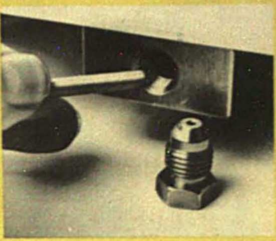

Filter accessible for servicing

Send for the detailed ConstaMetric III brochure and the complete LDC pump catalog.

LABORATORY DATA CONTROL
Division of Milton Roy Co.
P.O. Box 10235
Riviera Beach, FL 33404
305/844-5241, telex 513479

European office:
LABORATORY DATA CONTROL
Milton Roy House, High Street
Stone, Staffs., ST 15 8AR,
England
Telephone 0785-83-3542,
telex 36623

LABORATORY DATA CONTROL
P.O. Box 10235, Riviera Beach, FL 33404

Please send me the ☐ ConstaMetric III brochure
☐ Pump catalog

Name ____________________ Title ____________

Institution ____________________ Phone ____________

Address ________________________________

City ________________________________

State ____________________ Zip ____________

LDC

CIRCLE 127 ON READER SERVICE CARD

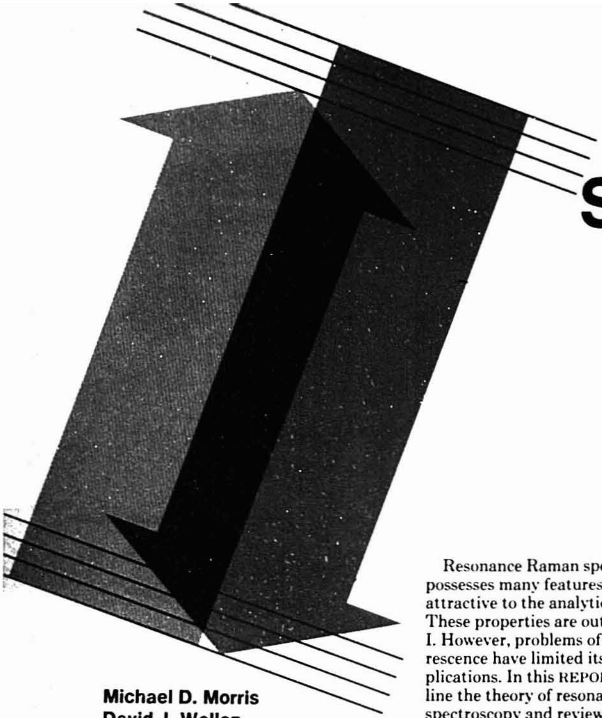

Resonance Raman Spectroscopy

Michael D. Morris
David J. Wallan
Department of Chemistry
University of Michigan
Ann Arbor, Mich. 48109

Resonance enhancement of Raman scattering occurs when the excitation wavelength corresponds to the wavelength of a dipole-allowed electronic transition of a molecule. Vibrations responsible for the usually unresolved vibronic structure of the absorption band as well as totally symmetric vibrations are enhanced. The enhanced Raman bands may have intensities 10^2–10^6 times greater than normal Raman intensities. Consequently, resonance Raman spectra have low detection limits and are much simpler than normal Raman spectra, since only bands related to the "chromophore" are enhanced. The power of resonance enhancement is shown in Figure 1. The sample is 5×10^{-6} M cyanocobalamin and 0.05 M sodium nitrate aqueous solution. The spectrum is obtained with 514.5-nm (Ar^+ laser) excitation, a wavelength within the intense lowest $\pi - \pi^*$ transition of cyanocobalamin, but well removed from any nitrate absorption bands. Thus, the strong ring vibration (1504 cm^{-1}) has about half the integrated intensity of the strongest nitrate band at 1055 cm^{-1}, despite a concentration difference of four orders of magnitude.

Resonance Raman spectroscopy possesses many features that make it attractive to the analytical chemist. These properties are outlined in Table I. However, problems of sample fluorescence have limited its practical applications. In this REPORT we will outline the theory of resonance Raman spectroscopy and review the published analytical applications. We will also describe the most promising approach to fluorescence rejection, coherent resonance Raman spectroscopy, and summarize the current applications and the prospects for the future.

Resonance Raman spectroscopy is the only high-resolution spectroscopic technique that is routinely applicable to dilute aqueous solutions. For example, detection limits of 2×10^{-7} M for vitamin B_{12} have been obtained using only a simple photon-counting system (*1*). Recently, detection limits for β-carotene were pushed below 10^{-8} M, by use of a multipass cell (*2*). Structural studies are routinely carried out on solutions in the 10^{-4}–10^{-5} M range.

Resonance-Enhanced Raman Spectra

The period of early exploration of applications of resonance Raman spectroscopy included vigorous debate about the origin of the effect and the form of its governing equations. Most of the controversies have been resolved, and several recent reviews discuss the theory clearly (*3–7*). The resonance Raman effect results from the promotion of an electron into an excited vibronic state, accompanied by immediate relaxation into a vibrational level of the ground state. The process is not preceded by prior relaxation to the lowest vibrational level of the excited state as in ordinary fluorescence. The distinction is shown in Figure 2. Consequently, the resonance Raman emission process is essentially instantaneous, and the resulting spectra consist of narrow bands. For molecules in solution, electronic states are broadened by many closely spaced vibrational states. Excitation with radiation anywhere within this continuum will give rise to the same resonance Raman spectrum, with an intensity proportional to the absorption intensity. Spectra may be obtained using an excitation frequency just below the absorption band. Such spectra display smaller resonance enhancement, typically less than tenfold, and are called preresonance Raman spectra.

Not all of the normal Raman bands are equally enhanced. Only those vibrations that exhibit a large change in equilibrium geometry upon electronic excitation will produce strongly resonance-enhanced Raman bands. In practical terms, this means that two classes of vibrational modes will produce intense resonance-enhanced spectra. These are totally symmetric vibrations, and those nontotally symmetric vibrations that vibronically couple two electronic states. The resulting two classes of enhancement are called A-term and B-term enhancement, respectively. They can be distinguished experimentally by their intensity vs. excitation frequency dependences (called excitation profiles) in the preresonance region.

Note that although resonance enhancement involves a true electronic excited state of a molecule, the vibrational frequencies observed are the

0003-2700/79/0351-0182A$01.00/0
© 1979 American Chemical Society

Current Applications and Prospects

Report

Table I. Advantages of Resonance Raman Spectroscopy

Table I. Advantages of Resonance Raman Spectroscopy
Works well in aqueous solution
Works well with solid samples
Good detection limits, 10^{-6}–10^{-8} M
Good resolution, 10–20 cm^{-1} (0.3–0.6 nm at 500 nm)
Structure-sensitive spectra
Simple spectra. Only "chromophore" vibrations contribute
No special equipment needed. Spectra obtained on conventional Raman spectrometers
Fast data acquisition. Scan rate 20–100 cm^{-1}/min
Multichannel detector sometimes usable

ground state frequencies of the molecule, as observed in infrared absorption or normal Raman spectroscopy. The reason is that the resonance-enhanced scattering process starts and terminates in the ground electronic state of the molecule. Resonance Raman spectroscopy can therefore be considered a form of high-resolution vibronic spectroscopy.

Since an electronic transition is often more or less localized in one part of a complex molecule, the resonance Raman effect provides a way to selectively enhance the Raman bands due to vibrations of this chromophore. This selectivity is quite apparent in molecules such as the heme proteins, whose resonance Raman spectra have been extensively studied (*8*). It is easily shown that the resonance Raman bands are due solely to vibrational modes of the tetrapyrrole chromophore. None of the bands associated with the protein is enhanced, and at the concentrations employed for biochemical studies (10^{-4}–10^{-5} M), protein bands are too weak to be observed.

The sensitivity of resonance Raman spectroscopy to only chromophore vibrational modes may be considered either a strength or a weakness. On the one hand, spectra are greatly simplified, and a series of molecules containing slightly different chromophores will give spectra that are easily distinguished. On the other hand, if a series of molecules contains the same chromophore with, for example, different aliphatic side chains, the resonance Raman spectra will be nearly identical.

The analytical advantages of resonance Raman spectroscopy were suggested as early as 1959 (*9*). At that time, sample self-absorption and the lack of a multiline source of sufficient intensity limited resonance Raman spectroscopic research to a handful of specialists. The argon ion and krypton ion lasers, which became available in the late 1960's, were quickly adopted as the intense excitation sources needed for resonance Raman applications. Almost immediately, resonance Raman spectroscopy became a valuable tool for the study of such diverse biochemical systems as heme derivatives and the poly-ene visual pigments. Applications to the study of inorganic molecules also quickly appeared (*10*).

Today commercially available dye lasers cover the wavelength range from about 300 nm into the near infrared. Frequency doubling extends this wavelength range down to about 220 nm. Thus, resonance Raman spectra can now be obtained over almost the entire range in which conventional electronic absorption spectra can be taken.

Clearly, one should be able to substitute the high resolution of resonance Raman spectroscopy for some or most of the separation steps and interference removal reactions needed for low-resolution techniques such as fluorimetry or spectrophotometry. In fact, resonance Raman spectra of dyes and pesticides have been observed at the micromolar level in such media as

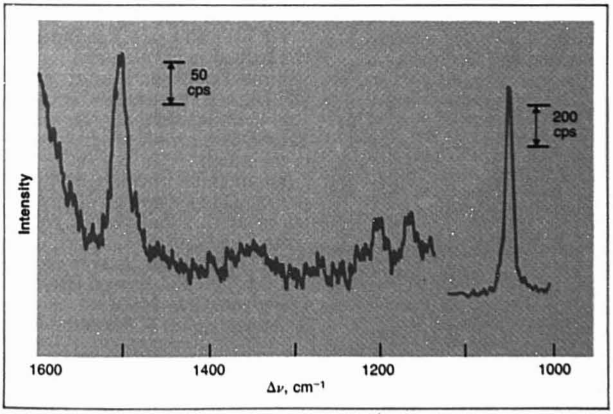

Figure 1. Resonance Raman spectrum of 5×10^{-6} M cyanocobalamin and 5×10^{-2} M nitrate ion in 0.1 M HCl. Excitation frequency: 19436 cm^{-1} (514.5 nm)

WE MADE AUTOMATIC TITRATION A SOFT TOUCH.

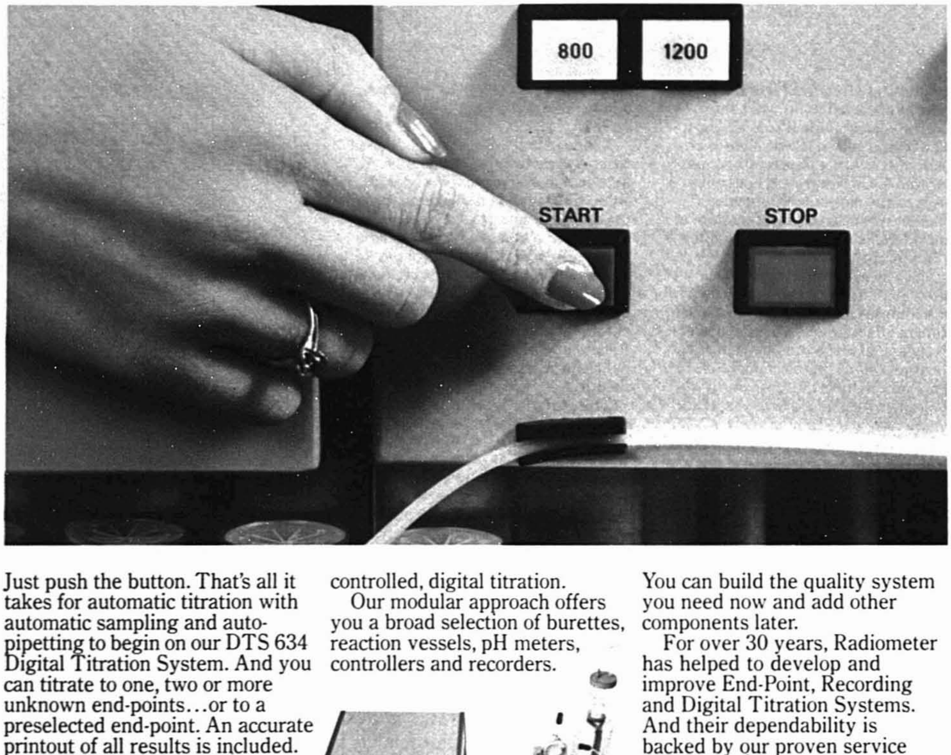

Just push the button. That's all it takes for automatic titration with automatic sampling and auto-pipetting to begin on our DTS 634 Digital Titration System. And you can titrate to one, two or more unknown end-points…or to a preselected end-point. An accurate printout of all results is included. Automatically.

Only Radiometer can offer such unsurpassed speed, accuracy and precision in titration.

But this is only one of our many systems. We offer a wide range of titration systems that are accurate, automatic and flexible. And we bring some unusual features to titration. Such as proportional band control, Radiometer's incremental titrant addition, stepped titration curves (patented), and micro processor-controlled, digital titration.

Our modular approach offers you a broad selection of burettes, reaction vessels, pH meters, controllers and recorders.

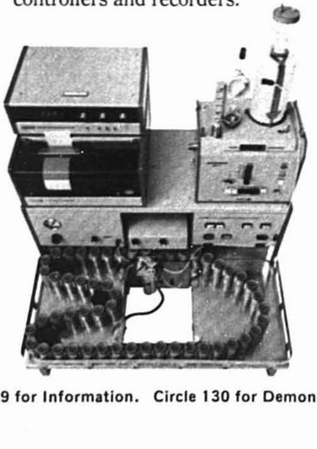

You can build the quality system you need now and add other components later.

For over 30 years, Radiometer has helped to develop and improve End-Point, Recording and Digital Titration Systems. And their dependability is backed by our proven service organization.

For more information or a personal demonstration of any of our many titration systems, call or write The London Company, U.S. Representative for Radiometer-Copenhagen, 811 Sharon Drive, Cleveland, Ohio 44145. Telephone (216) 871-8900.

RADIOMETER
COPENHAGEN

Circle 129 for Information. Circle 130 for Demonstration.

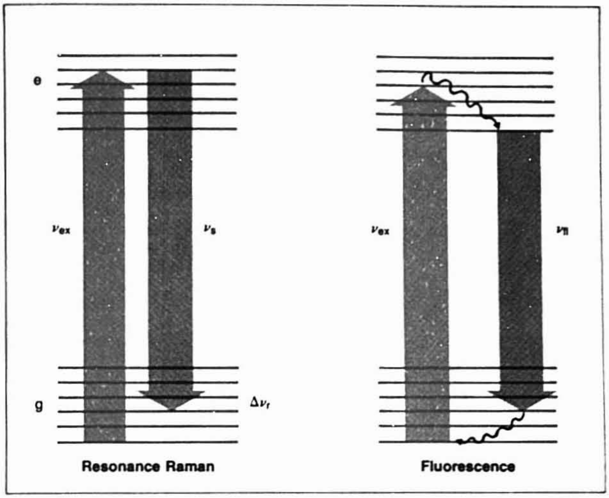

Figure 2. Energy diagram showing difference between resonance Raman emission and fluorescence

Relaxation to ground vibrational state, which precedes fluorescent emission, depicted by undulating arrow

river water and cherry soda with little or no matrix interference (*11–13*).

The combination of resonance Raman spectroscopy and some simple "chromophore developing" chemistry could result in many practical analytical methods. The catecholamines are an example of a system of closely related compounds amenable to this technique. The aminochromes, which are formed by oxidation of catecholamines with air or one of several common oxidizing agents, are useful for this purpose (*14–16*). Many molecules, such as heme derivatives, vitamin B_{12}, poly-ene visual pigments and antibiotics, have suitable absorption spectra and are easily studied with no chemical transformations at all.

Resonance Raman spectroscopy is also being used to investigate temporal changes in chemical systems. Several groups have used this method to examine generated species at electrochemical diffusion layers (*17, 18*). Spectra have been obtained using multichannel detectors, such as vidicons (*19*), and 7-ns time resolution has been observed (*20*).

Vibrational spectra of solids are readily obtained using resonance Raman spectroscopy. Recently, the technique has been employed to probe the olefin adsorption on a zeolite substrate (*21*). The chemical transformations of rose bengal adsorbed on a ZnO sinter electrode have also been investigated (*22*).

Resonance Raman spectroscopy is now established as a useful tool for a wide variety of problems. Nonetheless, analytical chemists have not often employed it, largely because many potentially interesting samples are fluorescent. Fluorescence appears as a broad band background signal and may be so intense as to completely obscure Raman signals. Urine and serum, for example, are sufficiently fluorescent that resonance Raman spectroscopy in these common matrices is generally difficult or impossible. The same problem may occur with paint samples, colored fabrics, or pharmaceutical preparations.

Sample fluorescence has long plagued Raman spectroscopists, and many have developed ad hoc techniques for dealing with the problem. Extensive sample purification or destruction of fluorescent impurities in a laser beam is sometimes helpful. However, if the fluorescent culprit is the species of interest, these techniques are useless, and even addition of quenching agents is usually not sufficient. Recently, time resolution of Raman signals from the much slower fluorescence emission has been proposed (*23–27*). However, fluorescence rejection is generally only ten to one hundredfold, an insufficient factor for many analytical applications. In some cases, time resolution actually lowers signal-to-noise ratios (*27*).

Coherent Raman Spectroscopy

Recently, coherent Raman spectroscopy (*28–31*) has been proposed as a method for obtaining Raman spectra of fluorescent samples. The fluorescence rejection of these techniques is indeed spectacular. An early report presented spectra of samples deliberately spiked with laser dyes (*32*), and the spectra of dyes themselves have been reported. Spectra of many other highly fluorescent molecules have since been observed. Coherent Raman spectroscopy appears to provide the most promising approach to analytical Raman spectroscopy.

The term *coherent Raman spectroscopy* has come to include several closely related techniques. These include coherent anti-Stokes Raman spectroscopy, CARS (*32–34*), Raman-induced Kerr effect spectroscopy, RIKES (*35, 36*), and inverse Raman spectroscopy, IRS (*37, 38*). Several other techniques suggested recently are all closely related to these three. All the techniques depend on the interaction of two intense, generally pulsed, laser beams with a sample. When the frequencies of the lasers differ by a Raman-active frequency, then one can observe coherent emission (CARS), absorption out of one beam (IRS) or a change in the polarization state of one of the beams (RIKES).

Although CARS, and with it fairly broad interest in coherent Raman spectroscopy, is only 4 or 5 years old, the advantages and problems of coherent Raman spectroscopy are already becoming clear. The advantages are summarized in Table II. For our purposes, the excellent fluorescence rejection is the most important.

Some of the problems are merely those of a new technology. At present, one must assemble one's own instrument, which usually lacks the convenience features of commercial devices. More serious is the presence in CARS of a nonresonant background signal, which limits its sensitivity. At this writing, detection limits are at least

Table II. Advantages of Coherent Raman Spectroscopy

- High conversion efficiency
  - Strong signals in most cases
  - Low average incident power required
  - Short spectral acquisition time—even single pulse
- Collimated output signal
  - Nearly 100% collection of signal
  - Good spatial rejection of fluorescence
- Anti-Stokes signal, or signal at *highest*
  - Good spectral rejection of fluorescence
- Resolution determined by laser bandwidths
  - Only low-resolution single or double monochromator needed
  - Interference filter adequate in some cases

two orders of magnitude higher for CARS than for conventional Raman spectroscopy under equivalent conditions. Refinements in instrumentation could improve detection limits somewhat. Newly emerging coherent techniques, to which we shall return later, may soon provide the sensitivity needed to exploit the full potential of resonance Raman spectroscopy.

The CARS apparatus used in our laboratory is similar to systems used by most investigators for CARS of solutions. A 1-MW nitrogen laser pumps two dye lasers. The dye laser, which generates the beam ω_2, has a motor-driven grating, allowing spectral scanning. The other dye laser is manually tunable only. For reasons of economy, reliability, and ease of operation, the two transversely pumped dye lasers are driven by a single nitrogen laser and form the most common CARS laser system.

Virtually any sort of sample cell can be used for CARS. We have used spectrophotometer cells of 1- or 2-mm path length. Melting point capillaries are useful, both because they are inexpensive and because they act as very short focal length lenses and help in aligning the system (*39*). Capillaries can also serve as flow cells for CARS.

Nitrogen laser-pumped dye lasers have very short pulses, typically 5–10 ns long, depending on design. Moreover, the repetition rate is low, typically 10–25 pulses per second. Because of this short pulse length and low duty cycle, CARS data must be processed through a gated integrator. For strong signals the detector can be a PIN diode. More frequently, it is necessary to use a photomultiplier. The common 1P28 is suitable. Because CARS signals show large pulse-to-pulse variations, it is useful to ratio to a reference signal. Typically, ω_1 is monitored, but a cell filled with solvent can be used to generate a reference background signal.

The gated integrator itself is a weak link in the coherent Raman experimental system. The device is linear to no more than 0.1% and operates over about three orders of magnitude of signal intensity. These linearity and dynamic range constrictions limit the effectiveness of background subtraction, averaging over many pulses or digital filtering.

Table III. Relative CARS Background Intensities[a]

Solvent	Background
Water (reference)	1.0
D_2O	1.0
Methanol	1.0
Ethanol	1.8
Chloroform	2.6
Carbon tetrachloride	2.6
Benzene	0.09
Toluene	0.09
m-Xylene	0.09
Benzyl chloride	0.12

[a] Reprinted with permission from ref. 40. Copyright 1976 National Academy of Sciences.

The presence of the nonresonant background signal is a fundamental limitation of CARS and is the origin of the poor sensitivity of this technique. CARS nonresonant background signals relative to water are shown for selected solvents in Table III. The key factor is that the nonresonant background signal for aromatic solvents is about an order of magnitude below the signals for most other solvent systems. Therefore, lower detection limits have been reported for samples in benzene than for those in other common solvents. Overcoming the nonresonant background is the object of intensive research. We will summarize progress in this area at the end of this review.

Resonance-Enhanced Coherent Raman Spectra

Coherent anti-Stokes Raman spectra can be resonance enhanced under the same conditions as spontaneous (conventional) Raman spectra (*40, 41*). The ω_1 (pump) frequency is made coincidental with an electronic absorption maximum, and ω_2 (probe) is scanned to generate the spectrum. Excitation profiles have been measured and found to conform to theory quite well (*42*). Resonance inverse Raman spectra have also been reported (*43*), but very little work has been done in this area.

The spectra of laser dyes themselves have been obtained and demonstrate the power of coherent resonance Raman spectroscopy. These molecules fluoresce with high quantum efficiency, approaching unity in the case of perylene, and conventional resonance Raman spectra of these molecules cannot be obtained (*44*).

Biochemical applications of resonance-enhanced CARS are now beginning to appear. Recently, resonance CARS spectra of several flavins, including FAD, glucose oxidase, and riboflavin binding protein, have been reported (*45, 46*). Partial band assignments and some preliminary structural correlations have been presented. The resonance-enhanced CARS spectrum of adriamycin has been used to reinterpret the electronic spectrum of that molecule (*47*), an important antitumor drug. Flavins and adriamycin are highly fluorescent, and their resonance Raman spectra cannot be obtained by conventional means.

Resonance CARS spectra are particularly susceptible to distortion by interference between the Raman signal of the solute and the nonresonant background of the solvent. Since these spectra are obtained with solute concentrations of 10^{-3} *M* or lower, there is an enormous excess of solvent, and negative and dispersive peaks are common. Figure 3 shows part of an adriamycin spectrum in which the Raman bands appear dispersive. The midpoints between the maximum and minimum emission correspond to the positions of the conventional Raman bands. As ω_1 is moved away from the origin of the electronic transition, the CARS bands are gradually transformed to negative peaks (*47*). The same transition from positive bands

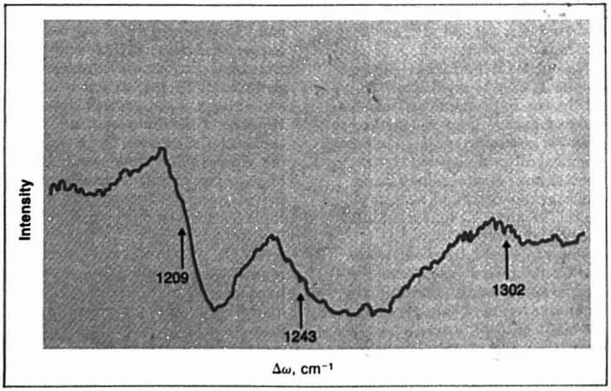

Figure 3. Resonance CARS spectrum of 3×10^{-3} *M* adriamycin in pH 6 buffer
$\omega_1 = 20\,000$ cm^{-1} (500 nm), origin of electronic transition. At this concentration, bands appear dispersive. Arrows show midpoint of each band, which corresponds well to bands observed in preresonance Raman spectrum of molecule

Presenting:

Finnigan 4023 Automated GC/MS

Unmatched GC/MS Performance and Data Acquisition/Processing Capability.

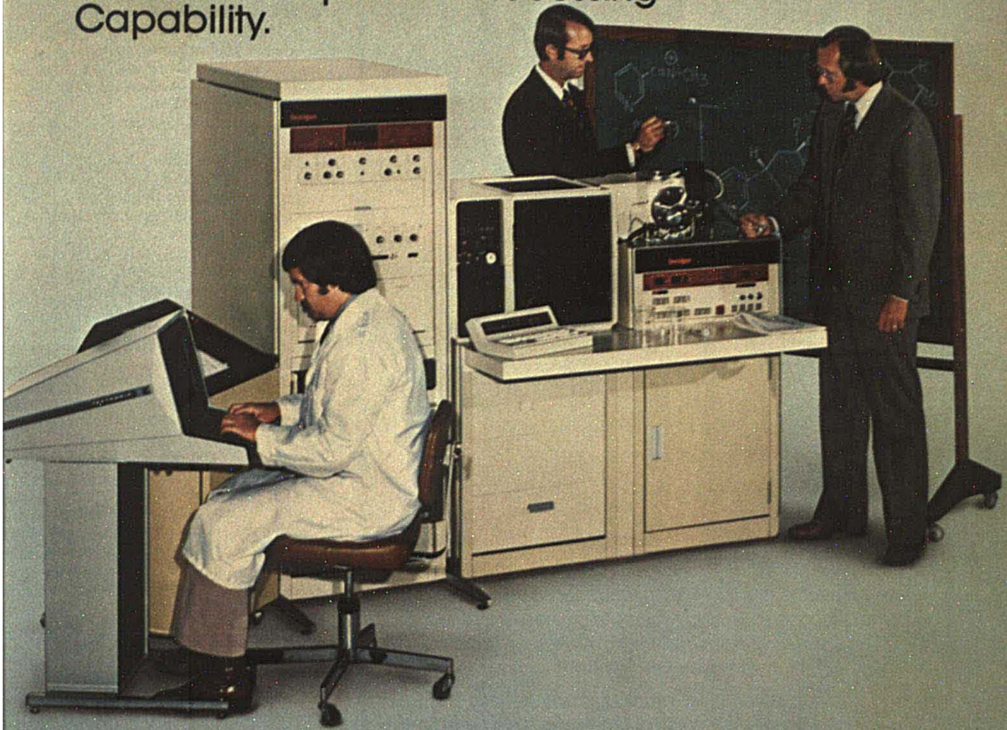

Finnigan's 4023 Automated GC/MS system is the most advanced of the 4000 Series instruments which have made Finnigan the recognized leader in the GC/MS field.

The 4023 provides the finest GC/MS performance available by any criterion, whether sensitivity, spectral quality, reliability, selectivity, or adaptability to special applications.

This GC/MS performance is coupled with a data acquisition/processing capability unequalled for speed, sophistication, choices in output formatting, and capability for chaining commands for individualized automation procedures.

Recent innovations include liquid chromatograph interfacing (LC/MS) and combined positive ion/negative ion mass spectrometry (PPINICI).

Finnigan users with previous Series 4000 GC/MS systems can update their present equipment by incorporating these and all other Finnigan advances. Finnigan's policy of maintaining adaptability of advances in the art to existing Finnigan equipment gives you the assurance you need that the system you acquire today will meet your needs for years to come.

Inquire today how Finnigan—the GC/MS people—can keep you at the forefront of research in your field.

finnigan
Instruments
A DIVISION OF FINNIGAN CORPORATION
845 WEST MAUDE AVENUE
SUNNYVALE, CALIFORNIA 94086
(408) 732-0940

©Finnigan Instruments, 1979

CIRCLE 79 ON READER SERVICE CARD

A FULLY AUTOMATIC
MICROPROCESSOR CONTROLLED
X-RAY SPECTROMETER

DIANO HAS IT!

DIANO now offers completely unattended instrument control at a price even lower than competitors' outdated manual systems! The secret — a powerful microprocessor coupled to a new torque drive system.

A universal bi-directional interface also allows easy communication with most available I/O devices. This permits fuller utilization of existing laboratory computers and software. In addition, DIANO offers a full range of Digital Equipment Corporation's PDP-11 computers with DIANO's ACUPAK™ Fortran language software — the most extensive and advanced package of x-ray fluorescence software available.

See the automatic spectrometer with the highest Performance/Cost Ratio in history at Cleveland or let us have one of our local sales representatives contact you with full details.

DIANO CORPORATION
8 COMMONWEALTH AVENUE
WOBURN, MASSACHUSETTS 01801 U.S.A.
TEL.(617)-935-4310 TELEX 94-9306

CIRCLE 46 ON READER SERVICE CARD

to dispersive to negative can also be observed at fixed pump wavelength, simply by diluting the sample.

Although resonance-enhanced CARS was first reported only 2 years ago, the technique is already proving valuable for mechanistic and structural studies. Because of the nonresonant background signal, detection limits in aqueous solution are seldom below $10^{-5}\ M$ and can be pushed to $10^{-7}\ M$ in benzene solution in exceptional cases. These high detection limits preclude widespread use of resonance CARS for trace analysis.

Development of a background-free or at least low background coherent Raman spectroscopic method is an area of active research. Optical cancellation of nonresonant signals and techniques free of nonresonant signals are being explored in several labs. Raman induced Kerr effect spectroscopy (RIKES) can be used to cancel the background optically (*35, 36*). This technique exploits birefringence induced in a sample when the two incident laser beams differ in frequency by a Raman active frequency. A major experimental problem with RIKES is that it requires the use of linearly polarized light with an extinction ratio of 10^5 or better. Ordinary Glan laser prisms are not capable of such high extinction ratios, and expensive polarizing optics are required.

An alternative approach called "CW stimulated Raman" (*48–50*) has been demonstrated. It is essentially inverse Raman or Raman gain spectroscopy. The absorption from a laser beam or the energy gained by a laser beam is measured under inverse Raman conditions. The gain or absorption from an argon ion laser is measured. The second tunable laser beam is chopped, and a lock-in amplifier is used to measure only the component of the argon beam synchronous with the chopped beam. By this technique very small induced intensity changes can be measured.

Another inverse Raman technique uses the induced absorption generated on an argon laser beam by a pulsed dye laser. The high peak power available from a pulsed dye laser means that the observed signal is much larger than that found by the CW technique (*51*). Signal-to-noise ratios are thus higher.

Raman gain and inverse Raman measurements require absorption of energy by the sample and therefore are intrinsically free of any nonresonant background. Measurement of Raman spectra by means of these phenomena should allow generation of undistorted spectra down to very low concentrations.

The Kerr effect and the inverse Raman/Raman gain techniques are

INTRODUCING

The Model 384-1 Polarographic Analyzer System...

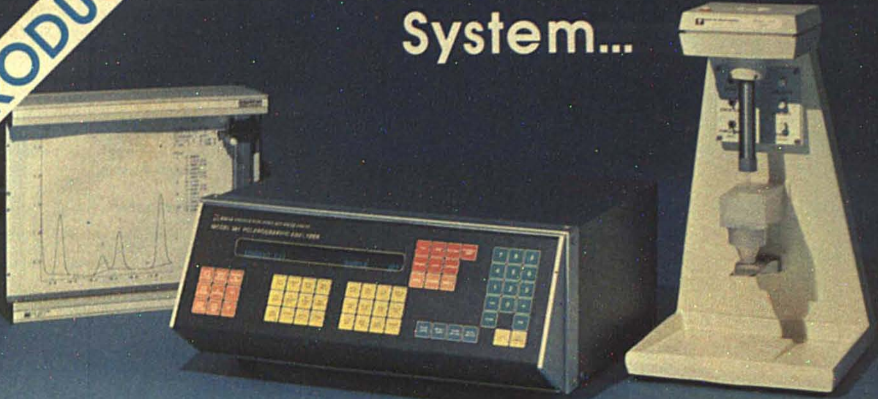

...because your analyses are not getting any easier.

The 384 has the MOST ADVANCED SOFTWARE for polarography

- Stores and recalls as many as 12 different analytical methods
- Stores and recalls as many as 9 complete analytical curves
- Accommodates up to 9 peaks in each scan
- Calculates concentration automatically by either standard addition or multi-point standard curve
- Labels header sheet with 24 experimental parameters
- Permits blank subtraction capability with unique blank for each curve
- Fits tangents for most accurate peak height measurements

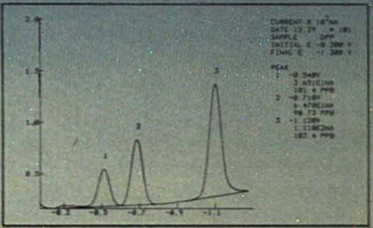

The 384 has the MOST ADVANCED HARDWARE for polarography

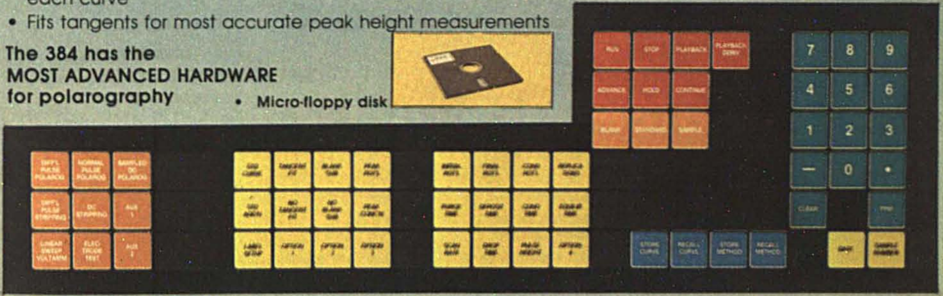
RUN
STOP
PLAYBACK
PLAYBACK DERIV
ADVANCE
HOLD
CONTINUE
BLANK
STANDARD
SAMPLE
7
8
9
4
5
6
1
2
3
—
0
.
CLEAR
STORE CURVE
RECALL CURVE
STORE METHOD
RECALL METHOD

- **Micro-floppy disk**
- **64 button control panel**
- **40 character alphanumeric display**

TANGENT FIT
STANDARD-1 DPP

For more information on the Model 384-1 System, write or call today:

EG&G PRINCETON APPLIED RESEARCH
P. O. BOX 2565 • PRINCETON, NJ 08540 • 609/452-2111

Circle #173 for additional information only
See us at the Pittsburgh Conference, March 5-9, Booths #113-#120

Peak separation you've never seen before.

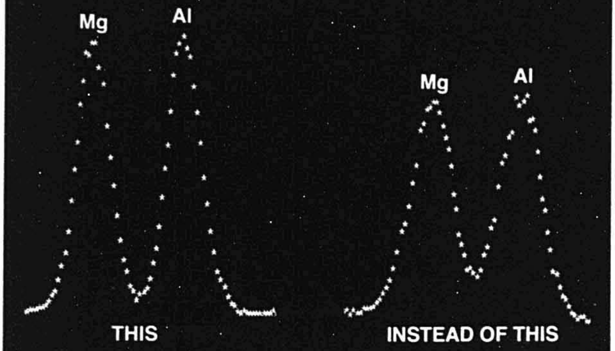

New from this X-ray fluorescence analyzer.

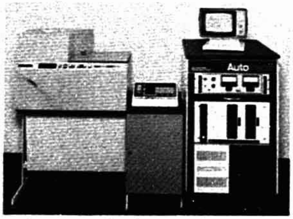

A new and unique pulse processor gives our SPECTRACE™ analyzer guaranteed resolution of 150 eV—the best ever achieved in an energy-dispersive X-ray fluorescence analyzer. This resolution, coupled with peak shifts no greater than 3 eV at maximum count rate, lets you detect light elements more reliably and quantify them more accurately.

The spectrum at left above shows an actual peak separation using the new pulse processor. That at right, with overlapping peaks, was made using a conventional processor in the same analyzer.

SPECTRACE 440 can make automatic unattended analyses of up to 40 samples—solids, liquids, powders or deposits on filter paper. Makes qualitative and quantitative analyses of all elements from Na to Pu. Handles samples from 1 mm in diameter to a foot high. Has superb sensitivity, repeatability and long-term stability.

Our applications laboratory and engineering group will work with you to help solve your analytical problem. That way you *know* you'll get the results you want after your SPECTRACE is delivered.

Over 50 SPECTRACE analyzers are now in use. And we'll give you the name of every single user—because we know every one will give you a favorable report. One thing they'll report is the service they get: personal instruction, an applications school, software school—and follow-up visits just to make sure you're getting the most out of your SPECTRACE.

Send for our highly informative brochure now. Contact United Scientific Corporation, Analytical Instrument Division, Dept. C, 1400 Stierlin Road, P.O. Box 1389, Mt. View, California 94042. Phone (415) 969-9400.

See SPECTRACE at the Pittsburg Conference, Booths 1702 & 1704

USC UNITED SCIENTIFIC
ANALYTICAL INSTRUMENTS DIVISION

CIRCLE 212 ON READER SERVICE CARD

in their infancy. Both look quite promising. One or both of these variants of coherent Raman spectroscopy may give analytical chemists the means to obtain Raman spectra of fluorescent materials at trace concentrations within the next year or two.

Acknowledgment

The authors thank G. Patrick Ritz and Jeanne Haushalter who have been extensively involved in the development and applications of our coherent Raman system.

References

(1) C.-W. Tsai and M. D. Morris, *Anal. Chim. Acta*, **76,** 193 (1975).
(2) L. C. Hoskins and U. Alexander, *Anal. Chem.*, **49,** 695 (1977).
(3) J. Behringer, in "Molecular Spectroscopy, Specialist Periodic Reports," R. F. Barrow, D. A. Long, and D. J. Millen, Eds., The Chemical Society, pp 170–3, London, England, 1974.
(4) J. Behringer, *ibid.*, Vol. 3, pp 163–280, 1975.
(5) B. B. Johnson and W. L. Peticolas, *Ann. Rev. Phys. Chem.*, **27,** 465 (1977).
(6) T. G. Spiro and P. Stein, *ibid.*, **28,** 501 (1977).
(7) A. Warshel, *Ann. Rev. Biophys. Bioeng.*, **6,** 273 (1977).
(8) T. G. Spiro, in "Vibrational Spectra and Structure," J. R. Durig, Ed., pp 101–20, Elsevier, Amsterdam, The Netherlands, 1976.
(9) J. Brandmüller, *Z. Anal. Chem.*, **170,** 29 (1959).
(10) R.J.H. Clark, in "Advances in Infra-Red and Raman Spectroscopy," R.J.H. Clark and R. E. Hester, Eds., Vol. 1, pp 143–72, Heyden, London, England, 1975.
(11) C. W. Brown and P. F. Lynch, *J. Food Sci.*, **41,** 1231 (1976).
(12) L. VanHaverbeke, P. F. Lynch, and C. W. Brown, *Anal. Chem.*, **50,** 315 (1978).
(13) R. J. Thibeau, L. VanHaverbeke, and C. W. Brown, *Appl. Spectrosc.*, **32,** 98 (1978).
(14) M. D. Morris, *Anal. Chem.*, **47,** 2453 (1975).
(15) M. S. Rahaman and M. D. Morris, *Talanta*, **23,** 65 (1976).
(16) M. D. Morris, *Anal. Lett.*, **9,** 469 (1976).
(17) D. L. Jeanmaire, M. R. Suchanski, and R. P. Van Duyne, *J. Am. Chem. Soc.*, **97,** 1699 (1975).
(18) J. L. Anderson and J. R. Kincaid, *Appl. Spectrosc.*, **32,** 356 (1978).
(19) W. H. Woodruff and G. H. Atkinson, *Anal. Chem.*, **48,** 186 (1976).
(20) W. H. Woodruff and S. Farquharson, *ibid.*, **50,** 1389 (1978).
(21) P. J. Trotter, *J. Phys. Chem.*, **82,** 2396 (1978).
(22) H. Yamada, Y. Amamiya, and H. Tsubomura, *Chem. Phys. Lett.*, **56,** 591 (1978).
(23) P. P. Yaney, *J. Opt. Soc. Am.*, **62,** 1297 (1972).
(24) R. P. Van Duyne, D. L. Jeanmaire, and D. F. Shriver, *Anal. Chem.*, **46,** 213 (1974).
(25) F. E. Lytle and M. S. Kelsey, *ibid.*, p 855.
(26) J. M. Harris, R. W. Chrisman, F. E. Lytle, and R. S. Tobias, *ibid.*, **48,** 1937 (1976).
(27) S. Burgess and I. W. Shepherd, *J. Phys., E,* **10,** 617 (1977).
(28) A. B. Harvey, *Anal. Chem.*, **50,** 905A (1978).

NICOLET MX-1

IR SPECTROSCOPISTS...
Thinking of buying a
dispersive spectrometer?

Think Again!

Come to Booths 513-519 at the 1979 Pittsburgh Conference for the unveiling of an FT-IR masterpiece from Nicolet at a price that will probably change your mind! (If you can't attend the unveiling, please phone or write Nicolet for complete details.)

**NICOLET
INSTRUMENT
CORPORATION**

5225 Verona Road
Madison, Wisconsin 53711
Telephone: 608/271-3333

CIRCLE 150 ON READER SERVICE CARD

(29) W. M. Tolles, J. W. Nibler, J. R. McDonald, and A. B. Harvey, *Appl. Spectrosc.*, **31,** 253 (1977).
(30) M. D. Levenson, *Phys. Today*, **30** (5), 44 (1977).
(31) H. C. Andersen and B. S. Hudson, in "Molecular Spectroscopy, Specialist Periodic Reports," R. F. Barrow, D. A. Long, and D. J. Millen, Eds., Vol. 5, The Chemical Society, London, England, 1977.
(32) R. F. Begley, A. B. Harvey, R. L. Byer, and B. S. Hudson, *J. Chem. Phys.*, **61,** 2466 (1974).
(33) P. R. Regnier and J.P.E. Taran, *Appl. Phys. Lett.*, **23,** 240 (1973).
(34) R. F. Begley, A. B. Harvey, and R. L. Byer, *ibid.*, **25,** 387 (1974).
(35) D. Heiman, R. W. Hellworth, M. D. Levenson, and G. Martin, *Phys. Rev. Lett.*, **36,** 189 (1976).
(36) M. D. Levenson and J. J. Song, *J. Opt. Soc. Am.*, **66,** 641 (1976).
(37) W. J. Jones and B. P. Stoicheff, *Phys. Rev. Lett.*, **13,** 657 (1964).
(38) E. S. Yeung, *J. Mol. Spectrosc.*, **53,** 379 (1974).
(39) L. B. Rogers, J. D. Stuart, L. P. Goss, T. B. Malloy, Jr., and L. A. Carreira, *Anal. Chem.*, **49,** 959 (1977).
(40) J. Nestor, T. G. Spiro, and G. Klauminzer, *Proc. Nat. Acad. Sci.*, **73,** 3329 (1976).
(41) B. J. Hudson, W. Hetherington, S. Kramer, I. Chalsay, and G. K. Klauminzer, *ibid.*, p 3798.
(42) L. A. Carreira, T. C. Maguire, and T. B. Malloy, *J. Chem. Phys.*, **66,** 2621 (1977).
(43) S. H. Lin, E. S. Reid, and C. J. Tredwell, *Chem. Phys. Lett.*, **29,** 389 (1974).
(44) L. A. Carreira, T. C. Maguire, and T. B. Malloy, Jr., 32nd Symp. on Molecular Spectroscopy, Paper No. WE7, Ohio State University, Columbus, Ohio, June 1977.
(45) P. B. Dutta, J. R. Nestor, and T. G. Spiro, *Proc. Nat. Acad. Sci.*, **74,** 4146 (1977).
(46) P. B. Dutta, J. R. Nestor, and T. G. Spiro, *Biochem. Biophys. Res. Commun.*, **83,** 209 (1978).
(47) G. P. Ritz and M. D. Morris, *J. Raman Spectrosc.*, submitted for publication.
(48) A. Owyoung, *Opt. Commun.*, **22,** 323 (1977).
(49) A. Owyoung and E. D. Jones, *Opt. Lett.*, **1,** 152 (1977).
(50) A. Owyoung, *IEEE J. Quantum Electron.*, **QE-14,** 192 (1978).
(51) M. D. Morris, D. J. Wallan, G. P. Ritz, and J. P. Haushalter, *Anal. Chem.*, **50,** 1796 (1978).

Financial support by the National Institutes of Health (Grant GM22604).

Michael Morris (right) is associate professor of chemistry at the University of Michigan. His research interests are coherent Raman spectroscopy and other applications of laser spectroscopy. **David Wallan** (left) is a graduate student in chemistry at the University of Michigan. He holds a full-year ACS Division of Analytical Chemistry Fellowship, sponsored by the Procter & Gamble Co.

The laboratory performers from Houston Atlas.

- The hallmark of the Houston Atlas performers is the achievement of superior accuracy, reliability, and effortless precision performance . . . without the need for skilled technicians. Plus - application flexibilities that deliver even more performance for your dollar.
- Whether you work with gases or liquids or solids, in low ppb or high %, Houston Atlas has a "can-do" performer for you.
- Such as the versatile Total Sulfur Analyzer that also measures H_2S, SO_2, NO_x, and other pollutants with just a change of tape. Its patented Photorateometric® brain routinely reads trace concentrations in less than 6-minutes.
- Or . . the PPM Reference Standard Generator. This non-permeation instrument automatically generates fresh, uniformly blended calibration standard samples the instant they are needed, with unrestricted ppb, ppm, or % rangeability.
- Or, the Microjector Syringe Drive that beats anything on the market today. You get precise motion control with this versatile linear motion injection/retraction device with digital timing.
- As your applications get tougher, your choice of instruments can get easier with your selection of a Houston Atlas performer.
- **Get complete details by calling Marketing at 713/462-6116 . . or write Houston Atlas, Inc., 9441 Baythorne Drive, Houston, TX. 77041. Do it today!**

HOUSTON ATLAS, INC.

Or better yet, see these performers perform for you at the
PITTSBURGH CONFERENCE in CLEVELAND
SPACES 1502-1504.

Model 601
PPM REFERENCE
STANDARD GENERATOR

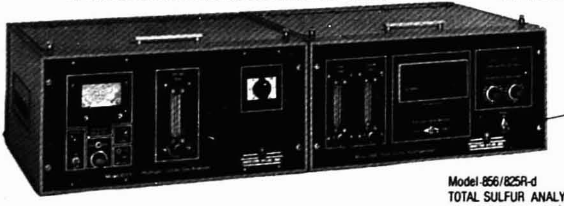

Model-856/825R-d
TOTAL SULFUR ANALYZER

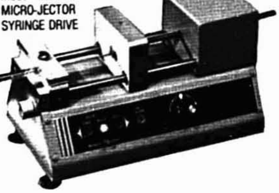

Model 1001
MICRO-JECTOR
SYRINGE DRIVE

CIRCLE 99 ON READER SERVICE CARD

There are many reasons why we have already updated over 3000 DU's®.

And why your DU® or DU-2® should be next.

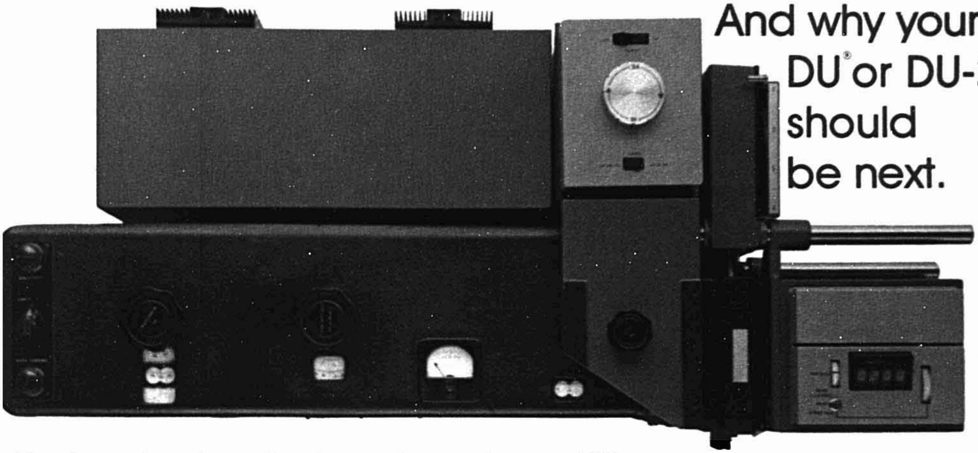

Though it may be gathering dust, the monochromator from your DU® or DU-2® is a good one, rugged and reliable. Above all, it's useful, whether you're into industrial or biomedical research, quality control, pollution studies, or similar disciplines. By replacing everything *except* the monochromator with a Gilford Series 252 update, we create for you a complete, modern spectrophotometer.

Solid-state linear absorbance photometer:

L.E.D. display to 3.000*A*; readout in absorbance *and* concentration units; recorder calibration controls; BCD output for interface with printers, computers; easy operation, no need for sensitivity or dark current adjustments, no shutters.

NBS-traceable absorbance standards:

Easy absorbance calibration at three points in absorbance range; routine determination of photometric linearity.

Four-place manual cuvette positioner:

Precise cam-operated positioning and sliding aperture mask for routine measurement with standard, micro, or flow-through cuvettes; integral full-flooding thermoplates for circulation of fluids from constant temperature source; economical option for automatic cuvette positioning.

Optical bench adapter/dual light source:

Tungsten and deuterium lamps plus new optical components for enhanced energy throughput; easy interchangeability of standard positioner with optional accessories for enzyme analysis, gel electrophoresis, thermal melts, rapid sampling, and more.

Solid-state power supply:

Stable, transistorized power for entire spectrophotometer; no batteries, reduced maintenance.

You'll find nothing with matching capabilities at anything NEAR the price.

For further information, call or write GILFORD INSTRUMENT LABORATORIES INC., Dept 5-7-12, Oberlin, OH 44074 (216) 774-1041.

® Registered trademark of Beckman Instruments, Inc.

gilford® INSTRUMENT

Oberlin, Ohio 44074
Paris (Malakoff), France
Düsseldorf, W. Germany
Teddington, Middx., England
(216) 774-1041 Telex: 98-0456

CIRCLE 85 ON READER SERVICE CARD

Introducing the $895 Milli-R/Q™ Water Purifier. It produces 3 liters of Type II* water per hour – with better quality than even double distillation.

Comparably equipped stills cost about $1,500, need weekly cleaning, and don't give you water of consistent quality. The best thing about them is they'll help us sell the new Milli-R/Q Water Purifier.

The system runs unattended directly off your tap, storing purified water in a built-in 20 liter self-contained tank. When you turn the spigot on, a resistivity monitor indicates purity.

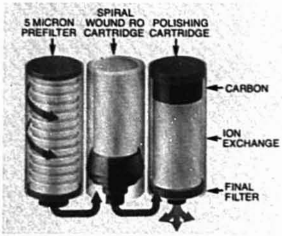

Here's the way the Milli-R/Q Water Purifier works. Water first passes through a pre-filter, followed by a reverse osmosis membrane. And then it flows into a unique three-stage polishing cartridge – carbon removes the organics; a nuclear-grade ion exchange resin takes out the inorganics; and a Millipore membrane filter stops bacteria and particulates.

And because this whole cartridge system is disposable, the Milli-R/Q Water Purifier is easy to maintain. In a typical application, cartridge replacement is necessary only a few times a year.

Installation is just as easy. The whole unit is 53 cm long by 42 cm wide by 41 cm high, so it fits almost anywhere. And because it comes complete, including cartridges, all you do is attach it to a tap. In a few minutes the system is fully operational. And since it operates on water pressure at room temperature, the Milli-R/Q Water Purifier saves on energy and water consumption.

So instead of spending a lot of money on a still, spend less and get something a lot better. To learn more about the Milli-R/Q Water Purifier, call this toll-free number (800) 225-1380. Or write to us for more information: Millipore Corporation, Water Systems Division, Bedford, MA 01730. (In Canada, call 800-268-4881 toll-free; in Massachusetts, call 617-275-9200.)

Water
Systems
Division
MILLIPORE®

CIRCLE 145 ON READER SERVICE CARD

™Trademark of Millipore Corporation
*Greater than 1 megohm-cm resistivity. Meets CAP/ASTM standards.

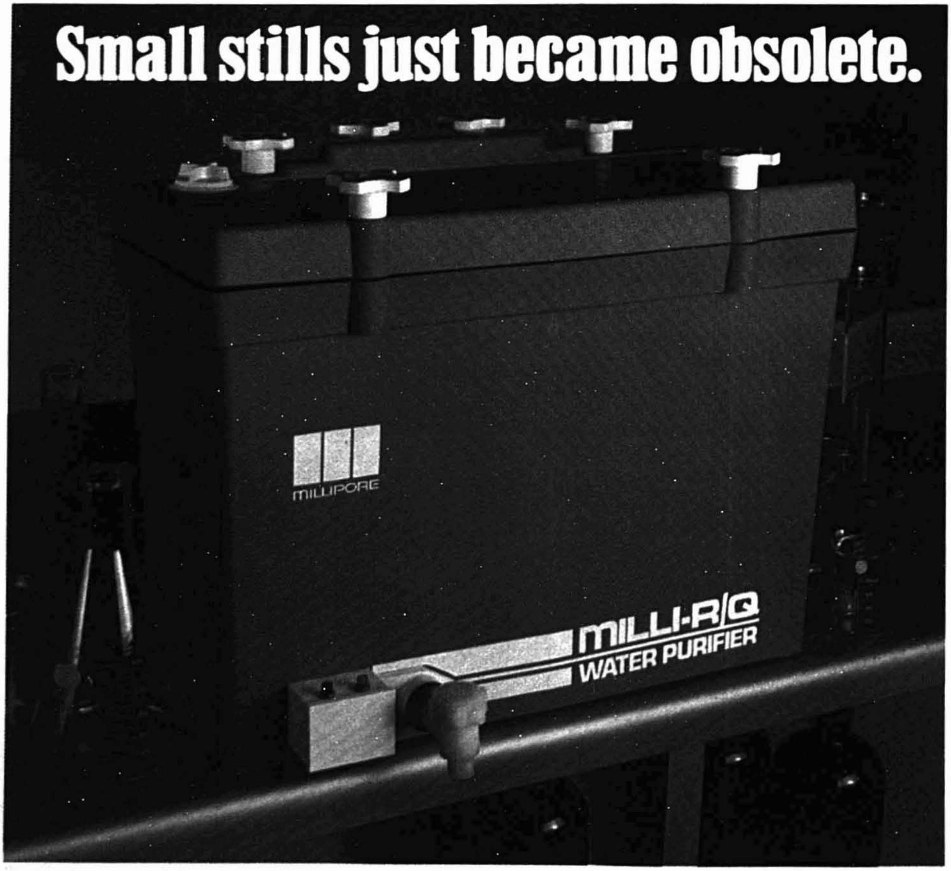

ANALYTICAL CHEMISTRY Appoints Three New Instrumentation Advisory Panel Members

ANALYTICAL CHEMISTRY has appointed three new members to its Instrumentation Advisory Panel. They are Tomas Hirschfeld, Block Engineering, Cambridge, Mass.; Carter L. Olson, College of Pharmacy at the Ohio State University; and Thomas H. Ridgway, University of Cincinnati.

Members who are leaving the panel after serving three-year terms are Nathan Gochman, Veterans Administration Hospital and University of California, San Diego; Gary Horlick, University of Alberta, Canada; and James N. Little, Waters Associates.

The six members who will continue to serve on the panel are Gary D. Christian, University of Washington; Catherine C. Fenselau, the Johns Hopkins University School of Medicine; Gary M. Hieftje, University of Indiana; Peter T. Kissinger, Purdue University; C. David Miller, American Instrument Co.; and Sidney L. Phillips, Lawrence Berkeley Laboratory, University of California.

The Advisory Panel members lend their expertise to the continued development of interesting and provocative editorial coverage of the interdisciplinary field of instrumentation. They aid both in the selection of subject matter and possible authors and in the development of the scope and aims of the feature itself. Panel members also review material for the feature and sometimes contribute directly as authors or coauthors of articles.

The goal of the instrumentation feature is to help broaden and deepen the reader's knowledge in related disciplines so that cross-fertilization of ideas might provoke original and useful thinking in the area of instrumentation for solving analytical problems. The articles are written by the specialist but directed toward the nonspecialist. They are not intended to be lengthy review articles but should serve to introduce and promote interest in the subject under discussion. Areas of interest include not only instrument design but also specific applications. Experts in disciplines other than chemistry are often invited as authors when the topic has great potential application to analysis. Although articles are normally invited, unsolicited articles are also considered if the topic is appropriate.

Brief biographical sketches of the new panel members follow.

Tomas Hirschfeld is currently chief scientist of Block Engineering, Cambridge, Mass., and a visiting professor at Indiana University, Bloomington. He received his PhD summa cum laude in 1967 from the National University, Uruguay. Dr. Hirschfeld has taught spectroscopy courses at several universities and has over 200 papers or patents in reflection, Raman, fluorescence, and Fourier transform spectroscopy. A Fellow of the Optical Society of America and a senior member of the Institute of Electronic and Electric Engineers, he is also a member of the Editorial Boards of the *Journal of Applied Spectroscopy* and the *Journal of the Optical Society of America*, and editorial advisor to *Optics Letters* and *Applied Spectroscopy*. Dr. Hirschfeld received the IR-100 award in 1975 for development of the CIRA gas chromatographic infrared analyzer and again in 1977 for the Virometer rapid virus detection system. He is a 1978 ACS and Society for Applied Spectroscopy tour speaker, and is the recipient of the 1978 Meggers award from the Society for Applied Spectroscopy.

Carter L. Olson is professor of pharmaceutical analysis in the College of Pharmacy at the Ohio State University. In 1956 he received his BS degree from Wisconsin State University, Stevens Point, and his PhD in 1962 from the University of Kansas where he worked under the direction of Ralph N. Adams. He then did two years of postdoctoral research with Walter J. Blaedel at the University of Wisconsin, Madison. Since 1963 Dr. Olson has been on the faculty of the Ohio State University, College of Pharmacy. His research interests include the development of electroanalytical methods for measuring clinically important enzyme reactions, flowstream spectroelectrochemistry, and methods for measuring membrane transport utilizing two-dimensional vidicon spectroscopy. He is also working on the development of a GEMSAEC-type multichannel centrifugal analyzer using electrochemical sensors. Dr. Olson is a member of ACS, Sigma Xi, and Rho Xi.

Thomas H. Ridgway is assistant professor of chemistry and director of instrumentation at the University of Cincinnati. He received his BS degree from the University of Michigan and his PhD degree from the University of North Carolina under the direction of C. N. Reilley. In 1973–76 Dr. Ridgway was assistant professor of chemistry at Texas A & M University, and in 1976 he joined the Department of Chemistry at the University of Cincinnati. His research interests include electrochemical methods of analysis and the application of mini- and microcomputers to chemical instrumentation. Dr. Ridgway is a member of ACS and the Electrochemical Society.

Tomas Hirschfeld

Carter L. Olson

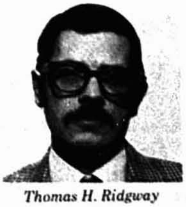

Thomas H. Ridgway

Determination of Lithium Levels by AA Spectrometry

At the University of California's School of Medicine in Los Angeles, researchers are developing an analysis method that will allow clinical laboratories to provide very accurate lithium determinations on blood samples of patients suffering from manic depression. Lithium helps to control manic depression, although the mode of operation is still unknown. The difficulty with lithium treatment is that too great a dosage is dangerous and too little is ineffective. A therapeutic dose might be 1 mmol/L plasma, whereas a toxic dose would be only 2 mmol/L plasma of lithium carbonate. Barbara Ehrlich, a PhD candidate who has been doing research on membrane transport biophysics for the past three years, is analyzing the drug's effect on patients' moods by studying the way lithium affects red blood cells, the rate at which it enters and then leaves these cells, and the change in lithium concentration in the whole body over a 24-h period.

Using a Varian Model 1200 atomic absorption spectrometer in the flameless mode, a carbon rod atomizer (CRA 90), and an automatic sampling device (ASD 53), Ehrlich measures plasma, red cell lithium levels, and lithium movement across the cell membrane with just 10 mL of blood. Using standard methods of analysis would have required 400 mL. Ehrlich does a minimum amount of preparation to test her blood-lithium samples. First, she separates the plasma from the red cells and then dilutes the plasma and the cells with ammonium nitrate to remove interfering ions. The sample goes into the spectrometer which has a hydrogen enhancement device that helps atomize more lithium by changing the gaseous environment around the sample chamber. In the spectrometer the sample is dried, reduced to ashes to remove any remaining protein and interfering ions, and is atomized into the absorption beam. There is an absorption readout, which Ehrlich converts to lithium concentrations.

Ehrlich found that lithium does affect cell membranes and possibly nerve membranes too. This finding, coupled with other research, suggests a biochemical basis for manic depressive illness. Learning the exact mechanism of lithium's action is important because manic depression is the only psychiatric illness that can be controlled with a specific drug.

Research work of this kind could lead to the development of a spectrometer that would let a clinical laboratory technician tell a doctor exactly how much lithium the patient needs to rapidly achieve a therapeutic response. Because lithium has fewer side effects, it is also being tested as treatment for other medical problems such as premenstrual tension, alcoholism, and explosive personality.

Barbara Ehrlich is putting blood serum samples into the spectrometer's automatic sampler in preparation for lithium analysis

Biotechnology Resource

One of the nation's most versatile centers for analyzing complex chemicals is now open for regional and national business in the Biochemistry Building at Michigan State University (MSU). The million-dollar facility is one of seven mass spectrometry laboratories designated as "biotechnology resources" by NIH. It is supported by the NIH's Division of Research Resources and, as such, serves all researchers funded by NIH. Although the MSU facility is considered a regional one, it has certain capabilities that are utilized by researchers from other regions, says Charles C. Sweeley, MSU professor of biochemistry. He and John F. Holland, associate professor of biochemistry, are codirectors of the facility, which was established in 1968 by NIH as part of Dr. Sweeley's laboratory. Recent growth in equipment and use necessitated the move to the new location.

Use of the facility by scientists from other institutions has been numerous and broad. One regular user has been the U.S. Army Laboratories at Natick, Mass., where preservation of food by radiation is being studied. Other off-campus users include researchers from the University of California at Berkeley, Mt. Sinai Medical School in New York, Washington University, University of Texas, University of Minnesota, University of Guelph in Ontario, Vanderbilt University, University of Houston, Johns Hopkins University, and the University of Oklahoma. The facility also trains young scientists in the use of mass spectrometry.

J. T. Baker Chemical Co. Nobel Laureate Lecture

Yale University's Chemistry Department sponsored the inaugural J. T. Baker Chemical Co. Nobel Laureate Lecture on Nov. 29, 1978. Christian Anfinsen, chief of the Laboratory of Chemical Biology at the Institutes of Arthritis, Metabolic and Digestive Diseases in Bethesda, Md., and Nobel prize winner in chemistry in 1972, delivered the first lecture in a series called "Perspectives for the Future." He spoke on the development of synthetic immunogens and stimulants of the immune response. These investigations promise to yield highly specific agents for the cure and prevention of viral diseases, he said. Dr. Anfinsen summed up his lecture in this way:

Our current knowledge of the chemical and three-dimensional structures of macromolecules, and the resulting opportunity to interpret biological function in terms of struc-

HIGH MAGNIFICATION MAY BE IMPORTANT, BUT . . .

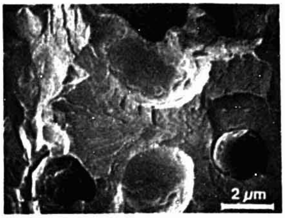

Secondary electron micrograph of a cast iron fracture surface.

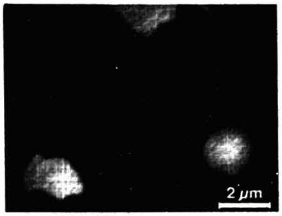

Carbon Auger image identifies the graphite nodules on the fracture surface.

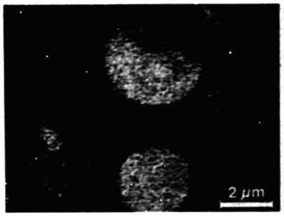

Antimony image reveals a thin layer of Sb segregation in the nodule craters.

. . . For Many Materials Problems, It's Just Not Enough. Where structure or topography is the key, a good SEM is indispensable. But where surface compositions are critical, a SEM doesn't provide the needed information. And accessories such as SIMS offer small improvement. For one reason or another — poor vacuum, ambiguous data, poor chemical spatial resolution, or instrumental restrictions — little useful information on surface chemistry is provided.

That's Where The SuperSAM Comes In.

SuperSAM — the PHI Model 590, Scanning Auger Microprobe — was designed as a high performance surface analysis instrument. In addition to a SEM capability, it provides spatially resolved data on surface chemistry — data that leads to solutions of real-world materials problems. It often adds that critical piece of information that means the difference between success and failure.

A typical SEM, for example, would provide a good micrograph of the cast iron fracture surface similar to the one above obtained with the SuperSAM. But, it is unlikely that a SEM, with or without accessories, could identify the surface chemistry with the precision demonstrated in the images of C and Sb, also obtained with the SuperSAM. The C image identified the graphite nodules present in the cast iron. The Sb image revealed the presence of antimony in the craters, left when carbon nodules were pulled away on fracture. Antimony had segregated to the interface between the nodules and the metal in a layer approximately 30Å thick.

SuperSAM Offers A Complete Analysis.

Topographical data and a variety of chemical data are easily obtained. Point analyses, elemental images and line scans, depth profiles, and quantitative analyses combine to supply a complete picture of surface composition. Instrument operation can also be automated for expanded data manipulation and operating ease.

SuperSAM Is Backed By PHI Expertise.

SuperSAM is backed by a well-established Analytical Laboratory and a technical staff with unparalleled experience in the surface analysis field.

So if surface chemistry is as important as high magnification pictures, and you want the best in surface analysis, contact the leader in surface analysis instrumentation. Write Physical Electronics Division, Perkin-Elmer Corporation, 6509 Flying Cloud Drive, Eden Prairie, MN, U.S.A., 55344, or call (612) 941-5540.

PERKIN-ELMER
Physical Electronics

CIRCLE 176 ON READER SERVICE CARD

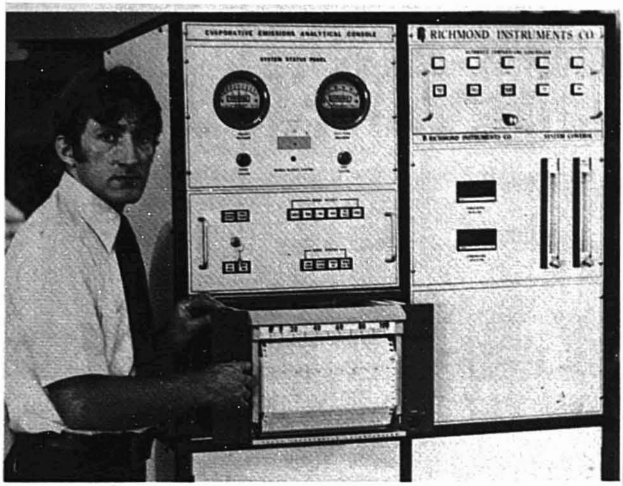

"TI recorders help our systems operate 24 hours a day."

. . . says Dennis Mach, General Manager of Richmond Instruments Company, manufacturers of emission control monitors.

"We have no problems with TI recorders. They are reliable, easy to mount, clean, and easy to handle. That's why we use them in the vast majority of our emission monitors. We like the resolution of the wide chart and the good inking system. In addition, the removable back panel makes special modifications easy."

"We especially like the reliable heavy-duty construction because our systems must operate with little or no down-time to keep our customers satisfied."

Richmond Instruments is only one of many satisfied users of TI strip chart recorders. The chances are good that you, too, can profit from the high quality, accuracy and heavy-duty construction of the TI recorders. There's a broad selection of designs to choose from.

Drives include unidirectional and bidirectional synchro systems. Wide and dual-grid *servo/riter*II* models give a choice of one to five full overlapping channels on a 8.75" grid. And if space saving is a requirement, the Lab/Test recorders use only 7 inches of panel height.

Options include full scale adjustable zero, variable spans and inputs, electric pen lifters, felt tip or capillary inking, bidirectional take-up system, synchro or digital drives, and stepper.

TI recorders are backed by more than twenty years of proven quality, reliability, accuracy and performance plus a nationwide network of sales and service offices to serve you.

For further information, please contact Texas Instruments Incorporated, P.O. Box 1443, M/S 619, Houston, Texas 77001. Or phone (713) 491-5115, ext. 3333, TWX 910-867-4702, Telex 775938.

*Trademark of Texas Instruments Incorporated

TEXAS INSTRUMENTS
INCORPORATED

CIRCLE 210 ON READER SERVICE CARD

ture, has made possible many exciting new approaches to the understanding of cell function and of human disease and its treatment. We know that large polypeptides, direct one-dimensional translations of genetic information, can fold spontaneously into functional and reproducible geometries. This fortuitous aspect of evolutionary design permits us to undertake the chemical synthesis of enzymes, large hormones, and molecules with receptor or recognition properties. A particularly interesting spin-off of macromolecular chemistry is the development of synthetic immunogens and stimulants of the immune response. These investigations promise to yield highly specific agents for the cure or prevention of viral diseases.

The new Nobel Laureate Lecture Series follows a recent announcement by ACS and J. T. Baker Chemical Co. of a Nobel Laureate Signature Award to be granted to outstanding doctoral candidates in the fields of science and medicine. The award, to be administered by ACS, will include a $2000 grant to the winner and a plaque bearing the signatures of more than 50 Nobel winners. J. T. Baker's Warren K. Kinglsey, chairman of the lecture series, announced the new program and stated, "It is our hope that we may be able to schedule the Nobel Laureate Lecture Series at various major learning centers in the U.S."

New York Society for Applied Spectroscopy Medal Awardee

Bernard J. Bulkin, dean of arts and sciences and professor of chemistry at Polytechnic Institute of New York, is the recipient of the 1978 New York Society for Applied Spectroscopy Medal. The medal is awarded each year to recognize excellence for research in spectroscopy. Dr. Bulkin has conducted research on infrared and Raman spectroscopy for 12 years and has coauthored more than 40 papers in this area. His major interest is in the spectra of liquid crystals and ordered fluids. A graduate of Polytechnic, he has been dean of arts and sciences for three years. Prior to becoming dean, he was on the faculty of City University of New York. Dr. Bulkin earned a PhD in physical chemistry from Purdue University and did postdoctoral work at the Swiss Federal Institute of Technology. Recipient of the 1975 Coblentz Award, he is a member of the Society for Applied Spectroscopy, ACS, Optical Society of America, New York Academy of Sciences, and the Coblentz Society.

Simultaneous I.C.P.A.E.S. Elemental Analyzer

Designed for routine use, the JY-48 offers rapid analysis of up to 48 elements simultaneously and uses time-proven techniques to enhance reliability and speed.

Will accept two sources. For example: a spark stand plus an Inductively Coupled Plasma source. Use for analysis of ferrous and non-ferrous metals and alloys, oils, industrial effluent, coals, ores and rare earths. Holographic diffraction gratings. Fully computer operated. Also ask about our JY-38 Sequential Plasma Spectroanalyzer.

Instruments SA, Inc., J-Y Optical Systems Division, 173 Essex Avenue, Metuchen, N.J. 08840 (201) 494-8660. Telex 844-516. In Europe, Jobin Yvon, Division d'Instruments SA, 16-18 Rue du Canal, 91160 Longjumeau, France. Tel. 909.34.93 Telex JOBYVON 842-692882.

JOBIN YVON **Instruments SA, Inc.**
J-Y Optical Systems Division

CIRCLE 108 ON READER SERVICE CARD

Raman

SEE THE LIGHT!

The Ramanor HG-2S double monochromator Raman system offers the greatest throughput in the industry, the simplest optical design and the largest, most accessible sample chamber. The Ramanor and its full line of accessories ensures dramatic results.

Call or write for more information on the most advanced Raman system in the world at Instruments SA, Inc.

Instruments SA, Inc., J-Y Optical Systems Division, 173 Essex Avenue, Metuchen, N.J. 08840 (201) 494-8660 Telex 844-516. In Europe, Jobin Yvon, Division d'Instruments SA, 16018 Rue du Canal, 91160 Longjumeau, France. Tel. 909.34.93 Telex JOBYVON 842-692882

JOBIN YVON **Instruments SA, Inc.**
J-Y Optical Systems Division

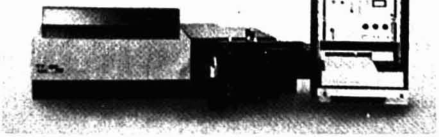

CIRCLE 109 ON READER SERVICE CARD

MODERNIZE YOUR OLD SPECTROMETER

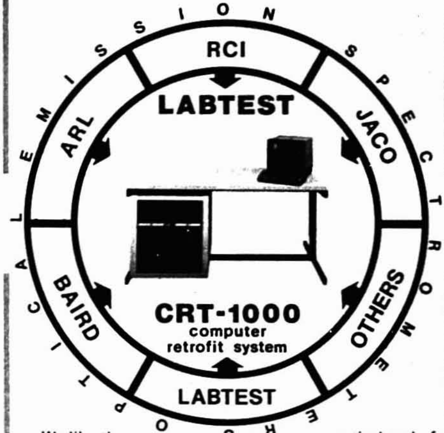

We like the optical end of OLD spectrometers made by ARL, Baird, JACO, RCI, and others. By-and-large they are still doing a good optical job. But technological advances have obsoleted their readout equipment. And modern laboratory demands have outpaced their capability. To solve this problem we designed the CRT-1000 Data Acquisition and Readout System. It is a highly reliable microprocessor controlled data acquisition, spectrometer control, and readout system designed specifically for use with optical emission spectrometers. IT WILL BRING YOUR SPECTROMETER UP TO CURRENT TECHNICAL STANDARDS FOR ABOUT 1/3 THE COST OF A COMPLETE NEW SYSTEM. The CRT-1000 will satisfy your existing readout requirements and provide additional features such as video display and/or hard copy printout of percent concentration, interelement corrections, averaging, automatic standardization, daily logging, and many other features. And you don't need a computer programmer to run it.

Over 100 major corporations have selected Labtest computer products and Labtest software. And Labtest computer installations have already logged hundreds of thousands of hours of field operation.

If reliability, low maintenance, flexibility, speed, and freedom from operator error are important in YOUR laboratory—modernization of your existing spectrometer system with the CRT-1000 may be the answer to your needs. Call us collect today to discuss your application. Ask for the Retrofit Project Manager.

LABTEST
EQUIPMENT
COMPANY
11828 La Grange Avenue, Los Angeles, CA 90025
Telephone (213) 478-2518 478-1610
subsidiary **SYSTRON DONNER** corporation

CIRCLE 126 ON READER SERVICE CARD

The EG&G PARC Photoacoustic Spectrometer can measure:

- Gels
- Clays
- Fabrics
- Plastics
- Polymers
- Catalysts
- TLC Plates
- Phosphors
- Cosmetics
- Paint Chips
- Suspensions
- Pharmaceuticals

Fast–with little sample preparation and it gives you BETTER RESULTS!

The EG&G PARC Model 6001

Features: • UV-VIS-IR Spectra automatically • Microprocessor memory and control • Flat Baseline • Variable Analysis Depth

FREE! ALL ABOUT PAS

EG&G PARC

EG&G
PRINCETON APPLIED RESEARCH
P. O. BOX 2565
PRINCETON, N.J. 08540
609/452-2111

442

Circle 177 for additional information only

News

1980 Pittsburgh Applied Analytical Chemistry Award Nominations

This award is sponsored by the Society for Analytical Chemists of Pittsburgh and consists of a $1000 honorarium given annually for an outstanding paper that was published in the previous five years and had an important impact in the field of applied analytical chemistry. Review papers and papers describing instrument construction are not considered to fall within the scope of this award. Papers published by members of the SACP are not eligible. Nominations for the award may be made by anyone, including the authors. Any paper published between Jan. 1, 1974, and Dec. 31, 1978, is eligible and may be nominated by sending five copies of the nominated paper, no later than June 15, 1979, to: Mr. Robert Mainier, Koppers Co., Inc., 440 College Park Drive, Monroeville, Pa. 15146.

15th Benedetti-Pichler Award Nominations

The American Microchemical Society is inviting nominations for its 15th annual Benedetti-Pichler Award. This award is given in recognition of service to microchemistry in its broadest sense, including research, application, administration, teaching, or other means of promoting the advancement of microchemistry. The nominee need not be a member of the society. Nominations, stating the reason for nomination and citing the work of the nominee, should be made in writing and must be received by June 1, 1979. Nominations and requests for further information should be addressed to: Lisa Hallquist, J. T. Baker Chemical Co., 222 Red School Lane, Phillipsburg, N.J. 08865.

Call for Papers

Photoacoustic Spectroscopy
Iowa State University, Ames, Iowa. Aug. 1–3, 1979. Sponsored by the Optical Society of America. Contributed papers covering original unpublished work on the meeting subjects will be accepted for presentation. Session topics will cover signal theory for various sample classes and measurement conditions, experimental methods for different types of measurements, and quantitative studies using the technique to characterize various sample properties and processes. Each author must submit a 25-word abstract plus a summary of the presentation of up to four pages including figures, tables, equations, etc. All abstracts and summaries must reach the Optical Society office by Apr. 20, 1979. Authors will be notified whether papers have been accepted by May 18. Send papers to: Optical Society of America, Photoacoustic Spectroscopy Meeting, 2000 L St., N.W., #620, Washington, D.C. 20036. 202-293-1420

9th Annual North American Thermal Analysis Society Meeting
Holiday Inn City-Centre, Chicago. Sept. 23–26, 1979. Sessions will include Industrial Applications of Thermal Analysis, Theoretical Aspects of Thermal Analysis, High-Pressure and Combustion Thermal Analysis, Applications of Thermal Analysis to Energy Conservation, New Techniques and Instrumental Advances, and Thermal Analysis of Inorganic, Organic, and Polymer Systems. Send 150–200-word abstracts by Mar. 1, 1979, to: Inez M. Johnston, Electromagnetic Industries, Square D. Co., P.O. Box 6440, Clearwater, Fla. 33518. For more information, contact: Barbara L. Fabricant, Glass Thermochemistry R&D, Owens-Corning Fiberglass Technical Center, P.O. Box 415, Granville, Ohio 43023. 614-587-0610

Meetings

The following meetings are newly listed in ANALYTICAL CHEMISTRY. *The 1979 meetings listed earlier appear in the January issue*

- **Air Pollution Control Association Conference on Quality Assurance in Air Pollution Measurement.** Mar. 12–13. Grand Hotel, New Orleans. *Contact: Gus Von Bodungen, Louisiana Air Control Commission, P.O. Box 60630, New Orleans, La. 70160*
- **16th Annual Chicago Chromatography Discussion Group Conference on Gas Chromatography.** Mar. 20–23. University of Illinois, Chicago. *Contact: J. B. Himes, Richardson Co., 2701 W. Lake St., Melrose Park, Ill. 60160*
- **National Conference for Control of Hazardous and Toxic Materials in the Environment.** Mar. 21–23. Deauville Hotel, Miami Beach. *Contact: B. D. Zucker, Information Transfer Inc., 1160 Rockville Pike, Suite 202, Rockville, Md. 20852*
- **ACS Pentasectional Oklahoma Meeting.** Mar. 24. Stillwater, Okla. *Contact: R. D. Freeman, Dept. of Chemistry, Oklahoma State University, Stillwater, Okla. 74074*

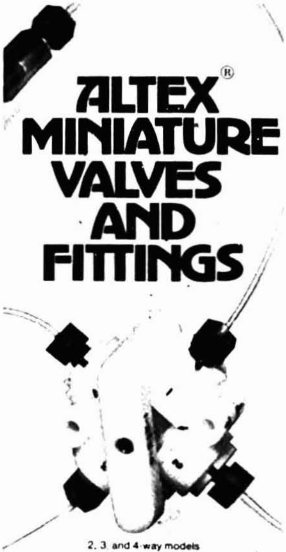

ALTEX® MINIATURE VALVES AND FITTINGS

2, 3 and 4-way models

Every inert component you need to quickly construct any liquid or gas flow system.

- ☐ CHEMICALLY INERT
- ☐ ZERO DEAD VOLUME
- ☐ LEAK TIGHT TO 500 PSI
- ☐ MATE PERFECTLY WITH GLASS-METAL-PLASTIC

Compatible with other micro-plumbing components, the Altex system includes: Tees and Crosses, Luer Adapters, Couplings, Stainless-steel and Glass Tube Adapters, Plugs, Pipe Connectors, TEFLON Tubing and Flanging Tool.

Also . . . a complete line of Liquid Chromatography Columns and Sample Injection Valves.

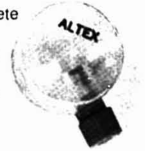

COMPLETE
CATALOG
on request

RAININ
INSTRUMENT CO, INC.

94 Lincoln Street • Brighton, MA 02135
1-800-225-4590 • TELEX 94-0687
CIRCLE 182 ON READER SERVICE CARD

ION? YAG?

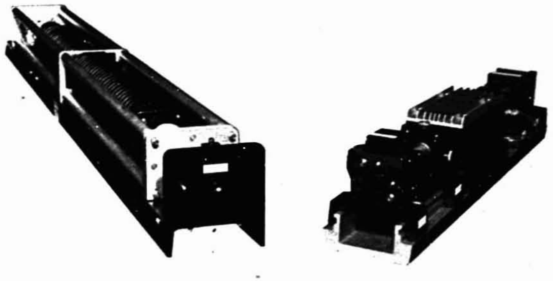

We've got'em all!

Whether you need an argon-krypton ion laser or a solid-state laser, Control Laser Corporation probably has a system to match your scientific/laboratory requirements. For work in the areas of photo-coagulation, blood plasma diagnostics, cauterization, particle analysis, primary pattern generation and the like, our ion laser line offers up to 20 W of output power with primary lines in the blue (488 nm) and the green (514 nm). On the other hand, our cw, pulsed and Q-switched lasers are ideal for tasks such as aligning laser fusion reactors, coherent anti-Stoke Raman spectroscopy, pollution monitoring and bloodless surgery. To make your job even easier, we will incorporate any of the lasers in to a laboratory work station containing (optionally) positioning stages, microscopes, cameras and the like.

For details, contact our Sales Department.

CONTROL LASER CORPORATION
HOLOBEAM® LASER, INC. - A Subsidiary

11222 Astronaut Blvd. ■ Orlando, Florida 32809
305/851-2636

CIRCLE 36 ON READER SERVICE CARD

Where Small Differences Make a Big Difference
0.007A difference on 2.6A background

New MIDAN™ Microprocessor Data Analyzer Enhances the Value of Data Generated by the DW-2a™ Spectrophotometer

Now you can expedite analyses of compounds in mixtures, correct baselines automatically, and perform other complex calculations using the new MIDAN Microprocessor Data Analyzer Accessory for our DW-2a Spectrophotometer.

With AMINCO's DW-2a Spectrophotometer, small sample differences can lead to new research territories in UV-VIS spectrophotometry. Our painstaking improvements in such parameters as photometric accuracy, stability, and system versatility extend your range of sample investigations and lead to substantial increases in overall system performance. And, the DW-2a Spectrophotometer's built-in flexibility and wide variety of capability-expanding accessories — like the MIDAN Analyzer — ensure continuing adaptability to your special applications needs.

AMINCO®

DIVISION OF TRAVENOL LABORATORIES, INC., Silver Spring, Md. 20910-Phone: 301-589-1727
European Headquarters' Rue Dautzenberg 36-38 1050 Brussels Belgium Phone (02) 648-50-02

© 1978 Travenol Laboratories, Inc.

- **EPA Oil Shale Sampling, Analysis, and Quality Assurance Symposium.** Mar. 26–28. Denver. *Contact: Jeannette King, Denver Research Institute, Chemical Division, University of Denver (Colorado Seminary), Denver, Colo. 80208*
- **Symposium on Electron Microscopy and X-Ray Applications to Environmental and Occupational Health Analyses.** Apr. 23–25. Aspen, Colo. *Contact: Philip A. Russell, Denver Research Institute, University of Denver, Denver, Colo. 80208*
- **3rd International Symposium on Control of Sulfur and Other Gaseous Emissions.** Apr. 24–26. Salford, UK. *Contact: R. Hughes, Dept. of Chemical Engineering, University of Salford, Salford, M5 4WT, UK*
- **70th Annual Meeting of the American Oil Chemists' Society.** Apr. 29–May 3. Fairmont Hotel, San Francisco. *Contact: American Oil Chemists' Society, 508 S. Sixth St., Champaign, Ill. 61820. 217-359-2344*
- **New York Microscopical Society Sessions.** May 30–June 1. Statler Hilton Hotel, New York City. *Contact: Ted Rochow, 3008 Charwood Pl., Raleigh, N.C. 27612*
- **13th Annual Conference on Trace Substances in Environmental Health.** June 4–7. University of Missouri, Columbia. *Contact: D. D. Hemphill, Environmental Trace Substances Research Center, Rte. 3, University of Missouri, Columbia, Mo. 65211*
- **XXI Colloquium Spectroscopicum Internationale/8th International Conference on Atomic Spectroscopy.** Jul. 1–6. University of Cambridge, UK. *Contact: The Secretariat, Association of British Spectroscopists, P.O. Box 109, Cambridge, CB1 2HY, UK*
- **AACC 31st National Meeting.** Jul. 15–20. New Orleans. *Contact: AACC National Office, 1725 K St., N.W., Washington, D.C. 20006. 202-857-0717*
- **1979 Symposium on Instrumentation and Control for Fossil Energy Processes.** Aug. 20–22. Denver Marriott, Denver. Topics include two-phase interface level measurement, on-line analysis and sampling, flow control systems, and reactor temperature measurement. *Contact: M. L. Holden, Director, Conference Planning and Management, Argonne National Laboratory, Bldg. 223, 9700 S. Cass Ave., Argonne, Ill. 60439. 312-972-5585*

The Preferred Source.

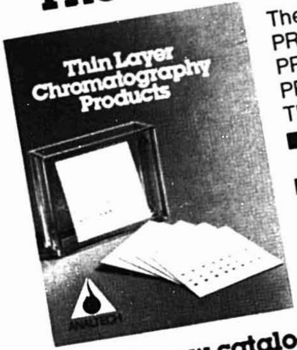

The Broadest Line of
PRE-Coated, PRE-Scored,
PRE-Absorbent, PRE-Printed,
PRE-Channeled
TLC Plates

- **Analytical and Preparative Layers**
- **Custom-Coated TLC Plates**
- **Full Line of TLC Accessories**
- **Same Day Shipments**

This new catalog is yours for the asking.

Toll Free: 1-800-441-7540 • (In DE) 302-737-6960
75 BLUE HEN DR., P.O. BOX 7558, NEWARK, DE 19711

ANALTECH

CIRCLE 1 ON READER SERVICE CARD

Glenco 3400 & 3500 Series Liquid Chromatography Columns

THE CHROMATOGRAPHERS' CHOICE

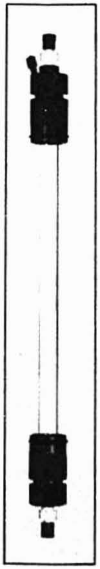

- Diameters from 6mm to 150mm ID - all available in standard lengths (15cm to 150cm) "off the shelf."
- Operating pressures to 150 psi.
- Borosilicate glass construction with polypropylene threaded collars and end plates.
- Aqueous and organic solvent systems available. Entire system autoclavable.
- Upper end plates with center inlet port and a side vent port which can be used to bleed air and to layer on sample with a long needle or tubing.
- Lower end plates with packing support of (10 micron) mesh cloth suspended over a woven grid and retained with snap ring.
- 1/8" or 1/16" Teflon Multifit connectors on each end plate for easy connection with polyethylene or teflon tubing.

Send today for our complete 60 page catalog of columns, fittings, valves, plungers, and accessories.

GLENCO®

Liquid Chromatography Specialists
since 1962

Glenco Scientific Inc.
2802 White Oak
Houston, Texas 77007
(713) 861-9123

CIRCLE 91 ON READER SERVICE CARD

free LC News

Agricultural Chemicals

Pesticide Metabolite Purification

LC purifies trace quantities of pesticide metabolites from soil. Purified metabolite is easily collected for positive identification by MS, IR, or other techniques.

Circle Reader Service No. 238

Analyze PCBs in Water

SEP-PAK Cartridges for rapid sample preparation allow direct, 1000:1 concentration of PCBs from water — at the sample site.

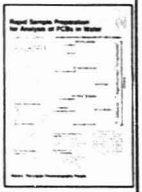

Circle Reader Service No. 239

Free Subscription

Pesticide Notes

"Pesticide Notes" keeps you updated on new LC methods for agricultural chemical analyses. Free applications literature is offered in every issue.

Circle Reader Service No. 240

Visit us at the Pittsburgh Conference, Booths 1201–6

Waters

The Liquid Chromatography People

Waters Associates, Inc.
Maple Street, Milford, MA 01757
(617) 478-2000

- **5th Australian Symposium on Analytical Chemistry.** Aug. 20–24. Perth, Western Australia. *Contact: Barry Codling, Analytical Division, Royal Australian Chemical Institute, 30 Plain St., Perth, Western Australia 6000*
- **27th IUPAC Congress.** Aug. 27–31. Helsinki, Finland. *Contact: J. Larinkari, P.O. Box 244, SF-00131 Helsinki 13, Finland*
- **XIV European Congress on Molecular Spectroscopy.** Sept. 3–7. Frankfurt/Main, Federal Republic of Germany. *Contact: Sec'ty Gen., EUCMOS 1979, Gesellschaft Deutscher Chemiker, J. Wendenburg, P.O.B. 90 04 40, D-6000 Frankfurt (Main) 90, West Germany*
- **Symposium on Atomic Spectroscopy.** Sept. 10–14. Tucson, Ariz. *Contact: J. O. Stoner, Dept. of Physics, University of Arizona, Tucson, Ariz. 85721*
- **9th North American Thermal Analysis Society Meeting.** Sept. 23–26. Holiday Inn City-Centre, Chicago. *Contact: Barbara L. Fabricant, Glass Thermochemistry R&D, Owens-Corning Fiberglass Technical Center, P.O. Box 415, Granville, Ohio 43023. 614-587-0610*
- **2nd European Symposium on Particle Characterization.** Sept. 24–26. Nuremberg, West Germany. *Contact: Secretariat, NMA Nurnberger Messe-und Ausstellungsgesellschaft mbH, Messezentrum, D 8500 Nuremberg, West Germany*
- **23rd ORNL Conference on Analytical Chemistry in Energy Technology.** Oct. 9–11. Gatlinburg, Tenn. *Contact: W. S. Lyon, Oak Ridge National Laboratory, P.O. Box X, Oak Ridge, Tenn. 37830*
- **3rd Symposium on Biological/Biomedical Applications of Liquid Chromatography.** Oct. 11–12. Boston. *Contact: Gerald L. Hawk, Waters Associates, Milford, Mass. 01757*
- **ACS 15th Western Regional Meeting.** Oct. 17–19. North Hollywood, Calif. *Contact: J. Quaglino, 5943 Lubao Ave., Woodland Hills, Calif. 91364*
- **International Exhibition on Laboratory Technology, Analyses, Procedures, and Automation in Chemistry.** Oct. 17–20. Graz, Austria. *Contact: Media Consult GmbH, Kongresse und Ausstellungen, Conventions and Exhibitions, Klopstockgasse 34, Postfach 404, A-1171 Vienna, Austria*
- **18th Annual Meeting of ASTM Committee E-19 on the Practice of Chromatography.** Oct. 21–24. Philadelphia. *Contact: Tim Bradley, Spectra-Physics, 2905 Stender Way, Santa Clara, Calif. 95051*

Short Courses

ACS Courses. For more information, contact: Department of Educational Activities, American Chemical Society, 1155 Sixteenth St., N.W., Washington, D.C. 20036. 202-872-4508

Carbon-13 NMR Spectroscopy
Cleveland (30th Pittsburgh Conference). Mar. 2–4. G. C. Levy and Paul Ellis. $280, ACS members; $330, nonmembers

Capillary Gas Chromatography
Cleveland (30th Pittsburgh Conference). Mar. 3–4. S. P. Cram and Milos Novotny. $250, ACS members; $300, nonmembers

CERAC
Manufacturer of Fine & Rare
INORGANIC CHEMICALS
OFFERS YOU

● Inorganics in Research Quantities, as well as in Production Quantities for Industry

● A Comprehensive Program
High Temperature Compounds, Vacuum Deposition Materials, Metal & Alloy Powders, Gas-Generating Alloys, Flame Spray Powders, Specialty Lubricants, Inorganic Chemicals, Hot-Pressed Parts.

● Our Literature
CERAC/PURE Catalog listing metals, intermetallics, salts, refractory compounds, oxides, phosphides, sulfides, selenides, tellurides, custom preparations. NEW UPDATED EXPANDED

CERAC Master Catalog, a unique handbook of inorganic and high temperature materials with properties not readily found elsewhere.

ATTENTION — Analysts & Research Personnel:
An extremely valuable, free service with every order . . .

● Our Certified Assurance of Quality Control
Each shipment from CERAC/PURE is certified with spectrographic analysis of trace metallic impurities, X-ray diffraction report on stoichiometry, and specialized items such as Fisher size, wet analysis, etc. when required.

Free pocket-size, plastic Periodic Table with every inquiry

CERAC, incorporated
P.O. BOX 1178 MILWAUKEE, WI 53201
TELEPHONE (414) 289-9800
TELEX 269452

CERAC, incorporated
P.O Box 1178
Milwaukee, WI 53201

Please send us your CERAC/PURE Catalog ☐
CERAC Master Catalog ☐

NAME ______
COMPANY ______
ADDRESS ______
CITY ______ STATE ______ ZIP ______

CIRCLE 33 ON READER SERVICE CARD

3300 Series electronic balance
$1395.00 Made in U.S.A.

Data Input Keyboard
$250.00 Made in U.S.A.

THE INTELLIGENT
ELECTRONIC
BALANCE
...ONLY $1395.00

Scientech's new dual range toploader has built-in microprocessor controlled data handling capabilities.

More than an electronic balance, Scientech's new 3300 Series is a data processing instrument that can be programmed to perform a wide range of complex weighing and data conversion functions . . . automatically, quickly and repetitively.

An optional data input keyboard is used to program the microprocessor "brain" in the balance, then the balance does the rest. The 3300 can store data, convert it from one unit to another, count parts and much more. A variable integration time feature assures accurate readings in hostile or unstable environments. And, since the balance does the "thinking", not the keyboard, one keyboard can serve many balances.

Even if you don't presently need the data handling capabilities of the 3300, you still get a full-featured toploader at a great price. For instance, BCD output is standard on the 3300. So is weighing in two ranges: 0-30.000g and 0-300.00g, instantaneous digital tare, clear LED display, all in a compact and attractive case.

Only Scientech can offer you an intelligent balance with these features for $1395.00. Call or write for descriptive literature.

For more information write or call
SCIENTECH, INC.
5649 Arapahoe Avenue · Boulder, Colorado 80303 · 303 444-1361

CIRCLE 196 ON READER SERVICE CARD

PRA's high intensity pulsed light sources.

The PRA 610 microsecond pulsed light sources offer maximum versatility for applications requiring high ultraviolet intensities.

- Discharge energy per pulse to 100 joules
- Repetition rate 1 to 100 pps
- Spectral range 200 nm to 1200 nm with peak intensities in UV
- Various pulse widths 1.5-50 μ sec.
- Non magnetic lens aperture for ESR/NMR applications
- Carefully designed for minimized RFI

PRA manufactures pulsed light sources with a variety of pulse widths and discharge energies and has people with broad experience in optical systems design to advise you.

PRA
Photochemical Research Associates Inc.
45 Meg Drive, London, Ontario
Canada N6E 2V2
(519) 686-2950 Telex 064-7597

CIRCLE 185 ON READER SERVICE CARD

Circular Dichroism turns us on

- ■ Very large sample compartment
- ■ Easy pushbutton operation
- ■ Measures CD or PM voltage on same chart
- ■ Photo (piezo) elastic modulator

JASCO Model J-500 Spectropolarimeter measures circular dichroism from either 180 to 700 nm or 180 to 1000 nm with high resolution, extreme sensitivity and excellent, fast scan speed. Optional attachments make measurement and data processing extremely simple. MCD, Low Temperature, micro, LCD and Stopped flow accessories available.

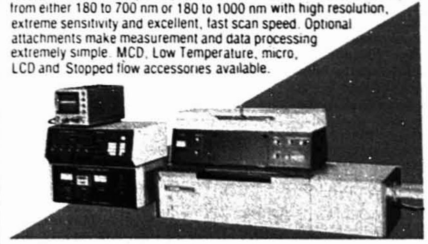

Jasco

JASCO INCORPORATED
218 Bay Street
Easton, Maryland 21601
(301) 822-1220

CIRCLE 114 ON READER SERVICE CARD

Gas Chromatography–Mass Spectrometry
Cleveland (30th Pittsburgh Conference). Mar. 3–4. J. Q. Walker, M. T. Jackson, and M.P.T. Bradley. $250, ACS members; $300, nonmembers

Maintaining and Troubleshooting Chromatographic Systems Workshop
Cleveland (30th Pittsburgh Conference). Mar. 3–4. J. Q. Walker, M. T. Jackson, and M.P.T. Bradley. $250, ACS members; $300, nonmembers

Systems Engineering in the Analytical Laboratory
Cleveland (30th Pittsburgh Conference). Mar. 3–4. Tomas Hirschfeld. $215, ACS members; $255, nonmembers

Thin-Layer Chromatography
Cleveland (30th Pittsburgh Conference). Mar. 3–4. V. W. Rodwell and D. J. McNamara. $215, ACS members; $255, nonmembers

Solving Problems with Modern Liquid Chromatography
Cleveland (30th Pittsburgh Conference). Mar. 9–11. J. J. Kirkland and L. R. Snyder. $230, ACS members; $280, nonmembers

Gas Chromatography, Theory and Practice
Blacksburg, Va. Mar. 12–15, Sept. 24–27. Harold M. McNair. $425, ACS members; $485, nonmembers

Microprocessors and Minicomputers—Interfacing and Applications
Blacksburg, Va. Mar. 18–23, June 10–15, Sept. 23–28, Dec. 9–14. R. E. Dessy and the Chemistry Dept. Instrument and Design Group of VPI&SU. $455, ACS members; $515, nonmembers

Flavor Research Workshop
Honolulu, Hawaii (ACS/CSJ Chemical Conference). Mar. 29–30. Roy Teranishi, R. A. Flath, and J. Sugisawa. $200, ACS members; $240, nonmembers

Planning for Safe Laboratory Handling of Highly Toxic Chemicals
Honolulu, Hawaii (ACS/CSJ Chemical Conference). Mar. 30–Apr. 1. N. V. Steere and Maurice Golden. $295, ACS members; $340, nonmembers

Modern Techniques in Gas Chromatography
Honolulu, Hawaii (ACS/CSJ Chemical Conference). Mar. 31–Apr. 1. H. M. McNair and S. P. Cram. $225, ACS members; $265, nonmembers

Solving Problems with Modern Liquid Chromatography
Honolulu, Hawaii (ACS/CSJ Chemical Conference). Mar. 31–Apr. 1. J. J. Kirkland and L. R. Snyder. $245, ACS members; $290, nonmembers

Toxicology for Chemists
Chicago. May 22–24. Morris Joselow. $485, ACS members; $555, nonmembers

Safety and Health for Academic Chemistry Laboratories
Chicago. June 2–3. Norman V. Steere. $130, ACS members and nonmembers

Liquid Chromatography, Theory and Practice
Blacksburg, Va. June 4–7, Dec. 10–13. Harold M. McNair. $450, ACS members; $510, nonmembers

Multinuclear NMR Spectroscopy
Los Angeles, June 7–9; Tallahassee, Fla., June 14–16. George C. Levy. $295, ACS members; $340, nonmembers

NEW! from GOW-MAC

a teaching LC good enough for QC

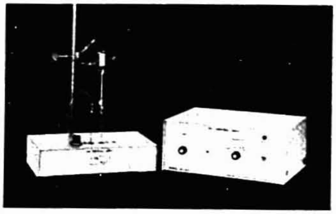

Model No. 80-500

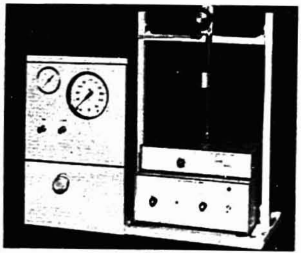

a QC LC good enough for research

Model No. 80-600

and both priced good enough for anybody

Both LC units employ rugged, modular GOW-MAC design for reliable operation. The basic Model 80-500 offers pulseless solvent delivery with a constant pressure pump (300 ml capacity to 1000 psi), a modular design for uniform manual injections, column holder, complete with 20 micron Silica Gel column, and reliable 254 nm, low volume (8 μl) UV detector. Only $1750.

The high-performance Model 80-600 offers a continuous solvent delivery system with constant volume, variable flow-rates from 0.5 $cm^3 min^{-1}$ – 5 $cm^3 min^{-1}$ with a low dead volume damping system. Pressures go to 3000 psi. For highly reproducible injections, a six-port rotary valve, modularly designed into column and detector system.

The 80-600 has a 10 micron Silica Gel column and a 254 nm, low volume (8 μl) UV detector. $3245.

Other detectors, columns and accessories are available. In addition, each unit shipped comes with a useful book, Elementary Theory of Liquid Chromatography with Bibliography and Experiments. For further information, inquire.

GOW MAC

GOW-MAC INSTRUMENT CO.
P.O. Box 32, Bound Brook, NJ 08805
Telephone: 201/560-0600
Shannon Free Airport, Co. Clare, Ireland
Telephone: 61632 Telex: 6254

CIRCLE 90 ON READER SERVICE CARD

Now. Make gas phase calibrations with NBS-traceable certainty

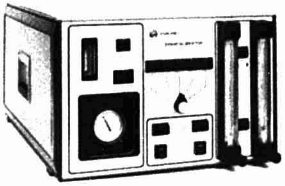

To get accurate, useful outputs from your gas analyzer or chromatograph, precise calibration is critical. So when you do calibrate, use the most accurate instrument available—the Metronics Dynacalibrator. It delivers accurate and precise gas concentrations ranging from 0.0001 ppm to over 1000 ppm. As a result, you can use it to get NBS-traceable calibrations of almost any instrument—in the lab or in the field.

Further, since calibration is our only business, you get an instrument that is coldly objective and easy to use. It's also competitively priced. Yet, it has features no other calibrator can match:

- Self contained design, no need for gas cylinders and related apparatus
- Oven control within ±.05°C, NBS traceable
- Oven temperatures variable to 50°C, 110°C optional
- Flow calibrated and stable to within ±1% (full scale) or ±3% (low scale) for each reading.
- Our own disposable, calibrated permeation devices, certifications traceable to NBS standards. Available for hundreds of gases.
- All controls and indicators logically grouped on front panel for fast, error free operation
- Fast, easy device change or replacement via front panel
- Continuous, unattended automatic or remotely controlled operation
- Dynamic gas concentration ranges of 60:1
- Optional, "in-transit" maintenance of purge and temperature

It all adds up to calibrations that are above suspicion—your best protection against costly measurement errors. Three models meet every requirement. For detailed literature and a demonstration, call or write today. Metronics, 2991 Corvin Drive, Santa Clara, CA 95051.
Phone: (408) 737-0550
Telex: 35-2129

SEE A DEMONSTRATION AT THE PITTSBURGH CONFERENCE, BOOTH 1936-1937.

Metronics
Calibration you can count on.

CIRCLE 136 ON READER SERVICE CARD

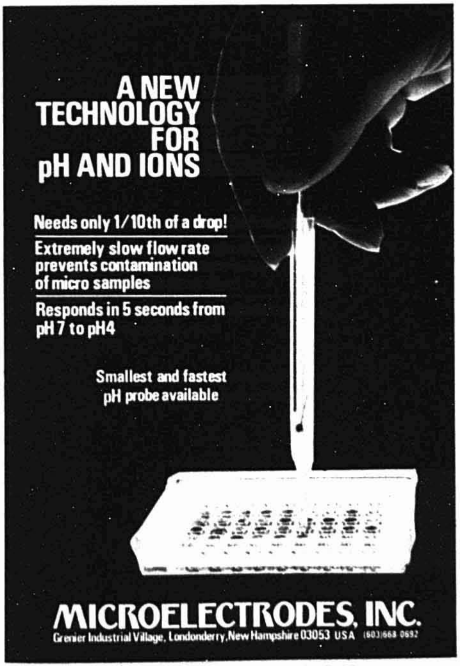
A NEW TECHNOLOGY FOR pH AND IONS
Needs only 1/10th of a drop!
Extremely slow flow rate prevents contamination of micro samples
Responds in 5 seconds from pH 7 to pH4
Smallest and fastest pH probe available

MICROELECTRODES, INC.
Grenier Industrial Village, Londonderry, New Hampshire 03053 USA (603)668 0692

CIRCLE 142 ON READER SERVICE CARD

PARR® BOMBS

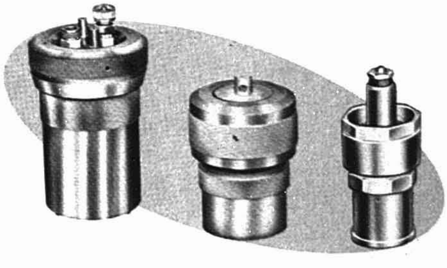

For Oxygen Combustion
For Acid Digestion
For Alkaline Fusion

Standard procedures for sulfur and halogens depend upon Parr oxygen or peroxide combustion bombs for oxidizing solid or liquid samples rapidly with complete recovery of all combustion products; while Parr digestion and fusion bombs give the analyst several effective systems for dissolving silicates, ores and other difficult materials in strong acids or alkalis without losing trace constituents. For details, write or phone: Parr Instrument Company, Moline, Illinois 61265. 309/762-7716

CIRCLE 171 ON READER SERVICE CARD

Laboratory Safety: Recognition and Management of Hazards
Washington, D.C. (178th ACS National Meeting). Sept. 7–9. N. V. Steere and Maurice Golden. $295, ACS members; $340, nonmembers

Experimental Design of Experiments
Philadelphia (FACSS Meeting). Sept. 14–16. John Hromi. $295, ACS members; $340, nonmembers

High-Pressure Liquid Chromatography Apparatus Workshop
Philadelphia (FACSS Meeting). Sept. 15–16. David H. Freeman. $250, ACS members; $300, nonmembers

Laboratory Automation: Micro-, Mini-, or Midicomputers?
Philadelphia (FACSS Meeting). Sept. 15–16. R. E. Dessy and the Chemistry Dept. Instrument and Design Group of VPI&SU. $225, ACS members; $265, nonmembers

Basic GC/MS/DS
Cincinnati. Feb. 12–16, Apr. 9–13. Q. Thomas. $625. *Contact:* Ann Woolley, Finnigan Institute, 11750 Chesterdale Rd., Bldg. #5, Cincinnati, Ohio 45246. 513-772-5500

Analysis of Organic Compounds in Water (Part I)
Cincinnati. Feb. 19–23. R. Foltz and D. Lin. $750. *Contact:* Ann Woolley, Finnigan Institute, 11750 Chesterdale Rd., Bldg. #5, Cincinnati, Ohio 45246. 513-772-5500

Atomic Absorption Spectrophotometry: Basic Concepts and Techniques
Cincinnati. Feb. 19–23, Mar. 26–30, Apr. 23–27. A. Knott or W. Stelzer. $625. *Contact:* Ann Woolley, Finnigan Institute, 11750 Chesterdale Rd., Bldg. #5, Cincinnati, Ohio 45246. 513-772-5500

Fundamentals of Industrial Hygiene
Pittsburgh. Mar. 6–8. $185, IHF/AIHA members; $245, nonmembers. *Contact:* George Reilly, Industrial Health Foundation, 5231 Centre Ave., Pittsburgh, Pa. 15232. 412-687-2100

Procedures for Sample Preparation and Cleanup
Cleveland. Mar. 7. Given in conjunction with the Pittsburgh Conference. *Contact:* Dexter Rogers, Kontes, P.O. Box 729, Spruce St., Vineland, N.J. 08360

Audiovisual Short Course on Liquid Chromatography
Cleveland. Mar. 7. Given in conjunction with the Pittsburgh Conference. *Contact:* Howard J. Sloane, SAVANT, P.O. Box 3670, Fullerton, Calif. 92634. 714-870-7880

Audiovisual Short Course on Atomic Absorption
Cleveland. Mar. 7. Given in conjunction with the Pittsburgh Conference. *Contact:* Howard J. Sloane, SAVANT, P.O. Box 3670, Fullerton, Calif. 92634. 714-870-7880

Chemical Derivatization for Chromatography and Mass Spectrometry
Cincinnati. Mar. 7–9. M. Quilliam. $400. *Contact:* Ann Woolley, Finnigan Institute, 11750 Chesterdale Rd., Bldg. #5, Cincinnati, Ohio 45246. 513-772-5500

Put The "Third Generation", Computer Compatible Injector On Your "Second Generation" HPLC

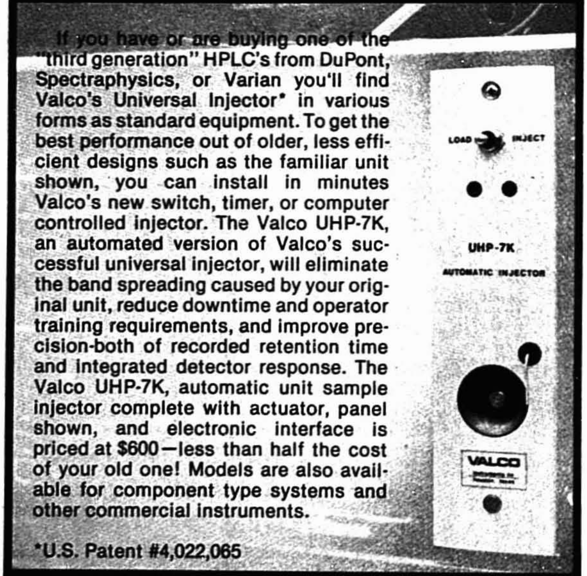

If you have or are buying one of the "third generation" HPLC's from DuPont, Spectraphysics, or Varian you'll find Valco's Universal Injector* in various forms as standard equipment. To get the best performance out of older, less efficient designs such as the familiar unit shown, you can install in minutes Valco's new switch, timer, or computer controlled injector. The Valco UHP-7K, an automated version of Valco's successful universal injector, will eliminate the band spreading caused by your original unit, reduce downtime and operator training requirements, and improve precision-both of recorded retention time and integrated detector response. The Valco UHP-7K, automatic unit sample injector complete with actuator, panel shown, and electronic interface is priced at $600—less than half the cost of your old one! Models are also available for component type systems and other commercial instruments.

*U.S. Patent #4,022,065

VALCO instruments co.
P.O. Box 19032 Houston, TX 77024
713-688-9345
TWX 910-881-5500
Telex 79-0033

Booth numbers 1630 & 1632 at the Pittsburgh Conference.

CIRCLE 225 ON READER SERVICE CARD

Digilab GC/IR

Digilab Means Sensitivity

In GC/IR, the most critical parameter is SENSITIVITY. GC fractions are measured in nanograms, so you need maximum sensitivity to obtain positive IR spectra. Digilab Fourier transform spectrometers with GC/IR provide better than 100 nanogram sensitivity on-the-fly; and better than 10ng in trap mode. These numbers are your assurance of receiving clear functional group identification of fractions virtually as fast as the GC separates them. The on-the-fly IR spectrum, below, of a 10ng fraction demonstrates Digilab's GC/IR sensitivity.

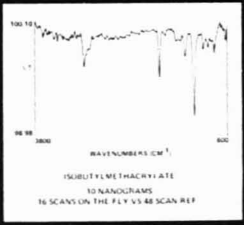

SYSTEM UTILITY and FLEXIBILITY are vitally important to GC/IR analysis. Digilab GC/IR uses your chromatograph and takes full advantage of its detector output. Digilab flexibility is evident in the switch-selectable external GC/IR on dual-beam FTS® instruments. Digilab's IMX-RDOS® software provides proven utility in GC/IR processing . . . from rapid data acquisition to spectral differentiation of the components in unresolved GC peaks. Digilab is the ultimate refinement in high sensitivity GC/IR.

External GC/IR sampling accessory on Digilab model FTS-15C spectrometer.

To learn more, see "High Sensitivity Infrared Spectroscopy of Gas Chromatographic Peaks," Wall and Mantz, APPL. SPEC *31*,6,1977,P.552.

3 GC = 4 GC/IR

Take a look at the chromatogram. It's a read-out of a four component mixture – with equal concentration of each component. Yet there are just three peaks. Without the help of Digilab's infrared Fourier Transform Spectrometer with GC accessory,

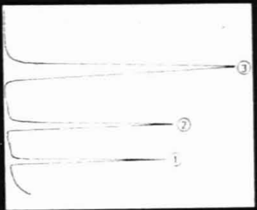

you'd never know that Peak 3 is a blend of two components – o-nitrotoluene and methylsalicylate (separated in the spectra below).

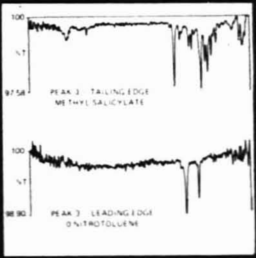

What you don't know can hurt you – and your research findings. But with Digilab you'll be sure.

But don't just take our word for it. Call or write us today for a free brochure and ask about our demonstration program.

DIGILAB INC

Subsidiary of Block Engineering, Inc.
237 Putnam Avenue, Cambridge,
MA 02139 Telephone (617) 868-4330

Put us to the test.

CIRCLE 45 ON READER SERVICE CARD

See us at the Pittsburgh Conference, Booths 950, 952, 1049 and 1051. Application seminars March 5 and 7, Room 243B.

NMR Interpretation: Proton & Carbon-13
Cincinnati. Mar. 12–15. D. Traficante. $440. *Contact:* Ann Woolley, Finnigan Institute, 11750 Chesterdale Rd., Bldg. #5, Cincinnati, Ohio 45246. 513-772-5500

Problem Solving by GC/MS/DS
Cincinnati. Mar. 12–16. Q. Thomas and G. Vander Velde. $625. *Contact:* Ann Woolley, Finnigan Institute, 11750 Chesterdale Rd., Bldg. #5, Cincinnati, Ohio 45246. 513-772-5500

Problem Solving by Chromatography: HPLC and GC
Cincinnati. Mar. 19–23, Apr. 23–27. W. Averill. $625. *Contact:* Ann Woolley, Finnigan Institute, 11750 Chesterdale Rd., Bldg. #5, Cincinnati, Ohio 45246. 513-772-5500

Interpretation of Mass Spectra
New Orleans. Mar. 26–28. Fred MacLafferty. $400. *Contact:* Bud Bromley, P.O. Box 1449, Kenner, La. 70062

Basic Mass Spectral Interpretation (Part II)
Honolulu, Hawaii. Mar. 28–30. D. De Jongh. $300. *Contact:* Ann Woolley, Finnigan Institute, 11750 Chesterdale Rd., Bldg. #5, Cincinnati, Ohio 45246. 513-772-5500

Forensic & Clinical Toxicology
Cincinnati. Apr. 2–6. B. Finkle. $625. *Contact:* Ann Woolley, Finnigan Institute, 11750 Chesterdale Rd., Bldg. #5, Cincinnati, Ohio 45246. 513-772-5500

Mass Spectral Interpretation: Applications
Honolulu, Hawaii. Apr. 6–7. D. De Jongh. $220. *Contact:* Ann Woolley, Finnigan Institute, 11750 Chesterdale Rd., Bldg. #5, Cincinnati, Ohio 45246. 513-772-5500

IR Interpretation
New York City. Apr. 18–20. H. Sloane. $330. *Contact:* Ann Woolley, Finnigan Institute, 11750 Chesterdale Rd., Bldg. #5, Cincinnati, Ohio 45246. 513-772-5500

Analytical Pyrolysis
Cincinnati. Apr. 18–20. R. Levy. $375. *Contact:* Ann Woolley, Finnigan Institute, 11750 Chesterdale Rd., Bldg. #5, Cincinnati, Ohio 45246. 513-772-5500

Metabolism & Pharmacokinetics: Quantitative & Qualitative Analysis
Cincinnati. Apr. 30–May 4. W. Braun. $625. *Contact:* Ann Woolley, Finnigan Institute, 11750 Chesterdale Rd., Bldg. #5, Cincinnati, Ohio 45246. 513-772-5500

X-Ray Spectrometry
State University of New York at Albany, Albany, N.Y. June 4–15. $500, one week; $950, two weeks. *Contact:* Henry Chessin, State University of New York at Albany, Dept. of Physics, 1400 Washington Ave., Albany, N.Y. 12222. 518-457-8339

Industrial Fatty Acids
Philadelphia. June 10–13. $285. *Contact:* Fatty Acids Short Course, American Oil Chemists' Society, 508 S. Sixth St., Champaign, Ill. 61820

X-Ray Powder Diffraction
State University of New York at Albany, Albany, N.Y. June 18–29. $500, one week; $950, two weeks. *Contact:* Henry Chessin, State University of New York at Albany, Dept. of Physics, 1400 Washington Ave., Albany, N.Y. 12222. 518-457-8339

Fiber analysis
Convenient and reproducible

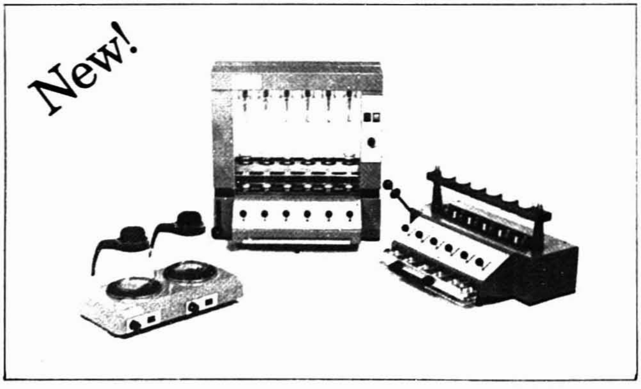

Fibertec – a Tecator invention – **determines the content of fiber and related parameters in food or feed efficiently and conveniently. Extraction and filtering is performed asbestos free** in place in the unit. **No handling or transfer of the sample,** even during a sequential extraction to determine cellulose, hemicellulose, lignin or other subfractions of the total fiber.
You choose the method yourself. Crude Fiber, Weende, Van Soest NDF or ADF. **Fibertec** can handle them all!

Fibertec is available in several models and in different price ranges.

tecator
2200 Central Avenue, Boulder, Colorado 80301
Phone: (303) 4439245

CIRCLE 205 ON READER SERVICE CARD

INTRODUCING

S/MAX

RIGAKU'S OUTSTANDING NEW
AUTOMATED X-RAY SPECTROMETER
ENGINEERED FOR **MAX**IMUM
- PERFORMANCE
- CAPABILITY
- VERSATILITY
- FLEXABILITY

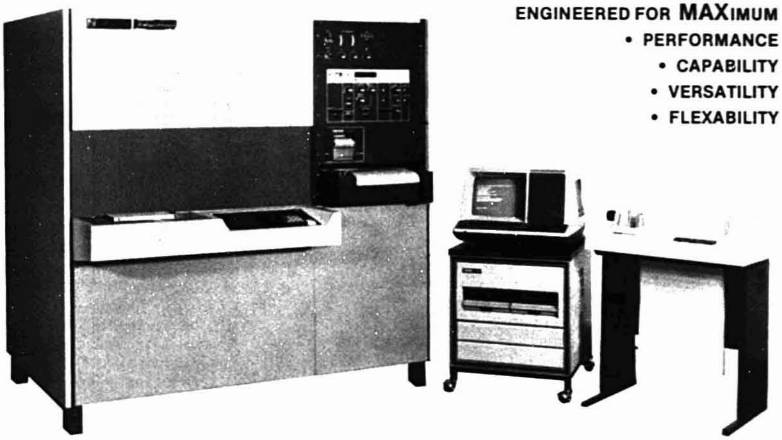

The Microprocessor controlled Automated X-Ray Spectrometer System that provides unmatched performance and versatility in sequential X-Ray Fluorescence Instrumentation.

- Sensitivity and Stability . . . End Window Rhodium Tube plus exciting new design concepts provide performance unsurpassed in the field.
- Versatility and Automation . . . A new, more sophisticated Microprocessor with Random Access Memory increases instrument capabilities while retaining all the advantages of human-engineered ease of operation.
- Computer Interfacing in minutes to any DEC11 family computer. Built-in Serial Line Interface is provided as standard equipment.
- Minicomputer Data Processing . . . A new and improved Software Package utilizing either a RT-11 or RSX-11 Operating System for comprehensive data analysis.
- 24 and 108 Sample Changers available for unattended operation.

Rigaku's S-MAX has been designed by an outstanding team of engineers who understand the needs of their fellow professionals and insist upon uncompromising excellence.

We care about technology . . .
that makes the difference!

Rigaku USA inc.

3 Electronics Avenue, Danvers, Massachusetts 01923, U.S.A.
Phone: (617) 777-2446

CIRCLE 181 ON READER SERVICE CARD

Building Integrity into Integration.

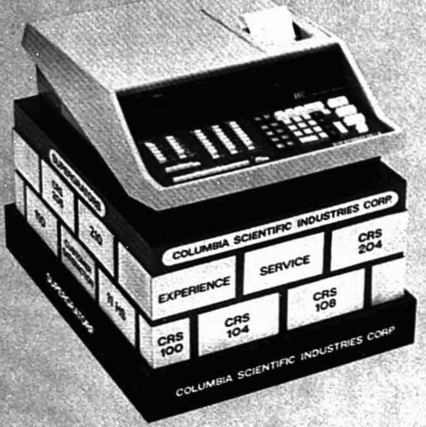
COLUMBIA SCIENTIFIC INDUSTRIES CORP
EXPERIENCE
SERVICE
CRS 204
CRS 108
CRS 104
CRS 100
COLUMBIA SCIENTIFIC INDUSTRIES CORP

CSI's Supergrator Series: 17 Years in the Making of Low Cost Reliability

The CSI Supergrator series is the result of 17 years of building digitizing instruments for the analytical laboratory.

The NEW Supergrator 3A provides new auto sampler capability at a price that justifies a stand-alone system. It automatically provides multi-program storage and all of the calculations that are necessary for accurate and precise results. The Supergrator 3A offers answers with user-designed flexibility and programming parameters for under $4,000.00. This is the only system in this price range offering this degree of versatility.

The Supergrator 1A, for less than $3,000.00, provides the same basic mainframe as the Super 3A, including all the baseline correction techniques as well as area allocation procedures, and area percent calculations. Should your needs expand, the Super 1A can be upgraded to a Super 3A at any time.

Compare with any other System

•Flexibility •Expandability •Reliability
•Versatility •Proven Design •Low Cost
•Built-in Self Diagnostics

Call or write today for complete information or free demonstration.

CSI COLUMBIA SCIENTIFIC INDUSTRIES

P.O. Box 9908, Austin, Texas 78766
Call toll-free 800-531-5003 or in Texas 512/258-5191 TWX 910-874-1364

If you attend the Pittsburgh Conference on Analytical Chemistry, please visit Booths 241, 243, 245, 247, and see how CSI can help you.

CIRCLE 34 ON READER SERVICE CARD

News

Capillary Gas Chromatography
Lausanne, Switzerland. Sept. 21–22. *Contact:* A. Zlatkis, Chemistry Dept., University of Houston, Houston, Tex. 77004

High-Performance Liquid Chromatography
Lausanne, Switzerland. Sept. 21–22. *Contact:* A. Zlatkis, Chemistry Dept., University of Houston, Houston, Tex. 77004

Gas Chromatography/Mass Spectrometry
Lausanne, Switzerland. Sept. 21–22. *Contact:* A. Zlatkis, Chemistry Dept., University of Houston, Houston, Tex. 77004

High-Performance Thin-Layer Chromatography
Lausanne, Switzerland. Sept. 21–22. *Contact:* A. Zlatkis, Chemistry Dept., University of Houston, Houston, Tex. 77004. 713-749-2623

For Your Information

The heads of four Federal regulatory agencies, EPA, FDA, OSHA, and the Consumer Product Safety Commission, have asked the Civil Service Commission chairman Alan K. Campbell to create a new Federal job classification for **toxicologists.** The agencies, all of whom regulate toxic substances, find it difficult to recruit toxicologists since Federal civil service registers do not list such an occupation. Agency officials estimate that the Federal Government will need about 2000 toxicologists by 1985, but the number now employed is uncertain since identification is a problem.

Members of the **London-based Chemical Society** and the **Royal Institute of Chemistry** have voted to merge. The new organization may be named the Royal Society of Chemistry and is expected to begin operating in 1980 with a membership of some 40 000. The merger will lead to single control of the two complementary functions of the existing organizations: the learned society, and the professional and qualifying institute.

Berghof/America has moved its operations to 2 Chester Road, Derry, N.H. 03038 (603-434-8688), according to Shirley Baker, managing director. The company manufactures and distributes PTFE Teflon labware and lab equipment.

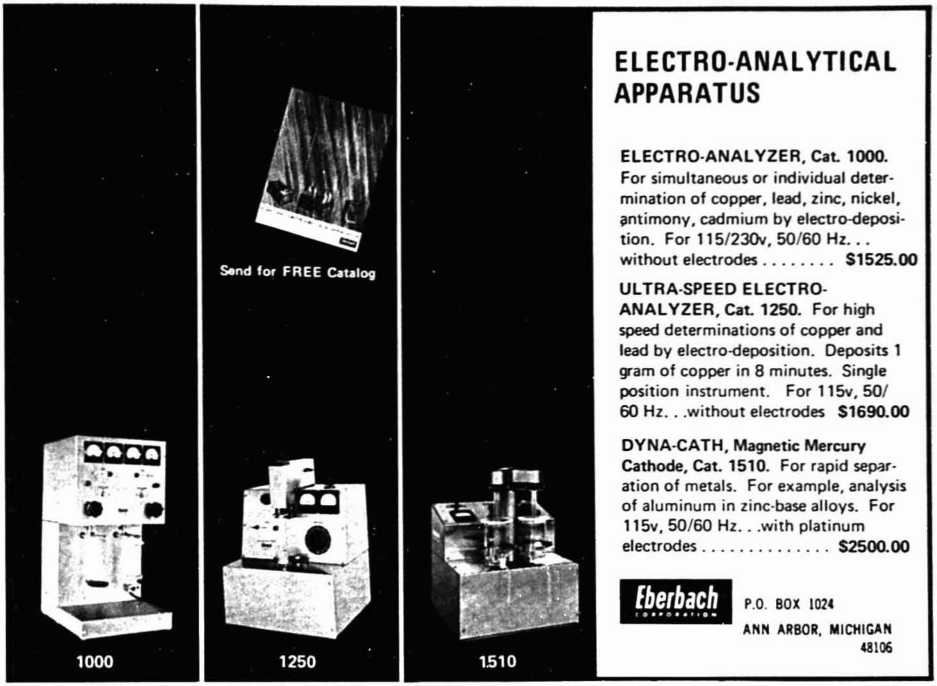

ELECTRO-ANALYTICAL APPARATUS

ELECTRO-ANALYZER, Cat. 1000. For simultaneous or individual determination of copper, lead, zinc, nickel, antimony, cadmium by electro-deposition. For 115/230v, 50/60 Hz. . . without electrodes $1525.00

ULTRA-SPEED ELECTRO-ANALYZER, Cat. 1250. For high speed determinations of copper and lead by electro-deposition. Deposits 1 gram of copper in 8 minutes. Single position instrument. For 115v, 50/60 Hz. . .without electrodes $1690.00

DYNA-CATH, Magnetic Mercury Cathode, Cat. 1510. For rapid separation of metals. For example, analysis of aluminum in zinc-base alloys. For 115v, 50/60 Hz. . .with platinum electrodes $2500.00

Eberbach CORPORATION
P.O. BOX 1024
ANN ARBOR, MICHIGAN
48106

See us at the Pittsburgh Conference, Booth #314 CIRCLE 75 ON READER SERVICE CARD

For perfect solutions... specify Alfa AA Standards

Alfa offers the most complete line of atomic absorption standards available for trace metal analyses—at new, lower prices. And shipment is guaranteed within 24 hours.

Included are standard solutions of 1000 ppm of metal in an aqueous matrix, as well as organometallic standards for use with heavy organic liquids.

Circle our reader service number for more information on Alfa's AA Standards.

Alfa Division, Ventron Corporation,
152 Andover Street, Danvers,
Massachusetts 01923
(617) 777-1970
(617) 289-9250

Alfa
DIVISION OF VENTRON CORPORATION

CIRCLE 233 ON READER SERVICE CARD

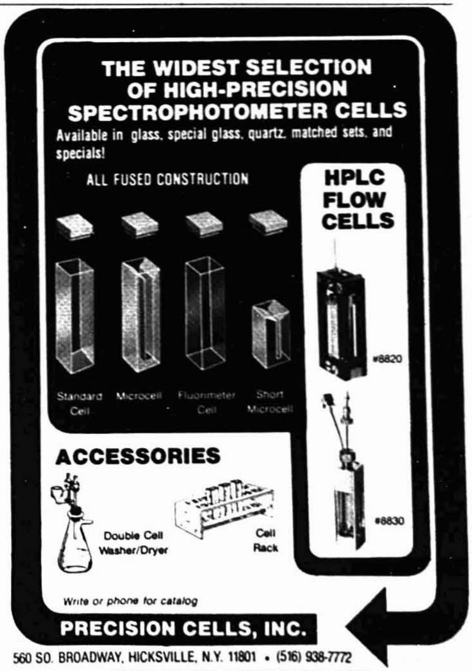

THE WIDEST SELECTION OF HIGH-PRECISION SPECTROPHOTOMETER CELLS

Available in glass, special glass, quartz, matched sets, and specials!

ALL FUSED CONSTRUCTION

HPLC FLOW CELLS

ACCESSORIES

Write or phone for catalog

PRECISION CELLS, INC.

560 SO. BROADWAY, HICKSVILLE, N.Y. 11801 • (516) 938-7772

CIRCLE 174 ON READER SERVICE CARD

The New...

See Us At Booth 810
"Pittsburgh 79"

NEC

EXAC™ 5000
Computer-Based
Energy Dispersive
XRF Systems

Built to perform reliably in the toughest industrial environments ... and to satisfy demanding research requirements

- Unique, down-looking, detector — x-ray tube geometry
  - analyze fragile briquettes, powders, and liquids conveniently, precisely, and without danger of system contamination
  - high-angle, detector x-ray tube geometry maximizes analytical sensitivity
- Uniquely flexible, computer-based system
  - complete library of qualitative (QUALEX™) and quantitative (EXAC) analysis programs
  - the system can be programmed to suit individual user requirements in NEC BASIC II (The Spectroscopy Language of Today)
- Computer controlled "Intelligent" sample changer maximizes throughput

Nuclear Equipment Corporation
963 Industrial Road
San Carlos, California 94070
Phone: (415) 591-8203

79/04

CIRCLE 149 ON READER SERVICE CARD

Whatman Inc., announces the establishment of a toll-free telephone line for its HPLC customers to discuss problems with Whatman experts. The technical staff, selected and trained to assist users of Whatman Partisil columns and other HPLC products, has access to computer data banks and applications laboratories. The toll-free number is 800-631-7290.

A newly produced film, ***What About Tomorrow?,*** explores the history of basic research as well as today's scientific endeavors and the people searching for new knowledge. Research topics include use of high-altitude balloons to measure ozone in the stratosphere, how a tiny fern converts nitrogen from air into fertilizers for crops, and the use of lasers in chemistry. The film is available on free loan from: Modern Talking Pictures Service, 2323 Hyde Park Rd., New Hyde Park, N.Y. 11040.

Sadtler Research Laboratories, Inc., has published a brochure that describes and illustrates its **High Resolution Evaluated Quantitative Infrared Spectra Collection.** Each compound in the collection is represented by two spectra; both are plotted linear in percent transmittance and in absorbance. Spectra are prepared in solution at two wavenumber resolution over the range of 4000–400 cm^{-1}, and are in accord with the Class II guidelines established by the Coblentz Society. For a copy of the 8-page brochure or more information on this collection, contact Sadtler Research Laboratories, Inc., 3316 Spring Garden St., Philadelphia, Pa. 19104 (215-382-7800).

Rofin, Ltd., Surrey, England, announces the establishment of a subsidiary, Rofin, Inc., Newton Upper Falls, Mass., to handle sales, service, warehousing, and distribution of the firm's line of electro-optics products in the U.S.

"Research Needs and Instrumental Requirements in Catalysis," published by the National Science Foundation's Division of Engineering, presents the results of a workshop held at the University of Maryland June 22–23. This report includes sections on catalysis by metals and nonmetals, the applications of spectroscopic techniques, and support of fundamental research in catalysis. Free copies may be obtained by writing to Marshall M. Lih, Engineering Chemistry and Energetics Section, NSF, 1800 G St., N.W., Washington, D.C. 20550.

Garland Way Advertising, Inc., has been appointed the advertising agency for Leybold-Heraeus Vacuum Products Inc., Monroeville, Pa. Leybold-Heraeus is a supplier of vacuum components and systems for industrial processing and research and development.

The JCPDS-International Centre for Diffraction Data, in cooperation with NIH and EPA, announces an interactive search system based upon its file of over 33 000 powder diffraction patterns. The Powder Diffraction Search Match System is available for use as a component of the NIH-EPA Chemical Information System on a cost-recovery basis. Searches are billed on an elapsed-time basis and cost between \$5.00 and \$20. For further information, contact the JCPDS at 215-328-9400 or the CIS at 800-645-1132.

Neutron Activation Analysis is offered as a contractural service by the Nuclear Analytical Services Laboratory of Science Applications, Inc. The scope of the laboratory's service capabilities includes preirradiation chemistry, radiochemical separations, methodology development, and computer-based data reduction and report format. Further details on the company's Neutron Activation Analysis services are available from: Dr. Vic Orphan, SAI Technology Co., 4060 Sorrento Valley Blvd., San Diego, Calif. 92121.

Elsevier Scientific Publishing Co. announces the forthcoming publication of the ***Journal of Analytical and Applied Pyrolysis,*** edited by H. L. C. Meuzelaar and H. R. Schulten. Subscription price is \$70.75. A free sample copy is available on request from Elsevier Scientific Publishing Co., P.O. Box 330, 1000 AH Amsterdam, The Netherlands.

Lake Shore Cryotronics, Inc., announces the availability of a new service for measurement of thermal properties of materials, specific heat and thermal conductivity, in the measurement range of 2–30 K, with an uncertainty of method less than ±5%. Measurements are performed in an adiabatic calorimeter, and all data are referenced to thermometer standards, calibrated to IPTS-68 and EPT-76. Samples supplied for measurements should be in the form of disks $\frac{3}{8}$ in. in diameter by $\frac{1}{4}$ in. thick for specific heat and $\frac{1}{8} \times \frac{1}{4} \times 1\frac{1}{4}$ in. for thermal conductivity. For complete details, request technical data SH-TC from

10 years ago it was the best analytical lab balance around. 2500 units later, the Torbal EA-1 still is.

The "All-American" Balance

Torbal EA-1 has been in continuous production since 1968. Almost every one made in those ten years is still in service, and most with never a service call.

What makes the Torbal so durable—so special—for laboratory use is its friction-free torsion design. There's no damage-prone knife edge to wear, or need replacement. Which is why **the Swiss and German makers are now switching to torsion suspension in their balances.** At Torbal we've been building torsion suspensions for over 80 years.

Unmatched reliability and quality.

Every Torbal balance is "new generation", combining the quality and the reliability of a non-fatiguing torsion band.

Now save as much as $1000 over copy-cat imports.

The EA-1's combination of uncompromising quality and repair-free operation has always provided for inexpensive, long-run operation. **And right now, thanks to dollar fluctuations, it will cost you a lot less than a copy-cat import.**

We'd like you to see the EA-1. Unfortunately, size, weight and set-up time present some difficulties for your distributor salesman. So drop us a line and tell us where you are. We'll introduce you to a Torbal user in your area for a hands-on demo.

What makes Torbal the best?

- **Friction-free torsion design.**
- **Electronic null indicator for fool-proof readouts.**
- **Large, easy-to-read digital readouts to 159.9999 grams.**
- **Accuracy to 0.1 mg without vernier or micrometer readings.**
- **8 to 10 grams of infinitely variable dial-in-tare (with extended tare options to 208 grams).**
- **No knife-edges—no "beam arrest" required.**

Write for illustrated brochure or a demonstration.
(And look for us at the Pittsburgh Conference, Booth 402, March 5th to 9th.)

TORBAL **THE TORSION BALANCE COMPANY**

Main Office and Factory: Clifton, N.J. 07012
Sales Offices: Chicago, IL; Temple City, CA

CIRCLE 203 ON READER SERVICE CARD

Imagine!
An automated continuous flow industrial analyzer for under $6500.

The jobs our CFA 200 will do won't surprise you. We produce well over 200 plug-in analytical cartridges for the CFA 200 to handle the very same automated colorimetric wet chemical procedures you feel comfortable with.

Yet our CFA 200 Analyzer was designed for industrial applications. So it's a lot less finicky.

Its direct gear drive pump wears less, and is a snap to maintain. Its unique prism optics improves photometric accuracy. Its prealigned flowcells slip in and out in seconds. And if you need greater sensitivity we will equip your CFA 200 with flowcells up to 75mm.

Also, you get an easy-to-read digital readout. And practically any standard chart recorder plugs in when you need hard copy.

All this packaged in a single, rugged compact case you can move from the lab, to the plant, to the field.

CFA 200—the less finicky wet analyzer from Scientific Instruments Corporation. More instrument, more service . . . for less money. Write for free details.

scientific INSTRUMENTS CORPORATION
25 Broadway, Pleasantville, NY 10570 • Phone: (914) 769-5700

SEE US AT THE PITTSBURGH CONFERENCE, BOOTH #1550-52
CIRCLE 197 ON READER SERVICE CARD

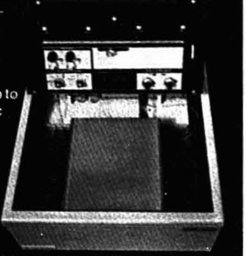

The little Chem/Meter: big on accuracy.

Take a look at all the outstanding features in our Series 20 Chem/Meter hydraulic diaphragm metering pump:

Metering accuracy within ± 1%.
Steady, continuous feeding of clear fluids.
Capacities of 14.7 ML/min.
Pressures to 1500 psi.
Zero to 100% capacity adjustment while operating.
Totally enclosed, leakproof design.
Wetted parts made of corrosive resistant stainless steel with sapphire ball-seats and teflon diaphragms.
Measures only 10½" × 5" × 3½".

The Series 20 Chem/Meter is ideal for machinery that requires the injection of precisely measured liquids. These include plastics, pharmaceuticals, chemical process, foods, beverages and fertilizers.

For larger measuring requirements from 23 to 3024 ML/min we have the Series 200 Chem/Meter. You can get all the details on the reliable Chem/Meter line by calling or writing Crane Co., Chempump Division, Warrington, Pa. 18976.

CRANE® CHEMPUMP

CIRCLE 32 ON READER SERVICE CARD

CR8-190

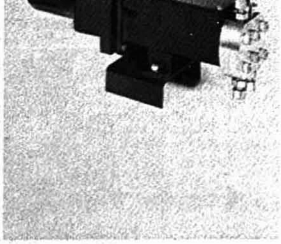

Lake Shore Cryotronics, Inc., 64 East Walnut St., Westerville, Ohio 43081 (614-891-2243).

Science Media announces an instructional program entitled "The Identification of Polymer Additives by Infrared Spectroscopy." Authored by Richard Nyquist of Dow Chemical Co., this is the second program in a new series (developed in a cooperative effort with the Coblentz Society) devoted to the interpretation of IR spectra of specific classes of compounds. Program materials consist of an audio taped lecture on cassette, workbook, problem spectra booklet, and text. Price is $45. Contact: Science Media, P.O. Box 910, Boca Raton, Fla. 33432.

Lab-Line Instruments, Inc., installed the Centrex System effective Dec. 4, 1978. Their new main number is 312-450-2600 or 312-LAB-LINE.

Astra Scientific International Inc., announces its appointment as the exclusive U.S. representative for Solea-Tacussel, a manufacturer of electrochemical instrumentation located in France. For more information contact: Astra Scientific International, Inc., P.O. Box 2004, Santa Clara, Calif. (408-244-9767).

Science Media, a division of J. Huley Associates, Inc., has expanded the utility of its spectra interpretation courses by offering a revised edition. Currently in use in over 500 higher level academic institutions, subjects include the interpretation of infrared, NMR (proton and C-13), mass, Raman, and electron spin resonance spectra. Newly adapted materials consist of seven audio cassettes, workbooks, and explanatory notes. The complete series is priced at $175.

ANALYTICAL CHEMISTRY is pleased to announce the availability of a combined reprint containing the 50th Anniversary Symposium contributions presented at Miami Beach in September 1978 and published in the November and December 1978 issues of the JOURNAL. The 42-page reprint also contains Professor Laitinen's editorials from Nov. and Dec. and the Report on editorial staffing over the 50-year period. For your copy, send $1.00 to cover postage and handling to Business Operations, American Chemical Society, 1155 16th St., N.W., Washington, D.C. 20036.

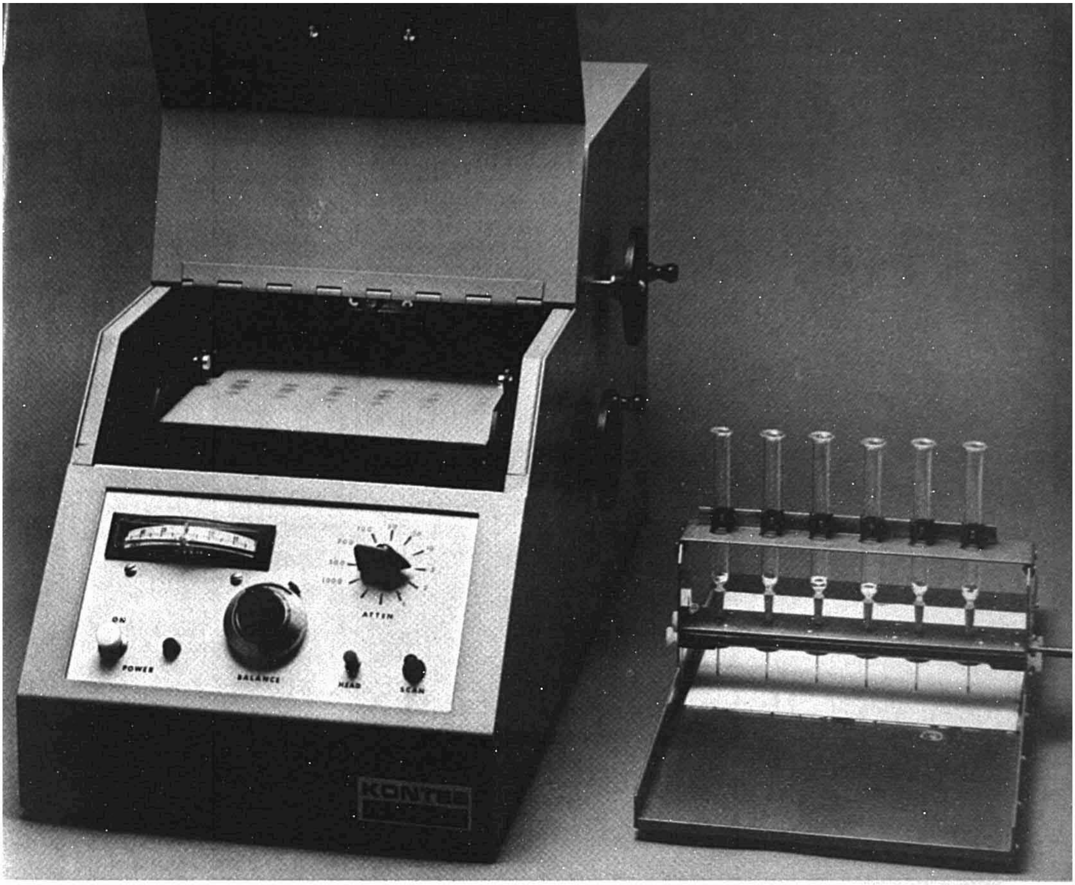

Patented and proven.

The Kontes low-cost, quantitative TLC system.

Here is the proven Kontes system that offers high resolution, quantitative TLC analysis at low cost.

The brain of the system is the unique and patented Kontes Densitometer*[1]. It utilizes a rugged and highly reliable fiber optic scanner to create outputs compatible with all conventional data processing. It features single or double beam scanning in four modes—diffused reflectance, visible transmission, fluorescence, and fluorescence quenching. The densitometer sells for $3463.20 in U.S.

Our air-manifold Chromaflex® Spotter**[2] is the heart of the system. It consistently makes uniformly-sized spots on all standard TLC plates. Up to 2 ml of solvent extract can be spotted to a controlled diameter of 6mm or less with a reproducibility of ±2%. The Chromaflex Spotter sells for $181.50 in U.S.

In combination, our densitometer and spotter afford reproducible, quantitative analysis at a cost unmatched by other methods. The practicality of the Kontes system is documented by a bibliography of applications and a comprehensive manual.

For further information contact your Kontes representative or send for our detailed literature.

1. *U.S. Patents 3,562,539 and 3,924,948. "Determination of Reflectance of Pesticide Spots on Thin-Layer Chromatograms, Using Fiber Optics", Morton Beroza, K. R. Hill, Karl H. Norris, ANALYTICAL CHEMISTRY, September 1968.
2. "An automatic spotter for quantitative thin layer and paper chromatographic analysis by optical scanning", Melvin E. Getz, Journal of the AOAC, Volume 54, No. 4, 1971. **U.S. Patent 3,843,053.

KONTES
Vineland, N.J. 08360

Exclusive Distributors: KONTES OF ILLINOIS, Evanston, Ill. • KONTES OF CALIFORNIA, San Leandro, Calif.
KONTES (U.K.) LTD., Carnforth, England

CIRCLE 117 ON READER SERVICE CARD

Seek peaks at 206 nm and get up to 200x the sensitivity of monitoring at 280 nm...

LKB
2138 UVICORD S
BASELINE ADJUST

...with the new Uvicord S UV monitor

Sensitivity is increased up to 200x for proteins when you monitor at 206 nm with LKB's new Uvicord® S UV-monitor. This unique instrument will detect non-aromatic peptides, polysaccharides, nucleotides, lipids and steroids as well as proteins. And, naturally, you can also monitor at 254 or 280 nm.

Enhanced versatility has required no compromise in stability. Quite the contrary. Sophisticated optics and solid state circuitry provide outstanding linearity. And you can monitor simultaneously at high and low sensitivities.

Unlike others, the new Uvicord S UV-monitor is contained in a single small case which mounts easily on a fraction collector or ring stand. And its low price matches its small size.

Contact LKB today for full details.

See us at the Pittsburgh Conference Booths 1223-5

LKB

LKB Instruments Inc.
12221 Parklawn Drive, Rockville, Maryland 20852
301: 881-2510

CIRCLE 131 ON READER SERVICE CARD

3A-300

CHEMISTS HAVE SOLUTIONS

CHEMISTRY T-SHIRTS

With the Original Periodic Table
Earth · Air · Fire · Water

The design is multi-colored and vibrant. The t-shirts are buff. They are made of 50% polyester/50% cotton and are available in adult sizes:

Small (34–36), Medium (38–40), Large (42–44), and Extra Large (46).

Price: $6.00, includes postage and handling. (10% discount for orders of 10 or more).

Send order to
Department of Educational Activities
American Chemical Society
1155 Sixteenth St., N.W.
Washington, D.C. 20036

Number of Shirts:

S ___ M ___ L ___ XL ___

Amount Enclosed $________

Name

Address

City **State** **Zip**

Make checks payable to the American Chemical Society.

pH
Electrode
Quiz

QUESTION
The most common cause of pH electrode failure is:
☐ Other people break them.
☐ Other people let the reference dry out.
☐ Cosmic forces de-energize them.

ANSWER
Eventually all pH electrodes age; response becomes slow and span is short. Unfortunately, most electrodes are broken or let dry out before old age takes its toll.

PRIZE
Sensorex Combination pH Electrodes are prize-winners. They have:
- Epoxy Bodies with Recessed Bulb/Safeguard Tips to minimize breakage.
- Sealed, gel-filled references that never need refilling.
- Fast response over the full pH range.

STANDARD SIZE MODEL S200C
$36

RECESSED BULB
SAFEGUARD TIP

Semi-micro, flask, flat surface, other models available. Send for Bulletin 200A

Sensorex®
9713 Bolsa Ave.
Westminster, CA
USA 92683
Phone: 714/554-7090

CIRCLE 192 ON READER SERVICE CARD

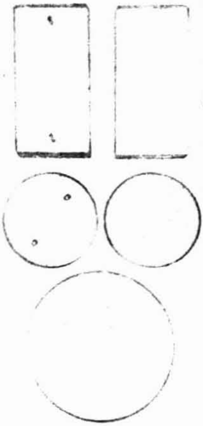

Why window shop? Get all your analytical accessories from Barnes.

What do you want from your supplier of windows and crystals?

Variety? We offer NaCL, KBr, KRS-5, Irtran-2, and a host of others. Round, Square, Rectangles. In all standard sizes to fit Beckman and Perkin-Elmer cells.

Quality? Each window is inspected, individually wrapped and identified, and meets the highest standards of purity.

Price? Since we specialize in Analytical Accessories, our prices are among the lowest in the industry.

Fast Service? Just call us, toll-free at (800) 243-3498 and ask for Peggy. She'll take your order and in most cases have it shipped to you within 48 hours.

For cells and windows, as well as other analytical accessories for IR Spectrophotometry, make Barnes your 1-stop place to shop.

Call or write for our catalog. Barnes Engineering Company, 30 Commerce Road, Stamford, CT 06904, (203) 348-5381. Out of state toll free (800) 243-3498.

BARNES

CIRCLE 29 ON READER SERVICE CARD

PRA's new arc lamp systems. More power at less cost per watt.

- 2 to 6 times more useable power for given lamps over conventional systems
- Water cooled
- Sealed to significantly reduce ozone health hazard
- Designed to allow direct imaging into monochromators without the use of lenses
- Allows for use of lower-powered lamps for Reduced Operating Cost

The regulated power supplies are:
- Modulatable up to 25 KHZ
- Pulsed mode operation and optical feedback capability
- Highly regulated – 0.1% ripple under full load
- Low RF, filtered single pulse starters

The supplies can power most arc lamps from 75W – 1000W.

PRA
Photochemical Research Associates Inc.
45 Meg Drive, London, Ontario
Canada N6E 2V2
(519)686-2950 Telex 064-7597

CIRCLE 186 ON READER SERVICE CARD

INNOVATIVE GAS

FROM

One of the world's oldest and largest manufacturers of gas chromatographs, Shimadzu, spent more than a quarter century developing and perfecting these instruments. The performance of Shimadzu's fine line of gas chromatographs and related equipment is outstanding. And the very latest electronics technology is used to ensure high reliability with easy maintenance.

Chromatopac C-R1A Recording Data Processor

Only the C-R1A can calculate calories, vapour pressure, specific gravity of liquid, deviations from standard values, mole concentration (%) —weight concentration (%) and others in addition to the standard routines. A thermal plotter printer for chromatograms, recording of names of components is equipped. Up to 393 peak area as well as measurement of peak heights or average peak heights can be processed. There is also an all new grouping function and a self-diagnostic function.

CIRCLE 118

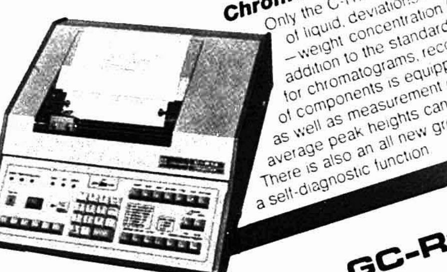

GC-R1A Computer Gas Chromatograph

This advanced gas chromatograph is controlled by a micro-computer with a data processing function and thermal recorder (printer-plotter). Up to 9 sets of analysis conditions can be established, and these can be filed and stored. Other features include automatic ghost-peak shutout, temperature control to near room temperature without coolant, multi-stage heating, a built-in pre-amp for TCD and a fully automatic GC system.

CIRCLE 119

GC-MINI2 Gas Chromatograph

Although very compact and lightweight, this GC system has the performance of much larger and more expensive types. Outstanding stability, sensitivity and accuracy are ensured by dual column flow and on-column/on-detector system, two different kinds sensors system in column oven, and contamination free type detector. And a unique oven temperature control system can maintain the oven at room temperature, even when the injection port temperature is high. Maintenance is also easier because the four main modules can be disassembled and the electric control broken down to its five sub-units.

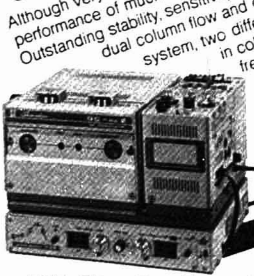

CIRCLE 120

•Write today for more information on these and other Shimadzu labor and cost saving instruments.

CHROMATOGRAPHS SHIMADZU

GC-7AG Series Ghost-Cut Gas Chromatograph

Truly state-of-the-art, this quality unit features the unique Shimadzu Ghost-Cut Sample Injection Port which eliminates ghost peaks and baseline fluctuations caused by substances evolved from the rubber septum and volatile substances absorbed by the sample residue on the inner surface of the injection port. This and the many other features enable results of unsurpassed accuracy and reliability.

CIRCLE 121

GC-6AM Series Cartridge Gas Chromatograph

The GC-6AM Series is an extremely versatile gas chromatograph that lets you change your entire analysis system without time-consuming cooling of the column, injection port and detector. Simply change cartridges and you're ready to begin a new GC run. FID, ECD, TCD (factory installed), backflush, precut, column conditioning and capillary column cartridges designed to handle any GC application offer more versatility, flexibility and performance than ever before.

CIRCLE 123

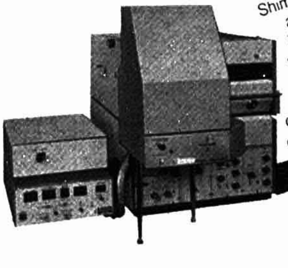

AOC-6B Auto Sampler

Shimadzu's AOC-6B automatically injects up to 100 samples in succession and provides suitable cleaning solvent for each sample

CIRCLE 122

Glass Capillary Column System

The new Shimadzu GDM-1B Glass Drawing Machine offers complete preparation of high performance glass capillary columns. The GDM-1B delivers a high drawing speed of 100 cm/min with a solid-state electronic temperature control system, digital setting and LED display of column length.

The MCT-1 Capillary Column Coating Stand and CLH Capillary Column Holder are also available. Installation is possible without reshaping of drawn columns.

CIRCLE 124

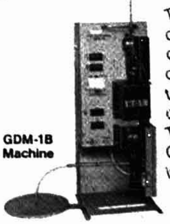

GDM-1B
Glass Drawing Machine

See SHIMADZU at the Pittsburgh Conference, Booths No.1409-1416

SHIMADZU
SCIENTIFIC INSTRUMENTS, INC.

SHIMADZU SCIENTIFIC INSTRUMENTS, INC.
9147 Red Branch Road, Columbia, Md. 21045, U.S.A. Phone: (301)596-6978 Telex: 2308795
SHIMADZU (EUROPA) GmbH
4000 Düsseldorf 1, Johannes-Weyer-Str. 1, F.R. Germany Phone: (0211)314061 Telex: 0858680
SHIMADZU SEISAKUSHO LTD.
1 Nishinokyo-Kuwabaracho, Nakagyo-ku, Kyoto 604, Japan Telex: 05422-166

the plasma people

They're yours with every Jarrell-Ash plasma system.

We sell **more than** plasma instruments. We sell **total** plasma capability. When you take on a Jarrell-Ash plasma spectrometer, you also take on a remarkable **support team,** whose collective expertise guarantees maximum return on your plasma investment.

Marketing specialists and demonstration laboratory staff work with you initially to **define** your needs.

Plasma scientists give your personnel intensive **training** after our installation veterans have set up your lab's instrument.

Applications people visit your lab to advise on **methods** (they're always on tap for phone consultation too).

Service engineers assure you of minimum downtime.

And, each quarter, you'll receive **Plasma Newsletter,** filled with valuable new developments in applications and technique.

Jarrell-Ash, the plasma people. Specialists you acquire for the life of your plasma system. Which makes **your** life a lot easier too!

Send for data on our distinguished Plasma AtomComp™ series today.

Jarrell-Ash Division
Fisher Scientific Company

590 Lincoln Street
Waltham, Massachusetts 02154
Phone (617) 890-4300

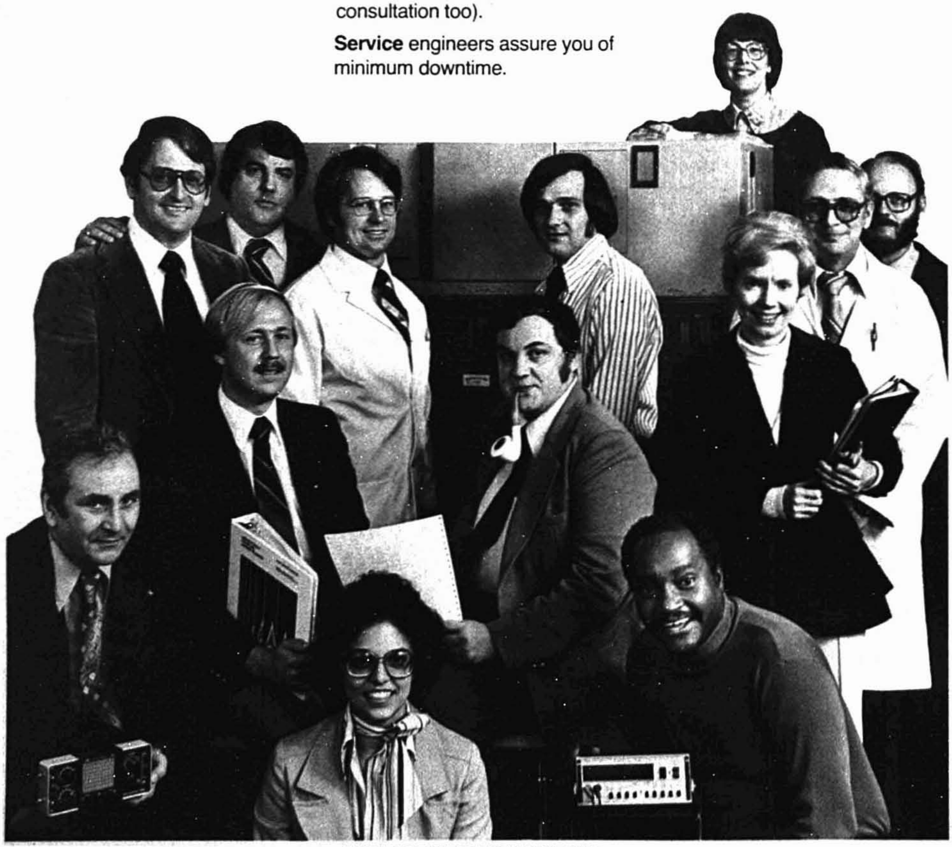

CIRCLE 112 ON READER SERVICE CARD

Priority Pollutant Analysis: Problems and Opportunities

R. O. Kagel, R. H. Stehl, and W. B. Crummett
Analytical Laboratory, Dow Chemical U.S.A., Midland, Mich. 48640

In 1972, with the enactment of PL 92-500, Congress directed the Environmental Protection Agency (EPA) to develop a program to improve the quality of the waters of the United States. After pressures brought to bear on the Agency (because of timetable slippage), a court-approved agreement, "The Consent-Decree," focused the attention of the Agency on section 307a of the act, which regulates "priority pollutants" (now called "toxic pollutants"). The administrator published a list of 65 compounds and categories (subsequently translated to 129 specific compounds or mixtures), and the Agency set about to collect and develop analytical methods to establish the presence or absence of these materials in industrial effluents and waterways of the United States. The Effluent Guidelines Division (EGD), a survey group established within EPA, was charged with the task of developing a program to establish effluent guidelines for these priority pollutants.

EGD initiated its two-phase program in 1976: The first phase involved screening of selected effluents to determine qualitatively which of the 129 were present; the second phase followed with verification or quantitation of those specific priority pollutants detected in the screening phase. The Agency solicited contributions and peer review of sampling and analysis protocol for both phases of the program. These were subsequently adopted as the March revised-April 1977 and June 1977, screening and verification protocols, respectively.

Since all parties recognized the necessity to avoid both false positive and false negative results, heavy emphasis was placed on GC/MS analysis for the determination of the organic components, with the Agency stressing attention to quality assurance of instrument operation. This program is being applied to 21 industrial categories (over 500 subcategories) by the Agency and its contractors. The screening phase was intended only to provide an initial qualitative data base to identify those types of effluent samples and specific compounds needing further work. It was recognized early in the program that these analytical methods and results would require subsequent validation.

As industry and EPA scientists jointly sought to generate a protocol for validation of verification phase methodology, the EGD suddenly and drastically departed from its original program. As of April–May 1978, the Agency had contracted for nearly every competent available GC/MS hour in the United States in order to complete the screening phase of the program. The Agency then undertook to simultaneously initiate the verification phase program. Lack of access to the data base from the screening phase, the scarcity of GC/MS instrumentation, and the few qualified analytical scientists experienced in this methodology forced the Agency to adopt less accurate methods based on untested GC/FID procedures. These procedures, unfortunately, were not subjected to peer review and have never been validated (noticeably, an Agency validation protocol for verification phase methodology has not yet emerged). Furthermore, EGD proposes that these GC/FID results be used to develop economic evaluation data in support of 1983 water treatment practices. EGD also proposes that the analytical verification of screening-phase data which will serve as the basis for the effluent guidelines are to be generated by these 21 industrial categories during a self-imposed 30-day monitoring program, also yet to be defined by the Agency.

The involvement of a variety of analytical chemists has progressed from one of collaboration (required under the consent-decree) to one emphasizing corroboration. If the trend continues along Agency pathways, the end result only can be an adversarial relationship centered around analysts from the Agency and both environmental groups and industry. The proliferation of untested, unvalidated analytical data will not lead to enforceable water treatment regulations, nor will it lead to an accurate assessment of the nation's water quality, but rather protracted litigation revolving about the analytical chemist.

The challenge to both industry and the regulatory agencies is to apply the state-of-the-art in sampling and analysis technology and to develop, validate, and apply appropriate analytical methodology that will give statistically meaningful results. The analytical scientist can and must impact more positively and forcefully on his profession. The most immediate mechanism is to make your views known to your employer (government, academe, or industry), the regulatory officials, state and local environmental planning units, and most important your elected senators and representatives.

EPA implements the directives of Congress: EPA scientists test their system, technically and legally, in much the same way as we test our own corporate systems. The difference is that we as "technical citizens" are the check and balance mechanism.

0003-2700/79/0351-223A$01.00/0
© 1979 American Chemical Society

The Analytical Approach

Edited by Claude A. Lucchesi

Assuring the Quality of Honey

Is It Honey or Syrup?

Honey, a natural product of limited supply and relatively high price, traditionally has been a target for adulteration. As a result, bulk honey markets are being lost to mixtures and substitutes in the form of sugar cane and corn-derived syrups. When such mixtures are appropriately labeled, there is no legal violation. However, the evidence of widespread mislabeling of these materials as pure honey represents a fraud to the consumer. The adulteration of honey with various sweet syrups without fear of detection is a great threat to the integrity of the honey markets, to the economic resources of beekeepers, and to the production of the more than 11.5 billion dollars worth of agricultural crops that depend on the honeybee for pollination.

The corn processing industry now produces a new low-cost sweetener, high fructose corn syrup (HFCS), in great amounts by making use of advances in bound enzyme technology. It has been estimated (*1*) that the food industry will use four billion pounds of HFCS annually by 1980, with per capita consumption reaching 18.2 lb, 14% of the total nutritive sweetener consumption. HFCS production involves the enzymatic isomerization of a portion of the glucose in conventional corn syrup to the sweeter sugar, fructose. The resulting syrup is then refined with activated carbon and ion-exchange treatment, and yields the two monosaccharide sugars, glucose and fructose, with only slight amounts of other materials.

A research program designed to develop methods for the detection of honey adulteration by HFCS was initiated at the Eastern Regional Research Center early in 1975. We considered several approaches with the hope that some would result in methods for HFCS detection in honey, regardless of improved production methods of this sweetener by the corn processing industry.

The Analytical Approach

Two general analytical approaches can be taken in attacking a problem such as the detection of mixtures of honey and HFCS.

Approach One: Identification of a constituent or property of the adulterant and detection of its presence in suspect honeys. Pure honeys would be shown either not to possess the chosen characteristic or to possess it at a much lower level.

Approach Two: Identification of a constituent or property of honey that is always present at a certain level. The addition of an adulterant without the characteristic would lower the concentration of the constituent or the value of the property.

Tests are available to detect the traditional adulterants of honey, including conventional corn syrup and commercial invert syrup (*2*). Approach One was used in the development of the official methods for identifying each syrup in honey. Conventional corn syrup (primarily glucose) contains appreciable amounts of higher molecular weight glucose polymers not present in honey, and these are detected by paper and thin-layer chromatography. Inverted cane syrups (consisting primarily of glucose and fructose) are detected in honey through the presence of hydroxymethylfurfural (HMF), which is present at significantly higher levels in acid-inverted cane syrups than in pure honeys.

Approach Two is of no value for the detection of adulterated honey because of the wide variability among the known constituents of honey. The most authoritative study of United States honey composition (*3*) illustrates the variability encountered. In that study, all commercially significant domestic honey types and blends

This article not subject to U.S. Copyright
Published 1979 American Chemical Society

Landis W. Doner, Irene Kushnir, and Jonathan W. White, Jr.
Eastern Regional Research Center, Agricultural Research, Science and Education Administration, USDA, Philadelphia, Pa. 19118

were analyzed, and the results can be considered truly representative of domestic honey composition with regard to the components determined. The concentration ranges for the major constituents of honey (490 samples analyzed) and of HFCS samples from a major commercial source are given in Table I. The ranges indicate that a considerable amount of a sweetener like HFCS, with its sugar composition resembling honey, could be added without the mixture exceeding normal honey concentration limits. The increased moisture content can be compensated for easily by a clever manipulator. In the survey (*3*) the presence of other honey constituents over a wide range precluded the use of dilution of a honey property for detecting adulteration. Approach Two was used for just two possibilities examined in our research, unsuccessfully both times, as indicated in Table II.

The composition of honey depends upon two most important factors, the floral source and the composition of the nectar. Less important are certain external factors, including climate and differences in processing. All factors contribute to the variability of honey composition and to its enormous complexity [22 minor di- and trisaccharides have been identified (*4*)] and make most approaches to the detection of adulteration unworkable.

Early in our research program we had to learn as much as possible about the properties and composition of HFCS from the various commercial sources. Our goal was to find a constituent or property common to the various HFCS samples but not found in any honeys. Little information regarding the minor HFCS constituents that may come through the rigorous refining process was available in the literature, and examination of significant numbers of representative honeys with respect to any candidate HFCS components was required. It was our expectation that no single test would serve the objective of this search, and the need to screen large numbers of suspect samples would require relatively simple indicator tests; confirmatory analysis could be more complex. Furthermore, tests, to obtain legal standing, would have to be subjected to formal collaborative testing by independent laboratories, under the auspices of the Association of Official Analytical Chemists.

Establishing tests for HFCS in honey proved more challenging than earlier methods for the traditional adulterants, since HFCS is simpler, more closely resembles honey composition with regard to major components, and is more highly refined. Complicating the problem is the fact that methods of HFCS production are continuing to evolve, and trace constituents found to be unique in present syrups may be eliminated by new refining processes. Accordingly,

Table I. Concentrations of Major Constituents of Honey and High Fructose Corn Syrup (HFCS)

Constituents	Honey Range (%)	Honey Mean (%)	HFCS Range (%)	HFCS Mean (%)
Moisture	13.4–22.9	17.2	23–29	26
Fructose	27.2–44.3	38.2	30–42	36
Glucose	22.0–40.7	31.3	31–35	33
Di-, tri-, and higher saccharides	4.6–23.3	10.1	3.1–5.7	4.4
Other		3.2		0.6

Table II. Approaches for Detection of Mixtures of High Fructose Corn Syrup and Honey

Method	Constituent determined	Found to be applicable
Approach One		
Differential scanning calorimetry	Organic compounds	No
Gas-liquid chromatography	Isomaltose/maltose ratio	Yes
Gel filtration, affinity chromatography	Polysaccharides	No
High-pressure liquid chromatography	Monosaccharide (psicose)	No
Immunodiffusion	Polysaccharides, proteins	No
Stable carbon isotope ratio analysis	$^{13}C/^{12}C$ ratio	Yes
Thin-layer chromatography	Dextrins, polysaccharides	Yes
Turbidimetry (with concanavalin A)	Polysaccharides	No
Approach Two		
Atomic absorption spectroscopy	Sodium/potassium ratio	No
Colorimetry	Proline	No

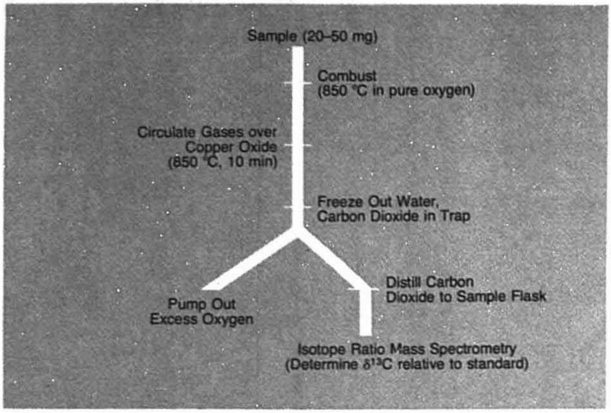

Figure 1. Flow diagram of method for $^{13}C/^{12}C$ determination

we applied Approach One to the problem of detecting HFCS in honey in eight separate investigations (Table II); three proved useful.

Evaluation of Various Approaches

Three approaches to the problem involved determining lower molecular weight ions and molecules and were not valid for judging honey purity. A suggestion had been made (*5*) that examination of the sodium/potassium ratio was useful because HFCS is refined by ion-exchange treatment, and the original cations present in HFCS are replaced by sodium. Honey has long been known to be relatively poor in sodium but rich in potassium. A paper evaluating literature data (*6*), however, demonstrated that the sodium/potassium ratio is of little use as the sole parameter because of the extreme variability of these elements in honey. The convenience of atomic absorption analysis would have made this a very attractive approach, but this variability precluded its use.

Early in our research, we were optimistic that a useful test might be the determination of the monosaccharide sugar psicose, which in early production lots of HFCS had been reported (*7*) to be present at levels to 1% because of base-catalyzed isomerization of fructose. This sugar is not present in honey, and HPLC methods were available for its detection in standard mixtures with the major honey sugars, fructose and glucose. The presence of psicose in HFCS, however, indicated to the corn sweetener manufacturers that the process was not ideal, and they were successful in producing syrups free of this sugar and other by-products considered detrimental to the quality of their product. This was our first experience with a potential method being eliminated because producers were obtaining better (from their viewpoint), more highly refined syrups. This was not our last such experience because, in a sense, we were shooting at a moving target.

The amino acid proline is present in unusually high levels in honey and absent from HFCS. Consequently, proline was measured in 740 honey samples (*8*) to determine whether it is present over a sufficiently narrow concentration range to permit the use of Approach Two. A convenient colorimetric method is available for such a test, but the wide range of values found precluded the use of proline determination as an indicator of honey purity.

Several methods were designed to reveal differences between the minor macromolecular (polysaccharide and protein) fractions of honey and HFCS. In one approach, we constructed an autoanalyzer to determine the molecular weight distribution of polysaccharides from honey and HFCS. Initially, this approach appeared to be very promising. In a second method based on the differences in the polysaccharide fractions from honey and from HFCS, we took advantage of the unusually high degree of branching present in polysaccharides from some HFCS samples. The soybean lectin, concanavalin A, associates with terminal glucose units in branched polysaccharides through a multivalent interaction and leads to precipitation and quantification by turbidity. Interesting results were obtained (*9*) but, as with the other macromolecular approaches, were rendered useless for the adulteration problem when HFCS containing no high molecular weight carbohydrate polymers became commercially available.

An immunochemical approach wherein rabbits were injected with HFCS materials and tested for elicitation of antibodies was attempted. HFCS polysaccharides were conjugated with bovine serum albumin and keyhole limpet hemocyanin and, after being administered to rabbits, produced immune sera, which were isolated by scientists at the Western Regional Research Center of the U.S. Department of Agriculture. Unfortunately, interaction between the immune sera and the injected materials was not inhibited by HFCS polysaccharides. Efforts to prepare a protein concentrate from HFCS for preparation of an immune serum in rats and rabbits were unfruitful. Considering the standard immunodiffusion techniques available, we were disappointed that these sensitive and convenient approaches to the problem did not work.

We also attempted to apply differential scanning calorimetry to the adulteration problem. However, the virtually identical profiles obtained for honey and HFCS again reflected the similarity in composition of the two products.

Stable Carbon Isotope Ratio Method

Clearly, we needed to identify a property of HFCS that would not be affected by new refining processes but would be characteristic of products derived from the corn plant. The breakthrough came when we evaluated the ratios of the stable isotopes of carbon in representative samples of honey and HFCS. This approach had been used (*10*) in detecting the illegal addition of cane sugar to Israeli citrus juice, and it was suggested (*10*) that the $^{13}C/^{12}C$ ratio might be useful in detecting fraudulent substitutions of various types of plant products with corn-derived materials. Methods for detecting the adulteration of maple syrup with cane sugar (*11*) and the adulteration of natural bean vanillin with synthetic vanillin (*12, 13*) had utilized $^{13}C/^{12}C$ analysis.

The reasons for differences in $^{13}C/^{12}C$ ratios among members of the plant kingdom are now beginning to be understood and result primarily from the three different pathways by which carbon dioxide is fixed into organic compounds via photosynthesis. In plants using the classic Calvin (C_3) cycle, the primary photosynthetic product is the 3-carbon acid, 3-phosphoglycerate. In plants using the Hatch-Slack (C_4) cycle, the initial products of carbon dioxide fixation are the 4-carbon acids oxalacetate, malate, and aspartate. Plants in a third category, crassulacean acid metabolism, have the enzymatic capability for initially fixing carbon dioxide by

RAPID SPECTRAL ANALYSIS

The TN-1710-I-DARSS* is a complete, computer-based system for rapid analysis of UV-Vis-NIR spectral data.

Complete spectra are acquired in milliseconds. Using the sequential scan module, *up to 64 different spectra* can be recorded at nearly 400 spectra/second for Time Resolved Spectroscopy and Chemical Kinetics measurements.

High spectral resolution measurements are accommodated with the TN-1149 spectrograph which can provide a dispersion *as high as 0.036 nm per channel.*

Highest S/N Ratio: The new TN-1223-4I large area intensified array has 2.5 mm x 0.025 mm channels for up to 15 times better S/N than other I-DARSS detectors.

Programmable operation: NBS traceable calibration sources are combined with advanced radiometric/photometric routines for correction of intensity data in Raman and general purpose QC measurements including CIE calculations. Programs and spectral data can be stored on an optional floppy disk device.

Highest Sensitivity: The I-DARSS is more sensitive than SIT and ISIT devices over most of its operational bandwidth. Further, the Gen II Intensifier gain can be varied from 200 to nearly 40,000 with a single control while maintaining a 4096:1 A-D conversion range.

In addition to speed, sensitivity and fine resolution, the I-DARSS offers the unique advantages of an all solid state design: bloom free and target-lag free operation, thermo-electric cooling, and a geometrically stable configuration for microphonic free operation.

As the only multichannel optical spectroscopy system to win the prestigious IR-100 award for 1978, the I-DARSS offers unmatched performance at an unbeatable price.

For descriptive literature or more information, contact:

Tracor Northern

CIRCLE 207 ON READER SERVICE CARD

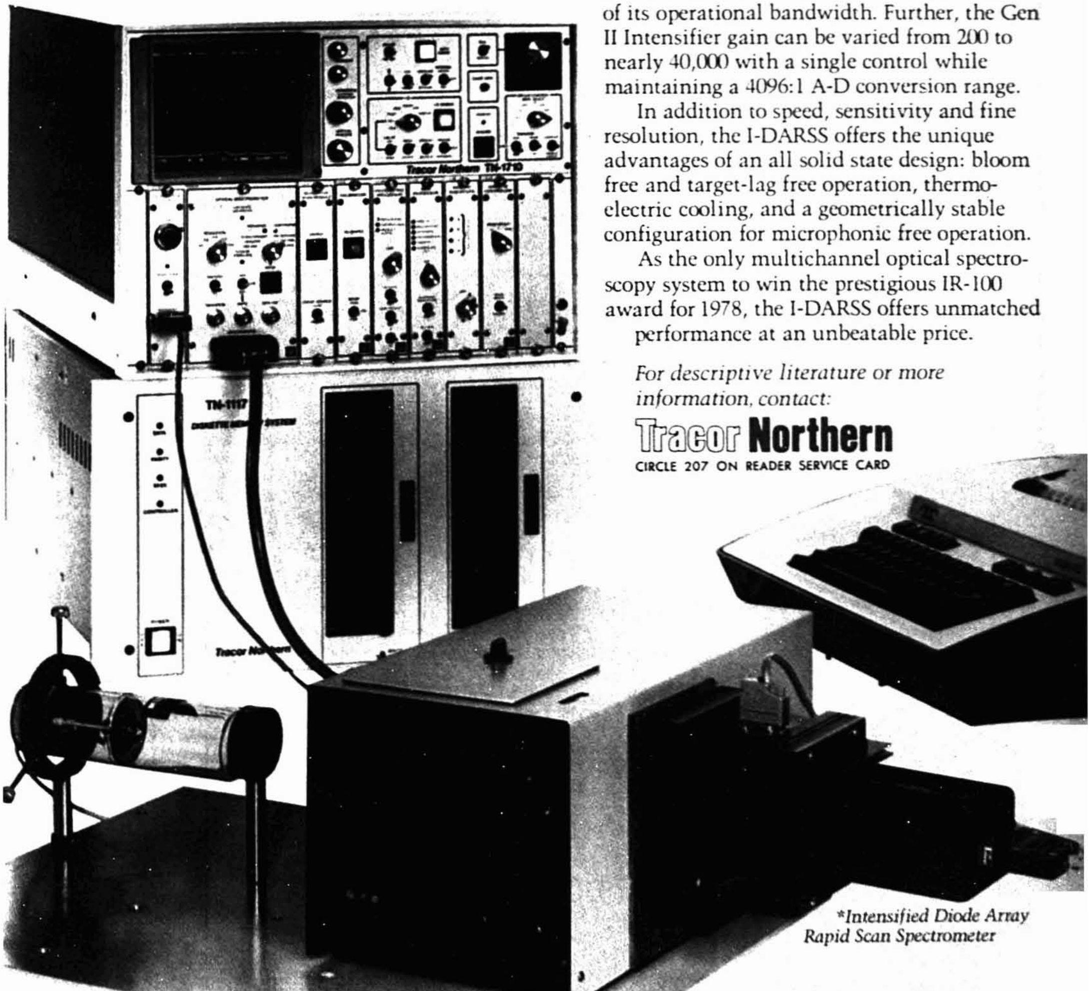

Intensified Diode Array Rapid Scan Spectrometer

2551 West Beltline Highway / Middleton, Wisconsin 53562 / (608) 831-6511 / TWX-910-280-2521
Tracor Europa B.V. / Schiphol Airport Amsterdam / Building 106, The Netherlands / Telephone (020) 41 1865 / Telex 13695

SPECTROSCOPY FROM VERLAG CHEMIE

FUNDAMENTAL ASPECTS OF ORGANIC MASS SPECTROMETRY
K. Levsen
A detailed introduction into the theoretical aspects and methodological concepts of organic mass spectrometry.
Progress in Mass Spectrometry Series.
1978 approx. 316 pp. with 87 fig., 25 tab., 63 schematic drawings
$42.00 cloth

13C NMR SPECTROSCOPY, 2nd Ed.
Methods and Applications
E. Breitmaier & W. Voelter
Deals with basic principles, methods, and techniques as well as structural correlations for many organic molecules and natural compounds. Includes pulsed and Fourier transform methods and double resonance techniques, chemical shifts, coupling constants, spin-lattice relaxation times, more.
Volume 5, Monographs in Modern Chemistry.
1978 approx. 336 pp. $50.30 cloth

POLYMER SPECTROSCOPY
Edited by Dieter O. Hummel
CONTENTS: The Subject of Polymer Spectroscopy. Vibrational Spectroscopy. High Resolution Nuclear Magnetic Resonance Spectroscopy. Electron Spin Resonance. Mass Spectrometry.
Volume 6, Monographs in Modern Chemistry.
1974 401 pp. with 262 fig., 76 tab.
$55.55 cloth

RAMAN/IR ATLAS OF ORGANIC COMPOUNDS
3 issues in 2 loose-leaf binders
1974, 1975, 1976 1090 pp. with 1001 spectra $404.60

ATOMIC ABSORPTION SPECTROSCOPY
Bernhard Welz
This revised second edition treats fundamentals, instrumentation, technique, and individual elements and their specific applications.
1976 267 pp. with 73 fig., 46 tab.
$34.80 cloth

Visit us at Booth 1228
or write:
Verlag Chemie International
175 Fifth Avenue
New York, New York 10010

Prices subject to change without notice

CIRCLE 219 ON READER SERVICE CARD

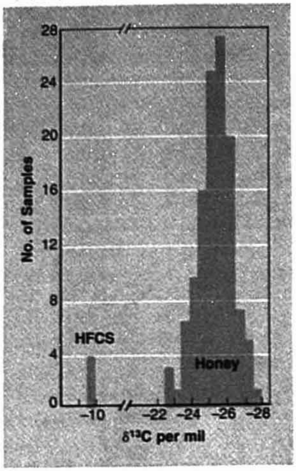

Figure 2. Distribution of $\delta^{13}C$ values for honey and HFCS

Reprinted with permission from ref. *17*. Copyright 1978 Association of Official Analytical Chemists

the C_4 pathway and then shuttling it into the C_3 system. All plants are slightly lighter in ^{13}C than the carbon dioxide of the atmosphere, and Calvin (C_3) plants discriminate to a greater extent than do Hatch-Slack (C_4) or crassulacean acid metabolism plants. The $^{13}C/^{12}C$ ratios of a sample are reported as per mil (‰) deviations from a limestone standard and are defined as:

$$\delta^{13}C \text{ (per mil, ‰)} = \left(\frac{^{13}C/^{12}C \text{ sample}}{^{13}C/^{12}C \text{ standard}} - 1\right) \times 10^3$$

These values are determined by isotope ratio mass spectrometry after complete sample combustion to carbon dioxide. A flow diagram of the procedure is shown in Figure 1. Calvin (C_3) plants have $\delta^{13}C$ values of −22 to −33‰, and Hatch-Slack (C_4) plants have values from −10 to −20‰ (*14, 15*). Crassulacean acid metabolism plants have intermediate $\delta^{13}C$ values.

Corn, sugar cane, sorghum, and other grasses native to the tropics fall into the Hatch-Slack category with $\delta^{13}C$ values in the upper range. Pure HFCS then would have a similar value. It was our hope that all honey samples would be in the range expected for Calvin plants and that this might be a characteristic of all flowering, nectar-bearing honey sources. To test this, we selected 84 samples from our collection of pure honeys to represent all commercially important United States honey sources from wide geographical areas. We analyzed 35 imported honey samples from 15 countries, with geographical latitude the primary consideration in their selection. Details of the method and results of $\delta^{13}C$ analysis of these samples are described elsewhere (*16–18*); the distribution of values are diagrammed in Figure 2. The coefficient of variation for all honey samples was 3.86%, the smallest yet encountered for any constituent or physical property of honey. Mixtures of HFCS and honey would be expected to have $\delta^{13}C$ values equal to the sum of the fractional contribution of each. This was found to be the case.

A collaborative study of the method was conducted (*17*) by seven laboratories, each testing four prepared honey–HFCS mixtures and a pure honey. Because of the excellent agreement among the collaborators, the Association of Official Analytical Chemists has adopted the method as official first action for handling cases of honey adulteration by HFCS. The beauty of this method is that it is noncircumventable and will apply regardless of new refinements in HFCS production. The only requirement is that these syrups continue to be produced from corn or other Hatch-Slack (C_4) plants. This procedure is now being used by regulatory agencies and by the honey industry for self-policing. The $\delta^{13}C$ values indicate to them whether samples are pure or adulterated honeys. The upper (least negative) limit for authentic honey may be set with any desired degree of certainty; Table III indicates the confidence with which a honey of a certain $\delta^{13}C$ value may be considered pure. A sample with a value less negative than −21.5‰ can be classified as adulterated.

Screening Methods Developed

The carbon isotope ratio test is moderately expensive. Only a few laboratories possess the required instrumentation, and none is in the regulatory field. A need existed for more routine tests that could be conducted

Table III. Probability of $\delta^{13}C$ Value of Authentic Honey Sample Being Lower Than a Stated Limit

Probability of a sample lower than limit	(%)	Limit $\delta^{13}C$ (per mil, ‰)
5 of 6	84.1	−24.4
43 of 44	97.7	−23.4
769 of 770	99.87	−22.5
24 999 of 25 000	99.996	−21.5

Reprinted with permission from ref. *17*. Copyright 1978 Association of Official Analytical Chemists.

Puzzled about the best X-ray system for your electron microscope?

PGT PUTS IT TOGETHER with the PGT-1000 XCEL

Rapid Analysis • Ease of Operation • Versatility • User Programmability • Reliability

No other system offers as wide a range of simple, push-button operations—from automatic element identification to automatic peak ratios. Routine qualitative or semi-quantitative analyses are performed in seconds.

As your needs change, so does the XCEL. Basic qualitative systems go fully quantitative in a matter of hours. Specialized quantitative software for your applications is available too.

And if that's still not enough, write your own programs easily with PGT BASIC. We give you all this, plus the finest after-the-sale service available from any manufacturer.

PUZZLED ABOUT MICROANALYSIS?

We'll give you a free book about energy dispersive X-ray spectroscopy. Simply bring this coupon to Booths 522-528 at the Pittsburgh Conference in Cleveland. (Not coming to the Conference? Mail us the coupon and we'll send you the book.)

Name ____________________
Title ____________________
Company ____________________
Address ____________________
City/State/Zip ____________________
Phone ____________________
☐ Please send other literature

PGT
PRINCETON GAMMA-TECH
Box 641 ▪ Princeton, NJ 08540 ▪ 609 924-7310 ▪ Cable PRINGAMTEC ▪ Telex 843486

CIRCLE 175 ON READER SERVICE CARD

NIH/EPA
Chemical Information System
CIS

WORLD'S LARGEST COLLECTION OF SPECTROSCOPIC DATA BASES:

- **MASS SPECTRAL SEARCH SYSTEM (MSSS)**
- **CARBON-13 NMR SEARCH SYSTEM (CNMR)**
- **POWDER DIFFRACTION SEARCH-MATCH SYSTEM (PDSM)**
- **X-RAY CRYSTALLOGRAPHIC SEARCH SYSTEM (CRYST)**

CIS is an interactive system designed to provide the international scientific community with online access to a series of structurally-searchable numeric chemical data bases. All chemical substances in the CIS data bases are identified with their Chemical Abstracts Service Registry Number providing a direct link to the chemical literature as abstracted by CAS.

See us at the Pittsburgh Conference, Booth 1725, or call (800) 424-9600 for more information.

CIRCLE 104 ON READER SERVICE CARD

Finally!
Routine In-Plant
THERMAL ANALYSIS Instrumentation
and Back-up Service
at a Low Cost.

Basic Model
$6650.00
cell not included

INSTRUMENTATION

The Q. C. 25 Controller and Programmer for DSC, TGA or TMA Analysis features –

- Low cost DSC with one pen X, Y recorder and cell for $10,000.00
- Easy to use push button controls
- Linearized output and digital readout of sample temperature
- Failsafe temperature protection eliminating accidental furnace overheating
- Also available with the following options: Program Cool, Automatic Gas Switching, Step Programming and Rapid Return to Start

SERVICE

In addition to servicing the Q. C. 25 System, our service group has eight years of experience in servicing, repairing and training on DuPont 990 and 900 systems and maintains a full complement of parts and supplies for on site repairs. We also offer a comprehensive service contract designed to suit the customer's needs for preventative maintenance and/or emergency service.

OMNITHERM CORPORATION, 65 E. Palatine Rd., Building 307
P.O. Box 878, Wheeling, IL 60090 Phone (312) 459-0001

CIRCLE 172 ON READER SERVICE CARD

DELIVERY FROM STOCK

WINDOWS, LENSES & ATR PLATES

NaCl · KCl · KBr · CaF_2 · MgF_2 · BaF_2 · Ge · Si · ZhSe · KRS-5 · ZnS · CsBr · CsI · LiF · SrF_2 · Cultured Quartz · Sapphire · Fused Silica · Irtran 2

INFRARED ACCESSORIES

Sealed Liquid Cell Holder · Gas Cell · Precision Cell · Demountable Cell · KBr Pellet Press & Holder

INTERFERENCE FILTERS

UV · Near UV · Visible · Near IR · IR

STANDARD & CUSTOM ITEMS

REPOLISH & RECONDITIONING SERVICES

JANOS
OPTICAL CORPORATION

RT. 35 TOWNSHEND, VT. 05353
TEL: (802) 365-7714
TWX: 7103636777

CIRCLE 111 ON READER SERVICE CARD

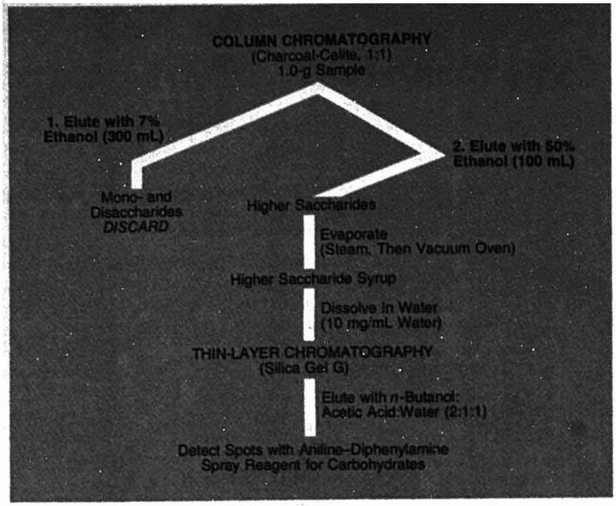
COLUMN CHROMATOGRAPHY
(Charcoal-Celite, 1:1)
1.0-g Sample
1. Elute with 7% Ethanol (300 mL)
2. Elute with 50% Ethanol (100 mL)
Mono- and Disaccharides DISCARD
Higher Saccharides
Evaporate (Steam, Then Vacuum Oven)
Higher Saccharide Syrup
Dissolve in Water (10 mg/mL Water)
THIN-LAYER CHROMATOGRAPHY
(Silica Gel G)
Elute with n-Butanol: Acetic Acid:Water (2:1:1)
Detect Spots with Aniline–Diphenylamine Spray Reagent for Carbohydrates

Figure 3. Thin-layer chromatographic test for honey adulteration

in ordinary laboratories for selecting samples sufficiently suspicious to justify the confirmatory isotope ratio test. Recently, we developed two such methods, one using thin-layer chromatography and the other gas-liquid chromatography.

The thin-layer chromatographic method (*19*) has been subjected to successful collaborative testing (*20*) and recommended for adoption as an official method of analysis. A flow diagram of the procedure is given in Figure 3. This very sensitive procedure involves isolation of a fraction containing oligo- and polysaccharides from both honey and HFCS by column chromatography on charcoal-Celite. After concentration, these fractions were examined by silica gel thin-layer chromatography; consistent differences between honey and HFCS fractions were revealed. Whereas pure honeys yielded only one or two blue-grey or blue-brown spots of R_f greater than 0.35, a series of spots or blue streaks extending from the origin characterized adulterated samples. The method detects HFCS and the traditional honey adulterants, even when present as 10% or less of the total mixture. An added advantage is that this procedure should detect in honey the presence of all starch-derived sugar syrups tested, regardless of the plant source. Figure 4 shows the differences in the chromatographic profiles of honey, HFCS, and adulterated mixtures. This procedure is being used routinely to screen samples, not only for HFCS but also for other adulterants of honey, including conventional corn syrup and inverted sucrose syrups.

A gas-liquid chromatographic method (*21*) based on the determination of maltose and isomaltose has been useful in our laboratory. However, in view of the small number of successful collaborative tests (*20*), it could not be

Table IV. Gas Chromatographic Determinations of Maltose and Isomaltose in Honey (80 U.S. Samples, 35 Imported Samples) and in HFCS (21 Samples)

	Maltose		Isomaltose	
	Mean (%)	SD	Mean (%)	SD
Domestic honey	1.93	0.51	0.64	0.37
Imported honey	2.17	0.53	0.87	0.50
HFCS	0.72	0.26	1.50	0.82

Reprinted with permission from ref. *21*. Copyright 1979 Association of Official Analytical Chemists.

GFS CHEMICALS

YOUR MOST
DIRECT
SOURCE
FOR THE FINEST
COMMERCIALLY
AVAILABLE

ANALYTICAL
CHEMICALS

IT'S WISE TO KNOW
YOU CAN
BUY DIRECT
in ANY
QUANTITY
FROM THE
MANUFACTURER

ANALYTICAL CHEMICALS SINCE 1928

G. FREDERICK SMITH
CHEMICAL COMPANY

867 McKinley Ave.
Columbus, Ohio 43223

FOR PROMPT SHIPMENT
614 224-5343

Contact us or circle
Reader Service Card for
YOUR 50th ANNIVERSARY
GENERAL CATALOG
...it's FREE

GFS CHEMICALS

CIRCLE 198 ON READER SERVICE CARD

NOW!
A DRY BLOCK HEATER THAT
STIRS!

PIERCE Reacti-Therm

FOR
ACCELERATING
AND PRECISELY
CONTROLLING
MINI AND MICRO
REACTIONS

For more information on
Pierce's new Reacti-Therm®
Heating/Stirring Module
please circle number below
on response card.

18900 Reacti-Therm®
Heating/Stirring Module, *110 volts* $162

PIERCE
CHEMICAL COMPANY
Box 117 Rockford, Illinois 61105

CIRCLE 178 ON READER SERVICE CARD

With the new
PIPETMAN™
You're all set...

... Digitally

SET ANY VOLUME (even odd volumes like 11.5 μl or 2,354 μl) with micrometer precision. Pipette with consistent accuracy (0.2 to 1% full range).

- One PIPETMAN replaces more than 30 fixed volume pipettes
- Simple Push-button Operation
- Disposable Pipette Tips
- No lubrication or routine maintenance

Built-in Tip Ejector
for Safe, Non-Contact
Disposal

Model	Recommended Ranges	Price
P-20D	0 - 20 μl	$110.00
P-200D	20 - 200 μl	110.00
P-1000D	200 - 1000 μl	110.00
P-5000D	500 - 5000 μl	137.50

All models supplied with 10 disposable tips
Tip ejector supplied with Models P-20D, 200D, 1000D

Name __________
Institution __________
Address __________
City __________ St. _____ Zip _____

CIRCLE 180 ON READER SERVICE CARD

WESCAN'S NEW MOLECULAR WEIGHT APPARATUS..

COMBINES EASE WITH PRECISION.

- Molecular weights 100 to 25,000
- Temperature range 25°C to 130°C
- Digital readout with analog recorder output
- Aqueous or organic solvents with no change in thermistors
- Priced under $5000

The WESCAN Model 233 Molecular Weight Apparatus is a convenient and easy means for routine determination of molecular weights up to 10,000, and with slightly greater care, up to at least 25,000. It works on the well established principle of differential vapor pressure measurement using two thermistors in a closed chamber.

Incorporation of the latest circuitry, and the same measurement chamber used in the Corona/Wescan Model 232A, provides an instrument which is more precise and stable than earlier designs. Yet the Model 233 includes a number of operating conveniences which make it easy to use.

For more information, contact

WESCAN
INSTRUMENTS, INC.

WESCAN INSTRUMENTS, INC.
3018 Scott Blvd. • Santa Clara, CA 95050
CIRCLE 232 ON READER SERVICE CARD

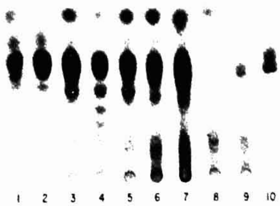

Figure 4. TLC plate of oligo- and polysaccharide fractions from honey, honey–HFCS mixtures, HFCS and standard trisaccharides

1, 2: Pure orange and clover honeys. 3–6: Mixtures of honey with 5, 10, 25, and 50% HFCS, respectively. 7: Mixture of honey with 5% conventional syrup. 8, 9: HFCS samples from two manufacturers. 10: Mixture of trisaccharides raffinose and melizitose

recommended for adoption as an official method. The results of the maltose and isomaltose determinations in honey and in HFCS samples are given in Table IV. A discriminatory equation was developed from these data, and 81% of authentic honey samples and 78% of adulterated honey samples (as determined by $\delta^{13}C$ analysis) were correctly classified.

Society Benefits

We are optimistic that awareness of these convenient new methods for detecting honey adulteration will minimize the threat to the integrity of honey markets. This will help protect the many thousands of beekeepers whose economic resources depend on confidence in the purity of their product. As a result, the population of honeybee colonies will be maintained at the high level so essential for the pollination of billions of dollars in food, feed, and fiber crops.

Since its advent about 30 years ago, isotope ratio mass spectrometry has been a powerful tool, particularly in the realm of basic research. Now it has been applied to a major problem for the food and agricultural industries. Undoubtedly, numerous applications will be forthcoming as more is learned regarding natural variations in $^{13}C/^{12}C$ ratios and ratios of other stable isotopes among plants and their derived products.

The adulteration of natural vanilla extract with synthetic vanillin has been revealed by $\delta^{13}C$ measurements (*12, 13*); detection will hopefully result in this practice being discouraged. More recently, U.S. Customs authorities have been confronted with the problem of determining whether shipments of imported candied pineapple and papaya are processed with honey or inexpensive syrups from C_4 plants. A method was developed (*22*) to determine the nature of the processing syrup by $\delta^{13}C$ analysis. The method also has been applied by the apple juice industry to determine whether HFCS has been mixed with apple juice before production of apple juice concentrates.

The thin-layer chromatographic method (*19*) is both highly sensitive for the detection of honey adulteration by HFCS and convenient for use by regulatory agencies and the honey industry. Added advantages of this method are its detection of inexpensive C_3 plant-derived syrups in honey and its potential for further development and application to future honey adulteration by new sweeteners. It has been recommended that this method replace the old paper chromatographic method (2) for detecting the presence of commercial glucose, one of the traditional adulterants, in honey.

References

(1) *Chem. Eng. News*, **54** (17), 13 (1976).
(2) "Official Methods of Analysis," 12th ed., sections 31.134–31.136, 31.138–31.139, Association of Official Analytical Chemists, Washington, D.C., 1975.
(3) J. W. White, Jr., M. L. Riethof, M. H. Subers, and I. Kushnir, "Composition of American Honeys," Tech. Bull., U.S. Dept. Agric. No. 1261, 1962.
(4) L. W. Doner, *J. Sci. Food Agric.*, **28** (5), 443–56 (1977).
(5) R. S. Shallenberger, W. E. Guild, Jr., and R. A. Morse, *N.Y. Food Life Sci.*, **8** (3), 8–10 (1975).
(6) J. W. White, Jr., *Bee World*, **58** (1), 31–5 (1977).
(7) J. M. Newton and F. K. Wardrip, "Symposium: Sweeteners," G. E. Inglett, Ed., Chap. 8, pp 87–96. Avi Publ., Westport, Conn., 1974.
(8) J. W. White, Jr., and O. N. Rudyj, *J. Apic. Res.*, **17** (2), 89–93 (1978).
(9) L. W. Doner, *J. Agric. Food Chem.*, **26** (3), 707–10 (1978).
(10) A. Nissenbaum, A. Lifshitz, and Y. Stepek, *Lebensm. Wiss. Technol.*, **7**, 152–4 (1974).
(11) C. Hillaire-Marcel, O. Carro-Jost, and C. Jacob, *J. Inst. Can. Sci. Technol. Aliment.*, **10** (4), 333–5 (1977).
(12) J. Bricout and J. C. Fontes, *Ann. Falsif. Expert. Chim.*, **716**, 211–5 (1974).
(13) P. G. Hoffman and M. Salb, *J. Agric. Food Chem.*, in press, 1979.
(14) M. M. Bender, *Phytochemistry*, **10**, 1239–44 (1971).
(15) B. N. Smith and S. Epstein, *Plant Physiol.*, **47**, 380–4 (1971).
(16) L. W. Doner and J. W. White, Jr., *Science*, **197**, 891–2 (1977).
(17) J. W. White, Jr., and L. W. Doner, *J. Assoc. Off. Anal. Chem.*, **61** (3), 746–50 (1978).
(18) J. W. White, Jr., and L. W. Doner, *J. Apic. Res.*, **17** (2), 94–9 (1978).
(19) I. Kushnir, *J. Assoc. Off. Anal. Chem.*, in press, 1979.
(20) J. W. White, Jr., I. Kushnir, and L. W. Doner, *ibid.*
(21) L. W. Doner, J. W. White, Jr., and J. G. Phillips, *ibid.*
(22) L. W. Doner, D. Chia, and J. W. White, Jr., *ibid.*

THE ANATOMY OF A QUALITY HPLC COLUMN

End cap for tight seal during storage.

1/16" "reverse nut" inlet/outlet, adaptable to virtually any chromatograph.

4 mm ID 316 stainless steel tubing with Lichroma* interior finish.

Choice of packings for adsorption, reverse phase, ion exchange and exclusion chromatography.

Zero dead volume end fitting for minimum band spreading.

FROM BIO-RAD, OF COURSE!

You can have complete confidence in the performance of Bio-Rad's HPLC columns for the best of all possible reasons: we *guarantee* it. Specifically, we guarantee column efficiency, peak symmetry, and flow resistance. Furthermore, every Bio-Sil® column comes with a test chromatogram and a test solution sample so that you can verify performance yourself.

Bio-Rad offers a wide selection of columns— all competitively priced— and a wide choice of top quality packings including: • Bio-Sil HP-10 for adsorption • Bio-Sil ODS-10 for reverse phase • Bio-Sil GFC 100 for exclusion • Aminex® HP-C and Aminex A-9 for cation exchange • Aminex A-27 for anion exchange • A variety of custom packings for specific applications (HPX-87 and HPX-42 for carbohydrate analysis are two examples).

Request Bio-Rad Bulletin 1056 for details and our guide to HPLC column evaluation. Contact:

BIO·RAD *Laboratories*

2200 Wright Avenue
Richmond, CA 94804
Phone (415) 234-4130

Also in: Rockville Centre, N.Y.; Mississauga, Ontario; London; Milan; Munich; Vienna.

CIRCLE 28 ON READER SERVICE CARD

New Products—A Preview

Exposition of Modern Laboratory Equipment

Cleveland Convention Center
Cleveland, Ohio

March 5-9, 1979

Microprocessor-based sample processor, Model 1560, can process up to 210 samples each through 960 discrete events like reagent addition from more than 40 sources, agitation, incubation, control of reaction times, and transfer of samples into peripheral instruments such as a chromatograph or spectrophotometer. The user can develop programs by communicating in chemical terminology; no computer language is needed. The processor can be interfaced with other instruments to measure pH and optical absorbance, and can automatically vary the program according to measured results. Instrumentation Specialties Co. 407

AA Spectrophotometers

Models AA-475 and 275 use an 8-bit microprocessor to control instrument functions and data handling. The AA-475 is a double-beam instrument; the AA-275 is its single-beam counterpart. The instrument panel includes keyboard control of hollow cathode lamp current. An automatic gas control unit facilitates programmed ignition and safe shutdown, and a running mean data output mode provides optimum precision. The selection of calibration methods includes three standard calibrations by the company's patented Rational method, and resloping for fast recalibration against a single standard. Varian Instrument Division 417

Monochromator

The DH-20 double monochromator uses the type IV aberration corrected concave holographic gratings and is designed primarily for applications where very high spectral purity is required in a small package. The DH-20 is available in either additive or subtractive dispersion and in four versions covering from 200 to 3200 nm. Instruments SA, Inc. 422

For more information on listed items, circle the appropriate numbers on one of our Readers' Service Cards

---

Vapor Generation Kit

Model 65 vapor generation kit is designed for use with the company's AA spectrophotometers. The kit provides for the determination of mercury by cold vapor generation and arsenic and selenium by hydride generation. It uses solid sodium borohydride pellets and a quartz absorption cell that is heated by an air–acetylene flame for arsenic and selenium measurements. The polypropylene chamber provides an inert reaction vessel and includes a magnetic stirrer. Varian Instrument Division 415

HPLC Columns

The range of ultraperformance prepacked columns offers high efficiencies (typically greater than 50 000 plates/m), peak shapes with asymmetry factors better than 1.6, and extended lifetimes. The columns are packed with spherical silica particles of nominal 5-μm diameter with uniform pore structure. Four types are available: a maximum surface coverage ODS material, an octyl phase, a silica adsorption phase, and a column especially designed for separations where complexing agents are added to the mobile phase. Altex Scientific, Inc. 418

Scanning Accessory

A scanning system for the concave holographic grating monochromators is available. The stepping motor is completely enclosed in a metal housing and is easily mounted on both new and older models of the H-10/H-20 series monochromators. The programmable controller offers 10 discrete scanning speeds (1 nm/mm to 1000 nm/min), continuously variable wavelength scanning range, and four different internal modes of operation. Instruments SA, Inc. 421

COMPARE YOUR IDEA OF A WORKHORSE RECORDER TO OURS.

The rugged Gould 105 General Purpose Strip Chart Recorder delivers such reliable performance, with so many unexpected features, that it goes beyond the traditional definition of a workhorse unit.

Die-cast to handle the day-to-day rigors industrial analytical instrumentation must face, the 105 still offers you a full complement of features you might not expect on such a competitively priced recorder.

Full scale linearity is 99.9%. Rectilinear data presentation is available in either single or dual 10-in. channels. Response time (10% to 90% full scale) is less than 350 ms.

The Model 105 uses disposable felt tip pens available in four colors. It easily takes Z-fold or roll paper without modification. Chart speeds range from 1 in./hr. to 20 in./min. It even makes chart annotation simpler with a flatbed, "write-on" design and event marking standard.

And of course you have the Gould/Brush sales and service organization should you ever need us. Check Gould's 105 — a workhorse of a recorder with a tradition of thoroughbreds.

For more information contact, Gould Inc., Instruments Division, 3631 Perkins Ave., Cleveland, Ohio 44114. Or Gould Alco S.A., 57 rue St. Sauveur, 91160, Ballainvilliers, France. **For brochure, call toll free (800) 325-6400, Ext. 77.** In Missouri: (800) 342-6600.

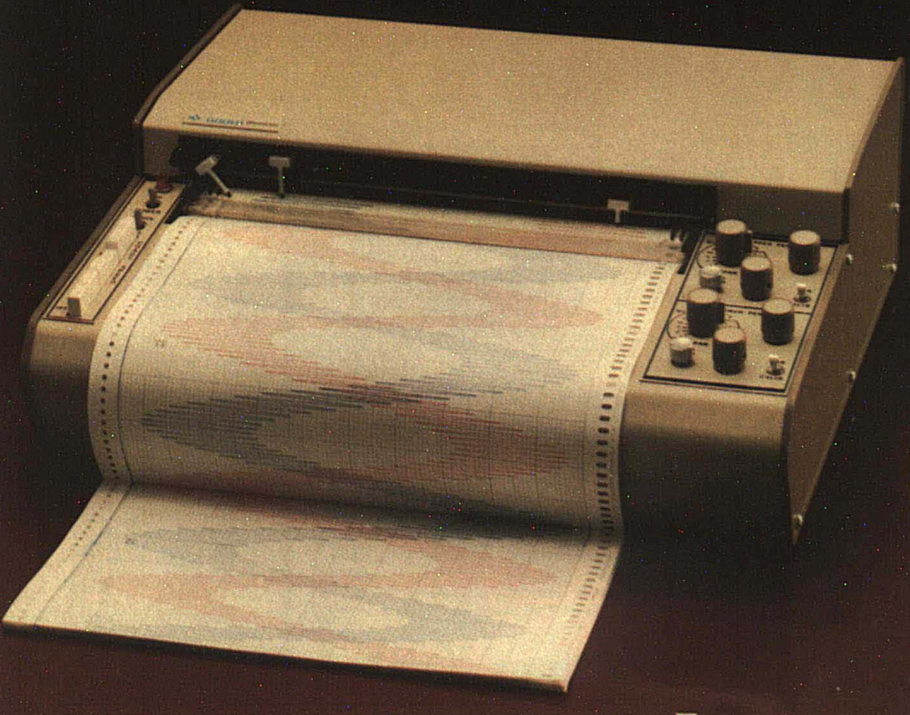

GOULD

CIRCLE 92 ON READER SERVICE CARD

GC/MS Systems

The capability of acquiring CI mass spectrum for high-sensitivity or molecular ion formation and EI mass spectrum for fingerprint or structural information is offered in Model series 200 Simulscan GC/MS systems. Certainty that the sample is identical for each ionization technique is provided and does not depend on the similarity of two consecutive GC runs. Other advantages include provision of the extra dimension of the CI information for manual and computer library searches with improvement in the recognition of correct "hits" or unresolved GC peaks. Two models are available: Model 276-1 comes without the GC, and 276-2 with the GC. Extranuclear Laboratories, Inc.
449

UV–VIS Spectrophotometer

Model 100-80 double-beam recording spectrophotometer features wavelength scanning, repeat scanning, derivative, printing, and a complete enzyme program. The automated system provides acquisition, data processing, and data presentation in the spectrophotometer. NSI/Hitachi Scientific Instruments, Inc.
459

KBr Windows

Two standard sizes of KBr windows are available: 38.5 × 19.5 × 4 mm rectangular windows and 25 × 5 mm round windows. They are guaranteed to transmit 90% or better from 2.5 μ to the cutoff point of KBr. McCarthy Scientific Co. **447**

pH Meter

Model 811 uses a microprocessor to automate every step in pH measurement. Standardization is carried out using an electronic "look-up table" containing pH buffer valves as a function of temperature; pH readings are continuously adjusted for changes in sample temperature. Error codes indicate defective pH electrodes and user mistakes. Additional modes allow reading of electrode potential, percent slope, and sample temperature. Orion Research **450**

Computer Interface for MS

Interlink, an interface for mass spectrometers and computers, uses 16-bit DAC for mass command, a 12-bit ADC for analog data acquisition, and "ping-pong" scalers for pulse counting acquisition. Extranuclear Laboratories, Inc.
452

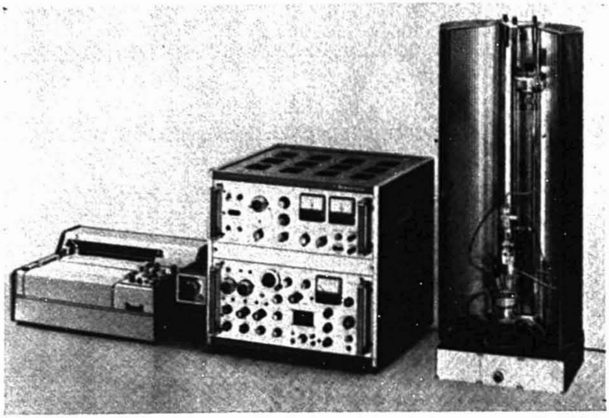

The polarographic system is composed of a polarographic unit, UAP3, a potentiostat PRT30-01, and a potentiometric recorder. The dc voltage programming circuit allows the voltage scanning limits to be set at will in the anodic or cathodic zone providing single-, double-, or multiple-cycle scanning modes. The superimposed ac signal can be continuously adjusted between 3 Hz and 3 kHz with an adjustable amplitude of 0–500 mV. The demodulation phase angle is adjustable from −45 to 135°. The mercury drop time can be adjusted between 0.01–100 s. The potentiostat has a background noise of less than 10 μV peak to peak with available output voltage of ±30 V and output current of ±100 mA. Concentrations of 10^{-7}–10^{-8} *M* in reversible systems and 10^{-6} *M* in nonreversible systems can be achieved, and separation of substances whose peak potential is 30–50 mV apart can be possible. Astra Scientific International, Inc. **408**

UV Detector

A dual-beam, dual-channel UV detector permits simultaneous monitoring in the UV region at two different and selectable wavelengths. Each wavelength is in the double-beam mode and is presented as individual recorder traces on a two-pen recorder. It provides eight push-button wavelength selections across the 210–280-nm region with scale expansions of up to 0.005 A with less than ±1% noise. NSI/Hitachi Scientific Instruments, Inc. **461**

Liquid Chromatograph

Model CLC-5 liquid chromatograph uses centrifugal force rather than gravity, capillary action, or high solvent pressure to separate. Separation of over 500 theoretical plates on sample weights of 5–10 g is provided. The system, which may be used with most column packing materials including silica gels and porous polymers, also includes a UV monitor and fraction collector. NSI/Hitachi Scientific Instruments, Inc.
462

For more information on listed items, circle the appropriate numbers on one of our Readers' Service Cards

MOST USED...
because it's most useful.

The annual ACS **LabGuide** is the definitive directory to scientific instruments, equipment, chemicals, services, books, trade names, manufacturers and their sales offices.

It leads all others in editorial pages, in advertising pages, and in reader usage: **more than 70,000 inquiries every year.**

THE PLOT TO SAVE YOU MONEY.

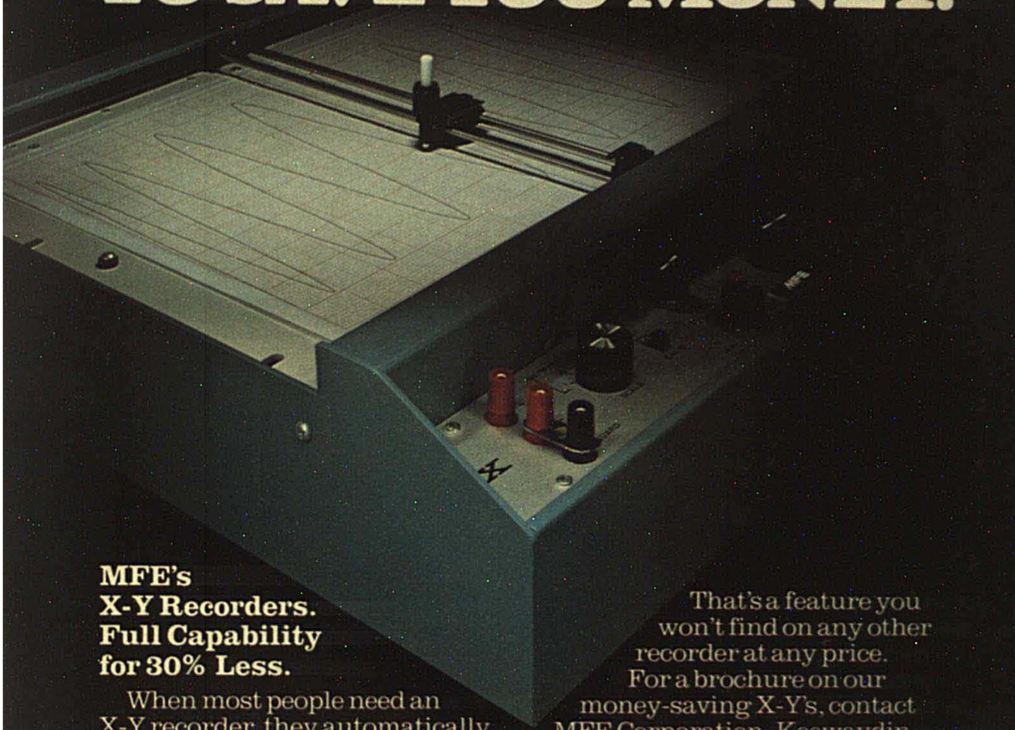

MFE's X-Y Recorders. Full Capability for 30% Less.

When most people need an X-Y recorder, they automatically turn to the biggest name in the business. Which is a very expensive habit.

Because MFE has two X-Y's that give you the same full capability for up to 30% less. A savings of up to $400!

Our X-Y's offer rugged, field-proven performance. In both English and metric. General purpose or OEM dedicated. With five colors of ink. Either 11" x 17" or 8½" x 11" formats. And we guarantee delivery within two weeks.

The plot thickens: our 8½" x 11" X-Y even has a pad/load paper feed system that operates three times faster than conventional single sheet machines. That's a feature you won't find on any other recorder at any price.

For a brochure on our money-saving X-Y's, contact MFE Corporation, Keewaydin Drive, Salem, NH 03079. Tel: 603-893-1921. TWX 710-366-1887/TELEX 94-7477. In Europe: MFE Products Sa, Vevey, Switzerland, Tel. 021 52, 80, 40/TELEX 26238. (MFE has complete worldwide representation. Contact us for the rep nearest you.)

MFE

CIRCLE 137 ON READER SERVICE CARD

Gel Scanner

The gel scanner accessory is designed for use with the company's Cary 210 or 219 UV-VIS spectrophotometers. It can accommodate stained or unstained gels and autoradiographs up to 20 cm long. Measurements can be done at various wavelengths with a choice of three slit widths (0.2, 0.1, 0.05 mm) and 10 scanning speeds (0.01–10 mm/s). Varian Instrument Division **416**

Liquid Chromatographs

The Miniprep is designed for semipreparative LC and uses a twin solvent delivery system so that instantaneous solvent system changes can be made for trivial gradient elution. The column is 20 mm i.d. and 500 mm long with a sample capacity in the range of 1 mg to 1 g. Typical efficiencies are in the 28 000 theoretical plates/m range. The Chromatospac Prep 10 preparative LC is intended for use in the 50 mg to 10 g range. The column is 40 mm i.d. with usable length up to 500 mm. The maximum amount of stationary phase for the Prep 10 is 225 g, and for the Miniprep, 50 g. The column can be interchanged with existing Prep 100 instruments. Instruments SA, Inc. **424**

The Infrared Data Station is a single-station intelligent terminal designed to operate, process data, and display spectra and output data from the company's infrared spectrophotometers. It can be used with Models 580B, 283B, 281B, 599B, 399B, and 299B. Principal features of the data station allow the user to collect data from an infrared spectrophotometer, store spectral data on a microfloppy disc, retrieve spectral data from the disc, perform mathematical operations on data, view spectra and display peak tables on a cathode ray screen, perform repeated runs under one command, and replot spectra on the recorder. The CRT display monitors keyboard entry and displays status and gives "setup" instructions to the user. In addition, the CRT display shows file and data listings, plots up to three spectra, and overlays spectra following data manipulation. Perkin-Elmer **401**

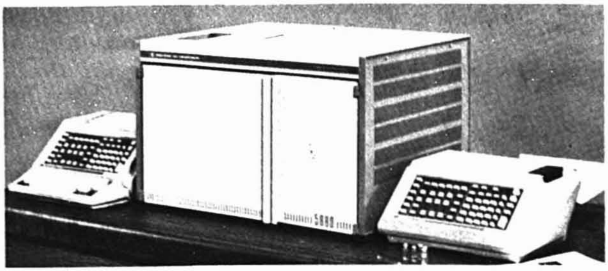

The HP 5880 series microprocessor-based gas chromatographs begin with a basic single-detector, single-column, isothermal GC model with a print/plot terminal that can be expanded in increments to a fully automated GC system with multiple keyboards, detectors and columns, and dual-channel data handling and programming capabilities. The modular design allows other features to be added as applications grow. Four levels of keyboard control are available: level one is for isothermal operation; level two permits temperature, flow, and pressure programming; level three features two-channel integration and area percent; level four adds GC method calculation capability, normalization, external and internal standards with multiple standards, reference peaks, and multipoint calibration procedures. The integrator redefines peak area allocation, valley, and baseline points without rerunning the sample. All GC parameters can be programmed through BASIC. The autoignition flame-ionization detector has a dynamic range of 10^7. The technology that allows the construction of silicon on sapphire chips produces high-speed single microprocessors that have up to 48K ROM and 16K RAM. Prices start at about $9000. Hewlett-Packard **402**

Microcomputer for Sample Changer

LabMate LM-2 is a portable microcomputer designed to interface with any instrument with an analog output. Three to eight standards generate a fitted calibration curve in memory when measurements are taken by integration or peak height. LabMate with option A (LM-2A) allows single-point standardization of curves to occur automatically when the unit is coupled to a sample changer on the instrument. Spectro Products Inc. **427**

ICAP AtomComp Systems

Series 955 and 965 inductively coupled argon plasma AtomComp systems are available. Model 955 determines up to 30 elements simultaneously, and Model 965, up to 48 samples. Model 955 features ICAP source with high temperature/low background, 0.75 spectrometer, DEC PDP-8A computer with 8K core memory, and TI Silent 733 terminal with tape cassette mass storage for fast program loading/simultaneous data storage capability. The system runs on plasma analytical language (PAL) that features simple, mnemonic operation. Software commands can be user linked and stored. Model 965 features PAL software with background correction capability and LA36 DEC writer terminal with dual floppy disks for speedier operation. Jarrell-Ash Division, Fisher Scientific Co. **425**

Liquid Chromatographs

Programmable liquid chromatographs, by use of the Z80 microprocessor, are available. Model 330 provides a 6000 psi, constant flow pumping system, a choice of detectors, and a sample injector. Model 332 provides an almost infinite number of solvent compositions and flow profiles to tackle difficult separation problems. The microprocessor offers control of solvent reservoir selection, automatic sample injection, column switching, and sample collection; up to 19 methods can be stored in memory for recall in any sequence. Altex Scientific, Inc. **419**

Sample Injector

The injector is based on a four-port valve constructed in 316 SS and chemically inert polymers, and is designed for pressures up to 10 000 psi. The design provides easy access to all fittings and requires very little force to actuate from the load-to-inject positions. Sample loops from 5 to 2000 μL are available, and smaller samples can be injected by partially filling the loop with a standard chromatographic syringe. Altex Scientific, Inc. **420**

For more information on listed items, circle the appropriate numbers on one of our Readers' Service Cards

---

INTRODUCING TOTAL CHEMICAL ANALYSIS. ONE BUTTON AND TWO MINUTES AWAY.

BECKMAN
Microlab™ 600
Computing Infrared Spectrophotometer

4000 723
ENTER ANALYSIS #
ENTER NUMBER OF READINGS TO AVERAGE
ENTER PATHLENGTH
PUSH START
ANALYSIS
NORMAL SLIT
GAIN SETTING

Rapid precise qualitative and quantitative final answers by IR analysis are now available at the push of a button on the new Microlab™ 600 Computing Infrared Spectrophotometer.

High precision double beam optics under self-contained automatic computer control analyze most solid, liquid, and gaseous multi-component samples in under two minutes.

Once you've entered your analysis protocol using the Microlab keyboard, the complete analytical procedure is stored right on board for immediate one-button recall.

No outside computational power is needed. Microlab optimizes your scanning parameters, computes quantitative final answers, and reports a complete analysis in analog (chart), digital, and printer modes while storing your program for future use.

High speed, precision, and repeatability are accompanied by features like Repetitive Scanning with selectable Cycle, Time Delay and Wavelength Span, Peak Pick Routine and Automatic Gain Set.

And finally, operator training time is reduced to a minimum by the teaching printer that instructs the user, inquires, and reports on completed operational steps.

So don't wait two minutes more to start saving hours of analysis time. Get complete information. Contact your local Beckman Representative or Scientific Instruments Division, Beckman Instruments, Inc., P.O. Box C-19600, Irvine, CA 92713.

Innovation in IR since 1940.

BECKMAN®

See our complete line of IR products at the Pittsburgh Conference

Monochromators

Model 234 is a compact single-reflection monochromator that covers the wavelength range from the vacuum ultraviolet to the midvisible with a single aberration-corrected holographic grating. Model 248 is a 1-m grazing incidence monochromator or spectrograph. Wavelength coverage is from the soft X-ray region through the vacuum ultraviolet with either photoelectric or photographic detection. Wavelength coverage from 10 to 900 Å is chosen by appropriate selection of the grating and the angle of incidence. GCA Corp. **428**

Resins

A broad line of macroporous polystyrene–divinylbenzene resins for liquid chromatography is available. Rigid spherical beads are synthesized and classified to a narrow range of particle sizes to make them compatible with the high flow rates used in LC. Resins with molecular weight exclusions from greater than 10^7 to less than 10^3 are produced. Functional groups have been introduced into the polymers to produce resins with ion-exchange properties. Dionex Chemical Corp. **433**

Flow Controller

The DFC 100, a dual-channel flow controller designed for chromatographic systems, measures gas flows from 4 to 100 standard cm^3/min. It can be factory calibrated to measure any three of the following gases—hydrogen, helium, and nitrogen and 5% methane in argon. Electronically controlled, the DFC 100 has accuracy and linearity of ±2% full scale and repeatability of ±0.2%. Operating temperature for the flow controller is 50–140 °F, and the temperature coefficient of calibration is less than or equal to ±0.1%/°C. Tylan Corp. **434**

Modular Systems for Amino Acid Analysis

A series of modular systems for amino acid analysis with single microcolumn methodology is available for both hydrolysate/peptide and physiological fluid analyses. Available options include ninhydrin or fluorescence detection, manual or automatic sampling, split stream analysis for fraction collection, and single- or dual-head pumping system. Price starts below $9000. Glenco Scientific, Inc. **435**

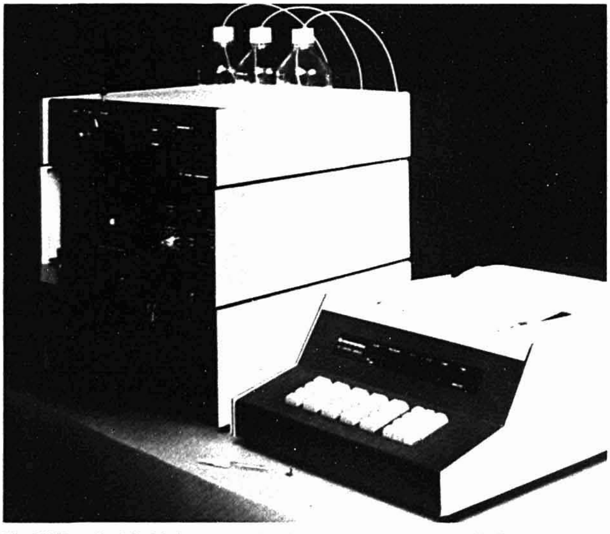

The 7500 gradient liquid chromatograph, with the microprocessor-based 740 control module, initiates analyses by the user entering all operating parameters such as flow rate, pressure limits, solvent concentration, and column temperature. An alphanumeric display continually informs the user of entry status. A printer/plotter located in the 740 produces a total analyses report that contains gradient/solvent conditions, flow rate, pressure, temperature, and operational status. An optional data reduction package prints complete report information describing sample retention times, peak area and height, percent of concentration, and sample and injection numbers. Micromeritics Instrument Corp. **403**

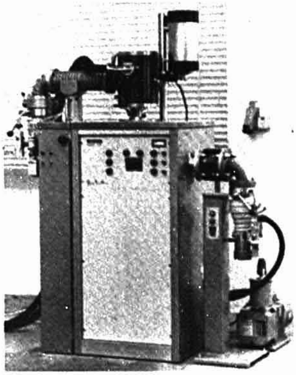

Combined simultaneous TG–DTA apparatus and quadrupole mass spectrometer with coupling system has a two-stage pressure-reduction system that allows gas analysis by simultaneous operation of the TG–DTA instrument and mass spectrometer to 1550 °C. For measurements under high vacuum, pressure-reduction systems are removed, and by direct view between test body and ion source, a high sensitivity is achieved. Netzsch Brothers, Inc. **405**

Balance

The RT 200 is a top-loading electronic balance featuring 200-g capacity, 1-mg readability, large digital display, and an output connector to permit data to be transmitted to printers, computers, or data processors. Operation is from a single bar, and when pressed, the balance "zeros" to allow automatic taring of containers. Sauter **426**

Recorder

The BD 40/41 flat bed strip chart recorder series includes as standard recorder pens with automatic power cutoff in case the pen goes off scale. Other features include multiple voltage spans from 1 mV, 14 chart speeds, and stepping motor chart drives with internal/external control. Kipp & Zonen, Division of Enraf-Nonius Service Corp. **430**

HPLC Columns

The 5-μ spherical ODS, CN, and NH_2 columns are warranted to produce 40 000 plates/m or 10 000 plates/column. Typical back pressures are 30% lower than irregular particle columns of comparable dimensions (250 × 4.0 mm). Columns are available for the adsorption, reverse, polar-bonded, and adsorption-size exclusion phases. Chromanetics Corp. **431**

"Why the Altex 2-pump, microprocessor controlled gradient HPLC is a better system for your lab."

Peter Mansfield,
Director of Marketing

"Two pumps are better than one."

"The Altex Model 332 two-pump system generates solvent composition very close to the inlet of the column so that gradient profiles are sharp, and complete solvent changeovers can be made quickly and efficiently. The microprocessor-controller uses a unique command sequence to ensure accurate solvent concentrations — even at extreme ends of the gradient. In addition, two pumps mean you can operate the system as two isocratic HPLCs when your workload demands.

"Microprocessor control means tight reproducibility plus almost unlimited flexibility."

"While each Altex component is capable of 'stand-alone' performance, the Model 332's microprocessor-controller integrates them into a system with unbeatable reproducibility and speed. This is the concept of 'Distributed Intelligence'. Up to 19 different programs can be stored and later combined into any sequence for automated methods development. Plus an almost infinite variety of gradient shapes and flow profiles assures maximum resolution of any sample.

"You can buy a spectrophotometer with the money you'll save! Not only does the Model 332 represent a moderate initial cost, it will also stretch your lab money in the years ahead, because complete obsolescence is impossible. You will always be operating at the highest levels of performance by replacing individual modules as advances in instrumentation become available. Let me send you full details on this and all the Altex HPLC products."

ALTEX

ALTEX SCIENTIFIC INC.
1780 Fourth Street
Berkeley, California 94710
415-527-5900, Telex 33-5403

CIRCLE 10 ON READER SERVICE CARD

See us at the 1979 Pittsburgh Conference in Booths 1013–14–15–16

Spectrometer

Model DL-203 triple spectrograph has superior stray light rejection and very fast f/5 optics. The optical system, allowing variable dispersions and resolutions by use of turreted optics, eliminates the need to change gratings for varying experimental parameters. Accessories make the DL-203 useful for kinetics, Raman, and fluorescence studies. Instruments SA, Inc. **423**

Monochromators

Model VM-502 vacuum monochromator is a 0.2-m spectral instrument for the vacuum UV–UV–VIS region. It is equipped with a standard aberration-corrected concave holographic grating and wavelength-optimized optical coatings. The instrument can be set up in the conventional "V" configuration or in a straight through configuration that allows the entrance and exit slits to be 180° apart. The VM-505 is a modified half-meter Czerny-Turner type evacuable scanning monochromator with wavelength range from the vacuum ultraviolet (1050 Å) to the far infrared. Model VM-505 with a 1200 g/mm grating has a mechanical scanning range from zero order to 12 000 Å. The resolution is 0.3 Å or better with the standard 1200 g/mm grating installed. Acton Research Corp. **429**

Conductivity Meter

Model 212 conductivity meter is a direct-reading meter with digital display. An analog recorder output also permits continuous monitoring of conductivity. Operating at a frequency of 10 000 Hz, polarization problems are minimized, and the need for platinized electrodes is eliminated. Accuracy is 1% full scale, and measurement ranges are 1–10 000 $\mu\Omega$. Wescan Instruments, Inc. **432**

Gas Calibration Kit

Model 722-K gas calibration kit aids in the preparation of standard gas mixtures of known composition. The heart of the system is a movable, sealed piston within the cylindrical acrylic chamber with calibrated scale units. The piston is raised by gas pressure, or lowered by vacuum, through the inlet fitting at the bottom of the cylinder. The calibration kit includes pump, tubing, an assortment of precision hyperdermic syringes, and a fitted carrying case. Houston Atlas, Inc. **436**

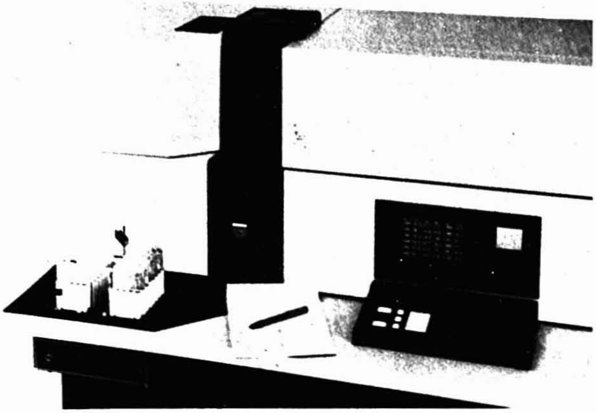

The IL Plasma-100 automated inductively coupled multielement plasma spectrometer determines any number of elements at any wavelength. Using a typewriter-style keyboard, one selects the wavelength for each element by answering questions put by a 23 × 17 cm video display. Background correction and the portion of the plasma to be observed can also be selected. In operation, two rapid-scanning double monochromators are driven by stepping motors from one wavelength to the next, with emission lines from a mercury source used as the wavelength reference. Price is near $40 000. Instrumentation Laboratory Inc. **404**

GC–IR Detector

The Miran GC–IR detector monitors separate multichannel chromatograms for components differentiated by molecular functional groups. It is highly sensitive to specific gases and generally interference free from other substances. Accuracy is unaffected by flow, pressure, and temperature changes. The detector provides supplementary information as to the chemical nature of the eluted components. Foxboro Analytical **437**

Liquid Sampling Valve

The RotaSphere high-pressure liquid valve is intended for liquid phase sampling of pressurized mixtures up to 1500 psig at temperatures to 50 °C. The design is based on a stainless steel ball pierced by two ports of equal dimension. Each port acts as a chamber containing a metered volume of sample. Rotating the sphere connects each chamber with either the sample/vent lines or to the column with the carrier gas. The steel chamber does not change as a function of time, ensuring sample repeatability. Carle Instruments, Inc. **444**

For more information on listed items, circle the appropriate numbers on one of our Readers' Service Cards

Specific Analyzer

The portable acrylonitrile/benzene specific analyzer, developed in response to new OSHA standards, has detection limits less than 0.5 ppm in the presence of common industrial interferences. The analyzer has continuous direct readout of total organic vapor and uses GC for the analysis of acrylonitrile or benzene in the air sampled. Century Systems Corp. **438**

Plasma Excitor

Plasma excitor 300-1 can be used for cleaning and treatment of surfaces and for ashing of organics prior to chemical analysis. The 300-W RF power supply and the long chamber permit processing of several samples simultaneously. Technics **439**

Environmental Analyzer

Model 1560 automated analyzer can be designed to separate and analyze the material of interest from all interferences in the sample environment in the percent to ppb concentration range. Data may be recorded permanently via strip chart as a bar graph in addition to the digital display. Current applications include the automatic analysis of benzene, vinyl chloride, phosphine, and other environmental and industrial pollutants. Analytical Instrument Development, Inc. **442**

Visit our booth 1717 at the
1979 "Pittsburgh" Conference

FOR ELEMENTAL MICROANALYSIS THE

PERKIN-ELMER MODEL 240 ELEMENTAL ANALYZER

IS THE RECOGNIZED LEADER.

C-H-N-S-O

BUT IT IS A TEDIOUS AND TIME DEMANDING INSTRUMENT TO OPERATE UNLESS IT IS AUTOMATED. AND THIS IS WHERE WE EXCELL.

If you already have a 240, we can offer several alternatives:

1. Single sample data handling system (all calculations) with solid state timing control of the 240 to increase production by 25% (5 samples per hour instead of 4), including single sample automatic injector and input/output printer	$ 8,810.
2. Full automation of sample injection and all calculations of an existing 240 to handle 64 samples without operator attendance	$11,550.
3. Or we can rejuvenate your old 240 to include the features of the new Model 240B (See Alt. 4)	
— With single sample automation	$13,310.
— With 64 sample automation	$16,910.

If you wish to buy a 240, you have 2 basic options:

4. We can supply you with a reconfigured 240, rebuilt from bottom up with new upgraded electronics and incorporating the latest improvements in the 240B (vertical scrubbers & traps, 2 additional valves)	
— With single sample automation	$15,310.
— With 64 sample automation	$18,910.
5. Or you can buy a 240B from Perkin-Elmer with fewer features and for more money.	

We stock glass ware, supplies and service parts for the 240 analyzers and our prices are up to 50% less than the Perkin-Elmer prices.

INSTALLATION:	Included above, except travel and living expenses portal-portal, charged at cost.
WARRANTY:	One year on parts and labor, F.O.B. our factory, except input/output printers where manufacturers warranty applies.
TERMS:	1% 10-Net 30 Days. F.O.B. Lowell, Mass. Prices valid in continental U.S.A. only.

CONTROL EQUIPMENT CORPORATION
171 LINCOLN STREET, LOWELL, MASS. 01851 • (617) 459-0573

CIRCLE 41 ON READER SERVICE CARD

Chart Recorders

Model 47-TR series of strip chart recorders can take digital data directly from computer or instrument bus. It converts digital input into a smooth analog curve at a writing rate of 75 cm/s. Paper advance and pen lift are under digital control. Model 57-DS chart recorder, with a high-speed electronic data storage built in, is used in obtaining hard copy recordings of either recurring or single-shot transients. It continually converts an analog voltage into 10 bit digital words, stores them in RAM, and retains the most recent 4096 words; upon receiving a trigger signal, the recorder will plot 4096 words. The plot may be allocated to all before, all after, or a portion before and a portion after the trigger. Applications areas are stopped flow, temperature jump, flash photolysis, and anodic stripping. Price of the Model 47-TR is $785. Pedersen Instruments **448**

Balance

Model 1201 MP-BCD electronic top-loading balance offers a weighing range of 30 g with an accuracy of 0.1 mg. It features a 7-segment digital readout, full range push-button taring, chamber with three accessible sides, and BCD-output permitting interfacing with printers and calculators. Sartorius, Division of Brinkmann Instruments, Inc. **453**

Pump-Colorimeter Analyzers

Two continuous sampling pump flow analyzers for the colorimetric analysis of free and total chlorine in water and wastewater are available. The colorimeter uses a single-beam, dual-wavelength, ratio optical system that corrects for a substantial amount of turbidity. A piston in the colorimeter cell works to measure and transport the sample, expel air bubbles, and clean the inside surface of the cell continuously. Method of analysis is based on *N,N′*-diethyl-*p*-phenylenediamine, with three testing ranges to choose from: 0–0.5, 0–1, and 0–2 mg/L. Hach Chemical Co. **440**

Capillary Columns

The split/splitless capillary injection system combines the all-glass splitter system of German and Horning and the splitless inlet design system of Grob. The four three-way solenoid valves allow changing from one mode of operation to the other. A push-button switch controls the inject-purge function, whereas a three-way toggle switch selects split, splitless, or remote operation. Three models are available: Model 560 with single capillary inlet system and single conventional inlet, and two versions of Model 550 with either dual- or single-capillary inlet system. Tracor Instruments **451**

The Cary 210 UV–VIS spectrophotometer has an absorbance range of −0.6000 to +4.000. The electronic-based baseline corrector is programmable for different scan conditions. Operating parameters such as scan speeds, slit widths, and absorbance ranges are varied using the front panel. The roomy sample compartment can accommodate two five-cell turrets, microcells, and cylindrical cells. Price is $11 995. Varian Instrument Division **406**

Calorimeter

Setaram C 80 calvet microcalorimeter features expanded temperature range to 300 °, pressure operation to 100 bars, isothermal or scanning temperature operation, removable sample cells, sample size to 15 mL, and rapid cool down by fan. Optional equipment includes joule calibration system and computer interface for data reduction. Marche Instruments, Inc. **441**

LC and GC Fitting

A fitting of type 316 stainless steel, featuring low dead volume, is available in $^{1}/_{16}$- and $^{1}/_{8}$-in. o.d. tubing. The fitting has a perfluoroelastomer seal of Du Pont's Kalrez that can withstand 500 °F and is chemically inert. The basic unit of the series 20 fitting consists of a Kalrez sealing disc, a nut, and a 6-in. length of tubing with one welded head and one plain end for interfacing with other fitting systems. General Valve Corp. **443**

FT–IR Spectrometer

Model fx-6200 dual-beam, rapid-scan Fourier spectrometer has spectral coverage from 4000 to 600 cm^{-1} with a resolution of about 2.0 cm^{-1} and a minimum scan time of less than 2 s. Single-scan amplitude resolution is better than 2%, and averaging of up to 256 scans is provided. User input is by a solid state keyboard with a CRT display and an XY plotter provided. Price is less than $20 000. Laser Precision Corp. **445**

Gas Chromatographs

Series-Sx gas chromatograph operation is based on automatic sample injection and column switching by motor-driven valves. Thus, the instrument has four separate control channels for operation of up to four valves or a combination of valves and other functions such as recorder on-off and solenoid operation. The Series-Sx is controlled by the user's in-house computer or microprocessor integrator. Carle Instruments, Inc. **446**

pH/Ion Meter

Model 135 microcomputer-controlled pH/ion meter has memory capability for storing calibration points to enable users to cycle determinations from one mode to another without recalibrating between measurements. Temperature variations are automatically compensated. Instrument control is done through the flat keypad. Corning Glass Works **456**

UL
®
HYDROGEN GENERATOR
GENERAL ELECTRIC
DESICCANT
WATER
REGULATED OUTPUT PRESSURE
GENERATING
SYSTEM OFF
OUTPUT PRESSURE ADJUST 0-60 PSIG
REFILL
LINE ON
OFF

GENERAL ELECTRIC'S HYDROGEN GENERATORS ARE UL LISTED

General Electric's hydrogen generator sets unmatched standards for performance and dependability. For users of gas chromatographs, ionization detectors and related equipment, it provides the on-site, on-demand source of high-purity hydrogen they need.

UL Listed–plus all these advantages

- Low-pressure, low-volume generation simplifies compliance with OSHA requirements
- Eliminates the need for high-pressure storage cylinders
- Solid polymer electrolyte eliminates gas stream contamination and ensures long life
- Maintains gas purity without palladium diffuser
- Uses distilled water instead of caustic soda
- Provides accurate output pressure control— ± 0.5%—150 or 225 cc/min STP Units
- Compact and lightweight
- Proven performance with previous units—over 3,500 in use

Get all the facts

Write General Electric Company,
Direct Energy Conversion Programs,
50 Fordham Road, Wilmington,
Massachusetts 01887

AIRCRAFT EQUIPMENT DIVISION

170-35

GENERAL ELECTRIC

CIRCLE 93 ON READER SERVICE CARD

New Disposable Gas Purifier

The economical method of producing high purity, oxygen free gas for laboratory, analytical instruments and production applications.

The Diamond disposable gas purifier, a polished aluminum canister containing an oxygen "getter"... removes oxygen, trace amounts of organics and water from standard bottled gas, including Nitrogen, Helium, Argon or Hydrogen, to less than 1 ppm. A single canister treats 3 standard 300 cu ft cylinders and is available with ⅛" or ¼" Swagelok type fittings for ease of inline hook-up.

$84.00—quantity discounts available ... truly an economical addition to your lab.

Write for complete information and quantity prices—
Dealer inquiries invited.

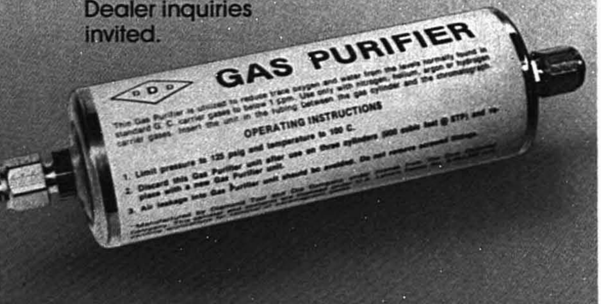

Diamond Tool & Die Inc.
508 - 29th Avenue, Oakland, California 94601 (415) 534-7050
Toll Free: (800) 227-1085 (except California)
Manufactured under license from Dow Chemical Co.

CIRCLE 49 ON READER SERVICE CARD

New Products

Titration System

Titrimax, a modular titration system, comprises an automatic titration controller and buret. Volumetric titrations can be plotted with reagent delivery rate controlled by the slope of the titration. Titrations with automatic detection of the inflection point and automatic end point titrations, as well as titrations with controlled increment addition of the reagent, can also be produced. Astra Scientific International, Inc. **457**

Fluorescence Flow Cell

U fluorescence flow cell, constructed with a fluorescence-free grade of fused silica, is designed to facilitate monitoring of HPLC fractions while using a spectrofluorimeter. The sample cavity is constructed to keep the volume to a minimum (20 μL nominal), and enables the cell to fit any cuvette holder. The cell has a large aperture capable of accepting the full exciting and fluorescent radiation. Precision Cells Inc. **454**

HPLC Gel Filtration Columns

Three types of Bio-Sil GFC packing columns are available: GFC-10, 50, or 100 with 100, 500, and 1000 Å pore sizes, respectively. Each type of packing is available in two column sizes: analytical columns (250 × 4 mm) for rapid molecular weight estimation, and high-resolution/preparative columns for demanding separations or purification of milligram quantities of materials. Bio-Rad Laboratories **455**

HPLC Columns

Reverse phase columns packed with Bio-Sil ODS-10 are guaranteed to provide at least 5000 theoretical plates, to have peak asymmetry or tailing no greater than 1.5, and to have a flow resistance parameter, ϕ, in the 1000–2000 range. Each column is shipped with a test chromatogram and a sample vial of the test mixture used so that the test results can be verified. Bio-Rad Laboratories **458**

Water Purifier

Milli-R/Q water purifier produces 3 L/h of CAP/ASTM Type II water, exceeding the purity of double-distilled water. A molded polypropylene case holds three cartridges. The first is a prefilter, followed by a spiral-wound reverse osmosis membrane. Water then flows through a three-stage polishing cartridge in which a dry-pack carbon removes organics, and a mixed membrane filter removes particles and microorganisms. Price is $895. Millipore Corp. **460**

For Creative Chromatography Specify Spectra-Physics.

SP 4100: the first intelligent integrator

Our new single-channel SP 4100 Computing Integrator is really sophisticated, and yet costs far less than other units with fewer features. **SP 4100 is easy to use**—plug it in, touch a button, and you get Area and Area % report. If you want more, **it has truly intelligent dialog**—it asks only relevant questions for the data manipulation you want. **Dynamic integration is standard**—automatic integration with dynamic evaluation of parameters will integrate each peak optimally.

Let us show you how SP 4100 can help you do more creative chromatography. It's what you'd expect from Spectra-Physics, the company that invented the computing integrator.

BASIC programmability is standard—You can use SP 4100's extensive capability and flexibility to fit your individual needs.

Programmable X-Y plotting—You can enhance your data presentation with graphs such as this multilevel calibration.

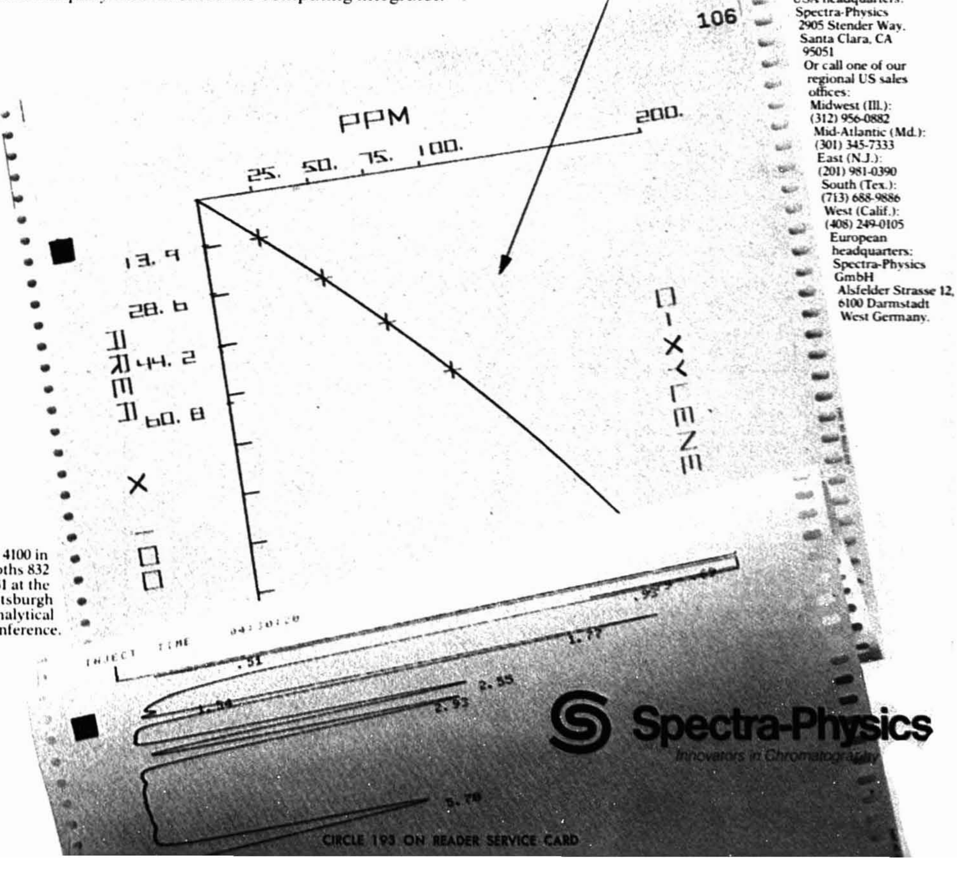

USA headquarters:
Spectra-Physics
2905 Stender Way,
Santa Clara, CA
95051
Or call one of our regional US sales offices:
Midwest (Ill.):
(312) 956-0882
Mid-Atlantic (Md.):
(301) 345-7333
East (N.J.):
(201) 981-0390
South (Tex.):
(713) 688-9886
West (Calif.):
(408) 249-0105
European headquarters:
Spectra-Physics
GmbH
Alsfelder Strasse 12,
6100 Darmstadt
West Germany.

See SP 4100 in Booths 832 and 931 at the Pittsburgh Analytical Conference.

Spectra-Physics
Innovators in Chromatography

CIRCLE 193 ON READER SERVICE CARD

the ideal GC/MS

PRESSURE MEASURING INSTRUMENTATION

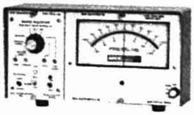

Accurate total inlet pressure measurement can be the key to your success in realizing accurate results from analytical instrumentation such as gas chromatographs and mass spectrometers.

The MKS Baratron® Type 170 capacitance micro–manometer is widely used for accurate pressure measurement in such applications.

Inlet temperatures ambient to 300°C.

TYPE 310 SENSOR HEAD

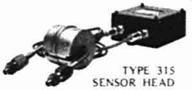

TYPE 315 SENSOR HEAD

Send for data on our 170 Series

MKS

MKS INSTRUMENTS, INC.

precision vacuum measurement & control
22 THIRD AVENUE, BURLINGTON, MASS 01803
Tel. 617 272 9255 Telex 94-9375

CIRCLE 135 ON READER SERVICE CARD

---

pH & Temperature

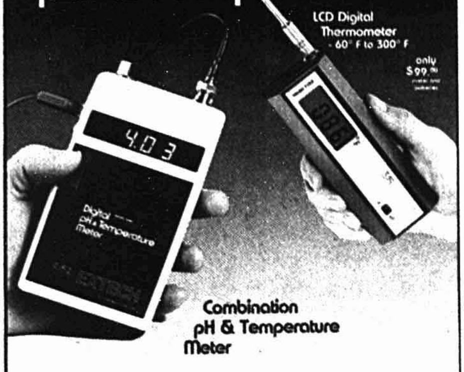

Request FREE Catalogs on these and EXTECH's other portable meters & probes.

EXTECH

EXTECH INTERNATIONAL CORPORATION
114 State Street, Boston, Mass. 02109, U.S.A.
Tel. (617) 227-7090 • Cable EXTECH • Telex 94-0913

See us at the Pittsburgh Conference, Booth #1813

CIRCLE 63 ON READER SERVICE CARD

Parker CPI Single Ferrule Fittings: Why Fewer Places To Seal And Fewer Parts To Assemble Give You More In A Tube Fitting.

Parker single ferrule fittings have only three pieces. Fewer surfaces to seal and fewer parts to assemble. It's a simple design that keeps your system secure. *That's* reliability!

You get other advantages too. Low torque assembly. Available off-the-shelf in 316 stainless steel, brass, steel, aluminum and monel. Other materials on request. Heat Code Traceability. All configurations from 1/16" to 1".

There really is a difference in tube fittings. Ask your local Parker CPI Distributor or write to the Instrumentation Connectors Division,
Parker Hannifin Corporation, 9400 S. Memorial Parkway, Huntsville, AL 35802.

Parker
FluidConnectors

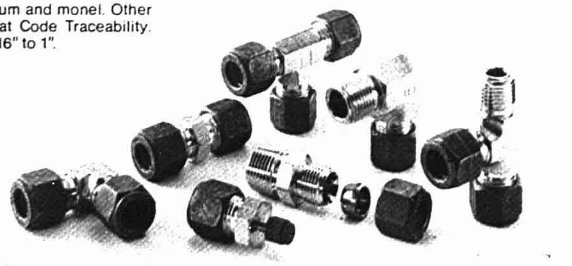

CIRCLE 165 ON READER SERVICE CARD

MCI Automatic Moisture Meter.
Reliable, Fast and Easy.

Incorporates coulometry principle applied to Karl Fischer titration. Operation is full-automatic. Measuring time is shortened. Accuracy is within 5μg for 10μg—1mg H_2O and within 0.5% for 1—30mg H_2O. Wide-range applications include measurement of ultra-trace water content in liquids, solids and gases. Range: 10μg—30mg H_2O.
An optional water vaporizer for speedy and accurate measurement of water content in plastics, grain, etc.

Printer (optional)

CA-02 Moisture Meter with Printer

MITSUBISHI CHEMICAL INDUSTRIES LIMITED
Instruments Dept., Mitsubishi Bldg., 5-2, Marunouchi 2-chome, Chiyoda-ku, Tokyo, 100 Japan Telex: J24901 Cable Address: KASEICO TOKYO

CIRCLE 144 ON READER SERVICE CARD

Parker CPI Ball Valves

Features:
- True ball valve design.
- Pressure compensated design ball valve/ low operating torque.
- C_v ranges from .8 to 1.4.
- Pressure range to 5000 psig.
- Temperature range: −65° to +350°F
- Available in brass or 316 stainless steel (Heat Code Traceable) in popular sizes and end configurations.

Ask for Catalog #4250 from your local CPI Distributor or write to the Instrumentation Connectors Division, Parker Hannifin Corporation, 9400 S. Memorial Parkway, Huntsville, AL 35802.

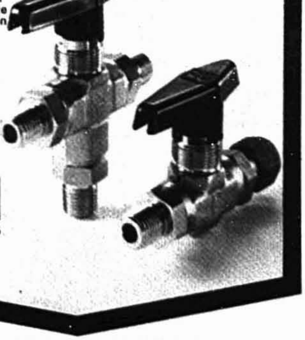

Parker
FluidConnectors

CIRCLE 166 ON READER SERVICE CARD

HIGH RESOLUTION MONOCHROMATOR

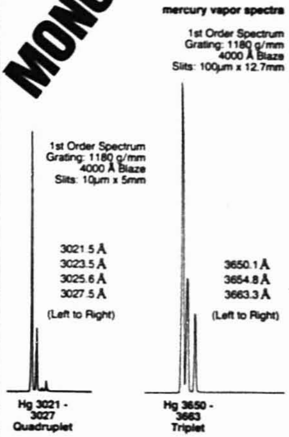

UNDER $2,000

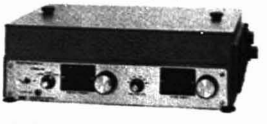

MODEL MP-1018B CZERNY-TURNER MONOCHORMATOR for UV, Visible, and Near-Infrared. 1180 groves/mm standard. Wavelength readout directly in angstroms. Variable slit width readout in microns. Six switch-selectable scanning speeds; bidirectional. Computer compatible. *Brochure available.*

PACIFIC
PRECISION
INSTRUMENTS
Formerly McKee Pedersen Instruments
1040 Shary Court
Concord, California 94518
(415) 827-9010

CIRCLE 170 ON READER SERVICE CARD

AT THE PITTSBURGH CONFERENCE WE'RE UNVEILING THE COST EFFECTIVE GC/MS DATA SYSTEM THAT REALLY WORKS.

Before you shell out a lot of money for a data system, we think you should see our latest system. It can be easily adapted to any quadropole, magnetic, time of flight or site mass spectrometer installations.

The Riber 150 is a state-of-the-art system that will keep pace with your state-of-the-art work.

You'll be able to acquire and analyze data in half the time plus eliminate downtime because we've duplicated the system to do away with single component failures. You'll get the total interaction of two CPUs without interdependence of the system.

And, you'll be able to use Simultaneous Acquisition and Data Reduction (SADR), a revolutionary new foreground/background software system.

You'll receive all of these benefits and more at a cost that is comparable to lesser data systems.

So, if you plan to automate your mass spectrometer installation call or write Riber Data Systems today.

RIBER DATA SYSTEMS

1020 Corporation Way
Palo Alto, CA 94303
(415) 961-2021
Telex 910-379-6474
See us at the Pittsburgh Conference, Booths 1738, 1740

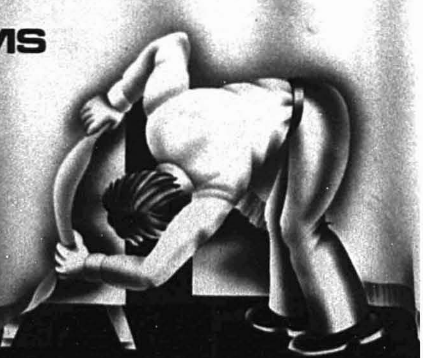

CIRCLE 184 ON READER SERVICE CARD

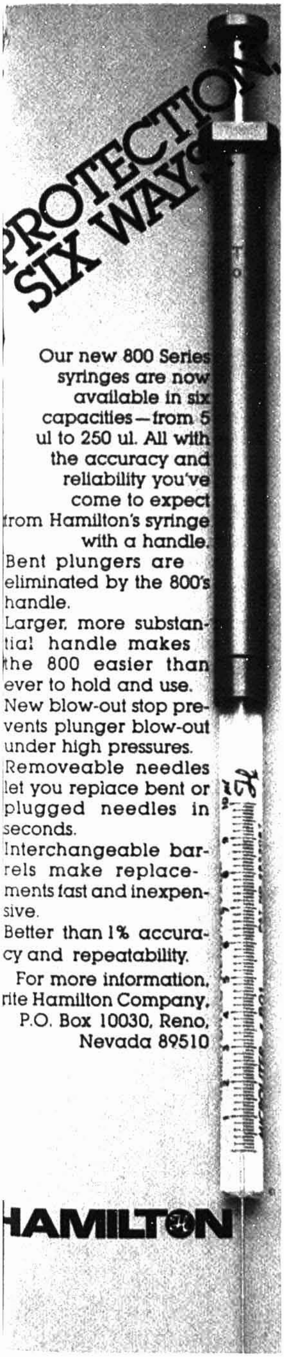

PROTECTION SIX WAYS

Our new 800 Series syringes are now available in six capacities—from 5 ul to 250 ul. All with the accuracy and reliability you've come to expect from Hamilton's syringe with a handle.

Bent plungers are eliminated by the 800's handle.

Larger, more substantial handle makes the 800 easier than ever to hold and use.

New blow-out stop prevents plunger blow-out under high pressures.

Removeable needles let you replace bent or plugged needles in seconds.

Interchangeable barrels make replacements fast and inexpensive.

Better than 1% accuracy and repeatability.

For more information, rite Hamilton Company, P.O. Box 10030, Reno, Nevada 89510

HAMILTON

CIRCLE 95 ON READER SERVICE CARD

FEBRUARY 1979 VALID THROUGH JUNE 1979

ADVERTISED PRODUCTS:					1	2	3	4	5	6
7	8	9	10	11	12	13	14	15	16	17
18	19	20	21	22	23	24	25	26	27	28
29	30	31	32	33	34	35	36	37	38	39
40	41	42	43	44	45	46	47	48	49	50
51	52	53	54	55	56	57	58	59	60	61
62	63	64	65	66	67	68	69	70	71	72
73	74	75	76	77	78	79	80	81	82	83
84	85	86	87	88	89	90	91	92	93	94
95	96	97	98	99	100	101	102	103	104	105
106	107	108	109	110	111	112	113	114	115	116
117	118	119	120	121	122	123	124	125	126	127
128	129	130	131	132	133	134	135	136	137	138
139	140	141	142	143	144	145	146	147	148	149
150	151	152	153	154	155	156	157	158	159	160
161	162	163	164	165	166	167	168	169	170	171
172	173	174	175	176	177	178	179	180	181	182
183	184	185	186	187	188	189	190	191	192	193
194	195	196	197	198	199	200	201	202	203	204
205	206	207	208	209	210	211	212	213	214	215
216	217	218	219	220	221	222	223	224	225	226
227	228	229	230	231	232	233	234	235	236	237
238	239	240	241	242	243	244	245	246	247	248
249	250	251	252	253	254	255	256	257	258	259
NEW PRODUCTS:				401	402	403	404	405	406	407
408	409	410	411	412	413	414	415	416	417	418
419	420	421	422	423	424	425	426	427	428	429
430	431	432	433	434	435	436	437	438	439	440
441	442	443	444	445	446	447	448	449	450	451
452	453	454	455	456	457	458	459	460	461	462
463	464	465	466	467	468	469	470	471	472	473
474	475	476	477	478	479	480	481	482	483	484
485	486	487	488	489	490	491	492	493	494	495
READER SURVEY:				301	302	303	304	305	306	307
308	309	310	311	312	313	314	315	316	317	318
319	320	321	322	323	324	325	326	327	328	329
330	331	332	333	334	335	336	337	338	339	340
341	342	343	344	345	346	347	348	349	350	351

TO VALIDATE THIS CARD, PLEASE CHECK ONE ENTRY FOR EACH CATEGORY BELOW:

Intensity of product need:

☐ 1. Have salesman call
☐ 2. Need within 6 mos.
☐ 3. Future project

Primary field of work:

☐ A. Energy
☐ B. Environmental
☐ C. Medical/Biological
☐ D. Drug/Cosmetic
☐ E. Forensic/Narcotic
☐ F. Textile/Fiber
☐ G. Metals
☐ H. Pulp/Paper/Wood
☐ I. Soaps/Cleaners
☐ J. Paint/Coating/Ink
☐ K. Electrical/Electronic
☐ L. Instrument Dev./Des
☐ M. Plastic/Polymer/Rub
☐ N. Agricultural/Food
☐ O. Inorganic Chemicals
☐ P. Organic Chemicals

Primary area of employment:

INDUSTRIAL
☐ A. Research/Development
☐ B. Quality/Process Control
MEDICAL/HOSPITAL
☐ C. Research/Development
☐ D. Clinical/Diagnostic
GOVERNMENT
☐ E. Research/Development
☐ F. Regulate/Investigate
COLLEGE/UNIVERSITY
☐ G. Research/Development
☐ H. Teaching
INDEPENDENT/CONSULTING
☐ I. Research/Development
☐ J. Analysis/Testing

This copy of Analytical is:

☐ 1. Personally addressed to me in my name.
☐ 2. Addressed to other person or to my firm.

NAME: ____________________
TITLE: ____________________
FIRM: ____________________
STREET: ____________________
CITY: ____________________
STATE: ____________ ZIP ____________
PHONE: (____ ________) ____________

COUNT Photons ON THE DPC-2

DIGITAL PHOTOMETER

SPEX
DIGITAL PHOTOMETER

DO NOT SETTLE FOR NOISE!

Select PMT pulses by their amplitude and detect signals, not electronic interference.

The DPC-2 delivers a 3-fold improvement over dc at vanishingly low light levels; but should photons start flying fast, it offers dc at the flick of a switch.

Call us for a demo or 14-day approval order

SPEX INDUSTRIES, INC./P.O. BOX 798/METUCHEN, N. J. 08840/☎ (201) 549-7144

CIRCLE 187 ON READER SERVICE CARD

NO POSTAGE
NECESSARY
IF MAILED
IN THE
UNITED STATES

BUSINESS REPLY CARD

FIRST CLASS Permit #27346 Philadelphia, Pa.

POSTAGE WILL BE PAID BY ADDRESSEE

analytical chemistry

P.O. BOX #7826
PHILADELPHIA, PA 19101

NO POSTAGE
NECESSARY
IF MAILED
IN THE
UNITED STATES

BUSINESS REPLY CARD

FIRST CLASS Permit #27346 Philadelphia, Pa.

POSTAGE WILL BE PAID BY ADDRESSEE

analytical chemistry

P.O. BOX #7826
PHILADELPHIA, PA 19101

YOUR "READER SURVEY" VIEWS ARE VITAL

Analytical Chemistry occasionally presents a Reader Survey section that provides you with an opportunity to indicate your interests and activities. Your answers help us in planning editorial material that will be useful to you in your work.

To express your Reader Survey views, simply circle your answers on one of these adjacent reply cards and drop it in the mail. No postage is required.

FEBRUARY 1979

VALID THROUGH
JUNE 1979

ADVERTISED PRODUCTS: 1 2 3 4 5 6
7 8 9 10 11 12 13 14 15 16 17
18 19 20 21 22 23 24 25 26 27 28
29 30 31 32 33 34 35 36 37 38 39
40 41 42 43 44 45 46 47 48 49 50
51 52 53 54 55 56 57 58 59 60 61
62 63 64 65 66 67 68 69 70 71 72
73 74 75 76 77 78 79 80 81 82 83
84 85 86 87 88 89 90 91 92 93 94
95 96 97 98 99 100 101 102 103 104 105
106 107 108 109 110 111 112 113 114 115 116
117 118 119 120 121 122 123 124 125 126 127
128 129 130 131 132 133 134 135 136 137 138
139 140 141 142 143 144 145 146 147 148 149
150 151 152 153 154 155 156 157 158 159 160
161 162 163 164 165 166 167 168 169 170 171
172 173 174 175 176 177 178 179 180 181 182
183 184 185 186 187 188 189 190 191 192 193
194 195 196 197 198 199 200 201 202 203 204
205 206 207 208 209 210 211 212 213 214 215
216 217 218 219 220 221 222 223 224 225 226
227 228 229 230 231 232 233 234 235 236 237
238 239 240 241 242 243 244 245 246 247 248
249 250 251 252 253 254 255 256 257 258 259

NEW PRODUCTS: 401 402 403 404 405 406 407
408 409 410 411 412 413 414 415 416 417 418
419 420 421 422 423 424 425 426 427 428 429
430 431 432 433 434 435 436 437 438 439 440
441 442 443 444 445 446 447 448 449 450 451
452 453 454 455 456 457 458 459 460 461 462
463 464 465 466 467 468 469 470 471 472 473
474 475 476 477 478 479 480 481 482 483 484
485 486 487 488 489 490 491 492 493 494 495

READER SURVEY: 301 302 303 304 305 306 307
308 309 310 311 312 313 314 315 316 317 318
319 320 321 322 323 324 325 326 327 328 329
330 331 332 333 334 335 336 337 338 339 340
341 342 343 344 345 346 347 348 349 350 351

TO VALIDATE THIS CARD, PLEASE CHECK ONE ENTRY FOR EACH CATEGORY BELOW:

Intensity of product need:
- ☐ 1. Have salesman call
- ☐ 2. Need within 6 mos.
- ☐ 3. Future project

Primary field of work:
- ☐ A. Energy
- ☐ B. Environmental
- ☐ C. Medical/Biological
- ☐ D. Drug/Cosmetic
- ☐ E. Forensic/Narcotic
- ☐ F. Textile/Fiber
- ☐ G. Metals
- ☐ H. Pulp/Paper/Wood
- ☐ I. Soaps/Cleaners
- ☐ J. Paint/Coating/Ink
- ☐ K. Electrical/Electronic
- ☐ L. Instrument Dev./Des
- ☐ M. Plastic/Polymer/Rub
- ☐ N. Agricultural/Food
- ☐ O. Inorganic Chemicals
- ☐ P. Organic Chemicals

Primary area of employment:

INDUSTRIAL
- ☐ A. Research/Development
- ☐ B. Quality/Process Control

MEDICAL/HOSPITAL
- ☐ C. Research/Development
- ☐ D. Clinical/Diagnostic

GOVERNMENT
- ☐ E. Research/Development
- ☐ F. Regulate/Investigate

COLLEGE/UNIVERSITY
- ☐ G. Research/Development
- ☐ H. Teaching

INDEPENDENT/CONSULTING
- ☐ I. Research/Development
- ☐ J. Analysis/Testing

This copy of Analytical is:
- ☐ 1. Personally addressed to me in my name.
- ☐ 2. Addressed to other person or to my firm.

NAME: ____________________

TITLE: ____________________

FIRM: ____________________

STREET: ____________________

CITY: ____________________

STATE: ____________ ZIP: ________

PHONE: (___ ___ ___) ___ ___ ___ - ___ ___ ___ ___

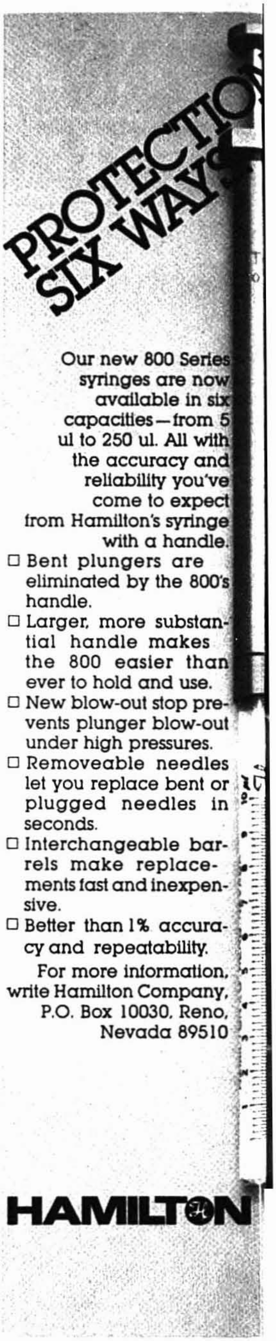

Our new 800 Series syringes are now available in six capacities—from 5 ul to 250 ul. All with the accuracy and reliability you've come to expect from Hamilton's syringe with a handle.

- ☐ Bent plungers are eliminated by the 800's handle.
- ☐ Larger, more substantial handle makes the 800 easier than ever to hold and use.
- ☐ New blow-out stop prevents plunger blow-out under high pressures.
- ☐ Removeable needles let you replace bent or plugged needles in seconds.
- ☐ Interchangeable barrels make replacements fast and inexpensive.
- ☐ Better than 1% accuracy and repeatability.

For more information, write Hamilton Company, P.O. Box 10030, Reno, Nevada 89510

HAMILTON

CIRCLE 95 ON READER SERVICE CARD

ION CHROMATOGRAPHY

DATELINE: FEBRUARY, 1979

AutoIon™

Hardly a week passes at Dionex without our research staff discovering another new application for Ion Chromatography (IC). The technique is as versatile as it is powerful. To keep our users and prospective users as up to date as possible, we'll be publishing a series of informative *Datelines*, backed by application notes. Perhaps what you see here will be 100% on target for you. But we'll be happy if it just triggers your imagination and starts you thinking about the enormous potential of IC.

A word about the technique

Ion Chromatography analyzes ions in solution. Its unique characteristics include: *specificity*, and *rapid, sequential* analysis. Based on ion-exchange chromatography, IC uses conductimetric detection to achieve unprecedented sensitivity levels...e.g. less than 10 ppb. IC is especially suited for the analysis of • complicated matrices • several ions in a single sample • ions in low concentration in the presence of a large concentration of other ions • trace (ppb) levels of ions • several samples of a given type, then several of a different type. Dionex offers this powerful analytical technique in three practical instruments that contain all you need to perform Ion Chromatography rapidly and routinely either manually or automatically.

Applications areas

Air Pollution
Analysis of ambient aerosols for nitrate and sulfate; trace ions in rain water; SO$_2$ in the atmosphere; anions in auto/diesel exhaust; sulfuric acid (SO$_3$) in stack gas; sulfite, sulfate in scrubber liquors.

Water Pollution
Ion characterization of waste effluents; routine ion analysis of ground waters; nitrate-N and phosphate-P in hatchery and bio-pond water; chloride, sulfate and oxalate in paper mill effluent and Kraft black liquors.

Elemental Analysis
Trace level and interference free analysis of organic fluorine, chlorine, bromine, iodine, sulfur and phosphorus after combustion of organic compounds, polymers, and coal.

Soil Analysis
Direct anion analysis in KCl, LiCl, ammonium acetate, ammonium fluoride, sulfuric acid or bicarbonate soil extracts.

Brine Analysis
Direct analysis of chlorate, sulfate, calcium and magnesium in 25% brine and 50% caustic solutions; phosphate, bromide, nitrate, sulfate, calcium and magnesium in 2% brine.

Power Production
Trace chloride, phosphate, sulfate, sodium, potassium, magnesium and calcium analysis in boiler, boiler feed, steam generator, turbine condensate; fuel cell effluents. Anions in geothermal waters, coal liquification and gasification.

Quality Control/Process
Oxalate in Bayer liquors; phosphate, ammonia in fertilizers; fluoride, sulfate, chromate in plating baths; trace anions, cations, amines in electronic device process water; glycolate in surfactants; monobutyl, dibutyl phosphates in uranium refining; halides and sulfates in foods and food additives; primary, secondary, tertiary, quaternary amines in monomers; nitrite, nitrate in spent sulfuric acids, cutting fluids and engine coolants; amines in DMF.

New AutoIon™ System 12 Analyzer

Performs automatic IC analysis at ppm and ppb levels. Twelve different programs of 15 steps each may be stored in the Program Controller. Once initiated by the push of a button, up to 99 samples may be analyzed without operator supervision. Two sub-programs can also execute periodically during any main program. Electronic peak integrator prints out all data.

Auxiliary sample pump enables continuous on-line monitoring; when coupled with an on-line sample concentrator, automatic trace analysis is possible. The determination of trace anions (below) is one example of an AutoIon™ continuous analysis which yields precision of 3% RSD.

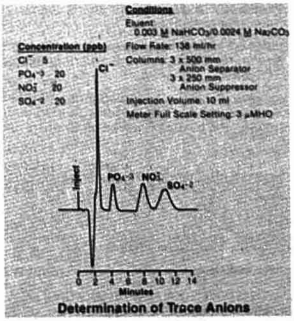

Concentration (ppb)
Cl$^-$ 5
PO$_4^{-3}$ 20
NO$_3^-$ 20
SO$_4^{-2}$ 20

Conditions
Eluent: 0.003 M NaHCO$_3$/0.0024 M Na$_2$CO$_3$
Flow Rate: 138 ml/hr
Columns: 3 x 500 mm Anion Separator
3 x 250 mm Anion Suppressor
Injection Volume: 10 ml
Meter Full Scale Setting: 3 μMHO

Determination of Trace Anions

Spring 1979 Pittsburgh Conference Booths 1105-1107-1109

Symposium and Training Courses

A Symposium on Ion Chromatography (the first ever at the Pittsburgh Conference) will feature the co-inventors of the technique—Hamish Small and Tim Stevens of Dow Chemical Corporation, U.S.A.

Dionex will be conducting a training course and applications lectures at the Conference, March 4–9. Please call (408) 737-0700 x224 for registration information.

Seminar Schedule

Dionex will be conducting a one day seminar series in the following cities. There will be a formal slide presentation on the technique and on applications of Ion Chromatography. An instrument will be available for demonstration and sample running. Please call 408-737-0700 (x224) or write to register or request further information.

CITY	DATE
Philadelphia/ Wilmington	Monday, March 19
Richmond, VA	Tuesday, March 20
Raleigh/ Durham, NC	Wednesday, March 21
Atlanta, GA	Friday, March 23
Birmingham, AL	Monday, March 26
Los Angeles, CA,	Tuesday, March 27
San Diego, CA	Wednesday, March 28
Gainesville, FL	Wednesday, March 28
Miami, FL	Friday, March 30
Phoenix, AZ	Friday, March 30
New Orleans, LA	Monday, April 2
Albuquerque, NM	Monday, April 2
Baton Rouge, LA	Tuesday, April 3
Amarillo, TX	Wednesday, April 4
Memphis, TN	Thursday, April 5
Dallas, TX	Friday, April 6
Knoxville, TN	Monday, April 9
Houston, TX	Monday, April 9
Beaumont, TX	Tuesday, April 10

For information regarding applications of IC, circle the appropriate number.

Air Pollution	#54	Brine Analysis	#58
Water Pollution	#55	Power Production	#59
Elemental Analysis	#56	Quality Control	#60
Soil Analysis	#57	System 12	#61

DIONEX

1977 Pittsburgh
Applied Analytical Chemistry Award

Dionex Corporation

In the US: 1228 Titan Way,
Sunnyvale, CA 94086, 408-737-0700

In Europe: c/o-4, The Buchan, Camberley,
Surrey, GU15 3XB England

NEW HOLLAND
HONEYEATER
Melionoris
Novae
Hollandiae.
MJSS.
MNVU,

So you thought GC/MS interfacing was strictly for the birds.

Until now, interfacing your gas chromatograph with your mass-spectrometer has been one task to steer clear of. Thanks to SGE that has changed!

SGE has developed a patented molecular jet separator and a range of micro needle valves which combine to give you a remarkably fuss and trouble free "all-glass" system of interfacing.

The SGE molecular jet separator has been designed to produce accurate, reproducible jet sizes, alignment and spacing. All with the capability of being temperature cycled up to 450°C - depending on the type of connections used — and without any peak broadening or tailing effects to mar your results.

The SGE micro needle valve range will impress you too. In fact, for accurate critical capillary flow control they're on their own. What's more, the valves have virtually no dead volume and can double as leak tight shut-off valves for high vacuum MS applications as well as for use at high pressures (to 100 atmospheres) and temperatures up to 300°C.

Write for our accessories catalogue;

Scientific Glass Engineering Pty. Ltd.

Head Office
Scientific Glass Engineering Pty. Ltd.,
111 Arden St., North Melbourne, Australia. 3051
Tel: (03) 329 6633

European Office
Scientific Glass Engineering (U.K.) Ltd.,
657 North Circular Road, London NW2 7AY.
Great Britain
Tel: 01-452 6244

U.S.A Office
Scientific Glass Engineering Inc.,
2800 Longhorn Blvd., Suite 104.
Austin, Texas, 78759 U.S.A.
Tel: (512) 837 7190

SGE

CIRCLE 188 ON READER SERVICE CARD

Manufacturers' Literature

Reversed-Phase HPLC. Bulletin #124, "Reversed-Phase HPLC—Which Column?" discusses modes in reversed-phase HPLC, differences in microparticle R-P bonded phases and the functionalities used, mobile phase considerations, and a guide for selecting optimum reversed-phase and column required for the separation. The bulletin has two appendices. Appendix I covers applications of reversed-phase HPLC such as pharmaceuticals, pesticides, biologicals, nucleic acid constituents, and proteins. Appendix II discusses ion pair chromatography, theory, and practice on reversed-phase columns. 40 pp. Whatman Inc. **466**

Sulfur and Chlorine Analyzer. Application report no. 2 describes the PGT sulfur and chlorine analyzer, which is based on energy-dispersive X-ray fluorescence. Precision is better than ±0.25% for samples containing up to 5% of S and 7% of Cl, by weight. 2 pp. Princeton Gamma-Tech **472**

Strip Chart Recorder. Model 105 strip chart recorder, featuring a left margin event marker, automatic pen lift when chart drive is turned off, 1.0 mV to 10 V measurement range, and response time of less than 350 ms, is illustrated in bulletin 456–7. 6 pp. Gould Inc. **468**

Metal Tester. General alloy ID lab #1599 metal tester identifies most of the common steels by a colog spot test for 14 alloying elements: C, Cr, Co, Cu, Fe, Mn, Mo, Nb, Pd, S, Ti, W, Ni, and V. These tests are used to characterize stainless steel series 303, 309, 316, 321, 347, and 400; Hastelloys; Inconels; tool steels; and low alloy and carbon steels. 8 pp. Koslow Scientific Co. **469**

Baths. In addition to the company's standard water, oil, and refrigerated models, bulletin 784 includes data on baths for thermal shock. Temperature ranges of units run from −100 to 260 °C. 8 pp. Blue M Electric Co. **473**

Flame Retardant. Data bulletin #353 describes Thermoguard CPA flame retardant, a free-flowing white powder, which can serve as a replacement material for antimony oxide. It has been used to impart flame resistance for polystyrene, polyvinyl chloride, polypropylene, and ABS formulations. 4 pp. M&T Chemicals Inc. **470**

Pyrolyzing Samples for IR. An application note entitled "Pyrolyzing Samples for Infrared Analysis" describes the principles of operation by which samples of such materials as polystyrene and other plastics, epoxy resins, or various types of synthetic or natural rubbers can be prepared for an IR spectrophotometer. 6 pp. Barnes Engineering Co. **471**

For more information on listed items, circle the appropriate numbers on one of our Readers' Service Cards

The AutoAnalyzer is the standard*

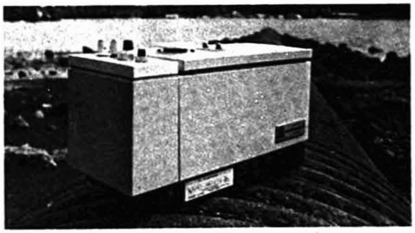

and ALPKEM rebuilds the standard.

- ✱ Rebuilt AutoAnalyzer instruments
- ✱ Full line of accessories & supplies
- ✱ Applications Engineering

ALPKEM Corporation

14625 S.E. 82nd St., Clackamas, OR 97015
503-657-3010 or 800-547-6275

*Trademark Technicon Corp.

CIRCLE 5 ON READER SERVICE CARD

prevent vacuum leaks . . . stop laboratory glassware breakage use **APIEZON**

GREASES • OILS • WAXES

Apiezon lubricants are especially formulated for use with high vacuum laboratory equipment. These easily applied, high purity, low vapor pressure, stable products are resistant to organic solvents, most chemical vapors.

GREASES—anti-seize greases which eliminate costly breakage: for high vacuum use down to 5×10^{-11} torr at 15°C and moderate vacuum use to 10^{-1} torr. They won't leach out of ground glass joints or stop cocks.

OILS—ideal as vapor diffusion pump fluids. They greatly minimize the need for a cold trap, permit maximum pumping speeds, reduce operating and maintenance costs.

COMPOUND Q: a low cost, putty-like, versatile sealant.

WAXES—for sealing vacuum joints more permanently.

Write or call for your free copy of Bulletin 43a

JAMES G. BIDDLE CO.
Plymouth Meeting, Pennsylvania 19462
Phone: (215) 646-9200

413

CIRCLE 30 ON READER SERVICE CARD

REPLACE TAP WATER PROBLEMS
FIT A CFT-25 INTO YOUR BUDGET

CFT - 25 Refrigerated Recirculators will cool:

- **Rotary Evaporators**
- **Condensers**
- **Small Lasers**
- **Diffusion Pumps**
- **Aquaria**
- **Electrophoresis**

NEW FROM NESLAB ONLY $795.00

CFT-25 — the compact, economical, benchtop closed loop recirculator designed to replace tap water. Runs continuously.

Range - −5 °C to +35 °C
Stability - ±1 °C
Cooling Capacity - 1900 BTU's/hr.

Call the leader — toll free
1-800-258-0830
In N.H. call collect 603-436-9444
NESLAB the name in circulation

NESLAB INSTRUMENTS, INC. 871 ISLINGTON STREET, PORTSMOUTH, N.H. 03801 U.S.A.

CIRCLE 152 ON READER SERVICE CARD

It's Axiomatic!

Many leading manufacturers of liquid chromatography systems prefer the Schoeffel SF 770 UV-VIS absorption monitor for use with their own instrumentation.

The Schoeffel SF 770 has become the industry standard for HPLC detection.

And for good reason:

- ✓ Patented optical design maximizes energy transmission.
- ✓ Continuously variable wavelength, 190-700nm.
- ✓ High sensitivity; low noise and drift.
- ✓ Double beam system for true sample absorbance measurements.
- ✓ Compact size; easy to operate.
- ✓ Interfaces easily with any liquid chromatograph.
- ✓ Wide choice of useful accessories.
- ✓ Provision for baseline and background compensated wavelength scanning.

We appreciate the confidence these manufacturers have in our products, and we'd like to gain yours. If you're looking into a variable wavelength HPLC detector, take a close look at Schoeffel. You'll be in very good company!

Call or write for our new comprehensive brochure.

U.S.A.: 24 Booker Street, Westwood, New Jersey 07675
(201) 664-7263, Telex 134356
EUROPE: 2351 Trappenkamp, Celsiusstrasse 5, W. Germany
(04323) 2021, Telex 299660

KRATOS Inc.
SCHOEFFEL
INSTRUMENT DIVISION

CIRCLE 190 ON READER SERVICE CARD

Manufacturers' Literature

Septum Flush Head for GC. Bulletin 105 describes the Septum Flush Head that is used to eliminate spurious chromatographic peaks due to septum bleed and solvent peak tailing. Analabs, Unit of Foxboro Analytical **467**

Petroleum Analyzers. Performance specifications for Model 100 series petroleum analyzers are provided in a bulletin. The X-ray fluorescent units are factory-tuned to measure one, two, or three user-specified elements. They provide direct push-button measurements of S, V, Pb, Cl, and metal additives in gasolines, oils, and cokes. 2 pp. Princeton Gamma-Tech **474**

Catalogs

Chromatographic Supplies and Pollution Standards. Features Ultra-Bond GC phases and other GC accessories such as capillary drawing machines and capillary columns, and over 700 environmental pollution standards and kits including pure PCB isomers, PCB metabolites, PCB chlorinated diphenyl ethers, chlorinated dibenzo-*p*-dioxins, and chemical carcinogen standards. 62 pp. RFR Corp. **475**

Scientific Apparatus. The fall 1978 catalog includes a microprobe digital thermometer, audiovisual aids in instrumentation—AA, HPLC, and RIA—homogenizers, and a liquid sample concentrator. 32 pp. Tekmar Co. **476**

Direct Drive Pump. Company's expanded line of rotary vane direct drive vacuum pumps is covered. Sizing information, installation, maintenance tips, pump accessories, and double-distilled pump oils are also included. 12 pp. GCA Corp. **477**

Chromatography and Mass Spectrometry Products. The complete line of microliter syringes, capillary columns, molecular jet separators, microneedle valves, and a variety of accessories is described in the 1979 catalog. Scientific Glass Engineering, Inc. **478**

Gases and Gas Handling Equipment. Catalog 88 is organized into five sections covering industrial gases, research grade gases, gas mixtures, electronic gases, and equipment such as regulators, valves, and other controls. Charts of gas safety standards and OSHA concentration limits for gases are also included. 100 pp. Scientific Gas Products, Inc. **480**

. . . and "baby" makes three

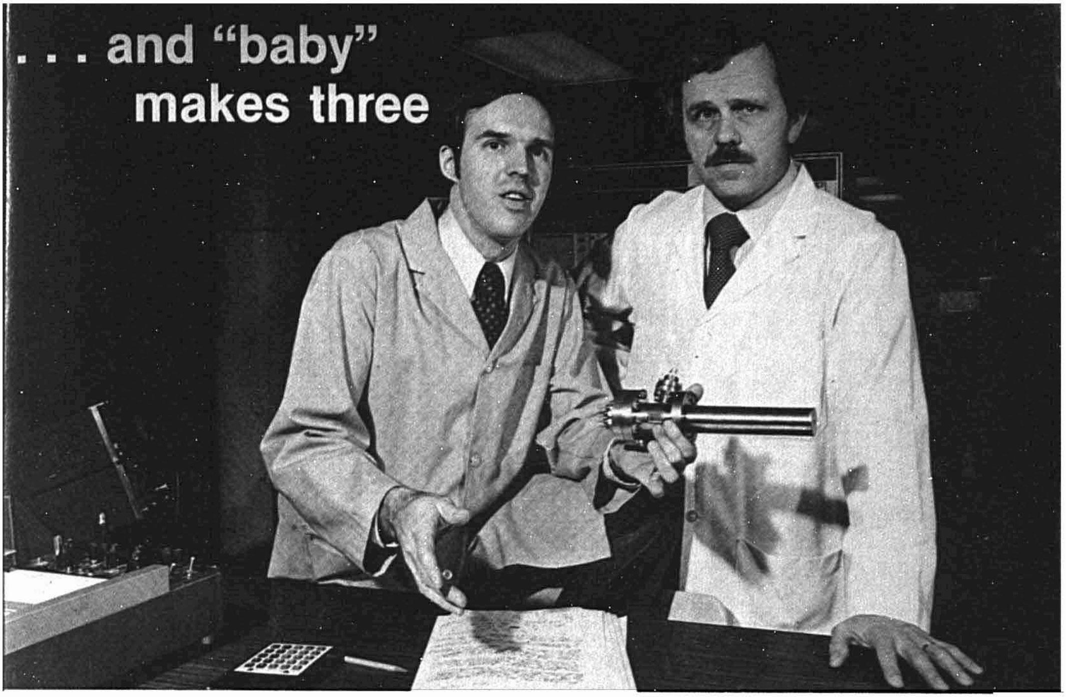

Research specialists Dr. Tom Rusch and Dr. Jerry Sievers sometimes call the 3M MiniBeam Ion Gun "our baby."

Because they invented it. And they're proud of it.

It's easy to see why. Their objective was to develop (1) a compact, adaptable and easy to use ion gun system, (2) a gun system with scanning capabilities, and (3) a system to provide substantially improved spatial resolution at a cost much lower than any other available.

Well, their work paid off.

After months of thought and experimentation, computer simulation and an occasional dose of educated guesswork, the MiniBeam was born.

3M's MiniBeam Ion Gun can give you much more precise surface analysis data because it produces an ion beam less than 125 microns in diameter to allow pinpoint accuracy. Compare that to competitive ion guns with beam diameters of several **thousand** microns.

What's more, you'll find the surprisingly inexpensive MiniBeam compatible with your existing surface analysis equipment. And because it's compact in size, you'll find the MiniBeam Gun attaches easily.

Find out more about Jerry and Tom's precocious "baby." Write for 3M's free information kit called "New Dimensions in Surface Analysis."

There's no cost or obligation, so let us hear from you today.

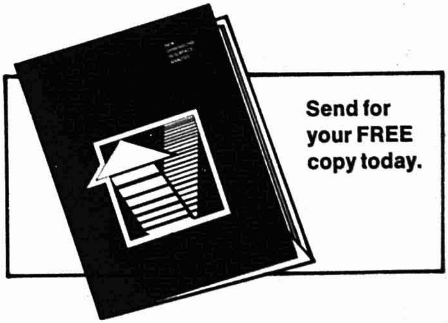

Analytical Systems / 3M
Building 53-3S 3M Center
Saint Paul, Minnesota 55101
612 / 778-4009

In Europe
Cambridge Instrument Company GMBH
D 4600 Dortmund 1
Postfach 1404
West Germany
(0231) 126086-89

3M

CIRCLE 143 ON READER SERVICE CARD

Automatic
Sizing
Analyzer
Plotter

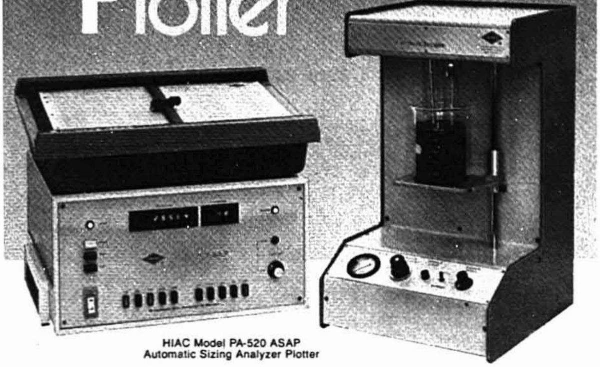

HIAC Model PA-520 ASAP
Automatic Sizing Analyzer Plotter

Measures particle size/volume (weight) distributions with pushbutton simplicity—delivers X-Y plots in 40 seconds!

Just put in the sample, insert a chart and press a button. In less than a minute ASAP measures particle size and computes, in its microprocessor, particle size and volume (weight) distributions. 11" x 17" X-Y plots are automatically delivered in your choice of any or all of six different modes of data presentation, cumulative or differential.
NON-ELECTROLYTIC HIAC® PRINCIPLE/ You don't have to use electrically conductive carrier fluids. You can use water, alcohol, oil, solvents—almost any liquid—even viscous fluids, with HIAC accessories. Standard sensors cover from 1 micron through 1000 microns!
HIGH RESOLUTION PRECISION/ ASAP can analyze up to one million particles per sample, with an accuracy traceable to NBS certified materials. Wide-range sensors analyze broad size distributions quickly, easily.
DIVERSE APPLICATIONS/ Include powdered materials of all kinds—pigments, pharmaceuticals, metals, abrasives, ceramics, sediments, fillers, cement, ash, toners, food products. Liquid applications include emulsions, synthetic fibers, resins, agricultural chemicals, catalysts. Research and Development or Quality Control, ASAP can analyze your material quickly, accurately and easily.

GET A FREE DEMONSTRATION—ASAP!
In your lab on your material—
or send a sample for free analysis
in our Applications Laboratory.

PACIFIC SCIENTIFIC™
HIAC INSTRUMENTS DIVISION
P.O. Box 3007, 4719 Brooks St., Montclair, Calif. 91763 Phone: (714) 621-3965
CIRCLE 164 ON READER SERVICE CARD

Manufacturers' Literature

Automatic Chemical Analysis Systems. Complete systems and modules for automatic continuous flow analysis of water, soil, plant, food, and pharmaceutical samples are available in catalog CFA 5000. Technical details on 1, 2, 3, 4 channel systems of an automatic sampler, peristaltic proportioning pump, UV–VIS spectrophotometer (200–850 nm), one and two pen recorders, single- and multichannel digital reduction units, and a list of analytical cartridges (EPA approved) are included. Lachat Chemicals, Inc. **479**

Chemical Standard Kits. Catalog CS-101 gives details on the environmental and pollution kits as well as others in the company's 8000 lab chemical line. On display at the Pittsburgh Conference are EPA water pollution, OSHA carcinogen and regulated chemicals, EPA "Consent Decree" priority pollutants, polynuclear aromatics, nitrosoamine compounds, and pesticide standards kits. Chem Service, Inc. **481**

Magnetic Drive Gear Pumps. All pumps shown include photo, performance curve, dimension drawing, materials of construction, and motor characteristics. An assortment of electric and air motors for use with the pumps is also described. 24 pp. Micropump Corp. **482**

Glassware and Apparatus. Catalog TG-50 features Airless-ware, Bantamware, biomedical, chromatographic, cryogenic and distillation apparatus, flow meter, Kem-kits, precision bore products, and vacuum apparatus. 300 pp. Kontes **483**

Vacuum Pumping Systems. Central to these pumping systems is a unit that combines in one vacuum-brazed assembly a diffusion pump, baffle, and valve. For these packaged pumping systems, three sizes are available. 4 pp. Edwards High Vacuum, Inc. **484**

Adsorbents for Gas Purification. Catalog F-4240 gives a wide selection of adsorbents for drying and purifying many types of gases, gas mixtures, and liquids. A brief summary of physical characteristics and typical applications for each of the adsorbents appears in the catalog. Seven types of the company's molecular sieves are listed: types 3A, 4A, 5A, and 13X for drying and purifying petroleum-derived gases; type AW-500 which is resistant to acidic impurities, and types 4A-XH-5 and 4A-XH-6 for dehydration of a system containing R-12 or R-22 refrigerant gases. 16 pp. Union Carbide Corp. **487**

Zoom into the 80's with the new MS80

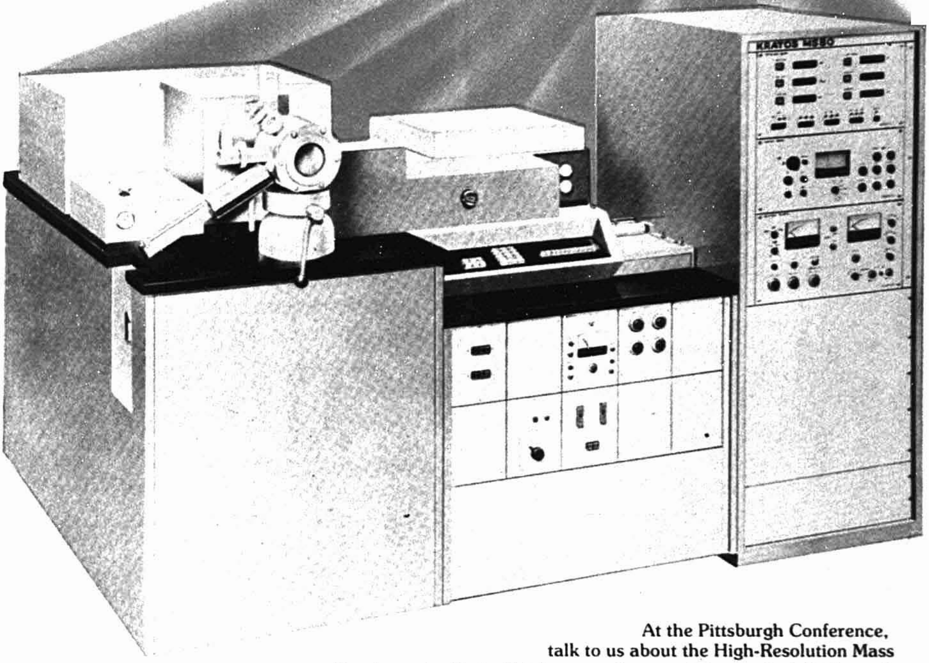

At the Pittsburgh Conference,
talk to us about the High-Resolution Mass
Spectrometer that will take care of your requirements right through
the next decade...*the new KRATOS MS80.*

Here are just a few of the reasons you shouldn't operate in the 80's without the MS80...

- Fast, *all-electronic* CI/EI switching (no mechanical ion-source adjustments)
- Digital control of all major functions
- Rapid scanning
- High sensitivity
- Wide solid angle source access
- Microprocessor gas chromatograph
- Super-accurate mass measurement

And...while you're in Cleveland for the Conference...we would also like to tell you about KRATOS's other instruments—products that have become laboratory standards around the world in these disciplines...

- ESCA/Auger
- X-Ray Diffraction
- GC/MS
- Data Handling

KRATOS Scientific Instruments

24 Booker Street • Westwood, NJ 07675 • (201) 664-5702

Circle 115 for literature. Circle 116 for salesman to call.

AIR HAS ITS USES

BUT NOT WHEN ACCURACY COUNTS

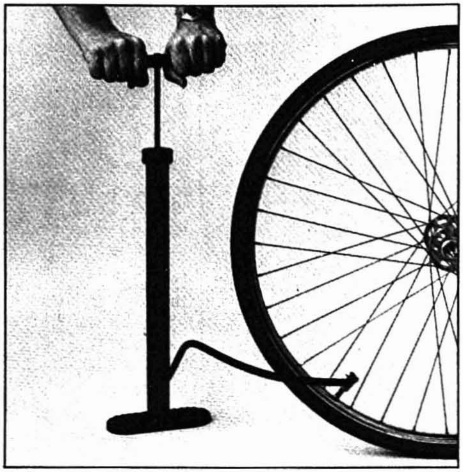

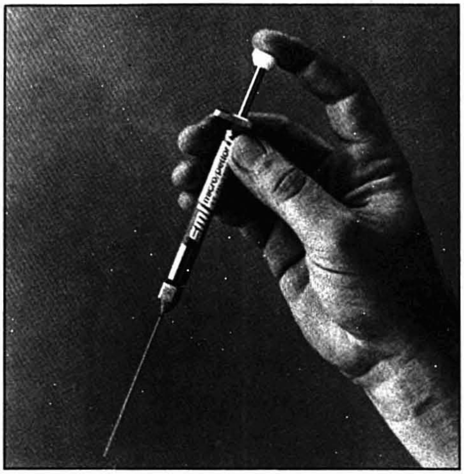

With MICRO/PETTOR®

WE'RE POSITIVE

Air is great for inflating bike tires and breathing, but it's not a particularly efficient means of dispensing fluid from a pipet. Air displacement systems leave too much residue in the tip, and depending on viscosity, seriously reduce transfer accuracy.

The SMI **Positive Displacement MICRO/PETTOR Pipetting System,** on the other hand, employs a precision bore capillary in which a precisely manufactured plunger operates to draw fluid into and dispense it from the capillary. The capillary is filled to a pre-set length by the plunger. Because there is no air space, the capillary will contain and the plunger will forcibly dispense, the same amount of fluid every time, virtually any viscosity. The plunger tip extends beyond the end of the capillary assuring complete delivery. And the MICRO/PETTOR system is specifically designed to deliver with ½% or less carryover from sample to sample.

SMI makes positive displacement pipets for virtually every application—ratings from 1 μl to 3 ml. MICRO/PETTORs for many clinical uses; Adjustable Volume MICRO/PETTORs for research; RE/PETTOR®s for repetitive dispensing of reagents. All are accurate; all are economical. We're Positive. And we'll send you a free reprint "How to Use and Check Pipetting Equipment."

Check your distributor or call SMI toll free (800) 227-0650, (In California) (800) 772-3937, Area Code (415) 548-8000.

Visit SMI Booth #1238 at the Pittsburgh Conference

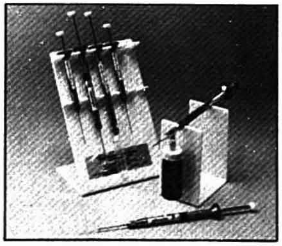

smi scientific manufacturing industries inc.

800 University Ave., Berkeley, CA 94710

SMI holds Patent #3815790.

CIRCLE 195 ON READER SERVICE CARD

DEXSIL®

High Temperature
GC Phases

Extended column life at 400°
and beyond

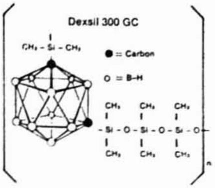

Separate amino acids, drugs, paraffins, hydrocarbons, natural waxes, pesticides, fatty acids, steroids, alcohols, etc. – at column temperatures of 400° C and more. Routinely. With outstanding selectivity.

Columns packed with Dexsil 300GC have shown negligible bleed from 20° to 450° C. Limited life applications can be performed at temperatures to 500° C. Two other Dexsil polymers – 400GC and 410GC – can be selected according to application, and used at temperatures to 400° C.

When used at lower temperatures up to 350° C, the Dexsils offer the advantages of using more sensitive GC settings and increasing column life because of the Dexsils' low bleed. Users report column life under routine conditions at 2, 3, 4 years and more.

Dexsil is available NOW, either directly or from your regular supplier. Write for details, and an exhaustive bibliography of over 200 Dexsil applications.

DEXSIL 295 Treadwell Street • Hamden, CT 06514
(203) 288-3509

® Registered Trade Mark Dexsil Chemical Corporation Hamden CT.

CIRCLE 44 ON READER SERVICE CARD

GARRICAST TYPE IS 825
GENERATOR IPS/ST

GARRICAST

MELTING AND
CENTRIFUGAL CASTING
EQUIPMENT
for preparing samples
for spectrographic analysis

The Garricast is capable of producing samples from chips, wires, scales, rods, filings, etc.

The unit employs induction melting and casting under pressure of metals and alloys to ensure homogeneous composition of sample.
The rapid melting under a protective gas atmosphere reduces the duration of contact of the molten material with its crucible to a minimum, and thereby reduces the chances of contamination to negligible proportions. Synchronised melting and casting control allows complete cycles of operations to be achieved within an average total time of two minutes.

See Demonstration Model
at BOOTH 628
PITTSBURGH CONFERENCE
to be held in CLEVELAND
MARCH 1979

THE GARRICAST IS MANUFACTURED IN THE U.K. BY INTERTHERM.

SOLD WORLDWIDE BY
GARRICK EQUIPMENT CO. LTD.
13 Garrick Street London WC2E 9AR Tel.01-240 2393/4 Telex:23623

CIRCLE 84 ON READER SERVICE CARD

HEYDEN

NEW JOURNAL
FREE SAMPLE OFFER

Maiden Issue
Vol.1/1 February

Surface and Interface Analysis

Editors:

David Briggs, ICI Plastics Division,
Bessemer Road, Welwyn Garden City,
Hertfordshire, U.K.

Gerald P. Ceasar, Xerox Corporation,
Webster Research Center,
Building 114,
Webster, NY 14580, U.S.A.

Editorial Board:

D. Allara, A. Barrie, A. Benninghoven, J.E. Castle, C.A. Evans, Jr., P. Holloway, R. Holm, J.W. Mayer, N.S. McIntyre, J. Morabito, C.J. Powell, M.P. Seah, C.J. Todd, H.W. Werner, N. Winograd

A new breed of 'analyst' interested in characterizing surfaces, interfaces and thin films has emerged. His techniques include electron and ion spectroscopy/microscopy (XPS, ESCA, UPS, AES, ELS, SIMS, ISS, SEM, SAM, ion probe etc.), Rutherford back scattering, reflection infrared spectroscopy, ellipsometry and electron microprobe analysis, EDXA, ion sputtering and methods of depth profiling. Development of these techniques is rapid and often technology driven so that new knowledge is scattered.

Surface and Interface Analysis is devoted to reporting developments and applications of techniques to meet the new needs of the materials scientist.

Publication on Schedule for 1979
Bi-monthly (6 issues p.a.) $ 120.00

To: HEYDEN & SON INC.,
247 South 41st Street,
Philadelphia, PA 19104

Journal of Surface & Interface Analysis -

☐ send free sample copy
☐ enter annual subscription

Name. . . . .
Address. . . . .
. . . .
. . . .

CIRCLE 96 ON READER SERVICE CARD

The Ultimate Moisture Analyzer...

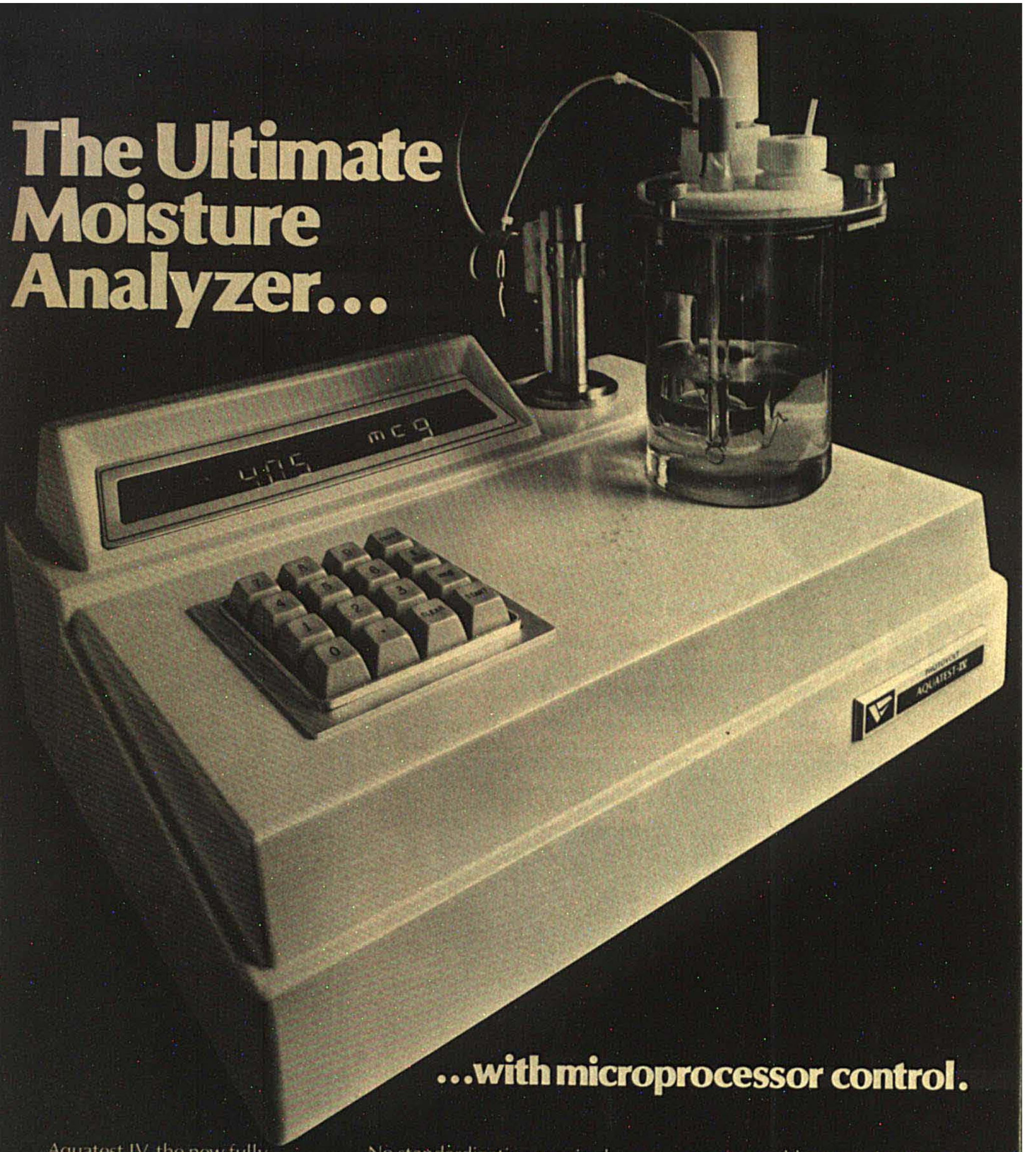

...with microprocessor control.

Aquatest IV, the new fully automated Karl Fischer titrator with digital readout, displays water content without calculations in ppm, percentages or micrograms.

No standardization required.

Aquatest IV automatically corrects for interfering reactions.

And has automatic blank correction when extracting, plus programmable extraction time.

For a free demonstration in your lab, call toll-free (800) 221-5182. In New York State, call collect (212) 989-0484.

After you lift a finger, you don't have to lift a finger.

Photovolt Corporation
1115 BROADWAY, NEW YORK, N.Y. 10010
See us March 5–8 at the Pittsburgh Conference, Booths 712–714
CIRCLE 167 ON READER SERVICE CARD

Books

Vibrational Data for Molecules

Infrared and Raman Spectra of Inorganic and Coordination Compounds. 3rd ed. Kazuo Nakamoto. xv + 448 pages. John Wiley & Sons, Inc., 605 Third Ave., New York, N.Y. 10016. 1978. $24.50

Reviewed by Ira Levin, Bldg. 2, Rm. B1-27, NIH, Bethesda, Md. 20014

In assembling a tractable review of vibrational data for several classes of chemical compounds, an author often places himself in the unenviable position of trying to balance a current, comprehensive survey of the material against a necessarily concise account that adequately reflects the trends, directions, and spectroscopic "flavor" of the various disciplines covered. As a consequence of the flourishing applications of Raman spectroscopy within the last decade, the author of a collection of vibrational frequencies is now confronted with an almost overwhelming source of literature references from which to cull, organize and, finally, report cogently. In spite of these literary hurdles, Professor Nakamoto admirably succeeds in the present volume in updating the previous editions of his widely used compilations of vibrational data for inorganic, coordination, and, now, organometallic molecules. For both the student and established research worker, the availability in a manageable form of over 2000 compiled and categorized references strongly suggests that a handbook of this nature be afforded an accessible position in one's laboratory. (Although the book was published in 1978, a cursory survey of the dates in the reference lists indicates, however, that the citations only generally cover the literature to about 1974.)

In addition to including more extensive discussions of Raman spectra throughout this edition, the first section, "Theory of Normal Vibration," which amounts to about one-fourth of the volume, has been significantly expanded in the number of topics discussed in comparison with earlier editions. This chapter contains introductory notions involved in specifying normal modes for oscillating systems and illustrates the pertinent prescriptions for applying elementary group theory to the vibrational problem. Approximately 25 pages are devoted to procedures concerning normal coordinate calculations. The mixture within specifically this subsection of somewhat eclectic topics with perhaps unnecessary details tends, in my judgment, to be too abbreviated and not suitably organized to be illuminating either to the student or to the newcomer to vibrational spectroscopy. Although background is required for following the points made later in discussions concerning force constants and intensity parameters, for example, the overall tone of the book is that of systematic discussions of primarily vibrational frequency data. Thus, the details of *s* vectors, Decius' formulas for *G* matrix elements, symmetry transformations, and the quite brief discussion of mathematical forms of model force fields, all of which exist elsewhere, could perhaps have been omitted or accommodated in the appendices, which already contain material relevant to actual computations. In this manner the pace and tenor of the chapter would not be needlessly broken.

Except for the previous objection, the overall discussion in the first 100 pages does in a broad way provide a foundation for understanding and appreciating the more subtle details in the succeeding chapters on the spectral properties of inorganic molecules and related systems. In particular, the author briefly introduces important topics, such as polarization properties of Raman transitions, resonance techniques in Raman spectroscopy (a fertile area of investigation), matrix effects and crystal concepts, which are later used in explaining trends in the spectral data and in clarifying the bond properties of intriguing molecular complexes.

In summary, for investigators interested in applying vibrational techniques to a wide range of structural and bonding problems, Professor Nakamoto has again provided the spectroscopic community with an extensive, carefully arranged review of contemporary research in several related areas of inorganic chemistry.

Analysis of Drugs and Metabolites by Gas Chromatography–Mass Spectrometry: Analgesics, Local Anesthetics and Antibiotics, Vol. 5. B. J. Gudzinowicz and M. J. Gudzinowicz. x + 541 pages. Marcel Dekker, Inc., 270 Madison Ave., New York, N.Y. 10016. 1978. $55

Reviewed by Donald F. Logsdon, USAF Environmental Health Laboratory, McClellan AFB, Calif. 95652

The combination of the gas chromatograph and the mass spectrometer has greatly expanded the capability of the analytical chemist. One group of compounds whose analysis is particularly suited to this combined procedure is drugs and their metabolites. This book is part of a growing series on the analysis of drugs and metabolites by gas chromatography–mass spectrometry. The objective of this series is to compile methods from the current literature and present them in sufficient detail to allow them to be reproduced faithfully in the reader's laboratory.

The contents of volume 5 include two chapters, an author index, a subject index, and a table of contents for the other volumes in the series. The first chapter presents analytical methods for narcotic, narcotic antagonist, and synthetic opiate-like drugs. The second and longer chapter presents analytical methods for antipyretic, antiinflammatory, antihyperuremic, local anesthetic, and antibiotic drugs. Each chapter includes extensive bibliographies to the referenced literature. The author index included in the book is for authors cited in the text, a somewhat unique feature.

This book is well done. It clearly meets the objective of the series and should be of direct and continuing value to those involved in the analysis of these drugs and their metabolites.

Physicochemical Applications of Gas Chromatography. R. J. Laub and R. L. Pecsok. xxi + 300 pages. John Wiley & Sons, Inc., 605 Third Ave., New York, N.Y. 10016. 1978. $23.50

Reviewed by Donald F. Logsdon, USAF Environmental Health Laboratory, McClellan AFB, Calif. 95652

The term *physicochemical* may be a new one for many individuals using gas chromatography as an analytical tool. This term is used to describe the application of gas chromatography to the study of physical and chemical attributes of matter, i.e., nonanalytical uses. The objective of this book is to discuss these physicochemical applications of gas chromatography in a user-oriented fashion and introduce research workers to this, perhaps unrealized, use of gas chromatography.

The book includes 10 chapters, a subject index, and a prefatory list of useful symbols. The first three chapters are grouped under a heading entitled Introduction. These chapters closely examine all aspects of gas chromatography from both theoretical and practical viewpoints. Chapters 4–6 discuss the application of the gas chromatographic method to thermodynamic studies such as viral coefficients, properties of solutions, complexation, and adsorption. The next two chapters focus on the application of gas chromatography to kinetic studies, and the last chapter discusses the use of gas chromatography for studies of the molecular properties of pure compounds. The chapters include numerous tables and figures, plus extensive reference lists.

This book presents a good discussion of the physicochemical applications of gas chromatography. Those involved in physical and chemical research should find much useful information.

New Books

Antibiotics. Isolation, Separation and Purification. M. J. Weinstein and G. H. Wagman, Eds. x + 771 pages. Elsevier Scientific Publishing Co., P.O. Box 211, Amsterdam, The Netherlands; 52 Vanderbilt Ave., New York, N.Y. 10017. 1978. $84.75

Volume 15 of the "Journal of Chromatography Library" series is contributed to by 24 eminent scientists in the field of antibiotic isolation on key chemical families of antibiotics, with emphasis on the isolation, separation, and purification of these substances. The book includes summaries of the biological, chemical, and physical properties, usage, and structural formulae of naturally produced antibiotics.

Analytical Chemistry of Liquid Fuel Sources—Tar Sands, Oil Shale, Coal, and Petroleum. P. C. Uden, S. Siggia, and H. B. Jensen, Eds. ix + 341 pages. American Chemical Society, 1155 16th St., N.W., Washington, D.C. 20036. 1978. $32

This book is number 170 in the Advances in Chemistry Series based on a symposium at the 173rd Meeting of the ACS in New Orleans, La., March 21–25, 1977. Reviews of on-going research in the areas of liquid fuel anal-

Ever tried to keep temperature drift within ±.0003°C per week?
TRONAC CAN!

Precision Temperature Controller PTC-40
Model 405 Bath

If you are interested in precision control of environmental temperature, our products can help you.

Tronac equipment measures and controls temperatures.
- Precision Temperature Controllers
- Temperature Controlled Baths
- Temperature Readout Bridges
- Isoperibal Titration Calorimeters
- Isothermal Titration Calorimeters
- Heat Conduction Microwattmeter
- Calorimeter Control & Data Acquisition Systems

TRONAC INC.
Builders of Precision Calorimeters
Write for Free catalog
1804 South Columbia Lane
Orem, Utah 84057
(801) 224-1131

CIRCLE 200 ON READER SERVICE CARD

NOW...
A Full Capability
CAPILLARY GC
For Less Than $5000

- Split/splitless injection system for glass capillary columns provides high resolution
- All glass system for maximum performance
- SCOT or WCOT column capability
- Easy capillary column installation
- Make up gas provided
- Linear temperature programming
- Versatility
- Ouststanding value

Model 467-LP

Call or write today for complete information
ANTEK INSTRUMENTS, INC.
6005 North Freeway
Houston, Texas 77076
TELEPHONE (713) 691-2265 TWX: 910-881-1792

Visit us at the Pittsburgh Conference booths 413 & 415
CIRCLE 11 ON READER SERVICE CARD

Volume 5 in Feb. 1979...Volume 6 due in April
...then four more per year to completion in 1983

New Third Edition–
KIRK-OTHMER
ENCYCLOPEDIA OF CHEMICAL TECHNOLOGY

Editorial Board
Herman F. Mark
Polytechnic Institute of New York
Donald F. Othmer
Polytechnic Institute of New York
Charles G. Overberger
University of Michigan
Glenn T. Seaborg
University of California, Berkeley

Executive Editor
Martin Grayson
Associate Editor
David Eckroth

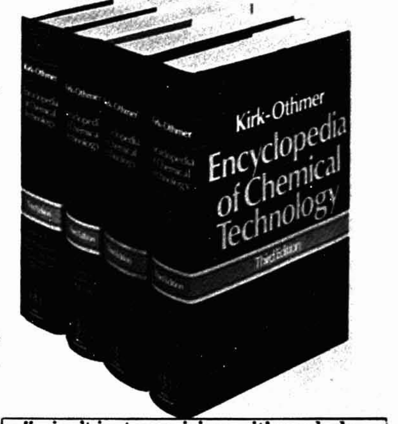

"impressed with the quality"–*Chemical Engineering*
"Invaluable...authoritative"–*Chemical Processing*
"wide ranging...packed with goodies"–*New Scientist*

The third edition of the **ENCYCLOPEDIA OF CHEMICAL TECHNOLOGY** is built on the solid foundation of the previous two editions. All of the articles in this new edition have been rewritten and updated and many new subjects have been added to reflect changes in chemical technology since the second edition. The results, however, will be familiar to users of the earlier editions: comprehensive, authoritative, accessible, lucid. This Encyclopedia remains the indispensable tool for all producers and users of chemical products and materials.

In many ways, this edition is an entirely new encyclopedia–yet its format is familiar to those acquainted with the earlier editions. New features include the use of SI units as well as English units, Chemical Abstracts Service's Registry Numbers, and a complete indexing based on automated retrieval from a machine-readable composition system.

New subjects have been added especially in polymer and plastics technology, fuels and energy, inorganic and solid state chemistry, composite materials, coatings, fermentation and enzymes, pharmaceuticals, surfactant technology, fibers, and textiles. As in the Second Edition, authors are acknowledged at the end of every article.

For prospectus, write to Nat Bodian, Dept. 092

WILEY-INTERSCIENCE
a division of John Wiley & Sons, Inc.
605 Third Avenue
New York, N.Y. 10016

> **"...isn't just a revision...it's a whole new encyclopedia...articles are well illustrated...layout of articles is very neat...(uses) common chemical names...seems to contain far more references...really impressed with the quality...Kirk-Othmer has long had a reputation for being authoritative; this new edition will indeed enhance that reputation."**
> **–*Chemical Engineering***

Vol. 1 (1-02037-0) A to Alkanolamines .... **1978...$120.00**
Vol. 2 (1-02038-9) Alkoxides, Metal to Antibiotics (Peptides) **1978...$120.00**
Vol. 3 (1-02039-7) Antibiotics (Phenazines) to Bleaching Agents .... **1978...$120.00**
Vol. 4 (1-02040-0) Blood to Cardiovascular Agents **1978...$120.00**
Vol. 5 (1-02041-9) Castor Oil to Chlorocarbons .... **Feb. 1979...$120.00**
Vol. 6 (1-02042-7) Chlorohydrins to Contraceptive Drugs .. **April 1979...$120.00**
Vol. 7 (1-02043-5) Coordination Compounds to Dietary Fiber.... **Aug. 1979...$120.00**
Vol. 8 (1-02044-3) Diffusion Separation Methods to Electrophotography .... **Nov. 1979...$120.00**

Subscription price per volume $95.00
(Subscription price saves approximately 20%)

In Canada: John Wiley & Sons, Canada, Ltd.
22 Worcester Road, Rexdale, Ontario **A3619-69**

CIRCLE 237 ON READER SERVICE CARD

IL551 Video I™
AA Spectrophotometer
Makes Operation Simple.

The IL551 Video I Atomic Absorption Spectrophotometer displays its data on a 23 × 17-cm video screen, which has at least two advantages over conventional data presentation. It makes the instrument very easy to use, by providing instructions to the operator. It also graphically shows the shape of the working curve, the form of absorbance peaks, and the nature of any background absorption. Methods development is greatly speeded up, and the instrument is without peer as an educational tool.

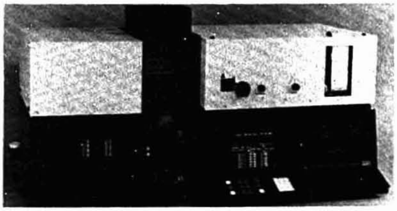

Instrumentation Laboratory Inc., Jonspin Road, Wilmington, Mass. 01887. Tel.: (617) 658-5125.

Instrumentation Laboratory

CIRCLE 107 ON READER SERVICE CARD

PHOTREX®
Spectrophotometric Solvents
(Where the proof of purity is right on the label.)

These J. T. Baker multi-purpose solvents are ideal in Quality Control and R&D for:

- determination and identification of organic compounds
- inorganic analysis • trace element analysis

They provide extremely reliable performance in UV, visible and IR spectrophotometry. Also excellent for high-performance liquid chromatography (UV detector).

47 unsurpassed spectrophotometric solvents are available with detailed definition by UV absorbances and GC assay.

Every label carries the actual lot analysis featuring the GC assay, trace impurity analysis, IR "windows", and lot absorbance values at key wavelengths in the UV region.

The 'Baker Analyzed' Photrex label provides proof of purity and spectro suitability, as well as valuable reference data.

Write for free brochure

For Instrumental Analysis
the professional chooses
J. T. Baker

See us at the Pittsburgh Conference, Booths 405, 407, 409 & 411.

J. T. Baker Chemical Co.
Phillipsburg, N.J. 08865
201 859-5411

J.T.Baker® CHEMICALS

CIRCLE 21 ON READER SERVICE CARD

ysis and characterization emphasize the latest advances in specific analytical methodology and instrumentation. Methods include high-resolution gas and liquid chromatography, electron microprobe, C-13 NMR, EPR, and computer modeling. Twenty-one chapters examine structural characterization of solvent-refined coals, the chemistry and composition of petroleum asphaltenes, and chromatographic studies on oil sand bitumens.

Particle Size Analysis. M. J. Groves, Ed. 440 pages. Heyden & Sons, Inc., 247 South 41st St., Philadelphia, Pa. 19104. 1978. $60

This book gives current developments in techniques and equipment used in particle size analysis as presented at the 1977 Third Particle Size Analysis Conference, held by the Analytical Division of the Chemical Society. In the 45 research and review papers presented, the areas of analysis include aerosol particles and spray droplets in flight, on-stream analytical control of industrial processes, characterization of shape, laser light scattering, laser doppler and holographic methods, and the light obscuration principle.

New Applications of Lasers to Chemistry. Gary M. Hieftje, Ed. x + 244 pages. American Chemical Society, 1155 16th St., N.W., Washington, D.C. 20036. 1978. $23.50

This is number 85 in the ACS Symposium Series based on a symposium at the 175th Meeting of the ACS in Anaheim, Calif., March 14–15, 1978. The 12 chapters contain four main subject areas—high-resolution spectroscopy, high sensitivity analysis, time-resolved or kinetic spectroscopy, and new techniques in laser Raman spectrometry. Included are specific discussions on luminescence, tunable diode lasers, molecular fluorescence, laser electrophoretic light scattering, and Raman scattering spectroscopy.

Chemical and Biochemical Aspects of Electron-Spin Resonance Spectroscopy. Martyn Symons. xii + 190 pages. John Wiley & Sons, Inc., 605 Third Ave., New York, N.Y. 10016. 1978. $19.50

Addressed to students, this book should be suitable for an undergraduate course. Topics covered include *g*-value, hyperfine coupling, linewidths and relaxation effects, examples from organic chemistry and of inorganic and organo-inorganic radicals, environmental effects, mechanisms,

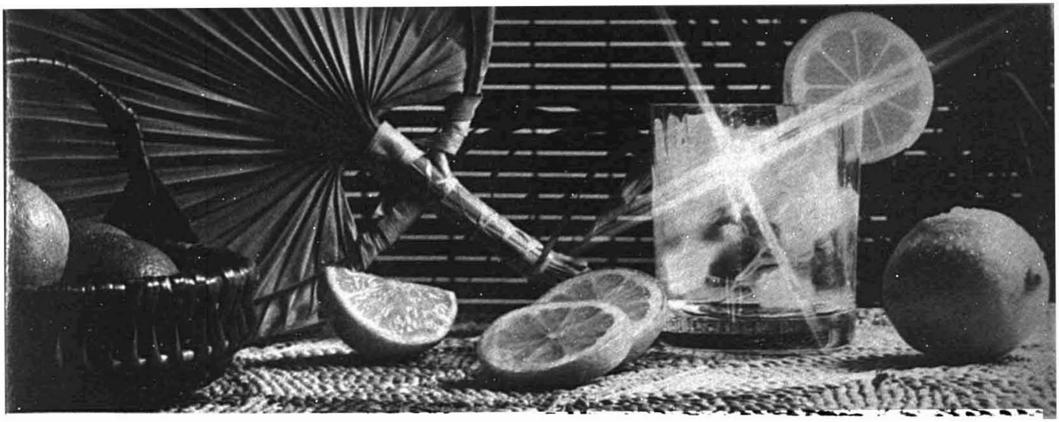

We took on the biggest cooling challenge we could find. The sun.

Not just ordinary sunlight, but concentrated rays hitting the lenses of a large telescope used in solar research. In a major observatory, the mirrors behind those lenses are cooled with baths and circulators from Forma Scientific.

Whatever the size of your cooling job, there's a Forma bath and circulator that has what the job needs. Capacities from 1 to 50 gallons, temperatures from −75°C to 100°C, proportional refrigeration—and a control sensitivity standard of ± 0.02°C or better. Write for more details on Forma's full line of baths and circulators.

Your work in medicine, biochemistry or microbiology deserves the precision and reliability Forma put up against the sun. Because we're all really studying the same thing—life.

CH/P
Forma Scientific
bath and circulator
model 2006

Model 2006
Refrigerated/Heated
Bath & Circulator

Where technology begins with imagination.

Forma Scientific
DIVISION OF MALLINCKRODT, INC.
BOX 649 MARIETTA, OHIO 45750 TELEX 24-5394
TOLL FREE USA 800-848-3080, OHIO 614-373-4763

Visit FORMA Booths 1729 and 1731 at the Pittsburgh Conference

CIRCLE 80 ON READER SERVICE CARD

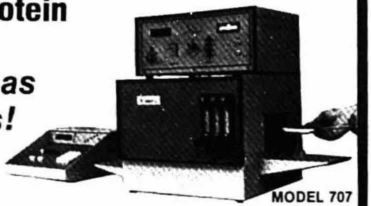

A FAST, EFFICIENT ALTERNATIVE TO KJELDAHL...

The Microprocessor Controlled MODEL 707 Provides Nitrogen/ Protein Analysis . . . In as Little as 30 Seconds!

MODEL 707

- Uses proven chemiluminescent detection principle
- Microprocessor controlled for greater stability and repeatability
- Programmed temperature parameters
- Handles from 5 to 120 samples per hour
- Accomodates up to 1g sample size
- 1 nanogram sensitivity with dynamic range of 10^6
- Extended range accessory (Model 732) allows combined nitrogen in percentage range

Visit us at the Pittsburgh Conference booths 413 & 415

ANTEK INSTRUMENTS, INC.
6005 North Freeway
Houston, Texas 77076
TELEPHONE (713) 691-2265 TWX: 910-881-1792

CIRCLE 12 ON READER SERVICE CARD

THERMOLYNE's Stir-Light is doubly useful as both a stirrer and a light source. Full stirring speed range from 60 to 1200 rpm plus evenly diffused cool light for positive end point determination. Also available as stirrer only.

Contact your Lab Supply Dealer or write to:

SYBRON | Thermolyne

Thermolyne Corp., a subsidiary of Sybron Corp., 2555 Kerper Blvd., Dubuque, IA 52001

Here's a dependable way to

stir, observe and analyze.

CIRCLE 204 ON READER SERVICE CARD

polyelectron systems, transition-metal complexes, and examples from biological systems. At the end there are four appendices on experimental hints, extracting data, electron-nuclear double resonance spectroscopy, and hyperfine coupling constants (G) for unit population of atomic orbitals calculated from Hartree-Fock atomic wave functions. Close to 200 references are cited; most of them are before 1975.

Blood Drugs and Other Analytical Challenges. Eric Reid, Ed. xi + 355 pages. John Wiley & Sons, Inc., 605 Third Ave., New York, N.Y. 10016. 1978. $47.50

Evolved from the Bioanalytical Forum held in Sept. 1977 at the University of Surrey, this book emphasizes chromatography with sample preparation as an underlying theme. The contents include gas chromatography—capillary and packed columns, detectors, and derivatization; mass spectrometric methods—GC-MS, negative-ion MS, and HPLC-MS; and HPLC, TLC, and nonchromatographic methods—ion pair operation, electrochemical detection, sample handling, derivatization, and choice of approach. A special feature is a section on notes and comments related to the foregoing topics made at the Forum on which this book is based, together with supplementary material. The up-to-date references include some published in 1978.

Statistics. R. F. Hirsch, Ed. viii + 308 pages. Franklin Institute Press, Box 2266, Philadelphia, Pa. 19103. 1978. $21

Eleven authors contributed to this 1977 Eastern Analytical Symposium series monograph, which offers guidance in the application of modern techniques of experimental design and statistical analysis. The book's four parts deal, respectively, with experimental design; basic statistical analysis; techniques for analyzing larger quantities of chemical data—factor analysis, pattern recognition, and cluster analysis; and the ultimate disposition of analytical data.

Applications of Inductively Coupled Plasmas to Emission Spectroscopy. R. M. Barnes, Ed. vii + 188 pages. Franklin Institute Press, Box 2266, Philadelphia, Pa. 19103. 1978. $18.95

This 1977 Eastern Analytical Symposium series monograph, contributed to by 16 chemists, contains eight invited application papers. Topics covered

Solve Your Materials Problems 6 Ways

More R&D and QC labs use Micromeritics proven, precision instruments to measure physical properties of material than those of any other manufacturer in the world. These measurements include:

1 **Automatic particle size distribution** gives rapid analysis from 100 to 0.1 μm diameter.

2 **Manual and automatic physical adsorption** for B.E.T. surface area from 0.001m²/g up; adsorption and desorption isotherms; pore structure (volume, size and shape) from 600 to 20Å diameter.

3 **Manual and automatic chemisorption** measures active material availability; percent metal dispersion.

4 **Mercury porosimetry** measures pore structure (volume, size and shape) from 354 to 0.0035μm diameter; density, surface area and average particle size.

5 **Manual and automatic density** determines absolute volume to ± 0.02cc.

6 **Electorophoretic mass-transport analysis** to study flocculation and dispersion; particle-liquid systems behavior; zeta potential.

We also invite you to use our complete Materials Analysis Laboratory Services. Let us show you how to solve your material problems. Call or write Micromeritics Instrument Corporation, 5680 Goshen Springs Road, Norcross, Georgia 30093. U.S.A. (404) 448-8282. Telex: 70-7450.

micromeritics®

CIRCLE 133 ON READER SERVICE CARD

EUROPEAN SALES OFFICE
2 Orchard Way
Eaton Bray
Bedfordshire
England
Telex 851-826249

AFRICA
North
Coultronics France S A
Margency 95580 Andilly
France
Telephone 989-9030

South
Coulter Electronics PTY , Ltd
Transvaal
South Africa
Telephone 805-2046 55 56

ARGENTINA
Instrumentalia S R L
Buenos Aires
Telephone 85-3121 86-1436

AUSTRALIA
Townson & Mercer Ltd
Lane Cove N S W
Telephone 428-1199

BELGIUM
Anais S A
Namur
Belgium
Telephone 081-22 50 85

BRAZIL
Danon-Socidade Importadora
Equipmentos Cientificos LTDA
Rio de Janiero
Telephone 221-4480

DENMARK
Bie & Berntsen, Ltd
Roedovre
Telephone 45-294-8822

EASTERN EUROPE
Medata AB
Stockholm
Sweden
Telephone 08-303370

ENGLAND
Coulter Scientific Ltd
Hertsford
Telephone Harp 63151

FINLAND
OY Tamro AB
Helsinki
Telephone 90-544011

FRANCE
Coultronics France S A
Margency 95580 Andilly
Telephone 989-9030

GERMANY
Coulter Scientific GmbH
Gahlingspfad
West Germany
Telephone 02156-755011

GREECE
The GG Forum
Thessaloniki
Greece
Telephone 542-371

GUADELOUPE
Coultronics France S A
Margency 95580 Andilly
France
Telephone 989-9030

INDIA
Blue Star Limited
Bombay
Telephone 45-7887 or
45-6799

ITALY
Coulter Scientific S p A
Milano
Telephone 98-80-108

JAPAN
Shimadzu Seisakusho Ltd
Kyoto
Telephone (075) 8111111

KUWAIT
Bader Sultan & Bros. Co
Kuwait
Telephone 421291 92 93

MALAYSIA
Delta Electronics SDN BHD
Bangsar Baru
Kuala Lumpur
Telephone 943629

MARTINIQUE
Coultronics France S A
Margency 95580 Andilly
France
Telephone 989-9030

NETHERLANDS
Chemical Laboratory Instruments
Schijndel
Netherlands
Telephone 04104-4035

NEW ZEALAND
Selby-Wilton Scientific, Ltd
Lower Hutt
Telephone 697-099

REUNION
Coultronics France S A
Margency 95580 Andilly
France
Telephone 989-9030

SPAIN
Izasa S L
Barcelona 15
Telephone 2548100

SWITZERLAND
IG Instrumenten-Gesellschaft
Zurich
Telephone 0166331

TAIWAN
Vertex Corporation
Taipei, Taiwan
Telephone 752-6452(3)

U.S.S.R.
Coultronics France S.A.
Margency 95580 Andilly
France
Telephone 989-9030

UV/VISIBLE SPECTROPHOTOMETRY

The new SP8-200. Research performance at your fingertips!

Keyboard operation combines with the flexibility of microprocessor control in this brand new, high performance UV/Visible spectrophotometer from Pye Unicam.

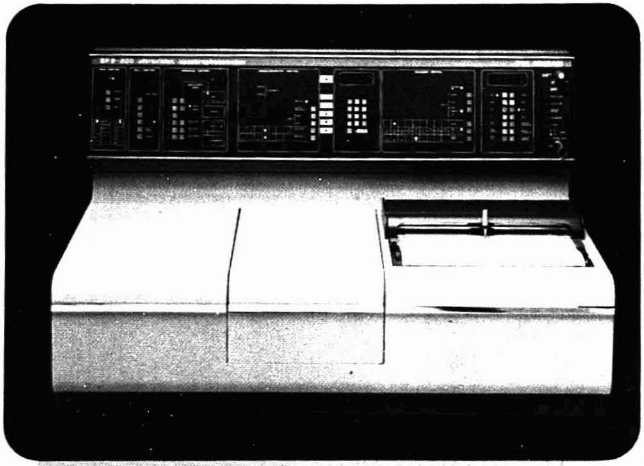

The latest advances in optical design and microprocessor technology have been incorporated in the outstanding new SP8-200 UV/Visible scanning spectrophotometer. Microprocessor control brings convenience features such as digital baseline correction, autozero, autoconcentration and error detection to research instrumentation. The fine optical design of the proven SP8-100 has been upgraded by the introduction of a unique master, blazed, holographic grating to provide resolution and stray light figures that can only be significantly bettered by more expensive double monochromators. Any program can be set up or changed in a matter of seconds by keyboard or controlled remotely by calculator or computer.
The SP8-200 provides high analytical performance over the full 185-950nm range and is accompanied by a very versatile set of sample handling accessories.
Ask for details of the SP8-200 . . . the spectrophotometer with the touch of greatness.

PHILIPS

Pye Unicam

A SCIENTIFIC INSTRUMENT COMPANY OF PHILIPS

York Street Cambridge CB1 2PX England
Telephone (0223) 58866 · Telex 817331

CIRCLE 168 ON READER SERVICE CARD

PYE

GAS CHROMATOGRAPHY

5+1= versatility

Each of the five versions of the Pye Unicam GCD dual column gas chromatograph is a compact, self-contained package designed for a specific method of detection. Each offers proven performance at a sensible price.

While suitable for countless applications, the GCD is ideal for repetitive and routine usage, and achieves real economy in this area.

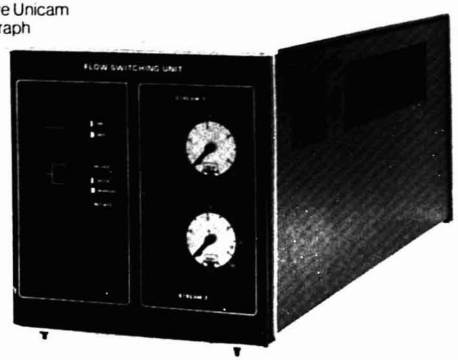

Now add the remarkable advantages of multidimensional chromatography: the Pye Unicam Flow Switching Unit, which permits backflushing, heart-cutting and by-passing, to save you valuable time and effort in the laboratory.

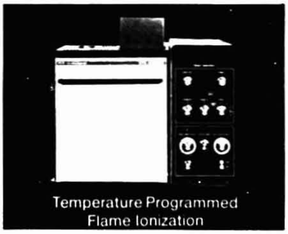

Temperature Programmed Flame Ionization

If it's time to replace your present gas chromatograph and you require an instrument for a specific detection method, the GCD is an excellent choice at a reasonable price. And the Flow Switching Unit will add that much more versatility.

Write to Pye Unicam for details of the five versions of the GCD and related accessories, and for our brochure on Multi-dimensional Gas Chromatography.

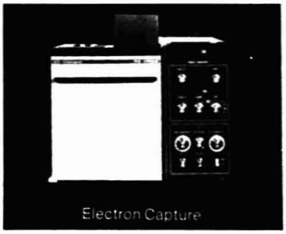

Electron Capture

Isothermal Flame Ionization

Thermal Conductivity

Autodoor Temperature Programmed Flame Ionization

PHILIPS

Pye Unicam

A SCIENTIFIC INSTRUMENT COMPANY OF PHILIPS

York Street, Cambridge, England CB1 2PX
Telephone (0223) 58866 Telex 817331

CIRCLE 169 ON READER SERVICE CARD

With your interests,
you'll want to read:

Chemistry in Medicine

The Legacy and the Responsibility

Just when the entire field of health care is being scrutinized and discussed, this unique and valuable study report makes its appearance.

Sponsored by the Committee on Chemistry and Public Affairs of the American Chemical Society, this well-documented study shows what chemical research related to health care has accomplished in the past and how it operates today.

The study report is packed with information and makes fascinating reading. Its contents include:

Social Attitudes and the Future for Drugs . . . Health Care Needs, Organizations, and Research . . . The Origins of Drugs . . . The Contributions of Basic Research . . . Drugs for Heart Patients . . . Chemistry in the Attack on Cancer . . . Therapeutic Uses of Polypeptide Hormones . . . The Control of Human Fertility . . . The Prostaglandins in Therapy . . . Prevention and Treatment of Genetic Disease . . . Chemicals vs. Mental Illnesses . . . The Relief of Pain . . . Chemical Immunosuppressants in Transplantation and Immunoinflammatory Diseases . . . Diagnostic Tests and Modern Therapy.

All you have to do to receive **Chemistry in Medicine** is to fill out the form below and mail it back to us!

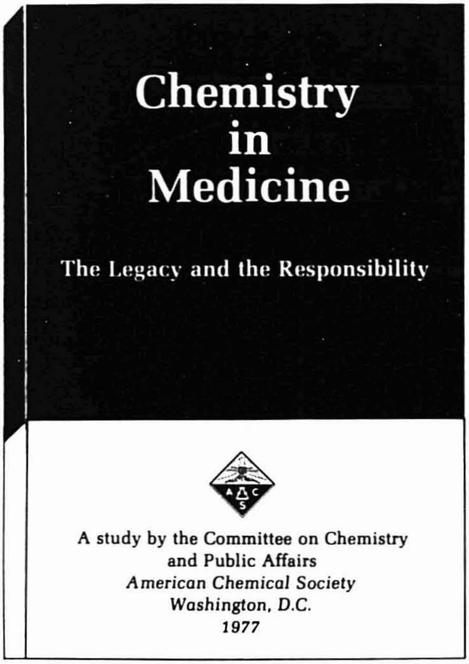

Chemistry
in
Medicine

The Legacy and the Responsibility

A study by the Committee on Chemistry
and Public Affairs
American Chemical Society
Washington, D.C.
1977

Special Issues Sales
American Chemical Society
1155 Sixteenth Street, N.W.
Washington, D.C. 20036

Price: $7.50 Paper bound (Foreign orders . . . add $.50)

Please send me ______ copies of **Chemistry in Medicine — The Legacy and the Responsibility**

☐ My payment is enclosed.

Name ____________________

Address ____________________

City ____________________

State ____________________ Zip Code ____________________

CM 77

CURRENT TITLES FROM

Academic Press, Inc.

A Subsidiary of
Harcourt Brace Jovanovich, Publishers
111 FIFTH AVENUE, NEW YORK, N.Y. 10003
24-28 OVAL ROAD, LONDON NW1 7DX

Send payment with order and save postage and handling charge.

Prices are subject to change without notice.

FOURIER TRANSFORM INFRARED SPECTROSCOPY:

APPLICATIONS TO CHEMICAL SYSTEMS

Edited by JOHN R. FERRARO and LOUIS J. BASILE

Volume 1—*1978, 311 pp., $29.75*
ISBN: 0-12-254101-4

Volume 2—*1979, in preparation*
ISBN: 0-12-254102-2

OPTOACOUSTIC SPECTROSCOPY AND DETECTION

Edited by YOH-HAN PAO

1977, 244 pp., $22.25
ISBN: 0-12-544150-9

PHYSICAL METHODS IN MODERN CHEMICAL ANALYSIS

Edited by THEODORE KUWANA

Volume 1—*1978, 336 pp., $33.00*
ISBN: 0-12-430801-5

Volume 2—*in preparation*

ANALYSIS OF FOODS & BEVERAGES: HEADSPACE TECHNIQUES

Edited by GEORGE CHARALAMBOUS

1978, 394 pp., $23.00
ISBN: 0-12-169050-4

GAS CHROMATOGRAPHY WITH GLASS CAPILLARY COLUMNS

By WALTER G. JENNINGS

1978, 184 pp., $19.75
ISBN: 0-12-384350-2

SIMPLIFIED DIGITAL AUTOMATION WITH MICROPROCESSORS

By JAMES T. ARNOLD

1978, in preparation
ISBN: 0-12-063750-6

LIQUID CHROMOTOGRAPHIC ANALYSIS OF FOODS & BEVERAGES

Edited by GEORGE CHARALAMBOUS

Volume 1—*1979, in preparation*

Volume 2—*in preparation*

ACADEMIC PRESS BOOKS ARE ON DISPLAY AT THE PITTSBURGH CONFERENCE BOOK SERVICE BOOTH.

CIRCLE 9 ON READER SERVICE CARD

Tailor-Made Monochromator

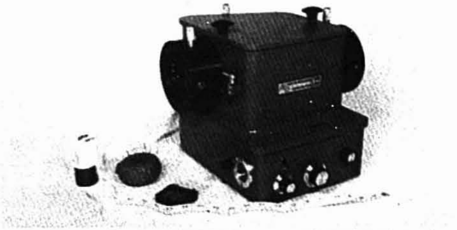

TAILOR-MADE MONOCHROMATOR for your experimental requirements...
a flexible 0.2m Vacuum Monochromator

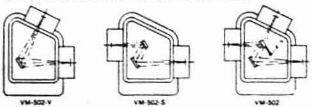

- spectral scanning of UV laser and fluorescence emission
- dispersion of synchrotron radiation
- absorption and emission spectroscopy
- calibration of detectors and films
- tunable UV radiation sources
- laboratory astrophysics
- plasma diagnostics
- optics calibration
- double beam applications

Vacuum UV-UV-VIS-IR operation (from below 300A)

Aberration-corrected concave holographic grating, kinematically mounted

Fabricated housing UHV model available

Fast optical system F/4.5 nominal

Wavelength-optimized optics*

Interchangeable diverter mirrors may be coated as individual reflective filters (e.g. for VUV-UV laser lines at 1460, 1720, 1930, 2484, 3080, or 3511A) for high peak efficiency and low out-of-band reflectance; kinematic mounts allow quick replacement without realignment.

Standard broad-spectrum Al-MgF_2 coatings allow efficient operation above 1150A, with 80% typical reflectance at 1216A. Extreme UV coatings of **Osmium** are supplied for short-wavelength operation.

Compatible ARC accessories: ☐ Light Sources, ☐ Power Supplies, ☐ Diffusion Pumping System, ☐ Sample Chambers, ☐ Detector Assemblies, ☐ Model 50 Filter Assembly.

ACTON RESEARCH CORPORATION
BOX 215•525 MAIN STREET•ACTON, MASSACHUSETTS 01720
(617)263-3584•TELEX 94-0787 ARC ACTO
IN EUROPE, CONTACT ORIEL

PRECISION
OPTICAL INSTRUMENTS
COMPONENTS
AND COATINGS

See Action Research Corp. at the Pittsburgh Conference, Booths 1909-1910

CIRCLE 6 ON READER SERVICE CARD

Our
Quality

STAINLESS STEEL
TWO STAGE REGULATOR
MILLAFLOW DSG-750 SERIES
Corrosion & Diffusion Resistant Pressure Regulator

▶ MILLAFLOW OFFERS THE FIRST TWO STAGE REGULATOR CONSTRUCTED FROM 316 STAINLESS STEEL, THIS SERIES OFFERS PRECISION REGULATION WITH LONG LIFE AND EXCELLED DEPENDABILITY.

▶ MAXIMUM INLET PRESSURE: 2,200 psig.

▶ OUTLET PRESSURE RANGES: 1-15 psig, 2-75 psig and 5-150 psig.

▶ LEAKAGE RATE: LESS THAN 2 x 10^{-9} cc/sec HELIUM.

VERIFLO
CORPORATION
INSTRUMENT DIVISION • 250 Canal Blvd., Richmond, CA 94804, (415) 235-9590

CIRCLE 220 ON READER SERVICE CARD

are analysis of metals, soil extracts, plant tissue ash, geochemical samples, air particulates, and foods, sampling approaches, and factors influencing precision and accuracy.

Continuing Series

Encyclopedia of Electrochemistry of the Elements: Organic Section. Vol. 12. A. J. Bard and H. Lund, Eds. xii + 512 pages. Marcel Dekker, Inc., 270 Madison Ave., New York, N.Y. 10016. 1978. $88

Volume 12 continues the organic section which in four volumes will complete this long-standing series on electrochemistry of the elements. This book contains three review chapters: carbonyl compounds; carboxylic acids, esters, and anhydrides; and organic sulfur compounds. All chapters have sections on electrode potential, voltammetric properties, and electrochemical studies. The chapter on carboxylic acids, esters, and anhydrides includes a section on applied electrochemistry. Each section includes tables of available thermodynamic, kinetic, voltammetric, and other electrochemical data, and a critical discussion on the known electrochemical reactions. Most of the references do not extend much beyond 1974. The book is reproduced from typewritten text.

U.S. Government Publications

Order copies of the following PRE-PAID at the price shown by SD Cat. No. from Superintendent of Documents, U.S. Government Printing Office, Washington, D.C. 20402. Foreign remittances must be in U.S. exchange and include an additional 25% of the publication price to cover mailing costs

Atomic Energy Levels—The Rare-Earth Elements. W. C. Martin, R. Zalubas, and L. Hagan. vii + 411 pages. 1978. $9.50. SD Cat. No. C13.48:60

Energy level data are given for 66 atoms and atomic ions of the 15 elements lanthanum (Z = 57) through lutetium (Z = 71). Only experimentally determined energy levels are included; energies are restricted to excitations of outer-shell electrons and to inner-shell excitations up to the soft X-ray range. The levels are taken from analyses of the spectra of atomic gases wherever possible; however, the levels for several of the triply ionized rare earths are from analyses of the spectra of the

THE NEW MODEL 240B ELEMENTAL ANALYZER– A REFLECTION OF EXCELLENCE

The new Model 240B is a second-generation analyzer for the automatic determination of carbon, hydrogen, nitrogen, oxygen, and sulfur. The Model 240B retains the proven combustion and detection design that made the Model 240 the accepted industry standard — while incorporating features for ease of operation and reliability.

SPEED AND PRECISION

Based on proven classical techniques, the Model 240B automates the process — increasing speed, assuring higher reproducibility, and eliminating the tedium and errors involved in weighing absorption tubes. And because it accepts sample weights in the most convenient range (up to 3 mg), it yields more precise results than other instrumental systems.

EASY TO USE AND MAINTAIN

The 240B is designed to assure that technicians of reasonable training and skill can obtain excellent results. All controls are located on the front panel, including a switch that allows the selection of automatic extended combustion times, for those hard-to-burn samples. An external programmer index wheel provides an immediate update of the program position and simplifies routine maintenance. And an oxygen control valve makes it easy to convert from C, H and N to oxygen analysis.

ALL-NEW DESIGN

The design of the new Model 240B has other features to save you time and trouble. Faster heating furnaces provide rapid equilibration. The new pneumatic system permits gas scrubbers and gas supplies to be changed without instrument shutdown. And a redesigned detector and thermostatted electronics eliminate bridge drift, assuring excellent stability.

VERSATILITY AND AUTOMATION

The Model 240B can be used on virtually any material in which C, H, N, O, or S need to be determined — not just for pure organic compounds. Coal, fuel oil, oil shales, ocean sediments, soils, filtered particulate matter, gasoline, copolymers, algae, sewage, food, feeds, and fertilizers are among the many materials which can be analyzed routinely. Moreover, the Model 240B is available with either recorder operation or automatic data reduction that provides a printed analytical report.

FIND OUT MORE

A free literature package gives you all the details on the Model 240B and its full line of accessories. Just write Perkin-Elmer Corporation, Main Avenue, Norwalk, CT 06856. Or phone (203) 762-4629.

PERKIN-ELMER

Expanding the world of analytical chemistry

CIRCLE 159 ON READER SERVICE CARD

Advanced technology

ion selective electrodes

New sensing membrane designs, developed by HNU Systems, represent fundamental advances in ion electrode technology and result in improved analytical performance in virtually all key areas.

For example:

- Detection limits are extended 2X-10X lower
- Fewer interferences for most electrodes
- Response times up to 5X faster
- New solid matrix membranes replace old style liquid ion exchange membranes
- Simpler constructions reduce failures and extend operating lives

A twelve page technical manual describing the new performance standards for gas sensing, solid matrix and solid state electrodes and the technology advances behind them is available from:

hnu

HNU Systems, Inc.
30 Ossipee Road, Newton, MA 02164
Tel. 617-964-6690; TWX. 710-335-7692

HNU Systems, Inc./Europe
Via Boccaccio 2, 20123 Milano, Italy
Tel. (02) 87 11 86080 08 61;
TWX. 34343 EXECMIL

CIRCLE 97 ON READER SERVICE CARD

ions in crystals or solutions. Level value, parity, J-value, configuration and term assignments, experimental g-value, and ionization potentials for most of the spectra are listed. Complete references for the tabulated data are given.

ASTM Publications

The following are available from the American Society for Testing and Materials, 1916 Race St., Philadelphia, Pa. 19103 (USA, Canada, and Mexico add 3% shipping charges. Other countries add 5%)

Part 12 of Annual Book of ASTM Standards on Chemical Analysis of Metals, and Sampling and Analysis of Metal Bearing Ores. 880 pages. 1978. $28

Part 12 contains 81 standards of which 36% are new, revised, or changed in status since the 1977 edition. The American National Standard designation is also carried by 28 of the standard documents. Chemical analyses of metals standards in Part 12 cover Al and Al alloys; Cd, Nb, Cu, and Cu alloys; ferroalloys; Fe, Ni, and Co alloys; Pb, Sn, Sb, and their alloys; Mg and Mg alloys; metal powders; and Ni and Ni–Cu alloys. Also addressed within the standards are Ni–Cr Fe alloys; Ag solders and other brazing alloys; steel; cast, open-hearth, and wrought iron; W, Zn, and Zn alloys; and Zr and Zr alloys.

Part 42 of Annual Book of ASTM Standards. 602 pages. 1978. $18

Part 42 on emission, molecular and mass spectroscopy, chromatography, resinography, and microscopy contains 73 standards of which 58 are approved as American National Standards. The new standards include optical emission spectrometric analysis of aluminum and aluminum alloys by the point-to-plane technique, nitrogen atmosphere, practice for sampling zinc and zinc alloys for optical emission spectrochemical analysis, and guidelines for developing functional requirements, and implementing, evaluating, and documenting computerized lab systems. In addition, ASTM publishes three related publications: special technical publication *Flameless Atomic Absorption Analysis: An Update 1977* (STP 618); and E-2 compilation, *Methods for Emission Spectrochemical Analysis, 1977 Supplement and 6th Ed. 1971.*

GET MORE "INFRAMATION" FROM YOUR SAMPLE

The compact unit displaying the spectrum in such detail is our new Perkin-Elmer Infrared Data Station. It's a microcomputer that lets you process spectral data on the spot. Spectra can be displayed right on the CRT screen or replotted on the spectrophotometer's own recorder. And the best news is that it costs less than $10,000.

SIMPLE TO OPERATE

You need no special programming skill to operate the Data Station. We provide an applications program consisting of more than 32 different routines. Twenty-four special function keys further simplify operation. Just push a key to initiate a dialog in which the screen asks you for any additional information needed to process your spectrum. Such routines as difference, smoothing, accumulation, average, multiply, subtract, add, divide, flat, etc., are made easy with the Data Station.

When you start a scan, the Data Station goes into action. Single or repetitively scanned spectra are taken into memory. In a matter of seconds, the spectra can be smoothed, averaged or flattened. Difference spectra can be obtained rapidly by using the special function key, while automatic scaling speeds the process. You can view the spectra on the CRT screen at any point in the process; when satisfied, plot the final spectrum on your instrument's own recorder for a permanent record. Or, if you prefer, save it in digital form on a microfloppy disk. The unique OBEY command lets you specify a sequence of operations to be performed on a single sample or series of samples. This is especially powerful when coupled with our multisampling accessory.

GRAPHIC DISPLAY OF SPECTRA

The graphics capability lets you follow the scan of the spectrophotometer on the CRT. You can display up to three spectra simultaneously on the screen; for example, component A, component B, and the mixture of A plus B. You can overlay two spectra (as shown) highlighting the differences. The GRID command superimposes grid lines with wavenumber calibrations corresponding to the spectrum of interest. Any portion of a spectrum's X-axis can be expanded to fill the screen.

What won't the Infrared Data Station do? Just about nothing. It was designed by infrared specialists to make your work easier, faster, and more accurate – to relieve you of time-consuming chores. It's directly compatible with the Model 283 Infrared Spectrophotometer in your lab and can also be used with our X99B Series and our Model 580B. Find out more about what the Infrared Data Station can do for you. For a brochure, contact your nearest Perkin-Elmer representative or write to Perkin-Elmer Corporation, MS-12, Main Avenue, Norwalk, CT, 06856. To arrange for a demonstration, just phone (203) 762-6126.

PERKIN-ELMER

Expanding the world of analytical chemistry.

CIRCLE 163 ON READER SERVICE CARD

PERKIN-ELMER BRINGS YOU SIGMA BASIC... MORE MEANING FROM CHROMATOGRAPHY DATA

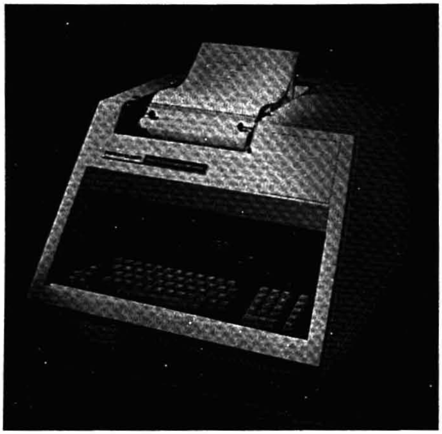

Ordinary data handling systems for chromatography can give users the ability to get large amounts of data from a chromatograph, but not the flexibility to reduce that data to meaningful information. SIGMA BASIC, an exclusive feature of the Model SIGMA 10 Chromatography Data Station, provides that flexibility. Imagine taking standard chromatography data and converting it into almost any form you need. It's possible with the SIGMA 10.

IMAGINATION—THE KEY.

SIGMA BASIC lets you use imagination to create solutions according to your needs. You can choose how much computer power to use, choose one of many programs in Perkin-Elmer's SIGMA BASIC library, or choose to write your own programs exactly matched to your specific needs. You can call on SIGMA BASIC to pull you through both routine and special laboratory procedures. And you decide just how far you want to tailor the results.

Actual printouts are about three times larger than shown here.

GO FROM STANDARD TO SPECIALIZED CALCULATIONS.

The SIGMA 10, preprogrammed to plot annotated chromatograms and to integrate the data, provides a fully-documented quantitative report on a single sheet of paper for as many as four data channels simultaneously. A typical report looks like this.

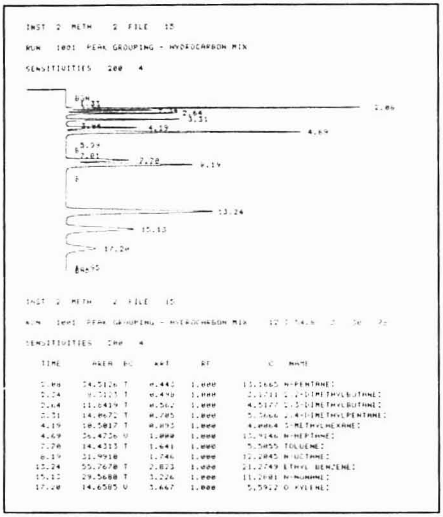

```
INST  2  METH    2  FILE   15

RUN   1001  PEAK GROUPING - HYDROCARBON MIX

SENSITIVITIES   200   4
```

BGN
2.33
2.64
3.31
4.19
4.69
2.06
5.39
7.01
7.70
8.19
13.24
15.13
17.20
END

```
INST  2  METH    2  FILE   15

RUN   1001  PEAK GROUPING - HYDROCARBON MIX    12 : 54.6   3   30   78

SENSITIVITIES   200   4

  TIME      AREA  BC    RT       RF             C   NAME

  2.06    24.5126 T   0.443    1.000     13.1665 N-PENTANE:
  2.34     9.3123 T   0.496    1.000      3.1711 2,2-DIMETHYLBUTANE:
  2.64    11.6419 T   0.562    1.000      4.5177 2,3-DIMETHYLBUTANE:
  3.31    14.0672 T   0.705    1.000      5.3666 2,4-DIMETHYLPENTANE:
  4.19    10.5017 T   0.893    1.000      4.0064 3-METHYLHEXANE:
  4.69    36.4736 V   1.000    1.000     13.9146 N-HEPTANE:
  7.70    14.4313 T   1.641    1.000      5.5055 TOLUENE:
  8.19    31.9910     1.746    1.000     12.2045 N-OCTANE:
 13.24    55.7670 T   2.823    1.000     21.2749 ETHYL BENZENE:
 15.13    29.5680 T   3.226    1.000     11.2601 N-NONANE:
 17.20    14.6585 V   3.667    1.000      5.5922 O-XYLENE:
```

However, often you need further specialized calculations. A short, simple program written in SIGMA BASIC makes them possible. You can turn the data in the typical report into concise. meaningful information.

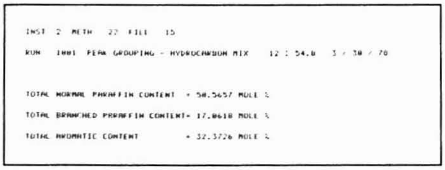

```
INST  2  METH   22  FILE   15

RUN   1001  PEAK GROUPING - HYDROCARBON MIX    12 : 54.6   3 / 30 / 70


TOTAL NORMAL PARAFFIN CONTENT  = 50.5657 MOLE %

TOTAL BRANCHED PARAFFIN CONTENT= 17.0618 MOLE %

TOTAL AROMATIC CONTENT         = 32.3726 MOLE %
```

LABORATORY DATA HANDLING AND AUTOMATION SYSTEMS

WHAT ELSE CAN SIGMA BASIC DO?

Rarely is the analysis complete after the chromatogram is run and the standard quantitative data is made available. The required information must be extracted from the data. SIGMA BASIC provides a limitless combination of ways to *unlock* this information. For example, with SIGMA BASIC you can convert molar quantities in a natural gas mixture into compressibility factor, gross caloric value, relative density, Wobbe number, and much, much more.

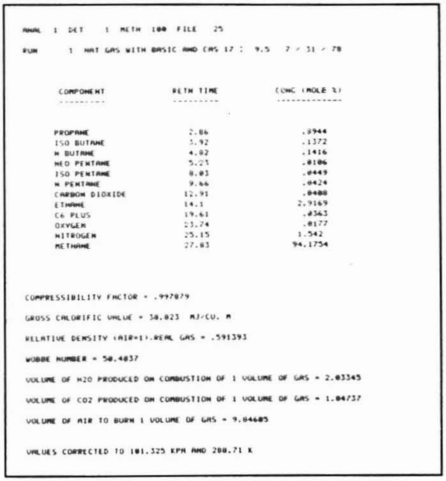

```
ANAL  1  DET     1  METH  100  FILE   25

RUN       1  NAT GAS WITH BASIC AND CAS 17 :   9.5   7 / 31 / 78


        COMPONENT              RETN TIME            CONC (MOLE %)
        ---------              ---------            -------------


       PROPANE                   2.86                   .3944
       ISO BUTANE                3.92                   .1372
       N BUTANE                  4.82                   .1416
       NEO PENTANE               5.23                   .0106
       ISO PENTANE               8.03                   .0449
       N PENTANE                 9.66                   .0424
       CARBON DIOXIDE           12.91                   .0408
       ETHANE                   14.1                   2.9169
       C6 PLUS                  19.61                   .0363
       OXYGEN                   23.74                   .0177
       NITROGEN                 25.15                  1.542
       METHANE                  27.03                 94.1754


COMPRESSIBILITY FACTOR = .997079

GROSS CALORIFIC VALUE = 38.023  MJ/CU. M

RELATIVE DENSITY (AIR=1).REAL GAS = .591393

WOBBE NUMBER = 50.4037

VOLUME OF H2O PRODUCED ON COMBUSTION OF 1 VOLUME OF GAS = 2.03345

VOLUME OF CO2 PRODUCED ON COMBUSTION OF 1 VOLUME OF GAS = 1.04737

VOLUME OF AIR TO BURN 1 VOLUME OF GAS = 9.84605

VALUES CORRECTED TO 101.325 KPA AND 288.71 K
```

Perhaps a graphic presentation of data, such as a plot of normalized molecular weight distribution by gel permeation chromatography, is more meaningful for you.

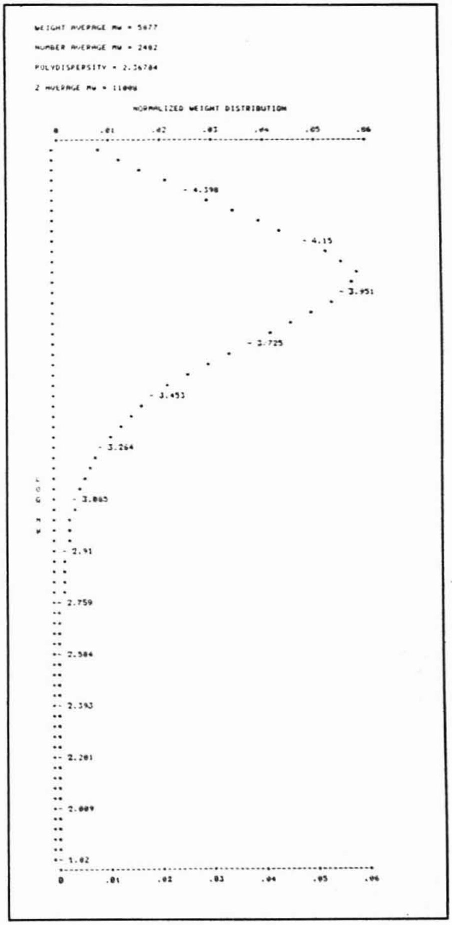

```
WEIGHT AVERAGE MW = 5677

NUMBER AVERAGE MW = 2402

POLYDISPERSITY = 2.36784

Z AVERAGE MW = 11006
```

Continued on the next page

Or, you may want a standard compilation of several runs of data, automatically stored and summarized, to help you test the validity of your data.

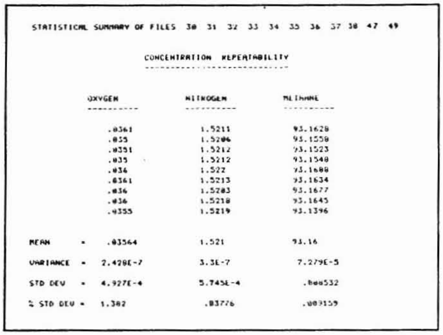

```
STATISTICAL SUMMARY OF FILES  30  31  32  33  34  35  36  37  38  47  49

                     CONCENTRATION  REPEATABILITY
                     ----------------------------

            OXYGEN               NITROGEN             METHANE
            ----------           ----------           ----------

               .0361                1.5211               93.1628
               .035                 1.5206               93.1558
               .0351                1.5212               93.1523
               .035                 1.5212               93.1548
               .036                 1.522                93.1688
               .0361                1.5213               93.1634
               .036                 1.5203               93.1677
               .036                 1.5218               93.1645
               .0355                1.5219               93.1396


MEAN      =     .03564              1.521                93.16

VARIANCE  =   2.428E-7              3.3E-7                7.279E-5

STD DEV   =   4.927E-4              5.745E-4               .008532

% STD DEV =   1.382                  .03776                .009159
```

With SIGMA BASIC, you can operate the SIGMA 10 as a totally automated *custom* system – the SIGMA 10 can request the information needed to do a specific series of analyses – in an unattended manner, overnight or over weekends. You define the precise form of dialog to match the level of the instrument operator.

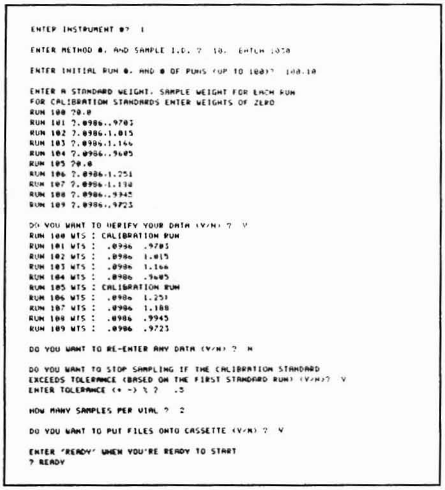

```
ENTER INSTRUMENT #?  1

ENTER METHOD #, AND SAMPLE I.D. ?  10,  BATCH 1030

ENTER INITIAL RUN #, AND # OF RUNS (UP TO 100)?  100,10

ENTER A STANDARD WEIGHT, SAMPLE WEIGHT FOR EACH RUN
FOR CALIBRATION STANDARDS ENTER WEIGHTS OF ZERO
RUN 100 ?0,0
RUN 101 ?.0986,.9703
RUN 102 ?.0986,1.015
RUN 103 ?.0986,1.166
RUN 104 ?.0986,.9605
RUN 105 ?0,0
RUN 106 ?.0986,1.251
RUN 107 ?.0986,1.188
RUN 108 ?.0986,.9945
RUN 109 ?.0986,.9723

DO YOU WANT TO VERIFY YOUR DATA (Y/N) ?  Y
RUN 100 WTS : CALIBRATION RUN
RUN 101 WTS :  .0986  .9703
RUN 102 WTS :  .0986  1.015
RUN 103 WTS :  .0986  1.166
RUN 104 WTS :  .0986  .9605
RUN 105 WTS : CALIBRATION RUN
RUN 106 WTS :  .0986  1.251
RUN 107 WTS :  .0986  1.188
RUN 108 WTS :  .0986  .9945
RUN 109 WTS :  .0986  .9723

DO YOU WANT TO RE-ENTER ANY DATA (Y/N) ?  N

DO YOU WANT TO STOP SAMPLING IF THE CALIBRATION STANDARD
EXCEEDS TOLERANCE (BASED ON THE FIRST STANDARD RUN) (Y/N)?  Y
ENTER TOLERANCE (+ -) % ?   .5

HOW MANY SAMPLES PER VIAL ?  2

DO YOU WANT TO PUT FILES ONTO CASSETTE (Y/N) ?  Y

ENTER 'READY' WHEN YOU'RE READY TO START
? READY
```

SOME QUESTIONS YOU MIGHT HAVE.
CAN SIGMA BASIC DO MORE? YES. The applications are virtually limitless. With its ability to access raw data, SIGMA BASIC can even produce information from data generated by instruments other than chromatographs.

WHAT IS SIGMA BASIC? A SPECIAL CHROMATOGRAPHY-ORIENTED EXTENSION OF BASIC. BASIC is a simple-to-use yet powerful programming language. It has become the standard for both laboratory and home computers.

CAN I SELECT RATHER THAN WRITE PROGRAMS? YES. If you prefer, you can select a program from our Users' Library. You may find a program already written to suit your needs. If not, it is easy to modify an existing program.

WHY DO I NEED SIGMA BASIC? IT OFFERS GREAT FLEXIBILITY IN A SMALL PACKAGE. To try to provide all the flexibility available with SIGMA BASIC as a standard part of a chromatography data system would require a large and therefore costly system. Also, SIGMA BASIC is multi-user and reentrant: several BASIC programs can be run simultaneously.

FIND OUT MORE.
Learn how the SIGMA 10 with SIGMA BASIC can simplify laboratory data handling. Request our literature describing its long list of benefits.
Ask for a demonstration. Call (203) 762-4487. Or write Perkin-Elmer Corporation, Main Avenue MS-12, Norwalk, CT 06856.

PERKIN-ELMER

Expanding the world of analytical chemistry.

CIRCLE 153 ON READER SERVICE CARD

Editors' Column

Publication Times

Through 1978, 62.9% of ANALYTICAL CHEMISTRY's research contributions were published within six months (37% in less than five months), 23.6% between six and eight months, and 13.5% in over eight months. Comparable figures for 1977 are 67.2, 25.2, and 10.6%. The JOURNAL had tightened procedures so stringently in the earlier period that the best we could hope for was minimal slippage. Further insight into our publication processing times is provided by data from Books and Journals Division. Four times a year (February, May, August, and November), B&J's Journals Department studies processing data for all of the ACS publications. For November 1978 the median publishing time (receipt to publication) for ANALYTICAL CHEMISTRY was 24 weeks with a range of 13–63 weeks. Receipt-to-acceptance (essentially the peer review and revision process) median time was 13 weeks with a range of 4–51 weeks. Acceptance to publication had a median time of 11 weeks with a range of 7–18 weeks.

In a November 1978 editorial, Russell Christman, editor of our sister publication, *Environmental Science & Technology* (*ES&T*), discussed manuscript processing time. He cited some of the difficulties faced by his own journal and called attention to the shorter processing times enjoyed by ANALYTICAL CHEMISTRY. Without attempting to comment on the particular circumstances that apply uniquely to *ES&T*, we can discuss factors that go into shortening processing times for ANALYTICAL CHEMISTRY.

There is much to be said for momentum. Readers may have noticed the differing sizes of individual issues of the JOURNAL. On the last possible, reasonable date for our "list of order" for an issue, we include ALL manuscripts for which corrected galleys are back from the authors and even some for which corrected galleys are expected any day. We have NO backlog. This means, of course, that all of us working with the manuscripts must move right along. Otherwise, we will have a month with no papers!

A commitment to speed manuscript processing begins with the editor who then conveys this importance throughout the operation so that everyone is motivated to act promptly all along the line. We acknowledge particularly our debt to the ACS Books & Journals Administration for exerting extra efforts in our behalf to make sure that our manuscript-into-print times were not extended when we moved galley and page preparation from the Mack Printing Co. to the Chemical Abstracts Service (CAS) in May 1976. If anything, the time from acceptance to publication has been reduced by this move. Credit for this also goes to Chemical Abstracts personnel; Charles F. Bertsch, head of the Journals Department; Marianne Brogan, his associate, located at Chemical Abstracts in Ohio; and Elizabeth Rufe, ANALYTICAL CHEMISTRY's associate editor in Easton, Pa. Mrs. Rufe copy edits and marks for the printer accepted manuscripts just as fast as she receives them from the Washington headquarters office and speeds them off to CAS for galley production.

Let us now backtrack to the initial submission of the manuscripts: manuscripts are usually out to reviewers within a week. Reviewers are prodded on a regular basis. Lengthened processing times may mean slow reviewers, the need for a third review, or time used by the authors in revision. This is not to say that any particular manuscript might not run into trouble. An especially novel research contribution may be difficult to get reviewed. Controversy between reviewers and authors takes time to resolve. Or a manuscript may be lost in the mail. Authors should not hesitate to call the editorial office and inquire about the status of their manuscripts if the times involved seem overlong.

The people working with ANALYTICAL CHEMISTRY, from Professor Laitinen through the editorial and production offices, are all striving for the shortest possible manuscript processing times consistent with careful peer review.

Josephine M. Petruzzi

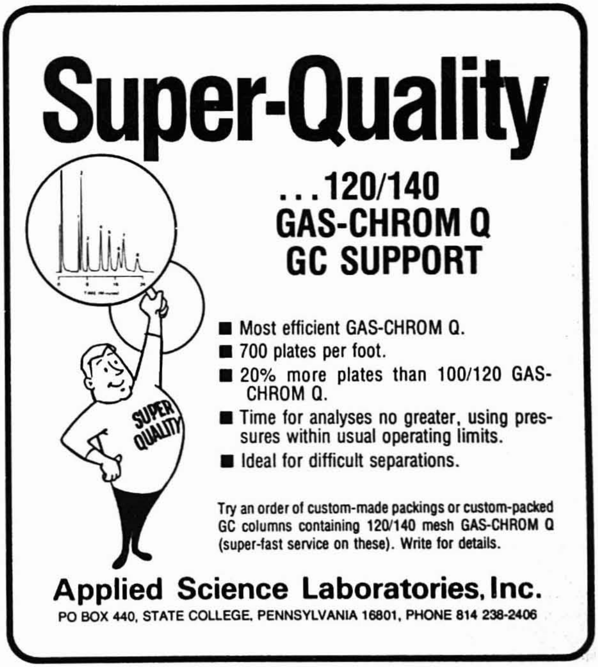

Super-Quality

...120/140
GAS-CHROM Q
GC SUPPORT

- Most efficient GAS-CHROM Q.
- 700 plates per foot.
- 20% more plates than 100/120 GAS-CHROM Q.
- Time for analyses no greater, using pressures within usual operating limits.
- Ideal for difficult separations.

Try an order of custom-made packings or custom-packed GC columns containing 120/140 mesh GAS-CHROM Q (super-fast service on these). Write for details.

Applied Science Laboratories, Inc.
PO BOX 440, STATE COLLEGE, PENNSYLVANIA 16801, PHONE 814 238-2406

CIRCLE 2 ON READER SERVICE CARD

A new weighing concept from Mettler...

DeltaRange

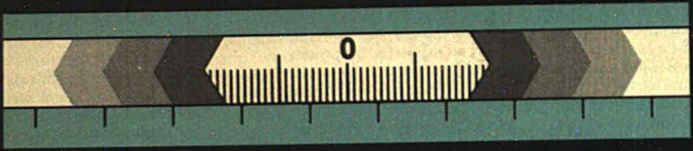

A movable fine range that's ten times as accurate as the coarse range.

▲ Remember that axiom that says one must sacrifice balance readability as capacity goes higher? Forget it. With the new electronic Mettler PC4400 DeltaRange balance, the user has two readability ranges—a 400 g fine range that is movable along a 4000 g coarse range. The fine range is readable to .01 g; the coarse range reads to .1 g.

DeltaRange adds a new measure of versatility to precision weighing. At any point in the 4000 g weighing range, the operator simply presses the single control bar of the PC4400 and gets a 400 g fine range to work with—giving readings 10 times as accurate as those in the coarse range. And he can do this as often as he wishes.

The DeltaRange concept is thus analogous to a 400 g slide on a 4000 g slide rule.

What this means to you is that one balance, the PC4400—first of a family of Mettler DeltaRange balances—can serve numerous applications that previously required several balances. Weigh heavy and light objects on the same balance.

PC balances are available with plug-in microprocessor-based Application Input Devices that accept keys for programming the balance to count small parts, measure moisture loss in percent, do reference comparison weighing, or to highlight intermediate and final results during compounding or formula weighings.

To get DeltaRange versatility working for you, contact your Mettler representative. Or write for a brochure to Mettler Instrument Corporation, Box 71, Hightstown, NJ 08520.

CIRCLE 146 ON READER SERVICE CARD

Delta Delta Del
Range Range Ra
Mettler
Mettler PC 4400
+
DeltaRange
1.26 g

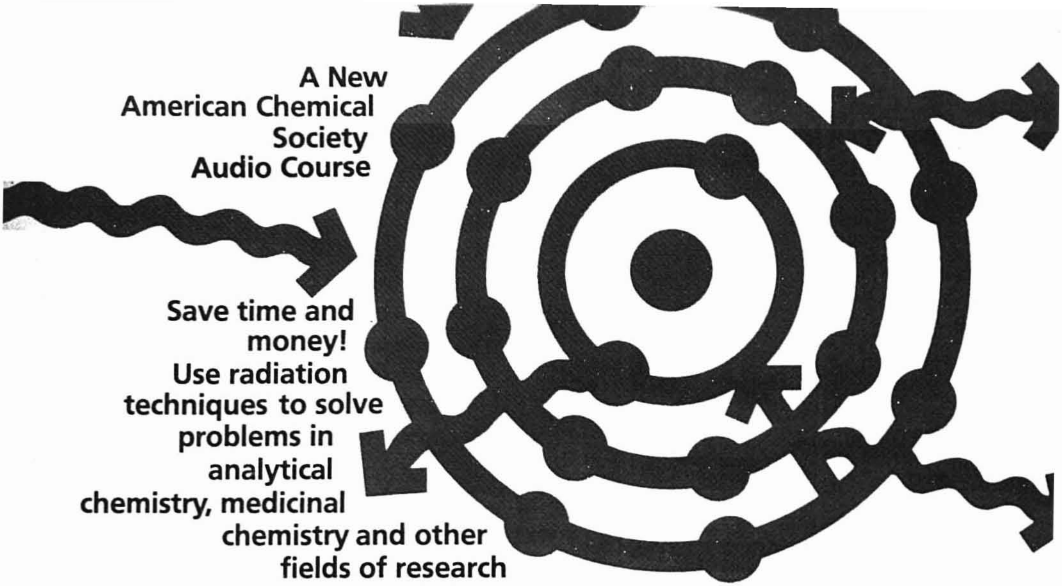

A New
American Chemical
Society
Audio Course

Save time and
money!
Use radiation
techniques to solve
problems in
analytical
chemistry, medicinal
chemistry and other
fields of research

RADIOCHEMISTRY

Covering a wide variety of topics, this course is designed as an in-depth introduction to this important sub-discipline of chemistry. The course provides rigorous, yet concise, treatments of general nuclear concepts, nuclear stability and radioactivity, and the interaction of radiation with matter including a discussion of radiological safety. The course also contains sections on counting radioactive samples, sample purification and preparation, and various types of detectors such as gas-filled and solid-state detectors and scintillation counters.

Other important topics include pulse-height analysis, gamma-ray spectroscopy, induced nuclear reactions, radionuclide production, activation analysis, tracer methodology, and liquid scintillation counting.

American Chemical Society
Educational Activities
Department
1155 16th Street, N.W.
Washington, D.C. 20036
(202) 872-4588

YES, please send ______ copy(ies) of the ACS Audio Course *Radiochemistry* @ $155.00 each.
Please specify course number C-4OU when ordering.
______ Additional manuals: 1-9 @ $23.00 each; 10-49 @ $18.50 each; 50 or more @ $17.25 each.

☐ Payment enclosed. ☐ Bill company.

Name ______________________

Organization ______________________

Address ______________________

City ____________ State ____________ ZIP ____________

All customers outside the U.S. and Canada who are not ACS members should address their orders to Pergamon Press, Headington Hill Hall, Oxford OX3 OBW, England.

LEARN BY DOING
Problem sets, complete with answers, follow each section of the course to aid in the learning process.

WHO SHOULD TAKE THE COURSE
Analytical chemists, medicinal chemists, medical researchers, teachers and students whose work involves them in radioactivity and its relationship to chemistry. No previous knowledge of the subject is presumed.

THE INSTRUCTORS
Dr. Gregory R. Choppin, Chairman, Department of Chemistry, Florida State University, is the author of numerous research publications.

Dr. Patricia A. Baisden, Department of Chemistry, Florida State University, recently completed her doctoral studies.

ACS Triple-Impact Audio Courses
combine the ease of ***listening***
the reinforcement of ***reading***
the challenge of ***doing***
as you learn from the leaders — renowned authorities — teaching the subjects they know best in their own words and voices.

FOR INDIVIDUAL OR GROUP USE
Excellent for use by individuals or groups, the course consists of six audiotape cassettes (5.3 hours playing time) and a 332-page manual . . . $155.00. Additional manuals for group use, 1-9 copies . . . $23.00 each; 10-49 copies . . . $18.50 each; 50 or more . . . $17.25 each.

NO-RISK, 10-DAY, FREE TRIAL OFFER
Order your course on Radiochemistry now. If you are not completely satisfied, just return the unit to us within ten days for full credit or refund.

Meet Joyce Loebl

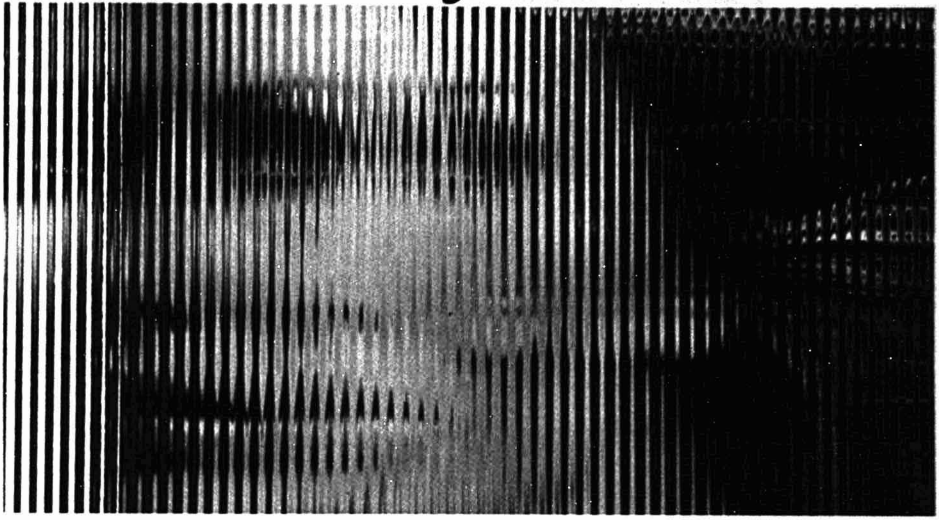

who has 4 degrees in image analysis.

When it comes to image analysis, Joyce Loebl is at the head of the class. Our complete line of instruments can handle virtually any requirements in the field of image analysis. Check out these instruments and see why Joyce Loebl is top!

1. Microdensitometer 3CS

The *Microdensitometer 3CS* is a versatile double beam, high resolution, flatbed recording microdensitometer providing an output in the form of an analog graph on an integral X-Y recorder. Modular options allow digital output onto magnetic tape recorder or complete computer control. The 3CS features bilaterally adjustable pre and post specimen slits (1 x 25 microns to 1 x 4 millimeters), specimen to record expansion from 1 to 1 up to 1000 to 1 and density measurement up to 6 0 D in 11 ranges. Provision is made to accept colour filters and a wide range of accessories for special applications.

2. Scandig 3/Filmwrite 2

The *Scandig 3* and *Filmwrite 2* are a hi-speed rotating drum microdensitometer and photographic recorder, respectively. Interfaced to a digital computer, they form an image analysis system that can digitize, enhance, and record photographic imagery. *Scandig 3* features Joyce-Loebl's "state of the art" solid state photometrics system providing repeatability not previously possible. Scandig has sampling apertures from 12 5 to 200 micrometers and accommodates transmission or reflection samples up to 250mm x 250mm (350mm x 425mm as an option). /*Filmwrite 2* generates instant hard copy on 250mm x 250mm photographic paper. Pixel size is variable down to 125 micrometers. The integral photographic processor gives you instant prints without need for a darkroom. Joyce-Loebl's famous FSPP software provides simple control of both Scandig and Filmwrite as well as a range of picture processing algorithms.

3. Microdensitometer 6

The new *Microdensitometer 6* combines the best features of the now world famous Microdensitometer 3CS, with the latest advances in electro-optical techniques and computer data processing. It's a classical flatbed microdensitometer, utilizing double microscope optics in transmission and a dark field system in the reflectance mode. Optical density measurements are made using a double-beam optical principle to assure high linearity and precision over a wide range of optical density. Optical density or transmission data are recorded in digital form at a data rate of up to 1000 points per second. The table can accommodate samples up to 250mm x 250mm. A large area of sample may be viewed through an ocular or on a rear projection screen. Sample illumination is provided from a secondary light source for high intensity illumination of a large sample area without the need to adjust the source aperture setting. With the proprietary Joyce-Loebl "Wizard" software language, the user has full control of the microdensitometer. The Digitized data is stored on magnetic tape, floppy-disc or any other mass storage medium. A large range of options is available.

4. MAGISCAN

The *Magiscan* is a television based turn-key quantitative image analysis system with integral scanning processing, and display facilities. Magiscan has separate digital processors: a high speed Image Processor to do the difficult feature extraction task and a powerful minicomputer to do the arithmetic oriented quantitative analysis task. The Image Processor operates on the full range of the image and can therefore perform complex procedures involving varying background levels, gradients, and textures. Magiscan can handle feature extraction tasks other systems are incapable of such as defining cell boundaries in a non-uniformly stained sample, separating overlapping spheres, and rejecting out-of-focus particles. There are 12 standard field and feature measurements. Other measurments can be added in software without the need for additional hardware. Standard detection methods include grey level thresholding, tracking detection, and edge detection. Magiscan is easy to use. The only operator controls are a 14 button keypad and a single pixel light pen that permits precise editing of the detected image. For more flexibility, it may be programmed in Basic, a human readable programming language, or Fortran, a scientific programming language. Many useful options are available.

JOYCE LOEBL

Joyce-Loebl
A Division of Vickers Limited

Great Britain Team Valley, Gateshead, NE11 0QW ENGLAND, Telephone 0632-822111 • Telex 53257
North America 100A Commerce Way, Woburn, MA 01801 USA, Telephone (617) 935-3113 • Telex 94-9413
West Germany Niederlassung fur Deutschland, 7417 Pfullingen/Reutlingen, Romerstrasse 90 WEST GERMANY, Telefon 07121/73021 • Telex 0729 651

CIRCLE 113 ON READER SERVICE CARD

Finnigan's Organics-in-Water Analyzer: a breakthrough.

Finnigan's new OWA™-Series (Organics-in-Water Analyzer) is your answer to meet the requirements of the water regulatory acts:

- Complete measurement of GC or ion data from samples with both high and low concentration constituents.
- Provides correct isotope ratio data for signals of very low ion abundance.
- Capable of calibration to EPA protocol.
- EPA compatible data format and medium.

Meets Laboratory Operational Requirements

- Simplified pre-programmed operating procedures.
- High sample throughput.
- High reliability and resulting low maintenance expense.
- Low capital investment and low operating cost.

Vacuum System

- Use of a high reliability turbomolecular pump results in low residual vacuum background and low energy and water consumption.

Data System

- Proven Nova 3 computer used for system control, data acquisition and data processing.
- High speed interactive graphic display terminal.
- Highly efficient software routines.
- Chained commands for automated processing.
- Data compatible with Incos system.

GC/MS System

- Proven quadrupole analyzer (over 1000 installations).
- Automated ion source optimization with operator override capability.
- Reliable microprocessor controlled GC with full complement of options.

Sample Handling

- Bellar – Lichtenberg liquid sample concentrator.
- Optional auto sample changer or autoinjector.
- Optional solid probe.

The result: a system simpler to operate and simpler to maintain, but which does not sacrifice any of the analytical capabilities of systems which cost thousands of dollars more. For further details on how an OWA system can meet your organics-in-water analysis problems, please contact us directly.

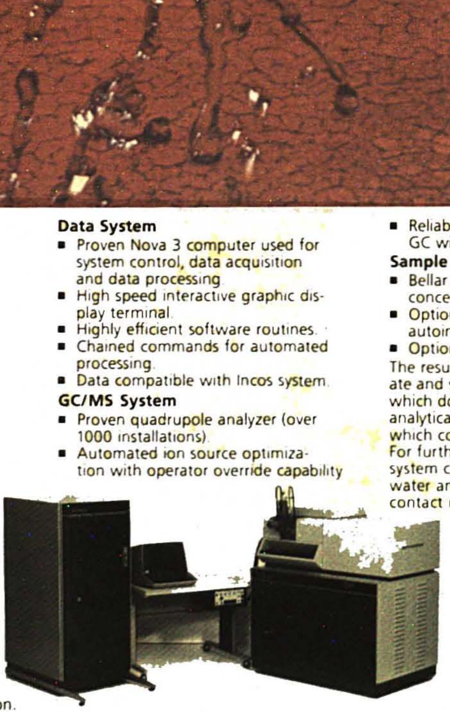

CIRCLE 78 ON READER SERVICE CARD

finnigan
Instruments
A DIVISION OF FINNIGAN CORPORATION
845 WEST MAUDE AVENUE
SUNNYVALE, CALIFORNIA 94086
(408) 732-0940

© Finnigan Instruments, 1979

Instrumentation

Field Desorption Mass Spectrometry

Warren D. Reynolds
National Center for Toxicological Research
Jefferson, Ark. 72079

A recent advance in the application of mass spectrometry to biomedical and environmental research has been the development of the field desorption ionization technique. Although its potential has not been fully realized, the simplicity of the field desorption (FD) spectra, and its applicability to a wide range of analytical problems that encompass a multitude of compounds from inorganic salts to polar metabolites has become its trademark. The growing use of this technique is amply demonstrated by the increasing number of publications, workshops, reviews, and books during the period 1971–78 (*1–8, 16*). In this brief report, the principles and analytical applications will be included for this important mass spectrometric technique.

Field desorption mass spectrometry's unique properties arise from the behavior of chemical compounds under high potential fields. When a high field is applied to an absorbed organic layer on a metal surface, it experiences an electrostatic force similar to that on the plates of a charged condenser. If the metal surface (anode) has the proper geometry (sharp tip) and under high vacuum (10^{-6} torr), this force can be sufficient to eject particles as positive ions that can be analyzed via a mass spectrometer (Figure 1). This, in essence, is the basis for field desorption mass spectrometry. However, if the compound to be ionized reaches the anode via the gas phase instead of being surface applied, the process is called field ionization.

In comparison with other ionization techniques, the smaller amount of transferred energy in the FD process (~0.1 eV) increases the probability of detecting intact molecular ions. Thus, the salient feature of field desorption spectra is normally the predominance of the molecular ion. Fragment ions can also be produced through thermal decomposition and field induced surface reactions.

Emitters

Early investigations by Müller on field ionization microscopy and Inghram and Gomer's subsequent work led H. D. Beckey to a systematic study of the parameters required for field desorption mass spectrometry of organic compounds (*8–10*). The intense electric fields (10^7–10^8 V/cm) necessary for field desorption are produced with positively charged emitters having at their surface multipoint needles of very great curvature (10^2–10^3 Å radii) on which an intense electric field is established.

Emitter Properties. It will be helpful in understanding the basis for obtaining field desorption spectra of organic compounds to consider the development and limitations of the emitters. Early in the development of this technique, several different emitter configurations were used such as thin metal blades, etched foils, and needle-sharp metal points (*6*). Sharp point emitters have the advantage over the other configurations in producing extremely high field strengths. The local microfield strength (F_0) at the tip of the microneedle, as defined by Speier et al. (*11*), is a function of the applied voltage (V), radius of curvature of the tip (r) as well as the distance to the counter electrode (d):

$$F_0 = V\left(\frac{1-\alpha}{\frac{r}{2}\ln\frac{4d}{r}} + \frac{\alpha}{r}\right)$$

where α = shape factor ≃ 0.006.

For an applied voltage of 5000 V and an electrode distance of ~2.3 mm,

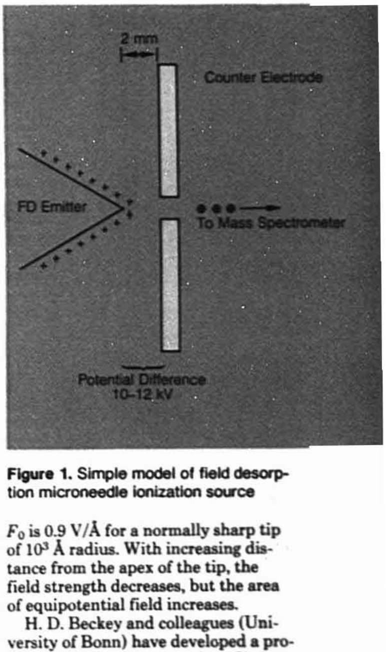

Figure 1. Simple model of field desorption microneedle ionization source

F_0 is 0.9 V/Å for a normally sharp tip of 10^3 Å radius. With increasing distance from the apex of the tip, the field strength decreases, but the area of equipotential field increases.

H. D. Beckey and colleagues (University of Bonn) have developed a procedure for growing multiple ("Christmas-tree") polymeric needles, using benzonitrile, from the vapor phase on a fine tungsten wire (10 μm) under the influence of high electric fields (*12*) (Figure 2). Subsequent in-situ high-temperature carbonization resulted in structurally strong carbonaceous needles with improved efficiency of ionization. Although similar dendritic needles of other types of materials such as germanium, nickel, and other metals have been tried, these metal

This article not subject to U.S. Copyright
Published 1979 American Chemical Society

CuSO4
H2O
K MnO4

Tygon® tubing

The one tubing that's right throughout the lab.

Tygon laboratory tubing is specifically formulated to meet the high standards of quality and reliability required by laboratories everywhere.

Tygon is versatile enough to excel in almost any application. It has a broad range of chemical compatibility and safely handles most chemicals found in the lab.

But that's just part of the Tygon story. Tygon tubing is built tough to last. It resists aging and oxidation for a superior service life . . . which makes Tygon economical for even routine uses like with water and air. And because Tygon is glass-clear, you can check flow at any point.

But most important, Tygon will not affect the solutions or gases it carries. That's because it's non-contaminating, and has a smooth inner bore that resists residue build-up. You're assured of reproducible results, even when tests are made over a period of time. Tygon is available in popular vacuum tubing sizes as well.

Tygon Tubing Hot-Line: 800-321-9634

Specify the one tubing that's right throughout the lab — Tygon tubing. Call us toll-free for complete chemical resistance information, and the location of your nearest Tygon lab supply house. In Ohio, call collect 216-630-9230.

NORTON PLASTICS AND SYNTHETICS DIVISION
P.O. BOX 350 AKRON, OHIO 44309 TEL: (216) 630-9230

See us at the Pittsburgh Conference, Booths 813, 815.

CIRCLE 151 ON READER SERVICE CARD

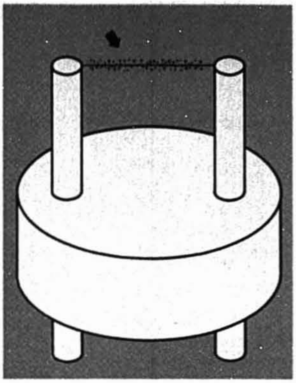

Figure 2. Field desorption emitter holder and 10-μm tungsten emitter with carbonaceous needles (arrow)

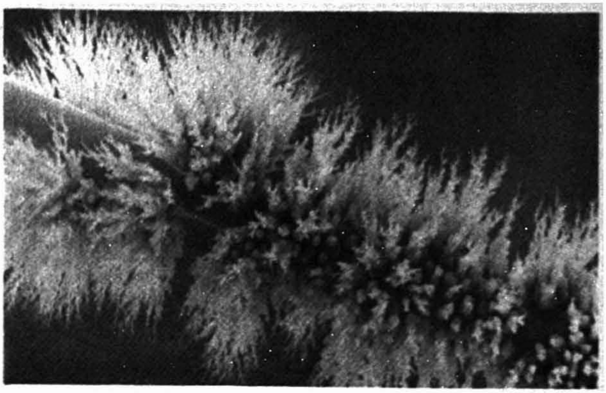

Figure 3A. Scanning electron micrograph (500×) of high-temperature emitter
Tungsten wire (10 μm) covered with carbon "microneedles" grown in benzonitrile vapor under high field conditions

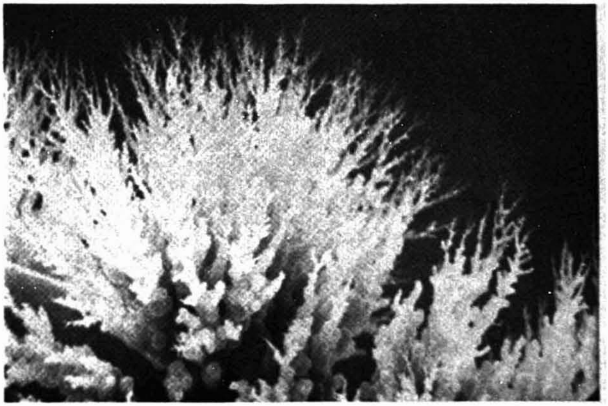

Figure 3B. Scanning electron micrograph of high-temperature activated emitter at higher magnification (1000×)

needles yield ions that are less energy homogenous than those from carbon emitters (*6*).

The procedure for forming relatively good carbonaceous emitters is dependent upon a number of factors. Cleanliness of the emitter preparation apparatus and tungsten wire as well as purity of the benzonitrile is important for successful emitter preparation. The high-temperature activation process for preparing carbonaceous emitters is conducted in a small vacuum chamber under carefully controlled conditions of temperature, pressure, electric field strength, and time. The temperature of the fine tungsten wire (10 μm), which is controlled by the dc current, is adjusted to a value sufficient to achieve a high temperature (800–1000 °C) on the emitter wire. The hot emitter wires thermolyze the benzonitrile (~10 torr) at various points on each wire. These points act as centers for further cationic polymerization during the high-voltage operation (7–10 kV). By monitoring the field ion current on a plate opposite to the emitters, the growth of the microneedles can be followed. Normally, after a short period of time, the wire temperature is raised in a programmed fashion to a specified limit (~1500 °C) as determined by direct current during the activation process. Activation time varies (6–10 h) and is dependent on the desired needle length. Long activation periods with reduced field strengths generate long needles. Short, sharp needles are preferred to long, blunt ones for most efficient ionization.

The ionization ability of the "activated" emitters is largely dependent on the structural and morphological composition of the microneedles. The structural ordering determines the chemical and mechanical stability, whereas the morphology determines the efficiency of the microfields during ion production (*13, 14*).

Figures 3A and 3B show two scanning electron micrographs of the morphology of the high-temperature prepared emitters. These micrographs illustrate the "tree-like" formation of these microneedles. The branches appear to be solidly grown together near the base. Electron diffraction studies have shown that these needle structures correspond to an arrangement of layers of graphite-like regions concentric to the needle axis (*13*).

Due to the nonhomogeneity of the microneedle size and directional orientation, the surface ions generated during the FD process possess an energy distribution and spreading over a small angle. This creates focusing problems during the subsequent recording of FD spectra. Refocusing of the mass spectrometer after repetitive scans is necessary for good FD spectra.

Emitter Surface Processes

Currently, there is no quantitative theory for field desorption processes of organic molecules from structural and graphitized microneedle surfaces. The present theoretical understanding of the dynamics of field desorption remains to be clarified due to the complex nature of the emitter surface processes. However, there are several proposed mechanisms by which organic molecules can be converted to ions or ion clusters during the FD process, i.e., resonance electron tunneling and field induced surface reactions (*6*).

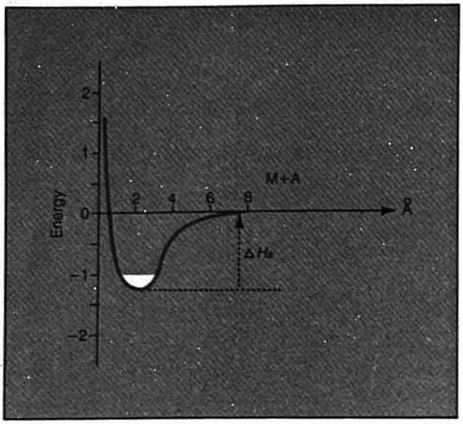

Figure 4A. Potential energy curve for interaction of organic molecule (M) with surface (A) in absence of electrostatic field

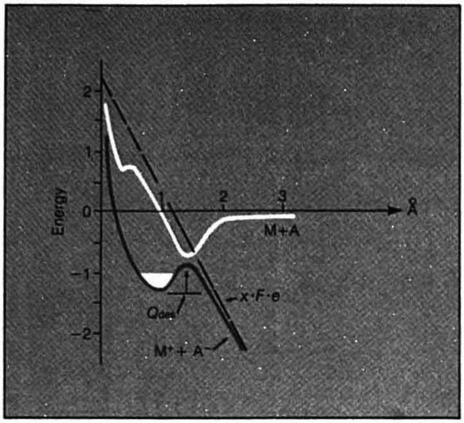

Figure 4B. Potential energy curves in presence of electrostatic field

Ionic potential energy curve is downward, and its intersection with the ground state curve produces a Schottky saddle, $x \cdot F \cdot e$ = potential energy of external field, F

Reprinted with permission from ref. 5. Copyright 1975 Verlag Chemie International

Electron Tunneling. Tunneling is a quantum mechanical process without a classical mechanics analog. In the field desorption process, this quantum tunneling involves surface substrate such as a metal or carbon. The electron from the adsorbed organic molecule can only enter the substrate at or above the Fermi level, since below this level there are, at ordinary temperatures, no vacant quantum states for it to enter (*15*). Potential energy diagrams depicting this process are shown in Figures 4A and 4B.

The occurrence of the field desorption of an organic molecule is related to the tunneling probability (D) of the nonbonding electron in the molecular orbital. This probability is dependent on a number of factors including surface work function (Φ), ionization potential (I), barrier potential (V_R), and a local microfield (F) and can be written (*16, 17*):

$$D = \exp \int_{r_1}^{r_2} \sqrt{\frac{8\,m}{\hbar^2}\,(eV_R - E)}\,dr$$

$$\simeq \exp - \left[\frac{0.68\,(I - \Phi)^{3/2}}{F}\right]$$

Generally, for carbon emitters and high field strengths ($3\text{–}15 \times 10^3$ applied volts), the probability for "tunneling" lies in the range of $10^{-4}\text{–}10^{-1}$ for most organic compounds. Consequently, ion currents (C/g) obtained from this type process are less by a factor of 10–100 as compared to the normal 70 eV electron impact ionization.

The "tunnel effect" has been attributed as the first step in many field ionization/field desorption surface reactions. For example, alcohols (ROH) generally yield high ion currents for the $(M+H)^+$ and $(2M+H)^+$ ions that result from a series of reactions as shown in Figure 5. The fate of the $ROH^{\cdot +}$ ion can take several pathways. If it reacts in a concerted mechanism with a nearest neighbor and a free radical center on the carbon matrix, then a ROH_2^+ ion is generated. A secondary reaction with additional nearest neighbor participation leads to cluster-ion formation [$(ROH)_2H^+$]. For surface concentration depleted areas, the $ROH^{\cdot +}$ is removed to give an $M^{\cdot +}$ ion current as seen in Figure 6 for ethanol (*18*).

Field and Temperature-Dependent Surface Reactions. The fate of surface generated ions and radicals is complex. The effect of the field can play a dominant role on the mechanism of these surface reactions. Other factors affecting the outcome are the electronic properties of the compound, e.g., tautomerism, temperature, and surface environment.

Certain fragmentation reactions with relatively low activation energies have been found to be field dependent. As an example, the elimination of water to generate a $C_2H_5^+$ ion after protonation of C_2H_5OH by direct $(C_2H_5\text{—}OH_2)^+$ bond rupture increases with increasing field strength (*18*). Other studies with acetone, acetonitrile, hydrocarbons, and others have yielded a number of general observations concerning field-dependent processes in the absorbed layers (*18*):

- Excluding emitter surface interactions, the primary processes are proton transfer reactions.
- All ions formed are immediately removed from the reaction zone due to the high potential gradient at the emitter surface.
- Most field reactions take place without activation energy.
- The products of field induced ion-molecule reactions are generated by simple bond rearrangements.

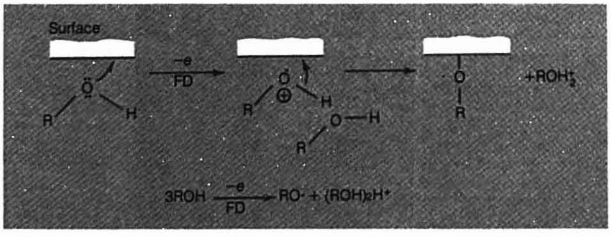

Figure 5. Upper: Diagram illustrating a three-step concerted surface mechanism of electron resonance tunneling and generation of protonated molecular ion, ROH_2^+. Lower: Reaction indicating nonsurface interaction of RO· radical after electron tunneling and cluster-ion formation $(ROH)_2H^+$

Reprinted with permission from ref. 18. Copyright 1974 Verlag der Zeitschrift fuer Naturforschung

ON SALE NOW!

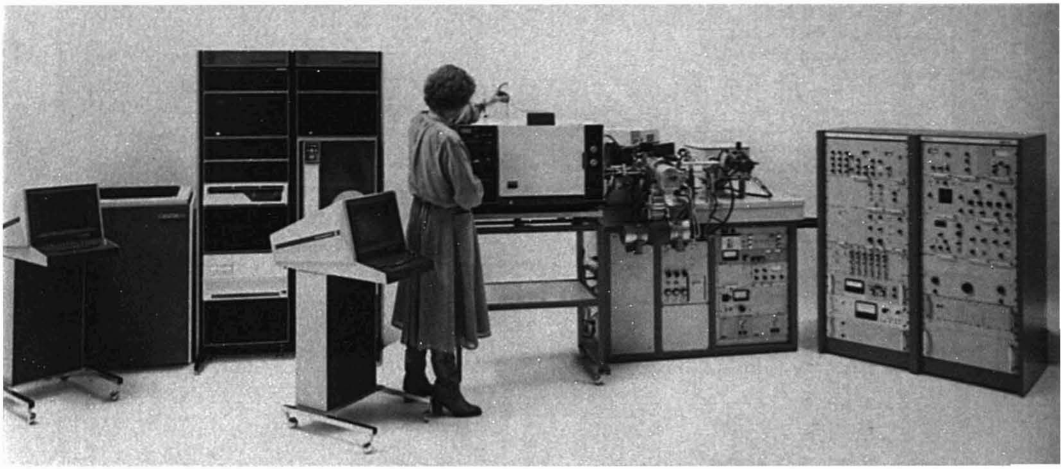

The new Varian MAT 212 and 312 mass spectrometers are so attractively priced you'll think they're on sale.

If you've always been a Varian admirer, now's an excellent opportunity to be a Varian owner.

Reason: Varian has put together some great "packages" combining our new MAT 212 and 312 mass spectrometers with our popular SS200P* data systems which feature simultaneous data acquisition and evaluation.

And, whether a 212 or 312 package catches your eye, you'll like our irresistibly low prices.

The MAT 312 is an advanced version of our popular MAT 311A. It has an improved source with more accessories and greater versatility for applications including field desorption studies.

The versatile MAT 212 brings a proven track record to CI/EI studies, not to mention such great options as GC/MS analysis with packed columns (jet separator); multi-ion selection analysis, DCI (direct chemical ionization or desorption CI) collisional activation analysis, negative ion detection and much more.

Now, to the bottom line . . . price. We suggest you call us. You'll be pleasantly surprised and may want to arrange a demonstration. For information or literature contact:

Performance at a glance!

MAT 312	
Resolving power:	up to 35,000 (10% valley)
Mass Range:	1 to 3600 amu
Accuracy:	better than 2 ppm
MAT 212	
Resolving power:	up to 20,000 (10% valley)
Mass Range:	1 to 1200, switchable to 3600 amu
Accuracy:	better than 3 ppm

*Outside U.S. — SS 188.

Varian MAT Mass Spectrometry, 25 Hanover Road, Florham Park, NJ 07932. Phone (201) 822-3700

Varian MAT GmbH, Postfach 14 4062
Barkhausenstr 2, 2800 Bremen 10
West Germany. Phone (0421) 5493-1

Varian Associates, Ltd., 28 Manor Road
Walton-on-Thames/Surrey
United Kingdom. KT12, 2QF
Phone (43741)

varian

On Display at the Pittsburgh Conference
CIRCLE 221 ON READER SERVICE CARD

Temperature dependence of FD spectra is illustrated by a variety of saturated and unsaturated carboxylic acids containing 12 or more carbons. At low-to-moderate anode temperatures (0–8 mA), the $M^{+\cdot}$ and $(M+1)^+$ ions dominate the spectra of the individual acids while at higher temperatures (10–20 mA), peaks representing $(M-17)^+$ and $(M-44)^{+\cdot}$ are quite evident. For mixtures of acids, reactions between constituents are possible. For example, a 1:1 mixture of *cis*-5-icosenoic acid (M_1) and elaidic acid (M_2) behaved normally at low temperatures yielding both $M_1^{+\cdot}$ and $M_2^{+\cdot}$ ions. At higher anode temperatures (>15 mA), both "dimer ions" and their cross product dimer $[(M_1 + M_2 + H—H_2O—COOH)^+]$ were present (*19*).

An interesting class of thermally activated, field induced reactions is the ion attachment or "cationization" reactions. The most stable "quasimolecular" ions occur when cations such as the alkali ions are attached to the adsorbed organic molecules. The stability of the $(M+C)^+$ ions is due to strong charge localization at the alkali atom. Thus, the charge shift by rearrangement of the bonding electrons within the ion necessary for decomposition is prevented (*20*). The resulting mass spectra display a high abundance of cations $(C)^+$ and cluster-ions, i.e., $(M+C)^+$ and $(nM+C)^+$, $n = 2, 3 \ldots$, at field strengths ($\leq 10^6$ V/cm) that are insufficient for ionization of adsorbed organic molecules. Under FD conditions the observed intensity distribution and maximum size of the cluster ions depend on how the molecules diffuse into the ionization zone at the emitter tip, i.e., neat or as complexes. Thus, the FD mass spectra of cationized organic molecules are sensitive to the influences of the experimental conditions such as temperature, organic compound/cation ratio, distribution, and thickness of absorbed layer (*8*, *20*). Figure 7 shows an example of a Li^+ cationized spectrum of adenosine (1:1 mixture) (*20*).

Analytical Applications

In comparison with electron impact mass spectra, less intense and often fluctuating ion currents are generated in FD. This has a limiting influence on both the ultimate sensitivity and precision. Since nearly 100% of the total ion current is frequently carried in the molecular ion group $[M^{+\cdot}$, $(M+H)^+$, or $(M+C)^+]$, one has a favorable condition for specificity with minimization of disturbance due to impurities. Subsequently, the fluctuating ion currents require integration techniques for good analytical measurements. For example, mixtures containing glucose and glucose-1-^{13}C as an internal standard were analyzed using predominantly the $(M+Na)^+$ ion group with a multichannel integration technique. Individual measurements had a mean error of ±7.2%, whereas the mean error of the average value (100 scans) was ±0.7% (*21*). Mixtures of dopamine added to urine at the 10-ng/µL level have been determined via the FD method using dopamine-d_4 as the internal standard. After formation of the tris-bansyl derivative and TLC cleanup, the relative error was 5% (*22*).

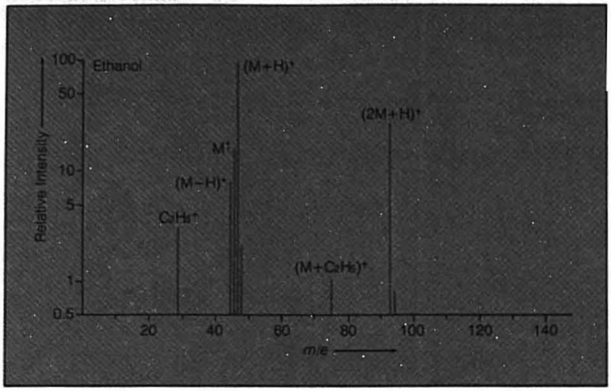

Figure 6. Pulsed field desorption mass spectrum of ethanol (−6 kV pulse, 0.1 µs, emitter at −100 °C)

Reprinted with permission from ref. *18*. Copyright 1974 Verlag der Zeitschrift fuer Naturforschung

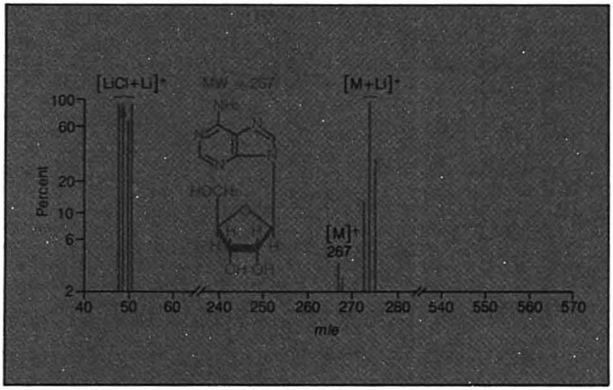

Figure 7. Field desorption mass spectrum of adenosine (1 *M*) with added lithium chloride (1 *M*)

Water solvent. Note weak parent ion at *m/e* 267 and cationized molecular ion at *m/e* 274 (*19*)
Reprinted with permission from ref. *20*. Copyright 1975 Heyden and Son

Measurements on the degree of stable label isotopic incorporation can be done accurately via the FD method. Glucose-1-d_1 was determined to have 97.4% deuterium incorporated at this position using the cationized molecular ion group $[(M+Na)^+$, $(M+Na+1)^+]$ after correction for the $(M-1+Na)^+$ ion (*23*).

The excellent sensitivity of the FD process toward alkali metal cations was discovered during early studies on organic and inorganic salts. The ion currents for the alkali metals are several orders of magnitude more intense than the FD-generated organic ions. For example, cesium was determined in several solvents, body fluids, and water samples at the 0.3–1000-pg/µL range with a minimum detectability in the low femtogram range. Since cesium is monoisotopic, an external calibration curve was used with a precision of ±10% (*24*). FD spectra of other inorganic salts have shown strong ions suitable for trace quantitative analysis. KF gave $(KF)K^+$ and $(KF)_2K^+$ ions, whereas KBr gave $(KBr)K^+$ and Br^+ ions; $NaNO_3—(NaNO_3)_nNa^+$ where $n = 1, 2, 3$; $NaN_3—(NaN_3)Na^+$ and $CaCl_2—CaCl^+$, $Ca^{+\cdot}$ and $CaCl_2^{+\cdot}$ (*25*).

INTRODUCING
the Varian 5000 family of liquid chromatographs

It makes LC responsive and simple

The Varian 5000 Series is a family of powerful microcomputer-CRT-based liquid chromatographs that make LC easy for anyone.

It makes tough separations seem simple. The helpful CRT continuously displays *all* instrument conditions. Tells you everything you need to know, right now. Responds to you. Helps you build programs. Prompts and leads you. Makes LC easier than ever before.

It comes with full support. With your Model 5000 you receive a commitment from Varian to provide strong, continuing support—training, service and applications assistance—that will assure successful solution of your liquid chromatography problems.

Price/performance. There are six basic models in the 5000 Series: from simple isocratic to completely automatic gradient systems. Each is designed to offer unbeatable price/performance; to provide a new level of LC capability at system prices lower than most LC components.

Upward expandability. 5000 Series chromatographs are upward expandable and offer many options. You can configure a 5000 that is exactly right for your laboratory. Later, as your needs change, you can add whatever new capability you require.

For full details on a 5000 that may be exactly right for you, circle Reader Service Number 222.

To have a Varian representative contact you, circle Reader Service Number 223.

varian

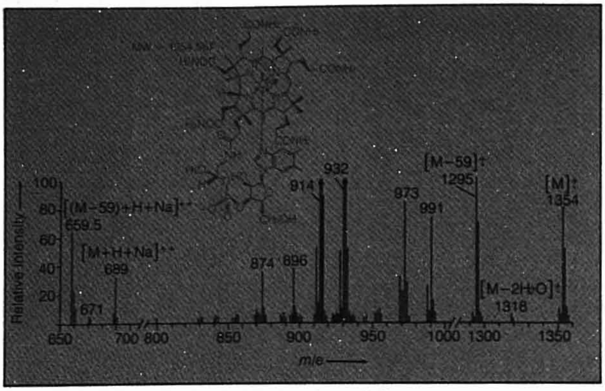

Figure 8. Field desorption mass spectrum of vitamin B_{12}

Indirect heating by laser-supported FD-MS (0–200 mW). Mass resolution 8000 (10% valley). Note doubly charged ions *m/e* 689 and 659.6 (*27*)

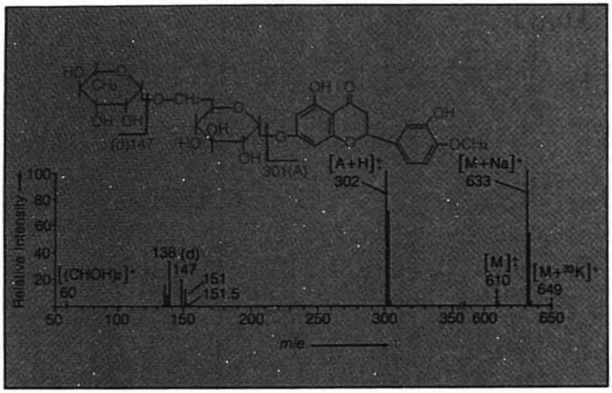

Figure 9. FD mass spectrum of the flavanone glycoside, hesperidin

Resolution >15 000 (10% valley), photographic detection. Note molecule-cation complexes at *m/e* 633 and 649

Reprinted with permission from ref. 29. Copyright 1977 North-Holland Publishing Co.

Nonvolatile and thermally labile organic molecules with molecular weights up to 2100 daltons are promising candidates for FD analysis. In recent years, much of the difficulty in assigning structures to peptide antibiotics has been due to an inability to determine accurate molecular formulas. Recently, FD studies have been conducted on several cationized (^{7}Li, ^{23}Na, and ^{39}K) triacetates of antiamoebin I to ascertain its molecular ion (MW 1796). By utilizing the high-resolution peak-matching technique, the molecular formula: $C_{88}H_{38}N_{17}O_{23}Na$ − 1818.9596 was confirmed (*26*). The FD spectra of vitamin B_{12}, a complex macrocyclic ring system, has recently been completed (*27*). The structure and FD spectrum are shown in Figure 8. As indicated, the molecular ion is present with high relative intensity at *m/e* 1354 with additional thermal/field induced fragments at lower amu's. The high-resolution measurement at 914.445 agrees with the ion of composition: $C_{45}H_{65}N_{11}O_6Co$ that results from a loss of the nucleotide side chain.

A number of research groups have applied the FD/MS technique to biological and natural product analytical problems. The peptides (through nona-) have been studied for sequencing information as well as 50 other compounds representing a wide variety of phospholipids and related biochemical materials (*28, 29*). The natural product, hesperidin, is an example of several surface FD mechanisms operating simultaneously, which is indicated by the presence of both $M^{+\cdot}$ and $(M+Na)^+$ ions as seen in Figure 9 (*30*). Various antibiotics representing several classes, e.g., macrolides, polyenes, ansamycins, aminocyclitols, and acyltetramic acids, have also been studied (*31*). In all cases, members of the molecular ion group [$M^{+\cdot}$ or $(M+H)^+$] were present as base peaks. This is an advantage since most of the EI spectra of these compounds do not yield this molecular weight information.

Summary

The fundamental advantage of field desorption mass spectrometry is the "soft" ionization process for thermally sensitive and relatively nonvolatile compounds. For many organic compounds, the FD mass spectra produced show the molecular ion or molecule-cation complex alone or as the peak of highest relative intensity. The relative absence of fragmentation except under thermal surface conditions aids in the molecular weight determinations but becomes a disadvantage when structure determinations are attempted.

The assessment of the FD/MS technique for rapid organic mixture analysis is limited and subject to matrix interactions. The presence or absence of nearest neighbor interactions, e.g., protonations, cationization, etc., in the mixture does alter the FD spectra of the sought-for constituent. In spite of these limitations, good quantitative analyses have been conducted utilizing the stable isotope dilution technique.

The attainment of the FD mass spectra of large intact molecules, such as the antibiotics and vitamin B_{12}, has been a challenge and landmark. It represents a significant advance in the application of mass spectrometry to high molecular weight constituents.

Acknowledgment

I thank Ben Lau (NCTR) and Dave Brent (Burroughs-Wellcome Corp.) for many interesting and valuable discussions. I also express my appreciation to Tom Grafton (NCTR) for his accomplishing the scanning electron micrographs of the field emitters.

References

(1) H.-R. Schulten, "Advances in Mass Spectrometry in Biochemistry and Medicine," Vol. 1, Chap. 25, Spectrum Publications, Holliswood, N.Y., 1976.
(2) W. D. Lehmann and H.-R. Schulten, *Anal. Chem.*, **49**, 1744 (1977).
(3) S. Pfeifer, H. D. Beckey, and H.-R. Schulten, *Fresenius Z. Anal. Chem.*, **284**, 193 (1977).
(4) H. D. Beckey, S. Bloching, M. D. Migahed, E. Ochterbëck, and H.-R. Schulten, *Int. J. Mass Spectrom. Ion Phys.*, **8**, 169 (1971).
(5) H. D. Beckey and H.-R. Schulten, *Angew. Chem. (Int. Ed.)*, **14**, 403 (1975).
(6) H. D. Beckey, K. Levsen, F. W. Röllgen, and H.-R. Schulten, *Surf. Sci.*, **70**, 325–62 (1978).

See the light–
The new Varian Cary 210
UV-Vis Spectrophotometer...
It's surprisingly affordable

For the low introductory price of $11,995*, you can explore new avenues in UV-Vis measurements with the powerful new Varian Cary 210 Spectrophotometer.

See low level enzyme activities

The high signal-to-noise ratio, excellent photometric stability and sensitivity of the Cary 210 allow the measurement of small absorbance changes. Enzyme activity levels as low as 0.0005 Abs per minute can be monitored.

See scattering samples

Low stray light means high absorbances can be measured accurately. The versatile Cary 210 encompasses the complete range from −0.6000 to +4.0000 Abs. Scattering samples can be scanned without the use of special sampling locations or accessories. Highly turbid material need not be diluted.

See microsamples

Cary 210's high energy throughput and patented sample space optics minimize sample volume requirement and permit efficient energy utilization. Measure samples as small as 200 μl directly, and 70 μl with beam masks.

Total sample handling capabilities

Roomy sample compartment can accommodate two five-cell turrets. You can automate measurements with our Cell Programmer and Wavelength Programmer. Monitor more than 300 samples per hour at controlled temperatures with the Routine Sampler. Scan gels up to 20 cm long . . . and more.

Seeing is believing

Look for the Varian Cary 210 at the upcoming Pittsburgh Conference. See the Cary 210 and complete accessories at work.

Circle **17** for more information on the new Cary 210.
Circle **18** if you would like a representative to call.
Varian Associates, Inc., 611 Hansen Way, D-070,
Palo Alto, Ca. 94303

varian

*U.S. only.

How Varian's 3700 series takes the risk out of buying a gas chromatograph

Varian's 3700 is designed to give you the efficiency and flexibility to build the precise gas chromatography system you need to meet changing analytical requirements. There is no risk because the 3700 can change as your needs change. It is completely modular and upgradeable, and it continues to grow.

In addition, the 3700 system is unique in that the major components—(1) chromatograph, (2) data system, and (3) AutoSampler®—can be purchased and used separately or they can be combined in many different configurations to meet specific needs. Result: You can start your GC system wherever you want to. And you don't have to buy anything that you don't need.

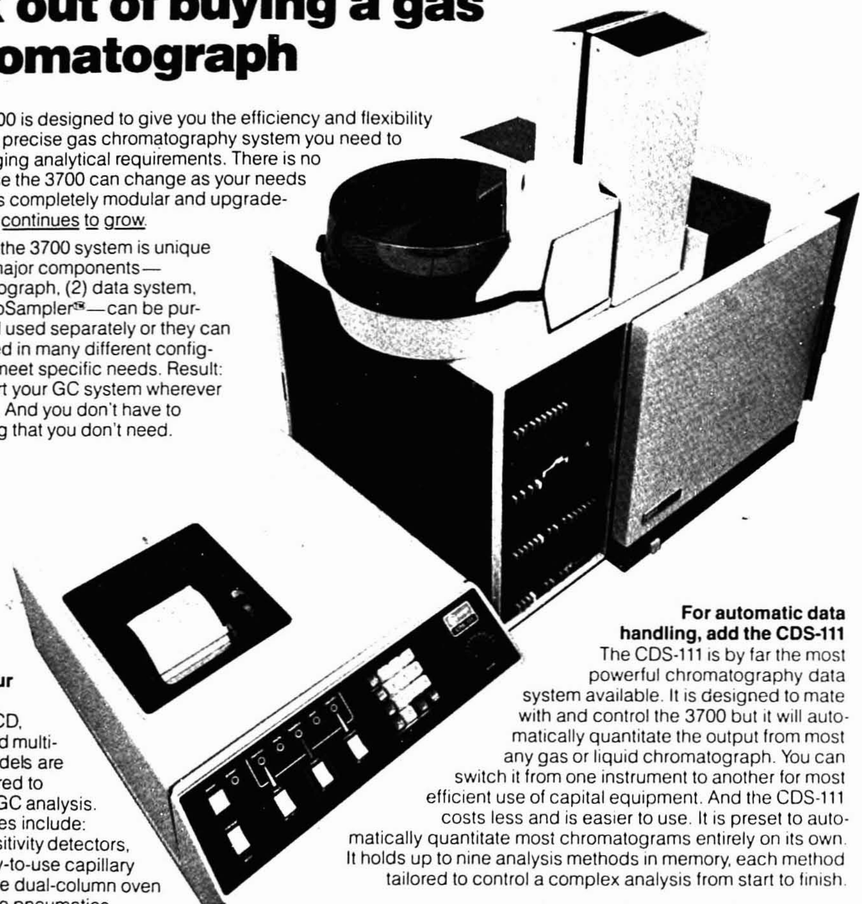

Choose a 3700 for your application

TCD, FID, ECD, FPD, TSD and multi-detector models are offered tailored to handle any GC analysis. Major features include: highest sensitivity detectors, the first easy-to-use capillary system, large dual-column oven and separate pneumatics compartment for versatility and convenience. You can begin with a basic dual-column unit and add capability as you need it. Or you can start right now with the world's most powerful and fully automatic GC system by combining the 3700 with the CDS-111 data system and the 8000 AutoSampler.

For automatic data handling, add the CDS-111

The CDS-111 is by far the most powerful chromatography data system available. It is designed to mate with and control the 3700 but it will automatically quantitate the output from most any gas or liquid chromatograph. You can switch it from one instrument to another for most efficient use of capital equipment. And the CDS-111 costs less and is easier to use. It is preset to automatically quantitate most chromatograms entirely on its own. It holds up to nine analysis methods in memory, each method tailored to control a complex analysis from start to finish.

For total automation, add the AutoSampler

The reliable, proven Model 8000 AutoSampler obtains injection reproducibility that sets the standard for automatic gas chromatography. Sample cross contamination is virtually eliminated. It will handle up to 60 samples in a single unattended run. Model 8000 can be used with any gas chromatograph. Or it can be microproccesor controlled by the CDS-111 in a completely automatic fail-safe system with the Model 3700 Gas Chromatograph.

Let us help you select a gas chromatography system that will meet your changing analytical needs.

varian

For detailed information circle the indicated **Reader Service Numbers:** **226** CDS-111 Chromatography Data System, **227** Model 8000 AutoSampler, **228** Model 3700 Gas Chromatographs, **229** Model 3711 Automatic Gas Chromatographs, **230** Have a representative call.

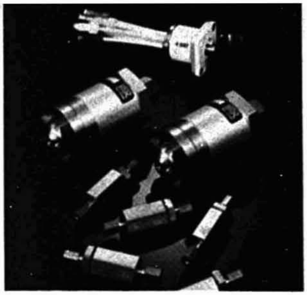

Little things mean a lot in HPLC

Inlet filters. Rheodyne inlet filters can be connected between the sample injection valve and the column to protect the column from plugging. The 2 micron filter element prevents plugging caused by particles in the samples or by injection valve wear particles. Pressure rating of the filter assembly is 7000 psi (500 bar). Only type 316 stainless steel and PTFE contact the stream.

U.S. prices are $45 for the Model 7302 Column Inlet Filter and $20 for a package of 5 2$\mu$m filter elements and gaskets.

Pressure Relief Valve. Rheodyne's Model 7037 Pressure Relief Valve protects your equipment against damage from over-pressure. You can set it anywhere in the range of 2000 to 7000 psi (140 to 500 bar). U.S. price is only $270. So, when you consider the fact that you can blow a pressure gauge in less than 1 second, it's a real bargain.

Teflon Rotary Valves. Type 50 Rheodyne Valves are real workhorse accessories for your LC equipment.

Use them for sample injection, column switching, recycling, reagent switching, fraction collection, stream sampling and quantitive reagent injection. Available in four different versions, these valves are chemically inert with zero dead volume, operate at 300 psi. They are offered in 0.8 or 1.5 mm bore and in either manual or automatic versions.

U.S. price of 0.8 mm bore 3 and 4-way valves is $80. The 6-position and sample injection valves are priced at $95. Cost of 1.5 mm bore valves is $2 more.

Write for more data. For full information, please address Rheodyne, Inc., 2809 Tenth Street, Berkeley, CA 94710. Phone (415) 548-5374.

RHEODYNE

THE LC CONNECTION COMPANY

CIRCLE 183 ON READER SERVICE CARD

(7) Third Annual Field Desorption Mass Spectrometry Workshop, Burroughs-Wellcome Corp., Research Triangle Park, N.C., Feb. 2–3, 1976.

(8) H. D. Beckey, "Principles of Field Ionization and Field Desorption Mass Spectrometry," Pergamon, London, England, 1977.

(9) E. W. Müller, *Z. Phys.*, **131**, 136 (1951).

(10) M. G. Inghram and R. J. Gomer, *J. Chem. Phys.*, **22**, 1279 (1954).

(11) F. Speier, H. J. Heinen, and H. D. Beckey, *Messtechnik*, **80** (6), 147 (1972).

(12) H. D. Beckey, A. Heindrichs, E. Hilt, M. D. Migahed, H.-R. Schulten, and H. U. Winkler, *ibid.*, **78** (9), 196 (1971).

(13) D. M. Taylor, F. W. Röllgen, and H. D. Beckey, *Surf. Sci.*, **40**, 264 (1973).

(14) B. Ajeian, H. D. Beckey, A. Maas, and U. Nitschke, *Appl. Phys.*, **6**, 111 (1975).

(15) E. Müller and S. V. Krishnaswamy, *Surf. Sci.*, **36**, 29–47 (1973).

(16) H. D. Beckey, "Field Ionization Mass Spectrometry," pp 3, 207–10, 228–38, Pergamon Press, Elmsford, N.Y., 1971.

(17) C. B. Duke, "Tunneling in Solids," pp 39–45, Academic Press, New York, N.Y., 1969.

(18) F. W. Röllgen and H. D. Beckey, *Z. Naturforsch.*, **29a**, 230–38 (1974).

(19) G. W. Wood, E. J. Oldenburg, P. Y. Lau, and D. L. Wade, *Can. J. Chem.*, **56**, 1372–7 (1978).

(20) F. W. Röllgen and H.-R. Schulten, *Org. Mass Spectrom.*, **10**, 660 (1975).

(21) W. D. Lehmann and H.-R. Schulten, *Angew. Chem. (Int. Ed.)*, **16**, 184 (1977).

(22) W. D. Lehmann, H. D. Beckey, and H.-R. Schulten, *Anal. Chem.*, **48**, 1572 (1976).

(23) W. D. Lehmann and H.-R. Schulten, *Biomed. Mass Spectrom.*, **5**, 208 (1978).

(24) H.-R. Schulten, R. Ziskoven, and W. D. Lehmann, *Z. Naturforsch.*, **33c**, 178 (1978).

(25) H.-R. Schulten and F. W. Röllgen, *Angew. Chem. (Int. Ed.)*, **14**, 561 (1975).

(26) K. L. Rinehart, J. C. Cook, Jr., H. Meng, K. L. Olsen, and R. C. Pandey, *Nature*, **269**, 832 (1977).

(27) H.-R. Schulten and H. M. Schiebel, *Naturwissenschaften*, **65**, 223 (1978).

(28) J. Asante-Poku, G. W. Wood, and D. E. Schmidt, Jr., *Biomed. Mass Spectrom.*, **2**, 121 (1975).

(29) G. W. Wood, P. Y. Lau, G. Morrow, G.N.S. Rao, D. E. Schmidt, Jr., and J. Tuebner, *Chem. Phys. Lipids*, **18**, 316 (1977).

(30) H.-R. Schulten and D. E. Games, *Biomed. Mass Spectrom.*, **1**, 120 (1974).

(31) K. L. Rinehart, Jr., and J. C. Cook, Jr., *J. Antibiot.*, **27**, 1 (1974).

Warren D. Reynolds is chief, Bioanalytical Methods Branch, NCTR. His interests include high-pressure liquid chromatography, gas chromatography, and computerized instrumentation development.

Varian announces training courses in gas chromatography

Schedule for February, March and April 1979:

Basic Gas Chromatography

Feb. 21–23, Florham Park, NJ
March 7–9, Houston, TX
April 10–12, Chicago, IL
Lecture & Lab, 3 days, $225
Lecture only, 2 days, $155

Gas Analysis by Gas Chromatography

March 12–13, Houston, TX
Lecture & Lab, 2 days, $225

Automatic Gas Chromatography*

March 14–16, Houston, TX
April 18–20, Chicago, IL
Lecture & Lab, 3 days, $200

Glass Capillary Gas Chromatography

Feb. 13–14, Denver, CO
March 1–2, Florham Park, NJ
Lecture & Lab, 2 days, $225

Maintenance of the Gas Chromatography

Feb. 26–27, Florham Park, NJ
April 16–17, Chicago, IL
Lecture & Lab, 2 days, $225

To enroll in Chicago, Denver and Houston courses, please contact the Varian Instrument Division Training Department, 2700 Mitchell Drive, Walnut Creek, CA 94598; Telephone (415) 939-2400, ext. 225. Enroll in Florham Park courses at Varian Instrument Division Training Department,
25 Hanover Road,
Florham Park, NJ 07932;
Telephone (201) 822-3700.

varian

**One tuition-free course per Model 3711 purchase.*

CIRCLE 231 ON READER SERVICE CARD

Look for us
in
Cleveland
at the

Pittsburgh Conference
March 5–8

...to say hello ...to discuss your solvent-related technical problems.

We'll be looking for you.

Booth 1133

BURDICK
& JACKSON
LABORATORIES, INC.
MUSKEGON, MICHIGAN 49442 (616) 726-3171

CIRCLE 24 ON READER SERVICE CARD

HELLMA
...tomorrow's designs today!

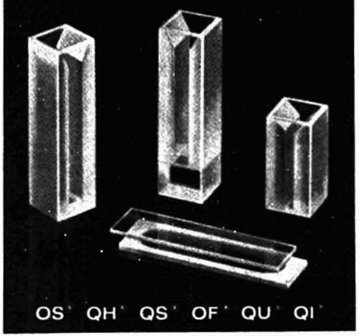

Hellma—the largest assortment of highest precision glass and quartz cells.
Standard · Flow-through · Constant-temperature
Anaerobic · Special Designs
Also available—ULTRAVIOLET LIGHT SOURCES
Deuterium Lamps · Mercury Vapor Lamps
Hollow Cathode Lamps · Power Supplies

HELLMA
CELLS, INC.

Write for literature
Box 544
Borough Hall Station
Jamaica, New York 11424
Phone (212) 544-9534

CIRCLE 98 ON READER SERVICE CARD

Bring State of the Art Gas Analysis to your GC
at a fraction of the cost of a brand new GC.

VALCO'S MODEL-140B* WIDE-RANGE ELECTRON-CAPTURE DETECTOR SYSTEM can indeed bring state of the art capabilities to your GC freeing you from the baseline drifts, sensitivity changes, and linear dynamic range limitations of other ECD designs. This proven system extends the linear dynamic range to five or six decades of sample concentration. Used with a suitable GC column, this detector permits quantitative analysis from picograms to micrograms with no need for expensive reruns or critical sample sizing.

*The Valco 140B — formerly manufactured by Analog Technology Corporation. Now covered by Valco, Patent No. RE. 28,951

Valco's Model-140B Offers:

■ MORE PERFORMANCE
1. Larger linear dynamic range: Five to six decades.
2. More stable baseline.
3. High-temperature operation — up to 320°C. through use of tritiated scandium foil.
4. Better peak reproduction and overload recovery.

■ MORE CONVENIENCE
1. Easily connected to **your** GC.
2. Requires no radioactive source license.
3. Stands alone as separate accessory providing all its own required functions and controls.

VALCO instruments co.
P.O. Box 19032 Houston TX 77024
713/688-9345
TWX: 910-881-5500
Telex: 79-0033

Booth numbers 1630 & 1632 at the Pittsburgh Conference.

CIRCLE 224 ON READER SERVICE CARD

NEW!

CUSTOM PACKED HPLC COLUMNS

OUR HPLC COLUMNS ARE INDIVIDUALLY TESTED BY COMPUTER & ARE SUPPLIED WITH A SAMPLE OF THE TEST MIXTURE & THE ACTUAL CHROMATOGRAM....

ALL THIS AND YOU SAVE $ TOO!

WRITE FOR OUR LATEST CATALOG..

ALLTECH ASSOCIATES

202 CAMPUS DR./ARLINGTON HEIGHTS, ILLINOIS 60004
312/392-2670

CIRCLE 4 ON READER SERVICE CARD

RECYCLED Instruments Save Money!

- **YOU CAN HAVE INSTRUMENTS** pre-owned but completely refurbished and fully warranted.... Save 50% of the new replacement cost from the nation's leader in REBUILT Atomic Absorption, Infrared and Ultraviolet-Visible Spectrophotometers.
- **WE CURRENTLY STOCK** reconditioned instruments from: Beckman, Coleman, Hitachi, Leads & Northrup, Perkin-Elmer, Varian and Others.
- **WE PROVIDE SERVICE** repair and preventative maintenance at rates lower than the original equipment manufacturers.

Call or write for our latest FREE brochure of REMANUFACTURED ANALYTICAL INSTRUMENTS.
See us at the Pittsburgh Conference, Booths 317-319

BUCK Scientific, Inc.

58 Fort Point Street, East Norwalk, Conn. 06855
(203) 853-9444

CIRCLE 27 ON READER SERVICE CARD

Topics in . . .

Chemical Instrumentation—II

An ACS Reprint Collection

A volume of reprints from the *Journal of Chemical Education*

Galen W. Ewing, *Editor*

310 pages (1977)
hardback $12.00
ISBN 0-8412-0367-9
LC 73-153064

This new collection of selected reprint articles from the "Topics in Chemical Instrumentation" column in the JOURNAL OF CHEMICAL EDUCATION provides excellent coverage of the field from January 1970 through November 1975.

In order to furnish the most complete, up-to-date information on the subject many of the authors have added supplemental material to their papers. The 36 reprints are listed according to subject matter rather than by chronological order.

This useful collection will be of particular interest to analytical chemists, college chemistry faculties, research chemists, librarians, and those seeking an introduction to the state of the art.

SIS/American Chemical Society
1155 16th St., N.W./Wash., D.C. 20036

Please send ________ copies of *Chemical Instrumentation—II* at $12.00 per copy.

☐ Check enclosed for $ ________. ☐ Bill me. Postpaid in U.S. and Canada, plus 40 cents elsewhere.

Name

Address

City State Zip

FMI METERING PUMPS

The FMI LAB PUMP line of valveless, variable metering pumps is available from stock at catalog prices. Models are available with maximum flow rates as low as microliters per minute or as high as one liter per minute at pressures to 200 PSIG. A wide variety of pump head materials offer superb chemical resistance. New items include: RYTON® liners, miniature panel mount pumps, and water flush gland option for use with problem fluids.

Price of model shown: $305*.

*Model RP-D-2SSY (0 to 1000 ml/min, 50 psig) with Micrometer Flow Kit.

FMI FLUID METERING, INC. SINCE 1959
P. O. BOX 507, OYSTER BAY, NEW YORK 11771 • (516) 922-6050

See us at the Pittsburgh Conference, Booths 318 and 320

CIRCLE 82 ON READER SERVICE CARD

New from Varian...
Low cost, microcomputerized AA-475 and AA-275

The pacesetters in atomic absorption

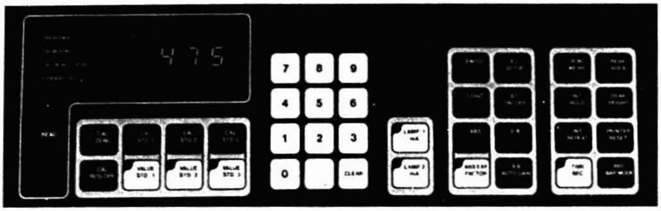

Routine AA analysis has never been this easy, this sensitive, this economical. The AA-475 and AA-275 fully exploit their powerful 8-bit, 10K microcomputers to give you high quality data quickly and simply.

The AA-475 and AA-275 are designed with the novice operator in mind. Prompts on the interactive instrument panel provide step-by-step guidance through set-up and calibration procedures. Operator errors are identified and flagged. Ten vital flame functions are monitored continuously for programmed ignition and safe shutdown.

Computerized signal processing gives you reliable data every time. Varian's unique Rational Method allows rapid, accurate calibration, with a reslope function for recalibration against a single standard. The running mean mode simplifies data collection.

Totally versatile, the AA-475 and AA-275 adapt readily to your requirements. Select from the single beam AA-275 or the double beam AA-475. Customize your system with powerful Varian AA accessories such as the CRA-90 carbon rod atomizer, automatic sample changers for flame and furnace, and programmable calculators. The new M-65 Vapor Generation Accessory greatly simplifies hydride analyses, bringing new levels of convenience and throughput.

There is no compromise in performance. The low cost AA-475 and AA-275 provide a sensitivity level that matches or exceeds that of competitive models at twice the price.

Find out more about the AA-475 and AA-275 today. Circle **235** for product literature. Circle **236** if you wish a representative to call. Or write: Varian Associates, Inc., 611 Hansen Way, D-070-2, Palo Alto, CA 94303.

SEE US AT THE PITTSBURGH CONFERENCE.

varian

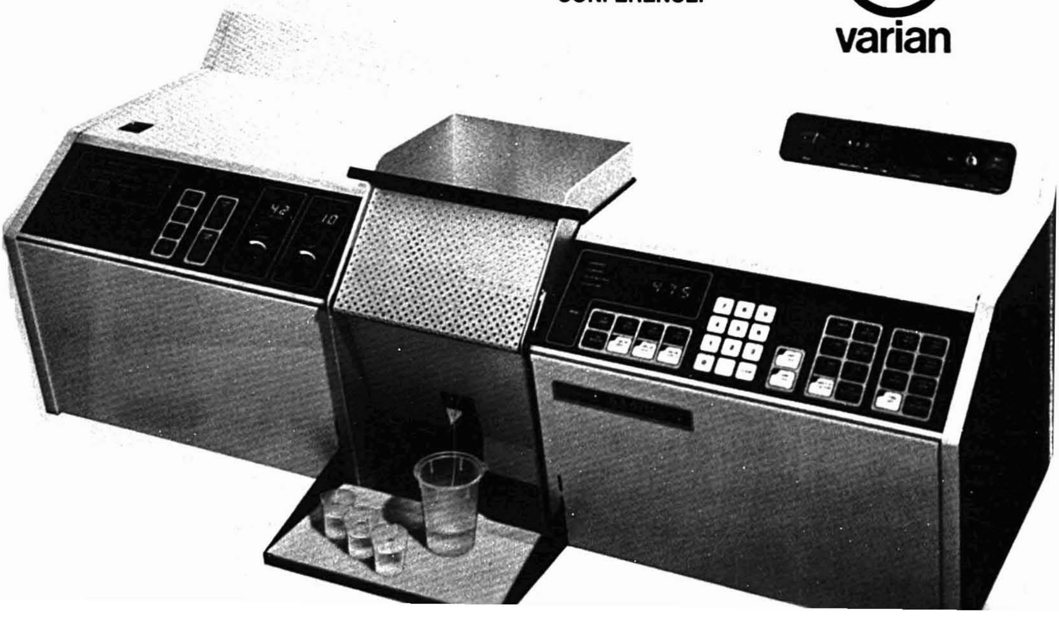

Patent Policy
Government, Academic, and Industry Concepts

ACS Symposium Series No. 81

Willard Marcy, *Editor*
Research Corporation

A symposium sponsored by the Division of Industrial and Engineering Chemistry of the American Chemical Society.

This new, practical guide provides historical insight into and traces the evolution of a broad spectrum of existing patent policies in government, industry, and academia — an essential reference for professional chemists and chemical engineers as well as patent lawyers, legislators, inventors, science researchers, and administrators.

Specific questions are asked and answers are given concerning existing patent policies and how they are working to reward all of the parties at interest while safeguarding the public, and constructive approaches which may enhance the usefulness of the patent system in the future are outlined.

CONTENTS

GOVERNMENT: Federal Patent Policy • Government Patent Policy • H R 8596 • Government R&D Contracting

ACADEMIC: University Technology Transfer • University of California Patent Program • Economic Benefits for Minority-Run Universities • Educational and Nonprofit Scientific Institutions

INDUSTRY: Patent and Licensing Policies at Ford Motor Company, Battery Industry, Petroleum Industry, Pharmaceutical Industry • Protection of Intellectual Property

GENERAL: Impact of Patent Policies on Creativity in Industrial Research Laboratories • The Inventor's Interest • Experiences with Industrial Patent Policy

173 pages (1978) clothbound $19.00
LC 78-9955 ISBN 0-8412-0454-3

Order from:
SIS/American Chemical Society
1155 16th St., N.W.
Wash., D.C. 20036

Supervisor Chemical Stability

G.D. Searle & Co., Research & Development Division, has an immediate opportunity available within our chemical stability evaluation function.

Responsibilities include:

- **Supervisory duties in the development of stability indicating methods;**
- **Stability analysis of new chemical drug substances and raw materials;**
- **Regulatory submission documentation and expiration dating.**

Qualifications include Ph.D. in Analytical Chemistry specializing in chromatographic methods of analysis coupled with one to two years pharmaceutical analysis chromatographic instrumentation experience.

Forward resume in strictest confidence with salary history or requirements to:

Peter J. Vozas

SEARLE **G. D. Searle & Co.**
Research & Development Division
P. O. Box 5110
Chicago, IL 60680

Equal Opportunity M/F...
A Practice, Not Just A Policy

LABORATORY SERVICE CENTER

WANTED—ANALYTICAL BALANCE WITH AUTOMATIC PAN DUMPING AND ELECTRONIC READ-OUT. PLEASE CONTACT KENT SHAH AT COLOR CONVERTING INDUSTRIES, P. O. BOX 4804, DES MOINES, IOWA 50306 515-266-2626

LAB SAFETY

Send for 1979 Catalog
LAB SAFETY SUPPLY CO.
P.O.Box 1368, Janesville, WI 53545

ANALYTICAL SERVICES

• Gas Analysis: GC, Org. Mass Spec, LC
• Industrial Hygiene, Pollution Tests

GOLLOB ANALYTICAL SERVICE

47 Industrial Rd.
Berkeley Heights, NJ
(201) 464-3331

SOLVENTS—Highest Purity

Call or write for prices.

Pollard & Co. Box 7131 Wilmington, DE 19803
Phone: 302-656-0060

2-Amino-5-chlorobenzophenone • 4-Aminoantipyrine • Bromoacetal
p-Bromoaniline • 1-Bromonaphthalene • 2-Chloro-4-nitrobenzoic Acid
Dichloroacetic Acid • trans-1,2-Dichloroethylene • 2,2'-Dipyridyl
Glycolic Acid • Hydroxylamine HCl & Sulfate • 3-Indolebutyric Acid
Inulin • Malonamide • Maltose • o- & p-Nitrobenzaldehydes • Orcinol
Oxamide • Potassium & Sodium m-Periodates • Sodium-p-Aminohippurate
Sodium Dithionate • Succinimide • Tetrachlorofluorescein • Thoron
Tetraiodoethylene • 3,4,5-Trimethoxyaniline • iso-Vanillin • Xylose

Write for our Products List of over 3000 chemicals

Tel: 516-273-0900 TWX: 510-227-6230

EASTERN CHEMICAL BOX 2500 K
Division of GUARDIAN CHEMICAL CORP. HAUPPAUGE, N. Y. 11787

Laboratory Service Center (Equipment, Materials, Services, Instruments for Leasing). Maximum space — 4 inches per advertisement. Column width, 2-3/16"; two-column width, 4-9/16". Artwork accepted. No combination of directory rates with ROP advertising. Rates based on number of inches used within 12 months from date of first insertion. Per inch: **1" — $69; 12" — $68; 24" — $65; 36" — $64; 48" — $63.**

CALL OR WRITE BARBARA AUFDERHEIDE

ANALYTICAL CHEMISTRY
25 Sylvan Road, So.
Westport, Ct. 06880
203-226-7131

INDEX TO ADVERTISERS IN THIS ISSUE

CIRCLE INQUIRY NO.	ADVERTISERS	PAGE NO.
9	*Academic Press Flamm Advertising	269A
6	Acton Research Corporation Bell & Wilson, Inc.	270A
7	*Airco Industrial Gases Hammond Farrell Inc.	165A
4	*Alltech Associates, Inc. Chromad	295A
5	*Alpkem Corporation Alpkem Advertising Company	255A
10	*Altex Scientific, Inc. Oliver Smith Advertising, Inc.	241A
xxx	*The American Instrument Company Industrial Advertising Associates	202A
1	*Analtech, Inc. Robert J. Allen	203A
11, 12	*Antek Instruments, Inc. Cooley & Shillinglaw, Inc.	264A, 268A
3	*Applied Research Laboratories Illustrated Design Services	143A
2	*Applied Science Laboratories, Inc. Science Advertising Associates	277A
22	Baird Corporation Buck & Berglund, Inc.	159A
19, 21	J. T. Baker Chemical Company Naimark & Barba, Inc.	123A, 266A
31	Balzers Corporation Business Development Services	138A
29	Barnes Engineering Company Jarman, Spitzer & Felix, Inc.	219A
26	*Bausch & Lomb Blair Advertising, Inc.	120A–121A
xxx	*Beckman Instruments, Inc. N W Ayer ABH International	239A
30	James G. Biddle Ferguson Advertising	255A
28	*Bio-Rad Laboratories Fred Schott & Associates	233A
16	*Brinkmann Instruments, Inc. Blatt Advertising, Inc.	OBC
xxx	*Bruker Instruments, Inc. Schwietzer Advertising	300A
25	*Buchler Instruments Jud Jaffe Advertising	176A
27	*Buck Scientific, Inc. Leif W. Hansen	295A
24	*Burdick & Jackson Laboratories, Inc. Studio 5 Advertising	294A
33	Cerac, Incorporated The Barry Agency Advertising	204A
37–40	*Chromatix, Inc. David R. McClurg	113A
34	Columbia Scientific Industries Bonner McLane Advertising, Inc.	212A
41	Control Equipment Corporation Art/76	243A
36	Control Laser Corporation Sphere Advertising	201A
32	Crane Company Doremus & Company	216A
44	*Dexsil Chemical Corporation Kenyon Hoag Associates	261A
49	Diamond Tool & Die Webb & Associates, Inc.	246A
46	Diano Corporation Design Associates	188A
45	Digilab, Inc. Conrad, Inc.	209A
47	Digital Equipment Corporation Creamer, Trowbridge, Case & Basford, Inc.	152A
54–61	*Dionex Corporation Fred Schott & Associates	253A
50	*Dohrmann Fred Schott & Associates	107A
51–53	*DuPont N W Ayer ABH International	132A–133A, 134A–135A, 136A–137A
75	*Eberbach Corporation Drury, Lacy Inc.	213A
65–73	Environmental Sciences Associates Marketing Dimensions, Inc.	169A
63	*Extech International The Yankee Group	248A
74	Extranuclear Laboratories, Inc. R. E. Johnson Studios	122A
78, 79	*Finnigan Instruments Robert Pease & Company Adv.	187A, 282A
76, 241–248	*Fisher Scientific Company Tech-Ad Associates	148A–149A, 166A–167A
82	Fluid Metering, Inc. Arnold H. Nachman Associates	295A
80	Forma Scientific Fahlgren & Ferriss, Inc.	267A
81	*Foxboro Analytical Shepherd, Tibball, Galog	171A
84	Garrick Equipment Co., Ltd., U.K. Adcounsel Ltd.Adv.	261A
93	General Electric Company A & SPO	245A
85	*Gilford Instrument Laboratories, Inc. Oberlin Industrial Advertising	193A
87–89	*Gilson Medical Electronics, Inc. Fred Schott & Associates	141A
91	*Glenco Boone Advertising, Inc.	203A
92	*Gould, Inc. Carr Liggett Advertising	235A
90	*Gow-Mac Instrument Kenyon Hoag Associates	206A
100	Haake, Inc. Conceptual Marketing, Inc.	150A
95	*Hamilton Company Mealer & Emerson Adv.	251A, 252A
98	*Hellma International, Inc. Miller Advertising Agency, Inc.	294A
96	Heyden & Son Inc.	261A
97	*HNU Systems, Inc. Demon Advertising	272A
99	Houston Atlas Harold Siegel Consultants	192A
94	*Houston Instruments Cooley & Shillinglaw, Inc.	IFC
105	Inficon Paul, John & Lee, Inc. Adv.	179A
107	Instrumentation Laboratory Aries Advertising, Inc.	266A
108–109	*Instruments SA, Inc., J-Y Optical Systems Div. Kathy Wyatt & Associates Adv.	199A
104	Interactive Sciences Corporation Polo Advertising	229A
106	*ISCO Farneaux Associates Advertising	175A
110, 112	*Jarrell-Ash Div., Fisher Scientific Co. Tech-Ad Associates	145A, 222A
111	Janos Optical Corporation International Design	230A
114	Jasco Incorporated S. M. Sachs & Associates, Inc.	205A
113	Joyce-Loebl S. & M. E. Winship	281A
117	*Kontes The Aitkin-Kynett Co., Inc.	217A
115–116	*Kratos, Inc. Mesa Copy	259A
127	Lab Data Control Kelleher, Bamberger, Terry Adv.	180A–181A
126	Labtest Equipment Company Clarke Advertising	199A
xxx	Leco Corporation LECOM	162B–162D
131	LKB Instruments, Inc. The Matlin Company, Inc.	218A
129–130	The London Company Brand Advertising, Inc.	184A
143	3M Company-New Business Ventures D'Arcy, MacManus & Masius, Inc.	257A
138–141	*Matheson Kenyon Hoag Associates	118A, 119A
136	*Metronics Murphy Advertising, Inc.	207A
146	*Mettler McKinney, Inc.	278A–279A
137	MFE Corporation Schneider Parker Jakuc Inc.	237A
142	*Microelectrodes, Inc. Aries Graphics	207A
133–134	**Micromeritics Adgraphics	130A–131A, 268B

INDEX TO ADVERTISERS IN THIS ISSUE

CIRCLE INQUIRY NO.	ADVERTISERS	PAGE NO.
145	***Millipore Corporation** Schneider Parker Jakuc Inc.	194A
144	***Mitsubishi Chemical Industries Ltd.** Global Advertising Co., Ltd.	249A
135	**MKS Instruments, Inc.** Research Associates	248A
152	***Neslab Instruments** The Ramphastos Agency	256A
150	**Nicolet Instrument Corporation** Technical Communications	191A
13–15, 101–103	***Nissei Sangyo Instruments** Kaneko-Murakami, Inc. Adv.	177A
151	**Norton** Northlich, Stolley of Akron, Inc.	284A
149	***Nuclear Equipment Corporation** KREatiVELy Designed	214A
157	***Ohaus Scale Corporation** Michel-Cather Inc.	115A
172	**Omni-Therm**	229A
156	***Orion Research** OBC Advertising	111A
170	**Pacific Presicion Instruments** Bocek Associates	249A
164	**Pacific Scientific** Allen, Dorsey & Hatfield, Inc.	258A
165–166	**Parker-Hannifin** Media Marketing Service Center, Inc.	248A, 249A
171	**Parr Instrument Company** F. Willard Hills Advertising Service	207A
153, 158–161, 163	***Perkin-Elmer Corporation** Marquardt & Roche, Inc. Adv.	127A, 128A, 129A, 271A, 273A–276A
162	***Pharmacia Fine Chemicals** Cummins, MacFail & Nutry, Inc. Adv.	147A
147	***Philips Electronic Instruments** S. T. Communications	178B
185–186	**Photochemical Research Associates** Quantum Communications	205A, 219A
167	**Photovolt Corporation** Michel-Cather Inc.	262A
155	**Physical Data, Inc.** Commark Group	178D
176	***Physical Electronics** Visual-Media Inc.	197A
178	***Pierce Chemical Company** Pierce Ad-Graphics	231A
174	**Precision Cells Inc.** Arnold H. Nachman Associates	213A
173, 177	***Princeton Applied Research Corporation** The Message Center	189A, 200A
175	***Princeton Gamma-Tech**	229A
168–169	****Pye Unicam Ltd.**	268C, 268D
180	***Rainin Instrument Co., Inc.** Amsterdam Advertising, Inc.	231A
182	***Rainin Instrument Co., Inc.** Robert J. Allen	201A
183	***Rheodyne** Bonfield Associates Adv.	293A
184	***Riber Data Systems** Marken Communications	250A
181	**Rigaku** Harry B. Hill Co.	211A
194	***Schleicher & Schuell, Inc.** Jarman, Spitzer & Felix, Inc.	173A
190	***Schoeffel Instrument** Mar-Bet Associates	256A
196	***Scientech, Inc.** Prescott Purcell Karsh & Hagan	205A
188	***Scientific Glass Engineering** Arden Advertising Agency	254A
197	**Scientific Instruments** J. M. Ferrazza Associates, Inc.	216A
195	**SMI Scientific Manufacturing Ind.** McArthur Associates	260A
xxx	**G.D. Searle** Bentley, Barnes & Lynn	297A
192	***Sensorex** 10346 Agency	219A
118–124	**Shimadzu Seisakusho Ltd.** General Advertising Agency, Inc.	220A–221A
191	***Siemens** Hogan Gazzara Associates	161A
198	***The G. Frederick Smith Chemical Co.** Andrew Show Advertising	231A
193	***Spectra Physics** Paul Pease Advertising, Inc.	247A
187	**SPEX Industries** Seymour Nussenbaum	251A
205	**Tecator, Inc.**	210A
202	***Techne, Inc.** Brunswick Advertising	174A
210	**Texas Instruments, Inc.** Morris & Adams	198A
204	**Thermolyne Corporation** E. R. Hollingsworth & Associates	268A
206	**Tokyo Kasei** Global Advertising Co. Ltd.	178D
203	***The Torsion Balance Company** Douglas Turner, Inc.	215A
208–209	***Tracor Analytical Instruments** Aim Advertising Agency	156A–157A
201, 207	***Tracor Northern, Inc.** Aitchnew Energetics	117A, 227A
200	**Tronac** Western Advertising Agency	264A
212	**United Scientific** Bonfield Associates	190A
213	**U.S. Divers Co., Lif-O-Gen Div.** International Communications Inc.	116A
224, 225	***Valco** Cooley & Shillinglaw	208A, 294A
17–18, 222–223, 226-231, 235–236	***Varian** Moran, Lanig & Duncan Adv.	289A, 291A, 292A, 293A, 296A
218	***Varian, LSE Division** Tycer-Fultz Ltd.	154A
221	**Varian M.A.T.** Shepherd, Tibball Galog	287A
233	***Ventron/Alfa Division** Impact Advertising Inc.	213A
220	**Veriflo Corporation** CGA Advertising Agency	270A
219	**Verlag Chemie International Inc.**	228A
238–240	***Waters Associates** Marketing Dimensions, Inc.	203A
232	***Wescan Instruments, Inc.** W. W. Love Advertising	232A
234	***Whatman, Inc.** J. S. Lanza & Associates	108A
237	***John Wiley & Sons, Inc.** 605 Advertising Group	265A

** See ad in ACS Laboratory Guide*

*** Company so marked has advertisement in Foreign Regional edition only.*

Advertising Management for the American Chemical Society Publications

CENTCOM, LTD.

Thomas N. J. Koerwer, President; James A. Byrne, Vice President; Clay S. Holden, Vice President; Benjamin W. Jones, Vice President; Robert L. Voepel, Vice President, 25 Sylvan Rd. South, Westport, Connecticut 06880 (Area Code 203) 226-7131

ADVERTISING SALES MANAGER
James A. Byrne

SALES REPRESENTATIVES

Atlanta, GA . . . Robert E. Kelchner, CENTCOM, Ltd. Telephone: 203-226-7131

Boston, MA . . . Don Davis, CENTCOM, LTD. Telephone 203-226-7131

Chicago . . . John W. McGuire, CENTCOM, LTD., 540 Frontage Rd., Northfield, Ill. 60093, 312-441-6383.

Cleveland . . . Bruce E. Poorman, CENTCOM, LTD., 17 Church St., Berea, Ohio 44017, 216 234-1333.

Houston . . . Robert LaPointe, CENTCOM, LTD., 415-781-3430

Denver . . . Clay S. Holden, CENTCOM, LTD., 213-325-1903.

Los Angeles 90045 . . . Clay S. Holden, CENTCOM, LTD., Newton Pacific Center, 3142 Pacific Coast Highway, Suite 200, Torrance, CA 90505, 213-325-1903

New York 10017 . . . Don Davis, Richard L. Going, CENTCOM LTD., 60 East 42nd St., 212-972-9660

Philadelphia . . . Richard L. Going, CENTCOM LTD., GSB Building, Suite 510 1 Belmont Avenue Bala Cynwyd, Pa. 19004. Telephone: 215-667-9666

San Francisco, CA . . . Robert E. LaPointe, CENTCOM, Ltd., Suite 303, 211 Sutter Street, San Francisco, CA 94108. Telephone: 415-781-3430

Westport, CT . . . Robert E. Kelchner, CENTCOM, Ltd., 25 Sylvan Rd. South, Westport, Ct. 06880. Telephone: 203-226-7131.

Come and see
the exciting NEW
spectrometer from
BRUKER
ODCB/TMS
at the Pittsburgh Conference
BOOTHS 1115 - 1119

Use this card to receive 1979
your own monthly copy of

ANALYTICAL CHEMISTRY

Toll Free: New Orders: 800-638-2000/Md. only 301-949-1551

	U.S.	Canada**	Foreign**
ACS Members*	☐ $12.00	☐ $21.00	☐ $21.00
Nonmembers	☐ $16.00	☐ $25.00	☐ $33.00

☐ Bill me ☐ Bill Company ☐ Payment enclosed
(Make payable: American Chemical Society)

Name ______________________

Position ______________________

Your Employer ______________________

Address ☐ Home ☐ Business ______________________

City ____________ State ________ ZIP ________

Employer's business ☐ Manufacturing ☐ Academic ☐ Government ☐ Other ______

If manufacturer, type of products produced ______________________

____

*Subscriptions at ACS member rates are for personal use only
**Payment must be made in U.S. Currency, by international money order, UNESCO coupons, U.S. bank draft, or through your book dealer

Allow 60 days for your first copy to be put in the mail 9998-G

Mail this postage-free card today

Use this card to receive 1979
your own monthly copy of

ANALYTICAL CHEMISTRY

Toll Free: New Orders: 800-638-2000/Md. only 301-949-1551

	U.S.	Canada**	Foreign**
ACS Members*	☐ $12.00	☐ $21.00	☐ $21.00
Nonmembers	☐ $16.00	☐ $25.00	☐ $33.00

☐ Bill me ☐ Bill Company ☐ Payment enclosed
(Make payable: American Chemical Society)

Name ______________________

Position ______________________

Your Employer ______________________

Address ☐ Home ☐ Business ______________________

City ____________ State ________ ZIP ________

Employer's business ☐ Manufacturing ☐ Academic ☐ Government ☐ Other ______

If manufacturer, type of products produced ______________________

____

*Subscriptions at ACS member rates are for personal use only
**Payment must be made in U.S. Currency, by international money order, UNESCO coupons, U.S. bank draft, or through your book dealer

Allow 60 days for your first copy to be put in the mail 9998-G

Mail this postage-free card today

NO POSTAGE
NECESSARY
IF MAILED
IN THE
UNITED STATES

BUSINESS REPLY MAIL

FIRST CLASS PERMIT NO 10094 WASHINGTON, D C

POSTAGE WILL BE PAID BY ADDRESSEE

AMERICAN CHEMICAL SOCIETY
Attn: Gayle Hebron
1155 Sixteenth Street, N.W.
Washington, D. C. 20036

NO POSTAGE
NECESSARY
IF MAILED
IN THE
UNITED STATES

BUSINESS REPLY MAIL

FIRST CLASS PERMIT NO 10094 WASHINGTON, D C

POSTAGE WILL BE PAID BY ADDRESSEE

AMERICAN CHEMICAL SOCIETY
Attn: Gayle Hebron
1155 Sixteenth Street, N.W.
Washington, D. C. 20036

analytical
chemistry

Editor: **Herbert A. Laitinen**

EDITORIAL HEADQUARTERS
1155 Sixteenth St., N.W.
Washington, D.C. 20036
Phone: 202-872-4570 Teletype: 710-8220151

Managing Editor: Josephine M. Petruzzi
Associate Editors: Andrew A. Husovsky, Barbara Cassatt
Associate Editor, Easton: Elizabeth R. Rufe
Editorial Assistant: Andre D'Arcangelo
Associate Editor, editing: Nancy J. Oddenino
Production Manager: Leroy L. Corcoran
Art Director: John V. Sinnett
Designer: Alan Kahan

Advisory Board: L. S. Birks, Peter Carr, David Firestone, Kurt F. J. Heinrich, Philip F. Kane, Barry L. Karger, J. Jack Kirkland, Marvin Margoshes, Robert S. McDonald, James W. Mitchell, Royce W. Murray, Harry L. Pardue, Garry A. Rechnitz, Walter Slavin, John P. Walters

Instrumentation Advisory Panel: Gary D. Christian, Catherine Fenselau, Gary M. Hieftje, Tomas Hirschfeld, Peter T. Kissinger, C. David Miller, Carter L. Olson, Sidney L. Phillips, Thomas H. Ridgway

Regulations, Analytical Division Ad Hoc Committee: Robert A. Libby (Chairman), Warren B. Crummett, William T. Donaldson, Donald T. Sawyer

Contributing Editor: Claude A. Lucchesi
Department of Chemistry, Northwestern University, Evanston, Ill. 60201

Published by the
AMERICAN CHEMICAL SOCIETY
1155 16th Street, N.W.
Washington, D.C. 20036

Books and Journals Division
Director: D. H. Michael Bowen
Journals: Charles R. Bertsch
Magazine and Production: Bacil Guiley
Research and Development: Seldon W. Terrant
Circulation Development: Marion Gurfein

Manuscript requirements are published in the January 1979 issue, page 171. Manuscripts for publication (4 copies) should be submitted to ANALYTICAL CHEMISTRY at the ACS Washington address.

The American Chemical Society and its editors assume no responsibility for the statements and opinions advanced by contributors. Views expressed in the editorials are those of the editors and do not necessarily represent the official position of the American Chemical Society.

The Black Box

The term "black box" has usually been applied to an instrument or device that operates in a mysterious manner, as far as the operator is concerned, to perform a desirable function. To the chemist not well practiced in electronics, the most familiar black box is an electronic circuit that manipulates input signals in some fashion to generate an output.

Recently we came upon a "chemical black box" in the form of a proprietary device to purify a gas to be used as a fuel in flame spectrometry. It evidently uses a selective wet oxidation procedure to remove an impurity from the gas by a process not divulged to the purchaser. This brings to mind that the "black box" concept can be generalized to include any aspect of the analytical operation that is used purely in a routine way to perform a function that is not central to the research.

In a particular research problem, the central focus might be on the variable experimental parameters in the measurement step, using well-established methods for sample preparation and data processing. In another, the emphasis might be on variables in sample pretreatment, using otherwise standard procedures. Thus, sample preparation, pretreatment, separations, mechanical manipulations, measurements, theoretical interpretations, or data processing could be either "black boxes" or the center of the research objective.

We can picture a crude analogy of a surgeon performing an operation on a particular organ of a patient. While he is concentrating on the target organ, he turns over to others the task of monitoring the function of other organs, and pretty much takes them for granted. Yet he must be conscious of the whole organism, to avoid the situation that the operation was successful but the patient died. In the same vein, the analytical research worker is well advised to understand the working of each "black box" in his operation, even if it is being used in a routine way, to be sure it is not causing the whole system to fail.

H. A. Laitinen

Determination of Trace-Level Vanadium in Marine Biological Samples by Chemical Neutron Activation Analysis

Alan J. Blotcky, Carl Falcone, Victor A. Medina, and Edward P. Rack*

General Medical Research, Veterans Administration Hospital, Omaha, Nebraska 68105, and Department of Chemistry, University of Nebraska Lincoln, Nebraska 68588

David W. Hobson

Department of Biology, Texas A&M University, College Station, Texas 77840

A pre-irradiation chemistry neutron activation analysis procedure employing cation-exchange chromatography is described for the determination of trace-level vanadium in marine biological specimens. The procedure, utilizing a low-power nuclear reactor ($\sim 1 \times 10^{11}$ n/cm^2-s), consists of wet digestion of the sample, cation-exchange chromatography employing nitric acid wash to remove the major radioactivatable contaminants (sodium and chloride ions), ammonium hydroxide elution to remove vanadium from the resin, and neutron irradiation and radioassay for ^{52}V. The limit of detection of the method is 30 ppb. The determinations of the vanadium content of NBS Standard Reference Material 1571 Orchard Leaves resulted in a value of 0.60 ± 0.02 ppm. Determinations of the vanadium content in shrimp, crab, and oyster (RSD $\leq$ 5%) from four sites off and near Galveston Island, Texas, showed that the vanadium content is greater in samples taken in the industrialized areas as compared to a non-industrialized section.

Analytical methodology for the determination of petroleum hydrocarbons in sediment (*1*) is evolving at a rapid rate. Unfortunately, there is no concomitant progress in developing highly sensitive techniques for measurement of the vanadium content of marine biological specimens, which have a tendency toward concentrating (*2, 3*) vanadium from the environment, for reasons not yet understood. Environmental mobilization of vanadium and its compounds occurs by a number of means in the net transport of vanadium into the oceans. Some of these transport processes include terrestrial run off, industrial emissions, atmospheric wash out (vanadium in the air comes only from industry, as there are no significant natural sources), river transport, and oil spills, resulting in a complex ecological cycle (*4*). There has been discussed (*5, 6*) the possibility of vanadium deposition due to oil spillage, but no evidence is yet available to confirm the release of vanadium from oil. Since crude oils are rather rich in vanadium (50–200 ppm), it is not inconceivable that some vanadium should be released upon the contact of oil with seawater (*7*).

While vanadium determinations may be accomplished in a variety of ways, including spectrophotometry, atomic absorption, X-ray fluorescence, and neutron activation (*7*), only a few of these methods are capable of detection limits which include natural concentrations of vanadium, without extensive pooling of samples. Because of favorable radioactivation properties of vanadium, neutron activation analysis, in theory, offers detection limits in the several parts per billion range.

The reason why vanadium determination by neutron activation requires a rather elaborate procedure, when applied to biological samples, is that the Compton contributions from the large amounts of sodium-24 and chlorine-38, almost always present in neutron-activated biological samples, cause a masking of the 1.434-MeV vanadium peak (^{52}V). This means that unless quantities of vanadium are very large, or the sodium and chlorine contributions are very small, vanadium cannot be accurately detected in a biological matrix. It then becomes necessary to devise means of sodium or vanadium separation from the sample, such as the pioneering method used by Meinke (*2*), involving post-irradiation chemistry. Unfortunately, post-irradiation chemical techniques have several drawbacks, especially in the case of a short-lived radioisotope such as ^{52}V ($T_{1/2}$ = 3.77 m), where appreciable quantities of activity are lost prior to radioassay.

In a recent study, Guinn and his co-workers (*8*) analyzed marine biological specimens and sediments for vanadium using pre-irradiation removal of sodium by hydrated antimony pentoxide (HAP). According to Guinn, the procedure worked fairly well but activation of antimony dissolved from the HAP made it difficult to detect low vanadium levels in small biological samples. Guinn also proposed an alternate method involving co-precipitation of vanadium with ferric hydroxide, but found that the reproducibility of the method was not very good.

At the present time, there is an unavailability of certified standard samples, such as freeze-dried Bovine Liver (SRM 1577), Orchard Leaves (SRM 1571), or Tuna (SRM 1591), assayed for vanadium. However, Nadkarni and Morrison (*9*) quote a value for vanadium in Orchard Leaves (SRM 1571) of 0.61 ppm, as compared to Guinn's values of 0.52 ± 0.02 ppm and 0.50 ± 0.07 ppm, and that of 0.58 ± 0.05 ppm, as obtained in six Japanese laboratories (*8*).

The main purpose of this study is to develop a sensitive neutron activation analysis procedure employing pre-irradiation chemistry to remove the major radioactivatable contaminants from marine biologicals such as oyster, crab, and shrimp, and to evaluate the procedure by analyzing NBS Orchard Leaves and comparing the values to those already reported. Rather than develop a procedure employing "shelf" specimens, we obtained "real world" shrimp, blue crab, and oyster from four areas off or near Galveston Island, Texas. One area was in pristine waters and the other three were areas of varying degrees of industrial pollution. The areas selected for the collection of the "polluted" samples were near or adjacent to Texas City oil refineries and proximal to both the Gulf intra-coastal waterway and the Houston ship channel.

EXPERIMENTAL

Sample Collection. All marine biological specimens were taken at four different sites on or around Galveston Island, Texas. One site was the rather non-industrialized or pristine San Luis Pass area off the westerly section of the island. The other three sites were in the industrialized area of Galveston. The Bolivar site is adjacent to the Texas City refineries and proximal to both

0003-2700/79/0351-0178$01.00/0 © 1979 American Chemical Society

the Gulf intra-coastal waterway and the Houston ship channel. The East Beach area is on the northeastern section of the island in the channel waterway. The Sportsman Road area is in the north central area of Galveston Island, south of the Texas City refineries.

Blue crab (*Callinectes sapidus*) and white shrimp (*Penaeus setiferous*) were collected by seine. Oysters (*Crassostrea virginica*) were pried off the rocks with a crowbar. All specimens were dried at 95 °C in an oven to constant weight, and then crushed into a powder with a mortar and pestle. Samples analyzed weighed on the order of 0.25 g.

Acid Digestion Procedure. All glassware was soaked in a 50% by volume aqueous (distilled water) solution of HNO_3 for at least 12 h, and then rinsed thoroughly with distilled deionized water to remove possible traces of vanadium prior to analysis.

A wet-ashing procedure utilizing concentrated HNO_3 was employed to digest the specimens prior to the chemical separation of vanadium. We compared the vanadium contents of several commercial brands of reagent grade nitric acid for their suitability in the ashing procedure. Since there appeared little difference between Baker (0.006 μg/mL V) and Baker Ultrex (0.006 μg/mL V) HNO_3, we employed the Baker Reagent grade acid. It appears that vanadium is one of the least troublesome elements with respect to contamination.

A comparison of 50 ppb undigested vanadium standards (as V_2O_5) with 50 ppb digested standards showed that there was no measurable loss of vanadium due to the digestion process at the temperatures employed in the procedure.

Samples weighing on the order of 0.25 g dry weight were placed in Vicor crucibles containing 10 mL of concentrated nitric acid. The crucibles were then placed in an ultrasonic bath for 30 min to increase the surface area of the sample, which enhances its ability to dissolve in the digestion process. The crucibles were then placed on a sand bath and heated to 65 °C until absolutely dry (approximately 48 h). The low ashing temperature was used in order to prevent volatilization losses of any vanadium compound in the multielement biological matrix.

To effect an efficient digestion, 10 additional mL of concentrated HNO_3 were added to the digested sample, after which it was again placed in the ultrasonic bath for 30 min and the sand bath digestion procedure repeated. After the sample was digested for the second time, 10 mL of 1 M HNO_3 was added to redissolve the sample, and the crucible was again placed in the ultrasonic bath for 30 min. The dissolved sample was then transferred to a centrifuge tube and centrifuged at 2500 rpm for 10 min to separate out the non-acid-soluble residue. Both the acid-soluble and the non-acid-soluble fractions were saved for analysis.

Resin Columns. Cation-exchange columns were prepared by loading a 0.7 × 10 cm polypropylene column (Bio-Rad) with 2.5 g of Bio-Rad AG 50W-X8 cation resin (200–400 mesh, hydrogen form) in 3 mL distilled deionized water. The resin was then equilibrated with 10 mL of 1 M HNO_3.

Vanadium Determination in Orchard Leaves. Two digestion procedures were evaluated, one involving concentrated HNO_3 as previously described and the other a mixture of 20% H_2O_2 by volume in a concentrated HNO_3 solution.

The acid-soluble part of the sample was added to a previously prepared AG 50W-X8 resin column and allowed to elute through the column. Two 3-mL aliquots of 4 M NH_4OH were then allowed to elute through the resin and each 3-mL eluent was collected in an irradiation vial for activation. The non-acid-soluble residue was transferred to an irradiation vial using 3 mL distilled deionized water.

Determination of Vanadium in Marine Biological Specimens. The acid-soluble part of the nitric acid-digested sample was added to the AG 50W-X8 resin column as described above. However, because of the large quantity of sodium and chlorine in the biological samples, it was necessary to wash the column with 10 mL of 0.5 M HNO_3 prior to eluting the vanadium off the resin with the 4 M NH_4OH. The two 3-mL aliquots of NH_4OH were then collected for irradiation as described above.

The non-acid-soluble residue was then transferred to an irradiation vial using 3 mL distilled deionized water. Instrumental neutron activation analysis of the residue showed minor quantities of sodium and chlorine; however, aluminum was a major radiocontaminant, probably the result of the $^{28}Si(n,p)^{28}Al$ reaction, if the insoluble vanadium-containing residue was a silicate.

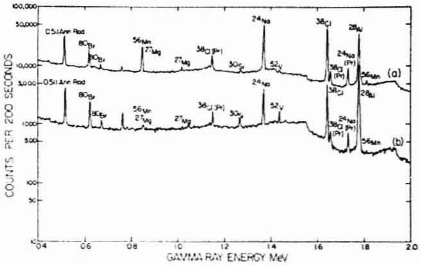

Figure 1. γ-ray spectra following neutron irradiation of white shrimp from Bolivar area. Photo peaks with a Pr designation indicate escape peaks. (a) INAA procedure, (b) after pre-irradiation chemistry

Neutron Irradiation. All samples were irradiated in the Omaha Veterans Administration Hospital TRIGA Mark I reactor operating at a thermal-neutron flux of $\sim 1.1 \times 10^{11}$ n/cm²-s. The samples were irradiated in the rotary specimen rack of the facility for 10 min and allowed to decay for 2 min before counting.

Radioassay. γ counting was done using a 80-cm³ coaxial lithium-drifted germanium detector (Harshaw Chemical) and a Nuclear Data ND 600 2048-channel analyzer, with a system resolution of 2.3 keV (FWHM), a peak-to-Compton ratio of 26/1, and a relative peak efficiency of 12.7% for the 1.332-MeV γ of ^{60}Co.

RESULTS AND DISCUSSION

Development of Procedure Parameters in Aqueous Solution. Shown in Figure 1a is the instrumental neutron activation analysis (INAA) γ-ray spectra following neutron irradiation of 0.25-g samples of white shrimp collected from the Bolivar area. It is obvious from inspection of this Figure that INAA procedures cannot be employed, because of the large contribution of sodium, chlorine, and aluminum activities. Consequently, it is necessary to employ either a pre-irradiation or post-irradiation wet chemistry procedure. We decided against the post-irradiation procedure developed by Fukai and Meinke (*2*) for various reasons. Because of the short half-life of ^{52}V ($T_{1/2} = 3.77$ m), any prolonged decay time after neutron irradiation will raise the limit of detection. Because vanadium exists in various oxidation states, neutron irradiation can result in Szilard–Chalmers reactions of vanadium with the medium, which can complicate any post-irradiation procedure (*10*). We decided against the Guinn et al. (*8*) pre-irradiation use of hydrated antimony pentoxide (HAP) for the reasons discussed in the introduction. From our previous experience, for trace aluminum in urine and bone (*11*, *12*), we found that a pre-irradiation cation-exchange chromatography procedure (employing HNO_3 elution) on digested biological samples resulted in a near 100% decontamination of sodium and chlorine. Vanadium is an element that can exist in multiple oxidation states; but while in the +5 oxidation state, it can exist as either a cation or anion species, depending on the pH of the system (*13*).

To study the feasibility of a cation-exchange chromatography procedure for vanadium in marine biologicals, it was first necessary to study the interrelationships of vanadium retention on the resin and sodium and chlorine decontamination at various HNO_3 concentrations. This was done with aqueous solutions of V_2O_5 and NaCl. For the purpose of the cation-exchange experiments, we employed a 0.7 × 10 cm polypropylene column, as compared to the 0.7 × 4 cm column in our aluminum studies (*11*, *12*). This resulted in a more efficient retention of vanadium on the cation column resin bed. Presented in Table I are the vanadium and sodium losses from the AG 50W-X8 cation resin at various HNO_3 elution concentrations, and the number of washes employed. The

Table I. Vanadium and Sodium Loss from Resin at Various HNO_3 Elution Concentrations and Number of Washes

HNO_3 wash	load	1st wash	2nd wash	3rd wash	total (2 washes)
vanadium loss from resin					
resin loaded with 1 mL of 1 μg/mL V + 10 mL distilled deionized water					
	% loss				
5 mL 1 M	3.8		64.0[a]		
5 mL 0.5 M	1.3	1.7	5.5	9.5	8.5
5 mL 0.2 M	ND[b]	3.9	ND[b]	ND[b]	3.9
sodium decontamination from resin					
resin loaded with 1 mL of 1 mg/mL Na + 10 mL distilled deionized water					
5 mL 1 M	24	58	22	0	104
5 mL 0.5 M	39	30	24	13	93
5 mL 0.2 M	38	19	9	9	66

[a] The sum of the first two washes was 64.0% indicating 1 M HNO_3 as a nonsuitable eluent. [b] Nondetectable.

ideal condition is to find an elution resulting in zero vanadium loss from the resin and 100% decontamination of sodium. As is generally known, and as we have found previously (*11*), the chloride ion readily passes through the resin. It is apparent from inspection of the Table that greatest vanadium retention is with 0.2 M HNO_3; however, at this concentration of HNO_3, the sodium decontamination is least efficient. It is unfortunate that appreciable vanadium loss occurs as the number of HNO_3 washes increases. We decided, for optimal results, to use a 10-mL 0.5 M HNO_3 wash, which results in a 93% decontamination of sodium and a vanadium retention of >91% in an aqueous solution. Since the retention is not 100%, there may be some question as to actual reproducibility in biological samples. This question will be answered in the following section. The main vanadium species is probably VO_2^+ under these conditions (*13*).

In the development of our cation-exchange chromatography procedure for aluminum in biological matrices (bone, urine) employing HNO_3 elution, we radioassayed the aluminum on the resin. Employing the method of Currie (*14*), the limit of detection using the vanadium captured on the resin is 0.006 μg/mL. It would seem that the ideal procedure would involve employing the resin. However, when we used actual marine biological samples, which contain significantly greater quantities of the radioactivatable contaminants sodium and chlorine, we found that the level of sodium and chlorine contamination on the resin after a 10-mL 0.5 M HNO_3 wash was too great to allow accurate vanadium determinations. We evaluated the possibility of eluting the vanadium from the resin and performing a radioassay on the eluent. This procedure would have the added advantage in that the resin radiocontamination would not be present in the assay. Since vanadium can exist as an anion at pH values greater than 4 (*13*), we evaluated the use of NH_4OH as an eluting agent to remove vanadium. We loaded various columns with 1 ppm vanadium in 5 mL of water. The amount of vanadium retained on the resin under these conditions was 100%. Presented in Table II are the NH_4OH elution yields at various NH_4OH molarities. It would seem that the yields were rather insensitive to the molarity and were generally >81%. We chose to use for our elutions 4 M NH_4OH. At this condition, the most probable vanadium species are anions such as VO_4^{3-} or $[V_2O_6(OH)]^{3-}$. In the procedure which we discussed in the Experimental section, we employed two 3-mL 4 M NH_4OH elutions for ease in sample handling in the radioassay steps.

Table II. Elution Yield vs. Molarity of Ammonium Hydroxide

molarity,[a] M	% yield[b]
2	83.7 ± 3.0
3	87.0 ± 1.2
4	87.8 ± 2.8
5	87.4 ± 2.0
6	85.7 ± 3.0
7	86.0 ± 2.0
9	81.6 ± 13.0

[a] Each elution was with 5 mL Baker Reagent Grade NH_4OH. [b] Resin loaded with 1 ppm V in 5 mL water.

Table III. Total Recovery of Vanadium in Marine Biological Specimens from the Bolivar Area

marine biological samples	white shrimp[a]	blue crab[a]	oyster[a]
load of resin[c]	ND[b]	ND[b]	ND[b]
first 0.5 M HNO_3 wash[c]	0.06	ND[b]	ND[b]
second 0.5 M HNO_3 wash[c]	0.05	0.02	0.03
first 4 M NH_4OH elution	ND	0.05	0.02
second 4 M NH_4OH elution	0.12	0.06	0.11
residue	0.22	0.13	0.02
resin	ND	ND	0.00
total vanadium in sample	0.45	0.28	0.18
marine biological samples + 1 μg vanadium " spike"			
load of resin[c]	ND[b]	0.03	0.03
first 0.5 M HNO_3 wash[c]	0.12	0.14	0.07
second 0.5 M HNO_3 wash[c]	0.11	0.15	0.09
first 4 M NH_4OH elution	0.06	0.60	0.07
second 4 M NH_4OH elution	0.81	0.16	0.89
residue	0.18	0.10	0.01
resin	ND[b]	ND[b]	ND[b]
total vanadium in sample	1.28	1.18	1.16
difference between "spike" and sample	0.83	0.90	0.98
elution yield, %[d]	75	65	83

[a] μg vanadium per gram, dry weight. [b] ND = nondetected. [c] Approximate values. Because of the large sodium and chlorine radiocontamination, a computer matrix was used to solve for the vanadium content. [d] Calculated for the NH_4OH elution.

Development of the Procedure for Marine Biological Specimens. As can be seen in Table III, employing "real world" marine biological samples, white shrimp, blue crab, and oyster specimens collected from the Bolivar area, we evaluated the vanadium procedure described in the Experimental section. We determined for these specimens and those containing a 1-μg vanadium "spike" as V_2O_5 the vanadium content of the various steps in the procedure. Because of the large sodium and chlorine contamination in the HNO_3 wash and the resin, these values can be considered only approximations. It is interesting to note that even with these approximations, the accountability of the 1-μg "spike" for white shrimp, blue crab, and oyster is 0.83, 0.90, and 0.98 μg. One interesting feature of this Table is that the vanadium content in the insoluble residue, probably a silicate, is constant within experimental error between the sample and the "spike". Using the NH_4OH elutions for both the sample and the spike, by the method of standard additions, we calculated vanadium elution yields. As can be seen in Table III the major loss of vanadium appeared to be in the HNO_3 washes. The total vanadium content in each sample is the NH_4OH elution fraction, corrected by employing an elution yield determined by the method of standard additions, and the vanadium content of the residue. In order for the procedure to be a viable one, it is important that the vanadium elution yields with the NH_4OH be reproducible. We determined relative standard deviations employing 16 different sets of marine

Table IV. Analyses of Marine Biologicals in the Galveston Island Area for Vanadium[a]

	Σ 4 M NH_4OH eluent[b]	NH_4OH elutions yield, %	residue	total V content
white shrimp[c]				
Bolivar	0.64 ± 0.06[d]	77	0.78 ± 0.13[d]	1.42 ± 0.19[d]
East Beach	2.05 ± 0.06	79	0.61 ± 0.18	2.67 ± 0.18
Sportsman Road	1.41 ± 0.09	88	1.64 ± 0.25	3.05 ± 0.34
San Luis Pass	0.28 ± 0.07	68	0.12 ± 0.04	0.40 ± 0.09
blue crab[e]				
Bolivar	0.62 ± 0.04	64	0.47 ± 0.05	1.09 ± 0.09
East Beach	1.00 ± 0.08	70	0.76 ± 0.18	1.76 ± 0.26
Sportsman Road	0.84 ± 0.03	88	1.00 ± 0.12	1.84 ± 0.14
San Luis Pass	0.84 ± 0.06	63	0.47 ± 0.07	1.31 ± 0.09
oyster[f]				
Bolivar	0.65 ± 0.11	81	0.18 ± 0.12	0.83 ± 0.02
East Beach	0.43 ± 0.13	90	0.26 ± 0.18	0.69 ± 0.24
Sportsman Road	0.62 ± 0.02	76	0.80 ± 0.06	1.42 ± 0.05
San Luis Pass	0.46 ± 0.05	94	0.07 ± 0.05	0.53 ± 0.03

[a] $n = 6$. [b] The sum of the two 3 mL 4M NH_4OH elutions. [c] *Penaeus setiferous*. [d] All values expressed in μg V/g of dry-weight sample. [e] *Collinectes sapidus*. [f] *Crassostrea virginica*.

Table V. Vanadium Content of NBS Standard Reference Material 1571 Orchard Leaves. Neutron Activation Analysis Procedures

destructive analyses	digestion procedure	vanadium content, μg V/g
reported procedure	*c*	0.60 ± 0.02[a]
modified reported procedure	*d*	0.44 ± 0.04[a]
V. P. Guinn procedures,		
HAP	*e*	0.50 ± 0.15[b] (8)
$Fe(OH)_3$	*e*	0.52 ± 0.02 (8)
six independent Japanese laboratories (mean)	*f*	0.58 ± 0.05[a] (8)
instrumental neutron activation analyses		
this study		0.65 ± 0.05
Nadkarni and Morrison		0.61 (9)

[a] 1 standard deviation. [b] 90% condifence limit. [c] Wet-ashed with 10 mL concentrated HNO_3. [d] Wet-ashed with 8 mL concentrated HNO_3 + 2 mL H_2O_2. [e] Wet-ashed (HNO_3 + H_2O_2) ratio unknown. [f] Unknown.

biological samples collected from all sites. Each set was composed of at least six individual samples of the same specimen. The average relative standard deviations of the determinations was better than 5%. It is our contention that these elution yields are acceptably reproducible quantities.

Determination of Trace Levels of Vanadium in Marine Biological Specimens. Employing the procedure described in the Experimental section, we determined the vanadium content in white shrimp, blue crab, and oyster from the four sites off and near Galveston Island. Figure 1b shows the combined spectra of the residue and the NH_4OH elution for a typical analysis of Bolivar area shrimp. The major contribution of aluminum was from the residue, probably the result of the $^{28}Si(n,p)^{28}Al$ reaction. The other radiocontaminants, ^{80}Br, ^{56}Mn, ^{27}Mg, and ^{30}Si, were mainly present in the residue. The total decontamination of radiocontaminants was greater than 90%. It is important to realize that ^{52}V can be produced from naturally occurring manganese. Since some of the samples contained manganese, we determined whether sufficient quantities of ^{52}V could be produced by fast-neutron activation. A 50-μg manganese sample irradiated under identical conditions resulted in nondetectable quantities of ^{52}V. Presented in Table IV are the vanadium results for the marine biological samples from the Galveston Island area. The vanadium contents in the NH_4OH elution and the residue were separately radioassayed for the 1.434-MeV ^{52}V γ photopeak. The activity under the vanadium photopeak was determined by a computer procedure (*15*) utilizing a simplex method of linear programming.

According to the method of Currie (*14*), the lower limit of detection in the procedure is 30 ppb. Although it was not our intention in this paper to comment on the environmental or marine biological significance of vanadium differences in the various species collected in the non-industrialized and industrialized areas, it is apparent from inspection of Table IV that the vanadium content of the species is greater in the industrialized areas as compared to the nonindustrialized San Luis Pass area.

Vanadium Content in NBS Standard Reference Material 1571 Orchard Leaves. Since there is no certified vanadium reference standard, it was of importance for us to determine the vanadium content in NBS Orchard Leaves SRM 1571. As can be seen in Table V, there are several reported values for the vanadium content of Orchard Leaves. Because of the low radiocontamination by other elements, vanadium can be readily determined by INAA. As discussed in the Experimental section, we employed two different experimental processes, the regular HNO_3 digestion procedure and one involving a mixture of NHO_3 and H_2O_2 similar to the Guinn digestion procedure (*11*). The remaining chemistry procedure was similar to that employed for the marine biological specimens. We note that our HNO_3 and H_2O_2 digestion procedure resulted in a value 0.44 ± 0.04, close to being within experimental error of the Guinn values of 0.52 ± 0.02 and 0.50 ± 0.07 μg V/g. These values were lower than the Japanese value of 0.58 ± 0.05 μg V/g and our value employing HNO_3 digestion of 0.60 ± 0.02 μg V/g. The Nadkarni and Morrison value of 0.61 μg V/g and our 0.65 ± 0.05 by INAA are within experimental error of our 0.60 ± 0.02 μg V/g value. We suggest that the use of HNO_3 and H_2O_2 results in vanadium loss during digestion, and that the vanadium content in the Orchard Leaves is closer to the 0.60 μg V/g value.

LITERATURE CITED

(1) L. R. Hilpert, W. E. May, S. A. Wise, S. N. Chesler, and H. S. Hertzog, *Anal. Chem.*, **50**, 458 (1978).
(2) R. Fukai and W. W. Meinke, *Limol. Oceanogr.*, **7**, 186 (1962).
(3) R. Soremark, *J. Nutr.*, **92**, 183 (1967).
(4) D. H. Klein, *Water, Air, Soil Pollut.*, **4**, 89 (1975).
(5) R. S. Barnes and W. R. Schell, "Cycling and Control of Metals", National Environmental Resource Center, Cincinnati, Ohio, 1973, p 45.
(6) M. Zerner and M. Gouterman, *Inorg. Chem.*, **5**, 1699 (1966).
(7) National Academy of Sciences, "Medical and Biological Effects of Environmental Pollutants: Vanadium", Washington, D.C., 1974, 117 pp.

(8) V. P. Guinn, E. R. Christensen, K. deLancey, W. W. Wadman III, J. H. Reed, N. Hansen, A. Abu Samra, and V. J. Orphan, *Proc. Third Int. Conf. Nucl. Meth. Environ. Res.*, in press.
(9) R. A. Nadkarni and G. H. Morrison, *J. Radioanal. Chem.*, **43**, 347 (1978).
(10) A. J. Blotcky, D. M. Duven, W. M. Grauer, and E. P. Rack, *Anal. Chem.*, **46**, 838 (1974).
(11) A. J. Blotcky, D. Hobson, J. A. Leffler, E. P. Rack, and R. R. Recker, *Anal. Chem.*, **48**, 1084 (1976).
(12) A. J. Blotcky, E. P. Rack, R. R. Recker, J. A. Leffler, and S. Teitelbaum, *J. Radioanal. Chem.*, **43**, 381 (1978).
(13) O. W. Howarth and R. G. Richards, *J. Chem. Soc.*, **1965**, 864.
(14) L. A. Currie, *Anal. Chem.*, **40**, 586 (1968).
(15) F. J. Kerrigan, *Anal. Chem.*, **38**, 1677 (1966).

RECEIVED for review September 14, 1978. Accepted October 30, 1978. Research supported by the Omaha Veterans Administration Hospital (MRIS 7319) and the University of Nebraska Research Council (NIH Biomedical Research Support Grant RR-07055). This is USDOE document number COO/1617-57.

Viscosity, Calorimetric, and Proton Magnetic Resonance Studies on Coal Liquid Fractions in Solution

Krishna C. Tewari, Nan-sing Kan, David M. Susco, and Norman C. Li*

Department of Chemistry, Duquesne University, Pittsburgh, Pennsylvania 15219

Two coal liquid products derived from the same Kentucky hvAb coal have been separated into toluene-insoluble, asphaltene, and pentane-soluble heavy oil fractions. Viscosity and calorimetric studies are reported of the interaction between heavy oil and asphaltene (A) and its acid/neutral (AA) and base (BA) components in solvent benzene. The increase in viscosity and molar enthalpy of interaction, $\Delta H°$, in the order BA > A > AA, correlates well with the proton magnetic resonance downfield chemical shift of the OH signal of *o*-phenylphenol, as a function of added asphaltene (A, AA, BA) concentration in solvent CS_2. The results suggest that when asphaltene and heavy oil are present together, hydrogen-bonding involving largely phenolic OH, is one of the mechanisms by which asphaltene–heavy oil interactions are achieved and, in part, is responsible for the viscosity increase of coal liquids.

The high viscosity at ambient temperature of coal liquids, derived from hydrogenation processes, has been a major concern in the direct use of the coal liquids as a boiler fuel. The viscosity of these liquid products has been related to the asphaltene (toluene-soluble, pentane-insoluble) and preasphaltene (toluene-insoluble, pyridine-soluble) fractions (*1–5*). Although the effect of preasphaltene concentration on the viscosity of coal liquids is dramatic, the increase caused by asphaltene materials has been suggested to be due to acid–base interactions (*2, 4*) between hydroxyl or acidic nitrogen and basic nitrogen functions causing molecular aggregation and a corresponding trend toward highly viscous liquids. Recently, the effect of the heavy ends of coal liquids on viscosity has been studied by Schiller et al. (*6*). They, however, observe that hydrogen bonding is more important in defining the effect of asphaltene on viscosity than are acid–base salt formation interactions.

We report here the effect of asphaltene concentration on the viscosity of benzene solutions containing pentane-soluble heavy oil (HO) fraction of the same coal liquid, and the observed correlation of viscosity change with calorimetric and proton magnetic resonance results. The data suggest that when asphaltene and HO are present together, hydrogen-bonding involving largely phenolic OH, is one of the mechanisms by which asphaltene–heavy oil interactions are achieved, and in part is responsible for the viscosity increase of coal liquids.

EXPERIMENTAL

Centrifuged liquid product (CLP) samples, FB53-59 and FB57-42 were obtained from the 450 kg (1/2 ton) per-day Process Development Unit at the Pittsburgh Energy Research Center, after 236 and 168 h, respectively, and were prepared from the same feed coal, Kentucky hvAb, from Homestead Mine, at 27.6 MPa (4000 psi) hydrogen pressure and 723 K reactor temperature. Run FB53-59 was made with the reactor packed with Harshaw 0402T CoMo catalyst, 11-min preheater and 3-min reactor residence time while run FB57-42 was made with the reactor charged with glass pellets, 17-min preheater and 6-min reactor residence time (residence time of coal slurry feed in preheater and reactor was calculated from Cold-Model studies). The isolation of toluene-insoluble (TI), asphaltene(A), and HO fractions from the two CLP samples was accomplished by solvent fractionation based upon solubility in toluene and pentane. The A fraction was further separated into acid/neutral (AA) and base (BA) components by bubbling dry hydrogen chloride gas through a stirred toluene solution. Details of these isolation methods have been previously described (*7, 8*). Traces of residual solvent from dried asphaltene samples were removed by freeze-drying a dispersion of the isolated fraction in benzene. For the liquid HO fraction, dry nitrogen was passed for 8–10 h at room temperature.

o-Phenylphenol (OPP) was obtained from Eastman Kodak Co., purified by recrystallization from ether and stored in a vacuum desiccator at 130 Pa (1 mm Hg) at room temperature. Benzene was of Fisher pesticide grade dried over 4A molecular sieves. Carbon disulfide (CS_2) was purified as described previously (*9*). The molecular weights were determined on a Mechrolab 301A vapor pressure osmometer at 10–20 g/dm^3 in toluene solutions. The solution viscosities were determined by Ostwald viscometer at 293 K. Viscosity data reported here are with respect to water whose viscosity (*10*) was taken as 1.002 cP at 293 K. Proton magnetic resonance (PMR) spectra were obtained at 220 and 60 MHz as CS_2 solutions with tetramethylsilane (TMS) as an internal reference.

Hydroxyl Silylation. Hexamethyldisilazane, 20 cm^3, and 10 cm^3 of *N*-trimethylsilyldiethylamine were added to 100 cm^3 of benzene containing 2 g of asphaltene or HO sample. The mixture was slowly refluxed under nitrogen for 18 h. The solvent and unreacted reagents were removed on a Rotavap at 333 K. Nitrogen was then flushed to ensure dryness. The residue was repeatedly dissolved in benzene and dried as before. To ensure nearly complete removal of reagents, the silylated asphaltene residue was finally freeze-dried from 10 cm^3 of benzene over a 3-h period. In the case of the silylated HO fraction, dry nitrogen was bubbled through the solution for 8–10 h. The formation of HO or asphaltene trimethylsilyl ether was checked by infrared spectrometry for complete disappearance of the free phenolic or alcoholic hydroxyl group absorption at 3600 cm^{-1}. Representative partial

© 1979 American Chemical Society

Table I. Ultimate Analyses (maf) and Molecular Weights of Asphaltene and Heavy Oil Fractions

source	fraction	C	H	O	N	S	Cl	atomic C/H ratio	$\overline{M}_n$ mol. wt.
FB 53-59	A	85.85	6.5	4.4	2.02	0.88	0.39	1.10	740
	AA	84.0	7.2	5.5	1.03	0.96	1.34	0.97	620
	BA	85.3	6.6	4.2	2.79	0.70	0.44	1.08	950
	HO	86.3	8.6	3.2	1.05	0.73	0.16	0.84	290
FB 57-42	A[a]	86.3	6.45	4.2	2.02	0.95	0.10	1.12	530
	AA[a]	85.45	6.75	4.7	1.21	0.77	1.16	1.06	430
	BA[a]	86.05	6.1	3.45	3.03	1.15	0.24	1.18	680
	HO	86.8	8.5	2.9	1.13	0.64	0.11	0.85	260

[a] Taken from Ref. (7).

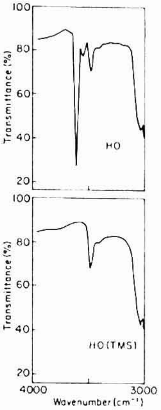

Figure 1. Partial infrared spectra of pentane-soluble heavy oil, (HO), and silylated heavy oil, HO (TMS), fractions in CS_2 solution

infrared spectra of the HO fraction before and after silylation are shown in Figure 1. No significant change in intensity of the infrared absorption band at 3480 cm^{-1}, assigned (*11*) to free NH groups of pyrrole or carbazole, was observed after silylation, indicating that the silylated HO or asphaltene derivative was substantially derived from hydroxyl moieties.

Calorimetric Measurements. The calorimeter was essentially that designed by Arnett (*12*), except that the systematic base-line drifts on the recorder were compensated by extremely slow passage of dry nitrogen through the Teflon top well over the solution surface in the cell. All solutions were prepared in a dry box. A gas-tight Hamilton syringe with Chaney adaptor was used for the introduction of the liquid sample of HO in benzene. The heat of reaction, corrected for the heat of dilution, was determined by injecting a benzene solution of HO of known concentration into the calorimeter cell containing a known amount of asphaltene fraction in benzene. Each successive measured heat and the moles of HO injected in the cell solution were added to the previous total measured heat and moles injected. The range of reactant concentrations was chosen to satisfy as nearly as possible the criteria outlined by Conrow et al. (*13*). The accuracy of the calorimeter was checked against the accepted value for the heat of solution of potassium chloride (*14, 15*) in water.

The molar enthalpy, ΔH°, and equilibrium constant, K, for a 1:1 complexation in a donor–acceptor type reaction $A + B \rightleftharpoons C$, were determined simultaneously from the Bolles and Drago (*16*) equation

$$K^{-1} = \frac{\Delta H'}{v\Delta H^\circ} + \frac{A_0 B_0 v \Delta H^\circ}{\Delta H'} - (A_0 + B_0) \qquad (1)$$

where A_0 and B_0 are the initial concentrations of A and B, respectively, v is the volume in dm^3 of the solution and $\Delta H'$ is the measured heat of formation for an unknown amount of complex corrected for the heat of solution of the added reagent at the corresponding concentration.

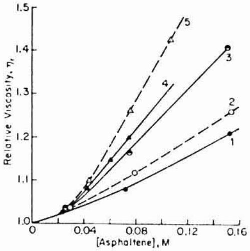

Figure 2. Relative viscosity change with added asphaltene concentration in C_6H_6 and in 0.305 M solution of HO in C_6H_6 at 293 K. Sample FB57-42: (1) AA in C_6H_6; (2) AA in HO + C_6H_6; (4) BA in C_6H_6; (5) BA in HO + C_6H_6; Sample FB53-59: (3) AA in C_6H_6

RESULTS AND DISCUSSION

The viscosities (*17*) at 355 K of the two CLP samples, FB53-59 and FB57-42, from the same feed coal Kentucky hvAb, were >700 and ~128 Saybolt seconds, respectively. The high viscosity of the catalytic run, FB53-59, may be attributed largely to partial deactivation of the catalyst bed. Solvent fractionation gave the weight percent distribution of TI, A, and HO fractions in FB53-59 as 10.4, 33.3, and 56.3, respectively, and in FB57-42 as 9.3, 28.3, and 62.3, respectively. Further separation of A from FB53-59 and FB57-42 into AA and BA components gave the weight ratio AA/BA of 53.1/46.9 and 46.7/53.3, respectively. The results indicate that the low viscosity liquid, FB57-42, contains lower weight content of TI, A, and higher weight percent of BA in A fraction. The long-residence-time preheater and reactor seem to favor conversion as well as decrease the viscosity of the product oil. The results of ultimate analyses and molecular weight determinations for the asphaltene and HO fractions are given in Table I. It is interesting to note that asphaltene (A, AA, BA) and HO fractions isolated from the low viscosity liquid, as compared to similar fractions from the high viscosity liquid product (FB53-59), have lower molecular weight, lower oxygen content, higher nitrogen content, and higher C/H ratio.

To understand the effect of the asphaltene fraction on the viscosity of the liquid product and the nature of the interaction involved, the viscosities at 293 K were measured for benzene solutions of HO (0.305 M) containing varying amounts of individual asphaltene fractions. The relative viscosity (η_r) changes with concentration of AA and BA, isolated from FB57-42, are shown in Figure 2 (curves 2 and 5). The results indicate that, at a given temperature and concentration (above 0.035 M), BA has a larger effect on viscosity than AA. Although the limited solubility of unfractionated A restricted the viscosity measurement above 0.035 M, where marked changes in viscosity were observed, it is interesting to note

Table II. Summary of Thermodynamic Constants[a] at 298 ± 0.5 K

source	system	K, dm^3 mol^{-1}	$-\Delta H^\circ$, kJ mol^{-1}
FB 53-59	HO + A in C_6H_6	9.3	19.12 ± 0.57
	HO + AA in C_6H_6	9.1	15.02 ± 0.48
	HO + BA in C_6H_6	9.4	25.90 ± 0.78

[a] Uncertainties in ΔH° values are standard deviations. Error in K is about 10%.

that Bockrath et al. (*4*), have shown that the viscosity values for BA in pure HO are slightly greater than that of A in HO. The observed order of increase in η_r (BA > AA) correlates well with the increase in molecular weight, nitrogen content, and decrease in oxygen content, Table I, of the added asphaltene fraction. Since coal-derived asphaltenes are known to associate even in dilute solution and more significantly in nonpolar solvent (*18, 19*), the contribution of molecular size and molecular weight on the observed viscosity could be seen qualitatively from the variation of η_r with concentration of added asphaltene fraction in pure benzene as solvent, as shown in Figure 2, curves 1, 3, and 4. It should be noted that at a given temperature and concentration, η_r varies linearly with the molecular weight of the added fraction (Figure 2, curves 1, 3, and 4 refer to asphaltene fractions of molecular weight 430, 620, and 680, respectively). At a given concentration, for a given fraction (AA or BA), the value of η_r in benzene as solvent is smaller than that for the same fraction in benzene containing HO as solvent. Furthermore, in the presence of HO and at a given concentration of asphaltene, the increase in η_r for BA is larger than that observed for AA. Since solvent benzene is less polar than benzene containing HO, and since nitrogen and oxygen are largely present (*2*) as basic ring nitrogen and ring or ether oxygen in BA and as acidic nitrogen and phenolic hydroxyl in AA, it is reasonable to assume that, in addition to the molecular weight of the added asphaltene fraction, part of the effect on viscosity is due to the functional groups. The HO fraction contains phenolic or alcoholic hydroxyl as well as acidic NH groups which serve as hydrogen donors in intermolecular association. PMR analysis of the silylated HO fractions from FB53-59 and FB57-42 shows, respectively, 83% and 80% of the oxygen present is in the form of phenolic and/or alcoholic hydroxyl. The contribution involving pyrrol type imino groups as hydrogen donors, however, is negligible since the pK_a of phenol and pyrrol in aqueous solution at 293 K are 9.89 and ~15, respectively. Furthermore, A, AA, and BA having phenolic groups can likewise act as proton donors to HO in these systems. It must be mentioned that contrary to the thin-layer chromatographic (TLC) analyses of Sternberg et al. (*2*), the infrared spectrum (*20, 21*) of the base component (BA) of coal-derived asphaltene shows distinct absorption for free phenolic and/or alcoholic OH and NH at 3600 cm^{-1} and 3480 cm^{-1}, respectively.

In order to obtain stronger evidence and substantiate further the hydrogen bonding nature of interaction, a calorimetric method was used to determine simultaneously the molar enthalpy, ΔH°, and equilibrium constant, K, for the interactions of A, AA, and BA with HO in benzene. The applicability of the calorimetric method and reliability of the assumed 1:1 complexation, can be seen from the excellent agreement, Figure 3, of the observed heat values with those calculated from Equation 1. The values for the thermodynamic constants are summarized in Table II.

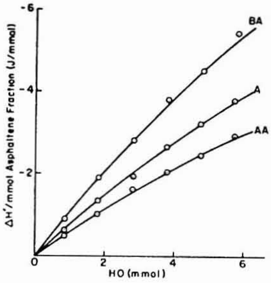

Figure 3. Plots of $\Delta H'$/(mmol of asphaltene) vs. heavy oil (mmol) added. Points are experimental; solid lines are calculated from Equation 1, using the values of K and ΔH° listed in Table II

It is interesting to note that the computed K values, within experimental error, are the same while the molar enthalpy of interaction, ΔH°, increases markedly with the increase in molecular weight, nitrogen content, and decrease in oxygen content of the asphaltene fraction, in the order AA < A < BA, and shows a direct correlation with the viscosity results shown in Figure 2. It must be realized that coal liquid fractions are complex mixtures of substituted heterocyclic aromatics. The interaction of HO with asphaltene (A, AA, BA) in solution can be viewed as a system involving varying degrees of hydrogen-bonding and other types of rapidly reversible intermolecular interactions. The observed values of K and ΔH°, therefore, correspond to the total interaction involving these equilibria.

To evaluate qualitatively, the hydrogen-bonding contribution in the observed ΔH°, asphaltene (A, AA, BA) and HO fractions isolated from FB53-59 were examined by high resolution proton magnetic resonance at 220 MHz in CS_2 solutions. The proton distribution and structural parameters such as aromaticity, f_a, the degree of substitution on aromatic rings, σ, the average length of alkyl substituents on the rings, $(H_0/H_\alpha) + 1$, and hydrogen/carbon ratio for the hypothetical unsubstituted aromatic nuclei, H_{au}/C_a, using Brown and Ladner (*22*) equations, are given in Table III. Both AA and HO fractions show a larger fraction of the hydrogens bound to aliphatic carbons, β or further from the aromatic rings, H_0. A and BA show larger aromaticities, larger percent of aromatic hydrogens and smaller aliphatic branches as compared to AA and HO fractions. It is interesting to note that both A and BA, within experimental error, show the same structural parameters and an even distribution of hydrogen bound to aromatic, benzylic, and aliphatic carbons. This is in agreement

Table III. Proton Distribution and Structural Parameters of Asphaltene and Heavy Oil Fractions Isolated from FB53-59

	area percent, PMR Spectra						
fraction	aromatic H_a	benzylic[a] H_α	aliphatic[a] H_0	f_a	σ	$(H_0/H_\alpha) + 1$	H_{au}/C_a
A	32.6	34.5	32.9	0.70	0.40	1.95	0.70
AA	25.6	22.9	51.6	0.62	0.39	3.25	0.70
BA	32.9	32.4	34.7	0.69	0.38	2.07	0.71
HO	23.8	31.9	44.3	0.54	0.43	2.39	0.93

[a] Separation point between H_α and H_0 chosen at 1.94 ppm.

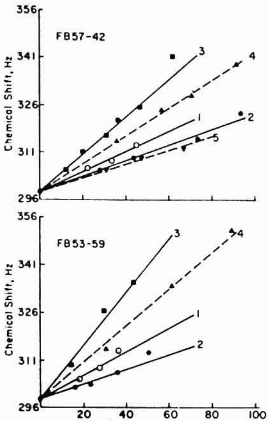

Figure 4. Chemical shift changes (at 60 MHz) of the proton-OH resonance of *o*-phenylphenol (0.2 M) as a function of asphaltene concentration in CS_2 solution. Added asphaltene: (1) A, (2) AA, (3) BA, (4) A(TMS), and (5) AA(TMS).

with the nearly constant C/H ratio for the two fractions (Table I). It could be inferred, therefore, that the contribution of the π-bonding form of associations to the observed $\Delta H°$ values of HO interaction with A and with BA, to a large extent, would be the same. The observed large increase of $\Delta H°$ value, in the order AA < A < BA, therefore, is due to the varying degree of hydrogen-bonding basicity of these fractions. In systems involving coal liquid fractions, the dominance of hydrogen-bonding effects, largely involving phenolic H as hydrogen donors, over other types of molecular interactions in solution is in line with our previous observations (*7, 8, 21*) on quinoline (Qu) interaction with coal-derived asphaltenes (A, AA, BA) and HO fractions in solvent benzene. It was observed that for a given system, Qu + asphaltene (A, AA, BA) and Qu + HO, the values of K, within experimental error, were the same while $\Delta H°$ of interaction increased linearly with the increase in the phenolic oxygen content of the coal liquid fraction.

As shown in Figure 4, additional support for the presence of the hydrogen-bonding interaction, involving phenolic hydroxyl protons, can be obtained from the PMR downfield chemical shift (δ) of phenolic OH signal of OPP, a model chosen for phenolic OH in HO, as a function of added asphaltene (A, AA, BA) concentration in solvent CS_2. OPP was chosen as the model because it is a moderately hindered phenol and any self-association (*23*) at the concentration (0.2 M) studied can be neglected. Although the chemical shift of a proton resonance is the sum of contributions from several factors (*24*), however, it is interesting to note that the observed shift of the OPP-OH signal at a given asphaltene (A, AA, BA) concentration is fairly large, downfield in the order BA > A > AA and correlates well with the viscosity and calorimetric results reported earlier. The extent of the observed OPP-OH downfield shift with asphaltene (A, AA, BA) concentration, therefore, represents a qualitative measure of the relative hydrogen-bonding basicity of the asphaltene fraction. The chemical nature of the hydrogen-bonding bases in asphaltenes, containing heteroatoms, is probably multifunctional so that any conclusions drawn from the present work would be merely speculative. However, since nitrogen in BA is largely present as free basic ring nitrogen as in pyridine and the aromaticity of BA is the same as that of A (Table III), the calorimetric and OPP-OH chemical shift results indicate that nitrogen is largely responsible for the high hydrogen-bonding basicity of BA fraction. The near absence of OH- -π interactions in systems involving ortho substituted hindered phenols and pyridine is well recognized (*25*). Furthermore, addition of silylated asphaltene, A (TMS), into 0.2 M OPP in CS_2, Figure 4, moves the OPP-OH signal considerably downfield compared to that observed for A addition. This is expected since the acid-base structure (*2*) of A involves hydrogen bonding between acidic phenols and basic ring nitrogens. Removal of phenolic hydrogens on silylation would leave an appreciable amount of basic ring nitrogens available for association with OPP-OH protons. On the other hand, oxygen is probably responsible for the hydrogen-bonding basicity of the AA fraction, since AA contains no basic nitrogens and addition of AA (TMS) shows no significant difference on the OPP-OH chemical shift compared to that observed as a function of AA concentration.

The above qualitative correlation of viscosity, calorimetric, and PMR results, therefore, suggests that in coal-liquids, asphaltene and pentane-soluble heavy oil fractions are associated intermolecularly through hydrogen-bonding involving largely phenolic hydrogens as proton-donors. The hydrogen bonding is, in part, responsible for the increase of viscosity of the product oil.

ACKNOWLEDGMENT

The authors are grateful to B. C. Bockrath for helpful discussion and advice. We thank J. T. Wang and H. J. C. Yeh for obtaining PMR spectra at 220 MHz, using the NMR spectrometer at the National Institutes of Health, Bethesda, Md.

LITERATURE CITED

(1) H. W. Sternberg, R. Raymond, and S. Akhtar, "Hydrocracking and Hydrotreating", *ACS Symp. Ser.*, **No. 20** (1975).
(2) H. W. Sternberg, R. Raymond, and F. K. Schweighardt, *Science*, **188**, 49 (1975).
(3) E. H. Burk, and H. W. Kutta, Preprints Coal Chemistry Workshop, Stanford Res. Inst., Aug. 1976, p 86.
(4) B. C. Bockrath, R. B. LaCount, and R. P. Noceti, *Fuel Process. Technol.*, **1**, 217 (1977/1978).
(5) M. G. Thomas, and B. Granoff, *Fuel*, **57**, 122 (1978).
(6) J. E. Schiller, B. W. Farnum, and E. A. Sondreal, *Prepr. Div. Fuel Chem., Am. Chem. Soc.*, **22** (6), 33 (1977).
(7) K. C. Tewari, L. G. Galya, E. M. Egan, and N. C. Li, *Fuel*, **57**, 245 (1978).
(8) K. C. Tewari, E. M. Egan, and N. C. Li, *Fuel*, in press.
(9) L. E. Glemser, in "Handbook of Preparative Inorganic Chemistry", G. Braver, Ed., Academic Press, New York, 1963, p 652.
(10) J. R. Coe Swindells, Jr., and T. B. Godfrey, *J. Res. Natl Bur. Stand.*, **48**, 1 (1952).
(11) J. C. Peterson, *Fuel*, **46**, 295 (1967).
(12) E. M. Arnett, W. G. Bentrude, J. J. Burke, and P. M. Duggleby, *J. Am. Chem. Soc.*, **87**, 1541 (1965).
(13) K. Conrow, J. D. Johnson, and R. E. Bowen, *J. Am. Soc.*, **86**, 1025 (1964).
(14) G. Somson, J. Coops, and M. W. Tolk, *Recl., Trav. Chim. Pays-Bas*, **82**, 231 (1963).
(15) R. G. Irving and I. Wadso, *Acta. Chem. Scand.*, **18**, 195 (1964).
(16) T. F. Bolles and R. S. Drago, *J. Am. Chem. Soc.*, **87**, 5015 (1965).
(17) P. M. Yavorsky, *PERC Int. Q. Progr. Rep.*, April–June, 1976, and Oct.–Dec. 1976.
(18) I. Schwager, W. C. Lee, and T. F. Yen, *Anal. Chem.*, **49**, 2363 (1977).
(19) W. C. Lee, I. Schwager, and T. F. Yen, *Prepr. Div. Fuel Chem., Am. Chem. Soc.*, **23** (2), 37 (1978).
(20) F. R. Brown, S. Friedman, L. E. Makovsky, and F. K. Schweighardt, *Appl. Spectrosc.*, **31**, 241 (1977).
(21) K. C. Tewari, J. T. Wang, N. C. Li, and H. J. C. Yeh, unpublished work, Duquesne University and National Institutes of Health, 1978.
(22) J. K. Brown and W. R. Ladner, *Fuel*, **39**, 87 (1960).
(23) F. K. Schweighardt, R. A. Friedel, and H. L. Retcofsky, *Appl. Spectrosc.*, **30**, 291 (1976).
(24) J. A. Pople, W. G. Schneider, and H. J. Bernstein, "High Resolution Nuclear Magnetic Resonance", McGraw-Hill, New York, 1959.
(25) T. S. Pang and S. Ng, *J. Magn. Reson.*, **17**, 166 (1975).

RECEIVED for review August 18, 1978. Accepted November 1, 1978. This research was supported by Contract No. EY-76-S-02-0063.A003 with the U.S. Department of Energy. However, any opinions, findings, conclusions, or any recommendation expressed herein, are those of the authors and do not necessarily reflect the views of DOE.

Determination of Tetraalkyllead Compounds in Water, Sediment, and Fish Samples

Y. K. Chau,* P. T. S. Wong, G. A. Bengert, and O. Kramar

Canada Centre for Inland Waters, Burlington, Ontario L7R 4A6, Canada

A simple and rapid extraction procedure to extract five tetraalkyllead compounds (Me_4Pb, Me_3EtPb, Me_2Et_2Pb, $MeEt_3Pb$, and Et_4Pb) from water, sediment, and fish samples is described. The extracted compounds are analyzed in their authentic forms by a gas chromatographic–atomic adsorption spectrometry system. Other forms of inorganic and organic lead do not interfere. The detection limits for water (200 mL), sediment (5 g), and fish (2 g) are 0.50 μg/L, 0.01 μg/g, and 0.025 μg/g, respectively. The methods were developed to investigate the occurrence of these compounds in environmental samples. Experiments have established that tetramethyllead can be accumulated by fish and remains in its authentic form for some time.

Organolead compounds are generally more toxic than inorganic lead compounds (*1*) and the toxicity of the alkylated lead compounds varies with the degree of alkylation, with tetraalkyllead being the most toxic (*2*). Recently several research laboratories (*3–6*) have reported the biological methylation of inorganic and organic lead compounds in the aquatic environment by microorganisms. Subsequently, methods are being developed to detect the occurrence of these compounds in water, sediment, and biological samples. Tetraalkyllead in fish samples has been determined by solvent extraction, followed by digestion of the extract and atomic absorption measurement of the total lead (*7*). The procedure is based primarily on the assumption that only tetraalkyllead compounds are extracted from fish tissues. It suffers from the interferences of other organolead compounds co-extracted in the solvent, and the lack of specific differentiation of the alkyl groups. Another procedure (*8*) employs vacuum extraction of the tetraalkyllead into a cold trap under liquid nitrogen, followed by solvent extraction of the condensate for gas chromatographic determination. In both methods, tetraalkyllead compounds have been found in fish and mussels. Fairly high concentration of tetraethyllead (30 ppm) was detected in mussels collected at a buoy near the S.S. Cavtat incident where a shipload of tetraethyllead was sunk (*9*) in the Adriatic Sea. High organolead concentrations, mainly of tetraethyllead, were also found in mussels in other parts of Italian seas. The presence of tetraethyllead in aquatic organisms may indicate that the alkyllead compounds are not immediately metabolized by living organisms and may remain in their authentic forms in the living tissues for a long time (*8*). The occurrence of tetraalkyllead compounds in aquatic biota is highly significant because of the possibility of their incorporation into the food chain.

The present study describes techniques for separation and speciation in the determination of tetraalkyllead compounds in water, sediment, and fish samples.

EXPERIMENTAL

The gas chromatograph-atomic absorption spectrophotometer (GC-AAS) system reported elsewhere (*10*) and specific for the analysis of tetraalkyllead compounds was used without the sample trap. The extract was injected directly into the column injection port of the chromatograph. Instrumental parameters were identical as previously described. A Perkin-Elmer Electrodeless Discharge Lead Lamp was used; peak areas were integrated with an Autolab-Minigrator (Spectra-Physics, Calif.).

Tetramethyllead, 80% in toluene, and tetraethyllead, 99%, were obtained from Alfa Chemicals (Beverly, Mass.). The mixed lead alkyls, Me_3EtPb, Me_2Et_2Pb, $MeEt_3Pb$, were provided by the Ethyl Corporation, Ferndale, Mich. The purity of these compounds was assessed by gas chromatography and standardization was done by atomic absorption determination of the lead content as described in a previous study (*11*). High purity hexane was used for all extractions. EDTA 0.1 M was prepared by dissolving 37 g $Na_2EDTA{\cdot}2H_2O$ in 1 L of distilled water.

Procedures. *Water Analysis.* Place 200 mL of lake water and 5 mL of hexane in a 250-mL separatory funnel. Shake rigorously for 30 min in a reciprocating shaker. Let stand for about 20 min for phase separation. Drain off approximately 195 mL of the water and transfer the remaining mixture into a 25-mL tube with a Teflon-lined cap. Without separating the phases, inject a suitable aliquot, 5–10 μL of the hexane, to the GC-AAS system.

Sediment Analysis. Place 5 g of wet sediment, 5 mL of EDTA reagent, and 5 mL of hexane in a 25-mL test tube with a Teflon-lined screw cap. Shake rigorously in a reciprocating shaker for 2 h. Centrifuge the sample for 10 min at 2000 × g. Inject a suitable aliquot, 5–10 μL, of the hexane extract to the GC-AAS system.

Fish Analysis. Homogenize fish tissue in a Hobart grinder and a Polytron homogenizer. Place 2 g of the fish homogenated with 5 mL of EDTA reagent and 5 mL of hexane in a 25-mL test tube with a Teflon-lined screw cap. Shake rigorously for 2 h in a reciprocating shaker. Centrifuge to facilitate phase separation. Carefully withdraw a suitable aliquot, 5–10 μL, of the hexane phase and inject to the GC-AAS system.

Calibration. Add a known amount of standard tetramethyllead, 5 μg, to the hexane layer after injection of the sample. Mix gently, centrifuge again if necessary. Inject into the instrument the same volume as used in sample analysis. The increase in peak area due to the standard added is used to calculate the amount of tetraalkyllead in the sample. It is not necessary to separate the phases or to know the volume of hexane after extraction.

The calibration curves for each of the five tetraalkyllead compounds expressed as Pb were identical and linear up to at least 200 ng above which overlapping of peaks occurred. If only one compound was present (e.g., tetramethyllead), the curve was linear up to at least 2000 ng.

RESULTS AND DISCUSSION

Extraction of Tetraalkyllead Compounds. As the authenticity of the compounds to be analyzed must be preserved, any of the digestion methods with acids or alkalis are not suitable. Solvent extraction seems to be the method of choice for removing these compounds from samples. Benzene has been used to extract tetramethyllead and tetraethyllead from fish homogenates suspended in aqueous EDTA solution (*7*). Quantitative recoveries for both compounds were reported. Ionic forms of lead such as Pb(II), diethyllead dichloride, and trimethyllead acetate were not extracted in the benzene phase. However, the possibility of extraction of other non-ionic forms of organolead into the benzene phase was not extensively investigated by these workers. Their method, therefore, determines any lead compounds that distribute into the benzene phase as tet-

0003-2700/79/0351-0186$01.00/0 © 1979 American Chemical Society

Table I. Extraction of Tetraalkyllead Compounds from Fish Tissue by Different Solvents[a]

solvent	averaged recovery, %
hexane	80.0
cyclohexane	54.0
octanol	90.0
butyl acetate	55.0
methylisobutyl ketone	30.0
chloroform	57.0
benzene	78.0

[a] Fish homogenate 2 g; EDTA, 5 mL; solvent, 5 mL.

raalkyllead. It has been found in this laboratory that there are other forms of organolead compounds extracted into the organic phase but they were not volatile enough to be analyzed by the GC-AAS techniques. A speciation-specific detection system is therefore necessary for the analysis of tetraalkyllead compounds.

Experiments were carried out to investigate the optimum solvent system for extraction. Fish homogenate, 2 g, spiked with approximately 10 μg each of the five tetraalkyllead compounds, Me_4Pb, Me_3EtPb, Me_2Et_2Pb, $MeEt_3Pb$, Et_4Pb, was suspended in 5 mL of EDTA reagent and extracted with 5 mL of each of the following solvents: hexane, cyclohexane, octanol, butyl acetate, methylisobutyl ketone, chloroform, or benzene. Hexane, benzene, and octanol gave the most satisfactory recovery of the tetraalkyllead compounds (Table I). There were only traces of tetraalkyllead compounds recovered in a second extraction which did not contribute significantly to the overall recovery. Such practice was therefore not considered necessary. Hexane was considered more suitable for extraction and for gas chromatographic analysis because of its relative insolubility, lower boiling point, and lower viscosity. Benzene produced an emulsified layer between the phases which may affect the distribution of the lead compounds in the organic extract. The resultant extract of octanol was too viscous to be suitable for gas chromatographic injection.

The use of tetramethylammonium hydroxide (*12*) to dissolve fish tissue prior to solvent extraction was also investigated. It was found that the resultant solution was a thick gel and the organic layer after extraction became very viscous. Its use was not investigated further.

The use of EDTA in the extraction served to disperse the sediment and fish homogenate in a suspension to provide better extraction and to produce a clarified organic phase and cleaner boundary between the aqueous and organic phases. It has no effect on the recovery of the tetraalkyllead compounds.

Calibration of the Method. When an extraction procedure is used to remove certain compounds from a sample, the solvent after extraction must either be separated and adjusted to its original volume, or its volume must be known in order to calculate the quantity of the analytes contained in the original sample. Unfortunately, in spite of the relative insolubility of hexane, the volume after extraction still varies and depends on the components in the sample. In addition, with biological samples, quantitative phase separation after extraction often presents difficulties. In the method presented here, phase separation after extraction is avoided through use of the standard addition method. After injection of an aliquot of the extract, a known amount of a standard (volume less than 50 μL) is added to the hexane phase. The same aliquot of extract is withdrawn for analysis. The increase in peak area represents the amount of standard in the extract and is used to calculate the total quantity of the analyte in the original sample not requiring knowing the volume of the extract.

Recovery of Tetraalkyllead Compounds from Environmental Samples. The recoveries of the alkyllead compounds from lake water, sediment, and fish samples were evaluated by adding a mixture of five tetraalkyllead compounds to respectively 200 mL of lake water, 5 g of sediment, and 2 g of fish homogenate. The spiked samples were equilibrated for approximately 1 h and processed as described in the procedures.

The recoveries of five tetraalkyllead compounds added to environmental samples are summarized in Table II. For water, the recoveries averaged about 89%. Addition of 5 g of sodium chloride to the water sample for "salting out" effect did not improve recovery to any significant extent. Sediment is a much more complex matrix and the recoveries of the five compounds ranged 81–85% at the concentration level of 2–3 ppm. The sediment used in this experiment was taken from Hamilton Harbor, Ontario, and was fine and silty, and high in organic matter. It is not known whether the loss of spiked compounds is due to adsorption or interactions with some components of the sediment.

There are several limitations in the evaluation of recovery of lead alkyls from fish tissues. It is difficult to assure that the spiked compounds are completely incorporated into the fish tissues. Another difficulty arises from the nonhomogeneous distribution of lipid and protein in different organs and tissues which exhibit variation in solubilization of the lead alkyl compounds. For accurate calculations of the concentration of these compounds in fish, assessment of extraction efficiency from a batch of similar samples should be made by adding a known amount of a standard to a separate aliquot of fish sample and analyzing in parallel with the other samples.

The recovery of the five alkylated lead from fish tissue averaged 74%. The reproducibility of the procedure was evaluated by analyzing 11 replicates of a fish homogenate, 1 g, each spiked with 5 μg of tetramethyllead. The coefficient of variation was 7.3%.

The detection limits based on the given procedures are 0.50 μg/L, 0.01 μg/g and 0.025 μg/g, respectively, for water, sediment, and fish.

Treatment and Storage of Samples. Tetraalkyllead compounds have high vapor pressures and are not stable in water. It is observed that water containing 4.2 μg/L Me_4Pb decreased to 2.8 and 3.9 μg/L when stored respectively at room temperature and at 4 °C overnight. For this reason, water samples should not be filtered by suction but should be extracted with hexane immediately after collection. It was

Table II. Recovery of Tetraalkyllead Compounds from Water, Sediment and Fish Samples[a]

		water		sediment		fish	
compound	added, μg	found, μg	recovery, %	found, μg	recovery, %	found, μg	recovery, %
Me_4Pb	10.00	8.78	87.8 ± 3	8.27	82.7 ± 9	7.22	72.2 ± 8
Me_3EtPb	13.15	11.80	89.7 ± 4	10.65	81.0 ± 5	9.15	72.3 ± 5
Me_2Et_2Pb	14.30	12.50	87.4 ± 3	11.68	81.0 ± 7	10.26	76.2 ± 5
$MeEt_3Pb$	10.15	9.08	89.5 ± 4	8.32	82.0 ± 2	7.22	75.2 ± 9
Et_4Pb	14.20	12.82	90.3 ± 7	12.09	85.2 ± 6	10.69	75.3 ± 8
		average	88.9 ± 7		83.7 ± 9		74.2 ± 9

[a] Four determinations for each sample.

Table III. Accumulation of Tetramethyllead in Rainbow Trout

			concn of Me_4Pb in		
exposure, day	wt. of fish, g	fish, alive or dead	water averaged, $\mu g/L$	fish, $\mu g/g$ wet wt.	concn factors[a]
1	0.1211	dead	3.46	0.43	124
2	0.3661	dead		1.08	312
	0.7982	dead		2.00	578
3	0.4116	dead		1.32	382
	0.6300	dead		2.09	604
7	1.3045	alive		2.94	850
	1.5466	alive		3.23	934
	0.8100	alive		2.25	650
	0.4926	alive		1.73	500

[a] Concentration factor = Concentration of Me_4Pb in fish/concentration of Me_4Pb in water.

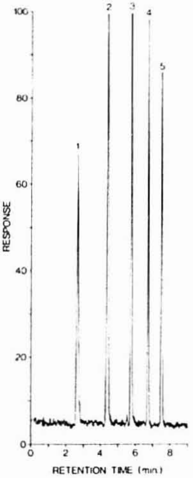

Figure 1. Recorder tracings of five tetraalkyllead compounds analyzed by the GC-AAS system. Each peak represents approximately 5 ng of the compound expressed as Pb. (1) Me_4Pb, (2) $MeEt_3Pb$, (3) Me_2Et_2Pb, (4) Me_3EtPb, (5) Et_4Pb

found convenient to add 5-mL hexane to the water sample (200 mL) and to shake the mixture briefly for 5 min. The sample can then be stored for at least up to one week for further process in the laboratory.

Similar practice is recommended for sediment samples. After collection, the sediment is weighed (5 g) and shaken with 5 mL of EDTA and 5 mL hexane for 5 min in a 25-mL stoppered tube. The treated samples can be stored for at least up to one week for further analysis.

Fish samples should be frozen immediately after collection. Extraction should be carried out immediately after homogenization.

Environmental Samples. Experiments were carried out to establish that tetramethyllead can be taken up by fish and can be recovered with hexane in its authentic form. Rainbow trout after exposure to water containing 3.5 $\mu g/L$ Me_4Pb for different periods of time were found to contain tetramethyllead, see Table III. Preliminary results show that this compound was mainly concentrated in the lipid layer of the tissues.

Many environmental samples, including water, sediment, and fish from high lead areas, have been examined for the presence of tetraalkyllead compounds. Of some 50 fish samples analyzed, only one sample (Ganaraska River, Ontario) so far was found to contain detectable amounts (0.26 $\mu g/g$) of Me_4Pb in the fillet. Since there is no known tetraalkyllead industry and tetramethyllead is not used in gasoline in this area, the source of Me_4Pb is not yet known. The possibility that Me_4Pb comes from in-vivo lead methylation in the sediment or in the fish cannot be totally disregarded. Analysis of more environmental samples for the occurrence of these compounds is now underway. Figure 1 illustrates the recording tracings of the tetraalkyllead compounds analyzed by the GC-AAS system operated according to the parameters described in a previous study (*10*).

LITERATURE CITED

(1) P. T. S. Wong, B. A. Silverberg, Y. K. Chau and P. V. Hodson, "Lead and the aquatic biota" in "Biogeochemistry of Lead", J. Nriagu, Ed., Elsevier Press, New York, 1978, Chapter 17, pp 279–342.
(2) B. G. Muddock and D. Taylor, "The acute toxicity and bioaccumulation of some lead alkyl compounds in marine animals", in Proceedings of the International Experts Discussion on "Lead—Occurrence, fate and pollution in the marine environment", Rovinj, Yugoslavia, 1977, in press.
(3) P. T. S. Wong, Y. K. Chau, and P. L. Luxon, *Nature (London)*, **253**, 263 (1975).
(4) A. W. P. Jarvis, R. N. Markall, and H. R. Potter, *Nature (London)*, **255**, 217 (1975).
(5) U. Schmidt and F. Huber, *Nature (London)*, **259**, 159 (1976).
(6) J. P. Dumas, LeRoy Pazdernik, S. Belloncik, D. Bouchard, and G. Vaillancourt, *Proc. 12th Can. Symp. Water Pollut. Res.*, **12**, 91–100 (1977).
(7) G. R. Sirota and J. F. Uthe, *Anal. Chem.*, **49**, 823–825 (1977).
(8) E. D. Mor and A. M. Beccaria, "A dehydration method to avoid loss of trace elements in biological samples", in Proceedings of the International Experts Discussion on "Lead—Occurrence, fate and pollution in the marine environment", Rovinj, Yugoslavia, 1977, in press.
(9) G. F. Harrison, "The Cavtat Incident", in Proceedings of the International Experts Discussion on "Lead—Occurrence, fate and pollution in the marine environment", Rovinj, Yugoslavia, 1977, in press.
(10) Y. K. Chau, P. T. S. Wong, and P. D. Goulden, *Anal. Chim. Acta*, **85**, 421–424 (1976).
(11) Y. K. Chau, P. T. S. Wong, and H. Saitoh, *J. Chromatogr. Sci.*, **14**, 162–164 (1976).
(12) L. Murthy, E. E. Menden, P. M. Eller, and H. G. Petering, *Anal. Biochem.*, **53**, 365–372 (1973).

RECEIVED for review September 25, 1978. Accepted November 9, 1978.

ANALYTICAL CHEMISTRY, VOL. 51, NO. 2, FEBRUARY 1979 • 189

Parametric Neutron Activation Analysis of Samples Generating Complex γ-ray Spectra

P. F. Schmidt*

Bell Telephone Laboratories, Incorporated, Allentown, Pennsylvania 18103

J. E. Riley, Jr.

Bell Telephone Laboratories, Incorporated, Murray Hill, New Jersey

D. J. McMillan

Northern-Tracor, Inc., Middleton, Wisconsin

The accuracy of multielement quantitative determinations by parametric neutron activation analysis using Fe-Ru flux monitors is compared with that obtained by relative measurements using Standard Reference Materials (SRMs) from NBS. Agreement is good. Isotopes with a large ratio of resonance integral/thermal cross section require empirical correction factors. Deviation of the resonance flux in the reactor reflectors from a 1/*E* distribution appears responsible for at least part of the necessary corrections. The correction factors were found invariant from reactor to reactor. Molybdenum and certain rare earths can be determined by parametric counting in the presence of comparable amounts of uranium; interference by fission products is eliminated by calculations including the fission yields.

Previous State of the Art. Conventional neutron activation analysis (NAA) uses relative measurements, i.e., standards for each element to be determined. These should be co-irradiated with the unknown sample, and later be measured in the same geometry as the unknown sample, and should have not too different count rates for the individual isotopes to be determined. This implies extensive work on the preparation of the standards before and after irradiation in order to achieve comparable activities in identical geometries for a multiplicity of isotopes.

Parametric counting avoids most of the work on standards. The concentrations of the various isotopes present are derived from the photopeak areas via the use of the pertinent nuclear constants, employing an equation which also contains the intensities of the thermal and resonance fluxes (or the fast flux for (n,p) reactions) in the reactor at the time and location of the irradiation. Light elements are mostly activated by the thermal flux, but many of the heavier elements have large cross sections for resonance activation. Parametric counting is thus critically dependent on the accuracy of the nuclear constants and on the accuracy of flux determination. The fluxes are measured by including monitors (such as iron and ruthenium) in the irradiation.

The nuclear constants for most isotopes have now been established with fair to very good accuracy. Except for some elements, such as gold or cobalt, the accuracy to be expected from parametric counting is still not quite as good as can be obtained from relative measurements. However, the speed and ease of the method make it very attractive in any kind of survey work involving a large number of samples. Thus the main obstacle to applying parametric counting consisted in finding a convenient and reliable method for measuring the thermal, resonance, and fast fluxes at the location and time of irradiation. The flux in a reactor is not constant but depends on the power level, motion of control rods, and the locations and age of fuel elements.

An accepted way of determining the thermal and resonance fluxes consists in making cadmium-difference and cadmium-ratio measurements on very dilute gold alloys. A bare sample is activated by both the thermal and the resonance fluxes, a cadmium-shielded sample only by the latter. The method, however, has its difficulties (possible non-uniformity of the gold alloy, possible leakage of thermal neutrons through cracks in the cadmium, absorption of epithermal neutrons in the cadmium, flux depression in the vicinity of the cadmium capsule). The very fact that parametric counting has so far not enjoyed any popularity in spite of its obvious conveniences testifies to the practical difficulties encountered with flux determinations via cadmium measurements on gold, especially for users without direct access to a research reactor.

In a recent publication (*1*) we described a convenient new method of determining the resonance-to-thermal flux ratio, *F*, in a nuclear reactor by co-irradiation of Fe-Ru monitors. The advantages of using the activities of three isotopes of the same element, Ru, for the calculation of the epithermal flux, as compared to any method using isotopes of different elements, were outlined in Reference 1. This flux determination, together with precise photopeak area and detector efficiency determinations, enabled us to apply parametric counting successfully to instrumental (i.e., nondestructive) NAA of trace elements in silicon and other high purity materials with relatively simple γ-ray spectra. While the accuracy of these determinations was adequate for the purpose at hand, a rigorous determination of the accuracy achieved by measurements on SRMs had not yet been carried out.

Original Purpose of This Work. The purpose of the present investigation was to apply the parametric counting approach to the analysis of samples yielding complex γ-ray spectra after irradiation, as well as to compare the concentrations calculated in this manner to those obtained by relative measurements. The "Trace Elements in Gelatin" Reference Materials, recently fabricated and described by Kodak (*2, 3*) are rather ideal for this purpose, since each of the three gelatins, TEG A, B, and C, contains up to 25 elements at the nominal 50-ppm level and the γ-ray spectra are not dominated by any one element, because of a fortuitous choice of the components. We participated in the cooperative effort initiated by Kodak to characterize these Reference Materials, and the results are reported here. By making relative measurements with SRMs, and using parametric counting on aliquots of the *same* sample, an excellent opportunity was

0003-2700/79/0351-0189$01.00/0 © 1979 American Chemical Society

afforded to evaluate the accuracy achievable with parametric counting while also evaluating its performance in analyzing extremely complicated γ-ray spectra.

A wide array of analytical techniques (*2, 3*) by researchers both in the United States and abroad was employed in the characterization of the "Trace Elements in Gelatin" coordinated by Kodak. In general, good agreement resulted with the nominal concentrations expected from the method of fabrication—gelling from aqueous solutions doped with measured amounts of impurities. However, the uncertainty of the values obtained by many different techniques at many different laboratories resulted in relative standard deviations which are decidedly too large for many applications. Our own work on the TEG materials was limited to one technique, NAA, and the relative measurements with SRMs covered only a fraction of the elements contained in the TEGs, but for the elements covered we were able to obtain significantly smaller relative standard deviations.

During the course of this work it was noticed that the concentrations obtained by parametric counting were consistently too low for both isotopes of antimony, provided that the antimony concentrations in the TEG-50 samples were as stated by Kodak. Silver, arsenic, molybdenum, and uranium appeared to follow the same pattern, but in the case of Ag and As we deemed our determinations somewhat uncertain because of interferences, uranium was contained in only one sample (TEG-50A), and the nuclear constants for molybdenum are not very well established as yet.

As a first step toward resolving this question, we irradiated the NBS SRM 364, having a certified antimony content, together with Fe-Ru monitors at the University of Missouri light water reactor and evaluated the antimony concentration both by relative measurements and by parametric counting using the Fe-Ru flux data. Parametric counting yielded antimony concentrations too low by the same factor as seen in the TEG samples. Setting the concentration of each certified element in SRM 364 = 100%, the following percentages were found: ^{59}Fe: 99.17 ± 2.7%; ^{60}Co: 95.17 ± 2.7%; ^{51}Cr: 106.14 ± 2.3%; ^{65}Zn: 115.54 ± (?)%; ^{122}Sb: 53.15 ± 0.2%; ^{124}Sb: 53.33 ± 0.1%. Clearly, an uncertainty in the true antimony concentrations in the TEG samples cannot be blamed for the anomalous antimony results.

Since each of the isotopes showing this anomalous behavior: ^{121}Sb and ^{123}Sb, ^{75}As, ^{109}Ag, and ^{238}U, has a large ratio R of resonance integral/thermal cross section, it seemed logical to assume that the ruthenium monitor indicated an artificially large resonance flux, thus leading to artificially low isotopic concentrations.

In order to clarify this question, a double-pronged approach was chosen. On the one hand, milligram quantities of the metallic elements were co-irradiated with Fe-Ru monitors in the highly thermal flux at Georgia Institute of Technology; on the other, cadmium-ratio and -difference measurements on well characterized Al(Au) flux wires at the University of Missouri light water reactor were combined with flux determinations by the Fe-Ru monitors in the same irradiation. The resultant two sets of flux data were used for concentration calculations of co-irradiated Reference Materials. The measurements at Georgia Institute of Technology would be little affected by uncertainties in the magnitude of the resonance integrals because of the low resonance flux; the measurements at the University of Missouri would show up errors in the magnitude of the resonance flux calculated from the ruthenium data. Both sets of measurements provided interesting results.

Other Investigations. A well known type of interference in NAA comes about when fissionable isotopes like ^{235}U are present: the fission fragments add to the concentration of some other radioactive species stemming from (n,γ) reactions. We found a simple way to overcome this problem by means of parametric counting.

Finally, the natural abundance of ^{58}Fe was not known accurately before, since it is very low. Co-irradiation of a natural iron foil with a Fe_2O_3 sample highly enriched in ^{58}Fe offered a simple and very accurate way to determine the natural abundance of ^{58}Fe. This method is, of course, applicable to any isotope that becomes radioactive upon neutron capture and is obtainable in enriched form. The ^{58}Fe results are described in an accompanying Aid in this Journal (*4*).

EXPERIMENTAL

The spectrometry system employed at Allentown has been described before (*1*). The system at Bell Labs, Murray Hill, consisted of a Tennecomp TP-5000 pulse height analyzing system, a Northern Scientific (Model 623), 100-MHz ADC, and a 60 cm^3 coaxial lithium drifted germanium detector. Detector efficiency as a function of energy was established by means of a certified multiple isotopes point source from the National Bureau of Standards, the same source as used at Allentown for this purpose.

The counting system at University of Wisconsin (UoW) consisted of a computer-based Tracor-Northern TN-11 multichannel analyzer, a Canberra model 2010 spectroscopic amplifier, and a 30 cm^3 lithium-drifted germanium detector. An automatic pneumatic tube-sample changer controlled by the TN-11 is also incorporated into the system, so that samples may be counted with the facility unattended. Detector efficiency was measured over the range 122 to 1407 keV by means of a calibrated ^{152}Eu source, and extended to 2754 keV by measurements on the ^{24}Na photopeaks.

Irradiation Conditions and Counting Procedures for the TEG Samples. These varied at the three locations depending on the delivery time from the reactor and on the method of investigation. At the University of Wisconsin, samples could be measured immediately after irradiation, and a short irradiation of 60 s, followed by 300-s acquisition was used for the short-lived isotopes (^{28}Al, ^{52}V, ^{66}Cu). In addition, a 15-min irradiation followed by decay times of one and of three days for the longer-lived isotope was used. All samples were counted as solids at a distance of 5 cm from the detector, except for the longest decay time when they were counted at contact.

Bell Labs, Murray Hill, is too far from a reactor to measure very short lived isotopes but close enough to measure isotopes like ^{56}Mn or ^{64}Cu with time to spare. All samples were dissolved and counted at a distance of 15 cm from the detector in a rigidly fixed geometry. Aliquots of the solutions were transported to Allentown where they were counted at a distance of 4.6 cm from the detector, also in a rigidly fixed geometry. Allentown is too far from any reactor for reliable measurements even on ^{56}Mn or ^{64}Cu for the given level of activity generated. The maximum duration of irradiation is set by the nature of the gelatin sample, i.e., 20 min at a flux of about 8×10^{13} n cm^{-2} s^{-1} (charring, pressure buildup during irradiation). Both solid and liquid samples were measured at Allentown, and a conversion factor for the different geometry was determined for the samples counted as solids.

The same geometry that was used for counting TEG samples after dissolution was also used for measuring SRM 364 and 127B, as well as the iron and gold monitors, and the Sb, As, Ag, Mo, Ga, and Se samples discussed later. Ruthenium is exceedingly difficult to dissolve, and it was counted only as a solid. However, the method of determining the epithermal-to-thermal flux ratio from the activity of the three ruthenium isotopes (^{97}Ru, ^{103}Ru, ^{105}Ru) does not depend on knowing the amount of ruthenium present, so that an inaccurate geometry factor is unimportant for the epithermal flux determination.

Evaluation of the spectra at Bell Labs, Murray Hill, was limited to those isotopes also covered by co-irradiated SRMs, and these measurements did not require counting times longer than 3 h. Evaluation at Allentown comprised all isotopes detected, i.e., also very long-lived species, and counting times up to 18 h were employed. Both at Murray Hill and at Allentown, samples were counted immediately after receipt and then again after about 2 and after about 10 days. SRMs co-irradiated with the TEG samples were #85B (aluminum alloy), #364 (high carbon steel),

Table I. Concentrations Obtained by Parametric Counting from Irradiations at Reactors with Different F Ratios

	irrad. position: D_2O reflector, irradiation at Georgia Tech, F ratio = 1.38%		irrad. position: graphite reflector, irradiation at University of Missouri F ratio = 7.17%		
isotope	TEG 50A	TEG 50B	TEG 50A	TEG 50B	R = resonance integral/thermal cross section
^{197}Hg	39.5 ± 1.7	48.52 ± 9.8	40.0 ± 0.18	55.44 ± 4.9	0.386
^{203}Hg	31.79 ± 3.7	43.78 ± 4.4	31.89 ± 5.5	43.03 ± 1.6	0.816
^{24}Na^{a}	108.1 ± 0.68	302.50 ± 1.6	125.7 ± 1.8	290.75 ± 12.3	0.685
^{51}Cr	48.2 ± 1.6	37.52 ± 0.77	51.5 ± 0.56	40.93 ± 0.50	0.566
^{65}Zn	44.5 ± 3.5		56.72 ± 1.8		2.42
^{60}Co		45.81 ± 0.79		47.52 ± 0.90	1.286
^{72}Ga	41.81 ± 0.75		42.71 ± 0.39		7.73
^{110m}Ag	24.9 ± 0.33		26.16 ± 0.28		10.89
^{75}Se	32.0 ± 0.32	30.84 ± 2.9	35.4 ± 2.1	32.16 ± 4.5	9.17
^{76}As^{b}	interfered	62.20 ± 0.06	interfered	58.94 ± 0.10	17.44
^{122}Sb	26.0 ± 1.2	27.54 ± 0.36	27.3 ± 0.13	28.72 ± 1.4	31.86
^{124}Sb	29.2 ± 0.93	28.20 ± 1.2	28.9 ± 0.07	28.38 ± 1.0	30.28
^{239}U (^{239}Np)	32.0 ± 0.03		31.3 ± 0.35		100.74
^{99}Mo^{c}	41.6 ± 0.11		39.8 ± 3.1		35.86

[a] Probably nonuniform. [b] All photopeaks interfered. [c] Calculated by hand from the total ^{99}Mo – ^{99}Mo due to fission of ^{235}U; see text.

and 1571 (orchard leaves). The TEG samples were equilibrated for 2 days in a controlled atmosphere clean room, 21 ± 1 °C, 40 ± 5% RH, before irradiation, as suggested by Kodak (*2*).

The nuclear constants used in the Absolute Counting calculations are listed in Table VII for all isotopes determined in this manner.

RESULTS

Multiple Trace Element Determination by Absolute Counting. Table I shows concentrations of impurities in TEG 50A and 50B as obtained by irradiation at the Georgia Institute of Technology heavy water moderated reactor, and at the University of Missouri (UoM) light water moderated reactor. Because of the different moderators, the F ratio (epithermal/thermal flux) is quite different at the two reactors. This ratio is shown in Table I, next to the irradiation facility, as determined by the Fe-Ru method. In spite of the large difference in F ratio, the concentrations calculated for isotopes with such different resonance integral/thermal cross section ratios as ^{203}Hg (= 0.816) and ^{238}U (= 100.74) are in good agreement for irradiations at the two reactors. This strongly suggests that the Fe-Ru method ought to be quite reliable.

Table II shows the factors by which the elemental concentrations for Sb, As, Ag, Mo, Ga, Se, and Au were found too low in the irradiation of milligram quantities of these elements at the Georgia Tech heavy water reactor (in the most thermal location, at a flux of 5.7×10^{11} n cm^{-2} s^{-1}). These factors turned out to be identical to those which would have to be used to make the concentration of these elements, as determined by parametric counting, coincide with the true concentrations in the Kodak TEG or NBS SRM samples. In calculating these factors, the small correction for self-shielding of thermal neutrons has been taken into account according to the equations given by Zweifel (*5*). Self-shielding of the approximately 1.4% epithermal flux detected by the ruthenium monitor has not been taken into account, though this would obviously decrease the magnitude of the correction. This self-shielding of the small resonance flux was disregarded because the ruthenium resonances occur at higher energies than the large resonances of the other isotopes. If the discrepancy is, in fact, due to the other isotopes not "seeing" the resonance neutrons still present at the higher Ru resonance levels, then it appears questionable whether such a correction should indeed be applied. Incidentally, calculations showed that while such self-shielding would reduce the magnitude of the discrepancy, it would certainly not eliminate it (except for Au).

Table II. Factors by Which the Amounts of the Metallic Elements, Irradiated in a Highly Thermal Flux of the Graphite Reflector of the Georgia Tech Heavy Water Reactor, Were Found Too Small When Using the Flux Data of the Co-irradiated Fe-Ru Flux Monitors for the Calculation[a]

elements	multiply by
antimony (^{122}Sb or ^{124}Sb)	1.923
arsenic (^{76}As)	1.652
gold (^{198}Au)	1.119
molybdenum (^{99}Mo(Tc))	1.802
silver (^{110m}Ag)	1.535
gallium (^{72}Ga)	1.300
selenium (^{75}Se)	1.413

[a] The calculated concentrations of the isotopes have to be multiplied by the factors indicated in order to arrive at the correct concentrations. These correction factors were found to be independent of the reactor neutron spectrum in which the samples were irradiated, see Tables I, III, IV, and V.

The correction factors determined for ^{122}Sb and ^{124}Sb, ^{76}As, ^{110m}Ag, ^{99}Mo(Tc), ^{72}Ga, and ^{75}Se have been used to correct the concentrations of these isotopes in the following Tables III–V.

It is worth noting that cadmium measurements on Al(Au) flux wires carried out in the same location at Georgia Tech indicated an epithermal flux 2 orders of magnitude smaller than derived from the ruthenium measurements (*6*).

The comparison between concentrations obtained by parametric counting (at BTL Allentown and at UoW) and those obtained by relative measurements using SRMs is given in Tables III–V. Not all isotopes detected and determined by parametric counting are listed; for a complete list of the components of the TEG samples, the reader is referred to Refs. (*2, 3*).

The data in Tables II–V need some explanation. Access to the UoW reactor enabled determination of very short-lived isotopes such as ^{52}V and ^{28}Al, but use of loaned equipment limited the acquisition time and hence the determination of very long lived isotopes with correspondingly low count rates. The situation at BTL Allentown was exactly the reverse of that at UoW, while the evaluation of isotopes at Murray Hill was limited by the number of SRMs that could be co-irradiated and co-evaluated with the TEG samples in the given number of runs executed.

The meaning of the standard deviation is also different for the relative measurements at BTL Murray Hill and for the

Table III. Intercomparison of Concentrations Obtained for TEG 50A by Parametric Counting (a and b), and by Relative Measurements Using NBS Standard Reference Materials (c), to the Values Quoted by Kodak (Average of Several Techniques) (d)[a]

	(a) Allentown (PFS)	(b) Univ. of Wisconsin (DJM)	ratio of resonance integral/thermal cross section	(c) comparison to NBS SRMs (JER)	(d) average of several techniques, Kodak (*2, 3*)
^{51}Cr	51.5 ± 6.0	43.0 ± 8.0	0.566	(51)	56 ± 9
^{65}Zn	56.7 ± 1.6		2.42	48.6 ± 2.3	53 ± 4
^{72}Ga[c]	55.5 ± 1.4	58.6 ± 0.6	7.73	47.4 ± 0.5	57 ± ?
^{110m}Ag[c]	40.15[b]	55.26 ± 9	10.89		46 ± 5
^{75}Se[c]	50.0 ± 0.8	56.5 ± 10	9.17		38 ± 5
^{56}Mn		47.8 ± 2	1.28	50.3 ± 1.4	52 ± 7
^{76}As	interfered	interfered	17.44	53.1 ± 4.1	48 ± 8
^{122}Sb[c]	53.36 ± 0.88	59.6 ± 0.5	31.86	54.7 ± 2.4	53 ± 4
^{124}Sb[c]	55.59 ± 0.93	74.4 ± 1.3	30.28	54.7 ± 2.4	53 ± 4
^{99}Mo(Tc)[c]	55.44[b]		35.86		55 ± 7
^{239}U(Np)	31.3[b]		100.74		49 ± ?
^{116m}In		45.3 ± 1.2	13.45		51 ± ?

[a] Note: Samples of all three runs shown were irradiated in graphite reflector positions. [b] Single determination. [c] Correction factors from Table II have been applied in the calculation.

Table IV. Intercomparison of Concentrations Obtained on TEG 50B by Parametric Counting (a and b), and by Relative Measurements Using NBS Standard Reference Materials (c), to the Values Quoted by Kodak (d) (Average of Several Techniques)[a]

	(a) Allentown (PFS)	(b) Univ. of Wisconsin (DJM)	ratio of resonance integral/thermal cross section	(c) comparison to NBS SRMs (JER)	(d) average of several techniques, Kodak (*2, 3*)
^{51}Cr	40.9 ± 0.5	51.3 ± 8.5	0.566	49.9 ± 3.0	49 ± 4
^{65}Zn			2.42	49.9 ± 2.2	50 ± 5
^{24}Na	290.8 ± 12.3	327 ± 2	0.685	378 ± 13	328 ± 45
^{56}Mn		43.9 ± 1	1.28	49.9 ± 1.5	50 ± 3
^{197}Hg	55.4 ± 4.9	60.5 ± 9	0.386		56 ± 5
^{203}Hg	43.0 ± 1.6	42 ± 15	0.816		56 ± 5
^{60}Co	47.5 ± 0.9	52.4 ± 2.7	2.016	47.8 ± 4.9	50 ± 3
^{75}Se[c]	45.5 ± 4.5	52.3 ± 7.4	9.17		35 ± 9
^{76}As[b,c]	97.3 ± 0.1	99.1 ± 0.5	17.44	99.6 ± 4.3	95 ± 10
^{122}Sb[c]	55.2 ± 1.4	63.1 ± 0.5	31.86	53.4 ± 5.2	50 ± 6
^{124}Sb[c]	54.6 ± 1.0	61.5 ± 3.0	30.28	53.4 ± 5.2	50 ± 6
^{28}Al		49 ± 11	0.662		54 ± 7

[a] Note: Samples of all three runs shown were irradiated in graphite reflector positions. [b] All ^{76}As lines interfered, the 657-KeV line by the 657.7 line of ^{110m}Ag, an unintended contaminant in TEG 50B. [c] Correction factors from Table II have been applied in the calculation.

Table V. Intercomparison of Concentrations Obtained on TEG 50C by Parametric Counting (a and b), and by Relative Measurements Using NBS Standard Reference Materials (c), to the Values Quoted by Kodak (d) (Average of Several Techniques)[a]

	(a) Allentown (PFS)	(b) Univ. of Wisconsin (DJM)	ratio of resonance integral/thermal cross section	(c) comparison to NBS SRMs (JER)	(d) average of several techniques Kodak (*2, 3*)
^{51}Cr	40.0 ± 2.5	47 ± 5	0.566	49.1 ± 2.1	49 ± 4
^{42}K	49.0[b]	57 ± 12	0.931	48.2 ± 1.4	64 ± 17
^{86}Rb	47.1 ± 0.5	82 ± 20	1.046		50 ± ?
^{110m}Ag[c]	54.8 ± 0.8	53.7 ± 3	10.89		60 ± 10
^{99}Mo(Tc)[c]	52.8 ± 1.0		35.86		60 ± 10
^{72}Ga[c]	52.0 ± 0.8	49.0 ± 0.5	7.73	46.5 ± 1.0	51 ± ?
^{24}Na	89.5 ± 0.1	100 ± 1	0.685	116 ± 1	120 ± 34
^{56}Mn		40 ± 2	1.28	45.7 ± 1.2	48 ± 3
^{52}V		64.5 ± 0.7	0.594		49 ± 3
^{64}Cu			1.356	56.8 ± 2.3	49 ± 4
^{116m}In		50.8 ± 1.1	13.45		49 ± ?

[a] Note: Samples of all three runs shown were irradiated in graphite reflector positions. [b] Single determination. [c] Correction factors from Table II have been applied in the calculation.

parametric counting measurements at BTL Allentown and at the University of Wisconsin. The standard deviation has its usual analytical meaning at BTL Murray Hill. At the two other locations, it refers *only* to the counting statistics of a single sample measured at three consecutive decay times. The systematic errors inherent in the nuclear constants are not included since these errors are largely unknown. If they were included, the standard deviation for the parametric counting would definitely become larger than shown in the tables. There is, however, agreement between parametric counting results at Allentown and at the University of Wisconsin, and also between results for irradiations at Atlanta and at the

University of Missouri. This indicates that the standard deviations obtained for irradiation of several batches of the same sample and evaluated by parametric counting would be very similar to the ones shown here in the tables. As already pointed out, the correction factors listed in Table II have been used to correct the concentrations of ^{122}Sb and ^{124}Sb, ^{76}As, ^{110m}Ag, ^{99}Mo(Tc), ^{72}Ga, and ^{75}Se. None of the other data have been corrected in any way.

Discrepancies between values obtained for sodium should not be taken too seriously, in view of the ubiquitous nature of the element and that it is not an intentionally added impurity in the TEG samples but contained in the gelatin. We also had some indication that a few other elements were not completely uniformly distributed, but those deviations were minor.

Comparative Flux Determinations. An irradiation run was carried out with the pneumatic tube facility at the University of Missouri light water reactor, in the same irradiation position which had been used for the TEG samples (the so-called "front-row" position). A Fe-Ru monitor couple, a bare Al (Au = 0.127%) flux wire, 15 mg of NBS SRM 127B and 51.60 mg of Al(Co = 0.116%) SRM 953 were co-irradiated, immediately followed by irradiation of another Al (Au = 0.127%) flux wire under 20-mil cadmium shielding (length of the capsule 2.0 cm, inner diameter 2 mm).

The concentration of gold in the Al(Au) flux wire was determined both by atomic absorption spectrometry and by relative neutron activation measurements vs. a dilute gold solution (volume 2 cm^3) of known concentration and using the most thermal flux available at the Georgia Tech heavy water reactor; both measurements agreed, giving the gold concentration = 0.127%. SRM 127b is a lead-tin based alloy containing small amounts of antimony, and very small amounts of arsenic. Unfortunately, it carries only a provisional certification but still appeared as the most suitable SRM for the particular purpose.

The thermal and epithermal fluxes were determined both from the Fe-Ru monitors and from the cadmium-ratio and -difference measurements on the Al(Au) flux wires. These flux data were then used to calculate the concentration of Sb and As in SRM 127B, and of Co in SRM 953. The results are shown in Table VI.

It is immediately obvious that the two sets of flux data are not in agreement with each other. Some of this discrepancy might be due to the difficulties noted before—some absorption of epithermal neutrons, possible leakage of thermal neutrons into the cadmium shield—but some more fundamental cause appears more likely.

The uncorrected antimony value is again found too low by approximately a factor of 2 from the Fe-Ru data, and approximately 30% too low from the gold data. For Co the two sets of data are in better agreement, though the Fe-Ru data give the better fit. The uncorrected arsenic value, too, is too low by more than a factor of 2, and the As value from the gold data is not much higher. We suspect that "100 ppm" is really only a nominal concentration, and that the true value is close to 73 ppm, the corrected value from the Fe-Ru flux data.

OTHER INVESTIGATIONS

Determination of Molybdenum in the Presence of Uranium. Because of the fission reaction on ^{235}U (which has a very large cross section, 280 b) producing fission fragments decaying to ^{99}Mo and ^{99m}Tc, the determination of Mo by neutron activation in the presence of uranium has been a problem in the past. Parametric counting provides a simple way to overcome this difficulty. In our particular example, analysis of TEG 50 A, we observed that only ^{103}Ru was present after irradiation; the ^{97}Ru and ^{105}Ru isotopes were missing or below our limit of detection. Since the fission yields for production of ^{103}Ru and ^{99}Mo are known, we only needed to convert, on a proportional basis, the number of ^{103}Ru atoms detected (at end of irradiation) into the number of ^{99}Mo atoms present at end of irradiation but due to fission. Subtraction of this number of ^{99}Mo from the total number of ^{99}Mo atoms present then gives the number of ^{99}Mo atoms due to activation by the (n,γ) reaction on ^{98}Mo, and hence the molybdenum concentration in the sample. It should be noted that this approach would still be valid in the presence of ruthenium in the original sample. In this case one would use only the fraction of ^{103}Ru in excess over the amount present in natural ruthenium as determined by the concentration calculated from ^{97}Ru and ^{105}Ru. The method could also be applied to the determination of certain rare earths which are likewise formed with high yield as fission fragments of ^{235}U.

As a check on our calculation, we calculated the amount of ^{235}U which in the given reactor spectrum (as determined with the Fe-Ru monitor) would have caused the observed number of ^{103}Ru atoms by fission. The amount of ^{238}U present was then obtained from the natural abundances of ^{235}U and ^{238}U and compared to the ^{239}Np activity detected in the TEG 50A sample. The two calculations checked within 26%, the ^{103}Ru branch giving the higher value. This is probably as good an agreement as can be expected for a calculation of this type, given also the uncertainty in the abundance of ^{235}U in the actual sample.

Table VI. Comparison of Fluxes and Concentrations Obtained by the Fe-Ru Method with Those Obtained by Cadmium Ratio and Cadmium Difference Measurements on Gold[a]

Thermal and epithermal flux	
from the Fe-Ru data	$\phi_{\text{thermal}} = 6.215 \times 10^{13}$ n cm^{-2} s^{-1}; $\phi_{\text{epi}} = 7.356 \pm 0.004\%$
from Au-Au/Cd data	$\phi_{\text{thermal}} = 7.733 \times 10^{13}$ n cm^{2} s^{-1}; $\phi_{\text{epi}} = 2.742\%$
Concentration of cobalt in NBS SRM 953 Al(Co) flux wire	
from Fe-Ru data	Co = 97.4 ± 0.8% of NBS value
from Au-Au/Cd data	Co = 88.4 ± 0.8% of NBS value
Concentration of antimony in NBS SRM 127 B	
from Fe-Ru data (both ^{122}Sb and ^{124}Sb)	Sb = 2095 ppm; = 4029 ppm if empirical correction factor is used.
from Au-Au/Cd data	Sb = 3038 ppm;
from SRM 127B spec.	Sb = 4300 ppm.
Concentration of arsenic in NBS SRM 127 B:	
from Fe-Ru data	As = 44.4 ppm; = 73.3 ppm if empirical correction factor is used.
from Au-Au/Cd data	As = 55.6 ppm;
from SRM 127 B spc.	As = "100" ± ? ppm.

[a] The University of Missouri light water reactor was used for this run. Irradiation position: front row of the graphite reflector.

DISCUSSION

Tables III–V compare the concentrations in the three TEG materials as obtained by parametric counting with those obtained by relative measurements using SRMs, and with those quoted by Kodak (*2*, *3*). It must, of course, be remembered that the nuclear constants of the various isotopes have not all been established with the same degree of accuracy. Some of the discrepancies in Tables III–V undoubtedly arise from the use of incorrect nuclear constants. The large discrepancy between the concentrations calculated for mercury

Table VII. Nuclear Constants Used in Calculating the TEG Impurity Concentrations as Given in Columns (a) and (b) of Tables II–IV

isotope & γ-ray energy	halflife & absolute intensity of γ-ray, %	% abundance	thermal cross section, barns	resonance integral, barns
^{198}Au	64.7 h[b]	100.0	98.8*E* + 00	1.540*E* + 03
411.8 keV	95.50			
675.9	0.84			
^{59}Fe	1080 h	0.31	1.14*E* + 00	1.20*E* + 00
1099.2	56.1			
1291.6	43.51			
^{97}Ru	69.0 h	5.51	2.08*E* − 01	4.80*E* + 00
215.7	85.30			
325.1	10.76			
^{103}Ru	955.2 h	31.61	1.29*E* + 00	4.30*E* + 00
497.1	86.80			
610.3	5.47			
^{105}Ru	266.3 m	18.58	4.47*E* − 01[a]	5.8*E* + 00[a]
724.2	49.00			
469.4	17.50			
676.3	16.66			
316.6	12.25			
^{51}Cr	667 h	4.35	1.59*E* + 01	9.00*E* + 00
320.1	9.90			
^{65}Zn	245.0 d	48.89	7.15*E* − 01	1.73*E* + 00
1115.5	50.60			
^{72}Ga	14.2 h	40.00	4.40*E* + 00	3.40*E* + 01
834.1	95.80			
2201.6	25.60			
629.9	26.20			
2507.6	15.00			
2490.9	8.65			
600.9	5.50			
894.2	10.30			
^{99}Mo(Tc)	66.2 h–6.0 h	23.78	1.45*E* − 01	5.20*E* + 00
140.5	88.00			
739.5	12.20			
777.9	4.30			
^{239}U	23.54 m	99.27	2.73*E* + 00	2.75*E* + 02
^{239}Np	56.52 h			
228.1 keV	10.70			
^{116m}In	54.0 m	95.72	1.57*E* + 02	2.11*E* + 03
416.9	24.20			
818.7	11.30			
1293.5	82.50			
2112.2	15.30			
^{24}Na	15.0 h	100	5.40*E* − 01	3.70*E* − 01
1368.6	100			
2754.0	100			
^{197}Hg	65.0 h	0.15	3.19*E* + 03	1.23*E* + 03
77.4	19.10			
191.4	0.50			
^{203}Hg	1130.0 h	29.80	4.90*E* + 00	4.00*E* + 00
279.2	81.00			
^{60}Co	1928.3 d	100	3.72*E* + 01	7.50*E* + 01
1173.2	99.88			
1332.5	100.00			
^{28}Al	138.6 s	100	2.34*E* − 01	1.55*E* − 01
1779.0	100			
^{42}K	12.4 h	6.70	1.45*E* + 00	1.35*E* + 00
1524.7	18.30			
312.8	0.31			
^{110m}Ag	6010.0 h	48.18	4.50*E* + 00	4.90*E* + 01
657.7	94.30			
744.3	4.88			
884.7	73.40			
937.5	35.20			
1384.3	25.20			
^{75}Se	2900.0 h	0.90	5.18*E* + 01	4.75*E* + 02
136.0	57.20			
264.7	60.85			
279.5	24.95			
121.1	17.65			
^{56}Mn	154.8 m	100	1.33*E* + 01	1.7*E* + 01
846.8	98.80			
2113.0	15.25			
1810.7	28.40			
^{76}As	26.3 h	100	4.30*E* + 00	7.50*E* + 01
559.1	42.90			
657.0	5.80			

Table VII. (*Continued*)

isotope & γ-ray energy	halflife & absolute intensity of γ-ray, %	% abundance	thermal cross section, barns	resonance integral, barns
1228.5	1.10			
2096.2	0.56			
^{122}Sb	65.76 h	57.25	$6.56E + 00$	$2.09E + 02$
564.1	71.20			
692.8	3.98			
1140.5	0.86			
^{124}Sb	1450.0 h	42.75	$4.26E + 00$	$1.29E + 02$
602.7	97.90			
1690.9	48.10			
722.8	10.74			
645.8	7.38			
^{86}Rb	449.0 h	72.17	$4.60E - 01$	$4.81E + 00$
1076.8	8.76			
^{64}Cu	12.8 h	69.09	$4.50E + 00$	$6.10E + 00$
1345.8	0.48			
^{66}Cu	306.0 s	30.91	$2.16E + 00$	$2.30E + 00$
1039.2	9.00			
833.5	0.34			
^{52}V	225.7 s	99.75	$4.88E + 00$	$2.90E + 00$
1434.0	100			
^{46}Sc	83.7 d	100.00	$2.60E + 01$	$1.20E + 01$
889.3	100.00			
1120.5	100.00			

[a] These values for the thermal and resonance cross sections make the Ru concentration calculated from ^{105}Ru coincide with those calculated from ^{97}Ru and ^{103}Ru for any reactor irradiation. [b] h = hour, m = minute, d = day, s = second.

from the activities of ^{197}Hg and ^{203}Hg almost certainly belongs in this class in view of the small resonance integral to thermal cross section ratio for both isotopes, since even a grossly inaccurate F ratio would not greatly affect the concentrations calculated. Other discrepancies are more baffling, like those for the two antimony isotopes ^{122}Sb and ^{124}Sb, for ^{76}As, ^{110m}Ag, and ^{239}U. All of these isotopes have large resonance integral/thermal cross section ratios, and for some of them the nuclear constants are known particularly well. Thus the most likely source of the errors ought to be an incorrect F ratio used in the calculation. This simple assumption, however, does not explain all of the facts, to wit:

(1) The relative standard deviation between the concentrations of ruthenium calculated from the activities of its three isotopes is reproducibly less than 1%, using the nuclear constants as listed in Table VII, and is *independent* of the actual composition of the neutron spectrum in which the ruthenium was irradiated (e.g., light vs. heavy water moderated reactors); in addition, the calculation yields the correct weight of the ruthenium, indicating that the determination of the thermal flux via the iron monitor is also acceptable. These observations simply must mean that the ruthenium monitor correctly measures the F ratio as seen by the resonances of its three isotopes.

(2) The concentrations of isotopes with low resonance integral/thermal cross section ratios are calculated correctly, proving again that the magnitude of the thermal flux assumed for the calculations is correct.

(3) The relative error in the concentration calculation is larger for large ratios of resonance integral to thermal cross section; however, this relative error appears to be independent of the ratio of thermal to resonance flux present during irradiation, i.e., of the ratio of thermal to resonance activation.

The ruthenium isotopes sample the resonance flux at much higher energies than does gold with its low lying resonance at 4.9 eV. It seems probable that this fact somehow constitutes the reason for the observed discrepancies, perhaps because of deviations of the resonance flux from its theoretical $1/E$ dependence. Such deviations from the $1/E$ shape have been noted by several authors (*7–12*), and an epithermal flux distribution proportional to $1/E^{1+m}$ has been proposed. Bereznai et al. (*12*) suggest that m is a negative quantity inside the core, and changes to a positive quantity in the (graphite) reflector. Ryves (*9*) states: "Well moderated systems containing hydrogen or deuterium have a nearly zero value of "m", but for graphite moderated assemblies "m" may vary from −0.1 to +0.1 . . ., which will have a pronounced effect on the relative resonance integral measured in these geometries". All of our measurements were carried out in the reflectors of the various reactors used, thus some deviation from a $1/E$ shape of the resonance flux was to be expected. Positive values of m would produce effects of the observed magnitude using the formalism suggested by Bereznai and MacMahon in a recent report (*13*); it should be noted, however, that negative values of m were observed in the reflector in that work, contrary to the predictions in Reference 12. Thus there does not seem to exist at this time an unambiguous treatment to take these deviations from a $1/E$ shape into account. From the practical point of view, however, application of empirical corrections factors appears to be adequate, at least for irradiation positions at core face or in a graphite reflector. Our results indicate that these correction factors were invariant for the three different reactors used.

CONCLUSIONS

Parametric counting in conjunction with flux determinations by means of the Fe-Ru monitor couple gives concentration values for isotopes with not too large resonance integral/thermal cross section ratios, R, which are in fair agreement with those obtained by relative measurements using SRMs, and which are certainly adequate for survey work. At large values of R, systematic deviations of the calculated concentrations towards too low values are observed. "Large" refers to R values of about 10 or larger. The percentage by which the concentration is found too low depends on the individual isotope and appears to increase with increasing values of R, though the largest deviation was observed for antimony with $R = 31$, not for uranium with $R = 100$. Our experience with isotopes with large R values has been that for a given isotope the concentration is *always* found too low by the same percentage, *independent* of the composition of the reactor flux in which the sample was irradiated. We do not understand the reason for this behavior, but we can arrive at the approximately correct concentration values by multiplication with an empirical factor. For antimony (both isotopes) this factor is 1.923, for gold it is 1.119. Values for ^{76}As, ^{109}Ag, ^{99}Mo(Tc), ^{72}Ga, and ^{75}Se are 1.652, 1.535, 1.802, 1.300, and 1.413 respectively.

We carried out a flux determination run simultaneously utilizing Fe-Ru couples and cadmium measurements on gold. The resonance flux is definitely found lower from the gold data. Concentration calculations from the Fe-Ru flux data (and using empirical correction factors for isotopes with large *R* ratios) were better than on the basis of cadmium-ratio and -difference measurements on gold; however, our experience with cadmium measurements is far too limited for any sweeping statements. We do not claim that determination of the actual epithermal flux distribution via the high-lying resonances of the three ruthenium isotopes yields necessarily a more accurate value than can be obtained via the low-lying resonances of ^{197}Au. We have, however, developed an internally consistent approach which yields the correct concentration values for all elements.

Parametric counting provides an easy way of determining molybdenum or certain rare earths in the presence of uranium, utilizing the known relative fission yields for the isotopes in question.

ACKNOWLEDGMENT

We are indebted to Norman Holden and others at Brookhaven National Laboratory and to Ronald Fleming of the National Bureau of Standards for very helpful discussions. Thanks are due to Richard Cashwell of the Nuclear Engineering Department at the University of Wisconsin for performing the irradiations carried out there, and for permission to use his measuring equipment. Appreciation is expressed to L. D. Blitzer, B. E. Prescott, and D. L. Malm for quantitative analysis of the Al(Au) and the iron foil monitors, and to A. M. Mujsce for the thermogravimetric analysis of the gelatin samples.

LITERATURE CITED

(1) P. F. Schmidt and D. J. McMillan, *Anal. Chem.*, **48**, 1962 (1976).
(2) D. H. Anderson, J. J. Murphy, and W. W. White, *Anal. Chem.*, **48**, 116 (1976).
(3) D. H. Anderson, J. J. Murphy, and W. W. White, *Eastman Org. Chem. Bull.*, **49**, 1 (1977).
(4) P. F. Schmidt and J. E. Riley, Jr., "Determination of the Natural Abundance of Iron-58 by Neutron Activation Analysis", *Anal. Chem.*, see paper in the Aids for Analytical Chemists section.
(5) P. F. Zweifel, *Nucleonics*, **18**, (11), 174 (1960).
(6) R. Kirkland, Georgia Institute of Technology Research Reactor, private communication.
(7) K. W. Geiger and L. van der Zwan, *Metrologia*, **2**, 1 (1966).
(8) T. B. Ryves and E. B. Paul, *J. Nucl. Energy*, **22**, 759 (1968).
(9) T. B. Ryves, *Metrologia*, **5**, 110 (1969).
(10) P. Schumann and D. Albert, *Kernenergie*, **8**, 88 (1965).
(11) J. W. Connolly, A. Rose, and T. Wall, **AAEC/TM 191** (1963).
(12) T. Bereznai, D. Bódizs, and G. Keömley, *J. Radioanal. Chem.*, **36**, 509 (1977).
(13) T. Bereznai and T. D. MacMahon, University of London Reactor Centre, Research Report, August 1977.

RECEIVED for review May 17, 1978. Accepted November 3, 1978.

Comparison of the Determination of Cobalamins in Ocean Waters by Radioisotope Dilution and Bioassay Techniques

G. M. Sharma,* Henry R. DuBois, Albert T. Pastore, and Stephen F. Bruno

New York Ocean Science Laboratory, Montauk, New York 11954

Application of two radioisotope dilution techniques to the direct determination of cobalamins in 1 mL of seawater is described. These techniques give results which are approximately 4–10 times higher than the results obtained by the standard microbiological assays. The disparity in results obtained by the biological and isotopic methods is explained by suggesting that the later technique measures both biologically active and inactive cobalamins indiscriminately. The combined sensitivity range of the two isotopic methods described in this paper is 0.5–400 pg B_{12}/mL. The accuracy ($X_i - \hat{X}$) of individual values at the 1.0 pg/mL level was found to lie in the range of 0.1–0.2 pg.

The concentration of cobalamins in ocean waters is usually measured by microbiological techniques (*1*). Although these techniques are highly sensitive (range: 0.05–3 ng B_{12}/L) they are technically tedious and time consuming. Furthermore, the precision of the bioassays depends largely upon the presence or absence of inhibitors in the samples being analyzed. Because of these drawbacks of the biological methods, there is need for a technique for the determination of cobalamins in seawater which should not only be rapid and highly sensitive but must also be immune to the presence of inhibitors in the medium. Several radioisotope dilution techniques developed for the determination of vitamin B_{12} in plasma have been shown to be endowed with these characteristics (*2, 3*). Recently one of these techniques has been used for the determination of benzyl alcohol extractable cobalamins from ocean waters (*4*). In this paper, we report our experience and results obtained in applying two radioisotope dilution techniques to the direct determination of cobalamins in a small volume (1.0 mL) of ocean waters.

The two isotopic methods tested for the determination of cobalamins in ocean waters are called competitive binding and sequential saturation analysis (*5, 6*). The B_{12}-specific binder used in the experiments was the porcine intrinsic factor (IF). Comparison of these IF-based radioassays with a standard biological assay (*1*) revealed that the former techniques give substantially higher values for the concentration of cobalamins in ocean waters. One explanation of unexpectedly higher values obtained by isotopic methods would be that these techniques measure the sum of the concentration of all cobalamin and cobalamin-like molecules. The cobalamin-like molecules may have been produced by environmental degradation of various naturally produced B_{12} molecules.

EXPERIMENTAL

Apparatus. Radioactivity was measured with a Beckman Gamma 8000 Counting System. This instrument has a factory

0003-2700/79/0351-0196$01.00/0 © 1979 American Chemical Society

installed program to give % bound radioactivities directly. Reagents used in the experiments were pipetted with a Schwarz/Mann biopipet. Polypropylene tubes (12 × 75 mm), logit-log graph papers, and a Cornwall 2 cm^3 syringe for adding aqueous charcoal suspension were purchased from Becton-Dickinson Co., Mountain View Ave., Orangeburg, N.Y. 10962. Whatman GF/C filter pads and 0.45-μm membranes for filtering seawater were obtained from VWR Scientific Company and Amicon Company.

Chemicals. Norite A (decolorizing charcoal) for stripping seawater and Human Serum Albumin (HSA) of cobalamins was purchased from Fisher Scientific Co. The unlabeled vitamin B_{12} was from Sigma Chemical Co. Lyophilized porcine intrinsic factor (IF), RIA grade charcoal, and aqueous solutions of ^{57}Co-labeled B_{12} containing 0.01% KCN were purchased from Becton and Dickinson Co. The concentration of KCN in labeled B_{12} solutions was considered to be sufficient to release cobalamins from endogenous protein binders when mixtures of 200 μL of labeled-B_{12} and 1.0-mL aliquots of the unknown samples were heated at 100 °C for 15 min. The 30% sterile HSA solution was purchased from Calbiochem, San Diego, Calif. 92112.

Reagents. *Vitamin-free Seawater.* One liter of seawater was obtained from the same area where samples to be analyzed were collected. This seawater was made vitamin-free by shaking with Norite A as described in the literature (7).

Vitamin-free HSA. To 3.0 mL of 30% HSA placed in a well cleaned plastic tube, 24 mL of sterile distilled water and 3.0 mL of 0.48 N HCl were added. The resulting solution was heated at 100 °C for 15 min. The reaction mixture was brought to room temperature and 0.5 g of Norite A added to it. The suspension was vortexed and left at room temperature for 30 min. After centrifugation, the clear HSA solution was decanted and filtered through a 0.22 μm millipore filter. The filtrate was stored aseptically at 4 °C. Standard tests revealed that the 3% HSA solution thus prepared contains neither vitamin B_{12} nor B_{12} binding factors.

Charcoal Suspension. The RIA grade charcoal, 1.25 g, was added to 100 mL of sterile distilled water. The suspension was stirred at 4 °C for 30 min before and during use. The unused suspension was stored at 4 °C for later use.

0.01 N KCN and 1 N HCl. These were prepared from reagent grade KCN and concentrated hydrochloric acid using sterile distilled water. The solutions were stored in glass bottles at room temperature.

Unlabeled B_{12} Standard Solutions. Serial dilutions of stock solution containing 100 mg B_{12}/L with sterile vitamin-free seawater gave working solutions containing 0.5–400 pg B_{12}/mL. The concentration of the stock solution was routinely checked by measuring extinctions at 278, 361, and 550 nm.

Competitive Binding Experiments. *(A) Preparation of the Standard Curve.* For duplicate runs, 18 sequentially numbered polypropylene tubes were arranged in pairs. One milliliter of sterile vitamin-free seawater was added to each tube of pairs 1 and 2. Using standard solutions, progressively increasing amounts (5, 10, 20, 50, 100, 200, and 400 pg) of unlabeled B_{12} were added to the tubes of pairs 3–9. Then 200 μL (50 pg) of labeled B_{12} and 100 μL of 1 N HCl were added to all tubes. After mixing, the tubes were allowed to stand at room temperature for 15 min. Final reagents to be added were: 400 μL of HSA to all tubes and 200 μL of intrinsic factor to pairs 2–9 only. After centrifugation, the supernatants which contained only complexed B_{12} were decanted and counted in a Beckman Gamma 8000 counting system to give % bound radioactivities directly. The logit-log plot of % bound radioactivities vs. pg unlabeled B_{12}/mL was a straight line (slope: −2.30; y-intercept: 4.20). The correlation coefficient for the regression line was 0.99.

In a separate experiment, the contents of the tubes after the addition of 1 N HCl and labeled B_{12} were heated at 100 °C for 15 min and then reacted with the intrinsic factor. The standard curve constructed from the data of this experiment was identical with the one obtained in the first experiment.

(B) Determination of Cobalamins in Seawater by Competitive Binding Technique. These determinations were carried out simultaneously with the preparation of the standard curve. The seawater samples were collected from the Peconic Bay estuary, Long Island, N.Y. The sampling stations were located throughout the estuary ranging from the mouth of the Peconic River (samples 1 and 2, Table I) to Cedar Point, East Hampton (samples 3–10). The samples were first filtered through GF/C filter pads and then through 0.45-μm Aminco filter membranes. One-milliliter aliquots of the filterates, 100 μL 1 N HCl and 200 μL labeled B_{12} were placed in two sets of paired polypropylene tubes. After mixing, one set of tubes was kept at room temperature and the other set was heated at 100 °C for the same period of time. The set heated at 100 °C was cooled to room temperature in a running water bath. Same amounts of HSA and intrinsic factor as used in the preparation of the standard curve were added to the tubes of both sets. After an incubation period of 30 min, % radioactivities bound to the intrinsic factor were determined and the concentrations of cobalamins were read from the standard curve. Columns 1 and 2 of Table I represent the results of duplicate analyses of 10 seawater samples carried out by incubating the samples with cyanide ions (present in labeled B_{12}) and HCl at room temperature and 100 °C, respectively.

Sequential Saturation Analysis. *(A) Standard Curve.* To obtain data in duplicate, 16 sequentially numbered polypropylene tubes were arranged in sets of two. One milliliter of vitamin-free seawater was added to each tube of sets 1 and 2. Using standard solutions, progressively increasing amounts of unlabeled B_{12} (0.5, 1, 2, 4, 6, 8, 12, and 15 pg) were added to the tubes of the remaining sets. Then 50 μL of 0.01% KCN and 200 μL of HSA solutions were added to all tubes. After mixing, the tubes were allowed to stand at room temperature for 15 min. Intrinsic factor, 50 μL, was added to tubes of sets 2–8 only and, after mixing, the tubes were incubated at room temperature for 30 min. Finally, 200-μL aliquots of ^{57}Co-B_{12} solution (50 pg, cpm = 6200) were added to all tubes and, after mixing, the contents of the tubes were incubated at room temperature for 45 min. The uncomplexed vitamin B_{12} was removed by adding 0.8 mL of charcoal suspension as described under competitive binding studies. After centrifugation, the supernatants which contained both labeled and unlabeled vitamin B_{12} bound to the intrinsic factor were decanted and the bound radioactivities measured. The bound counts in supernatants of tubes 1 and 2 were averaged and subtracted from the bound counts of supernatants of all other tubes. The plot of corrected bound counts (ordinate) vs. pg-unlabeled B_{12}/mL (abscissa) was a straight line (slope: −126. cpm/pg B_{12}; y-intercept: 3495 cpm). The absolute value of the slope of the regression line showed a high degree of agreement with the specific activity (124 cpm/pg) of labeled B_{12} used in the experiment.

(B) Determination of Cobalamins in Seawater Samples by Sequential Saturation Analysis. Seawater samples were diluted 1:10 with vitamin-free seawater. Aliquots, 50 μL, of the intrinsic factor were first reacted with 1.0-mL aliquots of the diluted samples and then with 200 μL of the ^{57}Co-B_{12} solution according to the procedures described under preparation of the standard curve. Radioactivities bound to the intrinsic factor were measured and the concentrations were determined by interpolation of the standard curve. The results were multiplied by 10 to express data as amounts per mL of the undiluted samples (See Table I, column 3).

Bioassays of Seawater Samples. The 10 seawater samples analyzed by isotopic methods were also bioassayed using clones 3H and 13-1 of the diatom *Thalassiosira pseudonana*. The procedure used was essentially the same as described by Carlucci (*1*). Glassware used for bioassays was cleaned in 3 N HCl, rinsed with distilled water, baked in a hot air oven at 250 °C for 4 h, and autoclaved for 20 min at 121 °C. Vitamin free seawater was prepared according to method described by Strickland and Parsons (*7*).

Samples for B_{12} (and B_{12} analogue) assay were dispensed in 5- or 10-mL aliquots into 50-mL microfernbach flasks (Bellco Inc.) with stainless steel caps. Each sample was diluted with 10 mL of vitamin free seawater (27–29‰) enriched with nutrients as described by Carlucci (*1*). External standards (calibration curve) for the bioassay contained 0, 0.1, 0.2, 0.4, 0.8, 1.0, 2.0, and 3.0 ng L^{-1} of vitamin B_{12}. Vitamin B_{12} was added to duplicate sets of each sample, resulting in an addition of 1 ng L^{-1}. These flasks served as internal standards to determine possible inhibition of the seawater to the assay organism. Flasks with samples, external standards, and internal standards were inoculated with ≈10^4 cells mL^{-1} of B_{12} depleted *T. pseudonana* cells.

The bioassay series was incubated in a temperature controlled room at 20 ± 1 °C below a bank of fluorescent lamps emitting 6000 lux. The assay was terminated after 5 days and vitamin B_{12} (and B_{12} analogue) concentrations were calculated on the basis of final cell density. Cell counts were made using a hemacytometer. The results of the analysis are collated in columns 4 and 5 of Table I.

RESULTS AND DISCUSSION

The determination of vitamin B_{12} by radioisotope dilution techniques has invariably been carried out in 0.9% NaCl solution (*8*). The salinity of seawater, on the other hand, lies in the range 2.8–3.5%. Major contribution to this salinity comes from chloride, sulfate, magnesium, potassium, calcium, and sodium ions. To evaluate the effect of the complex salt matrix of seawater on the precision and accuracy of isotopic methods, standard solutions of B_{12} prepared in charcoal-treated seawater were analyzed by competitive binding procedures (*4*). When experimentally determined %-IF-bound radioactivities were plotted vs. pg B_{12}/mL on a logit-log graph paper, a linear standard curve of slope −2.30 was obtained. The close correspondence of the slope of the experimental line to the theoretical value of −2.303 suggested (*9*) that the inorganic constituents of seawater do not interfere with the determination of vitamin B_{12} by the isotopic method. At an average standard deviation of ~10%, the detection limits of the competitive binding procedure were found to lie in the range 10–400 pg B_{12}/mL. The relative standard deviation at 5 pg/mL was ~30%. The competitive binding experiments designed to detect vitamin B_{12} at levels below 5 pg/mL were found to yield erratic results.

To develop a procedure capable of measuring the concentrations of B_{12} at levels below 10 pg/mL, standard solutions containing 0.1–50 pg B_{12}/mL were analyzed by the techniques of sequential saturation analysis (*6*). After several trials, the procedure described in the Experimental section was found to give IF-bound radioactivities which were inversely but linearly related to the concentration of B_{12} in the range 0.5–15 pg/mL. The regression line of IF-bound radioactivities, (Y), vs. the concentration of B_{12}, (X), was almost identical with the theoretical curve given by the equation $y = B_0 - sX$. In this equation, B_0 represents cpm bound to the intrinsic factor when the concentration of the unlabeled B_{12} was zero and the slope, s, is the specific activity of labeled B_{12} used in the experiment. The correlation coefficient for the regression line was 0.99.

By combining the results of the competitive binding and sequential saturation analysis, it may be concluded that seawater samples containing >0.5 pg cobalamins/mL can be directly analyzed for the concentration of this micronutrient by isotopic methods. In Table I, the results of the determination of cobalamins in 10 seawater samples by competitive binding, sequential saturation, and bioassay procedures are compared. Columns 1 and 2 of the table represent the data of the competitive binding experiments carried out by incubating the samples with KCN (present in the ^{57}Co-labeled B_{12} solution) at room temperature and at 100 °C, respectively. The samples were heated with KCN at 100 °C to free cobalamins from endogenous protein binders. For sequential saturation analysis, the samples were diluted 1:10 with charcoal-treated seawater. The results were multiplied by 10 to express data in amounts per mL of the undiluted samples (column 3). The clone 3H of the bioassay organism *Thalassiosira pseudonana* measures the sum of the concentrations of 5,6-dimethylbenzimidazole cobalamin (vitamin B_{12}), desdimethylbenzimidazole cobalamin, 5-hydroxybenzimidazole cobalamin, and 5-methylbenzimidazole cobalamin. Under the assay conditions, the clone 13-I of *T. pseudonana* measures the sum of 100% concentration of cobalamins listed above, 50% concentration of Factor B (B_{12} without the nucleotide), and up to 50% concentration of analogues of B_{12} containing, instead of benzimidazole, adenine (pseudo-B_{12}) and substituted adenine (e.g., 2-methyladenine) as the nucleotide (*10*). To obtain a rough estimate of the total concentration of Factor B, pseudo-B_{12} and other analogues of B_{12} in seawater samples, the difference between the values reported in column 4 and 5 of Table I should be multiplied by 2.

Table I. Comparison of the Results of Cobalamin Determinations of Seawater Samples by Isotopic and Bioassay Techniques[a]

	isotopic methods			bioassay	
	competitive binding				
sample no.	room temp.	100 °C	sequential saturation	*T. pseudonana*, 3H	*T. pseudonana*, 13-I
1	41.5	56.0	39.5	6.4	11.2
	46.0	52.0	38.0	4.8	10.4
2	53.0	55.0	31.0	<.05	13.8
	55.0	57.0	32.0	<.05	12.6
					12.0
3	23.8	26.5	19.5	1.8	4.9
	23.8	24.0	21.5	3.8	5.1
4	19.5	19.5	24.0	3.6	3.4
	20.2	--	27.5	4.0	3.4
					2.6
5	24.4	25.0	19.5	1.9	3.8
	23.4	25.2	27.5	3.1	3.3
					4.5
6	24.0	25.0	23.0	1.9	2.6
	19.6	24.0	23.5	2.9	2.6
					3.5
7	28.0	28.5	21.5	6.1	3.2
	27.7	26.5	26.0	6.5	2.9
					3.4
8	21.5	20.5	24.5	5.0	2.8
	18.8	22.0	21.0	7.0	2.8
					2.4
9	17.5	20.5	27.0	1.6	3.8
	19.0	21.0	23.0	2.6	3.9
					3.8
10	20.5	21.8	26.0	0.6	3.6
	18.5	23.5	21.0	0.6	3.6
					3.4

[a] The data by isotopic methods were collected in duplicates. The bioassays were carried out either in duplicate or triplicate. The results are reported as pg cobalamin/mL.

Recently, Beck (*4*) reported a competitive intrinsic factor binding assay technique for the determination of cobalamins in natural waters. In this technique, the seawater samples are first extracted three times with a small volume of benzyl alcohol. The combined benzyl alcohol extracts are then extracted with water and the aqueous phase thus obtained is used for the determination of cobalamins by the isotopic method. Interestingly, levels of cobalamins in seawater found by us using direct procedures are similar to those reported by Beck using the preconcentration procedure.

A comparison of the data reported under columns 1 and 2 of Table I revealed that there is no significant increase in the concentration of cobalamins when the samples are heated with KCN at 100 °C for 15 min. This suggests that either these samples contain no B_{12}-protein complexes or the cyanide extraction procedure used in the experiments is not vigorous enough to liberate cobalamins from their complexes.

The correspondence between the results of the analysis of samples 3–10 by competitive binding and sequential saturation analysis is within acceptable limits. The reason for the low values obtained for the concentrations of cobalamins in samples 1 and 2 by sequential saturation analysis is not clear. It may be noticed that compared to clone 13-I, the clone 3H of *T. pseudonana* gives higher values for the concentration of cobalamins in samples 7 and 8. These results are reverse of what is expected from the cobalamin specificities of the two bioassay organisms (*vide supra*). One explanation of these unexpected findings would be that the samples 7 and 8 contain ectocrines which inhibit the growth of clone 13-I but not that of 3H. In case the ectocrines are growth promoting substances, then they would be enhancing the growth of clone 3H specifically. The most important finding of this investigation is that, compared to bioassays, the isotopic methods give 4–10 times higher values for the concentrations of cobalamins. The disparity in the results of these methods may be explained as follows.

It has been reported that vitamin B_{12}, its various analogues and transformation products (e.g. lactam B_{12}, lactone B_{12}, etc.) all compete on almost an equal basis for binding to the porcine intrinsic factor (*11*). It may then be expected that isotopic methods would determine the sum of the concentration of all these molecules. Of the cobalamins detectable by isotopic methods, the transformation products of vitamin B_{12} and its analogues exhibit little or no biological activity. In view of this, it may be suggested that out of 18–50 pg/mL of cobalamins and cobalamin-like molecules determined by the isotopic methods only 25–40% are vitamin B_{12}, pseudo-vitamin B_{12}, and their analogues. The remaining 60–75% of the material may be a mixture of transformation products formed by the action of light and seawater on cobalamins. However, the possibility cannot be excluded that this 60–75% of the material may actually be some types of biologically produced cobalamins which are not utilized by the bioassay organisms used in these investigations. What is the actual chemical nature of this material and what is its ecological role is a subject of future research.

LITERATURE CITED

(1) A. F. Carlucci, "Handbook of Phycological Methods", J. R. Stein, Ed., Cambridge University Press, 1973, pp 387–394.
(2) D. M. Mathews, R. Gunasegaram, and J. C. Linnel, *J. Clin. Pathol.*, **20**, 683–685 (1967).
(3) H.-Y. Shum, A. M. Streeter, B. J. O'Neill, and M. C. Path, *Med. J. Aust.*, **1**, 1144–1148 (1970).
(4) R. A. Beck, *Anal. Chem.*, **50**, 200–202 (1978).
(5) A. Zettner, *Clin. Chem.* (*Winston-Salem, N.C.*), **19**, 699–705 (1973).
(6) A. Zettner and P. E. Duly, *Clin. Chem.* (*Winston-Salem, N.C.*), **20**, 5–14 (1974).
(7) J. D. H. Strickland and T. R. Parsons, "A Practical Handbook of Seawater Analysis", J. C. Stevenson, Ed., Fisheries Research Board of Canada, Ottawa, 1968.
(8) K. S. Lau, C. Gottlieb, L. R. Wasserman, and V. Herbert, *Blood*, **26**, 202 (1965).
(9) David Rodbard, *Clin. Chem.* (*Winston-Salem, N.C.*), **20**, 1255–1270 (1974).
(10) R. R. L. Guillard, *J. Phycol.*, **4**, 59–64 (1968).
(11) M. B. Bunge and R. F. Schilling, *Proc. Soc. Exp. Biol. Med.*, **96**, 587 (1957).

RECEIVED for review May 19, 1978. Accepted October 30, 1978. Work supported by New York State Contract No. C114053 and by grants from Nassau and Suffolk Counties. NYOSL Contribution No. 97.

Enzymatic Determination of Urea in Serum Based on pH Measurement with the Flow Injection Method

J. Ruzicka,* E. H. Hansen, and Animesh K. Ghose[1]

Chemistry Department A, The Technical University of Denmark, Building 207, DK-2800 Lyngby, Denmark

H. A. Mottola

Department of Chemistry, Oklahoma State University, Stillwater, Oklahoma 74074

A method based on the Flow Injection Analysis system incorporating a flow-through capillary pH-electrode is described and used for the enzymatic determination of urea in aqueous and serum samples. By maintaining a constant buffering capacity of the carrier stream solution, a linear relationship between the recorded pH signal and the urea content is obtained. Attaining the analytical readout within 30 s of sample introduction, the sampling rate was 60 samples per hour and the reproducibility of measurement was ±0.0029 pH unit corresponding to ±0.52%. When soluble urease was used in the carrier stream, the consumption was 25 units per analysis. The possibility of further reducing the enzyme consumption by using the merging zone principle in the Flow Injection stop-flow system is discussed.

Many enzyme catalyzed reactions involve proton exchange with the background electrolyte. Therefore, a pH sensor is the most appropriate as well as the simplest monitoring detector as it does not require an additional coupling of the primary reaction to an indicator reaction, such as, e.g., NAD-NADH. The drawbacks of pH sensing are, however, serious because (a) the resulting pH change may inhibit the enzyme function; (b) the pH response is a logarithmic function of the analyte concentration; and (c) any buffer present in the background electrolyte affects the pH response.

The first drawback is the least serious one since, as the pH change is usually small, one can design the chemistry so that only the initial part of the reaction is used for determination; but above all, by handling the process of mixing and measuring automatically, the small undesired influence of inhibition can be built into the calibration curve because each sample is handled in exactly the same way.

The second drawback of the pH electrode sensing is more serious as the logarithmic response is inherently less reproducible—an objection often made to all ion-selective electrode measurements—and very difficult to use, e.g., for derivative techniques where the measurement has to be made at a fixed signal level, while the fixed time method using a system with a *logarithmic* response is not readily applicable (*1*).

---

[1] Present address: Department of Chemistry, University of Allahabad, Allahabad-211002, India.

0003-2700/79/0351-0199$01.00/0 © 1979 American Chemical Society

As enzymatic assays are of principal interest in clinical and biochemical analyses, where sample materials frequently contain several buffer systems in different concentrations, one inevitably encounters considerable and *variable* background effects which can be summarized as a variable blank affecting both the position as well as the slope of the calibration curve.

Apart from these drawbacks, yet another group of well known difficulties is encountered if the enzymes are used on an immobilized form, whether contained in columns (*2–5*), tubular reactors (*6*) (where the enzymes are attached to the tube walls), or sensors covered by enzyme layers (such as enzyme amperometric (*7*) or potentiometric (*8*) electrodes, or enzyme covered thermistors (*9, 10*)). To avoid this second group of problems, it was decided to use a soluble enzyme in this work. This approach is justified not only because urease is rather inexpensive, but mainly because the recently designed multiinjection technique (*11*) allows the use of the merging zones principle (*12*) in Flow Injection enzymatic analysis (*13, 14*) where as little as 0.5 unit of enzyme in 25 μL of reagent solution is consumed per determination (*15*).

It was Mosbach and his co-workers (*16, 17*) who first made an enzyme electrode based on pH measurements with the conventional hydrogen ion glass electrode covered with a layer of gel (or trapped liquid) containing glucose oxidase, urease, or penicillinase. Already in this pioneering work, the influence of varying the background buffer concentration was observed and later confirmed in a more detailed study on the penicillinase electrode (*17*), which was used in practice for the continuous control of fermentation processes. Their sensor was reported to have a logarithmic response and was affected both by the buffering capacity within the enzyme layer as well as by the measured fermentation liquid.

However, a linear response can be obtained in two ways, both being based upon the concept of the buffering capacity

$$\beta = \mathrm{d}C_\mathrm{B}/\mathrm{dpH} \tag{1}$$

that is, this can be achieved either: (a) by keeping pH constant and volumetrically determine the amount of base (or acid) $\mathrm{d}C_\mathrm{B}$ used in the course of a measurement; or (b) by keeping the buffering capacity β constant and measure the pH change which thus becomes a linear function of the amount of protons produced or consumed.

The most recent example of the first approach is the work of Adams and Carr (*5*) who used an electrochemical pH stat (where protons were generated coulometrically) in connection with tubular and column reactors containing immobilized urease. Apart from the usual difficulties associated with the use of an immobilized enzyme, this careful study confirmed the interfering effect of variable buffering capacity of individual samples, which in the case of serum was exaggerated to such a degree that the determination of urea could not be practically performed.

The second approach was first used by Papariello and co-workers (*4*) who designed an immobilized enzyme continuous flow system in which the pH changes on a stream of constant buffering capacity were measured. Although their sample turnover was low (6 samples/h), sample consumption high (1.5 mL), and the blank so variable that they had to resort to clean-up by dialysis, their work indeed confirmed that one can obtain a useful linear range, and their theory correctly predicts the main factors influencing the readout.

When measuring with the glass electrode in the Flow Injection system, the recorded peak height reflects the pH increase between the base line $\mathrm{pH_{base\ line}}$ and the $\mathrm{pH_{max}}$ measured atop a peak:

$$\mathrm{dpH} = \mathrm{pH_{max}} - \mathrm{pH_{base\ line}} = \mathrm{d}C_\mathrm{B}\cdot 1/\beta \tag{2}$$

and this response can be related to the substrate concentration by means of the Michaelis equation:

$$\frac{\mathrm{d}P}{\mathrm{d}t} = \frac{V_\mathrm{m}S}{K_\mathrm{m} + S} \tag{3}$$

where P is the product concentration, t is the reaction time, K_m is the Michaelis constant, and S is the substrate concentration, while V_m is the maximum velocity of the reaction. Using an excess of enzyme ($K_\mathrm{m} \gg S$) and relating $\mathrm{d}P$ to $\mathrm{d}C_\mathrm{B}$ ($\mathrm{d}P = (1/q)\mathrm{d}C_\mathrm{B}$), one obtains—in the case that the product is a base—the expression:

$$\mathrm{dpH} = Sq\mathrm{d}t\frac{V_\mathrm{m}}{K_\mathrm{m}}1/\beta \tag{4}$$

where $\mathrm{d}t$ is the resident time T of a sample plug in the Flow Injection Analyzer (*13*) and q is a constant.

Equation 4 predicts that there will be a *linear* relationship between peak height (dpH) and substrate concentration (S), provided that the pH change is measured at the initial stages of the reaction with sufficient activity of enzyme present (i.e., that the $V_\mathrm{m}/K_\mathrm{m}$ ratio is constant). It also follows that an increase of the buffering capacity will decrease the slope of the calibration line. Thus high β is clearly undesirable, yet its *constancy* is a prerequisite for obtaining a linear response, since at very low or no buffering capacity, the electrode response would be logarithmic:

$$\mathrm{pH} = \mathrm{const} + \log S \tag{5}$$

where $S = k[\mathrm{OH^-}]$ (if the product is a strong base) leading to:

$$\mathrm{pH} = \log S - \log K_\mathrm{w} - \log k \tag{6}$$

Therefore, depending on the ratio between the buffering capacity and the amount of base (or acid) produced by the enzymatic reaction the calibration curve will have a shape described by Equation 4 or 5 and will also have a region of a mixed type of response.

In order to obtain the widest possible range of linear response (Equation 4) and maximum slope of the calibration curve, the buffer selected as carrier stream should have a pK value close to the $\mathrm{pH_{max}}$ value generated by the enzymatic conversion of a sample of medium concentration (i.e., in clinical analysis that of a normal sample), and its maximum buffering capacity β_max (= 0.576 c) should be equimolar with the amount of base (or acid) generated from the least concentrated sample. The pH of the carrier stream containing this buffer should then be adjusted (by addition of strong acid or base) to be 0.2 pH unit from this carrier buffer pK value in the *opposite* direction than the expected pH change. In this way β_max will be 94.8% at the base line, 100% for a typical or normal sample, and will decrease again to 94.8% when $\mathrm{pH_{max}} = \mathrm{pH_{base\ line}} + 0.4$ (88.9% β_max at $\mathrm{pH_{max}} = \mathrm{pH_{base\ line}} + 0.5$)(*18*). If there is another buffer present in various amounts in the individual samples, an additional requirement arises, that is, that the buffering capacity of this interfering buffer must be much smaller than that of the carrier stream so that its variations do not affect the overall buffering capacity of the carrier stream. This can be achieved by two means: (a) by diluting the sample solution by the carrier solution prior to injection; (b) by choosing a carrier buffer with a pK value and a pH-base-line value which both are much different from the pK of the buffer present in the sample solution.

Thus if the pK of the interfering buffer differs by 2 pH units from the pK of the carrier stream buffer, the interfering buffer will have 25 times lower buffering capacity even if both buffers have the same molarities (for 1.5 pH units difference, the buffering capacity will be ten times lower).

In clinical analysis, the main interfering buffer is bicarbonate (pK_1 = 6.3, pK_2 = 10.3) and therefore the pK of

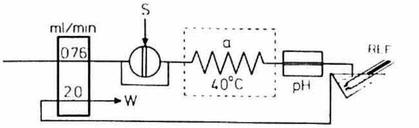

Figure 1. Flow Injection Analyzer for the enzymatic determination of urea by pH measurement. (S) Injection rotary valve (30 μL) furnished with a bypass, (a) reaction coil (0.75 m long, 0.5-mm i.d.) placed in a thermostated water jacket; (pH) capillary glass flow-through electrode; (REF) reference electrode. The overflow from the reference electrode vessel is pumped to waste (W). All connecting lines were 0.5-mm i.d. (D_t = 3.2, T = 30 s)

the carrier stream buffer should be around 8. For the determination of urea in the range of 2 to 20 mmol/L, the buffering capacity should be around 0.5 mmol/L to allow for the noncomplete enzymatic conversion of substrate. By choosing Tris as carrier buffer (K = 8.06 at 25 °C; 7.72 at 37 °C) and $\text{pH}_{\text{base line}}$ = 7.70, the above requirements will be fulfilled as during the enzymatic conversion of urea: $H_2NCONH_2 + 2H_2O + H^+ \rightleftharpoons 2NH_4^+ + HCO_3^-$, one proton is consumed, and this results in a shift of the pH through the region of maximum buffering capacity. By diluting the serum sample in the ratio 1:5 with 1 × 10^{-3} M Tris adjusted to pH 7.7 (β = 0.5 mmol/L), the typical serum sample will yield a concentration of 4 mmol of bicarbonate/L which at this pH will correspond to a buffering capacity of approximately 0.3 mmol/L, and this value will further decrease with increasing pH. Therefore, the buffering capacity will remain practically constant within the measuring range as the pK of the principal buffer (Tris) is situated almost exactly halfway between the two pK values of the interfering buffer. Additionally, the dispersion in the Flow Injection system which is a result of mixing of carrier solution and sample zone, will further affect the ratio between the interfering buffer and the carrier stream buffer in favor of the latter one. Thus in the system depicted in Figure 1 the total dispersion (D_t) measured by the color method (*18*) was found to be 3.2, i.e., while β_{buffer} remains constant $\beta_{\text{interf.}}$ will decrease to approximately one third of the nominal value of the diluted serum samples.

The presence of bicarbonate, however, will also influence the starting pH, which would be different from the $\text{pH}_{\text{base line}}$ of the carrier stream containing only Tris. Therefore, the peak height dpH must be corrected for the blank, pH_{blank}, to obtain the correct answer for the urea content:

$$\text{dpH} = \text{pH}_{\text{max}} - \text{pH}_{\text{blank}} = S\cdot\text{const} \qquad (7)$$

EXPERIMENTAL

The peristaltic pump was a four channel ISMATEC Minipuls, type 840. The pH electrode was a capillary glass Radiometer G299 A, of the type commonly used for blood gas measurement. The electrode was checked in the Flow Injection system by injecting 2 Radiometer Precision Buffer Solutions (S1510, pH = 7.383, and S1500, pH = 6.841). It is important to note that to avoid electrical noise the thermostating solution surrounding the pH glass capillary was made conductive by addition of KNO_3 (to ~0.5%) and electrically connected to the reference socket of the pH meter. The calomel reference electrode, type K401, the pH meter, type 64, as well as the Servograph recorder, type 310, furnished with an REA unit 100, were all made by Radiometer. A Heto thermostat 05E623 was used as a supply of circulating thermostated water. The injection valve was of the rotary type with a volumetric bore of 30 μL, furnished with a bypass of 10-cm, 0.5-mm i.d. polyethylene tubing (*13*). The Flow Injection manifold is described in detail in Results and Discussion.

Reagents. The carrier buffer solution containing 1 × 10^{-3} M Tris in 0.14 M NaCl had a pH of 7.70 and was prepared daily from a stock buffer by 50-fold dilution with 0.14 M NaCl. The stock buffer was made by mixing 50 mL of 0.1 M Tris (containing 12.114 g L^{-1} of Tris(hydroxymethyl)aminomethane) with 36.6 mL of 0.1 M HCl making the volume to 100 mL with distilled water (*18*).

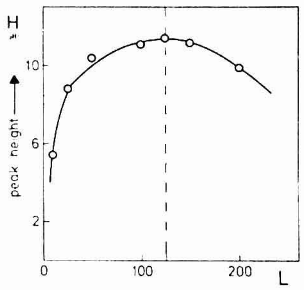

Figure 2. Dependence of the peak height H (i.e., dpH) on the reaction coil length L (in cm). Note that the peak height increases with increasing resident time (T), passes through a maximum at L = 125 cm, and then decreases because of the prevailing effect of the sample zone dispersion (D_t)

The urea standards were, for the preliminary experiments, prepared from a reagent grade urea (Merck) by dissolving the appropriate amount of urea in 0.14 M NaCl to obtain a 100 mM stock solution. For serum analyses, however, this stock solution was further diluted by a 0.14 M NaCl–0.02 M $NaHCO_3$ solution to obtain standards in the range of 4.0 to 20.0 mM urea. Both types of standards were, *prior* to injection, diluted 1:5 with the carrier solution.

The urease (Worthington Biochemical Corp.) contained 110 units/mg and was dissolved in the carrier solution in an amount of 30 mg/100 mL.

The serum standards were Monitrol I (lot LTD 144) and Monitrol II (lot PTD 46A), reconstituted according to manufacturers' instruction (Dade and Merz, Bern). It was, however, found that while Monitrol I contained the specified amount of bicarbonate (12 mM after reconstitution) Monitrol II did not contain any bicarbonate (it was not stated as a constituent either). For this reason, Monitrol I was dissolved in distilled water, while Monitrol II was dissolved in 0.02 M $NaHCO_3$ solution.

RESULTS AND DISCUSSION

All measurements were executed in the very simple experimental setup schematically shown in Figure 1. The carrier stream was pumped by the small peristaltic pump at a rate of 0.76 mL/min continuously through the injection valve which was furnished with a bypass (10 cm-long, 0.5 mm-i.d.) and which had a volumetric bore of 30 μL. While the sample was being filled into the valve (see Figure 1), the carrier solution streamed through the bypass and, after the valve was turned, the sample was injected into the system, carried through the thermostated coil *a* (0.5-mm i.d. polyethylene tubing) and then the resulting pH was measured during the passage of the sample zone through the capillary electrode. The calomel reference electrode was situated close by in a small vessel in which a constant level was maintained by back pumping (2 mL/min).

The optimum coil length was found by injecting 10 mM urea standards in 0.14 M NaCl into the carrier stream of Tris containing 30 mg urease/100 mL. The plot of peak height vs. coil length (Figure 2) yielded a typical curve with maximum at L = 125 cm. As there is not much difference between L = 125 and L = 100 cm, the latter coil length was used in all subsequent experiments as it would yield a resident time of 30 s and a sampling frequency of 60 samples/h. In order to find the optimum urease concentration while saving the enzyme, a carrier stream of 1 × 10^{-3} M Tris to which urea was added to the level of 10 mM was continuously pumped through the system. By injecting Tris solutions containing 5, 10, 15, 20, 25, 30, 40, and 50 mg of urease/100 mL, it was found that the peak height increased approximately loga-

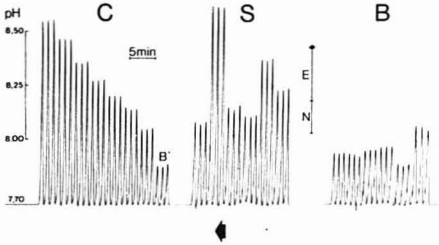

Figure 3. Recorder output showing from right to left: a series of serum blanks (B) recorded without urease in the carrier stream; a series of serum analyses (S); and a series of aqueous standards of urea (C). All samples injected in triplicate. The normal (N) and elevated (E) ranges of the urea levels in blood are indicated on the arrow between series S. and B. The blank value (B′) is that of an aqueous sample containing no urea, but only the interfering buffer (20 mM bicarbonate). All samples were diluted 1:5 with the carrier buffer *prior* to injection. The total dispersion in the system (D_t) was 3.2

rithmically with the "half-concentration" of enzyme corresponding to 10.8 mg/100 mL. As little is gained in peak height when increasing the enzyme concentration over three "half-concentrations", 30 mg of enzyme per 100 mL Tris were used as carrier solution (i.e., 33 units/mL) in all subsequent enzymatic assays. Additionally, higher concentrations of enzyme will lead to increased consumption of protons resulting in a shorter range within which the dpH will be a linear function of the urea concentration (Equation 7).

To develop a method which could be used for serum analysis, all three drawbacks of pH sensing outlined at the beginning of this paper must be overcome. The first two disadvantages are readily detected and evaluated from the calibration curve obtained in the absence of the interfering buffer, that is, by injecting urea standards prepared in Tris–0.14 M NaCl solution into the carrier stream consisting of Tris–0.1 M NaCl–urease. It was found that the recorded pH_{max} value, that is, the analytical readout is available 30 s after sample injection and the base line is reached within another 30 s, thus permitting a sampling rate of 60 determinations per hour. When the dpH (peak height) was plotted vs. the concentration of urea within the range of 4 to 15 mM, each sample solution being injected in triplicate (see Figure 3 C), the regression coefficient was 0.9998, the standard error of estimate amounting to 0.0029 pH unit. The reason for the 20 mM urea dpH value being lower than what would be obtained by extrapolating the straight line was found not to be due to the lack of enzymatic activity (or inhibition), but due to the fact that the amount of base produced affected the constancy of the buffering capacity of Tris. This conclusion was reached after plotting the same dpH values vs. the *logarithm* of the urea concentrations where it was found that the slope was 95% of the Nernstian value for the linear portion of the calibration curve situated between 15 and 30 mM urea. As would be expected, below 15 mM the deviation from linearity was the larger the lower the concentration of urea was, and at 4 mM the slope of the pH–log urea curve was close to zero. Thus it was confirmed that with the present experimental conditions (a) there is no inhibition of the enzyme function and (b) the pH response is a linear function of the urea concentration, can be obtained within 30 s, and is reproducible to 0.0029 pH unit.

For serum analysis, the main obstacle is the interfering effect of bicarbonate—which is the major component governing the serum buffering capacity—which still had to be overcome. Therefore, four series of urea standards, encompassing the range 4 to 20 mM urea, were prepared in 0.14 M NaCl solution, the first series containing no bicarbonate, the second series 5×10^{-3} M $NaHCO_3$, the third series 10×10^{-3} M $NaHCO_3$ and the fourth series 20×10^{-3} M $NaHCO_3$. Each sample from these series was diluted 1:5 with the carrier buffer solution (1×10^{-3} M Tris in 0.14 M NaCl) and assayed by Flow Injection Analysis in the manifold described above (Figure 1), using the carrier stream containing 30 mg urease/100 mL. When plotted, the resulting values of dpH yielded a series of straight lines within the range of 4 to 15 mM urea which were practically parallel and shifted toward higher pH with increasing contents of bicarbonate (Table I). With no bicarbonate present, the straight line intersects the ordinate of zero content of urea at a pH which corresponds to $pH_{\text{base line}}$ of the carrier stream, that is, dpH is zero (see also Figure 4). With increasing bicarbonate content, the blank increases also and its value, pH_{blank}, found by extrapolation, is in good agreement with the value found by injecting the blank solution of Tris–NaCl–$NaHCO_3$ with no urea present. The serum analysis developed on the basis of the previous experiments comprised three steps as shown in Figure 3. First, a series of blank experiments was run (B) by injecting the samples into the carrier buffer solution without urease and by pumping them through the manifold described above (Figure 1). The second series of serum samples (S) was then injected into the carrier buffer solution containing 30 mg urease/100 mL. Finally a series of aqueous standards containing 0.0, 4.0, 6.0, 8.0, 10.0, 12.0, 15.0, and 20 mM urea,

Table I. Regression Analysis of Urea-Calibration Curves in the Concentration Range 4–15 mM at Different Levels of Bicarbonate Added to the Sample Solutions[a]

$[HCO_3]$ level added to the sample soln. (mmol/L)	const.	$pH_{\text{base line}}$ ($C_{urea} = 0$)	dpH_{blank}	regression coefficient
0	0.0404	7.730	0.000	0.9997
5	0.0402		0.036	0.9994
10	0.0396		0.089	0.9997
20	0.0376		0.183	0.9996

[a] All samples (4.0, 6.0, 8.0, 10.0, 12.0, and 15.0 mM) were prediluted 1:5 with carrier buffer solution (1×10^{-3} M Tris in 0.14 M NaCl) and were injected in triplicate. $dpH = pH_{max} - pH_{blank} = \text{const.} \cdot C_{urea}$. $dpH = pH_{max} - pH_{\text{base line}} - (pH_{blank} - pH_{\text{base line}}) = \text{const.} \cdot C_{urea}$, i.e., $pH_{max} = \text{const.} \cdot C_{urea} + pH_{\text{base line}} + dpH_{blank}$.

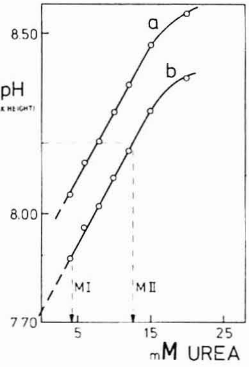

Figure 4. Calibration curves obtained by plotting dpH values from Figure 3, series C. Curve a includes the blank value B′ so that $dpH = pH_{max} - pH_{\text{base line}}$, while curve b is corrected by the B′ (so that $dpH = pH_{max} - pH_{blank}$). The latter curve is then used to read the urea contents in Monitrol I (MI) and Monitrol II (MII); for detail see text

respectively, and 20 mM bicarbonate was injected to obtain the calibration curve (C). All serum samples as well as aqueous standards were diluted 1:5 with 1×10^{-3} M Tris + 0.14 M NaCl carrier buffer solution *prior* to injection, and were all injected in triplicate.

The calibration curve, plotted as peak height vs. millimoles of urea:

$$\mathrm{dpH} = \mathrm{pH}_{\mathrm{max}} - \mathrm{pH}_{\mathrm{base\ line}} = C_{\mathrm{urea}} \cdot \mathrm{const} \qquad (8)$$

is shown in Figure 4, line a, while the same curve, corrected by blank, B′, ($\mathrm{dpH}_{\mathrm{blank}}$ = 0.183 pH), i.e.:

$$\mathrm{dpH} = \mathrm{pH}_{\mathrm{max}} - \mathrm{pH}_{\mathrm{blank}} = C_{\mathrm{urea}} \cdot \mathrm{const} \qquad (9)$$

is shown in Figure 4, line b. The const. has a value of 0.0372 pH/mM urea and the intersect of line b for zero urea content is 7.73 pH, i.e. only 0.03 pH unit higher than the $\mathrm{pH}_{\mathrm{base\ line}}$ of the carrier stream.

Thus, for accurate assay, the correction for blank values of individual serum samples must be made by using Equation 7 (or calibration line Figure 4b) as otherwise the urea values in the normal range would be elevated. This can be illustrated by referring to the two samples, represented by the first six injections on the right hand side of groups B and S in Figure 3, of which the first three represent the standard serum material Monitrol I and the second three are Monitrol II. The urea content of Monitrol I (lot LTD 144) was 4.64 mM (confidence limits 3.57–5.71) and of Monitrol II (lot PTD 46A) was 12.4 mM (confidence limits 10.5–14.3) as declared and found by the manufacturer on the basis of enzymatic assay. By the present method, comprising blank correction, 4.20 mM urea was found for Monitrol I, while 12.8 mM urea was found for Monitrol II. Without blanking, Monitrol II was found to contain 12.9 mM, while Monitrol I was elevated to 7.94 mM urea.

For the *rapid screening* or simple monitoring of the changes of the urea content in blood, the blanking could be avoided if the error caused by the variation of the bicarbonate content in the individual serum samples would be acceptable. This can be illustrated by refering to samples 1–4 which were injected following the above mentioned Monitrol serum standards. As their "average blank value" is 0.075 pH unit higher than $\mathrm{pH}_{\mathrm{blank}}$ (value B′ in the calibration group C), the use of Equation 9 or calibration curve b of Figure 4 would yield results higher by 2 mM urea, compared to the actual content. Considering the fact that the analytical readout is available within 30 s after sample injection and the instrument can be started up within a few minutes, this approach could well be considered for an emergency screening, by mean of a simple instrument.

The Flow Injection system with pH detection can be easily assembled from commercially available parts of high reliability. This is not the least true for the sensor, the capillary glass electrode, which has been used for years as a standard part of the Radiometer clinical gas blood analyzers. The use of soluble enzymes, a fresh portion of which is mixed with each sample during the analysis, is much more reliable than use of enzyme columns or enzyme covered electrodes in which the enzyme activity gradually decreases and which are difficult to maintain and prepare. (Use of insolubilized enzymes also makes the blanking more difficult.)

The reagent consumption is moderate, considering that the carrier stream containing 33 units of urease/mL is pumped at a rate of 0.76 mL/min, while the sampling rate is 60 determinations per hour. The enzyme consumption could, however, be further reduced by a factor of five or even ten by using the recently developed multi-injection technique termed merging-zone Flow Injection Analysis (*11*, *12*). In this variation, the carrier stream is buffer solution or water, into which both sample and reagent (urease) are injected simultaneously by means of a double injector, and the analytical reaction takes place as sample and reagent merge downstream on their way to the detector. Such a procedure is most economical with respect to consumption of reagent.

This approach will be used either in (a) the continuous flow mode described above, or (b) in the Stop-flow Injection system (*13*). In method (a), a separate sample zone, along with a second sample zone and an enzyme zone which merge and react in a coil, are injected simultaneously. While sample zone no. 1 allows the determination of the blank value ($\mathrm{pH}_{\mathrm{blank}}$), the subsequent passage of the two merging zones through the flow cell renders the analytical readout ($\mathrm{pH}_{\mathrm{max}}$). In method (b), sample and reagent zones are injected, allowed to merge immediately before entering the detector, in which they are stopped automatically by means of an electronic device which locates the top of the peak. The enzymatic reaction is monitored continuously, the change in pH as a function of time yielding the analytical result. The working cycle is completed when the pump is restarted and the sample thus flushed out from the system. The experience, gained during the work on the spectrophotometric determination of glucose in serum using glucose dehydrogenase coupled with NADH (*15*), suggests that a similar approach could be successfully applied when measuring urea by urease, provided that the sample zone could be stopped reproducibly within the pH sensing glass capillary electrode.

The drawbacks of the pH sensing mentioned at the beginning of this paper were successfully overcome, yet it is realized that a more exact choice of the concentration of the carrier buffer components can be made following the mathematical approach oulined in the theory of "one point titration" suggested by Johansson and co-workers (*19*, *20*). Such an approach would further increase the linear response range and might even lead to higher sensitivity of detection which might be needed for assays of and with enzymes of lower activity than the urease used in this work.

LITERATURE CITED

(1) H. H. Bauer, G. D. Christian and J. E. O'Reilly, "Instrumental Analysis", Allyn and Bacon, Boston, 1978, Chapter 18.
(2) S. J. Updike and G. P. Hicks, *Science*, **158**, 270 (1967).
(3) G. G. Guilbault, "Handbook of Enzymatic Methods of Analysis", Marcel Dekker, New York, 1976.
(4) J. F. Rusling, G. H. Luttrell, L. F. Cullen, and G. J. Papariello, *Anal. Chem.*, **48**, 1211 (1976).
(5) R. E. Adams and P. W. Carr, *Anal. Chem.*, **50**, 944 (1978).
(6) L. P. Leon, M. Sansur, L. R. Snyder and C. Horwath, *Clin. Chem.* (*Winston-Salem, N.C.*), **23**, 1556 (1977).
(7) L. C. Clark and C. Lyons, *Ann. N.Y. Acad. Sci.*, **102**, 29 (1962).
(8) G. G. Guilbault and J. Montalvo, *J. Am. Chem. Soc.*, **91**, 2164 (1969).
(9) B. Mattiasson, B. Danielson, and K. Mosbach, *Anal. Lett.*, **9**, 217 (1976).
(10) L. D. Bowers, S. S. Schifreen, and P. W. Carr, *Clin. Chem.* (*Winston-Salem, N.C.*), **22**, 1427 (1976).
(11) J. Mindegaard, *Anal. Chim. Acta*, in press.
(12) H. Bergamin, E. A. Zagatto, F. J. Krug, and B. F. Reis, *Anal. Chim. Acta*, **101**, 17 (1978).
(13) J. Ruzicka and E. H. Hansen, *Anal. Chim. Acta*, **99**, 37 (1978).
(14) D. Betteridge, *Anal. Chem.*, **50**, 832A (1978).
(15) J. Ruzicka and E. H. Hansen, *Anal. Chim. Acta*, in press.
(16) H. Nilsson, A. Ch. Åkerlund, and K. Mosbach, *Biochim. Biophys. Acta*, **320**, 529 (1973).
(17) H. Nilsson, K. Mosbach, S. O. Enfors, and N. Molin, *Biotechnol. Bioeng.*, **20**, 527 (1978).
(18) D. D. Perrin and B. Dempsey, "Buffers for pH and Metal Ion Control", Chapman and Hall, London, 1974.
(19) G. Johansson and W. Backen, *Anal. Chim. Acta*, **69**, 415 (1974).
(20) O. Åström, *Anal. Chim. Acta*, **88**, 17 (1977).

RECEIVED for review September 5, 1978. Accepted November 1, 1978. The authors express their gratitude to the Scientific Affairs Division of NATO which through Grant No. 1492 made this work possible. The gift of two capillary electrodes from Radiometer A/S, Copenhagen, is gratefully acknowledged.

Development and Application of a Thermistor Enzyme Probe in the Urea–Urease System

Steven Rich

Hofstra University, 1000 Fulton Avenue, Hempstead, New York 11550

Robert M. Iannielo and Neil D. Jespersen*

Chemistry Department, St. John's University, Grand Central and Utopia Parkways, Jamaica, New York 11439

A novel thermistor enzyme probe (TEP) has been developed for the determination of urea in solution. Response time is 1 min or less. Linear response in urea concentration has been obtained in the 5–30 mM range. Stability and factors influencing the response of the probe are examined. Finally, a design for a modified TEP, useful for small sample volumes, is described.

Potentiometric detectors have been developed for the analysis of urea which utilize well established enzyme immobilization techniques (*1*). Guilbault (*2*) has developed a urease coupled ammonia electrode for the analysis of urea in blood serum. Guilbault (*3*) and others (*4*) have developed probes which sense the product of the urea–urease hydrolysis reaction, namely ammonium ion. In addition, pH electrodes coupled within an immobilized enzyme layer have been used (*5*) for the analysis of urea. While these methods have found widespread application, they are limited by their difficulty of enzyme-entrapment procedure, susceptibility to interference by cations, and slow response time.

Continuous flow analyzers have been developed (*6–8*) which utilize a variety of detection techniques for the analysis of the products of the urea–urease reaction. In the use of a continuous flow analyzer, it is necessary to employ enzyme immobilization techniques (*9*) which may be time-consuming or expensive.

Mosbach (*10, 11*) has developed the "enzyme thermistor" which measures the temperature change at the site of the enzyme–substrate reaction. Again, the method uses a matrix bound enzyme which is time-consuming to prepare.

It has been shown (*12, 13*) that proteins in aqueous solution can be adsorbed onto a mercury surface via the interaction of disulfide bonds with the metal. It has also been shown by thermometric and electrometric means (*12*), that urease adsorbed at a mercury surface remains active, which indicates little or no modification of the active site.

With these facts in mind, it became of interest to develop the thermistor enzyme probe (TEP). The device consists of a glass encapsulated thermistor sealed in a U-shaped piece of glass tubing with epoxy cement. A small drop of Hg covers the thermistor and serves as both the enzyme immobilization and heat conduction sites. Thus, the TEP senses a temperature change at the Hg-solution interface during the enzyme catalyzed reaction. Provided that the heat of reaction is sufficiently high, the probe should respond quantitatively to substrate concentration. The TEP can be a very versatile probe since a wide variety of enzymes may be immobilized via a simple adsorption process. This study represents the use of the TEP as a urea specific detector by using the enzyme urease.

EXPERIMENTAL

Reagents. All solutions were prepared from freshly distilled water. All glassware was cleaned daily by rinsing with ethanolic KOH, followed by concentrated nitric acid, followed by 4–5 washes with distilled water. This procedure ensured the removal of both organic films and cations absorbed on the glass surface.

A stock solution of Na–K phosphate buffer was prepared by adding 1.48 L of 0.1 M NaOH (prepared from NaOH pellets, (Baker analyzed reagent, J. T. Baker Chemical Co., Phillipsburg, N.J.)) to 2 L of 0.1 M K_2HPO_4 (Baker analyzed reagent) and diluting to 4 L with distilled water. Urea solutions were prepared fresh daily by dissolving 9.3 g EDTA, disodium salt dihydrate (Baker analyzed reagent) and urea (Absolute grade, Research Plus Laboratories, Denville, N.J.) in phosphate buffer and diluting to 500 mL. Urease (Type IV from Jack Beans, Sigma Chemical Co., St. Louis, Mo.) solution was prepared by dissolving 0.15 g of the enzyme and 1.86 g Na_2 EDTA·2 H_2O in 100 mL of phosphate buffer. The solution was stored at 0 °C when not in use and could be used for 2–3 days without noticeable loss of activity. Mercury metal (triple distilled) was obtained from Belmont Smelting and Refining Works, Brooklyn, N.Y., and was used without any further purification.

Apparatus. Two TEP's were constructued by sealing a 2000-Ω Veco Thermistor (Victory Engineering Co., Springfield, N.J.) in a U-shaped glass tube with epoxy cement. Figure 1 shows the details of the TEP. A 1.0-V power supply (Heathkit Model 1P-27 Regulated dc power supply) powers the differential Wheatstone bridge, to which the TEP's are connected. When a change in temperature occurs at the surface of *one* TEP, the imbalance voltage of the bridge appears on the grid of the microvoltmeter (Keithley Instruments Microvoltmeter no. 155). The output of the microvoltmeter is then recorded by a Perkin-Elmer no. 56 Recorder as a displacement from an initial steady-state value.

A Perkin-Elmer Model 360 Atomic Absorption Spectrometer was used for all Hg(II) determinations.

Procedure. Urea and pure buffer solutions were placed in 500-mL Erlenmeyer flasks, which were allowed to come to thermal equilibrium by placement in a thermostated bath (25 ± 0.001 °C). One TEP was placed in 100 mL of urease solution for 5 min. Excess urease was then washed off the probe with phosphate buffer. The probes were then placed in the thermostated buffer solution and allowed to come to thermal equilibrium (10–20 min). The equilibrium temperature was noted on the strip chart recorder as the base line. The probes were then rapidly removed from the buffer solution and placed into the urea solution. The change in temperature was recorded as the final steady state temperature, relative to the bath temperature (base line).

Mercury (Hg(II)) in the urea solutions was determined by the standard additions procedure using flame atomic absorption spectrometry.

RESULTS AND DISCUSSION

Figure 2 illustrates the typical response of the TEP. It is noted that two probes are used so that a differential reading is made. This is to ensure that ΔT readings are indeed due to only the reaction at the Hg–urease interface and *not* to bath temperature fluctuations. The response of the probe is on the order of 10–60 s. It is presumed that the probe behaves in the following manner. Urease adsorbs to the surface of the mercury drop with some of its catalytic activity intact. When the probe is placed in an unstirred solution of urea, the hydrolysis reaction occurs with the simultaneous evolution of heat. Assuming a diffusion controlled reaction, the temperature increase at the interface depends upon the bulk

0003-2700/79/0351-0204$01.00/0 © 1979 American Chemical Society

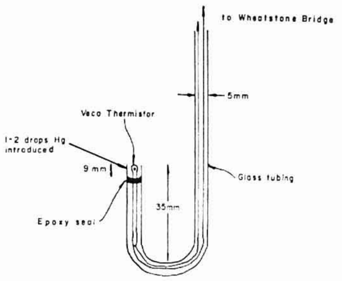

Figure 1. Construction of the TEP. Details given in text

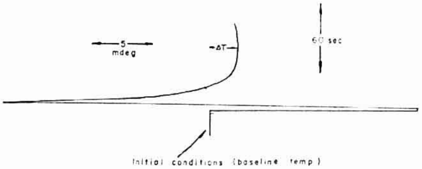

Figure 2. Recorder response of TEP for a 10.0 mM urea solution

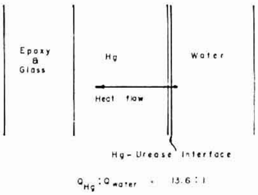

Figure 3. Schematic representation of the TEP surface and surroundings

concentration of urea plus the ΔH of reaction. Figure 3 gives a schematic description of the TEP surface and surroundings. Any heat produced at the interface will flow into both the mercury and analyte solution. Fortunately, the heat flow will be partitioned according to the thermal conductivity of water and mercury. Since this ratio is in favor of the mercury by a 13.6:1 factor (*16*), the mercury will rapidly assume the temperature of the interface. The temperature profiles of the regions surrounding the interface are given schematically in Figure 4. The dashed line in Figure 4 indicates the temperature profile if mercury is replaced with glass. This indicates why direct immobilization of enzyme onto the thermistor head would not work, since the heat flow is not preferentially directed toward the thermistor. In addition, the low heat capacity of mercury (*17*) allows the mercury temperature to more closely approximate the temperature at the interface.

Figure 5 illustrates the response of the TEP with urea concentration. A least squares plot of the data shows a correlation of 0.965. The nonzero intercept (−0.05) is well within the maximum accuracy of measurement and can, for all practical purposes, be neglected.

It was discovered that, at higher urea concentrations (40–70 mM), the response of the TEP decreased. Preliminary calculations have indicated that, in urea concentrations in excess of 30 mM, NH_3 is produced in such quantity at the interface (>1 mM) as to effectively inhibit the hydrolysis reaction (*15*). The truly nondestructive characteristic of the TEP is clearly demonstrated by a calculation which shows that, for a 10 mM urea solution, 230 trials (60 s/trial) would be necessary to obtain a 5% reduction in urea concentration.

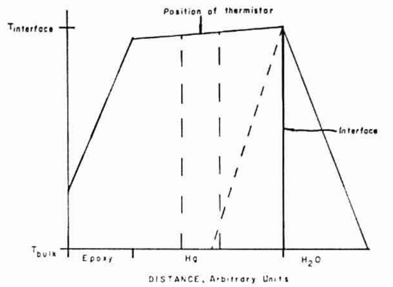

Figure 4. Schematic representation of temperature profile in the regions surrounding the Hg–solution interface. Dashed line represents profile if Hg is replaced with glass

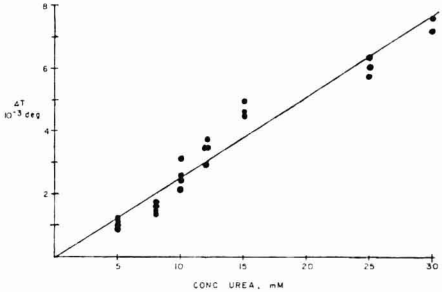

Figure 5. TEP response vs. urea concentration plot. Intercept of the data (−0.05) is negligible. Least squares slope and correlation were 0.260 and 0.965, respectively

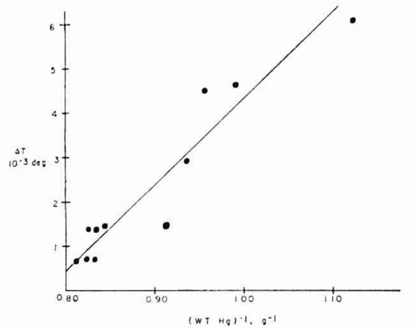

Figure 6. TEP response vs. reciprocal weight of Hg plot. Data were obtained for a 10.0 mM urea solution. Least squares slope and correlation were 0.0492 and 0.923, respectively

It was suspected that the mass of mercury would affect the response time and, more importantly, the average temperature sensed by the thermistor. This occurs since it would take more heat to cause a given temperature change as the mass of mercury increases. Since the heat evolved is directly proportional to the product of the mass of Hg and the change in temperature, a plot of ΔT vs. 1/mass should be linear.

Figure 6 demonstrates the response of the TEP with the reciprocal of the weight of Hg on a 10.0 mM urea solution. A least squares plot yielded a correlation value of 0.923 with

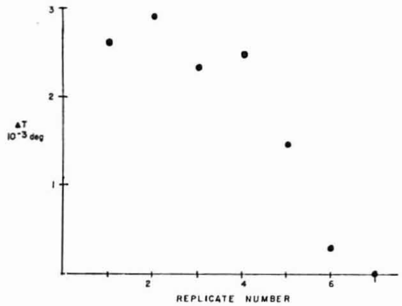

Figure 7. Response of TEP in a 10.0 mM urea solution, without urease renewal. Probe remains active for four trials

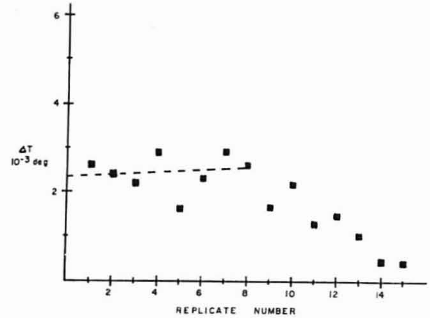

Figure 8. Response of TEP in a 10.0 mM urea solution after renewal of urease. Hg drop was not changed for renewal. Probe remains active for 8 trials

an X-intercept of −0.229. This somewhat poor corrleation value may be due to, in part, the difficulties of weighing the Hg drop after it has become wet. However, the correlation is sufficient to demonstrate the dependence of ΔT on the weight of Hg which corresponds to the model presented.

The stability of urease after adsorption onto the Hg drop was examined by recording the response of the TEP which was immersed, repetitively into a 10.0 mM urea solution. Figure 7 illustrates this point. It is shown that the probe remains active for about four trials and then tails off rapidly. This shows that the urease either degrades or dissolves after five trials. This is not a drawback, however, since the enzyme layer is easily renewed by immersion of the probe into the enzyme solution.

Since it was time-consuming to renew each Hg drop per trial, the response of the TEP was investigated when the same Hg drop was used for the adsorption site on a single trial. Figure 8 shows the response of the TEP, using the same Hg drop, on a 10.0 mM urea solution. The urease interface was renewed for each trial by immersion in the enzyme solution. Excluding trial no. 5, the response of the TEP appears to be constant for 8 trials. Loss of activity after this point may be due to modification of the enzyme–Hg interface and/or enzyme inhibition by the products of the hydrolysis reaction (*14*, *15*, *18*). In addition, it has been calculated that after 3 trials the effective concentration of EDTA is reduced to zero by complexation with Hg(II).

Table I. Determination of Hg(II) in Urea Solution by Flame Atomic Absorption Spectrometry

solution no.	wt Hg in 100 mL, μg	concn, ppm[a]
1	0.20	2.0
2	0.21	2.1
3	0.18	1.8
4	0.20	2.0

[a] Mean [Hg] = 2.0 ppm. Std. dev. = 0.13.

It has been shown that heavy metal ions seriously inhibit the reaction of urease and urea (*19–21*). This necessitated the careful cleaning procedure and the use of EDTA in all solutions. It was found that when EDTA was not used, the probe sometimes failed to respond. It was obvious that the Hg metal was a source of possible Hg(II) contamination. Table I shows that Hg(II) was indeed introduced to the solution by the mercury drops. A urea-buffer solution was used as the blank for all trials. A 2 ppm (1 × 10^{-5} M) concentration is indeed large enough to effectively inhibit urease (*22*).

CONCLUSIONS

At present, the probe has been used only on pure analyte solutions. The reason is that the construction of the probe necessitates the use of very large sample volumes. A new probe design is underway which utilizes the properties of a copper-clad "thinistor" wafer. Once a mercury–copper amalgam is made, urease will be easily adsorbed onto its surface (*12*). It appears that this probe will be ideally suited for small sample volumes. Results of this will be reported later.

LITERATURE CITED

(1) D. N. Gray, M. H. Keyes, and B. Watson, *Anal. Chem.*, **49**, 1067A (1977).
(2) G. Guilbault et al., *Anal. Chem.*, **49**, 795 (1977).
(3) G. Guilbault and J. Montalvo, *J. Am. Chem. Soc.*, **92**, 2533 (1970).
(4) S. A. Katz and J. A. Cowans, *Biochim. Biophys. Acta*, **107**, 605 (1965).
(5) H. Nilsson, A. Akerlund, and K. Mosbach, *Biochim. Biophys. Acta*, **320**, 529 (1970).
(6) R. Adams and P. Carr, *Anal. Chem.*, **50**, 944 (1978).
(7) A. Filippusson, W. Hornby, and A. McDonald, *FEBS Lett.*, **20**, 291 (1970).
(8) L. Bowers et al., *Clin. Chem. (Winston-Salem, N.C.)*, **22**, 1314 (1976).
(9) P. Savdaram and W. Hornby, *FEBS Lett.*, **10**, 325 (1970).
(10) K. Mosbach and B. Danielsson, *Biochim. Biophys. Acta*, **364**, 140 (1974).
(11) K. Mosbach et al., *Anal. Lett.*, **9**, 217 (1976).
(12) K. Santhanam, N. Jespersen, and A. Bard, *J. Am. Chem. Soc.*, **99**, 274 (1977).
(13) C. Tanford, *J. Am. Chem. Soc.*, **74**, 6036 (1952).
(14) K. M. Harmon and C. Niemann, *J. Biol. Chem.*, **77**, 601 (1949).
(15) J. P. Hoare and K. Laidler, *J. Am. Chem. Soc.*, **72**, 2487 (1950).
(16) "Handbook of Chemistry and Physics", 56th ed., Chemical Rubber Company, Cleveland, Ohio, 1976, p E 11-12.
(17) Ref. 16, D-62.
(18) W. Fishbein and P. Carbone, *J. Biol. Chem.*, **240**, 2407 (1964).
(19) J. Ambrose, G. Kistiakowsky, and A. Kridl, *J. Am. Chem. Soc.*, **73**, 1232 (1951).
(20) W. Shaw and D. Raval, *J. Am. Chem. Soc.*, **83**, 3184 (1961).
(21) S. N. Baldridge, Ph.D. Thesis, University of Texas at Austin, August 1977, pp 72–77.
(22) J. W. Webb, "Enzyme and Metabolic Inhibitors", Vol. II, Academic Press, New York, 1966, p 812.

RECEIVED for review August 10, 1978. Accepted October 30, 1978.

ANALYTICAL CHEMISTRY, VOL. 51, NO. 2, FEBRUARY 1979 • 207

Solvent Extraction Method for Determination of Thorium in Soft Tissues

Narayani P. Singh,* Shawki Amin Ibrahim, Norman Cohen, and McDonald E. Wrenn

Institute of Environmental Medicine, New York University Medical Center, 550 First Avenue, New York, New York 10016

A simple, precise and accurate analytical technique has been developed for the determination of thorium isotopes in soft tissues. The method consists of preliminary nitric acid digestion of tissues after adding ^{229}Th tracer, followed by a mixture of nitric and sulfuric acid with occasional addition of hydrogen peroxide; thorium is then coprecipitated with iron carrier by ammonium hydroxide. The precipitate is washed until free of sulfate ions, dissolved in 1:1 HNO_3 and finally adjusted to 4 M HNO_3. Thorium is extracted twice into 25% trilaurylamine (TLA) in xylene (pre-equilibrated with 4 M HNO_3) and backwashed twice with 10 M HCl. The aqueous phase is evaporated to almost dryness, treated with H_2SO_4 with frequent addition of a few drops of HNO_3, and electrodeposited onto a platinum planchet prior to α spectrometry with a surface-barrier silicon detector. The final total recovery ranged from 24–93% with a mean of 65% in 28 samples. Yield appeared to be independent of total iron when 10 to 100 mg Fe were added, and independent of the amount of added tracer. The natural ^{228}Th content of three different beef liver samples was 1.3, 1.4, and 3.0 pCi/kg wet weight.

The radiological impact of plutonium contamination in the environment has been discussed widely but thorium, another actinide element, chemically and biologically similar to plutonium, has been largely ignored. This may be due to the fact that the radiation dose to human tissues from natural thorium is significantly lower than that from other natural α-emitting nuclides.

Natural thorium is distributed widely in our environment; it is essential to quantitate the thorium content of human tissues because of our need to be able to evaluate the accumulation of this element by man from his environment. To assess the content of the thorium nuclides ^{228}Th, ^{230}Th, and ^{232}Th in human tissues, a new analytical technique has been developed. The methods available for the determination of thorium in tissues are limited. Petrow et al. (*1*) described an indirect technique for determining ^{228}Th which takes a considerable amount of time and is limited to only one isotope of thorium. Another procedure described by Petrow and Strehlow (*2*) is a colorimetric method for total thorium and again does not measure the isotopic composition. Sill (*3, 4*) has reported techniques for determining thorium in soil and ore samples and Percival and Martin (*5*) developed a method for assay of thorium isotopes in environmental and process waste samples. No method has been available, however, for the multiple isotopic determination of thorium in biological tissues. Therefore, a simple, precise and sensitive analytical technique has been developed in this laboratory for the simultaneous determination of all α-emitting isotopes in tissues. Trilauryl amine is chosen as the extracting agent because of its successful use for the determination of plutonium in soft tissues (*6*).

EXPERIMENTAL

Reagents and Apparatus. All the reagents used are of analytical grade. Trilauryl amine (TLA), Matheson, Coleman and Bell manufacturing chemicals (MC/B); a 25% TLA solution is prepared in xylene and shaken with $^1/_3$ volume of 4 M HNO_3 for 10 min. The organic phase is separated and centrifuged before use. A stock solution of TLA cannot be stored since it begins deteriorating after 24 h. Once it is equilibrated with 4 M HNO_3, it must be used the same day. Dilute acids such as 2 M H_2SO_4, 3 M HNO_3, and 10 M HCl are prepared by appropriate dilution of concentrated acids with deionized, distilled water. Thorium-229 tracer (this tracer has 8.1% ^{228}Th on activity basis), methyl red indicator, platinum planchet, nickel disks, electrolytic cell, electrolytic analyzer (motor driven platinum electrode and a power supply) were used.

Sample Preparation. Transfer 500–1000 g of tissue to a 4-L beaker and add 1–2 dpm ^{229}Th tracer. The suitability of this tracer has been demonstrated in our earlier work (*7*). Add just enough concentrated nitric acid to immerse the tissue, and cover the beaker with a watch glass. Heat gently on a hot plate with magnetic stirrer until frothing ceases. Raise the temperature slowly to approximately 100 °C and continue heating until the volume is reduced to approximately 100 mL. Heat at a higher temperature while occasionally adding concentrated nitric acid (a few drops at a time) until a clear solution is obtained. Add 200 mL 1:1 HNO_3 and H_2SO_4 mixture and heat vigorously until all the nitric acid is driven off. Add a few drops of HNO_3 occasionally with constant heating until a clear colorless solution is obtained ensuring almost complete decomposition of organic materials. (Addition of a few drops of H_2O_2 along with nitric acid helps in faster decomposition of organic materials.) Remove most of the sulfuric acid by evaporation, without going to dryness, before proceeding further. In case of lung and lymph nodes, heat the tissue samples further with HF, after HNO_3-H_2SO_4 digestion, and then remove HF by continuous heating.

Procedure. Add 200 mL of 1:3 HCl to the clear solution of the tissue and boil for several minutes. Cool and add 10 mg of iron carrier (as 1 mL $FeCl_3$) and swirl the beaker for proper mixing. Add concentrated ammonium hydroxide very gently until precipitation is complete. The precipitate must be allowed to settle completely overnight to avoid any loss of $Fe(OH)_3$ precipitate. Remove the supernatent by centrifuging the precipitate in a 50-mL centrifuge tube. Dissolve the precipitate in 4–5 mL of concentrated HNO_3 and reprecipitate $Fe(OH)_3$ with ammonia. Thorium is coprecipitated with iron along with some other metals present in the tissues. Repeat the precipitation and dissolution until the supernatent, after $Fe(OH)_3$ precipitations, is free of sulfate ions. Dissolve the precipitate in a minimum volume of concentrated nitric acid and determine the acidity of the solution by titrating an aliquot (100 μL) against a standard sodium hydroxide (0.1 N) solution. Adjust the acidity to 4 M by adding a calculated volume of nitric acid of appropriate concentration.

Solvent Extraction. Extract thorium from the solution, obtained after dissolving the $Fe(OH)_3$ precipitate in HNO_3 (acidity adjusted to 4M), with an equal volume of 25% TLA solution in xylene by shaking for 10 min in a 50-mL polyethylene tube (TLA solution was equilibrated with 4 M HNO_3 before use). Centrifuge for 10 min and remove the aqueous phase into another 50-mL polyethylene tube. Extract the aqueous phase once again with 25% TLA for 10 min and centrifuge for 10 min. Separate and discard the aqueous phase. Mix the organic phases from the first and second extraction and backwash thorium from the TLA phase by shaking it with 10 M HCl for 10 min (volume ratio 1:1). Centrifuge the tube and transfer the aqueous phase into a 100-mL beaker. Repeat the backwashing once again from the TLA phase with 10 M HCl and transfer the aqueous phase to the same beaker. Evaporate this aqueous solution to a smaller volume and then

0003-2700/79/0351-0207$01.00/0
© 1979 American Chemical Society

Table I. Recovery of ^{229}Th Added to Beef Liver as a Function of Iron Added to the Sample

sample no.	amount of tissue, g	amount of Fe added, mg	Amount of ^{229}Th, dpm added	Amount of ^{229}Th, dpm found	recovery, %
6	106	10	2.822	2.63 ± 0.12	93 ± 4
9	140	25	2.822	2.54 ± 0.13	90 ± 5
10	140	50	2.822	1.39 ± 0.09	49 ± 3
11	140	75	2.822	2.20 ± 0.12	78 ± 4
12	140	100	2.822	1.68 ± 0.11	59 ± 4

Table II. Recovery of ^{229}Th in Beef Liver with Variable Amounts of Added Tracer (^{229}Th)

sample no.	amount of tissue, g	amount of Fe added, mg	Amount of ^{229}Th, dpm added	Amount of ^{229}Th, dpm found	recovery, %
1	130	10	14.11	3.39 ± 0.14	24 ± 1
2	130	10	7.055	3.51 ± 0.14	50 ± 2
3	130	10	3.527	2.69 ± 0.15	76 ± 4
4	130	10	1.764	0.49 ± 0.06	28 ± 4
5	106	10	1.411	1.06 ± 0.09	75 ± 6
6	106	10	2.822	2.63 ± 0.12	93 ± 4
7	106	10	4.233	3.93 ± 0.16	93 ± 4
8	106	10	5.644	4.55 ± 0.17	81 ± 3
					mean 65%

add 10 mL of 2 M sulfuric acid and heat. Once the black droplets are seen floating on the surface, add concentrated HNO_3 and 30% H_2O_2, drop by drop, along the side of the beaker. This addition enhances decomposition of the organic material floating on the surface. Add HNO_3 occasionally, until all the organics are completely decomposed. Continue heating to almost dryness.

Electroplating. *Apparatus.* The plating apparatus (8) consists of an elongated 22-mm cap which holds a 1-oz polyethylene bottle with the bottom removed. The cap has space for an 18-mm diameter platinum plating disk and a nickel supporting disk. This may be firmly screwed into the polyethylene bottle forming a leak proof plating cell. A threaded brass brushing is molded into the cap which makes the electrical contact with the platinum disk cathode by clip leads. The entire cell is supported by a heavy brass base which is employed to fix the cell in the ice water bath. The anode is a 1.6-mm platinum-iridium rod, 4 inches long with a half-inch diameter platinum disk riveted at one end. (This dimension is not critical.) The disk is provided with a number of 0.3-mm holes. It is connected through a constant speed stirrer to the positive outlet of the power supply which furnishes a constant current ranging from 0–10 A and a voltage ranging from 0–36 V.

Procedure. After backwashing thorium from the TLA phase with 10 M HCl and decomposing the organic materials entrained with this HCl solution, evaporate it to dryness. Add 1 mL 2 M H_2SO_4 and heat gently at a low temperature on a hot plate. Transfer this solution to the plating cell. Wash two times with 1 mL 2 M H_2SO_4 and transfer the solution to the plating cell. Add one drop of methyl red indicator and titrate with 1:1 ammonia, drop by drop, to a yellow end point. Precautions should be taken not to add an excess of ammonia. Bring back to red by adding 2 M H_2SO_4 dropwise and add 3–4 drops in excess to get the required pH of the plating solution. The total volume of the plating solution should be restricted to 3–4 mL as larger volumes were found to produce poor electroplating recovery. Electroplate thorium at an initial current of 1.2 A for 1 h. Quench the electrolyte with 3–4 drops of ammonium hydroxide at the end of 1 h. Dismantle the cell and rinse the platinum disk with water followed by alcohol. Flame the disk to red heat over a burner. Determine the recovery and the isotopic composition of thorium by counting the disk in an α spectrometer with a surface barrier silicon diode.

RESULTS AND DISCUSSIONS

Since not much information was available on the isotopic determination of thorium, a new method was developed in which thorium was extracted into TLA, backwashed with 10 M HCl, converted to sulfate with H_2SO_4 and electrodeposited. Accordingly, it was essential to find the most favorable acid concentration for the extraction of thorium since every solvent extraction system is greatly influenced by acidity. In this system ^{229}Th tracer was extracted into 25% TLA solution in xylene from nitric acid ranging from 1–8 M. The best extraction efficiency occurred at 4 M. When the extraction was carried from the beef liver where thorium was coprecipitated with 100 mg Fe carrier, after the complete wet ashing of tissues with a mixture of H_2SO_4-HNO_3, the recovery of thorium was reduced. It was probably due to interference from iron, which was added into the system for coprecipitation of thorium, or the trace metals available in the tissues which are coprecipitated with iron along with thorium, or possibly both.

A separate experiment was conducted to investigate whether iron interfered in the extraction and, hence, in the final recovery of thorium. About 2000 g of tissue were wet ashed until free of all organics and the volume was made up to 1000 mL to give 100 g of tissue/50 mL of solution. Aliquots of 50 mL were placed into five different beakers and spiked with 2.8 dpm of ^{229}Th each. Iron was added in amounts varying from 10 to 100 mg for coprecipitation of thorium, and extraction and electrodeposition were carried out as described earlier. Comparing the results in Tables I and II shows that the range of variability in yield with low iron content (10 mg added) exceeded the different in yield observed when a range of 10–100 mg Fe is added. Hence, the extraction yield does not depend greatly on the iron content of the samples. One hundred mg of iron is the amount present in about 200 g of normal human blood (*9*). Accordingly, with tissue masses to be analyzed up to 500 to 600 g, it is unlikely that the endogenous iron content will exceed the amount we have added. In all further experiments, therefore, the amount of iron added for coprecipitation of thorium was maintained at 10 mg.

It is also possible that some of the trace metals which might be coprecipitated with iron may interfere in the extraction, backwashing, and electroplating of thorium which would accordingly differ depending upon the quantity of the tissues.

Thorium-232 can interfere with the electrodeposition process if present in amounts exceeding 100 μg (*5*). However, this large amount is unlikely in reasonable size samples of human or animal tissue. For example, it is estimated that the total body content of thorium of a normal man is <120 μg (*10*).

Since the specific activity of ^{232}Th is very low (1.09×10^{-7} Ci/g) compared to other thorium isotopes, any mass due to thorium in the electroplating step will be mainly due to ^{232}Th. To equal a mass of 100 μg, the activity of ^{232}Th required is 10.9 pCi. This is much higher than that expected in kilogram quantities of normal biological samples. Even though the

Table III. Recovery of ^{229}Th Added to Beef Liver with Varying Amounts of Tissue Mass

sample no.	amount of tissue, g	amount of Fe added, mg	Amount of ^{229}Th, dpm added	found	recovery, %
6	106	10	2.822	2.63 ± 0.12	93 ± 4
13	140	10	2.822	1.89 ± 0.10	67 ± 4
14	280	10	2.822	1.94 ± 0.11	69 ± 4
15	560	10	2.822	1.99 ± 0.11	71 ± 4

Table IV. Results of Replicate Analyses of Thorium-228 Content of Three Beef Livers with Varying Amounts of Added Thorium-229 Tracer

sample no.	percent recovery tracer ^{229}Th	total ^{228}Th,[a] dpm	natural ^{228}Th in liver, dpm	natural ^{228}Th pCi/kg beef liver
A-I	24 ± 1	1.65 ± 0.05	0.46 ± 0.22	1.59 ± 0.78
A-II	76 ± 4	0.62 ± 0.06	0.32 ± 0.08	1.12 ± 0.29
A-III	28 ± 4	0.76 ± 0.04	0.54 ± 0.16	1.86 ± 0.56
A-IV	75 ± 6	0.51 ± 0.06	0.38 ± 0.08	1.61 ± 0.33
A-V	93 ± 4	0.50 ± 0.01	0.27 ± 0.06	1.14 ± 0.25
A-VI	93 ± 4	0.66 ± 0.04	0.30 ± 0.07	1.27 ± 0.30
A-VII	81 ± 3	0.76 ± 0.05	0.29 ± 0.08	1.20 ± 0.35
	mean 67%			mean = 1.40 ± 0.29
B-I	90 ± 5	1.13 ± 0.07	0.89 ± 0.10	2.85 ± 0.33
B-II	49 ± 3	1.09 ± 0.09	0.84 ± 0.14	2.71 ± 0.44
B-III	78 ± 4	1.15 ± 0.07	0.91 ± 0.11	2.92 ± 0.37
B-IV	59 ± 4	1.38 ± 0.10	1.14 ± 0.16	3.65 ± 0.50
	mean 69%			mean = 3.03 ± 0.42
C-I	67 ± 4	0.70 ± 0.05	0.45 ± 0.08	1.46 ± 0.26
C-II	69 ± 4	1.10 ± 0.07	0.85 ± 0.11	1.37 ± 0.17
C-III	71 ± 4	1.65 ± 0.08	1.39 ± 0.14	1.12 ± 0.11
	mean 69%			mean = 1.32 ± 0.18

[a] Total ^{228}Th represents that naturally occurring plus that added as a contaminant in the tracer.

variation in the ^{229}Th activity should not significantly affect the mass, a number of analyses were performed with varying amounts of added ^{229}Th (1–14 dpm) and the recoveries did not show any correlation with the amount of ^{229}Th spiked (Table II). The analyses in Table II are useful to show the variability in yield with equal tissue masses.

We wished to show how sensitive the measurement might be made and accordingly investigated whether the analysis of masses larger than 100 g would result in a decreased extraction efficiency. Accordingly, varying masses of tissue from the same aliquot of beef liver in solution (from 100 to 560 g) were analyzed using equal activities of tracer for each analysis, and 10 mg of added iron for each aliquot. In Table III, the variability in yield with increased mass was less than the among eight roughly equal masses between 130 and 106 g. In fact, the yield was the same within counting error for masses of 140, 280, and 560 g of tissue. This was probably fortuitous, but demonstrates that wet weight of 0.6 kg can be analyzed without loss of yield.

Uranium is not extracted appreciably into TLA because of its low distribution coefficient and plutonium which is extracted into the organic phase is not backwashed with 10 M HCl. Thus thorium is separated from uranium and plutonium without any interference. The details have been included in our earlier paper (*6*). Also, ^{229}Th and ^{230}Th are well resolved without any spectral interference; however, a thick masseous plate may cause some interference (*7*).

Replicate analyses were performed on three different beef liver samples and the results are summarized in Table IV. The natural ^{228}Th content of three beef liver samples determined in replicate were 1.32 ± 0.18, 1.40 ± 0.29, and 3.03 ± 0.42/kg wet weight. Thorium-230 and -232 could not be detected in these liver samples which may be due to the fact that these animals were not old enough to have absorbed ^{232}Th or ^{230}Th in detectable amounts. The ^{228}Th observed probably was the decay product of ^{228}Ra which is absorbed much more readily.

The precision of this analytical technique can be seen from the results of replicate analyses on the same pooled liver samples (Table IV). The standard deviation was within the error of an individual analysis.

The activity associated with the individual analyses were calculated as follows:

$$A = \gamma \frac{R}{EY} \qquad (1)$$

where A = the activity of ^{228}Th in beef liver, R = the count rate in the ^{228}Th region from ^{228}Th in beef liver, E = the efficiency of the counter, and Y = the radiochemical yield. The product EY is equivalent to the cpm observed/dpm added of the tracer. γ is the factor to convert dpm to activity.

The propagated random error in A can be obtained from Equation 1 by the standard means of propagating error for products and quotients and is:

$$\frac{s^2A}{A^2} = \frac{s^2R}{R^2} + \frac{s^2(EY)}{(EY)^2} \qquad (2)$$

Since the count rate (R) in the ^{228}Th region includes that contributed by ^{228}Th contamination of ^{229}Th tracer, which is added in order to make a radiochemical determination of yield (^{228}Th/^{229}Th = 0.0814 on an activity basis) and also the background. Hence,

$$R = R_1 - R_2 - R_3 \qquad (3)$$

where R_1 = total count rate in the ^{228}Th region, R_2 = count rate in the ^{228}Th region due to tracer, and R_3 = count rate in the ^{228}Th region due to background.

The count rates of sample and background are simply:

$$R_1 = \frac{C_1}{t_1} \text{ and } R_3 = \frac{C_3}{t_3} \tag{4}$$

and the estimate of the standard deviation:

$$s(R_1) = \sqrt{C_1}\Big/t_1, \quad s(R_3) = \sqrt{C_3}\Big/t_3 \tag{5}$$

where C_1 is the total number of counts in the ^{228}Th region in counting time t_1.

$$R_2 = FR_o \tag{6}$$

where F is the ratio ^{228}Th/^{229}Th established from measurement of the tracer ($F = 0.0814$ and $s(F) = 0.0038$ for this work), and R_o is the count rate in the ^{229}Th region, and C_o = total counts in the ^{229}Th region in time t_o.

Again propagating the error for Equation 6 gives:

$$\frac{s^2(R_2)}{R_2{}^2} = \frac{s^2(F)}{F^2} + \frac{s^2(R_o)}{R_o{}^2} \tag{7}$$

R_3 is the background count in ~1000 min (the average counting time used for background); background counts are less than 1, so that $s^2(R_3)$ is of the order of 10^{-6} and can be neglected for our system.

By the standard rules for propagation of error for sums and differences, the random error associated with R from Equation 3 is:

$$s^2(R) = s^2(R_1) + s^2(R_2) + s^2(R_3) \tag{8}$$

and $s^2(R)$ can now be readily calculated by combining Equations 5 and 7 with 8.

The cpm observed/dpm added is the product EY, so that if E is known, then Y may be calculated. In fact,

$$Y = \frac{R_o}{ET} \tag{9}$$

The error is propagated in the usual fashion for products and quotients.

In short, the error in A (Equation 2) consists of two terms, comprising the contributions from the error in observed count rate and the product of yield and efficiency. The relative importance of the two as source of error depends on the activity in the sample and the amount of added tracer.

ACKNOWLEDGMENT

The authors thank Friedrich Steinhausler for his help in propagating the error and Sarah Hlavka for her technical assistance in sample preparation.

LITERATURE CITED

(1) H. G. Petrow, A. Cover, W. Schiessle, and E. Parsons, *Anal. Chem.*, **36**, 1600 (1964).
(2) H. G. Petrow and C. Strehlow, *Anal. Chem.*, **39**, 265 (1967).
(3) C. W. Sill, K. W. Puphal, and F. Hindman, *Anal. Chem.*, **46**, 1725 (1974).
(4) C. W. Sill, *Anal. Chem.*, **49**, 618 (1977).
(5) D. R. Percival and D. B. Martin, *Anal. Chem.*, **46**, 1742 (1974).
(6) N. P. Singh, S. A. Ibrahim, N. Cohen, and M. E. Wrenn, *Anal. Chem.*, **50**, 357 (1978).
(7) M. E. Wrenn, N. P. Singh, S. A. Ibrahim, and N. Cohen, *Anal. Chem.*, **50**, 1712 (1978).
(8) "Health and Safety Manual", Health and Safety Laboratory, U.S. Energy Research and Development Administration, 1976.
(9) M. E. Wrenn and N. Cohen, *Health Phys.*, **13**, 1075 (1967).
(10) M. E. Wrenn, *Proc. Int. Symp. Areas of High Natural Radioactivity, Pocos de Caldas, Brazil*, 131–157 (1975).

RECEIVED for review June 21, 1978. Accepted November 3, 1978. Research supported by Contract No. AT(49-24) 0358 from the U.S. Nuclear Regulatory Commission, Contract No. EY-76-S02-2968 from the U.S. Department of Energy and is part of a center program supported by Grant No. ES 00260 from the National Institute of Environmental Health Sciences and Grant No. CA 13343 from the National Cancer Institute.

Determination of Benzidine, Dichlorobenzidine, and Diphenylhydrazine in Aqueous Media by High Performance Liquid Chromatography

R. M. Riggin* and C. C. Howard

Organic, Analytical, and Environmental Chemistry Section, Battelle's Columbus Laboratories, 505 King Avenue, Columbus, Ohio 43201

A high performance liquid chromatographic method is described for the determination of benzidine, 3,3′-dichlorobenzidine, and 1,2-diphenylhydrazine in aqueous media. These compounds can be assayed either by direct injection, or by solvent extraction or resin adsorption of the aqueous sample prior to analysis with detection limits of less than 1 μg/L. Linearity, precision, and specificity of the method was excellent and no interferences were encountered in the several wastewater samples analyzed. Diphenylhydrazine was found to be extremely unstable (half time for disappearance approximately 15 min) in wastewater, thus making its analysis extremely difficult and of limited practical value.

The discharge of hazardous industrial effluents into the environment has focused a great deal of attention toward the monitoring and control of such effluents. In this vein, the U.S. Environmental Protection Agency (EPA) has established a list of hazardous organic chemicals (priority pollutants) which are likely to be present in certain industrial aqueous effluents, and thus should be monitored in these effluents. For this reason, there is need for relatively specific, sensitive procedures which can be utilized in the routine analysis for these compounds in aqueous media.

This paper deals specifically with the analysis of the three basic priority pollutants: benzidine, 3,3′-dichlorobenzidine (DCB), and 1,2-diphenylhydrazine (DPH). Benzidine and DCB, as well as various other aromatic amines, have been used extensively in the synthesis of dyes and DPH is an intermediate in the synthesis of benzidine. All three of these compounds are suspected carcinogens and thus their presence in the aqueous environment is of particular concern to human health (*1*).

Various methods have been published for the analysis of benzidine and DCB while no methods for DPH analysis have been reported. In one study, colorimetric, thin-layer, and gas chromatographic procedures were evaluated for the analysis

0003-2700/79/0351-0210$01.00/0 © 1979 American Chemical Society

of benzidines in natural waters (2). Gas chromatography with flame ionization detection (FID) was found to be the preferred method, with a detection limit of 2–3 μg/L. More recently, gas chromatography (FID) and spectrophotofluorimetry were used for benzidine analysis in a variety of matrixes, with detection limits in the low microgram per liter region (3).

Recent application of best available technology to remove toxic materials from industrial effluents has resulted in a need for more sensitive analytical techniques having submicrogram per liter detection limits for the analysis of benzidine, DCB, and DPH. Several approaches could be used to extend the detection limits of the gas chromatographic methods reported (colorimetric procedures are too nonspecific at low concentrations and will not be considered further). The use of a more sensitive and specific detection system such as alkali flame detection has been applied to certain amines at lower levels than are possible with FID (4). Fluoracylation of amines followed by gas chromatography with electron capture detection has also been employed at picogram levels (5). Neither of the above approaches has been reported for the compounds of interest. However, we have evaluated both of these approaches in our laboratory and have found: (1) that the free amines are not readily chromatographed at levels below 10 ng on column (and DPH decomposes instantaneously to azobenzene in the injection port), and (2) while DCB is easily derivatized by most fluoroacylating reagents, benzidine and DPH could not be satisfactorily derivatized.

An alternate approach which we have found far superior is the use of reversed phase high performance liquid chromatography (HPLC) with electrochemical detection. We have used this technique extensively for various compounds in biological media (e.g., catecholamines) and found it to be extremely sensitive (low picogram detection limits) and specific for readily oxidizable compounds (6). Since the three compounds of interest here are readily oxidized at a glassy carbon electrode, it was felt that this approach should be useful. The specific operational details of this technique have been reviewed and will not be described here (7).

EXPERIMENTAL

Apparatus. The HPLC system used in this study was assembled from modular components consisting of an Altex Model 110A Liquid Chromatographic Pump, a Rheodyne 7010 injector with a 50-μL loop, a 4.6-mm i.d. × 25 cm stainless steel column packed with Lichrosorb RP-2 (5-μm particle diameter), and an electrochemical detector (Model LC-2A) equipped with a thin-layer glassy carbon electrode (Model TL5) available from Bioanalytical Systems, West Lafayette, Ind. Data were recorded on a strip chart recorder and quantitative measurements were based on peak height. The mobile phase reservoir consisted of a single neck flask maintained at 30 °C to reduce the amount of dissolved air. A vortex evaporator (Model 3-2200, Buchler Instruments) was used for concentrating small volumes of organic solutions. The liquid chromatographic columns were slurry packed using established methods (8).

Procedure. In order to ascertain the stability of stock solutions of the three amines, 100-ppm solutions of each of the amines were prepared and 4-mL aliquots were sealed in 10-mL glass ampules. The ampules were stored in the dark at room temperature and at 0, 30, 60, and 90 days three ampules of each solution were opened and assayed by HPLC by comparing to freshly prepared standard solution. Figure 1 shows the separation of benzidine, DCB, and DPH by HPLC and lists the chromatographic conditions used throughout this study.

The extractability of the three compounds from aqueous solution was investigated using two different organic solvents and three different pH levels. Aqueous solutions were 0.1 M phosphate buffers at the appropriate pH. A 500-mL portion of the aqueous solution was spiked with 10 ppb of the amines and extracted with 50 and then 30 mL of organic solvent in a 1-L separatory funnel. The combined extracts were washed with 20 mL of water, mixed with 20 mL of methanol, and concentrated to 5–10 mL on a rotating evaporator at room temperature. The solution was then transferred to a 15-mL conical centrifuge tube and concentrated to 2 mL on a vortex evaporator at 35 °C. The solution was then diluted to 4 mL with acetate buffer and analyzed by HPLC. Benzidine and DPH were investigated separately throughout this study since DPH can be converted to benzidine at low pH.

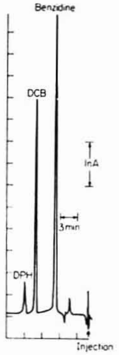

Figure 1. Separation of DCB, DPH, and benzidine by reversed phase liquid chromatography. Volume injected, 25 μL; amount injected, 3 ng each; flow rate, 0.8 mL/min; mobile phase, 50/50 acetonitrile/pH 4.7, 0.1 M sodium acetate buffer; stationary phase, 4.6 mm i.d. × 25 cm RP-2 (5 μm); electrode potential, 0.9 V

An alternate method which can be used for extraction of wastewater in the field was evaluated. Aqueous solutions were adjusted to pH 7 with 0.2 M phosphate buffer. Ten milliliters of the aqueous sample was passed through an ODS reversed phase cartridge (Sep Pak C-18, Waters Associates) at a flow rate of approximately 10 mL/min using a glass syringe. The cartridge was then washed with 5 mL of distilled water (discarded) and then eluted with 3 mL of methanol which was stored at −70 °C. When the sample was to be analyzed, the methanol was concentrated to 0.5 mL in a vortex evaporator, 1 mL of 0.1 M pH 4.7 acetate buffer was added, and the sample reconcentrated to 1 mL and analyzed by HPLC.

The stability of the three amines in dilute aqueous solution was investigated under various conditions including three pH levels, with or without chlorine, and two temperatures. The samples were spiked with 10 μg/L of the three amines (benzidine and DPH were studied separately as before) and stored at the appropriate temperature for 7 days. The samples were then extracted as described earlier. One half of the samples were spiked with 2 ppm of NaOCl. The samples stored at pH levels other than 7 were adjusted to pH 7 prior to extraction by the addition of either 0.1 M H_2SO_4 or NaOH.

A preliminary study was conducted to determine the feasibility of monitoring the benzidines in water effluents by direct injection (50 μL) onto the HPLC system. Several actual wastewater samples (1 L) were collected in half-gallon bottles containing 200 mL of methylene chloride, 5 g of $KHSO_4$, and 75 g of NaCl. The water samples were ~pH 2 (as a result of the $KHSO_4$) and were maintained at 4 °C until analyzed. Five milliliters of the water sample was spiked with 50 ng of benzidine and DCB, filtered through a 0.2-μm filter (Millipore type GS), and injected onto the HPLC system.

RESULTS AND DISCUSSION

The HPLC conditions shown in Figure 1 were found to be quite satisfactory. The RP-2 column was found to be superior to any other reversed phase or ion-exchange packing materials (e.g., VYDAC TP SCX, Whatman Partisil SCX, μ-Bondapak-18, and Lichrosorb RP-8 and RP-18). Column efficiencies of 5000 theoretical plates per 25-cm column for benzidines were commonly achieved using RP-2 whereas none of the other packing materials exhibited greater than 2500 theoretical

Table I. Solvent Effect on Stability

day	benzidine	DCB	DPH
	% recovery[a]		
		methanol	
0	85	90	81
	87	90	81
	84	90	81
	85 ± 2[b]	90	81
30	108	105	0
	94	93	
	95	105	
	99 ± 8	101 ± 7	
60	92	87	0
	95	87	
	93	86	
	93 ± 2	86 ± 1	
90	93	92	0
	97	90	
	95	90	
	95 ± 3	91 ± 1	
		acetonitrile	
0	100	102	109
	98	95	100
	101	98	80
	100 ± 2	98 ± 4	96 ± 15
30	96	88	0
	102	92	
	93	99	
	97 ± 5	93 ± 5	
60	100	98	0
	100	98	
	103	98	
	101 ± 2	98	
90	98	101	0
	99	100	
	98	101	
	98 ± 1	101 ± 1	

[a] Stability was determined by HPLC analysis after various storage periods by comparison to freshly prepared standards. [b] Average ± standard deviation.

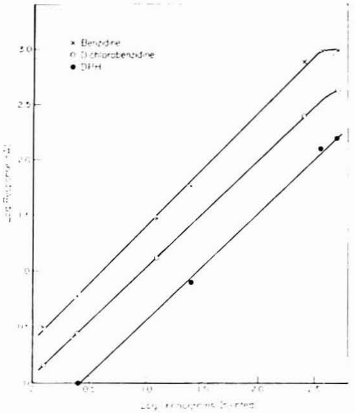

Figure 2. Linearity of response for DPH, DCB, and benzidine (See Figure 1 for conditions)

Table II. Extraction Studies[b]

pH	benzidine	DCB	DPH
	% recovery		
		methylene chloride	
2	0	80	9
	0	69	33
	0	77	0
	0	75 ± 7[a]	14 ± 16
7	68	99	75
	81	84	82
	81	99	58
	76	104	60
	76 ± 8	96 ± 9	68 ± 17
10	92	101	75
	103	104	79
	80	82	82
	92 ± 13	96 ± 12	79 ± 4
		chloroform	
2	0	93	35
	0	84	28
	0	89	41
	0	92 ± 3	35 ± 19
7	87	92	69
	89	92	70
	88	95	64
	92	99	37
	89 ± 2	94 ± 4	60 ± 24
10	79	88	81
	90	98	65
	88	94	67
	86 ± 7	93 ± 5	67 ± 16

[a] Average ± standard deviation. [b] Five hundred-milliliter volumes of aqueous solutions at the stated pH were extracted with the organic solvent and the extracts assayed by HPLC. Triplicate analyses were conducted in all cases.

plates. Column lifetime for the RP-2 was found to be greater than 6 months under the conditions used. Linear response for the three amines was achieved over the range of 1–1000 ng as shown in Figure 2. Repeatability of eight replicate injections was ±2.8% for each of the components at the 50-ng level at a signal to noise ratio of 10.

The results from the solvent stability study are summarized in Table I. It is readily apparent that benzidine and DCB are quite stable in both acetonitrile and methanol. DPH was found to be extremely unstable (half time of disappearance less than 24 h) in all the solvents evaluated, including benzene, methylene chloride, methanol, triethylamine, acetonitrile, and acetic acid. Therefore it was necessary to prepare DPH solutions fresh daily.

The extraction methodology was found to be a very delicate area since numerous unanticipated problems developed which led to low recoveries, especially for benzidine and DPH. The stability of DPH was found to be a major problem. The following are some of the other problems encountered.

(1) Benzidine is substantially adsorbed on Na_2SO_4 during the drying of organic extracts. Although use of K_2CO_3 corrected this problem, elimination of the drying step was found to be useful when using HPLC analysis.

(2) Benzidine is heat labile so that Kuderna Danish concentration techniques gave unacceptable results. The use of rotary evaporation and vortex evaporation eliminated this problem.

(3) Decomposition of benzidine occurred when concentrating it in methylene chloride or chloroform solutions. The addition of 15% MeOH prior to concentration stabilized the benzidine.

Table III. Preservation Date (after 7 Days Storage)

		% recovery[b]		
pH		benzidine	DCB	DPH
2	room temperature	80	90	0
		94	85	0
		87[a]	88	0
	4 °C	80	82	0
		80	82	0
		80	82	0
7	room temperature	64	110	0
		55	89	0
		60	99	0
	4 °C	79	97	0
		56	83	0
		68	90	0
10	room temperature	70	80	0
		73	82	0
		72	81	0
	4 °C	82	93	0
		38	44	0
		64	74	0
4.7	4 °C	72	81	10
		86	91	28
		79	86	19

[a] Average. [b] Zero recovery was realized for the samples spiked with 2 ppm NaOCl and therefore this data is not reported in the table. Five-milliliter volumes of distilled water at the stated pH were stored at either room temperature or 4 °C, in the dark, for seven days. The solutions were then extractedand assayed by HPLC.

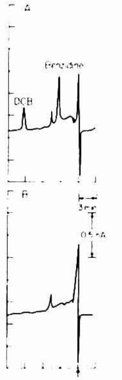

Figure 3. Chromatograms for direct injection of aqueous effluent from an organic chemical plant. (A) Spiked with 10 ppb DCB and benzidine. (B) Unspiked

The results of the extraction experiments are summarized in Table II. Chloroform at pH 7 was found to be the most satisfactory extraction condition and was used for all further work. DPH extraction was somewhat irreproducible due to its instability during concentration. However chloroform extraction at pH 7 gave an extraction efficiency greater than 50%.

The results of the preservation study are shown in Table III. DPH was not stable (<10% remaining) for longer than 1 day under any of the conditions studied and thus it is not included in the table. At each pH, DPH degrades to different components (based on HPLC retention times) indicating that several competing reactions are taking place in solution. At pH 10, DPH apparently decomposes primarily to azobenzene; at pH 2, it degrades to benzidine; and at pH 7, still a third unidentified (oxidizable) component is formed.

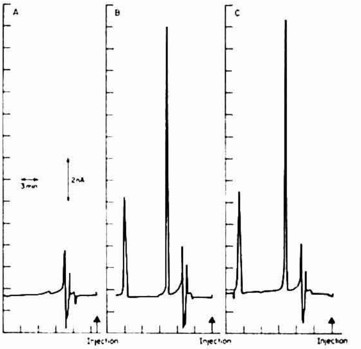

Figure 4. Chromatograms for solvent extraction of municipal sewage. (A) Unspiked. (B) Spiked with 10 ppb benzidine and DCB. (C) Standard corresponding to 100% recovery of spike

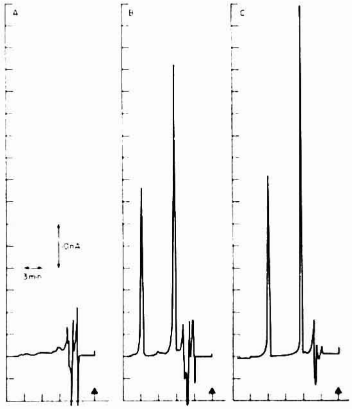

Figure 5. Chromatogram for resin concentration of municipal sewage. (A) Unspiked. (B) Spiked with 10 ppb benzidine and DCB. (C) Standard corresponding to 100% recovery of spike

None of the amines were detectable in the solutions to which chlorine was added. A pH of 2 was found to give the best results for benzidine and DCB. However, at pH 2, DPH degrades to benzidine thus creating an undesired artifact. This problem was overcome by employing 0.1 M pH 4.7 acetate buffer where both benzidine and DCB are well preserved, and DPH degrades to two unidentified components, not to benzidine.

The three analytical approaches, direct injection, solvent extraction, and resin adsorption were applied to actual wastewater and/or surface water samples and the results are shown in Figures 3, 4, and 5, respectively. Each of the approaches was found to be quite effective. Direct injection, while most susceptable to interferences, is very rapid and has a detection limit of approximately 1 μg/L. Solvent extraction serves to clean up and concentrate the sample to give a detection limit of 50 ng/L or better. However, DPH is not

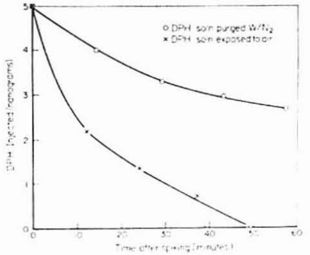

Figure 6. Stability curve for DPH in municipal sewage

efficiently recovered by this technique (as described previously). Resin adsorption offers a detection limit of approximately 100 ng/L and offers some degree of cleanup. The primary advantages of resin adsorption are its speed and the efficient recovery of DPH (at least from distilled water).

DPH was found to be quite unstable in aqueous solution and even more unstable in wastewater samples. Figure 6 shows the stability of DPH in a municipal sewage effluent at the 100 μg/L level. As shown, DPH disappears with a half time of approximately 15 min without removal of oxygen and a half time of 60 min when oxygen is removed by a nitrogen purge. This result indicates that DPH analysis in wastewater is virtually impossible and perhaps meaningless since it is so unstable. At least, the analytical result obtained will represent the portion of intact DPH remaining at the time of analysis, which will be quite different from the DPH level in the original effluent.

CONCLUSIONS

The results of this study clearly show that HPLC with electrochemical detection is a sensitive method for the analysis of benzidine, DCB, and DPH in aqueous samples. These compounds can be assayed by direct injection, solvent extraction, or resin adsorption techniques at the submicrogram per liter level. Direct injection is satisfactory in most cases where 1 μg/L sensitivities are adequate. Use of solvent extraction results in a detection limit of 50 ng/L, whereas resin adsorption affords a detection limit of 100 ng/L. The resin adsorption technique has the advantage of being used in the field, thus eliminating the need to preserve dilute aqueous solutions of the compounds of interest and also avoids the emulsion problems frequently encountered during solvent extraction of certain wastewater samples.

While benzidine and DCB are relatively stable compounds, DPH is extremely unstable and none of the approaches described herein gave entirely satisfactory results.

ACKNOWLEDGMENT

We thank Peter Mondron for packing the HPLC columns for this study.

LITERATURE CITED

(1) T. J. Haley, *Clin. Toxicol.*, **8**, 13 (1975).
(2) R. L. Jenkins, and R. B. Baird, *Bull. Environ. Contam. Toxicol.*, **13**, 436 (1975).
(3) M. C. Bowman, J. R. King, and C. L. Holder, *Int. J. Environ. Anal. Chem.*, **4**, 205 (1976).
(4) H. B. Hucker, and S. C. Stauffer, *J. Chromatogr.*, **138**, 437 (1977).
(5) M. Makita, S. Yamamoto, and M. Kono, *Clin. Chim. Acta*, **61**, 403 (1975).
(6) P. T. Kissinger, R. M. Riggin, R. L. Alcorn, and L. D. Rau, *Biochem. Med.*, **13**, 299 (1975).
(7) P. T. Kissinger, *Anal. Chem.*, **49**, 447A (1977).
(8) P. J. Mondron, and P. G. Bonnett, Pittsburgh Conference on Analytical Chemistry and Applied Spectroscopy, Cleveland, Ohio, Abstract No. 437, 1978.

RECEIVED for review August 18, 1978. Accepted October 27, 1978. Work supported by the U.S. Environmental Protection Agency, EMSL, Cincinnati, Ohio.

Determination of Trace Level Arsenic(III), Arsenic(V), and Total Inorganic Arsenic by Differential Pulse Polarography

F. T. Henry, T. O. Kirch, and T. M. Thorpe*[1]

Department of Chemistry, Miami University, Oxford, Ohio 45056

Speciation of As(III), As(V), and total inorganic arsenic (As(tot)) was achieved by differential pulse polarography. As(III) was determined directly in 1 M $HClO_4$ or 1 M HCl. Total inorganic arsenic was measured in either of these supporting electrolytes after prereduction of electroinactive As(V) with a boiling solution of $NaHSO_3$. As(V) was evaluated by difference. The efficiency of reduction ranged from 93% to 109% for concentrations of As(V) ranging from 24 ppb to 4.9 ppm. Standard deviations for the procedure were less than 5.2%. The detection limit in the $HClO_4$-HSO_3^- reduction medium was 20 ppb; in HCl-HSO_3^- it was 7 ppb. Relative errors for the determinations of As(III) and As(tot) ranged from 0% to 19.2%. Interferences from Pb, Sn, and Tl were accounted for by a blank determination employing Ce(IV); interference from the breakdown of monomethylarsonic acid (MMA) during the preliminary reduction was not significant at concentrations of MMA which normally occur in natural waters.

Traditionally, determinations of the total content of arsenic in environmental specimens have been considered adequate to assess the presence, amount, and behavior of this element. Spectrophotometry, atomic absorption, and neutron activation have been employed as the analytical techniques after pretreating samples to convert all of the arsenic present to inorganic arsenic (*1–3*). Recent research (*4–7*) has shown that the predominant arsenic-containing species found in natural aqueous systems are: inorganic arsenate and arsenite, and organic dimethylarsinic and monomethylarsonic acids. Furthermore, the distribution of arsenic among these chemical forms is dynamic with interconversions between the species taking place via chemical and biochemical oxidation–reduction reactions, and by means of biochemical methylation–demethylation (*4, 8–10*). These observations, coupled with recognition that the toxicity, carcinogenicity, transport, and bioavailability of As are highly dependent on the chemical form of the element, have prompted development of analytical methods capable of distinguishing between species of arsenic which exist as part-per-billion levels in environmental media.

Spectroscopic techniques, when used with preliminary oxidation or reduction reactions, hydride generation, or liquid–liquid extraction yield speciation data on arsenic (*1–3, 11–17*). The preliminary operations make it difficult to quantitatively recover very small amounts of As and they may be cumbersome when dealing with large numbers of samples.

Gas chromatographic procedures have been reported for the selective determination of organic and inorganic arsenicals (*5, 18–23*). These methods require preparation of volatile, thermally stable derivatives. While all of the arsenic-containing species mentioned previously have been determined chromatographically in nanogram and sub-nanogram quantities, molecular rearrangements of derivatives and consequent losses of accuracy have been observed (*21*).

Forsberg et al. (*24*), Davis et al. (*25*), Sulek, Zink, and Delude (*26*), and Holak (*27*) have used anodic stripping voltammetry (ASV) to determine As(III). Direct current polarographic measurement of arsenic has been reviewed extensively (*28*). Myers and Osteryoung (*29*) described the differential pulse polarographic (DPP) determination of as little as 0.22 μg/L As(III) in a 1 M HCl supporting electrolyte. This method has been employed to measure As in raw sewage and sewage sludge (*30*), fish (*27*), and foodstuffs (*27*). DPP is an advantageous technique because of its high sensitivity for elements, such as arsenic, which do not form mercury amalgams readily (*29*).

The polarographic determination of As(V) or total inorganic arsenic requires preliminary reduction of the electroinactive As(V) to electroactive As(III). Reducing agents which have been suggested for this purpose include $LiAlH_4$ (*31*), Zn-amalgam (*32*), cuprous ion, hydrazine salts, and acidic solutions of iodide ion (*24, 28, 29*). Sulfur dioxide, derived from an aqueous solution of HSO_3^- has also been recommended as a reductant. However, detailed reports describing the range of conditions over which bisulfite reduction is applicable to the determination of trace level As(V) have not been presented, nor have data on the use of such a prereduction to speciate As(III) and As(V).

In this paper we report a method for determination of As(III), As(V), and total inorganic arsenic by DPP. As(III) is measured directly in 1 M $HClO_4$ or 1 M HCl. Total inorganic arsenic is determined in either of these supporting electrolytes after prereduction of electroinactive As(V) with a solution of sodium bisulfite. As(V) is evaluated by difference. Bisulfite was selected as the reductant since it reduces As(V) rapidly and quantitatively, and excess HSO_3^- is readily removed from the reaction mixture.

EXPERIMENTAL

Reagents. High purity arsenic trioxide was obtained from ROC/RIC (Belleville, N.J.) and ultrapure arsenic pentoxide was purchased from Alfa Inorganics (Danvers, Mass.). Standard solutions containing 1×10^{-3} M As(III) or As(V) were prepared by dissolving an appropriate amount of oxide in a minimal amount of 3 N NaOH. The solution was acidified to pH 2 and diluted to the desired volume with triply distilled deionized water. These stock solutions were stable for at least three months. Working solutions of 1×10^{-4} M As(III) or As(V) were prepared weekly.

High purity dimethylarsinic acid and monomethylarsonic acid were obtained from Ansul Company (Weslaco, Texas).

A solution of 0.10 M Ce(IV) was prepared from reagent grade cerric ammonium nitrate. Sixty-three grams of $Ce(NH_4)_2(NO_3)_6$ were mixed with 30 mL of concentrated sulfuric acid. The paste formed from this mixture was dissolved by slowly adding 500 mL of triply distilled deionized water. After cooling the solution to room temperature, it was filtered through a fine porosity sintered glass filter. The filtrate was diluted to 1 L.

U.S. Environmental Protection Agency water reference standards were prepared according to the directions supplied with those samples. Solutions of a commercially available trace element standard (Eastman Kodak gelatin multicomponent trace element reference material TEG-50-B, Rochester, N.Y.) were prepared by addition of a weighed amount of the standard to 25 mL of triply

---

[1] Present address: The Procter & Gamble Company, Sharon Woods Technical Center, 11530 Reed Hartman Highway, Cincinnati, Ohio 45241.

0003-2700/79/0351-0215$01.00/0 © 1979 American Chemical Society

distilled deionized water. This mixture was heated gently until solution was complete.

All other chemicals were reagent grade. All solutions were prepared with triply distilled deionized water. Glassware was leached for 24 h with 1:1 HNO_3.

Instrumentation. A Princeton Applied Research Corporation (Princeton, N.J.) Model 174A polarographic analyzer and a Hewlett-Packard (Avondale, Pa.) Model 7040A X-Y recorder were used for all DPP determinations.

A Hach (Ames, Iowa) Model 8596 expanded scale pH meter was used for all pH measurements.

Reduction of As(V) with Bisulfite. The optimized procedure for determination of As(V) or for measurement of total inorganic arsenic is described below.

The pH of an aqueous sample is adjusted to 3, either with dilute HCl or with dilute NaOH. Equal volumes of the sample and 1 M $NaHSO_3$ are mixed to yield an HSO_3^- concentration of 0.50 M. Solid $NaHSO_3$ may be substituted for the solution of the reducing agent, if desired. The pH of the mixture is readjusted to a value of 3. The solution is boiled for 30 min with continuous stirring. An air condensor is used to minimize evaporation (*33*). After the reduction step is complete, the solution is cooled briefly and sufficient $HClO_4$ or HCl is added to neutralize the excess HSO_3^- and to provide a 100% excess of acid. The sample is boiled for 15 min, with the air condensor removed, and with nitrogen bubbling through the solution to facilitate removal of SO_2. After the purging step, the solution is cooled and the acid concentration adjusted to 1 M with $HClO_4$ or HCl.

Samples are split into two portions for the determinations of As(III) and As(III) plus As(V) (As(tot)). The first portion is used for determination of As(III) after it has been made 1 M in $HClO_4$ or HCl. The second portion is carried through the bisulfite reduction procedure to measure As(tot). Quantitation is performed by the method of standard additions.

Pb(II), Sn(II), Sn(IV), Tl(I), and Tl(III) are potential interferences to the DPP measurements. After recording polarograms for As(III) or As(tot) and for the standard additions used for quantitation, sufficient Ce(IV) is added to the solution to oxidize As(III) to polarographically inactive As(V). Another polarogram is recorded to give the "blank" response arising from the residual current and from reduction of Pb, Sn, and Tl. This blank is subtracted from the response obtained in the previously recorded polarograms. Ce(IV) does not interfere as it is reduced by the elemental mercury from the DME. A single addition of 0.20 mL of 0.10 M Ce(IV) usually oxidized As(III) completely. When dealing with samples having unfamiliar matrices or when high levels of As(III) are present, two 0.20-mL additions of 0.10 M Ce(IV) are made, with polarograms recorded after each, to assure quantitative oxidation of As(III). Caution must be exercised in the blank determination, especially when attempting to measure low concentrations of As, as large shifts in the base line may occur (*28*). Holak (*27*) recommended an ion-exchange procedure as an alternative to the Ce(IV) oxidation to reduce the background response from Pb, Sn, and other metals.

RESULTS AND DISCUSSION

Bisulfite Reduction of As(V). Quantitative reduction of As(V) was observed between pH 1.0 and 3.8. Beyond these limits, less than 90% of the As(V) was converted to As(III); if the total concentration of acid was increased to 1.5 M, no As(III) was detected after the bisulfite reduction. The hydrogen ion concentration directly affects the formal potentials of the H_3AsO_4/H_3AsO_3 and H_2SO_3/SO_4^{2-} couples, so that in the overall reaction:

$$H_3AsO_4 + H_2SO_3 \rightleftharpoons H_3AsO_3 + SO_4^{2-} + 2H^+ \quad (1)$$

a net decrease in production of As(III) occurs as the acidity increases. Furthermore, boiling a highly acidic solution of bisulfite (i.e., aqueous SO_2), to speed the red-ox process, results in rapid loss of SO_2, thereby making the active form of the reductant less available for reaction with As(V). These factors are responsible for the decrease in conversion of As(V) at pH's less than 1. At pH's greater than 3.8, deprotonation of H_2SO_3 and H_3AsO_4 occurs, lowering the availability of these species for participation in the red-ox reaction. A pH of 3 was optimum for the reduction of As(V) to As(III).

At concentrations of HSO_3^- from 0.075 to 1 M, the efficiency of reduction of As(V) averaged 96.8%; the efficiency dropped to 90% for 0.05 M HSO_3^-. To ensure an adequate supply of reductant for quantitative production of As(III) and to allow for potential competitive reactions with oxidants other than As(V), 0.50 M solutions of bisulfite were used in subsequent studies.

At room temperature the reduction reaction proceeded slowly and nonquantitatively; only 86% of the As(V) in a 6.5 × 10^{-7} M solution was reduced after 30 min. Reduction efficiency was increased to 95.8% ± 3.6% by boiling for 30 min, and more than 90% of the As(V) was reduced if solutions were boiled for 25–35 min. Low and erratic (68–82%) conversion of As(V) to As(III) was observed if boiling time was extended to 40 min or longer. This is thought to result from loss of As(III) through spattering as the solution evaporates during extended heating. Air oxidation of the spattered analyte may also contribute to the low recoveries.

The final step of the procedure is the removal of excess reductant. If this is not carried out, polarographically active SO_2 (E_P at −0.25 V to 0.30 V vs. SCE) will interfere with or completely obscure the peak due to As(III). Boiling the reduction mixture for 15 min after the unreacted HSO_3^- has been neutralized and a 100% excess of acid added was effective for SO_2 removal when used in conjunction with continuous bubbling of nitrogen through the solution. Shorter heating, lower temperatures, or omission of N_2 purging led to erratic removal of SO_2.

Electrochemical Characteristics of Bisulfite Reduction Systems. In $HClO_4$ and $HClO_4$-HSO_3^- (bisulfite blank acidified with $HClO_4$) media, the peak potential of As(III) was −0.49 V vs. SCE and linear working curves ($Y = 1.42\ (\mu A/ppm)X - 3.40 \times 10^{-4}$, correlation coefficient = 0.999) extended from 10 ppb to greater than 7.5 ppm. The detection limit, defined as the minimum concentration of As(III) producing a response that was two times the signal found at −0.49 V vs. SCE when analyzing the supporting electrolyte alone, was 20 ppb.

The As(III) peak occurred at −0.38 vs. SCE in the HCl and HCl-HSO_3^- electrolytes. Linear calibration curves extended from 1 ppb to greater than 7.5 ppm. However, these curves differed depending on the supporting electrolyte; in 1 M HCl the regression equation was $Y = 5.98\ (\mu A/ppm)X - 3.76 \times 10^{-3}$ (correlation coefficient = 0.999), and in 1 M HCl-HSO_3^-, the curve was described by $Y = 4.92\ (\mu A/ppm)X + 2.18 \times 10^{-2}$ (correlation coefficient = 0.999). These differences indicate that the DPP response to As(III) is more sensitive to changes in composition of the 1 M HCl supporting electrolyte than to alteration of the 1 M $HClO_4$ electrolyte. This conclusion was confirmed in analyses of water reference standards. The detection limit was 7 ppb in HCl and 4 ppb in HCl-HSO_3^-. Blanks were consistently smaller in the HCl-HSO_3^- system so that a lower detection limit was observed even though the slope of the calibration curve in 1 M HCl was approximately 30% larger than for HCl-HSO_3^-.

Efficiency of As(V) Reduction by HSO_3^-. The efficiency of As(V) reduction was examined in $HClO_4$-HSO_3^- and HCl-HSO_3^- media (Table I). Reductions were quantitative, with the average recoveries over the concentration ranges examined being 96% in $HClO_4$-HSO_3^- and 105% in HCl-HSO_3^-. Standard deviations were under 5.2%. Neither reoxidation of As(V) in the presence of $HClO_4$ nor volatilization losses of As(III) as $AsCl_3$ in the presence of HCl occurred.

Accuracy of As(III) and As(tot) Determinations. The accuracy of the analytical procedure was examined using U.S.

Table I. Efficiency of As(V) Reduction

As(V) present	As(III) found	recovery, %
perchloric acid-bisulfite media		
4.93 ppm	4.66 ppm	94.5
1.09 ppm	1.02 ppm	93.6
106 ppb	102 ppb	95.8
106 ppb	109 ppb	102
48 ppb	45 ppb	93
average recovery: 96		
standard deviation: ±3.6%		
relative standard deviation: 3.8%		
hydrochloric acid-bisulfite media		
247 ppb	265 ppb	107
169 ppb	178 ppb	105
53 ppb	58 ppb	109
51 ppb	49 ppb	96
24 ppb	26 ppb	108
average recovery: 105%		
standard deviation: ±5.2%		
relative standard deviation: 5.0%		

polarographic conditions

electrodes:
working: DME
reference: SCE
counter: Pt wire
drop time: 2 s
initial potential: -0.20 V
potential range: 0.75 V
scan rate: 1 mV/s
modulation amplitude: 100 mV

Environmental Protection Agency water reference standards, a commercial trace element reference material (Eastman Kodak, TEG-50-B, Rochester, N.Y.), and samples of "high purity" (*34*, *35*) dimethylarsinic acid (DMA) and monomethylarsonic acid (MMA) (Table II). Agreement between the measured and reported values for As(tot) was good except for the MMA and the commercial reference material. In the case of MMA, reduction conditions caused the organoarsenical to break down into an electroactive species, probably As(III), which prevented DPP determinations of the total inorganic arsenic impurity present in the sample. The relatively poor accuracy found in analyses of the commerical reference material resulted from difficulties in reliably interpreting base lines in the polarograms of the analyte and blank. This is attributed to the interference of the gelatin matrix with electrode processes.

Satisfactory agreement was found between the measured and reported (*35*) values for As(III) in MMA and DMA. In the cases of the water reference samples and the commercial reference material, the results for As(III) and As(tot) were in concordance.

The relative standard deviations for these determinations ranged from 2.5% to 10% for As(III) and from 3% to 32% for As(tot). Relative errors for As(tot), excluding results for MMA, averaged 7.9%.

Interferences. The primary interferences to the speciation of As by DPP arise from the ions of the elements Pb, Sn, and Tl (*29*). These interferences can, in general, be accounted for by means of the Ce(IV) blank determination. However, cases arise where the magnitude of the blank response is comparable to the signal from As(III). This results in poor analytical accuracy and precision. This was observed during the determination of As(III) and As(tot) in EPA #2 when 1 M HCl was the supporting electrolyte. By using 1 M $HClO_4$, the peak for As(III) was shifted cathodically to -0.49 V vs. SCE where the contribution of the blank to the total current was less significant. This approach to minimizing the effect of interferences is satisfactory provided the concentration of arsenic is not below the detection limit for As(III) in 1 M $HClO_4$.

Interferences may also arise when organoarsenicals break down during the bisulfite reduction to produce As(III) or other products which are electroactive at potentials where the DPP peak for As(III) occurs. The organoarsenicals DMA and MMA were examined for their potential as interferences. No decomposition of DMA was observed in the determinations of As(III) or As(tot) in solutions containing between 3 mg/mL and 10 mg/mL DMA either in 1 M $HClO_4$ or in 1 M HCl. MMA did not interfere with As(III) determinations, but did produce interfering material during the preliminary reduction procedure. Solutions containing 2 mg/mL MMA produced a DPP response at -0.38 V vs. SCE which was equivalent to 8880 μg/g of As(III) in the solid MMA. This occurred in HCl and $HClO_4$ media.

The level at which breakdown of MMA represented a significant interference to the determination of As(tot) was evaluated by preparing solutions in which the ratio of MMA to As(tot) was varied from 5 to 50. The solutions were analyzed for their As(III) and As(tot) content (Table III). As(III) was quantitatively recovered at all ratios. The same was true for As(tot) so long as the ratio of MMA/As(tot) did not exceed

Table II. DPP Determination of Arsenic in Standard Samples

	As(III), ppm		As(V), ppm		total inorganic As, ppm	
sample	found	reported	found	reported	found	reported
U.S. E.P.A. Water reference standards						
E.P.A. #1	0.023	- -	0.008	- -	0.031	0.026
E.P.A. #2	0.106	- -	0.007	- -	0.113	0.109
E.P.A. #3	0.154	- -	0.003	- -	0.157	0.154
high purity dimethylarsinic acid	4.5	<6	108	106	112	<112
high purity monomethylarsonic acid	163	180	N.D.[a]	160	N.D.[a]	340
commercial trace element reference material	116	- -	17	- -	133	115

[a] N.D. = not determinable.

Table III. Determination of As(III) and Total Inorganic As in Presence of Monomethylarsonic Acid (MMA)

	As(III)			total inorganic arsenic		
[MMA]/[As(tot)]	present, ppb	found, ppb	recovery, %	present, ppb	found, ppb	recovery, %
5	51	49	96	200	190	95
	102	104	102			
10	91	96	105	189	187	99
15	102	98	96	200	195	98
50	103	105	102	201	435	216

15. At a 50-fold excess of MMA (11 100 ppb) over As(tot), more than 200% of the initial amount of arsenic present was recovered. While the interference due to the breakdown of MMA becomes severe when determining small amounts of As in the presence of high levels of MMA (>1–2 μg/mL), MMA concentrations of this magnitude are not normally encountered in natural water samples (*4*).

ACKNOWLEDGMENT

Reference purity DMA and MMA were supplied courtesy of Edward Dietz of Hooker Chemical Company and James Warkentin of Ansul Company.

LITERATURE CITED

(1) Y. Talmi and D. T. Bostik, *J. Chromatogr. Sci.*, **13**, 231 (1975).
(2) Y. Talmi and C. Feldman in "Arsenical Pesticides", E. A. Woolson, Ed., *ACS Symp. Ser.*, **No. 7**, Chap. 2, 1975.
(3) M-D. Luh, R. A. Baker, and D. E. Henley, *Sci. Total Environ.*, **2**, 1 (1973).
(4) R. S. Braman in "Arsenical Pesticides", E. A. Woolson, Ed., *ACS Symp. Ser.*, **No. 7**, Chap. 8, 1975.
(5) R. S. Braman and C. C. Foreback, *Science*, **132**, 1247 (1973).
(6) R. S. Braman, D. L. Johnson, C. C. Foreback, J. M. Ammons, and J. L. Bricker, *Anal. Chem.*, **49**, 621 (1977).
(7) E. A. Woolson and P. C. Kearney, *Environ. Sci. Technol.*, **7**, 47 (1973).
(8) D. P. Cox in "Arsenical Pesticides", E. A. Woolson, Ed., *ACS Symp. Ser.*, **No. 7**, Chap. 6, 1975.
(9) J. E. Stolzenberg in "Arsenical Pesticides", E. A. Woolson, Ed., *ACS Symp. Ser.*, **No. 7**, Chap. 10, 1975.
(10) J. M. Wood, *Science*, **183**, 1049 (1974).
(11) M. G. Haywood and J. P. Riley, *Anal. Chim. Acta*, **85**, 219 (1976).
(12) S. S. Sandhu, *Analyst (London)*, **101**, 856 (1976).
(13) D. L. Johnson and M. E. Q. Pilson, *Anal. Chim. Acta*, **58**, 289 (1972).
(14) A. W. Fitchett, E. H. Daughtrey, and P. Mushak, *Anal. Chim. Acta*, **79**, 93 (1975).
(15) T. Kamada, *Talanta*, **23**, 835 (1976).
(16) R. Kaszerman and K. Theuer, *At. Absorp. Newsl.*, **15**, 129 (1976).
(17) J. Aggett and A. C. Aspell, *Analyst (London)*, **101**, 341 (1976).
(18) C. J. Soderquist, D. G. Crosby, and J. B. Bowers, *Anal. Chem.*, **46**, 155 (1974).
(19) J. D. Lodmell, Ph.D. Thesis, University of Tennessee, Knoxville, Tenn., 1973.
(20) L. D. Johnson, K. O. Gerhardt, and W. A. Aue, *Sci. Total Environ.*, **1**, 108 (1972).
(21) Y. Talmi and D. T. Bostick, *Anal. Chem.*, **47**, 2145 (1975).
(22) F. T. Henry and T. M. Thorpe, *J. Chromatogr.*, in press.
(23) M. O. Andreae, *Anal. Chem.*, **49**, 820 (1977).
(24) G. Forsberg, J. W. O'Laughlin, R. G. Megargle, and S. R. Koirtyohann, *Anal. Chem.*, **47**, 1586 (1975).
(25) P. H. Davis, G. R. Dulude, R. M. Griffin, W. R. Matson, and E. W. Zink, *Anal. Chem.*, **50**, 137 (1978).
(26) A. M. Sulek, E. W. Zink, and G. R. Delude, 89th Meeting, Association of Official Analytical Chemists, Washington, D.C., 1975.
(27) W. Holak, *J. Assoc. Offic. Anal. Chem.*, **59**, 650 (1976).
(28) J. P. Arnold and R. M. Johnson, *Talanta*, **16**, 1191 (1969).
(29) D. J. Myers and J. Osteryoung, *Anal. Chem.*, **45**, 267 (1973).
(30) D. J. Myers, M. E. Heimbrook, J. Osteryoung, and S. M. Morrison, *Environ. Lett.*, **5**, 53 (1973).
(31) S. S. Sandhu, R. S. Sandhu, and K. D. Sharma, *Fresenius Z. Anal. Chem.*, **237**, 32 (1975).
(32) M. V. Nosek, S. P. Buklman, and M. T. Kozlovskii, *Tr. Inst. Khim. Nauk, Akad. Nauk Kaz. SSR*, **9**, 131 (1962).
(33) H. Diehl, "Quantitative Analysis: Elementary Principles and Practice", 2nd. ed., Oakland Street Science Press, Ames, Iowa, 1974.
(34) E. A. Dietz and M. E. Perez, *Anal. Chem.*, **48**, 1088 (1976).
(35) J. Warkentin, Ansul Co., Weslaco, Texas, personal communication.

RECEIVED for review June 14, 1978. Accepted November 3, 1978. Work supported in part by funds from the University Faculty Research Committee of Miami University, Oxford, Ohio. Portions of this research were presented at the 29th Pittsburgh Conference on Analytical Chemistry and Applied Spectroscopy, Cleveland, Ohio, 1978.

Photometric Acid–Base Titrations in the Presence of an Immiscible Solvent

Frederick F. Cantwell* and Hussain Y. Mohammed

Department of Chemistry, University of Alberta, Edmonton, Alberta, Canada T6G 2G2

An apparatus is described which permits continuous monitoring of the UV absorbance of one phase in a vigorously agitated mixture of an aqueous and a water-immiscible organic solvent. Photometric titrations, using sodium hydroxide titrant, are performed in such a two-phase system on weak acid drug substances which show no spectral change upon deprotonation. Theoretical titration equations are derived and verified experimentally by titrating dextromethorphan hydrobromide. Four amine hydrohalide drugs are titrated by the new technique at concentrations between 8 × 10^{-4} M and 3 × 10^{-3} M with precision and accuracy of 1–2 ppt.

Heterogeneous titrations, in which acids and bases are titrated in a well-stirred aqueous solution in the presence of a second phase, have been described for systems in which the second phase is either an ion-exchange resin (*1, 2*) or a nonionic resin (*3*). Major alterations are produced in both potentiometric and photometric titration curves as a result of the heterogeneous distribution of acid–base conjugate species between the two phases. It is possible to alter the apparent strength of an acid or base and to differentially titrate mixtures of acids or bases with similar ionization constants but different charge types. A distinct advantage of heterogeneous photometric titrations is the fact that the two conjugate species of the sample compound do not need to have different molar absorptivities (*2*). This is true because the formal concentration of the sample compound is changing in the phase whose absorbance is monitored during the titration. Such titrations have been called "formal titrations" (*2*).

Potentiometric acid–base titrations have been reported in the presence of an immiscible liquid (summarized in references 1 and 3). However, the obvious experimental difficulty involved in achieving both rapid distribution equilibrium and rapid and complete phase separation before measuring the absorbance of one of the phases has apparently frustrated attempts to perform photometric acid–base titrations in two-phase liquid systems. In the present paper a simple titration apparatus is described which allows one liquid phase to be continually pumped out of a vigorously stirred two-phase solvent mixture, passed through a spectrophotometer flow cell, and returned to the mixture. Also, a theoretical equation describing the titration of weak acids BH^+ in such a heterogeneous titration medium is derived and verified experimentally. Finally, the new titration technique is used to assay

0003-2700/79/0351-0218$01.00/0 © 1979 American Chemical Society

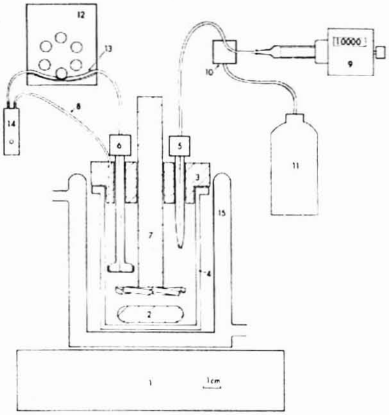

Figure 1. Diagram of the titration apparatus. (1) Magnetic stirrer, (2) stirring bar, (3) lid, (4) titration vessel, (5) buret tip, (6) filter-probe, (7) spoiler, (8) return line, (9) micrometer buret, (10) three-way valve, (11) titrant reservoir, (12) peristaltic pump, (13) Acidflex pump tubing, (14) flow cell, (15) water jacketed beaker. Only items 2–7 are drawn to scale

the weak acid hydrohalide salts of several pharmaceutical amines whose two conjugate acid–base species have nearly identical ultraviolet absorption spectra.

EXPERIMENTAL

Apparatus. The titration apparatus is shown in Figures 1 and 2. The magnetic stirrer (Model 4815, Cole-Parmer Instrument Co., Chicago, Ill.) must be one with a powerful magnet to avoid "spin-out" of the 1.5-inch Teflon covered stirring bar at the high speeds necessary to achieve rapid distribution equilibrium. The Teflon lid is held in place against the flat ground glass rim of the titration vessel with an aluminum clamp (not shown in figure). The lid need not be air tight but should provide a snug fit to minimize evaporation of the organic solvent and uptake of CO_2 from the atmosphere. Holes in the lid provide access for the glass buret tip, the filter-probe, the Teflon return tubing, and the shaft of the "spoiler". The latter is a 16-mm diameter Teflon rod, to the end of which a 39-mm diameter disk of Teflon is fastened with a force-fit glass pin. The Teflon disk is cut along six radii and the pie shaped sections twisted to give the disk a propeller shape. The "spoiler" does not rotate. Its purpose is to minimize vortex formation in the rapidly stirred solution and to increase the shearing effect which facilitates efficient dispersion of one solvent phase into the other. A properly stirred suspension will appear milk-white with no individual droplets of either solvent visible to the unaided eye. This is necessary for rapid achievement of distribution equilibrium after the addition of each increment of titrant. Stirring is continuous throughout the titration.

Titrant is delivered from a 1-mL micrometer buret (Digi-Pet, Monostat Corp., New York, N.Y.). The glass barrel of the buret is connected to a three-way valve (Model CAV 3031, Laboratory Data Control, Riviera Beach, Fla.). Another length of Teflon tubing connects the valve to the glass buret tip. The third valve port is connected to the titrant stored in a polyethylene reservoir bottle, and allows rapid refilling of the buret barrel between titrations by simply switching the valve and retracting the buret piston.

The filter-probe, shown in exploded view in Figure 2, is constructed by fusing a 13-mm diameter center-perforated glass disk to the end of a 1-mm i.d. by 6.5-mm o.d. glass tube (part no. G2–C, Laboratory Data Control). The bottom of the probe is grooved and a 6.3-mm diameter coarse Teflon mesh (Laboratory Data Control) is placed over its center. Three 18-mm diameter disks of filter paper are placed over the mesh and folded onto the probe by pressing into a short piece of 13-mm i.d. Teflon tubing which acts as a sleeve to hold the paper in place. The two innermost disks of filter paper are Whatman No. 5 and the outermost one is Whatman No. 1 paper. Disks of the correct size are conveniently punched out with a No. 10 cork borer. The upper end of the filter-probe is connected, via a short piece of Teflon tubing, to a 1.65-mm i.d. by 7 cm long piece of Acidflex peristaltic pump tubing (Technicon Corporation, Tarrytown, N.Y.). Connections of Teflon tubing to the glass buret tip and the filter-probe are made with a standard Cheminert fitting (Laboratory Data Control).

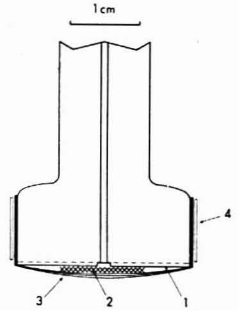

Figure 2. Exploded view of the end of the filter-probe. (1) Groove, (2) Teflon mesh, (3) Triple layer of filter paper, (4) Teflon sleeve

The Mini-Micro 2/6 peristaltic pump (Brinkmann Instruments Corp., Toronto) is adjusted to give a flow rate of about 1.5 mL/min. Solution from the pump passes via Teflon tubing into an 80-μL flow cell with a 1.00-cm pathlength (part 178-QS, Hellma Corp., Toronto) and then back into the titration vessel via the return line. A Cary 118 spectrophotometer (Varian Instruments, Palo Alto, Calif.) is used for absorbance measurements. The special cell compartment cover available for this instrument (part 01-640575-00) facilitates initial positioning of the flow cell. All Teflon tubing in the flow system is either 0.3- or 0.5-mm i.d. The total volume of the filter-probe, pump tube, flow cell, and associated transmission tubing is 0.42 mL.

The flat bottomed titration vessel is made from 51-mm i.d. Pyrex glass tubing with a wide rim that has been lapped flat. During an analysis the titration vessel is placed in a glass jacketed beaker filled with water, and water at 25 ± 0.1 °C is pumped through the glass jacket from a constant temperature bath.

The micrometer buret was calibrated at 6 points over the range 0 to 1 mL by filling it with 0.4763 M NaOH and potentiometrically titrating aliquots of accurately standardized 0.01510 M HCl solution. The buret was found to be accurate and precise to within 1 part per thousand over its entire range.

Reagents. The drugs dextromethorphan hydrobromide, molindone hydrochloride (Endo Laboratories, Inc., Garden City, N.Y.), diphenhydramine hydrochloride, and diphenylpyriline hydrochloride were all USP, NF, or equivalent grade and were assayed, without drying, by Fajan's argentimetric titration (*4*) and by the mercuric acetate method of nonaqueous titration using glacial acetic acid as solvent and perchloric acid in glacial acetic acid as titrant (*4*). All other chemicals were analytical reagent grade. Water was demineralized, distilled, and finally distilled from alkaline permanganate. Sodium hydroxide titrants were prepared from 1:1 solution with carbon dioxide-free water and were standardized against potassium hydrogen phthalate using phenolphthalein indicator.

Chloroform (Baker Analyzed Reagent) and carbon tetrachloride (Caledon Laboratories, Georgetown, Ontario) were mixed in a 1:1 volume ratio and the mixture was stored in gallon quantities for use as the organic solvent phase in heterogeneous titrations.

Distribution Isotherms. The distribution coefficient of dextromethorphan hydrochloride was determined between $CHCl_3/CCl_4$(1:1) and 0.01 M aqueous HCl (pH 2) that was also 0.10 M in NaCl, by agitating at 25 ± 0.1 °C and spectrophotometrically determining the dextromethorphan content of the phases. The distribution coefficients were measured at five

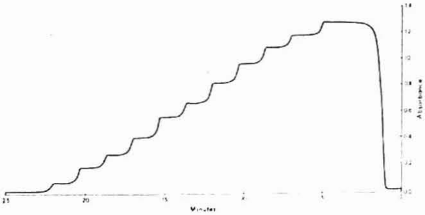

Figure 3. Spectrophotometer recorder tracing for the titration of dextromethorphan hydrobromide with sodium hydroxide at 275 nm

different equilibrium aqueous phase concentrations of dextromethorphanium ion ranging from 1 × 10^{-4} M to 1.3 × 10^{-3} M. The resulting isotherm plot of molarity in organic phase vs. molarity in aqueous phase is linear with zero intercept. The slope is numerically equal to the distribution coefficient.

Distribution coefficients of dextromethorphan hydrochloride were also measured at single points in 0.50 M NaCl and 0.01 M NaCl, both of which also contained 0.01 M HCl. Distribution coefficients that would prevail in 0.50, 0.10, and 0.01 M total chloride concentrations were calculated from these experimental values using the appropriate activity coefficients and Equation 2 (vide infra). The distribution isotherm of dextromethorphan base between $CHCl_3/CCl_4$ (1:1) and dilute NaOH (pH 13) that was also 0.1 M in NaCl, was measured in an identical manner to that described above, at equilibrium aqueous phase concentrations between 1 × 10^{-5} M and 1.5 × 10^{-5} M, and yielded zero intercept and a linear slope.

Titration Procedure. Distilled water to be used in the titration is sparged with nitrogen to remove CO_2. The $CHCl_3/CCl_4$ (1:1) solvent is shaken in a separatory funnel immediately before use with an equal volume of CO_2 free water and filtered through dry Whatman No. 2 paper. This washing removes both the ethanol preservative from $CHCl_3$ and the small amount of HCl that is usually formed in $CHCl_3$ upon standing. The spectrophotometer is set to 100% *T* with water pumping through the flow cell. Volumes of 60.00 mL of water, 10.00 mL of an aqueous NaCl solution, and 10.00 mL of drug solution are pipetted into the titration vessel along with 20.00 mL of $CHCl_3/CCl_4$ (1:1). The lid is fastened in place, with the filter-probe, spoiler, return line, and buret tip in place, and the titration vessel is placed in the water bath. Stirring and pumping are begun.

After about 4 min, the absorbance will have risen to a constant value as distribution equilibrium is reached in the titration vessel. Titrant is now added. After the addition of each increment of titrant, a period of about 1.5 min is required for the absorbance to decrease to its new plateau value (Figure 3). The titration curve is a plot of plateau absorbance values vs. moles of added titrant. As discussed below, a dilution correction may have to be made on the plateau absorbance values before making the plot.

RESULTS AND DISCUSSION

The filter-probe is successful in filtering the small droplets of organic solvent out of the aqueous phase because the paper is hydrophilic and once wetted with water it is not wettable with the organic solvent. If the pumping rate is made much higher or if a coarser textured paper is used, with larger capillary pores between the cellulose fibers, then it is more likely that small amounts of the organic phase will be drawn into the probe.

Proposed Model. Equation 1 summarizes the equilibria which prevail in the heterogeneous titration system.

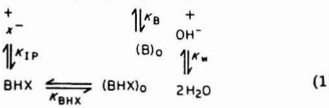

$$\begin{array}{ccccccc} BH^+ & + & H_2O & \overset{K_a}{\rightleftharpoons} & B & + & H_3O^+ \\ + & & & & \upharpoonleft\downharpoonright K_B & & + \\ x^- & & & & (B)_o & & OH^- \\ \upharpoonleft\downharpoonright K_{IP} & & & & & & \upharpoonleft\downharpoonright K_w \\ BHX & & \underset{K_{BHX}}{\rightleftharpoons} & & (BHX)_o & & 2H_2O \end{array} \tag{1}$$

Table I. Equilibrium Constant Expressions

thermodynamic constants	constant used
$K_a^T = \dfrac{a_B a_H}{a_{BH}}$	$K_a = \dfrac{[B]a_H}{[BH]}$
$K_w = a_H a_{OH}$	$K_w = a_H a_{OH}$
$K_B^T = \dfrac{a_{B,o}}{a_B}$	$K_B = \dfrac{[B]_o}{[B]}$
$K_{IP}^T = \dfrac{a_{BHX}}{a_{BH} a_X}$	
	$K_I = \dfrac{[BHX]_o}{[BH]}$
$K_{BHX}^T = \dfrac{a_{BHX,o}}{a_{BHX}}$	

Species without a subscript are in the aqueous phase and those with the subscript o are in the organic phase. Here x^- is the conjugate base of a strong acid (e.g., Cl^-). The thermodynamic constants appropriate to these equilibria are presented in the left-hand column of Table I. The formation of extractable ion pairs, BHX, has been well documented for a large number of protonated amines (5). In the titration equation, it is convenient to use concentrations, $[i]$, instead of activities, a_i, for all species *i*, except H_3O^+ and OH^-. In the right-hand column of Table I, the form of the equilibrium constant expressions used in the titration equation are presented. It is evident that $K_a = K_a^T\gamma_{BH}/\gamma_B$, where γ_{BH} and γ_B are the activity coefficient of conjugate species BH^+ and B in the aqueous phase. Since the species B is neutral $\gamma_B \approx 1$ at low electrolyte concentrations. Also, $K_B = K_B^T$, assuming that activity coefficients of B are equal to one in both phases. Now, if an inert electrolyte MX (e.g. NaCl) is present in the aqueous phase at concentrations much higher than the sample, all activity coefficients in the aqueous phase are constants and K_I is a constant:

$$K_I = K_{IP}^T K_{BHX}^T [X^-] \gamma_{BH} \gamma_x / \gamma_{BHX,o} \tag{2}$$

Furthermore, it has been found (5) for ion pairs involving organic ammonium ions that $K_{BHX}^T \gg K_{IP}^T[X^-]$. This means that the concentration of the species BHX is negligibly small in the aqueous phase.

Neglecting the concentration of BHX in the aqueous phase, the following titration equation is derived by combining the equilibrium constant expressions with mass balance equations and with Beer's law expressions for BH^+ and B in the aqueous phase.

$$n_{OH} = X + Y\frac{K_w V}{K_a \gamma_{OH}} - Z\frac{K_a V}{\gamma_H} \tag{3}$$

where:

$$X = \frac{[\epsilon'_{BH} n_{BH} - A_{obs}(V + K_I V_o)][V + K_B V_o]}{[\epsilon'_{BH}(V + K_B V_o) - \epsilon'_B(V + K_I V_o)]} \tag{4}$$

$$Y = \frac{n_{BH}\epsilon'_{BH} - A_{obs}(V + K_I V_o)}{A_{obs}(V + K_B V_o) - n_{BH}\epsilon'_B} \tag{5}$$

$$Z = 1/Y \tag{6}$$

In these equations, ϵ'_{BH} and ϵ'_B are the products of molar absorptivities, at the wavelength used, and cell pathlength for species BH^+ and B; A_{obs} is the observed absorbance, corrected for dilution if necessary; *V* and V_o are volumes of aqueous and organic phases in liters; n_{BH} and n_{OH} are moles of sample and titrant added to the titration vessel; γ_H and γ_{OH} are ionic activity coefficients for H_3O^+ and OH^-.

Table II. Assay Values (%) for Several Drugs by Three Titration Methods

compound	nonaqueous	Fajan's	photometric	molarity[b]
dextromethorphan·HBr	95.3 ± 0.07	95.4 ± 0.07	95.4 ± 0.1	8×10^{-4}
diphenylpyriline·HCl	98.5 ± 0.1[a]	98.4 ± 0.1	98.3 ± 0.2	3×10^{-3}
diphenhydramine·HCl	99.8 ± 0.1[a]	99.9 ± 0.1	99.8 ± 0.05	1.7×10^{-3}
molindone·HCl	99.0 ± 0.1	99.0 ± 0.2	99.0 ± 0.1	4.0×10^{-3}

[a] Average deviations are based on at least three replicate titrations in all cases except for these two nonaqueous titrations, where they are based in duplicate titrations. [b] Approximate molarity of the sample during the photometric titration, assuming that it is all in the aqueous phase.

The influence of each of the constants in Equations 3–6 can readily be seen by comparison with the ion-exchange system described in Reference 2. The influences of K_B and K_I in the present case are analagous, respectively, to those of $K_{IE,BH}$ and $K_{D,B}$ shown in Figures 1–4 in Reference 2. Since H_3O^+ and OH^- do not partition into the organic solvent phase, there are no constants in Equation 3 analogous to $K_{S,H}$ and $K_{S,OH}$. The symbol n_{Cl} in Reference 2 is replaced with n_{OH} in this case. The influence of K_a, the acid ionization constant, is the same as that described for the titration of acids in a homogeneous medium (*6*).

Dilution Correction. Addition of titrant results in an increasing volume of aqueous phase during the titration and a consequent dilution. In a photometric titration carried out in a homogeneous solution, this has a simple dilution effect on the absorbing species and can readily be corrected for by multiplying each absorbance value by the quantity $(V + V_{OH})/V$ before plotting the titration curve. Here V_{OH} is the volume of titrant added. In a two-phase titration medium, the situation is more complex. Photometric titration end points are usually evaluated by extrapolation of the linear portions of the curve before and after the end point. This means that over most of the length of the segment of the titration curve before the equivalence point the "X" term in Equation 3 is much larger than the other two terms on the right-hand-side of that equation. Therefore, the dilution correction before the equivalence point can be deduced for titration curves which do not show much curvature by considering only the "X" term in Equation 3.

Making the very likely assumptions that $\epsilon'_{BH}(V + K_B V_o) \gg \epsilon'_B(V + K_I V_o)$ and considering only the "X" term on the right-hand-side, then Equation 3 becomes:

$$n_{OH} \approx n_{BH} - \frac{A_{obs}(V + K_I V_o)}{\epsilon'_{BH}} \tag{7}$$

Now the constant K_I depends on the concentration of anion X^- according to Equation 2. If the dilution is only slight then γ_{BH} and γ_X will not change and it becomes evident that $K_I \propto [X^-]$. Since $[X^-]$ decreases directly with increasing dilution, provided that there is a large excess of inert salt MX present, then the initial value, $K_{I'initial}$, (i.e., that which prevails at the initial salt concentration at the beginning of the titration) should be multiplied by $V/(V + V_{OH})$ to correct it for dilution. At the same time, the volume V in Equation 7 should be replaced by $(V + V_{OH})$ to correct it for dilution.

Thus, to correct for both effects, before the equivalence point one should plot:

$$A_{obs} \frac{(V + V_{OH}) + K_{I,initial}\left(\dfrac{V}{V + V_{OH}}\right)V_o}{[V + K_{I,initial}V_o]} \text{ vs. } n_{OH} \tag{8}$$

to obtain the titration curve. The dilution correction given by Equation 8 can take two limiting forms. If the extraction of ion pairs is slight so that $K_I V_o \ll V$, then the correction is made by multiplying A_{obs} by $(V + V_{OH})/V$. At the other extreme, if ion pair extraction is extensive and $K_I V_o \gg V$, then the correction is made by multiplying A_{obs} by $V/(V + V_{OH})$.

The value of $K_{I,initial}$ need not be measured in a separate experiment, since a good approximation can be obtained from the titration curve itself. If the straight line portion of the curve is extrapolated back to the A_{obs} axis where $n_{OH} = 0$, the intercept will have the value:

$$A_{obs,extrap.} = \frac{n_{BH}\epsilon'_{BH}}{(V + K_{I,initial}V_o)} \tag{9}$$

If the extent of dilution is not very great, then a fairly accurate value of n_{BH} can be had from the end point obtained before dilution correction. Therefore, if the value of ϵ'_{BH} is known for the compound, it is a simple matter to obtain $K_{I,initial}$ from Equation 9. This method of obtaining $K_{I,initial}$ assumes that other absorbing compounds are absent from the sample. In the present case the initial aqueous phase volume was 80.42 mL and the titrant volume required to reach the end point was only about 0.7 mL so that dilution corrections, though used, are relatively small.

The linear segment of the titration curve obtained after the equivalence point is given by the equation:

$$A_{obs} = \frac{n_{BH}\epsilon'_B}{(V + K_B V_o)} \tag{10}$$

It is a constant, independent of added titrant, except for the dilution effect which is compensated for by plotting:

$$A_{obs} \frac{(V + V_{OH}) + K_B V_o}{V + K_B V_o} \text{ vs. } n_{OH} \tag{11}$$

Normally, K_B is large so that A_{obs} is very small, and the dilution correction after the equivalence point is negligible.

Experimental Verification. Extensive studies have been reported on the ion pair extraction behavior of dextromethorphanium cation with halide ions (*7–9*) and they have demonstrated that 1:1 ion pairs are involved. Titration Equation 3 was verified by titrating dextromethorphan hydrobromide with 0.09526 M sodium hydroxide titrant in the presence of a 1:1 mixture of $CHCl_3$ and CCl_4 as organic phase. The titration was performed at three different concentrations of added NaCl to show the effect of ion pair extraction on curve shape. The results are presented in Figure 4. The points in Figure 4 are the observed experimental values, corrected for dilution using Equations 8 and 11, while the solid lines are the theoretical curves calculated from Equation 3 using known or measured values for the parameters K_I, K_B, ϵ'_{BH}, ϵ'_B, V, V_o, n_{BH}, γ_H, γ_{OH}, K_w, and K_a. The value of K_a is obtained by multiplying the literature value (*7*) of 5.0×10^{-9} by the activity coefficient, γ_{BH}, which is computed from tabulated values (*10, 11*) assuming an ionic size parameter of 8×10^{-8}. Values of ϵ'_B and ϵ'_{BH} were obtained from Beer's law plots, which were linear on the Cary 118 spectrophotometer up to absorbance values of at least 1.5. Values of K_I and K_B were obtained from batch equilibration measurements as discussed above, and the value of n_{BH} was equal to the weight of dextromethorphan hydrobromide taken multiplied by 0.954, the assay value found by nonaqueous and Fajan's titration

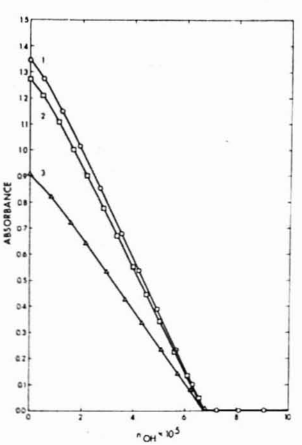

Figure 4. Photometric titration curves for dextromethorphan hydrobromide with sodium hydroxide titrant. Lines are calculated from Equation 3 and points are experimental. For all curves: $n_{BH} = 6.72 \times 10^{-5}$ mol; $\epsilon'_B = 1800$; $\epsilon'_{BH} = 1840$; $K_B = 2.70 \times 10^3$; $K_w = 1.00 \times 10^{-14}$; $V_o = 0.02000$ L; $V = 0.08042$ L; $\lambda = 275$ nm. For curve 1: $K_I = 0.30$; $K_a = 4.57 \times 10^{-9}$; $\gamma_H = 0.91$; $\gamma_{OH} = 0.90$; [NaCl] = 0.01 M. For curve 2: $K_I = 0.55$; $K_a = 4.11 \times 10^{-9}$; $\gamma_H = 0.83$; $\gamma_{OH} = 0.75$; [NaCl] = 0.1 M. For curve 3: $K_I = 2.49$; $K_a = 3.81 \times 10^{-9}$; $\gamma_H = 0.76$; $\gamma_{OH} = 0.69$; [NaCl] = 0.5 M

(the remaining $4._6$% of the drug is accounted for by water).

The agreement between predicted and observed results shown in Figure 4 demonstrates the validity of Equation 3 and clearly illustrates that accurate photometric titrations may be performed on amine salts which show no significant spectral change upon deprotonation. It should be noted that the concentration of sample, if it were all in the aqueous phase, would be 10^{-3} M.

In the region just before the end point, the experimental absorbance values fall slightly above the theoretical line. The reason for this is not known but may be the presence of small amounts of CO_2 in the titrant. It is not seen when higher (e.g., 10^{-2} M) sample concentrations are used. It causes no error in locating the end point, if the steepest straight line consistent with the data is drawn through the points before the equivalence point when performing the linear extrapolation.

Assay of Drugs. Four common amine hydrohalide drug substances were each analyzed by three different titration techniques: Fajan's titration for halide, nonaqueous titration, and heterogeneous photometric titration. Results are summarized in Table II which shows the averages and average deviations obtained in replicate titrations. Sample concentrations were >0.01 M for the Fajan's and nonaqueous titrations. Approximate sample concentrations during the photometric titrations, assuming all of the compound is in the aqueous phase, are given in the last column of Table II. All photometric titrations were performed in 80.42 mL of 0.10 M NaCl and 20.00 mL of $CHCl_3/CCl_4$ (1:1) using as titrant standardized solutions of sodium hydroxide between 0.05 M and 0.5 M, depending on drug concentration. End points of the photometric titrations were obtained by linear extrapolation of plots of absorbance (corrected for dilution) vs. moles of added sodium hydroxide. Assay values found by the photometric titration and the two indicator titrations agree within 1–2 ppt. Precisions for all three methods, as indicated by average deviations, are also in the range of 1–2 ppt.

Advantages of the Method. Considering the additional instrumentation required, it might be asked why one would choose the photometric technique over an indicator titration. The answer is that the photometric titration contains both qualitative and quantitative information about the sample, while indicator titrations contain only quantitative information. For example, if an acid BH^+ with a pK_a of 8 happened to contain, as an unexpected impurity, another acid of the BH^+ charge-type with a pK_a of 5, an indicator titration would yield only one end point corresponding to the sum of both compounds. A potentiometric titration with NaOH titrant would give two end points in this case, but if it happened that the impurity had, instead, a pK_a near 8 then even a potentiometric titration would not detect the presence of the impurity. On the other hand if, as is likely, the impurity had a different molar absorptivity than the acid of interest then, whether or not it had the same pK_a, the shape of the titration curve of the sample would be different than that for a pure standard of this material. In particular, the ratio of the slope of the linear portion of the curve before the end point to the moles of titrant required to reach the end point would be different for the sample and standard. Looking at it in another way, a photometric titration provides both a photometric and a titrimetric assay, and if the two assay values do not agree the analyst is alerted to a peculiarity of the sample.

CONCLUSIONS

The proposed heterogeneous acid–base titration can be performed using water-immiscible organic phases other than $CHCl_3/CCl_4$. The organic solvent phase can be chosen to yield particular distribution coefficients for a given sample compound. For example, a solvent might be chosen which minimizes ion pair extraction. Also, it is possible to replace the hydrophilic paper on the end of the filter-probe with a hydrophobic silicone-treated paper which will pass the organic phase and filter out the aqueous phase. In this way the absorbance of the organic phase can be measured.

The method is applicable to the titration of other charge type acids (e.g., HA) with NaOH titrant, and to the titration of bases of various charge types with a strong acid titrant. Since the nonlinear portion of the titration curve in the vicinity of the equivalence point is related to the strength of the acid or base being titrated, it should be possible to evaluate the pK_a values of very weak acids and bases by this technique.

The same apparatus can also be used to perform complexometric titrations of metal ions using as titrants ligands which form extractable complexes. This application is under investigation.

The time required to achieve a constant plateau absorbance value after each addition of titrant depends upon the efficiency of stirring, the pumping rate, the fraction of the total aqueous phase which is contained in the pumping system and flow cell, and the flow pattern through these (e.g., laminar flow in tubing, efficiency of rinsing of the flow cell). Experiments suggest that the latter three factors are the major ones contributing to the equilibration time in the present system. Therefore studies are underway using faster flow rates and low dead volume flow cells such as those used in liquid chromatographic detectors. The titration apparatus is also being automated.

ACKNOWLEDGMENT

Samples of drugs were kindly provided by Lester Chatten of the College of Pharmacy, University of Alberta, and by C. F. Hiskey of Endo Laboratories, Inc.

LITERATURE CITED

(1) F. F. Cantwell and D. J. Pietrzyk, *Anal. Chem.*, **46**, 344 (1974).
(2) F. F. Cantwell and D. J. Pietrzyk, *Anal. Chem.*, **46**, 1450 (1974).
(3) S. Puon and F. F. Cantwell, *Anal. Chem.*, **49**, 1256 (1977).
(4) "United States Pharmacopea", 19th rev., Mack Publishing Co., Easton, Pa., 1975.
(5) G. Schill in "Ion Exchange and Solvent Extraction", Vol. 6, J. A. Marinsky

and Y. Marcus, Ed., Marcel Dekker, New York, 1974, Chapter 1.
(6) R. F. Goddu and D. N. Hume, *Anal. Chem.*, **26**, 1679 (1954).
(7) T. D. Doyle and J. Levine, *J. Assoc. Offic. Anal. Chem.*, **51**, 191 (1968).
(8) T. Higuchi, A. Michaelis, T. Tan, and A. Hurwtiz, *Anal. Chem.*, **39**, 974 (1967).
(9) T. Higuchi and A. F. Michaelis, *Anal. Chem.*, **40**, 1925 (1968).
(10) J. Kielland, *J. Am. Chem. Soc.*, **59**, 1675 (1937).
(11) R. A. Robinson and R. H. Stokes, "Electrolyte Solutions", 2nd ed., Butterworth, London, 1959.

RECEIVED for review July 17, 1978. Accepted November 8, 1978. Work supported by the National Research Council of Canada and the University of Alberta.

Measurement of Ions within a Pulsed Electron Capture Detector by Mass Spectrometry

E. P. Grimsrud,* S. H. Kim, and P. L. Gobby

Department of Chemistry, Montana State University, Bozeman, Montana 59717

Measurements of ions within an electron capture detector (ECD) have been made by the technique of atmospheric pressure ionization mass spectrometry (APIMS) where the ion source has been modified to be an actual ECD. By observing the dependence of ion signals on electrostatic fields applied to the ionization cell, new insight into the role of ions in influencing the measured ECD current is provided. It is shown that for this pulsed ECD, a positive current of significant magnitude exists which is an integral component of the normally measured ECD current, and that it is caused by the selective migration of positive ions to the sampling electrode during the period between pulses. The results are discussed relative to opposing views of the ECD, and are shown to strongly support one of these.

Electron capture detection (ECD) with gas chromatography (GC) has proved to be one of the most useful techniques available for the trace analysis of many environmentally important organic compounds. This success is due primarily to the very selective reactivity of the low-energy electron with certain classes of compounds in the gas phase. To improve our understanding of these reactions and the basis of ECD responses, several studies have had as their objective the identification of the negative ions formed under one-atmosphere, electron capture conditions. Using the technique called plasma chromatography, the formation of negative ions from substituted benzenes (*1*) and polychlorinated biphenyls (*2*), and the effects of oxygen (*3*) under electron capture conditions have been reported. By atmospheric pressure ionization mass spectrometry (APIMS), additional chemical (*4, 5*) and physical (*6*) detail of EC reactions have been made possible by the direct mass spectrometric analysis of one-atmosphere plasmas. In a recent study by Horning et al. (*5*), an APIMS ion source was modified to be an actual ECD complete with a cell electrode, so that the ECD function of this ion source could be obtained simultaneously with negative ion measurements. Not only might one expect this combination to provide an ideal means of studying EC reactions, but it also appears to constitute a promising technique in itself for the analysis of trace amounts of organic substances.

Because of the demonstrated success of APIMS for the sensitive measurement of ions formed within its ECD-like source, we have constructed a similar instrument designed specifically for the study of ECD chemistry. This instrument provides the simultaneous measurement of cell current and mass-analyzed ion currents as in the Horning study (*5*). With it, however, we have made new observations which provide a new source of information for ECD events. We have found that, under electron capture conditions within the ion source, the measured intensity of negative ions formed by electron-capture reactions is strongly affected by the simultaneous application of the pulsed field used to obtain the ECD function of the source. We believe these interactions reflect changes in the rates of ion transport to boundary surfaces of the ionization cell and, therefore, provide added insight into the basis of the currents measured within the ECD.

EXPERIMENTAL

The vacuum envelope, quadrupole mass spectrometer, and pumping system of our APIMS has been described previously (*7*). A detailed view of its ion source is shown in Figure 1. The stainless steel ion source bolts onto the front flange of the vacuum envelope. A $^5/_8$-inch nickel disk of 25-μm thickness and containing a 20- or 25-μm aperture in its center (Perforated Products, Inc., Brookline, Mass.) provides a controlled leak of the ion source contents into the vacuum region. Nitrogen carrier gas (Matheson, ultra high purity) flows continuously through the ion source at a rate of about 40–60 cm^3 min^{-1}. The carrier gas is further purified by passing it through a filter containing $CaSO_4$ and 5A molecular sieve. The volume of the active region of the ion source is about 1 cm^3, the approximate size of a conventional ^{63}Ni ECD. A platinum cylinder imbedded with 9 mCi of ^{63}Ni (New England Nuclear, Boston, Mass.) forms the wall of the active region. A $^1/_{16}$-inch stainless steel pin protrudes into the ion source as shown via a ceramic feedthrough. The diameter of the cylindrical source is 1.0 cm.

Samples are introduced to the carrier gas stream via either a 3.4-L stainless steel exponential dilution sphere or at the injection port of a gas chromatograph (Aerograph Autoprep A-700). For GC a $^1/_8$-inch, 1.5-foot stainless column packed with 3% OV-17 on Supelcoport 100/120 mesh was used. A heated, glass-lined stainless transfer tube connects the GC with the ion source.

For the ECD current measurement, a pulsed, positive voltage was applied to the ion source pin. The resulting total cell current was measured at the same pin using the circuit shown in Figure 2. Others (*8*) have used a similar approach to obtain the ECD signal from cells whose walls are electrically grounded. The operational amplifier shown is an RCA CA3140S. In all chromatograms reported here, the ECD current is the total unprocessed cell current. For the pulsed mode, 35-V, 2-μs pulses of variable period were used. With a pulse period of 300 μs, a standing current of about 2 nA was obtained at all temperatures. All ECD circuitry was home-built.

Ion measurements were usually made by monitoring one ion only during the course of an experiment. Detection of positive and negative ions was by the counting method (*9*) using a Channeltron 4039 electron multiplier (Galileo Electro-Optics Corp., Sturbridge, Mass.). An analog signal from a ratemeter (Ortec, Model 441) is recorded. The mass filter is a quadrupole

© 1979 American Chemical Society

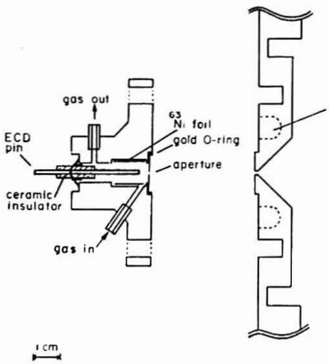

Figure 1. Electron Capture Detector ion source of mass spectrometer shown with the front flange of vacuum envelope

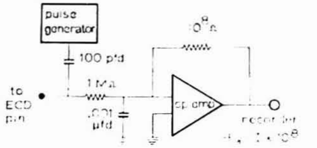

Figure 2. Circuit for measuring the ECD current at the ion source electrode

(Extranuclear, Model 162-8) capable of greater-than unit mass resolution up to about m/e = 500.

RESULTS AND DISCUSSION

Effect of Applied Fields on APIMS Signals. During our initial use of the specialized ECD/APIMS instrument described above, we looked for and usually found the negative ions of EC-active compounds which have been reported in other APIMS studies. These include the M and M − Cl + O negative ions of *p*-chloronitrobenzene and tetrachlorobenzene (*4*), the M$^-$ ion of SF$_6$ (*10*), and halide anions of simple aliphatic chlorocarbons and chlorofluorocarbons (*10*). With one exception (*5*), our instrument differs from other APIMS studies in that for the ECD function of the ion source, electrostatic fields can be applied to the ionization region. The presence of these fields was immediately noticed to have a pronounced effect on the negative ions observed under electron capture conditions. For example, in Figure 3 are shown two GC-ECD/MS analyses of azulene. In the first run, the elution of azulene is signaled by a reduction in the ECD standing current of about 10%. At mass 128, however, no negative ion corresponding to the M$^-$ species was detected. In searching for other possible negative ions of azulene, such as the M − H + O anion, none were found for this 0.5-ng sample as long as the ECD pulser was operative. In chromatogram b, however, the ECD pulser (+35 V, 300-μs period applied to the ion source pin) was turned off just prior to the elution of azulene. An intense negative ion current corresponding to M was then observed. This behavior has been the rule for all negative ions we have observed under electron capture conditions and is not unique to the example shown. Ions such as Cl$^-$, Br$^-$, SF$_6^-$, SF$_5^-$, and those of the type $[M - Cl + O]^-$ all are affected by the applied fields in the same manner.

In demonstrating further the effects of pulsed fields applied to the ion source, the example of *p*-chloronitrobenzene (PCNB) will be used most frequently where the sample introduction method is gas chromatography. To show, however, that the observations to be described are independent of compound type and sample introduction method, the case of SF$_6$ introduced directly into the carrier gas stream via an exponential dilution sphere is first shown in Figure 4. The injection of the SF$_6$ causes a drastic reduction in the ECD current and a simultaneous appearance of an intense SF$_6^-$ ion signal. As the SF$_6$ concentration decreases exponentially with time, the ECD current increases in a manner roughly similar to that predicted if a Beer's law relation between ECD current and SF$_6$ concentration is assumed. With the ECD pulser left on, the SF$_6^-$ ion current decreases prematurely and goes to zero when the ECD current has returned to about 90% of the original standing current. By turning the ECD pulser off intermittently, a simultaneous trace of the SF$_6^-$ current under the field-free ion souce condition was also obtained. This ion current does not differ drastically from the "pulse on" ion current in the large sample or saturation condition, but diverges continuously from it as the SF$_6$ concentration decreases. Under the small sample condition where the ECD current is restored to 90% or greater, a sizable SF$_6^-$ ion current is still measured only in the "pulse off" condition.

In Figure 5 is shown the effect of the pulsed field on the M$^-$ ion of *p*-chloronitrobenzene (PCNB) where this time the sample is introduced by gas chromatography. Again, as in the case of SF$_6$, the ion signal is decreased by the pulsed field

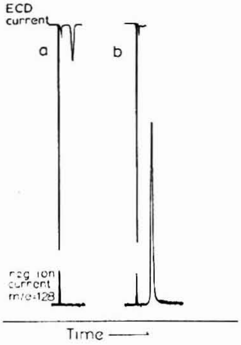

Figure 3. Two GC-ECD/MS analyses of azulene. (a) Both the pulsed, ECD current and the mass spectrometer ion current of the M$^-$ ion of azulene are monitored simultaneously. (b) The ECD pulser is turned off just prior to the elution of azulene. Sample size, 0.5 ng. Source temperature, 150 °C

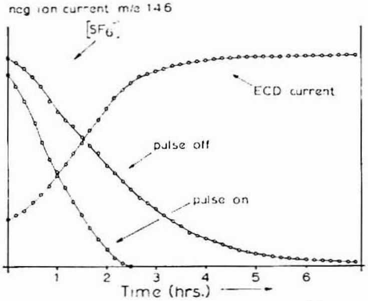

Figure 4. ECD current and SF$_6^-$ ion currents measured by ECD/MS with ECD pulser alternately turned on and off. Sample is introduced via a 3.4-L exponential dilution sphere. Initial SF$_6$ concentration 30 ppb (v/v) in nitrogen. Gas flow rate, 60 mL min^{-1}. Source temperature, 200 °C. Pulse period, 300 μs

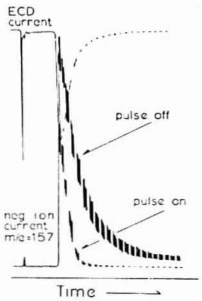

Figure 5. GC-ECD/MS analysis of *p*-chloronitrobenzene monitoring the molecular anion at $m/e = 157$. After the peak maximum, the ECD pulser is turned off and on alternately every 10 s. Sample size, 1.0 ng. Source temperature, 250 °C. Pulse period, 300 μs. Column temperature, 95 °C

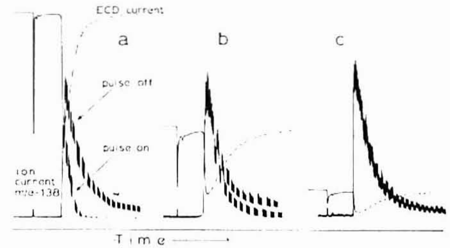

Figure 6. Effect of ECD pulse period on negative ion observed with the ECD/MS. Ion monitored is M − Cl + O negative ion of *p*-chloronitrobenzene. Pulse periods are (a) 300 μs, (b) 1.0 ms, (c) 2.5 ms. After the peak maxima, the ECD pulser is turned off and on alternately every 10 s. Sample size, 1.0 ng. Source temperature, 250 °C. ECD standing current in (a) is 2.2 nA

and is caused to go to zero as the ECD response returns to about 90% of the original standing current. Again, the ion signal observed with the pulser turned off seems to reflect better the degree of negative ion formation which might be predicted from the ECD response. In Figure 6 is shown the effect of varying the pulse period of the ECD pulser on the ion signal of the M − Cl + O anion of PCNB. Using a period of 300 μs, the ion signal is reduced by the field's presence in a manner precisely the same as that of the M^- ion. With longer pulse periods, the ECD current is lessened as expected (*11*). Also, with longer pulse periods, the perturbation of the ion signals by the field is observed to be not so severe. About 1 to 3 ms appears to be enough time to allow the perturbation caused by the pulse to relax significantly back toward an equilibrium position. Perhaps not coincidentally, this is about the same amount of time required for an apparent steady-state electron concentration to be achieved in ECD studies when ^{63}Ni ionization is used (*8, 12*).

In Figure 7 is shown the effect of the pulsed field (300-μs period) on the M + 1 positive ion of PCNB. The applied field clearly has no effect on the positive ions for all sample concentrations. In Figure 8 is shown the effect of reversing the polarity of the pulser (to −35 V) on the negative ions of PCNB. The fascinating result is that pulsing negative vs. positive makes no difference on the negative ion perturbation. Clearly, the cause of the negative ion perturbation cannot be related to a simple repeller field affect since, if it were, a negative field would assist the ejection of negative ions out of the ion source.

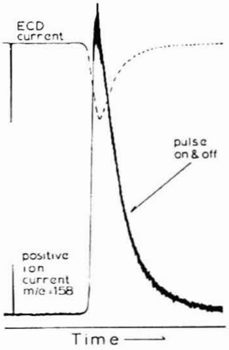

Figure 7. Effect of ECD pulser on positive M + 1 ion of *p*-chloronitrobenzene. Pulse period, 300 μs. Pulser turned on and off alternately every 10 s. Sample size, 0.3 ng. Source temperature, 250 °C. Column temperature, 87 °C

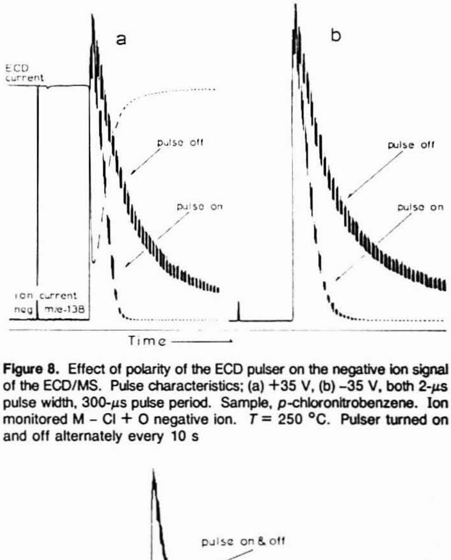

Figure 8. Effect of polarity of the ECD pulser on the negative ion signal of the ECD/MS. Pulse characteristics; (a) +35 V, (b) −35 V, both 2-μs pulse width, 300-μs pulse period. Sample, *p*-chloronitrobenzene. Ion monitored M − Cl + O negative ion. T = 250 °C. Pulser turned on and off alternately every 10 s

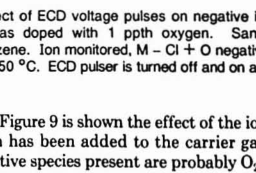

Figure 9. Effect of ECD voltage pulses on negative ions of sample with carrier gas doped with 1 ppth oxygen. Sample, 1 ng *p*-chloronitrobenzene. Ion monitored, M − Cl + O negative ion. Source temperature, 250 °C. ECD pulser is turned off and on alternately every 10 s

Finally, in Figure 9 is shown the effect of the ion source field when oxygen has been added to the carrier gas so that the negative reactive species present are probably O_2^- (*13*) instead of electrons. This saturated condition is indicated by the low ECD standing current which accompanies the addition of oxygen. Under this condition no perturbation of the negative ion signal is caused by the ECD field.

In summarizing the above set of measurements, it is clear that a pulsed field can alter APIMS signals under certain conditions of the ion source. These effects are strongest in the low-sample or weak-response condition where electrons are the predominant negatively-charged species. Under this condition using pulse frequencies of about 3 kHz or greater, the negative ion signals, only, are destroyed. Since an ECD response is observed, however, it seems likely that negative ions are actually being produced within the ion source.

Candidate Models of the ECD. If it is assumed that the ion measurements of our ECD/MS reflect the transport (diffusion and migration) of ions to the grounded walls of our ECD ion source, these measurements provide a means of adding further detail to physical events occuring within the ECD. Thus, we have tried to merge an explanation of the above experiments with the literature views of the ECD.

Conventional View. In the ECD, β radiation initiates a series of chemical reactions which, even in the absence of added sample, will produce steady-state concentrations of electrons, positive ions, negative ions (with sample present), free radicals, and molecular reaction products (*14*). For the pulsed ECD, a generally accepted model of the role of electrons and ions in determining the measured current has evolved (*8, 12, 15–21*) which states: (1) the current measured is due to electrons which are drawn to the more positive electrode during the application of short voltage pulses; (2) the relatively immobile ions contribute little to the current; and (3) the entire ionization cell is cleared of electrons during each pulse. Thus, this view holds that the ECD current is a direct measure of the steady-state electron concentration achieved at the end of the field-free period between pulses. Experiments such as those of Wentworth, Chen, and Lovelock (*16*), Devaux and Guiochon (*22*), and Simmonds et al. (*12*) in which the effects on the ECD currents of variations in the pulse width, pulse period, and pulse voltage were determined have provided persuasive evidence of the above general model. Further detail of ECD events, though not essential to its operation, has sometimes included: (4) positive ions will be in very large excess of electrons because the electrons diffuse quickly to cell boundaries (even during the field-free period between pulses); and (5) the charge associated with negative ions formed by electron capture is quickly lost because of a much faster recombination between positive ions and negative ions than exists between positive ions and electrons (*8, 18, 19, 21*).

Recently, Siegel and McKeown (*6*) have presented several criticisms of the above view. They argue that, under the ECD condition of relatively high ion density, positive and negative particles do not move independent of one another as they may in weakly ionized gases, but all move with one characteristic "ambipolar" diffusion constant. Using an APIMS with a ^{63}Ni ionization source, they provide experimental evidence indicating that strong electrostatic forces between ions and electrons (which are ignored in the conventional view of the ECD) cause the maintenance of charge balance in the field-free ionization source of their APIMS. Thus, it appears that point 4 of the conventional view is incorrect. Siegel and McKeown also argue with support from the literature and their APIMS experiments that point 5 is incorrect. Our own measurements by APIMS support Siegle and McKeown in this later point. For example, if during the GC elution of a large sample of CCl_4, the total positive ion intensity is monitored, this signal increases about 50% while the source is saturated with CCl_4. Apparently, the recombination of positive ions with negative ions (Cl^-) is actually slower than that of positive ions with electrons.

Modified View A. While Siegle and McKeown (*6*) did not address directly the effect of an applied field which must be present if the ionization call is to function as an ECD, they maintain that positive and negative charge densities must remain numerically equal in the ECD. Thus, within the view of Siegle and McKeown, it is more difficult to envision what the measured ECD current is due to. A view which may follow most naturally from Siegle and McKeown's concepts is that only a very small distance from the electrode surface (one Debye length) is sampled with each voltage pulse. According to McDaniel (*23*), a highly ionized volume of gas is to be considered a plasma where "when in contact with a physical boundary, a plasma forms a protective sheath about itself. The sheath, in effect, separates the main body of the plasma from its environment. Unlike the main body, the sheath is not electrically neutral and strong electric fields may be present in it. The thickness of the sheath is of the order of a Debye length". Thus, within Siegle and McKeown's concepts and McDaniel's description of a plasma, the current one measures from an ECD may reflect the motion of electrons and possibly ions only within one Debye length from electrode surfaces. This distance can be calculated from the equation (*23*).

$$\lambda_d = \sqrt{\frac{\epsilon k T}{4 \pi e^2 n}}$$

where n is the ion density, ϵ is the dielectric constant, e is the charge of an electron, k is the Boltzmann constant, and T is temperature. Assuming a reasonable value for n to be 2.4×10^8 cm^{-3} (*6*), λ_d becomes 33 μm at 300 °C. Since a typical ECD cell has an inside diameter on the order of 1 cm, this model suggests that only a minor portion of the total ECD volume is sampled during individual voltage pulses. This model contradicts point 3 of the conventional model and constitutes generally a radical departure from earlier ideas.

Modified View B. An alternative view might be considered which recognizes the importance of electrostatic forces between ions and electrons, but does not depart so drastically from the conventional view. This view insists that all electrons within the ECD are removed with each pulse, and then considers the effects of the positive space-charge field created by the excess positive ions during the period between pulses. We feel that this view has considerable merit, because point 3 of the conventional view is strongly supported in different ways by the ECD literature. Because this is a crucial detail of ECD theory, the support of point 3 might be recalled. The experiments of Wentworth, Chen, and Lovelock (*16*), Devaux and Guiochon (*22*), and Simmonds et al. (*12*) have already been referred to. Experiments by Hastings, Ryan, and Aue (*14*) and also by Lovelock (*19*) have shown that the electron capture reactions in an ECD cell can be stopped by the application of a continuous potential of about 50 V. These experiments suggest that the applied field's presence is felt throughout the cell, not just within a Debye length from the electrodes. In other experiments (*19, 24, 25*) it has been shown that a near-coulometric relationship exists between electrons lost and moles of sample present in the ECD's response to some polychlorinated molecules. Either point 3 of the conventional view is valid or this relationship is coincidental. Later in this article a theoretical argument supporting point 3 of the conventional view will also be presented.

Interpretation of Results. We would now like to consider how the mass spectrometric measurements reported here might be related to the ECD models discussed. As an aid for this discussion, in Figure 10 is shown a pictorial model of ions and electrons in a pulsed ECD which may be taken to represent modified view B if the events suggested are assumed to take place throughout the entire cell or, alternatively, may represent modified view A if the events pictured are thought to occur only at short distances (one Debye length) from the

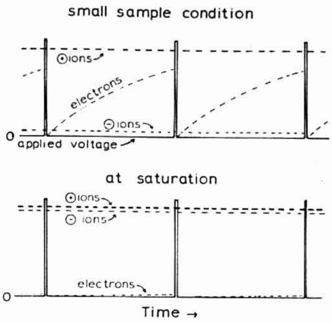

Figure 10. Representation of the concentrations of charged particles within a region of the pulsed ECD. This region exists throughout the entire cell volume or alternatively near the wall of the ECD. The saturated condition is caused by the presence of an adequately high concentration of electron capturing molecules in the carrier gas

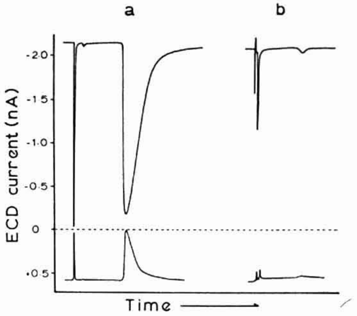

Figure 11. ECD current observed at the collection pin of the ion source using normal positive voltage pulses (upper trace) and using negative pulses (lower trace). During chromatograms of (a) 3 ng *p*-chloronitrobenzene, (b) 10 ng anthracene. ECD temperature, 250 °C. Pulse period, 300 μs

cell wall. During a short voltage pulse, the electrons are removed from the entire cell or from the region immediately adjacent to the cell wall. The relatively sluggish positive ions are not so strongly affected by the short pulses, and the result is that a positive space-charge is created. During the time immediately following the pulse, the positive space-charge will tend to hold the few negative ions which may be present in the small sample condition within the space-charge region, and the negative ions are not observed (thus, Figure 3). The positive ions, meanwhile, are allowed to diffuse to the cell boundaries (thus, Figure 7). With longer periods between pulses, electron concentration is allowed to increase to a point where charge neutrality may be achieved during the latter portion of the period and the effect of pulsing on the negative ion signals at this lower frequency is much less (thus, Figure 6). The positive space-charge which retards the negative ion signals is created by the removal of electrons, and it might be expected that this post-pulse condition could be created by pulses of either polarity. Thus, pulsing the pin positive or negative causes the identical effect on the negative ions (Figure 8). In the large sample condition, or with negative ions in large excess over electrons (saturation), electrons play a minor role in the maintenance of charge neutrality and the effect of pulsing the ECD on the negative ion signals vanishes (Figure 9).

The ECD/APIMS data cannot be explained solely by the conventional view of the ECD and clearly indicate the importance of electrostatic forces between charged particles. The data seem very consistent with modified view B, but, however, may also be explainable by the less-well defined modified view A. From the experiments we have described, one can make an interesting prediction which perhaps can be used to test the candidate views further. That is that at least some of the current measured in the pulsed ECD should be due to a selective positive ion migration to the sampling electrode during the period between pulses, when negative ions (as we have shown experimentally), and undoubtedly also electrons, are held within the space-charge region, while positive ions are allowed to diffuse out. This current would tend to subtract from the large negative current caused by drawing electrons to the pin during a positive pulse. We have tested this prediction by performing a simple experiment. The ECD pulser was altered to produce negative, 35-V pulses (as used in Figure 8). The negative pulses will repel electrons away from the sampling electrode, and a positive ECD current should be observed due to the arrival of positive ions to the pin during the period between pulses as we predict for the small- or no-sample condition. Two chromatograms using negative pulses are shown in Figure 11 in the lower traces while the normal ECD current caused by positive pulses during repeated analyses is shown in the upper traces. The very striking result is that in the backwards configuration, a remarkably high positive standing current results (0.28 as high as that of the conventional configuration). Furthermore, a very sensitive response to the electron-capturing compound, PCNB, occurs. The positive current goes to zero (and a response occurs) in the saturated condition because negative ions have replaced electrons, and the pulses then create no region of positive space-charge. That the response is due to an electron capture reaction is supported by the lack of response to the larger anthracene sample which captures electrons only weakly, but which we know from our APIMS measurements undergoes positive ion–molecule reactions very readily.

In determining whether this large positive ion current is consistent with either of the modified views, again modified view A has not yet been sufficiently defined as to allow this assessment to be made for it. It will be shown, however, that the magnitude of current observed with the application of negative pulses is in good agreement with modified view B. If the entire cell volume is cleared of electrons during a pulse, after this pulse a certain fraction of the positive ions will migrate to the sampling pin causing the positive current, and some will migrate to the cell wall which is electrically grounded. The fraction of the total positive ions present which will move toward the pin will be determined by the field generated by the positive ions themselves. If one assumes that initially following the removal of a pulse, positive ions are uniformly distributed throughout the cell, the electrical potential at any point within the cell can be calculated by solving Poisson's equation (*26*). Assuming infinite cylindrical symmetry, Equation 1 is thereby derived for the boundary conditions, that

$$V = \frac{\rho_0}{4\epsilon_0}\left[(b^2 - a^2)\,\frac{\ln(r/b)}{\ln(b/a)} + (b^2 - r^2)\right] \tag{1}$$

potential V, equals zero at radii, $r = a$ and $r = b$, where a is the radius of the sampling pin and b is the radius of the cylindrical cell cross section. ρ_0 is the density of the positive ions, and ϵ_0 is the permittivity of free space. For our cell, $a = 0.79$ mm and $b = 5.0$ mm. Assuming that ρ_0 is about 2.4×10^8 ions/cm^3 (*6*), the electrical potential calculated from Equation 1 is plotted as a function of r in Figure 12, curve

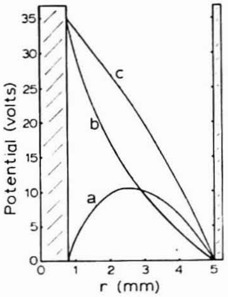

Figure 12. Calculated electrical potential, V, within our cylindrical ECD as a function of distance, r, from the center of the sampling pin as predicted by modified view B. Curve a shows the potential just as the pin is grounded after a voltage pulse, when all electrons have been removed, and a uniform distribution of positive ions remains. Curve a is calculated from Equation 1 in text. Curve b is the potential expected across the cell during the first instant a +35-V pulse is applied to the central pin. Curve b is calculated from the equation, V(volts) = 35 × ln (b/r)/ln (b/a). Curve c is also the potential expected during the applied pulse, but after all electrons have been removed, about 1 μs later. Curve c is the sum of curves a and b

a. This curve shows that the potential caused by the presence of the uniformly distributed positive ions rises from zero at the cell boundaries to a maximum which occurs at $r_{\max} = 2.57$ mm. Thus, we might expect space-charge repulsive forces to cause the positive ions within $r = 2.57$ mm to move toward the sampling electrode, and the ions beyond this distance to move toward the cell wall. The ratio of ions which may eventually arrive at the surfaces at $r = a$ and $r = b$ is equal to the ratio of the volumes of the cell within and beyond $r_{\max}$ and is given by

$$\frac{I^+_a}{I^+_b} = \frac{(r^2_{\max} - a^2)}{(b^2 - r^2_{\max})}$$

where I^+_a and I^+_b are the positive ion currents arriving at the sampling electrode and the grounded wall, respectively. For our cell this treatment predicts I^+_a/I^+_b to be 0.33. We can now compare this prediction of modified view B with the experimental result shown in Figure 11, in which the observed positive current, I^+_{net}, obtained with negative pulses is 0.28 as large as the negative current, I^-_{net} observed using positive pulses. According to modified view B, I^+_{net} might be viewed as being simply I^+_a, while I^-_{net} is equal to the electron current accumulated during pulses, I_e, minus the current due to the arrival at the pin of positive ions during the period between pulses, again equal to I^+_a. Thus,

$$\frac{I^+_{\text{net}}}{I^-_{\text{net}}} = \frac{I^+_a}{I_e - I^+_a}$$

A reasonable assumption within modified view B is that $I_e = I^+_a + I^+_b$. Thus, the last equation becomes

$$\frac{I^+_{\text{net}}}{I^-_{\text{net}}} = \frac{I^+_a}{I^+_b}$$

and the ratio of the two measured currents in Figure 11, noted to be 0.28, is a direct measure of I^+_a/I^+_b. This value compares very favorably with the predicted value, 0.33, and strongly supports the validity of modified view B.

Also shown in Figure 12 are the results of additional calculations which we feel further support modified view B over modified view A. Curve b in Figure 12 is the calculated potential throughout the cell during the application of a positive, 35-V pulse when the cell contains an equal number of positive and negative particles uniformly distributed. This is the condition we might expect to exist during the first instant of a pulse before any electrons have been removed. Curve c is the potential expected throughout the cell near the end of this same pulse (about 1 μs later) when all electrons have been removed by the pulse. Curve c is obtained by the simple addition of curves a and b. While curve c has some convex curvature as a result of the positive ion space-charge field, it still has a negative slope at all radii from the pin, supporting the assumption that all electrons within the cell will have been drawn to the anode. Only with the application of smaller voltages would curve c acquire a flat or positive slope, causing an incomplete collection of electrons at the pin. The insistence of modified view A that charge neutrality must be maintained at distances greater than one Debye length from the cell boundaries does not, therefore, seem appropriate to the pulsed ECD during the application of the pulse. The forces between charged particles appear to become dominant only during the period after the pulse.

CONCLUSIONS

We have demonstrated here the existence and theoretical basis of a previously unrecognized component of the current measured with a pulsed ECD. The importance of positive ions in affecting the ECD current is undoubtedly a function of the cell geometry and anode placement. In certain practical applications of the ECD, such as its use as a gas-phase coulometer (*19*, *24*, *25*), it is essential that either the positive ion contribution to the measured current be eliminated, or that its contribution be understood to the extent that a correction for its presence can be applied.

The incorporation of an ECD sampling pin into the ion source of an APIMS is very easily done and provides a powerful combination of functions which should be useful for trace organic analysis. In the use of such an instrument, however, an appreciation of the interdependence of negative ion signals and the pulsed field used for the ECD function is advised.

ACKNOWLEDGMENT

The authors thank P. Callis, R. Geer, and R. Howald for numerous discussions leading to this paper.

LITERATURE CITED

(1) F. W. Karasek, O. S. Tatone, and D. M. Kane, *Anal. Chem.*, **45**, 1210 (1973).
(2) F. W. Karasek, *Anal. Chem.*, **43**, 1982 (1971).
(3) F. W. Karasek and D. M. Kane, *Anal. Chem.*, **45**, 576 (1973).
(4) I. Dzidic, D. I. Carroll, R. N. Stillwell, and E. C. Horning, *Anal. Chem.*, **47**, 1308 (1975).
(5) E. C. Horning, D. I. Carroll, I. Dzidic, S.-N. Lin, R. N. Stillwell, and J.-P. Thenot, *J. Chromatogr.*, **142**, 481 (1977).
(6) M. W. Siegel and M. C. McKeown, *J. Chromatogr.*, **122**, 397 (1976).
(7) E. Grimsrud, *Anal. Chem.*, **50**, 382 (1978).
(8) A. Zlatkis and D. C. Fenimore, *Rev. Anal. Chem.*, **2**, (4), 317 (1975).
(9) D. I. Carroll, I. Dzidic, R. N. Stillwell, M. G. Horning, and E. C. Horning, *Anal. Chem.*, **46**, 706 (1974).
(10) M. W. Siegel and W. L. Fite, *J. Phys. Chem.*, **80**, 2871 (1976).
(11) D. C. Fenimore and C. M. Davis, *J. Chromatogr. Sci.*, **8**, 519 (1970).
(12) P. G. Simmonds, D. C. Fenimore, B. C. Pettitt, J. E. Lovelock, and A. Zlatkis, *Anal. Chem.*, **39**, 1428 (1967).
(13) E. P. Grimsrud and and R. G. Stebbins, *J. Chromatogr.*, **155**, 19 (1978).
(14) C. R. Hastings, T. R. Ryan, and W. A. Aue, *Anal. Chem.*, **47**, 1169 (1975).
(15) J. E. Lovelock, *Anal. Chem.*, **35**, 474 (1963).
(16) W. E. Wentworth, E. Chen, and J. E. Lovelock, *J. Phys., Chem.*, **70**, 445 (1966).
(17) W. A. Aue and S. Kapila, *J. Chromatog. Sci.*, **11**, 225 (1973).
(18) E. P. Pellizzari, *J. Chromatogr.*, **98**, 323 (1974).
(19) J. E. Lovelock, *J. Chromatogr.*, **99**, 3 (1974).
(20) P. L. Patterson, *J. Chromatogr.*, **134**, 25 (1977).
(21) F. W. Karasek and L. R. Field, *Res./Dev.*, **28**, 42 (1977).
(22) P. Devaux and G. Guiochon, *J. Gas Chromatogr.*, **5**, 341 (1967).
(23) E. W. McDaniel, "Collision Phenomena in Ionized Gases", John Wiley & Sons, New York, 1964, p 696.
(24) J. E. Lovelock, R. J. Maggs, and E. R. Adlard, *Anal. Chem.*, **43**, 1962 (1971).

(25) D. Lillian and H. B. Singh, *Anal. Chem.*, **46**, 1060 (1974).
(26) P. Lorrain and D. Corson, "Electromagnetic Fields and Waves", 2nd ed., W. H. Freeman and Co., San Francisco, Calif., 1970, p 51.

RECEIVED for review August 8, 1978. Accepted October 30, 1978. Research supported by the donors of the Petroleum Research Fund, administered by the American Chemical Society, by the Research Corporation, and by the National Science Foundation.

Mass Spectrum Dictionary for Library Searching

R. Geoff Dromey

Department of Computing Science, University of Wollongong, P.O. Box 1144, Wollongong, N.S.W. 2500, Australia

When data can be arranged according to some ordering principle (e.g., numerical or alphabetical), powerful searching techniques can be applied to retrieve information. An explicit set of procedures is proposed for constructing a precisely ordered mass spectrum dictionary. Performance tests on the proposed system show that on average less than 1% of the spectra need to be examined in searching for a given unknown. The mass spectrum dictionary is economical on storage and it will accommodate spectrum variability likely to be found in a library search environment.

Searching a large library of mass spectra for the best-match candidates with some particular query spectrum can be a time consuming process. A number of systems that perform well on this task have been proposed (*1–7*). One of the most successful of the library search techniques is the method due to Heller (*4*) which employs an inverted file structure. One of the only real criticisms of this system is that it is very costly both in terms of file generation and file maintenance. The other really serious problem is the size of the file (although there are ways to alleviate this problem (*8*)).

These problems have prompted the development of a system that is comparable in performance but which requires neither the overhead of file maintenance nor large amounts of storage for the search file.

Searching large amounts of data can be efficient provided the items can be ordered in some way. For instance, searching a file as large as a telephone directory by computer can be made a simple and efficient task using a binary search algorithm (*9*). The binary search algorithm guarantees to find *any* item in an ordered file of N items in at most $\log_2 N$ steps. For example only *16 comparisons* are necessary to locate any item in an ordered file of 32000 items. This efficiency is derived by taking advantage of the order in the file.

Returning to the mass spectrum context, we find that searching a library of mass spectra for the best match with some unknown spectrum is comparable to searching a telephone directory in which the names are in random order. Obviously such a search system is very inefficient because there is no way of taking advantage of any inherent order in the data. Series displacement indices (*7*) and ion series analysis (*5, 6*) have been suggested as ways of reducing the portion of the file that needs to be searched. These methods do not, however, possess the specificity that is desirable in searching large files; that is, *they do not eliminate enough candidates from the search.*

This leads to the question as to whether we can impose some ordering principle on a library of mass spectra. Any attempt at such a task must take into account the inherent variability in the data. In particular, there can be considerable differences in intensity information for representations of a mass spectrum measured on different instruments.

A careful examination of a large number of mass spectra reveals that, in general, there are considerable differences in both mass and intensity representations for compounds that are closely similar structurally. Grotch has shown that, when intensity information is discarded altogether, we still have a very selective representation (*10*). It might therefore seem reasonable that the mass information could be used in some way to order a file of spectra. However, using the mass information alone still does not completely remove the intensity variation problem. It will be shown in the next section that certain intensity related constraints can be placed on the selection of masses for an ordered representation.

MASS SPECTRUM DICTIONARY CONSTRUCTION

In order to construct a mass spectrum dictionary, a fixed range for selecting masses must be predetermined (for this to work the mass range 40 → 99 is used). This range is divided up into 6 ranges of 10 mass units (i.e. 40 → 49, 50 → 59, ...). The selection rules that are then applied to cope with spectrum variability are as follows.

(1) Select the mass of the most intense peak in each range (relative ion abundance is used for the intensity scale, range is 0 to 100%).

(2) Make the following checks to determine if there is any possibility of ambiguity in the selection made: (a) If the most intense peak in a range is less than or equal to 1%, assign it to the zero mass for the range and mark it as not ambiguous. (b) If the most intense peak in a range is greater than 1% and less than or equal to 10%, mark it as ambiguous. (c) If the ratio of the most intense to the second most intense peak in a given 10 amu range is less than 1.4, flag it as ambiguous. (The 1.4 criterion was a heuristic choice made after carefully examining over 200 spectra that included a number of duplicates.). (d) All other peaks that are the most intense in their respective ranges are considered as unambiguous.

The preceding steps divide the ranges and selected peaks into two categories: (1) those that are definitive and unambiguous, and (2) those for which instrumental variations may lead to either no mass or another mass being selected as the most intense for that particular range.

With this information in hand it is possible to consider how representations that can be ordered may be constructed.

Construction of Abbreviated Mass Spectral Representations Suitable for Ordering. The representation for each unambiguous range is just the value of the integer mass for that range modulo 10 (e.g., mass 43 has the representation 3, and 57 has the representation 7).

The representations for those ranges that have been flagged as possibly ambiguous must be treated differently. They are given *two* possible representations: (1) the representation they

0003-2700/79/0351-0229$01.00/0 © 1979 American Chemical Society

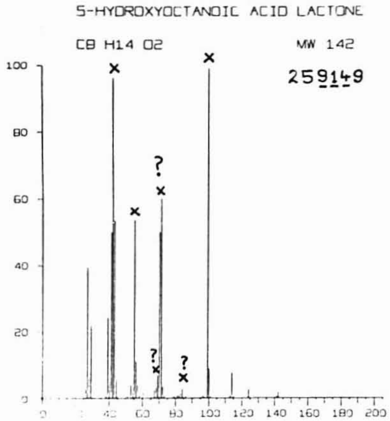

Figure 1. Numeric representation for 5-hydroxyoctonoic acid lactone

would assume if they were not classified as ambiguous (e.g., if the most intense peak in the range 40 → 49 amu is mass 43 at 5%, then 3 is its representation); (2) the second representation for the range is a standard default setting of 0. *This representation is vital for linking together spectra of the same compound that may be distorted with respect to one another because of instrumental variations.* The process must be taken a step further before we can construct suitable entries for an ordered mass spectrum dictionary.

Obviously we cannot expect to have single dictionary entries for any spectra that have one or more of their ranges flagged as ambiguous. Also we cannot expect that another representation of the same spectrum will have the identical ranges flagged as ambiguous as in the dictionary entry (e.g., the dictionary entry may have a peak of 9% [ambiguous] whereas another representation may have the same mass as 15% [unambiguous] and vice versa). *For this reason the dictionary must contain all possible permutations of the ambiguous and unambiguous representations.* The final representation for a given spectrum is therefore a set of six-figure numbers. *It follows that if n of the ranges have been flagged as possibly ambiguous or uncertain then 2^n representations for the spectrum will need to be placed in the dictionary.* These 2^n representations should be sufficient to cover all instrumental variability apart from impurity peaks.

The mass range 40 → 99 was chosen for the representation on the statistical grounds that most spectra tend to show considerable fragmentation in this region. Obviously other ranges may be more appropriate in specialized circumstances.

The choice of a six-figure representation was made because it was the smallest representation that gave considerable discriminating power. Longer representations could also be used if better resolution was required. However, they introduce the risk of many more dictionary entries per spectrum because of the way uncertain peaks are handled.

The six-figure representations can be sorted into numeric order along with their accompanying pointers to the corresponding original spectrum.

As an example, consider the dictionary entries for the spectrum of 5-hydroxyoctanoic acid lactone shown (*11*) in Figure 1.

Applying the selection rules previously described we obtain the representation $25\underline{9}\underline{1}\underline{4}9$ where the numbers underlined are possibly uncertain. The peaks at 69 (9) and 84 (4) are ambiguous because they are less than 10%. The peak at 71 is classified as uncertain because its ratio with the peak at mass 70 (the second most intense peak) is less than 1.4. There are therefore three of the six mass regions that contain representations which cannot be guaranteed to withstand variations due to instrument distortion. Obviously the peaks at masses 42, 55, and 99 would withstand any distortion. In this particular case, we must therefore generate eight ($2^{\text{no. of uncertain}} \equiv 2^3$) dictionary entries for this spectrum to accommodate all possible representations. The representations are given in Table I. These representations are entered into the dictionary at the appropriate place corresponding to ascending numeric order. Each entry is tagged with an address or label corresponding to the location of the complete spectrum in the master file.

Table I. Mass Spectrum Dictionary Entries for 5-Hydroxyoctanoic Acid Lactone Generated by Binary Multiplication

$X = 7$	$25\underline{9}\underline{1}\underline{4}9$ $\overline{1}\overline{1}\overline{1}$	259149
$X = 6$	$25\underline{9}\underline{1}\underline{4}9$ $\overline{1}\overline{1}\overline{0}$	259109
$X = 5$	$25\underline{9}\underline{1}\underline{4}9$ $\overline{1}\overline{0}\overline{1}$	259049
$X = 4$	$25\underline{9}\underline{1}\underline{4}9$ $\overline{1}\overline{0}\overline{0}$	259009
$X = 3$	$25\underline{9}\underline{1}\underline{4}9$ $\overline{0}\overline{1}\overline{1}$	250149
$X = 2$	$25\underline{9}\underline{1}\underline{4}9$ $\overline{0}\overline{1}\overline{0}$	250109
$X = 1$	$25\underline{9}\underline{1}\underline{4}9$ $\overline{0}\overline{0}\overline{1}$	250049
$X = 0$	$25\underline{9}\underline{1}\underline{4}9$ $\overline{0}\overline{0}\overline{0}$	250009

The uncertain digits are underlined.

Procedure for Generating Complete Sets of Dictionary Entries. The procedure for generating the permutations for any given spectrum can be formulated as a simple algorithmic sequence which has the following steps.

(1) Count the number of uncertain digits N in the basic representation generated using the prescribed selection rules.

(2) Calculate $2^N - 1$ and assign it to the variable X. The value of X is one less than the total number of dictionary entries to be generated for the spectrum.

(3) Calculate the binary representation of X (e.g., $7_{10} \rightarrow 111_2$).

(4) Moving left to right in both the binary representation of X and the decimal representation of the spectrum generated by the selection rules, multiply the uncertain decimal digits by the corresponding binary representation (see Table I).

(5) Subtract one from X (e.g., $X = X - 1$) and if the new value of X is greater than or equal to 0 go back to step (3) and calculate another permuted dictionary entry. If X is less than zero, all the necessary representations have been generated and so the process can halt.

Construction of an Efficient Search File. There are two basic options open for constructing an effective retrieval system based on the abbreviated spectrum representations that have been described. The first and perhaps most obvious approach is to sort and place the representations into ascending numeric order. The other alternative is to use what is known as a hashing method to determine where in the file a particular dictionary entry should be placed. At the expense of some additional storage, the latter approach can be guaranteed to be more efficient.

To minimize file maintenance costs (which are already small because of the highly compact nature of the representation), the hash table size should be overspecified to allow for easy additions. If the numerically ordered representation is chosen it can probably best be implemented as an indexed sequential file (*12*). The latter allows easy updates while restricting the rearrangement of the file.

Spectrum Retrieval from a Numerically Ordered File. The most practical and efficient way to search a numerically ordered file is to apply what is known as a binary search algorithm (*9*). This search procedure uses information about the order of the file to remove from further consideration half of the remaining entries in the file with each comparison made. The basic procedure is to take the number sought and compare it with the number in the middle of the file. If it is less than the middle value, we can discard from further consideration all the values in the top half of the file and vice versa if it is greater than the middle value. We then repeat the process with the remaining half of the file by dividing it in turn in two. With just two comparisons, three quarters of the file entries will be eliminated. The bisection procedure continues until we find the number we have sought or until we have established that it is not in the file. Analysis of the binary search procedure tells us that we never need to make more than $\log_2 N + 1$ comparisons and that on average only $\log_2 N - 1$ will be needed (*9*). If N is, for example, 60 000 which is probably typical for a large library of mass spectra, then on average only 16 entries in the file will need to be examined to find the address of any particular representation.

Spectrum Retrieval from a Hash-Stored File. It is common practice in computing science to use a hashing technique to retrieve data from a large file. It has also been used in chemistry for molecular formula retrieval (*4*). Hashing is usually favored because of its high efficiency for retrieval (*9, 13*). The basic idea of hashing is to take the numeric representation of the data to be stored and transform it in some way to produce a representation-dependent location at which the data are to be stored. Such hashing transformations are usually not unique. It is, however, usually easy to find a suitable transformation that will map the original data into a retrieval file that contains about twice as many locations as representations to be stored. Theoretical analysis of such systems indicates that *on average less than two positions in the table will need to be examined to locate any particular representation.* Detailed procedures for implementing hash files can be found in Knuth (*9*) and Severance (*13*). A linked overflow storage area (*13*) is the most suitable method for handling mass spectral data because of the fact that most representations occur more than once in the file.

To locate an item in a hashed file, the representation that is sought is hashed to produce a location at which to begin the search. The value stored in the calculated location is then compared with the number sought. If they match, the search terminates; otherwise adjacent locations are examined until the desired match is found. If in this subsequent search an empty location is encountered, this signifies that the representation sought is not present in the file.

The Search and Matching Procedures. The following steps must be carried out to locate the set of spectra most like some unknown spectrum being sought.

(1) The selection rules are applied to the unknown spectrum, establishing its numeric representation and its uncertain peaks.

(2) The permuted set of dictionary entries is then generated.

(3) The addresses of *all* the dictionary entries are then located by hashing or binary search depending on the file representation chosen. These addresses are pointers to where the complete spectra are stored.

(4) The selected set of *complete* spectra is then retrieved and *compared* against the unknown spectrum using some standard matching procedure.

The merging process is easily implemented with a bit vector which has as many bits as there are spectra in the file. As each spectrum number is found, the corresponding bit is set in the bit vector.

Table II. Number of Sample Spectra Requiring Less than X% of the File to Be Searched

no. of spectra requiring less than X% of file to be searched	percentage of file searched (X%)
26	0.1
41	0.25
50	0.5
68	1.0
82	2.0
92	3.0
100	over 3

RESULTS AND DISCUSSION

To test out the feasibility of the procedures that have been outlined a set of 10 000 mass spectra were studied and analyzed. The first parameter of interest for files of this type is the average number of representations per spectrum that are needed to cover all possibilities introduced by peak uncertainties. It was found that 60 894 representations were generated for the 10 000 spectra. That is, on average just over 6 dictionary entries per spectrum are needed to construct the dictionary. The size of the file processed to obtain this result should be large enough to guarantee its statistical significance for any *general* file of mass spectra.

The other important parameter for gauging the effectiveness of this method of spectrum retrieval is the average number of complete spectra that are required to be matched for a given query spectrum. To estimate this performance parameter, 100 spectra from the file of 10 000 were selected at random to remove any bias. Dictionary entries for each of these spectra were then generated and the corresponding number of spectra retrieved in each instance was calculated. The search results for the 100 spectra are summarized in Table II. Averaging the results for the 100 spectra searched for, it was found that 0.98% (~1%) of the file had to be matched.

The results in Table II indicate that we expect a quarter of the searches that are made to require searching of less than 0.1% of the file. The table also shows that, on average, *half* of the spectra will require less than 0.5% of the file to be searched and that a total of 92% of the spectra require less than 3% of the file to be searched.

One spectrum in the set took 5.88% and another spectrum required 7.92% of the file to be searched. The latter spectrum had 5 of its 6 peaks flagged as uncertain (e.g. $\underline{1}\underline{1}\underline{3}7\underline{9}\underline{1}$) with only the mass 77 being unambiguous. There were therefore 32 (i.e., 2^5) dictionary entries for this compound and so, because of the considerable number of aromatic compounds present, 7.92% of the file had to be searched.

There were nearly 1000 representations that had all zeros as their representation (e.g., 000000). The high number of these representations is due to a number of factors. A number of spectra in the data set do not have mass measurements taken until after mass 100. Ideally these anomalous data should be removed. Other spectra (mostly aromatics) have only a very few low intensity peaks below mass 100 while some have low molecular weights with only small peaks in the mass range 40 to 99. The latter groups obviously have 000000 as a legitimate representation. The most practical approach to this problem is to use another range (e.g., 100 → 159). The 000000 representation then disappears from many of the dictionary entries for the spectra in this group. An effective, although not strictly correct approach to the problem, is to ignore the 000000 representation when performing retrievals.

Where library spectra have not been recorded over the prescribed range (e.g., down to mass 40) obviously we cannot expect their representations to be accurately described in the file. This problem is an inadequacy in the data rather than in the search strategy and as such it is the responsibility of those in charge of maintaining the integrity of the data base.

One approach that will accommodate "incomplete" spectra is to separate them all from the main file and create a second file ordered on a mass range for which those spectra are defined. Both files would then need to be searched with their respective representations of the query spectra. In most instances presumably the latter file would be relatively small.

In discussing the performance of the system the preliminary searches of the dictionary have been ignored because of their very small overhead relative to spectrum matching operations. Further, the number of comparisons for retrieval from both a hash file and an ordered file are known and have been completely characterized by theoretical arguments (*9*).

ACKNOWLEDGMENT

The author thanks Ann Titus for typing the manuscript and S. R. Heller and G. W. Milne for providing the mass spectral data base.

LITERATURE CITED

(1) F. W. McLafferty, R. H. Hertel, and R. D. Villnock, *Org. Mass Spectrom.*, **9**, 690 (1974).
(2) S. Grotch, *Anal. Chem.*, **43**, 1362 (1971).
(3) H. S. Hertz, R. A. Hites, and K. Biemann, *Anal. Chem.*, **43**, 681 (1971).
(4) S. R. Heller, *Anal. Chem.*, **44**, 1951 (1972).
(5) L. R. Crawford and J. D. Morrison, *Anal. Chem.*, **40**, 1469 (1968).
(6) D. H. Smith, *Anal. Chem.*, **44**, 536 (1972).
(7) R. G. Dromey, *Anal. Chem.*, **48**, 1464 (1976).
(8) R. G. Dromey, *J. Chem. Inf. Comput. Sci.*, (November 1978).
(9) D. Knuth, "The Art of Computer Programming", Vol. 3, Addison-Wesley, Reading, Mass., 1973.
(10) S. L. Grotch, *Anal. Chem.*, **42**, 1214 (1970).
(11) B. H. Kennett, K. E. Murray, F. B. Whitfield, G. Stanley, J. Shipton, and P. A. Bannister, "Mass Spectra of *Organic* Compounds", CSIRO report, (1977).
(12) K. J. McDonell and A. Y. Montgomery, *Aust. Comput. J.*, **5**, 115 (1973).
(13) D. Severance and R. Duane, *Comm. ACM*, **19**, 409 (1976).

RECEIVED for review July 24, 1978. Accepted November 6, 1978.

Optimizing Precision in Standard Addition Measurement

Kenneth L. Ratzlaff

Department of Chemistry, The Michael Faraday Laboratories, Northern Illinois University, DeKalb, Illinois 60115

Equations are presented and plotted which describe the effect of the increment size on the precision of a standard addition or standard subtraction measurement. Linear, exponential, and logarithmic transfer functions are considered in which the uncertainty may take several forms.

The standard addition (SA) technique (also called known addition, standard increment, or known increment) is well known to be of value when solution conditions are not readily reproducible in reference media (*1*). In this technique, a measurement is made on the analyte followed by the addition of a known quantity of standard and a second measurement; the original quantity of analyte is then computed without reference to a calibration curve.

The increment size must be chosen such that good precision can be maintained in the measurement and the solution conditions are not disturbed (*1*). In this paper, the choice of increment size will be discussed as it relates to precision. Although SA is in common use, the increment size has received little or no attention except in dc polarography where, for example, Lingane suggests that the increment should double concentration (*2*).

There are several criteria which although seldom mentioned, must be satisfied for SA utilization.

(1) The instrumental technique must either have a linear response with concentration or must have a known transfer function over the range of concentrations encountered.

(2) The chemical system must be free of deviations from linearity over the range of concentrations observed; these deviations could be caused by effects related to complexation equilibria, ionic strength, pH, free electron concentration in flames, etc. A large increment may shift these equilibria and produce nonlinearity.

(3) The intercept must be known; generally it is considered to be zero.

The increment may be either positive or negative; a negative addition, or standard subtraction, occurs when the added reagent removes analyte from availability to the measurement system. This is in many ways similar to an incremental or Gran plot titration (*3*).

The advent of computer-controlled instrumentation has made possible automated SA measurements (*4, 5*). It is now feasible, after computing a first approximation of the concentration from the initial measurement, to determine an optimum addition based on the initial value. Consequently, a better understanding is needed of how precision relates to increment size. Because the increment size is to be determined after the first measurement, standard addition measurements in which two samples are taken and one is incremented before chemical workup are outside the scope of this study as are all errors and uncertainties associated with the sample preparation. Only the measurement step is included.

PRECISION OF SA MEASUREMENT

Factors affecting the choice of increment size are examined herein by considering the contribution of various types of uncertainty for each of several transfer functions. For any measurement the overall uncertainty, expressed as the relative standard deviation, is equal to the square root of the sum of the squares of the relative standard deviation due to each source of uncertainty. The relative standard deviation is determined using propagation of errors mathematics. This approach has been used on several occasions (*6–8*) for single measurement techniques so that certain types of uncertainty are well defined.

The following transfer functions will be considered.

(a) Linear. Examples include atomic or molecular fluorescence spectroscopy, flame emission spectroscopy, and voltammetric techniques.

(b) Exponential. An example is potentiometric measurement.

(c) Logarithmic. Molecular and atomic absorption spectroscopies are included.

0003-2700/79/0351-0232$01.00/0 © 1979 American Chemical Society

For spectroscopic measurements, the fundamental nature of the uncertainties has been discussed previously, and these uncertainties have been grouped into three categories (*6–8*).

(a) Independent. The uncertainty in the measured parameter is independent of the magnitude of the value.

(b) Square root. The uncertainty is proportional to the square root of the magnitude of the measured parameter.

(c) Proportional. The uncertainty is proportional to the measured parameter.

For electrochemical measurements and most others, there appear to be no fundamental sources of noise except for independent uncertainty generated by noise in electronic circuitry and either digitization or meter/recorder reading uncertainty.

Linear Transfer Function. A quantity of analyte, m_1 moles, in volume, V, is related to the readout, X_1 by a proportionality factor, k.

$$X_1 = km_1/V \tag{1}$$

After addition of m_2 moles of standard, the second measurement is made. The increasingly common use of micropipets which reproducibly dispense volumes under 10 μL makes reasonable the assumption of negligible dilution. Then,

$$X_2 = k(m_1 + m_2)/V \tag{2}$$

Solving for m_1,

$$m_1 = m_2X_1/(X_2 - X_1) \tag{3}$$

Since the variance in m_1 will be the result of the variances in the measured parameters, the variance in m_1 can be computed using propagation of error mathematics (*9*) if the contributing variances can be defined. The variance in m_1 $(\sigma_l)^2$, can be written as

$$\sigma_l^2 = \sigma_{X1}^2\left(m_2\frac{X_2}{(X_2 - X_1)^2}\right)^2 + \sigma_{X2}^2\left(m_2\frac{X_1}{(X_2 - X_1)^2}\right)^2 \tag{4}$$

where σ_{X1}^2 and σ_{X2}^2 are the variances in X_1 and X_2 respectively. The percent relative standard deviation, $\%\sigma_l = (\sigma_l/m_1) \times 100\%$ is then written in terms of m_1 and m_2 using Equations 1 and 2,

$$\%\sigma_l = ((\sigma_{X1}^2(m_1 + m_2)^2 + \sigma_{X2}^2m_1^2)V^2/k^2m_1^2m_2^2)^{1/2} \times 100\% \tag{5}$$

Independent Uncertainty. Where the uncertainty is independent of the measured parameter, the standard deviation of the measurement can be defined as a constant, σ_X, so that $\sigma_X = \sigma_{X1} = \sigma_{X2}$. Substituting into Equation 5, the percent relative standard deviation due to independent uncertainty, $\%\sigma_{l,i}$, is

$$\%\sigma_{l,i} = \frac{\sigma_XV(m_2^2 + 2m_1m_2 + 2m_1^2)^{1/2}}{km_1m_2} \times 100\% \tag{6}$$

It is useful to present $\%\sigma_{l,i}$ as a function of the ratio of increment to analyte, R, where $R = m_2/m_1$. Then

$$\%\sigma_{l,i} = \frac{\sigma_XV(1 + 2R^{-1} + 2R^{-2})^{1/2}}{km_1} \times 100\% \tag{7}$$

Equation 7 is plotted as curve A in Figure 1 vs. R for $\sigma_X = 2 \times 10^{-3}\ km_1/V$. It should be noted that R may assume negative values when a standard subtraction is carried out.

Square Root Uncertainty. When the standard deviation is proportional to the square root of the signal level, $\sigma_{X1} = (X_1/P)^{1/2}$ and $\sigma_{X2} = (X_2/P)^{1/2}$. The conversion factors grouped in P are discussed in references 6 and 8; X/P effectively represents the number of discrete events (photons or radioactive decay counts) included in the measurement, and is often termed "shot noise". Substituting into Equation 5, the relative standard deviation is

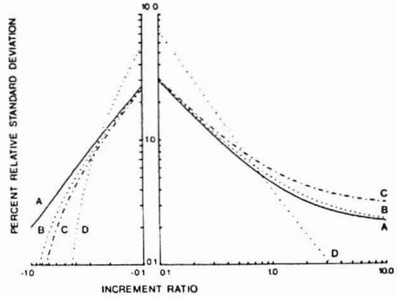

Figure 1. Percent relative standard deviation as a function of increment-to-analyte ratio. (A) Linear transfer function and independent uncertainty (Equation 7). $\sigma_XV/km_1 = 2 \times 10^{-3}$. (B) Linear transfer function, square root uncertainty (Equation 9). $Pkm_1/V = 2.5 \times 10^5$. (C) (i) Linear transfer function, proportional uncertainty (Equation 11). $\xi = 2 \times 10^{-3}$. (ii) Also represents exponential transfer function, independent uncertainty (Equation 15). $\sigma_X/S = 1.4 \times 10^{-3}$. (D) Exponential transfer function, independent uncertainty in slope (Equation 17). $\sigma_l/S = 1.4 \times 10^{-3}$

$$\%\sigma_{l,s} = ((2m_1^2 + 3m_1m_2 + m_2^2)V/Pkm_1m_2^2)^{1/2} \times 100\% \tag{8}$$

In terms of R,

$$\%\sigma_{l,s} = \left(\frac{(1 + 3R^{-1} + 2R^{-2})V}{Pkm_1}\right)^{1/2} \times 100\% \tag{9}$$

Equation 9 is plotted as curve B in Figure 1 vs. R for $km_1/V = 2.5 \times 10^5/P$.

Proportional Uncertainty. Where the standard deviation terms in Equation 5, σ_{X1} and σ_{X2}, are proportional to X_1 and X_2, respectively, $\sigma_{X1} = \xi X_1$ and $\sigma_{X2} = \xi X_2$ where ξ is the proportionality or "flicker" factor. The relative standard deviation becomes

$$\%\sigma_{l,p} = \sqrt{2}\xi((m_1 + m_2)/m_2) \times 100\% \tag{10}$$

In terms of R

$$\%\sigma_{l,p} = \frac{\sqrt{2}\xi(1 + R)}{R} \times 100\% \tag{11}$$

Equation 11 is plotted as curve C in Figure 1 for $\xi = 0.002$.

Exponential Transfer Function. For the common example of this function, potentiometric measurement, the measured value is proportional to the logarithm of the concentration, i.e., for the analyte,

$$X_1 = X_0 + S\ln(m_1/V) \tag{12}$$

and after the addition

$$X_2 = X_0 + S\ln((m_1 + m_2)/V) \tag{13}$$

In these equations X_0 is a constant, and S is the slope of the plot of potential against the logarithm of concentration; the theoretical value of S is the well-known RT/nF where R is the gas constant, T is the temperature, F is the value of the Faraday, and n is either the number of electrons transfered at a Redox electrode or the charge of the selected ion at an ion-selective electrode. Solving Equations 12 and 13 for m_1,

$$m_1 = m_2/(e^{(X_2 - X_1)/S} - 1) \tag{14}$$

Independent Uncertainty. Again applying propagation of error mathematics, the variance in m_1 for exponential transfer function, σ_e^2, is

$$\sigma_e^2 = \frac{(\sigma_{X1}^2 + \sigma_{X2}^2)m_2^2e^{2(X_2 - X_1)/S}}{S^2(e^{(X_2 - X_1)/S} - 1)^4}$$

The only type of uncertainty in the signal is independent, contributed by Johnson noise in the amplifiers and noise pickup in the electrodes. Consequently, both standard deviations can be written as σ_X. Including Equations 12 and 13, the percent relative standard deviation is then

$$\% \sigma_{e,i} = \frac{2\sigma_X(m_1 + m_2)}{Sm_2} \times 100\%$$

In terms of R

$$\% \sigma_{e,i} = \frac{2\sigma_X(1 + R)}{SR} \times 100\% \qquad (15)$$

Equation 15 has a dependence on R identical to that of Equation 10 so that it may be represented by Figure 1, curve C, where $\sigma_X = 1.4 \times 10^{-3}\ S$.

Slope Uncertainty. A second independent uncertainty to be considered in a potentiometric measurement is the standard deviation, σ_t, in the slope, S; S must be determined before Equation 14 can be applied, but is dependent on temperature and the condition of the electrode. The uncertainty in the entire measurement, $\sigma_{e,t}$, due to slope uncertainty is found from application of propagation of error mathematics to Equation 14.

$$\sigma_{e,t} = \sigma_t(X_2 - X_1)m_2e^{(X_2 - X_1)/S}/(S^2(e^{(X_2 - X_1)/S} - 1)^2)$$

Combining with Equations 12 and 13 and dividing by m_1, the relative standard deviation is

$$\% \sigma_{e,t} = \frac{\sigma_t(m_1 + m_2) \ln ((m_1 + m_2)/m_1)}{Sm_2} \times 100\% \qquad (16)$$

In terms of R,

$$\% \sigma_{e,t} = \frac{\sigma_t(1 + R) \ln ((1 + R)/R)}{SR} \times 100\% \qquad (17)$$

Equation 17 is represented in Figure 1 as curve D where $\sigma_t = 1.4 \times 10^{-3}\ S$; i.e., for a slope of 59.2 mV per decade, σ_t is about 0.1 mV.

Logarithmic Transfer Function. For absorption measurements, the measured values, transmitted and incident intensities, I and I_0, are logarithmically related to concentration. Thus, according to Beer's law, for the analyte of concentration of m_1/V,

$$\ln (I_0/I_1) = 2.303\epsilon b m_1/V \qquad (18)$$

where ϵ is the molar absorptivity and b is the path length. After the increment,

$$\ln (I_0/I_2) = 2.303\epsilon b(m_1 + m_2)/V \qquad (19)$$

Solving for m_1,

$$m_1 = m_2\frac{\ln (I_1/I_0)}{\ln (I_2/I_1)} \qquad (20)$$

At least three measurements must be made, I_2, I_1, and I_0. The latter may be made either once or twice depending on whether a single or double beam instrument is used; L will represent that number and may be 0 or 1.

The variance in m_1, σ_A^2 is

$$\sigma_A^2 = L\left(\frac{\sigma_{I_0}m_2}{I_0 \ln (I_2/I_1)}\right)^2 + \left(\frac{\sigma_{I_1}m_2 \ln (I_2/I_0)}{I_1(\ln (I_2/I_1))^2}\right)^2 + \left(\frac{\sigma_{I_2}m_2 \ln (I_1/I_0)}{I_2(\ln (I_2/I_1))^2}\right)^2$$

where σ_{I_0}, σ_{I1} and σ_{I2} are the standard deviations in the measurement of I_0, I_1, and I_2 respectively. Substituting for I_0, I_1, I_2

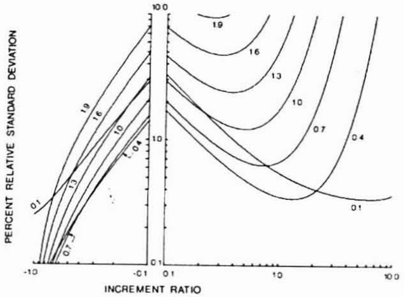

Figure 2. Percent relative standard deviation as a function of increment-to-analyte ratio for logarithmic transfer function, independent uncertainty (Equation 23) where $\sigma_I/I_0 = 4 \times 10^{-4}$

$$\sigma_A^2 = L\left(\frac{\sigma_{I_0}}{2.3kI_0}\right)^2 + \left(\frac{\sigma_{I1}(m_1 + m_2)}{2.3kI_0m_210^{-km_1}}\right)^2 + \left(\frac{\sigma_{I2}m_1}{2.3kI_0m_210^{-k(m_1+m_2)}}\right)^2 \qquad (21)$$

where $k = \epsilon b/V$.

Independent Uncertainty. If the uncertainty in I is independent of I, all standard deviations can be set equal, i.e., $\sigma_I = \sigma_{I_0} = \sigma_{I1} = \sigma_{I2}$. Then the relative standard deviation, $\% \sigma_{A,i}$ is

$$\% \sigma_{A,i} = \frac{\sigma_I}{2.303I_0km_1}\left(L + \left(\frac{m_1 + m_2}{m_210^{-km_1}}\right)^2 + \left(\frac{m_1}{m_210^{-k(m_1+m_2)}}\right)^2\right)^{1/2} \times 100\% \qquad (22)$$

Substituting $A = km_1$, $R = m_2/m_1$

$$\% \sigma_{A,i} = \frac{\sigma_I}{2.303I_0A_1}\left(L + \left(\frac{1 + R}{R10^{-A_1}}\right)^2 + \left(\frac{1}{R10^{-A_1(1 + R)}}\right)^2\right)^{1/2} \times 100\% \qquad (23)$$

This equation is plotted in Figure 2 for various values of A_1 where $\sigma_I = 4 \times 10^{-4}\ I_0$.

Square Root Uncertainty. If the uncertainty in I is due to shot noise, $\sigma_{I_0} = (I_0/P)^{1/2}$, $\sigma_{I1} = (I_1/P)^{1/2}$, $\sigma_{I2} = (I_2/P)^{1/2}$. Substituting into 21 and solving for the relative standard deviation,

$$\% \sigma_{A,s} = \frac{1}{2.3km_1}\left(\frac{L}{I_0P} + \frac{(m_1 + m_2)^2}{m_2^2I_0P10^{-km_1}} + \frac{m_1^2}{m_2^2I_0P10^{-k(m_1 + m_2)}}\right)^{1/2} \times 100\% \qquad (24)$$

In terms of R and A_1

$$\% \sigma_{A,s} = \frac{1}{2.3A_1}\left(\frac{L}{I_0P} + \frac{(1 + R)^2}{R^2I_0P10^{-A_1}} + \frac{1}{R^2I_0P10^{-A_1(1 + R)}}\right)^{1/2} \times 100\% \qquad (25)$$

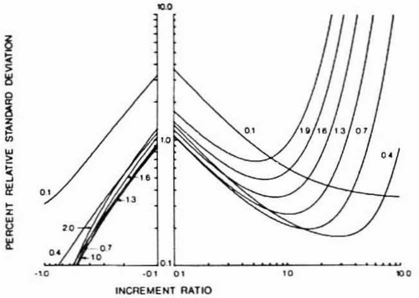

Figure 3. Percent relative standard deviation as a function of increment-to-analyte ratio for logarithmic transfer function, square root uncertainty (Equation 25), where $PI_0 = 4 \times 10^6$

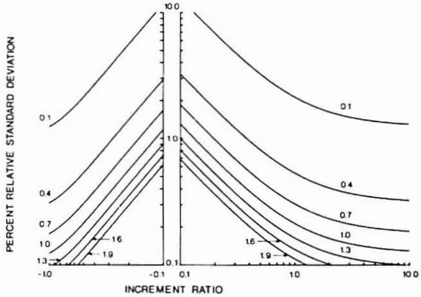

Figure 4. Percent relative standard deviation as a function of increment-to-analyte ratio for logarithmic transfer function, proportional uncertainty (Equation 27) for $\xi = 2 \times 10^{-3}$

Equation 25 is plotted in Figure 3 for various values of A_1 where $I_0 = 4 \times 10^6/P$.

Proportional Uncertainty. Finally, if the measurement is "flicker" limited, i.e., the standard deviation is proportional to the signal by the factor ξ, $\sigma_{I_0} = \xi I_0$, $\sigma_{I_1} = \xi I_1$, $\sigma_{I_2} = \xi I_2$. Then the variance in m_1 is

$$\sigma_{A,p}{}^2 = L\left(\frac{\xi}{2.303k}\right)^2 + \left(\frac{\xi(m_1 + m_2)}{2.303km_2}\right)^2 + \left(\frac{\xi m_1}{2.303km_2}\right)^2$$

The relative standard deviation is

$$\%\sigma_{A,p} = \frac{\xi}{2.303km_1}\left(L + \left(\frac{m_1 + m_2}{m}\right)^2 + \left(\frac{m_1}{m_2}\right)^2\right)^{1/2} \times 100\% \quad (26)$$

In terms of A_1 and R

$$\%\sigma_{A,p} = \frac{\xi}{2.303A_1}\left(L + \left(\frac{1 + R}{R}\right)^2 + \left(\frac{1}{R}\right)^2\right)^{1/2} \quad (27)$$

Equation 27 is plotted in Figure 4 for $\xi = 2 \times 10^{-3}$.

DISCUSSION

Aside from the equations which have been presented, there are several noteworthy points concerning the choice of increment size.

(1) When R is significantly less than unity, significant loss of precision results.

(2) The standard subtraction method is quite attractive although care must be taken to assure that R is less than one.

(3) In absorption spectroscopy, the uncertainty will always go through a minimum since the variances from each source are additive.

Although for some techniques, the uncertainty monotonically decreases with R, it is important to note that a large addition may change the solution conditions and consequently the slope of the transfer function (*1*). Consequently the equations developed herein should be used primarily to determine minimum values of R.

ACKNOWLEDGMENT

The author gratefully acknowledges the helpful comments of Arnold M. Hartley of the Institute for Environmental Studies, University of Illinois.

LITERATURE CITED

(1) Robert Klein, Jr., and Clifford Hach, *Am. Lab.*, **9** (7), 21 (1977).
(2) James J. Lingane, "Electroanalytical Chemistry", 2nd ed., Interscience, New York, 1958.
(3) Lester P. Rigdon, Gwilym J. Moody, and Jack W. Frazer, *Anal. Chem.*, **50**, 465 (1978).
(4) Axel Johansson and Sten Johansson, *Analyst (London)*, **103**, 305 (1978).
(5) Christian Stahli, John H. Wharton, and Hans Noll, *Anal. Biochem.*, **86**, 1 (1978).
(6) J. D. Ingle and S. R. Crouch, *Anal. Chem.*, **44**, 1375 (1972).
(7) H. L. Pardue, T. E. Hewitt, and M. J. Milano, *Clin. Chem.* (*Winston-Salem, N.C.*), **24**, 1028 (1974).
(8) K. L. Ratzlaff and D. F. S. Natusch, *Anal. Chem.*, **49**, 2170 (1977).
(9) P. R. Bevington, "Data Reduction and Error Analysis for the Physical Sciences", McGraw Hill, New York, 1969.

RECEIVED for review August 8, 1978. Accepted November 6, 1978.

Fluorescence and X-Ray Photoelectron Spectroscopy Surface Analysis of Metal Oxide Electrodes Chemically Modified with Dansylated Alkylaminesilanes

Henry S. White[1] and Royce W. Murray*

Department of Chemistry, University of North Carolina, Chapel Hill, North Carolina 27514

Dansyl chloride is coupled to an alkylaminesilane bound to a metal oxide electrode surface and the sulfonamide hydrolytically cleaved from the surface. Fluorometric analysis of the hydrolysate sulfonamide concentration assays its surface concentration at 0.5–2 × 10^{-10} mol/cm^2. XPES determination of sulfonamide reaction coupling efficiency yields an average alkylaminesilane coverage of 2.6 × 10^{-10} mol/cm^2. A small amount of coadsorbed dansyl chloride was detected and quantitatively distinguished from sulfonamide hydrolysate using the fluorescence spectrum.

SnO_2 (*1*), RuO_2 (*2*), Pt/PtO (*3*), Si/SiO (*4*), and TiO_2 (*5*) metal oxide electrode surfaces react with and bind chloro- and alkoxysilanes, of which 3-(2-aminoethylamino)propyltrimethoxysilane (en silane) is an example. The bonding is sufficiently stable that surface structure-elaborating procedures such as amide-coupling (*2, 3*) to the immobilized amine group can be carried out to attach electrochemically interesting molecules to the electrode surface. Such synthetic endeavors pose significant sensitivity problems for composition, molecular structure, and dynamical characterization of the chemically modified surface, since the electrode ordinarily is a flat surfaced material of a few cm^2 area, and monolayers of typical molecular substances, as deduced readily from molecular models, amount to only about 10^{-10} mol/cm^2. Spectroscopic methods which have been brought to bear on modified electrode surfaces include X-ray photoelectron spectroscopy (XPES) (*1, 6*), inelastic tunneling electron spectroscopy (*7*), Raman spectroscopy (*8*), and secondary ion mass spectrometry (*9*).

Many fluorescent coupling reagents exhibit sufficient sensitivity for analysis of solution concentrations at the 10^{-7}–10^{-9} M level. This paper selects one of these, dansyl chloride (dansCl) (*10, 11*) to explore the information which can be obtained on surface structure and coverage on silanized metal oxides using the reaction scheme

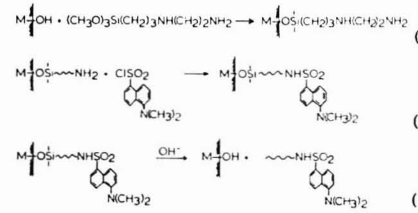
M–OH + (CH3O)3Si(CH2)3NH(CH2)2NH2 → M–OSi(CH2)3NH(CH2)2NH2
M–OSi~~NH2 + ClSO2 → M–OSi~~NHSO2
N(CH3)2
M–OSi~~NHSO2 OH⁻ → M–OH + ~~NHSO2
N(CH3)2

(1)

(2)

(3)

where the fluorescence spectrum of the surface hydrolysate solution from Reaction 3 is measured in a conventional manner, and its intensity is used to assay concentration of cleaved sulfonamide. This strategy is similar to that of Whitesides and co-workers in their studies of polymer surfaces (*12, 13*).

The fluorescence results support the sulfonamide bond formation indicated in Reaction 2, and in concert with complementary XPES experiments, are used to determine absolute coverage of the electrode by bonded alkylaminesilane.

EXPERIMENTAL

Electrodes. Fluoride-doped SnO_2 films on glass (*1*) were sonicated in heptane, water, methanol, and rinsed with water as a standard cleaning procedure. Some specimens for XPES were refluxed in concentrated HCl and heated at 450 °C for several hours to reduce N 1s and S 2p backgrounds. RuO_2 films on titanium metal disks (both sides) were prepared by a $RuCl_3$-butanol spray procedure (*2, 14*). Pt samples for XPES were mirror polished disks (1 μm diamond paste) vacuum dried at 50 °C; those for fluorescence were unpolished flags of geometrical area 1.9–3.4 cm.^{2} Oxide films were deposited by anodization at +1.9 V vs. SCE in 1 N H_2SO_4 after potential cycling had produced a stable oxide–hydrogen wave pattern. The microscopic roughness of the platinum electrodes was estimated at 1.34–1.62 from the charge under the hydrogen waves (*15*). Pt flags were recycled by brief exposure to aqua regia.

Chemicals. 3-(2-Aminoethylamino)propyltrimethoxysilane (en silane) (Petrarch, PCR) was vacuum distilled (ca. 4 Torr, 108 °C) immediately before use. Dansyl chloride (dansCl), 5-dimethylaminonaphthalenesulfonyl chloride (Pierce), was periodically recrystallized (bright orange) from heptane/acetone (*16*) to remove dansic acid contaminant. Pure dansic acid and dansyl sulfonamide (Pierce) were used as received. Benzene and toluene were dried over Na^0, acetonitrile over molecular sieves.

Reactions. *Silanization.* The vacuum oven dried (50 °C) oxide electrode was exposed as in "Method C" (*17*) to a 5% en silane solution in benzene or toluene for 5 min at room temperature (using syringe and serum cap techniques to exclude water), washed 5 times with dry toluene, soaked in water or methanol for about 5 min, and air dried.

Dansylation. Reaction 2 was carried out by exposing the silanized electrode to a ca. 4 × 10^{-3} M dansCl solution in dry acetonitrile plus a few drops of 2,6-lutidene. Reaction times of 20 h at room temperature and 5 h at 50 °C produced indistinguishable fluorescence-measured coverages. The dansylated surface was washed overnight in acetonitrile and then for 1 day in ethanol. Adsorption control reactions, using dansyl chloride with unsilanized surfaces and dansic acid with silanized material, followed the same procedures. Dansylation of surfaces using aqueous alkali solutions (*12*) was unsatisfactory because of XPES-indicated hydrolysis of the silane–electrode bonds.

Surface Hydrolysis. The dansyl sulfonamide was cleaved from Pt and RuO_2 surfaces (Reaction 3) by immersion in 3 mL 0.1 M KOH/ethanol for 2 h. Complete cleavage was ascertained by subsequent XPES observation of Si 2p and S 2p at background levels. For SnO_2, 1.5 mL of 0.1 M KOH/ethanol was confined to a 2.4-cm i.d. circle on dansylated SnO_2 using a glass ring barrier sealed to the SnO_2 with a thin layer of paraffin; after hydrolysis this solution was pipetted off, the surface rinsed with a fresh 1 mL, and the combined solution diluted to the 3.8-mL volume of the fluorescence cell.

Instrumental. XPES spectra were obtained using a DuPont 650B Electron Spectrometer. Fluorescence measurements were

---

[1] Present address, Department of Chemistry, University of Texas, Austin, Texas.

0003-2700/79/0351-0236$01.00/0 © 1979 American Chemical Society

Table I. XPES Results for Dansylated Surfaces and Dansyl Standards

standards	binding energies[a] S 2p, ev	N 1s, ev
dansyl chloride	168.4 ± 0.1	399.5
dansyl sulfonamide	168.5 ± 0.1	399.6
dansic acid	167.8 ± 0.1	402.2
dansylated surfaces		
SnO_2/en/(dansCl)	168.7 ± 0.1[b]	399.7
SnO_2/(dansCl)	~168.9[c]	399.2
SnO_2/en/(dansic acid)	~167.9[c]	399.3

	relative intensities I_N/I_S	atom ratio N/S	coupling efficiency,[f] %
dansyl sulfonamide	1.75[d]	2.00	- - -
SnO_2/en/(dansCl)	5.52, 4.42, 4.06, 3.45 4.10, 5.42, 4.91[e]	6.35, 5.08, 4.69, 3.97, 4.72, 6.23, 5.65, 5.77, 4.70	36, 47, 52, 65, 52, 37, 41 (av 47± 8)
Pt/PtO/en/(dansCl)	5.02, 4.09[e]	5.77, 4.70	40, 52 (av 46 ± 8)

[a] Referenced to C 1s as 285.0 eV. [b] Av of 14 samples. [c] Weak bands, approximate values. [d] For comparison, theoretical $I_N/I_S = 2\sigma_N(1254 - 400)^{0.75}/\sigma_S(1254 - 169)^{0.75} = 1.70$. [e] Corrected for background N 1s (ca. 30%) and S 2p (ca. 20%). [f] After correcting N/S for adsorbed dansCl, calculated from 200/[N/S − 1].

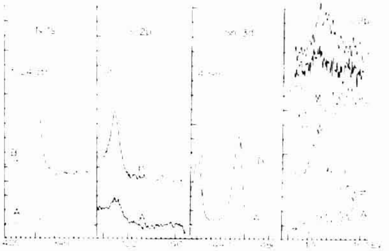

Figure 1. XPES spectra of indicated elements on Curves A: SnO_2; Curves B: SnO_2/en/(dansCl); S 2p XPES on Curve C: Pt/PtO; Curve D: Pt/PtO/(dansCl); Curve E: Pt/PtO/en/(dansCl)

made with a Perkin-Elmer Hitachi MPK-2A spectrometer using an excitation wavelength of 333 nm. Emission and excitation slits settings corresponded to 10-nm bandwidths.

Fluorescence Standards. A molar excess of *N*,*N*-dimethylethylenediamine (0.2 mL) (or en silane or *n*-butylamine) added to 10 mg dansCl in enough dry acetonitrile to make a 10-mL solution gave after 2–3 min of mixing a pale green sulfonamide solution which was then diluted 1/10000 with 0.1 M KOH ethanol. Further dilutions to 3×10^{-8} to 4×10^{-7} concentrations were used to prepare (linear) fluorescence intensity calibrations. Solutions of dansic acid in 0.1 M KOH/ethanol were similarly prepared.

RESULTS AND DISCUSSION

Surface Structure and Coverage. Preliminary XPES experiments were conducted to ascertain suitable conditions for Reaction 2 since the sulfonamide coupling reaction plus possible associated adsorption effects had not been previously studied on alkylaminesilanized surfaces. SnO_2 was used for these experiments for its low N 1s and S 2p background levels. The SnO_2 XPES spectrum after silanization (SnO_2/en surface) displays N 1s and Si 2p bands, and the Sn $3d_{5/2}$ band is reduced to 0.49 ± 0.27 of its original intensity, in line with previous experience (*1*, *17*). Following the dansylation Reaction 2 (conducted as in Experimental), further increase in N 1s is seen as is a new S 2p band at 168.7 eV as shown in Figure 1B. This binding energy is near that (168.5 eV) obtained for authentic dansyl sulfonamide (Table I and Figure 2). Binding energies for S 2p in standard dansyl compounds (Table I) show that sulfonamide is distinguishable from dansic acid but not from dansCl. Thus the XPES data support sulfonamide bond formation but do not cleanly separate it from possible interfering coadsorption of dansCl on the metal oxide surface. This question becomes resolved by the fluorescence measurements as shown below.

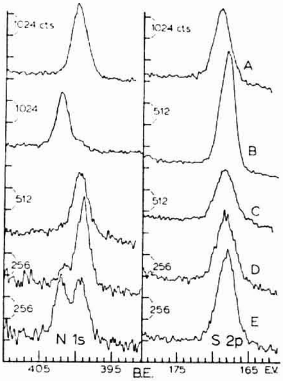

Figure 2. XPES N 1s and S 2p spectra for Curves A: pure dansyl amide; Curves B; pure dansic acid; Curves C: recrystallized dansCl; Curves D: dansCl with ca. 5% dansic acid; Curves E: dansCl with ca. 50% dansic acid

Table II. Fluorescence Sensitivities[a] of Various Dansyl Sulfonamide Models of Dansylated Surface Hydrolysate

	$K_{460} \times 10^{-8}$	$K_{510} \times 10^{-8}$
dansyl chloride + *N*,*N*-dimethylethylenediamine	0.69 ± 0.16	1.52 ± 0.01
dansyl chloride + *n*-butylamine	1.02 ± 0.04	2.56 ± 0.09
dansyl chloride + en silane	1.77 ± 0.64	3.37 ± 0.76
dansic acid	6.20 ± 0.40	2.83 ± 0.09

[a] Measured at 460 and 510 nm and given in arbitrary fluorescence intensity units; used to calculate hydrolysate concentrations from hydrolysate fluorescence with equations:

$I_{460} = K_{460(\mathrm{amide})}[\mathrm{sulfonamide}] + K_{460(\mathrm{acid})}[\mathrm{dansic\ acid}]$

$I_{510} = K_{510(\mathrm{amide})}[\mathrm{sulfonamide}] + K_{510(\mathrm{acid})}[\mathrm{dansic\ acid}]$

The dansyl sulfonamide formed by solution reaction of dansCl and *N*,*N*-dimethylethylenediamine yields in 0.1 M KOH/ethanol a fluorescence emission centered at 510 nm and with intensity permitting measurement at quite low con-

Table III. Surface Coverage Results for Dansylated Surfaces

samples	hydrolysate conc, M[a] dansyl sulfonamide × 10^7	hydrolysate conc, M[a] dansic acid × 10^8	surface coverage × 10^{10} Γ_{amide}[b]	surface coverage × 10^{10} Γ_{dansCl}[b]	surface coverage × 10^{10} Γ_{silane}[d]	$\Gamma_{amide}/\Gamma_{dansCl}$
Pt/PtO/en/dansCl)[c]	2.92	6.9	0.54	0.13	1.2	4.2
(illustrative examples)	1.32	3.4	0.97	0.25	2.1	3.9
	1.53	2.3	1.12	0.17	2.4	6.6
	1.63	1.95	1.20	0.14	2.6	8.6
	1.06	1.3	1.21	0.15	2.6	8.1
	1.92	1.7_5	1.41	0.13	3.0	10.8
	2.81	3.2	2.33	0.26	5.0	9.0
(average of 16 determ.)	--	--	1.21 ± 0.30	0.18 ± 0.05	2.6	6.7 ± 2.0
	(0.36)[e]	(0.9)[e]	(0.28)[e]	(0.07)[e]		(3.9)[e]
RuO_2/en/(dansCl)[f]	3.10	5.0	3.15	0.51	6.6	6.2
	4.25	6.1	4.11	0.59	8.6	7.0
SnO_2/en/(dansCl)[f]	3.11	1.3	3.61	0.11	7.5	32.8
adsorption controls						
Pt/PtO/(dansCl)[c]	--	0.7-1.8	--	$0.07_4 \pm 0.01_6$	--	--
RuO_2/(dansCl)[f]	--	1.9	--	0.18	--	--
Pt/PtO/en/(dansic acid)	--	0.2-1.2	--	$0.04_3 \pm 0.03_6$	--	--

[a] Concentrations in hydrolysate of dansylated as determined by two-component fluorescence analysis. [b] Calculated from hydrolysate concentration and volume (2-3.8 mL), and electrode area (1.9-3.4 cm^2). [c] Surface coverages on Pt include roughness correction factor (1.34-1.62) as measured with hydrogen adsorption waves. [d] Calculated from $\Gamma_{amide}/0.47$ where 0.47 is XPES estimated sulfonamide coupling yield. [e] Sample washed 20 h in 60 °C EtOH before hydrolysis. [f] Surface roughness not accounted for, geometrical electrode area used in coverage calculation.

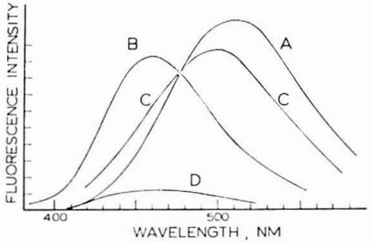

Figure 3. Background corrected fluorescence spectra for Curve A: 3.1 × 10^{-7} M dansyl sulfonamide derivative of *N*,*N*-dimethylethylenediamine; Curve B: 5.9 × 10^{-8} M dansic acid; Curve C: 2.0 × 10^{-7} M dansyl sulfonamide plus 2.4 × 10^{-8} M dansic acid, surface hydrolysate of Pt/PtO/en/(dansCl) on which Γ_{amide} = 1.09 × 10^{-10} mol/cm^2 and Γ_{dansCl} = 1.3 × 10^{-11} mol/cm^2; Curve D: 7 × 10^{-9} M dansic acid surface hydrolysate of adsorption control Pt/PtO/dansCl) on which Γ_{dansCl} = 6 × 10^{-12} mol/cm^2

centration (Figure 3A and Table II). Dansic acid is readily distinguished from the sulfonamide by an even more intense fluorescence at 460 nm (Figure 3B). The sulfonamide is stable toward base hydrolysis (spectrum unchanged after one day), whereas dansCl is quickly hydrolyzed and appears as dansic acid at 460 nm (*10*).

Figure 4 shows the fluorescence spectrum of hydrolysate Reaction 3) of a dansylated Pt/PtO/en surface. The fluorescence spectrum is readily measured above background. The background-corrected spectra (Figure 4C, D, E) for hydrolysate from RuO_2/en/(dansCl), SnO_2/en/(dansCl) and Pt/PtO/en/(dansCl) surfaces are similar to one another, and comparison of the Pt/PtO/en/(dansCl) hydrolysate spectrum to that of standards in Figure 3 shows that it is similar to the sulfonamide emission. Since a predominance in Reaction 2 of adsorbed dansCl would yield dansic acid emission at 460 nm, the Figure 3 comparison shows that most of the material in the surface hydrolysate must originate from bonded sulfonamide. The surface hydrolysate band maximum is, however, slightly shifted, to an intermediate 500-nm wavelength, and Figure 3C shows "extra" intensity at 460 nm in the hydrolysate spectrum. Admixture of a small amount of dansic acid to a solution of the sulfonamide standard produces a very similar spectrum. These results indicate that sulfonamide bond formation in Reaction 2 is accompanied by some coadsorption of dansCl.

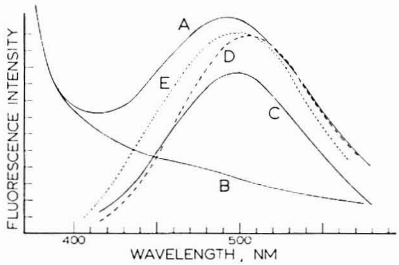

Figure 4. Fluorescence spectra. Curve A: surface hydrolysate of Pt/PtO/en/(dansCl); Curve B: background curve (solvent) for Curve A; Curve C: difference spectrum between Curves A and B; Curve D: background corrected surface hydrolysate of SnO_2/en/(dansCl); Curve E: for RuO/en/(dansCl)

Emission from dansic acid overlaps with that of the sulfonamide at 510 nm, as is evident from Figure 3. Consequently the surface hydrolysate spectra were analyzed, at 460 and 510 nm, as two-component mixtures of dansic acid and dansyl sulfonamide using standards as in Table II. Hydrolysate concentrations thus determined for the three electrode materials are given in Table III. The coadsorbed dansCl averages about 10% of the total on Pt/PtO/en, which was the most carefully studied. The fluorescence analysis is successful in determining from 1 × 10^{-10} to 1 × 10^{-9} mol of surface bonded dansyl sulfonamide and from 2 × 10^{-11} to 2 × 10^{-10} mol of coadsorbed dansCl, in absolute quantities.

Further and confirming data on dansCl adsorption was obtained by exposing Pt/PtO surfaces to dansCl. The hydrolysate from these surfaces exhibits a weak emission at 460 nm as shown in Figure 3D which when converted to concentration (Table III) is within a factor of two of that measured as dansCl coadsorbed with bonded sulfonamide on Pt/PtO/en/(dansCl) surfaces. Exposure of Pt/PtO/en surfaces to dansic acid yields a weak 460-nm emission so dansic acid also adsorbs. In parallel XPES adsorption tests on SnO_2 exposed to dansCl and SnO_2/en exposed to dansic acid, weak S 2p bands appear. Table I includes their estimated binding energies, which are insufficiently accurate to determine whether dansCl adsorbs as the acid chloride or as a sulfonate. The fluorescence results supplemented by XPES afford a satisfactory analysis of the sulfonamide binding vs. adsorption question, showing that the latter exists but in small proportions.

The surface coverage of bonded sulfonamide and coadsorbed dansCl on the dansylated electrode surfaces can be calculated from the hydrolysate concentrations of sulfonamide and dansic acid, respectively, using the hydrolysate solution volume and electrode area. Results are shown in Table III. On Pt, a microscopic roughness correction ranging from 1.3–1.6 was determined from the hydrogen adsorption waves observed in 1 N H_2SO_4 and is incorporated in the coverage results. Microscopic roughness of SnO_2 and RuO_2 surfaces is unknown and geometric areas were used. On Pt/PtO/en and RuO_2/en surfaces the coverage of coadsorbed dansCl, Γ_{dansCl}, is more or less constant.

The coverage by bonded sulfonamide, Γ_{amide}, is somewhat variable from sample to sample, probably due to variations in coupling efficiency in Reaction 2.

The choice of *N,N*-dimethylethylenediamine for preparation of the sulfonamide fluorescence intensity standard deserves comment. Reaction of dansCl with a solution of en silane or of *n*-butylamine yields very similar fluorescence spectra also centered at 510 nm but, as shown in Table II, the fluorescence intensity among the three amines differs by a factor of slightly more than two. Since previous data (*6*) have indicated that it is primarily the terminal amine site of surface-bonded en silane which is reactive in amide coupling reactions, the solution form of the en silane, with two active amine sites, is thought to be a less accurate model compound of the silanized surface than the *N,N*-dimethylethylenediamine. Fluorescence intensities for dansylated en silane solutions were also poorly reproducible. Nonetheless it is seen that the requirement of choosing a sensitivity-standardizing compound which accurately mimics coupling chemistry on the electrode surface introduces some level of uncertainty into the absolute values of fluorescence-measured surface coverages.

Determination of en Silane Surface Coverage, Γ_{silane}. Surface coverage (Γ_{amide}) achieved in the dansylation reaction can be converted to the overall Γ_{silane} resulting from the silanization step Reaction 1 if the dansylation Reaction 2 reaction yield, or coupling efficiency, is measured. Coupling efficiencies in surface modification reactions can be measured using XPES tag element relative intensities (*6*). On a dansylated surface, the relative intensities of sulfonamide S 2p and overlapping [en silane (two nitrogens) + dansyl nitrogen] N 1s measure reaction coupling efficiency. Conversion of I_N/I_S data to N/S atom ratios was effected by an elemental sensitivity calibration with authentic dansyl amide (Table I). The atom ratio was corrected for coadsorbed dansCl (Γ_{dansCl}) using the average (ca. 90%) proportion of sulfonamide bonded surface dansyl species measured fluorometrically. Reaction 2 coupling efficiencies given in Table I are calculated on the basis of one active site for coupling per en silane moiety (*6*).

Coupling efficiencies in Table I show some variation from preparation to preparation with an average efficiency on both Pt/PtO/en and SnO_2/en of ca. 50%. Combination of the average coupling efficiency percentage with Γ_{amide} data gives Γ_{silane} values presented in Table III. Γ_{silane} evaluated in this way averages 2.6×10^{-10} mol/cm^2 with outlying samples differing from this by a factor of about two. These results for Γ_{silane} are consistent with estimates from molecular models of en silane (these give ca. 7×10^{-10} mol/cm^2, extended perpendicular to the surface, and ca. 3×10^{-10} mol/cm^2 in lying-flat or cyclized (*6*) form), with other experimental determinations of Γ_{silane} by XPES (*1, 17*) and with combinations of XPES coupling yields with electrochemically determined coverages of a coupled redox moiety (*2, 18, 19*). Γ_{silane} on RuO_2/en (*2*) for example is 3–5 $\times 10^{-10}$ mol/cm^2 (no roughness correction) by the latter approach, and Γ_{silane} on Pt/PtO/en = 4–8 $\times 10^{-10}$ mol/cm^2 with roughness correction (*18*).

On a quantitative level, the results for Γ_{amide} and Γ_{silane} place the fluorescence technique on a competitive basis for surface coverage determinations with previous spectroscopic and electrochemical approaches. The surface coverage sensitivity limit for the dansCl reagent is ca. 5×10^{-12} mol/cm^2, which favorably compares with electrochemical sensitivities for surface waves. A considerable amount of surface structural information is accessible from the fluorescence experiment as well. Application of other available fluorescence reagents should be fruitful for understanding chemical and population details of chemically modified materials.

Dansyl Chloride Reagent Purity by XPES. The coadsorption of dansic acid and the interference of this hydrolysis product of dansCl with fluorescence sensitivity calibrations make regular recrystallization of the dansCl reagent essential. Interestingly, XPES of pure dansic acid (Figure 2) shows a much sharper distinction, from dansCl, in the N 1s band than by S 2p. Its 402.2-eV N 1s binding energy corresponds to protonated aromatic amine; from this and the known acidity of sulfonic acids, we see that dansic acid exists as a zwitterion in the solid state. The 402.2-eV N 1s band can be used to detect partial hydrolysis of dansCl reagent, as shown in Figure 2D for a ca. 50% contaminated sample and for a (freshly commercially procured) ca. 5% contaminated sample. The contamination detected is roughly representative of the bulk contamination since a fluorescence analysis is consistent with the XPES results.

LITERATURE CITED

(1) P. R. Moses, L. Wier, and R. W. Murray, *Anal. Chem.*, **47**, 1882 (1975).
(2) P. R. Moses and R. W. Murray, *J. Electroanal. Chem.*, **77**, 393 (1977).
(3) J. R. Lenhard and R. W. Murray, *J. Electroanal. Chem.*, **78**, 195 (1977).
(4) M. S. Wrighton, R. C. Austin, A. B. Bocarsly, J. M. Bolts, O. Haas, K. D. Legg, L. Nadjo, and M. C. Palazzutto, *J. Am. Chem. Soc.*, **100**, 1602 (1978).
(5) P. R. Moses and R. W. Murray, *J. Am. Chem. Soc.*, **98**, 7435 (1976).
(6) P. R. Moses, L. M. Wier, J. C. Lennox, H. O. Finklea, J. R. Lenhard, and R. W. Murray, *Anal. Chem.*, **50**, 576 (1978).
(7) A. F. Diaz, V. Hetzler, and E. Kay, *J. Am. Chem. Soc.*, **99**, 6780 (1977).
(8) V. S. Srinivasan and W. J. Lamb, *Anal. Chem.*, **49**, 1639 (1977).
(9) J. F. Evans, Symposium on Silylated Surfaces, Midland, Mich., May 1978.
(10) C. Gros and B. Labouesse, *Eur. J. Biochem.*, **7**, 463 (1969).
(11) J. P. Zarretta, G. Vincendon, P. Mandel, and G. Gombos, *J. Chromatogr.*, **51**, 441 (1970).
(12) J. R. Rasmussen, E. R. Stedronsky, and G. M. Whitesides, *J. Am. Chem. Soc.*, **99**, 4736 (1977).
(13) J. R. Rasmussen, D. E. Borgbreiter, and G. M. Whitesides, *J. Am. Chem. Soc.*, **99**, 4746 (1977).
(14) D. R. Rolison, K. Kuo, M Umana, D. Brundage, and R. W. Murray, *J. Electrochem. Soc.*, in press.
(15) T. Biegler, D. A. J. Rand, and R. Woods, *J. Electroanal. Chem.*, **29**, 269 (1971).
(16) R. F. Chen, *Anal. Biochem.*, **25**, 412 (1968).
(17) D. F. Untereker, J. C. Lennox, L. M. Wier, P. R. Moses, and R. W. Murray, *J. Electroanal. Chem.*, **81**, 309 (1977).
(18) J. R. Lenhard and R. W. Murray, *J. Am. Chem. Soc.*, in press.
(19) D. F. Smith, K. William, K. Kuo, and R. W. Murray, *J. Electroanal. Chem.*, in press.

RECEIVED for review September 11, 1978. Accepted November 9, 1978. This research was supported in part by a grant from the National Science Foundation. This paper is number XVIII in a series on chemically modified electrodes.

Pulse (Photon) Counting: Determination of Optimum Measurement System Parameters

E. J. Darland, G. E. Leroi, and C. G. Enke*

Department of Chemistry, Michigan State University, East Lansing, Michigan 48824

Linearity measurements and integral pulse height distributions have been used to evaluate the effects of electron multiplier voltage and discriminator coefficient (A_d) on the stability, sensitivity, and dynamic range of three pulse counting measurement systems. The data show that selection of the highest possible voltage has significant advantages for most experiments, but that the choice of an "optimum" value for A_d depends on the requirements of the particular experiment and requires careful evaluation of the trade-offs among stability, sensitivity, and dynamic range. Semiquantitative evaluation of these trade-offs on the basis of the experimental results is illustrated. The data also show clearly that measurements such as those reported here must be made on each system, since specific results for one system cannot be generalized to others.

Electron multipliers are widely used as particle flux transducers, whether incorporated into a photomultiplier (PMT) for measuring photon flux, or used "bare" for detecting ions, electrons, or vacuum ultraviolet photons. The particle flux can be determined either by measuring the average direct current output of the electron multiplier (the "dc" method) or by counting the individual charge pulses (*1*). The latter technique is often referred to as "photon counting", but the more general term "pulse counting" will be used throughout this paper.

When a pulse counting system is to be used for analytical measurements, several characteristics of the transfer function which relates measured count rate to incident particle flux may be important. Ideally, the transfer function would be a straight line (good linearity) which extends from zero to infinity (infinite dynamic range), would have a slope of one (high sensitivity), and would be invariant with time, temperature, etc. (high stability and freedom from noise).

Because of limitations inherent in the components of any real pulse counting system, such an ideal transfer function is unattainable. The extent to which the ideal is approached in practice is influenced not only by the limitations of the pulse counting system components, but also by the operating parameters of the system. For example, the accuracy with which a pulse counting measurement can be made is limited at high count rates primarily by pulse overlap counting losses (i.e., by nonlinearity of the transfer function). The percentage of pulses lost at a given count rate depends not only on the speed of the counter, the pulse arrival time distributions, and the pulse shape distributions (both amplitude and width) from the electron multiplier, but also on the discriminator coefficient, A_d (defined as the fraction of the pulses passed by the discriminator) (*1*, *2*). Thus, the user can adjust A_d to optimize the linearity of the system. Unfortunately, A_d also influences the sensitivity and stability of the pulse counting system in such a way that optimum linearity often results in less-than-optimum stability and sensitivity (*1*). Since the relative importance of linearity, stability, and sensitivity will vary depending on the type of experiment, there is unlikely to be a universally optimum setting for A_d. Instead, the "optimum" setting of this and other measurement system parameters must be selected while keeping in mind the particular experimental conditions likely to be encountered. The relationships between the measurement system parameters and the desired transfer function characteristics cannot be predicted in advance, since they depend on the characteristics of the individual electron multiplier, the multiplier power supply, component temperatures, component history, and so on. A careful selection of the parameters for the "optimum" operation of any pulse counting system will require an effective determination of the system characteristics.

In this paper, we present the results of pulse height distribution and linearity measurements made on several different pulse counting systems. Although these measurements do not provide a complete characterization of these systems, they do allow many of the trade-offs involved in selecting operating parameters to be evaluated on at least a semiquantitative basis. These examples illustrate the importance of such characterizations in making sound selections of the operating parameters.

EXPERIMENTAL

Equipment. Three different electron multipliers were used in these studies, an RCA 8850 PMT, an RCA 1P28 PMT, and a Johnston MM1 electron multiplier. The 8850 was mounted in a thermoelectrically cooled housing and powered with a Hewlett-Packard 6110A power supply. The 1P28 was housed in a Heath (now GCA-McPherson) EU-701-30 photomultiplier module, and used the integral power supply of that module. The MM1 was used as the ion transducer in a photoionization mass spectrometer (*3*) and was powered with a Power Designs 1543A power supply. All of the measurements reported here were made with the electron multipliers at room temperature.

The photon source used with the 8850 and 1P28 was made up of Heath (GCA/McPherson) 700 series components. The radiation from a tungsten lamp in an EU-701-50 light source module was dispersed by a model EU-700 monochromator. The monochromator slit width was used to control the photon flux. The MM1 detected a beam of Ar^+ ions which had an intensity determined by the Ar sample pressure in the ion source region of the mass spectrometer. For the linearity studies performed on the 8850 and 1P28 systems, a model EU-721-11 alternating cell module was inserted between the monochromator and PMT housing. This module contained a neutral density filter which was in the light beam whenever the sample cell carriage was in the sample position, but out of the beam in the reference position. The carriage position could be controlled by a computer. The shutter of the sample cell compartment was connected to a small solenoid so that it also could be computer controlled. All count rate data were acquired (under computer control) with an integrated-circuit based, dc-coupled pulse counter that has high sensitivity (130 μV) and a pulse pair resolution of ~11 ns. This pulse counter is described in detail in a companion paper (*4*).

Pulse Height Distributions. Relative integral pulse height distributions were measured for all three pulse counting systems by measuring the dark count rate and the light count rate (dark counts subtracted) at a constant photon or ion flux as a function of the pulse counter discriminator level. These measurements were made at a sufficiently low count rate that negligible pulse overlap errors occurred. Thus, a plot of count rate vs. discriminator level is proportional to the integral pulse height distribution.

0003-2700/79/0351-0240$01.00/0 © 1979 American Chemical Society

Linearity Measurements. The linearity studies reported here were performed using a method similar to that described by Heroux (5). The apparent transmittance of a neutral density filter was measured with the pulse counting apparatus as a function of light intensity. It is useful to define the following terms:

I_0	photon flux on the PMT without the filter, quanta s^{-1}
I	photon flux on the PMT with the filter, quanta s^{-1}
T	the actual transmittance of the filter, I/I_0, dimensionless
N_0	measured count rate without the filter, counts s^{-1}
N	measured count rate with the filter, counts s^{-1}
T'	the apparent transmittance of the filter, N/N_0, dimensionless.

From these definitions, it can be seen that while T is independent of light intensity, T' will be independent of light intensity (and equal to T) only when pulse overlap counting losses do not occur in the measurement of N and N_0. When such losses do occur, they will affect N_0 more than N, and T' will deviate from T by an amount which is indicative of the amount of dead time loss or pulse overlap gain in the measurement of N_0.

This method of analyzing the data assumes that pulse overlap loss in the measurement of N is small. Providing that T is small, this will be a good assumption, except perhaps at the very highest photon fluxes used. In any case, the data can be used to check the validity of the assumption, and to correct the results to any desired accuracy if the assumption turns out not to be "valid enough". The linearity of a pulse counting system can therefore be determined even when no other type of system is available for comparison measurements (such as an accurate dc measurement system). Furthermore, this method avoids the not-insignificant difficulty of ascertaining the accuracy and linearity of an analog dc system over many orders of magnitude.

A reasonable test of the linearity of a pulse counting system is to measure the count rate at which 1.0% of the counts are lost because of pulse overlap. In order to do so, the transmittance of the filter (about 0.013) must be known to an accuracy considerably better than 1.0% of its value, i.e., to better than ±0.0001. Since none of the analog spectrometers available were capable of this accuracy, the transmittance of the filter was measured with the photon counting system at very low light levels (about 10000 photons/s), where pulse overlap in the measurement of N_0 is certain to be negligible. However, the value of N then had to be measured at count rates of only 130 photons/s, which is comparable to the dark count rate for the 8850. Precise measurement of such low light intensities, especially in the presence of 1% light source instability, demanded the use of a synchronous measurement procedure similar to that of Arecchi et al. (6). Rather than measure N for sufficient time to accumulate a statistically significant number of counts and then measure N_0, both N and N_0 (as well as the dark count, D) were measured in rotation for periods of time (a few seconds each) much shorter than the period of the light source drift. The short integrations could be accumulated to produce an effective integration time of any desired duration. Errors caused by light source drift were found to be negligibly small with the above procedure, which was automated and controlled by a computer. After about 24 h of integration at low light levels, the value of T for the filter was determined to be 0.01304 ± 0.00004. This is an accuracy of ±0.3%, and thus the count rate for errors of 0.5% or greater could readily be determined.

RESULTS AND DISCUSSION

Pulse Height Distributions. In any real pulse counting system, there are several potential sources of instability. Any change in the discriminator setting relative to the mean pulse height at the discriminator input (or vice versa) may cause a variation in the measured count rate. Such a change may occur as a result of a change in the operating voltage or gain of the electron multiplier, in the gain of the preamplifier, or in the discriminator setting itself. These types of instability are the main sources of "excess noise" in the system (1).

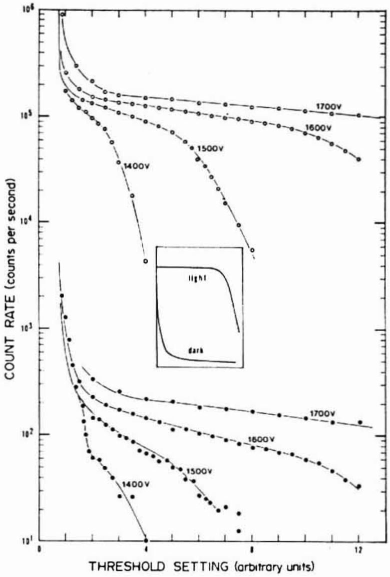

Figure 1. Integral pulse height distributions for the 8850 system at various PMT voltages. The open circles are light counts; the filled circles are dark counts. The inset shows the shape of "ideal" light and dark pulse height distributions

One of the advantages traditionally ascribed to pulse counting (as opposed to dc) measurements, however, is superior long-term stability (1, 7), which is especially important in low flux experiments. The reason usually stated to explain this stability is that it is possible to set the discriminator low enough that all "signal" pulses (those pulses originating at the first dynode of an electron multiplier or at the photocathode of a photomultiplier) have more than enough amplitude to be counted, while at the same time all of the (much smaller) "noise" pulses (those pulses originating at other dynodes or from other sources) are rejected. When this is the case (as it often is when bare electron multipliers are used at very high gains to detect electrons or high-energy ions), small fluctuations in the discriminator setting or mean pulse height will have no effect on the measured count rate, so that excess noise is usually assumed to be negligible compared to more fundamental noise such as quantum noise and signal and background flicker noise (1). Thus, the traditional "rule of thumb" in pulse counting is that the best stability is obtained when all the pulses are counted (i.e., when $A_d \simeq 1$), which is equivalent to operating on the "counting plateau" or on the horizontal portion of the integral pulse height distribution (see the "ideal" pulse height distribution in the inset of Figure 1). At the same time, counting all pulses ensures the best possible signal-to-noise ratio when shot noise is the main noise source (8). However, not all systems exhibit such ideal pulse height distributions. For example, pulse height distributions for the 8850 system at several different PMT voltages are shown in Figure 1. These data reveal a "plateau region" which is *not* flat, although it has a very shallow slope at higher voltages. Similar behavior for an RCA 8853 (a variant of the 8850) has been interpreted (9) as showing that there are very small signal pulses which are not counted at even the highest PMT voltage. The data of reference 9 were obtained with much higher PMT voltages than those used here, but with a much less sensitive pulse counter which had a fixed, 100-mV threshold. The data of Figure 1 do show a large number of noise pulses at the

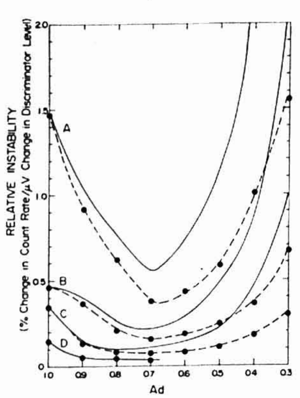

Figure 2. Relative light count instability of the 8850 system. The dashed lines are the unweighted curves, the solid lines are curves weighted by $1/A_d$ (see text). Curves A, B, C, and D were obtained at 1400, 1500, 1600, and 1700 V, respectively. Weighted and unweighted curves at 1700 V are virtually indistinguishable when plotted to this scale

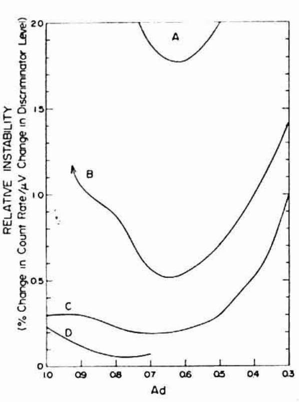

Figure 3. Relative dark count instability of the 8850 system. Only the weighted curves are shown. Curves A, B, C, and D were obtained at 1400, 1500, 1600, and 1700 V, respectively

lowest discriminator setting. However, since the "plateaus" observed in Figure 1 extrapolate to the same count rate (170 kHz) at all voltages, it is assumed that the extrapolated count rate represents "all the signal pulses". Therefore, this particular pulse counting system does have sufficient sensitivity to count virtually all of the pulses for PMT voltages above about 1500 V (half the recommended maximum of 3000 V). Rather than indicating a lack of sensitivity, these pulse height distributions indicate a fairly wide region of overlap between noise and signal pulses, with the smallest signal pulses being smaller than the larger noise pulses.

From a practical viewpoint, it is perhaps less important to understand the exact reasons for the shape of the pulse height distributions than to realize that a measured distribution can provide a great deal of information about the "best" operating parameters. For instance, since there is no portion of the pulse height distribution for the 8850 system which is completely horizontal, the excess noise contributed by discriminator instability, etc., may *not* be negligible, especially in experiments where long integration times are used (*4*). It is therefore important to evaluate the susceptibility of the pulse counting system toward such sources of drift for various operating conditions. This can be done by measuring the change in observed count rate for a unit change in either the mean pulse height or discriminator setting. The latter measure of "relative instability" is particularly convenient to use, since it is merely the slope of the integral pulse height distribution. It is important to note that relative instabilities measured in this way can be used to compare the susceptibility of a particular system to excess noise under different operating conditions, but that they cannot be used to compare different systems. This is because the actual change in measured count rate due to excess noise depends both on the susceptibility of the system and on the actual magnitude of drift in discriminator setting, amplifier and electron multiplier gain, and so forth.

The relative instability of the 8850 system (as measured from the light count pulse height distribution in Figure 1) is shown as a function of A_d in Figure 2 (dashed lines). These data show that in this case the best stability is not obtained at $A_d = 1$, but rather at $A_d \approx 0.6$–0.7, depending on the voltage. Unfortunately, at these lower discriminator coefficients, a large fraction of the signal pulses are lost (the slope of the transfer function is lower) so that longer integration times are required for a comparable signal-to-shot noise ratio. Therefore, these data should actually be weighted so as to show the changed susceptibility of the system to low frequency noise, due to the longer experiment duration, or decreased "noise equivalent bandwidth" (*1*). To do so accurately would require a detailed knowledge of the frequency distribution of the excess noise in the systems, which is difficult to measure. However, for low-flux experiments in which long integration times are used, high frequencies are averaged out quite well, and only low frequency ($1/f$) noise is much of a problem—the longer the integration time, the worse the drift problem. To illustrate the effect on the instability vs. A_d plots, the solid lines in Figure 2 show the same data as the dashed lines, but weighted by the relative integration time needed to reach a standard number of counts (i.e., by $1/A_d$). The point of best stability is indeed shifted toward higher values of A_d, but not very far. Similarly weighted dark count relative instabilities are shown in Figure 3.

The instability data of Figures 2 and 3 show not only that the best stability is obtained at values of A_d significantly less than 1, but also that operating at the highest PMT voltages has several advantages. Stability is better at higher voltages, and the slopes of the instability curves of Figures 2 and 3 are more gradual in the region of best stability. Thus, at the higher voltages, one could choose any A_d over a fairly wide range (e.g., to adjust for best linearity) without sacrificing too much stability. Furthermore, as seen from Figure 1, the counting "plateau" is broader at higher voltages (the change in A_d for a unit change in absolute discriminator level is lower) so that it is easier to adjust the discriminator to the desired A_d.

The data in Figure 1 also show that at equivalent light count rates (i.e., at equivalent A_d), there is a slightly higher dark count rate at the higher operating voltages. Thus, if one were to make measurements without background subtraction, a lower voltage would give a slightly wider dynamic range, since the dark count rate would determine the lower end of the dynamic range. However, if one does use some method of background subtraction, the lower end of the dynamic range can be well below the dark count rate (*10*). Then the important consideration is the amount of time which must be devoted to the measurement of the background. If the system is very stable, the background needs to be measured only once, just long enough to obtain the desired signal-to-noise ratio in the background measurement. If the system is not so stable, or if there is too much excess noise, then a synchronous

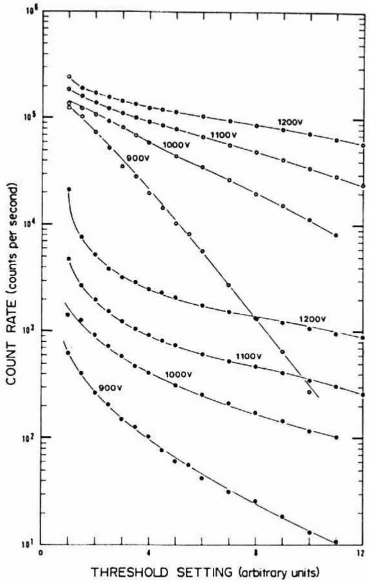

Figure 4. Integral pulse height distributions for the 1P28 system at various PMT voltages. The open circles are light counts; the filled circles are dark counts

demodulation technique must be used (*10*), and up to 50% of the time must be spent measuring the background count rate. The data of Figure 3 show that the excess noise in the dark count measurement associated with instability of the pulse counting system can be dramatically reduced by operating at higher voltages. This reduction in drift will far more than compensate for the slightly increased dark count rate. (Note that the dark count rate could be reduced considerably by cooling the PMT; whether the dark count rate and instability of a cooled PMT would behave the same as that of the room temperature PMT would have to be determined experimentally.)

Pulse height distributions for the 1P28 system, shown in Figure 4, contrast sharply with those of the 8850 system. There are again no noticeable plateaus at any voltage; even at the voltages indicated in Figure 4, which are near the maximum rating for the 1P28, stability is worse than for the 8850 system at voltages well below the recommended maximum for that PMT. Furthermore, the dark counts exhibited by the 1P28 system are higher than for the 8850 system, and the increase in dark count rate as a function of PMT voltage is more dramatic. Relative instabilities of the 1P28 system show roughly the same trends as those of the 8850 system, and are not shown here.

The behavior of the pulse height distributions for the MM1 system (not shown) is quite different from that of the 8850 and 1P28 systems. Changing the voltage not only alters the slope of the pulse height distribution (as in the 8850 and 1P28 systems), but also alters its relative shape—there is no plateau at lower voltages, but at higher voltages a plateau is quite evident. The reason is probably that as the voltage on the MM1 is increased, not only is the gain of the electron multiplier increased, but so is the energy of the ions striking the first dynode, which is known to have a marked effect on the secondary electron emission coefficients and pulse height distributions (*11*, *12*). Although at the highest voltage used (4700 V) the plateau was not quite flat, it is quite possible that higher ion impact energies would result in a nearly-ideal pulse height distribution, in which case the traditional rule of setting $A_d \simeq 1$ would be quite valid.

It should be emphasized that we do *not* claim that the characteristics observed in these systems are necessarily typical of the multiplier types employed. There is a great deal of variability in the behavior of different samples of the same type of multiplier, and the housing, power supply, pulse counter, and wiring details can drastically affect the performance of a given pulse counting system. Thus, any conclusions drawn here are expected to be valid only for the specific systems described. In fact, the most important point is not that the 1P28 system seems less suited to pulse counting than the 8850 system, or that even the 8850 system did not exhibit ideal behavior, but rather that the pulse height distributions must be measured to establish the actual behavior of a given system, and, once measured, they provide a great deal of information about the parameters affecting the relative stability of that system.

Linearity Studies. Pulse counting will always be limited at high particle fluxes by the inevitable count loss due to pulse overlap, either in the pulse counter electronics or in the electron multiplier itself. Thus, at very high particle fluxes, the dc method will be needed (*1*). However, if a dc system with high sensitivity and stability is not available, or if it is inconvenient to switch between pulse counting and dc techniques, it may be useful to extend the upper range of the pulse counting system as far as possible. For any given counter, this may be done in either of two ways: by employing some sort of "dead time compensation" (DTC) to make the system linear to higher count rates, or by employing appropriate count loss corrections (CLC) to the measured data to correct for the known nonlinearity of the system.

The CLC method has been discussed recently by Hayes et al. (*13*, *14*), who find that the amount of count loss can be regarded as being controlled by an "effective deadtime", which can be far different from the pulse pair resolution of the counter, and which is affected by the discriminator coefficient. The basic approach used by Hayes et al. is to measure the pulse counting system transfer function and to fit this function to an appropriate count loss equation which includes the effective deadtime as a parameter. The effective deadtime so measured can be used in the same equation to correct later measurements made on the same system, which extends the effective accurate dynamic range of the system to the point at which the assumptions made in deriving the count loss formula are no longer sufficiently valid. When employing the CLC technique, it is found that the uncertainty in the measured effective deadtime becomes an important factor in limiting the precision at high count rates. In fact, at high count rates, better precision is obtained in a shorter time by intentionally *reducing* the particle flux, so that beyond some point dc techniques remain clearly superior (*13*).

There are several methods of including some sort of automatic correction for pulse overlap loss in pulse counters. In counters which have a single discriminator, this can best be accomplished by setting the discriminator so as to exclude some of the pulses at low count rates. At higher count rates, some of the excluded pulses will overlap and become large enough to be detected. It was first suggested by Smit and Alkemade (*15*) that if this "pulse overlap gain" could be adjusted to counterbalance the pulse overlap loss of larger pulses, enhanced linearity should result. A practical demonstration of the technique was first described by Ash and Piepmeier (*2*), who named the technique "deadtime compensation". Both Ash and Piepmeier (*2*), and later Ingle

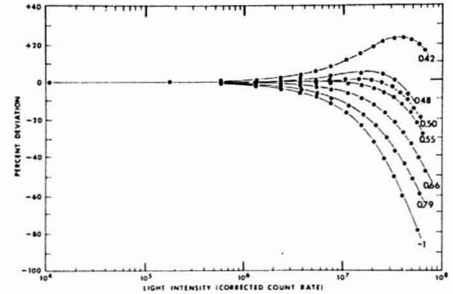

Figure 5. Linearity deviations of the 8850 system for various discriminator coefficients. The PMT was operated at 1500 V for these measurements

and Crouch (*1, 8*), showed that the discriminator coefficient for "optimum" DTC should be about 0.5, although the precise value depends somewhat on the individual measurement systems.

Figure 5 shows the results of the linearity studies performed on the 8850 system at several discriminator settings (and at 1500 V). Results for the 1P28 system are similar and are not shown; no linearity studies have yet been performed on the MM1 system, which is used for very low flux experiments. This figure is a plot of the deviation from linearity vs. light intensity, which shows pulse overlap losses (and gains) much more clearly than the conventional plot of count rate vs. light intensity. The ordinate is the percent deviation from the correct count rate, calculated as

$$\text{percent deviation} = ((T/T') - 1)(100)$$

so that -50 corresponds to loss of half the pulses due to pulse overlap. The corrected count rate used as a measure of light intensity for the abscissa of Figure 5 is essentially the count rate that would be obtained for N_0 if there were no pulse overlap gain or loss, and the discriminator coefficient were 1.0. Its calculation requires knowledge of the actual discriminator coefficient which is measured from the pulse height distribution of Figure 1. The corrected count rates were then determined from N and the known value of T as

$$\text{corrected count rate} = N/((T)(A_d))$$

The count rates at which various amounts of pulse overlap loss occurred for different discriminator settings are summarized in Table I. These results can be used to establish the upper limit of the dynamic range of the system for a given accuracy. An accuracy exceeding ±0.5% is obtained at all count rates up to 200 kHz for all discriminator settings. The linearity is even better at values of A_d less than 1.0. For instance, at $A_d = 0.5$, the linear range is more than two orders of magnitude higher than with $A_d = 1.0$, which demonstrates clearly the effectiveness of deadtime compensation. The corrected count rate of 24 MHz corresponds to a measured count rate of 12 MHz, and a measured photocurrent of 3×10^{-6} A. While this current is still below the upper limit of linearity for dc measurements (which can be extended to even higher light intensities by lowering the photomultiplier voltage), it is nonetheless a significant gain in the upper range of the pulse counting system.

The increased linearity obtained with DTC comes at a price, however. Since a large fraction of the pulses are thrown away to begin with, the signal-to-noise ratio of the measurement will be lower for a given integration time. This can be compensated for if it is possible to integrate for longer periods, but that may not be possible since the stability of the system is decreased under optimum DTC conditions, as shown in Figure 2. In this particular case, the stability is worse by a factor of 2 compared with the optimum; at higher operating voltages, the decrease in stability would not be as great. However, for systems which exhibit a flatter counting plateau, the loss of stability could be much worse. A final criticism of DTC (which applies also to CLC) is that its use requires that linearity measurements be performed in order to select the discriminator setting. This is not a very severe drawback, however, since the linearity should properly be checked whether or not one plans to use either DTC or CLC. Furthermore, the time to make such measurements is not as great as it might first appear. Once the transmittance of the neutral density filter has been measured, only measurements at high light fluxes are required, and since they can be made quickly with good precision, finding the optimum A_d will typically require less than an hour for a new system.

Table I. Limits of Linearity for Different Discriminator Coefficients

discriminator coefficient, A_d	upper limit of corrected count rate for indicated degree of linearity, MHz				
	±0.5%	±1%	±2%	±5%	±10%
~1	0.20	0.50	1.1	3.3	≈6.0
0.79	0.40	0.72	1.4	4.2	8.0
0.66	1.1	1.8	3.3	9.0	14.0
0.55	3.7	6.6	13.0	25.0	33.0
0.50	24.0	26.0	30.0	36.0	45.0
0.48	1.8	3.3	7.5	42.0	48.0
0.42	≈0.70	1.2	2.3	5.8	≈10.0

IMPLICATIONS FOR OPTIMIZING PULSE COUNTING SYSTEM PARAMETERS

If the 8850 system were to be used in low-light flux experiments, the implications of the data discussed above are fairly clear: one should use the highest voltage (1700 V or higher) and an A_d of about 0.8. Under these conditions, the system will exhibit the best possible stability (of utmost importance in low flux experiments) along with a fairly high sensitivity and a linear range extending to 400 kHz (±0.5% accuracy). At higher count rates, however, linearity becomes a worse problem than stability. If the experiment to be performed is fairly "slow", then DTC could be used to extend the linear range of the system more than an order of magnitude, using increased integration times to make up for the lower sensitivity. However, if the experiment is "fast" (for instance, monitoring the course of a fast reaction), then the decreased sensitivity may rule out the use of DTC so that the only choices would be to use CLC (if within the range of its applicability) or to switch to a dc measurement system. In any case, high flux pulse counting experiments should still be performed with the highest PMT voltage. Finally, if the experiment is likely to encompass both very low and very high count rates, one will be forced to make some sort of compromise in the choice of a discriminator coefficient, unless the voltage programmability of the discriminator setting of the pulse counter is exploited to allow a computer to select a high A_d for low count rate date acquisition and automatically switch to a lower A_d when the count rate becomes sufficiently high that DTC is needed.

CONCLUSIONS

We have shown how two relatively simple measurements (pulse height distributions and linearity studies) can provide valuable information about the optimum operating parameters for pulse counting measurement systems under different experimental conditions. The specific parameters found to be best for the particular systems studied are, however, not to be generalized; rather, they serve to demonstrate than even systems which use the same pulse counting electronics can behave quite differently, and that it is extremely important to characterize the behavior of any give pulse counting system to ensure that it does in fact satisfy the measurement requirements.

ACKNOWLEDGMENT

We thank S. R. Crouch for many helpful conversations during the preparation of this manuscript.

LITERATURE CITED

(1) J. D. Ingle, Jr., and S. R. Crouch, *Anal. Chem.*, **44**, 785 (1972).
(2) K. C. Ash and E. H. Piepmeier, *Anal. Chem.*, **43**, 26 (1971).
(3) E. J. Darland, Ph.D. Thesis, Michigan State University, East Lansing, Mich., 1978.
(4) E. J. Darland, J. E. Hornshuh, C. G. Enke, and G. E. Leroi, *Anal. Chem.*, following paper in this issue.
(5) L. Heroux, *Appl. Opt.*, **7**, 2351 (1968).
(6) F. T. Arecchi, E. Gatti, and A. Sona, *Rev. Sci. Instrum.*, **37**, 942 (1966).
(7) F. Robben, *Appl. Opt.*, **10**, 776 (1971).
(8) J. D. Ingle, Jr., and S. R. Crouch, *Anal. Chem.*, **44**, 777 (1972).
(9) L. Birenbaum and D. B. Scarl, *Appl. Opt.*, **12**, 519 (1973).
(10) D. C. Wenke, Ph.D. Thesis, Michigan State University, East Lansing, Mich., 1972.
(11) M. VanGorkom and R. E. Glick, *Int. J. Mass Spectrom. Ion Phys.*, **4**, 203 (1970).
(12) M. VanGorkom, D. P. Beggs, and R. E. Glick, *Int. J. Mass Spectrom. Ion Phys.*, **4**, 441 (1970).
(13) J. M. Hayes and D. A. Schoeller, *Anal. Chem.*, **49**, 306 (1977).
(14) J. M. Hayes, D. E. Matthews, and D. A. Schoeller, *Anal. Chem.*, **50**, 25 (1978).
(15) C. Smit and C. Th. J. Alkemade, *Appl. Sci. Res.*, **10B**, 309 (1963–64).

RECEIVED for review July 14, 1978. Accepted October 30, 1978. Two of the authors (E.J.D. and G.E.L.) are pleased to acknowledge the support of the National Science Foundation (MPS 75-02525) and the Office of Naval Research (N00014-76-C-0434).

Pulse (Photon) Counting: A High-Speed, Direct Current-Coupled Pulse Counter

E. J. Darland, J. E. Hornshuh,[1] C. G. Enke,* and G. E. Leroi

Department of Chemistry, Michigan State University, East Lansing, Michigan 48824

An amplifier/discriminator/prescaler module which forms a complete, high-performance pulse counter when combined with any standard TTL counter is described. It is constructed with readily-available integrated circuits and costs less that $150, yet has high sensitivity (130 μV) and is capable of very high count rates (>90 MHz with periodic input pulses; pulse pair resolution ≃ 11 ns). The entire circuit is dc coupled so that there is no base-line shift at any count rate. The discriminator level is voltage programmable and the amount of prescaling can be selected remotely. Extra precautions taken to ensure drift-free operation of the electronics result in a pulse counter with excellent long-term stability.

It is widely recognized that pulse counting is the best method for measuring the output signal from electron multipliers used as particle (photon, ion, electron, etc.) detectors when the incident particle flux is very low (*1–8*). Likewise, it is recognized that pulse overlap counting losses inherent in the pulse counting technique limit its accuracy at higher particle fluxes, so that direct current (dc) techniques are best used at these higher fluxes (*5–9*). In spite of the fact that dc measurement systems which are adequate for medium- and high-flux measurements are readily available, there are several practical reasons for the continued interest in developing pulse counting systems which can operate at ever higher count rates. For example, pulse counting systems may have significant signal-to-noise ratio and stability advantages over dc systems at equivalent fluxes (*3–8*). Furthermore, pulse counting is an inherently digital technique; pulse counting measurements require fewer data domain conversions (*10*) than dc measurements, and are thus less susceptible to the inevitable errors which accompany such conversions (*8, 10*). The development of faster pulse counting systems not only extends these advantages to measurements made at higher fluxes, but also has important consequences in terms of cost and convenience. The availability of a pulse counting system which is as fast as possible increases the probability that all necessary measurements (or at least an entire series of measurements) can be made without resorting to dc techniques. Thus, in some applications, the cost of a dc system may be eliminated entirely. Even when dc measurements must be made, a fast pulse counting capability will reduce the sensitivity requirements for the dc system.

The pulse counter described here has performance characteristics approaching the practical limits, but it can be built for a small fraction of the cost of present commercial pulse counting systems. The pulse counter has high sensitivity as well as stable and easily adjusted gain and discriminator levels, which are independent of pulse rate. The discriminator level is voltage programmed, and the amount of prescaling can be selected remotely. These features allow the possibility of real-time computer control of the measurement system parameters, which could be automatically optimized to meet changing experimental conditions (*11*).

PULSE COUNTER DESIGN

A block diagram of the pulse counter is shown in Figure 1. The digital counter is a standard TTL design, interfaced to a PDP8/I minicomputer, and the clock is the real-time clock of the computer (*12*). These units are not described in this paper. For the sake of brevity, the remainder of the circuitry (amplifier, discriminator, prescaler, and line driver) will henceforth be termed the "pulse counter", although it should be realized that some sort of frequency meter (or digital counter and clock) are also necessary to make a complete pulse counter.

---

[1] Present address: Central Research Department, Experimental Station, E. I. du Pont de Nemours, Wilmington, Del. 19898.

0003-2700/79/0351-0245$01.00/0 © 1979 American Chemical Society

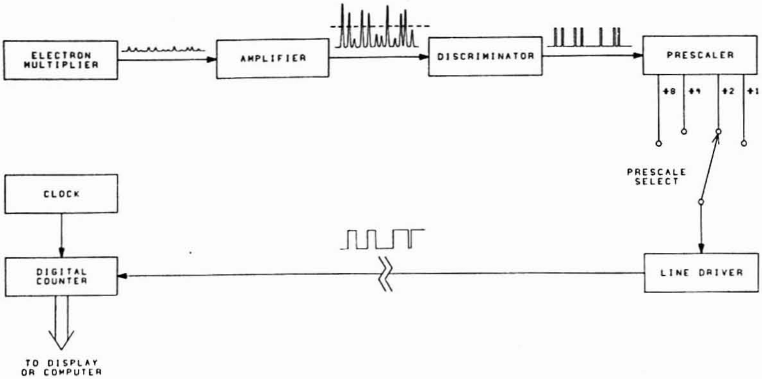

Figure 1. Block diagram of the pulse counter

Establishment of Performance Goals. The pulse counter described here was intended for use with a wide variety of computer-interfaced spectrometric instrumentation, at both very high and very low count rates. The primary design goals were high speed, sufficient sensitivity for use with common photomultiplier tubes, and sufficient stability for low count rate experiments lasting as long as several days.

The speed of the counter is important since pulse overlap in the counter circuits is usually the limiting factor in determining the maximum count rate at which accurate data can be obtained (*9*). State-of-the-art counters are capable of counting periodic pulses up to about 100 MHz, i.e., they can resolve pulses separated by as little as 10 ns. However, particles usually arrive at the electron multiplier with a random time distribution. In order to measure the average pulse rate accurately, the pulse counting electronics must be capable of responding at an instantaneous pulse rate which is greater than the average pulse rate by a factor which depends on the amount of pulse overlap counting loss that can be tolerated. The average pulse rate for which good accuracy can be obtained is only a few percent of the maximum count rate for the counter. Still faster pulse counting electronics might be expected to help the pulse overlap problem significantly. However, even with relatively fast electron multipliers, the full-width at half-maximum (FWHM) of the pulses observed at the counter input will be on the order of 2–3 ns. For most pulse counting, the best stability and signal-to-noise ratio will be obtained when the discriminator is set significantly below half of the mean pulse amplitude (*11*). Under these conditions, the mean pulse width may be significantly larger than the FWHM, or on the order of 6–10 ns. Thus, a 100-MHz pulse counter with a 10-ns dead-time approaches the practical limit set by pulse overlap within the electron multiplier and connecting cable, and a design goal of 100 MHz was adopted.

The sensitivity of the counter is important for two reasons. Pulse heights from a typical electron multiplier have a random and broad distribution. If the counter is not sensitive enough to count the smallest pulses, then some of the signal is wasted, increasing the measurement time or lowering the signal-to-noise ratio of the measurement (*8*). Furthermore, although the discriminator setting at which the best overall system stability is attained will vary from system to system (*11*), the optimum setting is likely to be near the "small" end of the pulse height distribution, so that the pulse counter should have sufficient sensitivity to count nearly all of the pulses.

Ease of use and restricted space within most photomultiplier housings dictated that the pulse counter not be mounted inside the housing, but rather in a separate nearby enclosure connected to the electron multiplier or photomultiplier with the shortest practical length of common 50- (or 100-) Ω coaxial cable. To minimize reflections, an anode load resistor of 50 (100) Ω must be used at the pulse amplifier input. The amplitude of the voltage pulses generated across this resistor by the anode current pulses determines the sensitivity required of the rest of the circuit. We performed pulse height measurements on several multipliers (RCA 1P28 and 8850 PMTs and a variety of "bare" electron multipliers used as mass spectrometer ion transducers). The multipliers which had the lowest gain at normal operating voltages produced pulses which were as large as 5–10 mV (50-Ω load), but also many pulses which were smaller than 1 mV. Therefore, a design goal of at least 500 μV sensitivity was adopted.

The pulse counter described here uses a fast binary counter between the discriminator and line driver to prescale the discriminator output, as depicted in Figure 1. The true number of counts must then be obtained by multiplying the recorded number of counts by the same factor by which the prescaler divides the pulse rate. Inclusion of prescaling has two very desirable effects. The first is that the average pulse rate at the input to the line driver is reduced by the scaling factor, so that succeeding circuitry does not have to be so fast. The second, and even more important, advantage is that prescaling reduces the probability of pulse overlap by *more* than it reduces the average pulse rate. This can be illustrated as follows. The probability that n pulses will occur within the resolving time t of a pulse counter is given by the Poisson distribution as

$$P(n,t) = \frac{(Rt)^n}{N!} \exp(-Rt)$$

where R is the average pulse rate. If zero or one pulse arrives during t, no pulse overlap occurs, but if two or more arrive during the same interval, pulse overlap counting loss has occurred. The probability of this happening is then

$$P_0 = 1 - \sum_{n=0}^{1} P(n,t)$$

If, however, the input pulses are prescaled by two (and the prescaler is so fast that no pulse overlap loss occurs in it), then three or more pulses must arrive at the prescaler input within

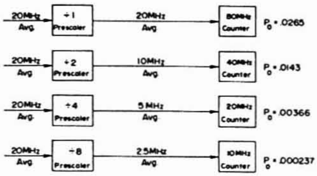

Figure 2. Probability of pulse overlap in the counter (P_o) for four combinations of prescaling factor and maximum counting rate

the resolving time of the counter to cause pulse overlap in the counter, and

$$P_0 = 1 - \sum_{n=0}^{2} P(n,t)$$

In general, for a prescaling factor I,

$$P_0 = 1 - \sum_{n=0}^{I} P(n,t)$$

The advantages of prescaling are illustrated in Figure 2. Note that, although the ratio of the pulse rate at the digital counter input to the maximum frequency of the digital counter is constant in the four examples in Figure 2, P_0 is reduced by a factor of more than 100 when a divide by eight prescaler is introduced.

The only disadvantage of prescaling is that the count resolution of the readout is lowered by the prescaling factor, so that longer integration times may be required to reach the desired count total and/or precision. This problem could be serious at low count rates except that, at low count rates, less prescaling is required. Therefore, three levels of prescaling are provided (in addition to the "no prescaling" or ÷1 option) so that the count resolution can be maintained as high as possible while keeping the maximum frequency within a range that the line driver and succeeding circuitry can handle.

Amplifier/Discriminator Circuit. The preamplifier-discriminator portion of the pulse counter is very simple; it is based on only two integrated circuits, as shown in Figure 3. A high-speed comparator (Advanced Micro Devices type AM685) with differential inputs and emitter-coupled logic (ECL) outputs is used as the discriminator. The amplifier is a Texas Instruments μA733 adjustable gain, high-speed differential video amplifier. When the counter is in its quiescent state (both amplifier inputs at essentially zero volts), the amplifier outputs have a common mode voltage, V_{Acm}, which is typically about 2.9 V, and are separated by an offset voltage, V_{Ao}, which depends on the gain of the amplifier, but is typically 0.6 V at the maximum gain of 400. These voltage levels are shown in the amplifier waveform plots of Figure 4. A negative pulse at the input of the amplifier causes the outputs to move closer together, and for sufficiently large pulses, the outputs will cross. A quiescent comparator input common mode voltage, V_{Ccm}, and an input offset voltage, V_{Co}, can be defined which are analogous to V_{Acm} and V_{Ao}. The comparator is triggered whenever its inputs cross, i.e., when the input pulse to the comparator is larger than V_{Co}.

Capacitive (or ac) coupling between the amplifier and comparator would allow V_{Ccm} and V_{Co} to be adjusted independently of V_{Acm} and V_{Ao}. However, ac coupled circuits exhibit base-line shift which changes the effective threshold level at higher count rates (*5*). The various diode clamp techniques which are commonly used to limit base-line shift do not completely eliminate it (*13*), and design of base-line correction circuits suitable for use at 100 MHz is not a trivial problem. Nor is simple direct coupling between the amplifier and comparator a possibility, since an amplifier gain of 1200 would be required if a 500-μV signal were to cause threshold crossing.

This pulse counter retains dc coupling, but through two simple resistor networks as shown in Figure 3. Resistors R3 and R4 (and similarly R6 and R7) act as simple voltage dividers, transmitting a large fraction of the amplifier output pulse to the comparator input. However, R5 and R8 allow the voltage at one end of each divider to be varied independently over a range of +6 V to −6 V, which in turn allows independent control of the quiescent values of the comparator input voltages. With the component values shown, V_{Ccm} can be reduced to approximately 1 V, which results in much improved overload characteristics. The comparator offset voltage, V_{Co}, can be adjusted continuously within a range of

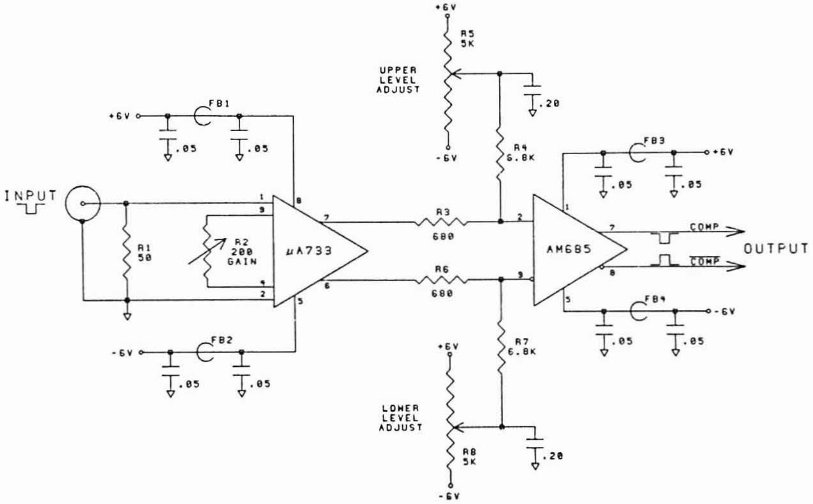

Figure 3. Preamplifier/discriminator circuit. All resistances in ohms; all capacitances in microfarads. FB1–FB4 are ferrite beads

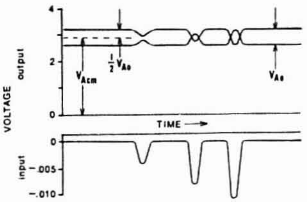

Figure 4. Relationship between amplifier input and output voltages. Note different scales for input and output waveforms

approximately ±300 mV. A typical value of 50 mV results in a tenfold gain in sensitivity compared with the directly coupled amplifier and comparator. Both V_{Ccm} and V_{Co} can be varied independently of the amplifier gain, which can be set so as to obtain the best compromise between bandwidth and temperature stability. Furthermore, *there is no base-line shift at any count rate.*

The comparator is essentially a high-gain, high-speed amplifier, and as such is particularly prone to oscillation. Oscillations will occur when the differential input voltage remains in some critical range near zero for longer than the propagation delay of the comparator (*14*). Therefore, the input signal must traverse the critical range in a time period which is less than the propagation delay of the comparator if oscillation is to be avoided. Fortunately, the rise time of the amplified anode pulses is much shorter than the comparator propagation delay time, so that hysteresis (which can only limit sensitivity and maximum speed) is unnecessary.

The tendency to oscillate does limit the overall sensitivity of the counter, however, since the critical range limits the minimum useful value of of V_{Co}. The width of the critical range (which may be as small as a few millivolts or as large as several hundred millivolts) depends on the (fixed) gain of the comparator, the extent to which the comparator's output is coupled back to its input via stray capacitance, and the source impedance seen by the comparator at its inputs (*14*). Careful construction techniques can help minimize the stray capacitance between comparator output and input. The use of a comparator with ECL outputs is also advantageous, since the voltage swing for an ECL logic transition is only about one fifth of that for a TTL logic transition, and thus there is less signal to couple back to the inputs. The width of the critical range is also found to be smallest when the comparator is driven by a balanced source with an output impedance of about a thousand ohms or a little larger. Coupling resistors R3 and R6 also serve to establish the desirable source impedance.

The inclusion of R3 and R6 has one major disadvantage. Every pulse from the amplifier must charge up the input capacitance of the comparator through these resistors, and if too large a resistance is used, the resulting RC time constant becomes the limiting factor in the frequency response of the counter. The value of 680 Ω was chosen as a compromise between high frequency response and small critical range (i.e., high sensitivity). Different values for these resistors could improve either of these characteristics at the expense of the other.

Prescaler/Linedriver Circuit. The prescaling and line driver circuitry of the pulse counter is shown in Figure 5. The signal from the comparator is converted into a TTL level signal (÷1) which is used to drive the light emitting diode (LED) that indicates the state of the comparator (it is on when the comparator is in its quiescent state). Since R5 and R8 (Figure 3) can be adjusted to make V_{Co} negative (so that the comparator is permanently triggered), the STATE LED is particularly useful when adjusting the threshold level of the pulse counter.

The output of the comparator also goes to a binary counter composed of three fast (140 MHz) ECL flip-flops which divide the pulse stream from the comparator by 2, 4, and 8. The output from each stage of the counter is also converted into a TTL level signal. A 74153 multiplexer passes one of these signals (or the ÷1 signal) to the 75109 differential current

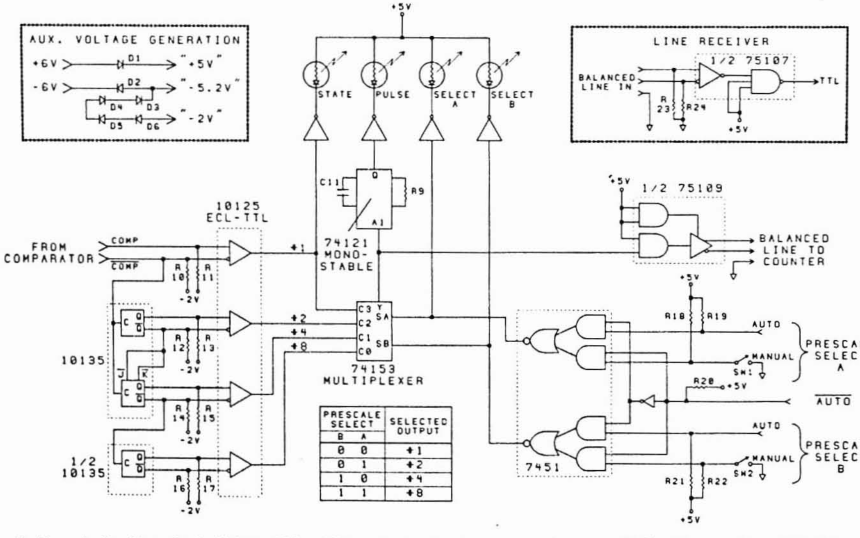
+5V
AUX. VOLTAGE GENERATION
+6V
D1
"+5V"
-6V
D2
"-5.2V"
D4
D3
D5
D6
"-2V"
STATE
PULSE
SELECT A
SELECT B
LINE RECEIVER
1/2 75107
BALANCED LINE IN
TTL
R 23
R24
+5V
C11
Q
R9
A1
74121 MONO-STABLE
+5V
1/2 75109
BALANCED LINE TO COUNTER
10125 ECL-TTL
FROM COMPARATOR
COMP
$\overline{\text{COMP}}$
R 10
R 11
-2V
÷1
÷2
÷4
÷8
C3
C2
C1
C0
Y
SA
SB
74153 MULTIPLEXER
10135
C
Q
$\overline{Q}$
$\overline{J}$
$\overline{K}$
R 12
R 13
R 14
R 15
-2V
1/2 10135
R 16
R 17
-2V
+5V
R18
R19
AUTO
MANUAL
SW1
PRESCALE SELECT A
R20
+5V
$\overline{\text{AUTO}}$
AUTO
MANUAL
SW2
PRESCALE SELECT B
7451
R21
R22
+5V

PRESCALE SELECT B	PRESCALE SELECT A	SELECTED OUTPUT
0	0	÷1
0	1	÷2
1	0	÷4
1	1	÷8

Figure 5. Prescaler/linedriver circuit. Values of R9 and C11 are not critical (see text). R10–R17 are 50-Ω pulldown resistors, R18–R22 are 3-kΩ, and R23 and R24 are each one-half the nominal impedance of the balanced line used to connect the line driver and reciever. D1–D6 are 1N4001 or equivalent

mode line driver, which transmits the pulse train to the digital counter. The line receiver circuit (used at the input of the digital counter) is shown in an inset in Figure 5. The signal selected by the multiplexer also triggers a monostable which flashes the PULSE LED. The output pulse width of the monostable is adjusted with R9 and C11 so that the LED emits a visible flash (a few milliseconds long), which is used to indicate whether pulses are being detected by the counter.

The amount of prescaling used (i.e., which signal is transmitted by the multiplexer) can be determined either manually or under computer control. When the $\overline{\text{AUTO}}$ line is HI, the manual prescale select switches, SW1 and SW2, control the multiplexer. When the $\overline{\text{AUTO}}$ line is LO these switches are disabled and the multiplexer is controlled instead from the computer via the remote prescale select lines. Two LEDs are used to indicate the status of the multiplexer control lines. It should be noted that the output pulses from the discriminator are so narrow (∼11 ns) that the "÷1" output of the prescaler does not trigger the line driver reliably, and single-count resolution should normally be obtained by counting both positive- and negative-going edges of the ÷2 output (*15*).

The entire circuit of the photon counter is designed so that only two main supply voltages (+6 V and −6 V) are needed. The auxiliary voltages needed for the TTL and ECL integrated circuits are derived on the circuit board using the simple diode circuits also shown in an inset in Figure 5.

Construction. When working with high frequency, low level signals, the construction methods used are as important as the rest of the circuit design, and some of the details of construction found to be necessary with the pulse counter are summarized here (*16*).

The entire circuit (except for the power supply) is built on a single, 4 inch × 9 inch, double-sided printed circuit board, on which as complete a ground plane as possible is maintained. Since the amplifier section of the circuit is very sensitive to high frequency signals, extra precautions are necessary to shield the amplifier and comparator from both internal and external noise sources. For instance, fast logic edges (such as normal TTL transitions) are very rich in frequencies above 30 MHz, which can be radiated very easily. It was found necessary to place a metal shield across the circuit board between the amplifier-comparator section and the ECL and TTL logic of the prescaler section to prevent noise radiated in the latter section from being picked up at the amplifier input. Better results were obtained when the input and output connectors (as well as the PULSE and STATE LEDs) were soldered directly to the circuit board instead of being connected with short wires, since such wires radiate and pick up unwanted noise more easily than does foil on a circuit board with a good ground plane. The main circuit board is shielded by internal partitions from the ac voltages present in both the power supply and temperature control circuits. The dc power to the circuit board is passed through the partitions via small feed-through capcitors which are used to bypass high frequency noise. Ferrite bead and capacitor filters are used to filter any remaining high frequency noise from the power inputs to both the amplifier and the comparator (see Figure 3).

Not only must the pulse counter be mounted in an enclosure which shields it from external radiated noise, but extreme care must be taken to ensure that no noise "sneaks in" on the 115-V ac power line. The pulse counter includes, at the power entrance to the enclosure, both a radio frequency interference (RFI) filter and transient suppressors which successfully eliminate such noise.

Preliminary experiments indicated that the thermal characteristics of the circuit could be important. The pulse counter was therefore built in an enclosure which was large enough to include a small circulating fan and proportional temperature control circuitry so that the thermal behavior of the counter could be easily studied and regulated. The completed pulse counter (shown in Figure 6) has overall dimensions of 11 × 3.5 × 7.5 inches. The total cost for all parts and materials in the pulse counter unit was less than $130.

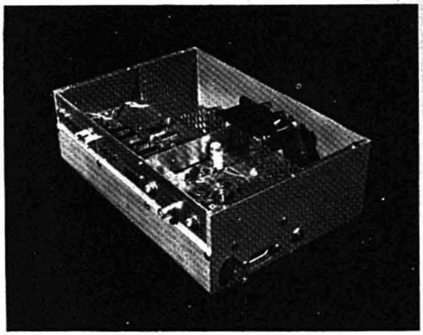

Figure 6. The completed pulse counter

PULSE COUNTER PERFORMANCE

Sensitivity. It is necessary to calibrate the sensitivity of a pulse counter using pulses with about the same width as the actual anode pulses from the multiplier to be used. The FWHM of the anode pulses from the 1P28 are about 5.5–6 ns; the pulses from the 8850 and the faster "bare" multipliers were similar at moderate voltages. The narrowest pulses obtainable from a Tektronix PG-501 pulse generator had a FWHM of just 5.5 ns, and an amplitude which was variable over a range of about 0–5 V. These pulses were connected to the counter via a calibrated 66-db attenuator, which reduced their amplitude to a range of 0–2.5 mV.

The input pulse amplitude necessary to cause reproducible triggering of the pulse counter (with a 50-Ω load resistor) was measured as a function of discriminator setting. The lower limit of sensitivity, determined by the onset of comparator oscillation, is about 130 μV. In practice, threshold settings lower than about 250 μV are not used, so that numerous small noise pulses which are picked up by the cable connecting the counter to the multiplier will not be counted. Measurement of V_{C_0} at the same threshold settings indicated that the effective gain of the amplifier for such narrow pulses is about 250, although the low frequency gain is nearly 400.

Speed. Pulse counter speeds are specified in several ways. One method is to specify the maximum frequency of a periodic waveform to which the pulse counter will respond. The waveform is often not specified, but if it is a series of very narrow pulses, then this method is equivalent to specifying the dead time or pulse pair resolution of the counter. The dead time can also be evaluated by measuring the width of the comparator output pulse for very narrow input pulses (assuming that the amplifier and/or comparator limit the speed of the counter). To specify that a counter is a "100-MHz counter" or that it has a "10-ns deadtime or pulse pair resolution" does not, of course, predict how fast a complete pulse counting system which uses that counter will be, since the behavior of such a system depends critically on numerous other factors (*6, 8, 9, 11, 17*). However, such specifications can be a useful basis of comparison between different counters of comparable sensitivity, cost, and stability, and such measurements are therefore worth making.

The sensitivity of this counter for 5.5-ns pulses showed no measurable change up to a pulse repetition rate of 57 MHz, which is the limit of the pulse generator used. The output pulse of the comparator when the amplifier was driven by such pulses was about 11 ns wide. The maximum frequency at which the counter would trigger reliably with a sinewave input was approximately 93 MHz, which is consistent with a pulse pair resolution of about 11 ns. The speed of several pulse counting systems incorporating this counter is examined experimentally in a companion paper (*11*).

Stability. Some of the results of preliminary experiments using this pulse counter circuit indicated that while the sensitivity was apparently sufficient to count all pulses when used in a photon counting system, the importance of good stability in the pulse counter electronics should not be neglected (*11*). An examination of the sources of instability in the two photon counting systems described in reference 11 revealed two major contributions. One was a low frequency variation in the light source output of some 1%. By far the worst type of instability exhibited by the electronics of the pulse counting measurement system itself was the variation in effective threshold with temperature. Several factors contribute to thermal drift of the effective threshold, but changes in the gain of the amplifier and in V_{A_0} (see Figure 4) were found to be most important. Direct measurement of the temperature coefficients of amplifier gain and offset voltage is extremely difficult because the changes are small and because so much low amplitude noise is introduced via the test probes that measurements anywhere near the (nonperturbed) critical range are impossible. A more sensitive (and perhaps more meaningful) method of measuring the change in effective threshold is simply to monitor the count rate at a "constant" light intensity as the temperature of the counter is varied. Such measurements were performed for several amplifier gain settings. The dependence of count rate on temperature was worst at low amplifier gain ($G \simeq 60$), exhibiting a 30% change from 30 to 50 °C. Much better results were obtained at full amplifier gain (the normal operating conditions), where any count rate changes between 32 and 40 °C were so small as to be totally obscured by the instability in the light source.

The temperature controller used with the pulse counter maintains the temperature to within ±0.5 °C indefinitely after an hour's equilibration time. The present data are insufficient to show whether such control is actually necessary for good stability. However, with this temperature control the instability of the counter is almost certainly negligible compared to light source instabilities, or to changes in photomultiplier cathode sensitivity with temperature (*18*).

ACKNOWLEDGMENT

The authors are grateful to B. K. Hahn for suggesting the use of the μA733 and AM685 integrated circuits.

LITERATURE CITED

(1) F. T. Arecchi, E. Gatti, and A. Sona, *Rev. Sci. Instrum.*, **37**, 942 (1966).
(2) A. T. Young, *Appl. Opt.*, **8**, 2431 (1969).
(3) F. Robben, *Appl. Opt.*, **10**, 776 (1971).
(4) M. K. Murphy, S. A. Clyburn, and C. Veillon, *Anal. Chem.*, **45**, 1468 (1973).
(5) M. L. Franklin, G. Horlick, and H. V. Malmstadt, *Anal. Chem.*, **41**, 2 (1969).
(6) K. C. Ash and E. H. Piepmeier, *Anal. Chem.*, **43**, 26 (1971).
(7) H. W. Werner, H. A. M. DeGrefte, and J. V. D. Berg, *Int. J. Mass Spectrom. Ion Phys.*, **8**, 459 (1972).
(8) J. D. Ingle, Jr., and S. R. Crouch, *Anal. Chem.*, **44**, 785 (1972).
(9) C. Smit and C. Th. J. Alkemade, *Appl. Sci. Res.*, **108**, 309 (1963-4).
(10) C. G. Enke, *Anal. Chem.*, **43** (1), 69A (1971).
(11) E. J. Darland, G. E. Leroi, and C. G. Enke, *Anal. Chem.*, preceding paper in this issue.
(12) E. J. Darland, Ph.D. Thesis, Michigan State University, East Lansing, Mich., 1978.
(13) L. B. Robinson, *Rev. Sci. Instrum.*, **32**, 1057 (1961).
(14) "Designing with High-Speed Comparators", AMD Application Note, Dec. 1975, Advanced Micro Devices, Sunnyvale, Calif., 94086.
(15) K. G. Harf, *Computer Des.*, **17**, 130 (June, 1978).
(16) Additional, more detailed, construction information can be obtained by writing the authors.
(17) J. M. Hayes, D. E. Matthews, and D. A. Schoeller, *Anal. Chem.*, **50**, 25 (1978).
(18) Photomultiplier Manual, Technical Series PT-61, RCA Corp., Harrison, N.J.

RECEIVED for review July 14, 1978. Accepted October 30, 1978. Two of the authors (E.J.D. and G.E.L.) are pleased to acknowledge the support of the National Science Foundation (MPS 75-02525) and the Office of Naval Research (N00014-76-C-0434).

Micromolar Voltammetric Analysis by Ring Electrode Shielding at a Rotating Ring-Disk Electrode

Stanley Bruckenstein* and P. R. Gifford

Chemistry Department, State University of New York at Buffalo, Buffalo, New York 14214

Ring electrode shielding at a rotating ring-disk electrode (RRDE) provides a sensitive solid electrode technique for the study of micromolar solutions of electroactive materials. At micromolar levels, shielded ring electrode currents are free of nonconvective diffusion current complications which obscure faradaic rotating disk electrode currents. Ag(I), Bi(III), Cu(II), and Fe(III) and mixtures of Ag(I) and Cu(II) can be determined in the concentration range 0.1 to 10 × 10^{-6} M.

In the determination of micromolar levels of electroactive species at solid electrodes, the convective diffusion-controlled current for the electrode reaction of analytical interest can be obscured by charging currents and/or surface processes occurring at the electrode. This problem can be minimized by use of the rotating ring-disk electrode (RRDE) in the ring shielding mode (*1–3*).

The RRDE has been shown to be of great utility in the study of metal ions in solution since the ring electrode can monitor electroactive species generated or consumed at the disk (*4*). Moreover, if the ring electrode is held at a fixed potential, complications due to charging and surface processes at the disk do not affect the ring current, thus making the ring electrode shielding technique a sensitive measure of the current due to the disk electrode process.

In this study, ring shielding at a RRDE was applied to the determination of Cu(II), Bi(III), Ag(I), and Fe(III). Simul-

0003-2700/79/0351-0250$01.00/0 © 1979 American Chemical Society

taneous determination of Cu(II) and Ag(I) was demonstrated. Quantitative results were obtained over the concentration range 10^{-7} to 10^{-6} M.

THEORETICAL

In order to describe our use of the RRDE shielding technique for the determination of micromolar levels of a species, the following reaction is considered:

$$M^{n+} + ae \rightarrow M^{(n-a)+} \qquad (1)$$

The expression relating the disk limiting current, $i_{D,L}$, to concentration for this process was first derived by Levich (*5*) and is

$$i_{D,L} = 0.62nF\pi r_1^2 D^{2/3}\nu^{-1/6}\omega^{1/2}C^b \qquad (2)$$

where r_1 is the disk radius (cm), D is the diffusion coefficient (cm^2/s), ν is the kinematic viscosity (cm^2/s), and ω is the electrode rotation speed (rad/s). The analogous expression relating the limiting current to concentration at a rotating ring electrode has been derived by Levich and Zaidel (*6*). Their result also applies to the ring electrode of a RRDE when the disk current is zero, and may be expressed as

$$i_{R,L} = \beta^{2/3} i_{D,L} \qquad (3)$$

where $i_{D,L}$ is the disk limiting current given by Equation 2 and β is a geometric function of r_1 and the inner and outer ring radii, r_2 and r_3, respectively, i.e.,

$$\beta = (r_3/r_1)^3 - (r_2/r_1)^3 \qquad (4)$$

If an intermediate, $M^{(n-a)+}$, is generated at the disk from a solution containing only M^{n+} according to Reaction 1 and detected at the ring by its reoxidation back to M^{n+}, then the ring current for a convective diffusion-controlled process is given by

$$i_R = -Ni_D \qquad (5)$$

where N is the collection efficiency (*2, 7*). For a convective diffusion-controlled process, the collection efficiency may be calculated from r_1, r_2, and r_3 (*8, 9*). When M^{n+} and $M^{(n-a)+}$ are both present in solution and M^{n+} is reduced at the disk electrode, the ring electrode current due to reoxidation of the intermediate is

$$i_R = i_{R,L} + Ni_D \qquad (6)$$

Thus, the ring current is the sum of two components—one arising from the current at the ring electrode when there is no disk process and one arising from the amount of $M^{(n-a)+}$ created at the disk. Analogously, if $M^{(n-a)+}$ in solution is oxidized to M^{n+} at the disk, the ring current for its reoxidation will be decreased by Ni_D. It is this ability to monitor the consumption of species at the disk electrode by changes in the ring current that is the basis for the ring electrode shielding technique.

Consider a solution of M^{n+} having no $M^{(n-a)+}$ in which the ring electrode is potentiostated so that Reaction 1 is convective diffusion-controlled. Initially, if no reaction occurs at the disk involving M^{n+}, the ring limiting current observed is given by Equation 3. As the disk electrode potential is scanned cathodically to produce the limiting current response for Reaction 1, the ring current decreases because of the consumption of M^{n+} at the disk. The ring current does not fall to zero since the disk cannot prevent all M^{n+} from reaching the ring. Rather, the ring current will fall to a value defined as the shielded ring current, $i_{R,sh}$ (*1–3*). Its value is

$$i_{R,sh} = (\beta^{2/3} - N)i_{D,L} \qquad (7)$$

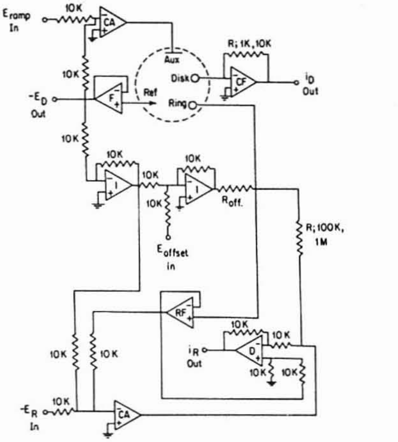

Figure 1. Circuit diagram for four-electrode potentiostat modified for ring current offset capability

According to Equations 2 and 7, the shielded ring electrode current is proportional to C^b. However, at low solute concentrations, the experimental measurement of the absolute value of $i_{R,sh}$ is difficult, while the measurement of the difference between the limiting (unshielded) and shielded ring currents, Δi_R, is much easier. The relationship between these currents is obtained by subtracting Equations 3 and 7 and substituting from Equation 2, i.e.,

$$\Delta i_R = i_{R,L} - i_{R,sh} = Ni_{D,L} = 0.62nF\pi r_1^2 D^{2/3}\nu^{-1/6} NC^b \qquad (8)$$

Because $i_{D,L}$ in Equation 8 represents the faradaic current associated with Equation 1, and Δi_R is measured at constant ring electrode potential, Δi_R is free of currents associated with charging and surface processes at both the disk and ring electrodes. Thus the measurement of Δi_R is a more sensitive analytical method than the direct measurement of $i_{D,L}$.

EXPERIMENTAL

Instrumental. The earlier circuit used for independent potentiostatic control of the ring and disk electrodes (*3*) was modified as shown in Figure 1 to allow an offset current to be summed into the ring current. This circuit still provided independent potentiostatic control of both electrodes and increased the sensitivity with which the small differences in ring currents could be measured.

Current–potential and current–time curves were recorded on an EAI X-Y-Y′ recorder (Electronics Associates, Inc.).

The analog voltage ramp for the potentiostat has been described elsewhere (*10*). Unless otherwise stated, a scan rate of 200 mV/s was employed for the ring shielding studies.

The electrochemical cell was constructed from borosilicate glass, had an approximate volume of 500 mL, and had five ports. One port provided an inlet for the RRDE and a polyethylene cover was fitted around the electrode over this port to minimize the introduction of oxygen and other contaminants. The other ports provided entrances for the auxiliary electrode compartment, a gas dispersion tube, Luggin capillary, and for the introduction of reagents to the cell. The cell was periodically cleaned with a 50–50 volume mixture of concentrated sulfuric and nitric acids by overnight soaking, followed by extensive rinsing with reagent grade water.

The RRDEs were rotated in a high-speed rotator (Pine Instruments Co., Grove City, Pa.). Precision pulleys allowed incremental steps of rotation speed from 400 to 10000 rpm. The rotator, with electrode and cell in place, was enclosed in an aluminum case grounded to the instrument ground to provide shielding against external noise. Connections to the cell from the instrument were made through the shield via double shielded

Table I. Rotating Ring-Disk Electrodes

electrode no.	type	R_1, cm	R_2, cm	R_3, cm	N	$\beta^{2/3}$
I	Au ring; Au disk	0.383	0.412	0.511	0.364	1.092
II	Pt ring; Pt disk	0.383	0.398	0.493	0.374	1.009
III	Au ring; Pt disk	0.380	0.402	0.523	0.409	1.269

coaxial cable and shielded BNC connectors. Experiments were performed at a rotation speed of 2500 rpm unless otherwise stated.

Electrodes. A coil of platinum or gold wire was used as an auxiliary electrode, depending on the metal composition of the ring-disk electrode being used. A commercial saturated calomel electrode (SCE) (Fisher Scientific Co.) was used for the reference electrode. All potentials are reported vs. the SCE. The RRDEs used in this study were constructed and polished by a previously described procedure (*11*). The various RRDEs used are described in Table I.

Before each set of experiments the RRDE was polished using 0.05 μm alumina. Next the ring and disk electrodes were potential cycled in supporting electrolyte until reproducible i–E curves were obtained. Then the ring electrode was potentiostated at the working potential for approximately 15 min before performing the shielding experiments. For electrode reactions involving metal deposition, this time deposits an average thickness of several atom layers of the metal over the ring electrode.

Reagents and Solutions. All reagents used were of AR grade and were used without further purification.

Solutions were prepared with water obtained from a Milli-Q Reagent Grade Water System (Millipore Corp., Bedford, Mass.).

Solutions were deoxygenated by bubbling with water-saturated nitrogen (boil-off from liquid nitrogen, Union Carbide, Linde Division). During experiments, nitrogen was passed over the surface of the cell solution.

Known volumes of stock solution were added to the cell with a Manostat micropipet.

Procedure and Data Interpretation. Values of Δi_R were determined for a series of concentrations in the range of 10^{-7} and 10^{-6} M M^{n+}. These values were obtained by taking the difference between the ring current at a disk potential where a ring limiting current was observed and the ring current at a disk potential where the ring was fully shielded. Values of Δi_R were plotted vs. concentration. Theoretically, one should obtain a straight line of slope $m_{\Delta i_R}$ with zero intercept. Experimentally we found that processes not of analytical interest (e.g., hydrogen and oxygen evolution at the disk) and solution impurities produced small nonzero intercepts.

Steady-state values of i_{DL} were obtained over the concentration range of 10^{-5} to 10^{-4} M M^{n+} and plotted vs. concentration to give linear plots of slope $m_{i_{DL}}$. An experimental value for the collection efficiency N was calculated from the ratio of $m_{\Delta i_R}/m_{i_{DL}}$ and compared to the theoretical N calculated from the electrode geometry.

RESULTS AND DISCUSSION

In this study the validity and utility of the RRDE ring shielding approach for micromolar determinations was tested for solutions containing Cu(II), Bi(III), or Ag(I), and mixtures of Cu(II) and Ag(I). Also, the Fe(III)/Fe(II) system was studied to show the validity of the ring shielding technique for a system not involving underpotential metal deposition.

Underpotential metal deposition is an important factor in the study of metal/metal ion couples at solid electrodes, e.g., Ag (*12*) and Cu (*13*) on Pt and Bi (*14*) on Au. At the low metal ion concentrations and fast scan rates employed in these studies, the disk electrode reaction for these systems was underpotential metal deposition, not bulk metal deposition. Therefore, the ring electrode became shielded at potentials more anodic than the formal reduction potential for the metal/metal ion couple.

Determination of Cu(II). Since the behavior of Cu(II) in 0.5 M KCl has been well characterized (*3*), this system was the first chosen to test the ring shielding technique. Electrode I was employed for these studies. Its ring was potentiostated at −0.50 V, where the reduction of Cu(II) to Cu(0) is convective diffusion-controlled.

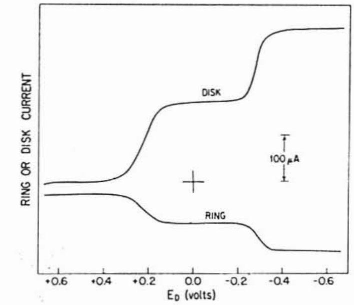

Figure 2. Current-potential curve for $C_{Cu(II)} = 5.0 \times 10^{-4}$ M–0.5 M KCl. Electrode I, potential scan rate 20 mV/s. Disk, upper curve; ring, lower curve

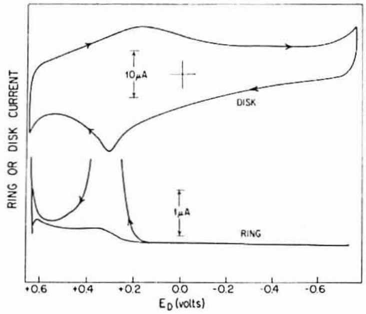

Figure 3. Current-potential curve for $C_{Cu(II)} = 9.70 \times 10^{-7}$ M–0.5 M KCl. Electrode I, potential scan rate 200 mV/s. Arrows indicate direction of potential scan. $E_R = -0.50$ V

The steady-state i–E curve at high concentrations of Cu(II) shows two waves (Figure 2) due to the reactions:

$$\mathrm{Cu(II)} + e \rightarrow \mathrm{Cu(I)} \qquad (9)$$

$$\mathrm{Cu(II)} + 2e \rightarrow \mathrm{Cu(0)} \qquad (10)$$

At $E_D = -0.4$ V, Reaction 10 is convective diffusion-controlled on the disk and the ring is fully shielded.

At low concentrations and fast scan rates, very different behavior is observed (Figure 3). The ring current is constant in the region of $+0.6 \text{ V} \leq E_D \geq +0.4$ V. The ring then begins to shield and at $E_D = 0.0$ V is completely shielded. Only a single wave is observed at the ring with low Cu(II) concentrations whereas two waves are observed with high concentrations. During the anodic scan, a single ring current peak occurs in the region $+0.5 \text{ V} \leq E_D \geq +0.2$ V corresponding to the oxidation of Cu(0) at the disk. The sharp increase in i_R at $E_D = +0.6$ V is due to dissolution of gold at the disk. Although a stripping peak is seen in the disk anodic scan, no reduction wave is detectable in the disk curve due to charging

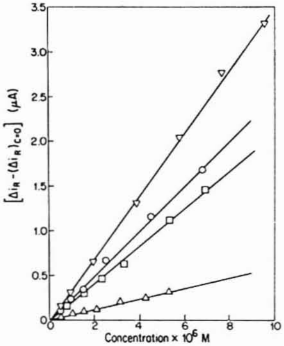

Figure 4. Plot of concentration of M^{n+} vs. $[\Delta i_R-(\Delta i_R)_{C=0}]$. (△) Fe(III), slope = 0.062 ± 0.002 μA/μM. (□) Ag(I), slope = 0.214 ± 0.002 μA/μM. (○) Cu(II), slope = 0.247 ± 0.004 μA/μM. (▽) Bi(III), slope = 0.350 ± 0.005 μA/μM

and surface currents at the disk.

No Cu(I) formation is observed until more than 500 μC of copper per cm^2 of electrode surface has been underpotentially deposited (*15*). Thus, at low concentrations, the shielding observed at the ring results from underpotential deposition of Cu(0) at the disk. The disk limiting current for Reaction 10 was determined for a series of 9.84×10^{-5} M ≤ $C_{\mathrm{Cu(II)}}$ ≤ 9.63×10^{-4} M solutions. A plot of $i_{\mathrm{D,L}}$ vs. concentration gave a straight line of slope 0.713 ± 0.001 μA/μM. Shielding studies were performed for a series of 2.19×10^{-7} M ≤ $C_{\mathrm{Cu(II)}}$ ≤ 6.82×10^{-6} M solutions. Values of Δi_R were plotted vs. concentration, giving a straight line of slope 0.247 ± 0.004 μA/μM (Figure 4). Calculation of *N* gives an experimental value of 0.346. The theoretical value of *N* is 0.364 for Electrode I.

Determination of Bi(III). The behavior of Bi(III) on Au in 0.1 M $HClO_4$ was originally studied by Cadle and Bruckenstein using a RRDE (*14*). They found that underpotential deposition of Bi(0) occurred in the region of 0.35 V ≤ E_D ≥ −0.23 V and ring collection curves yielded theoretical collection efficiencies.

In this study, Bi(III) in 0.1 M HNO_3 was determined using Electrode I over the concentration range of 10^{-7} to 10^{-6} M Bi(III). The ring was potentiostated at −0.25 V, a potential at which the reduction of Bi(III) to Bi(0) is convective diffusion-controlled.

A typical i_R–E_D curve for Bi(III) ($C_{\mathrm{Bi(III)}} = 4.86 \times 10^{-7}$ M) is shown in Figure 5. The ring does not shield until E_D = +0.35 V and is fully shielded in the region E_D ≤ −0.25 V. The anodic scan shows a ring current peak due to Bi(0) oxidation at the disk in the region +0.2 V ≤ E_D ≤ +0.5 V.

The disk limiting current for the reduction of Bi(III) to Bi(0) obtained in solutions 2.02×10^{-5} M ≤ $C_{\mathrm{Bi(III)}}$ ≤ 5.82×10^{-5} M gives a linear plot of slope 0.934 ± 0.004 μA/μM. Linear plots of Δi_R vs. concentration (Figure 4) are obtained for 4.86×10^{-7} M ≤ $C_{\mathrm{Bi(III)}}$ ≤ 9.63×10^{-6} M with a slope of 0.350 ± 0.005 μA/μ*M*, giving an experimental value of *N* = 0.375. Results at lower concentrations gave slightly poorer agreement, i.e., a value of 0.330 for *N* in the range 5×10^{-8} M to $5\ 10^{-7}$ M Bi(III). The theoretical *N* for Electrode I is 0.364.

Determination of Ag(I). The underpotential deposition of Ag on Pt has been studied at a Pt RRDE in 0.2 M H_2SO_4 by Tindall and Bruckenstein (*12*) by potentiostating the ring at E_R = +0.10 V.

In our investigation, Ag(I) was determined in 0.2 M H_2SO_4 at concentration levels of $C_{\mathrm{Ag(I)}} \geq 5 \times 10^{-8}$ M using Electrode II and a ring potential of +0.10 V, at which potential the reduction of Ag(I) to Ag(0) is convective diffusion-controlled at the ring.

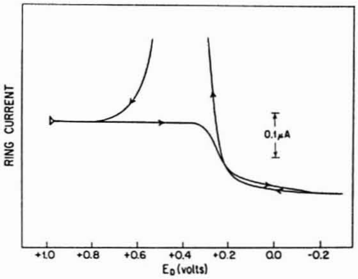

Figure 5. Ring current–disk potential curve for $C_{\mathrm{Bi(III)}} = 4.86 \times 10^{-7}$ M–0.1 M HNO_3. Electrode I, potential scan rate 200 mV/s. E_R = −0.25 V

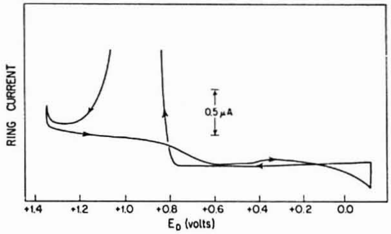

Figure 6. Ring current–disk potential curve for $C_{\mathrm{Ag(I)}} = 1.55 \times 10^{-6}$ M–0.2 M H_2SO_4. Electrode II, potential scan rate 200 mV/s. E_R = +0.10 V

A typical i_R–E_D curve is shown in Figure 6 ($C_{\mathrm{Ag(I)}} = 1.55 \times 10^{-6}$ M). A constant ring current is observed until E_D = +0.9 V, at which potential ring shielding begins because of underpotential deposition of Ag(0) at the disk. In the anodic scan, a peak at +0.8 V ≤ E_D ≤ +1.2 V occurs in the ring current due to the oxidation of Ag(0) at the disk.

Values of $i_{\mathrm{D,L}}$ obtained for the reduction of Ag(I) to Ag(0) in 9.57×10^{-5} M ≤ $C_{\mathrm{Ag(I)}}$ ≤ 1.88×10^{-4} M solutions gave a linear plot of slope 0.574 ± 0.002 μA/μM. Shielding studies were performed for $C_{\mathrm{Ag(I)}} \geq 5 \times 10^{-8}$ M. A plot of Δi_R vs. concentration was linear and had a slope of 0.211 ± 0.008 μA/μM for 4.88×10^{-8} M ≤ $C_{\mathrm{Ag(I)}}$ ≤ 6.78×10^{-7} M. This slope corresponds to a value of 0.368 for *N*. Experiments at slightly higher concentrations (7.88×10^{-7} M ≤ $C_{\mathrm{Ag(I)}}$ ≤ 6.90×10^{-6} M) yielded a slope of 0.214 ± 0.002 μA/μM, i.e., *N* = 0.373 (Figure 4). The theoretical *N* for Electrode II is 0.374.

Determination of Fe(III). The systems described above all involve underpotential metal deposition as the reaction of analytical interest. However, it is not necessary that this be the case for the ring shielding technique to be useful. To demonstrate this, determinations of Fe(III) were carried out for solutions of $C_{\mathrm{Fe(III)}} \geq 5 \times 10^{-7}$ M, in 0.2 M H_2SO_4 by the reduction of Fe(III) to Fe(II) at Electrode II. The ring was potentiostated at E_R = +0.05 V and a scan rate of 100 mV/s employed.

RRDE studies at 1 mM Fe(III) in 0.2 M H_2SO_4 show a well-defined reduction wave for Fe(III) to Fe(II) starting near E_D = +0.5 V and exhibit a limiting current at E_D = +0.05 V (Figure 7). With the ring potentiostated at +0.05 V, the ring reduction reaction of Fe(III) to Fe(II) is convective diffusion-controlled and the ring is shielded for E_D < +0.50 V. At ring potentials more cathodic than +0.05 V, hydrogen evolution interferes.

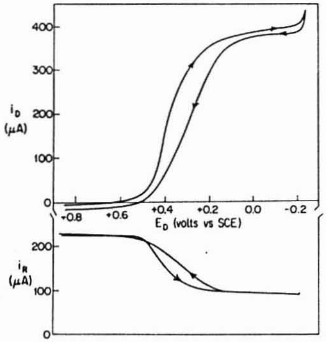

Figure 7. Current-potential curve for 1.5×10^{-3} M Fe(III)–0.2 M H_2SO_4. Electrode II, potential scan rate 10 mV/s. Disk, upper curve; ring, lower curve. Arrows indicate direction of potential scan. $E_R = +0.05$ V

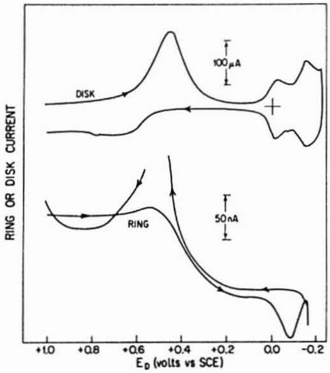

Figure 8. Current-potential curve for 1.06×10^{-6} M Fe(III)–0.2 M H_2SO_4. Electrode II, potential scan rate 100 mV/s. Disk, upper curve; ring, lower curve. Arrows indicate direction of potential scan. $E_R = +0.05$ V

Steady-state currents for Fe(III) reduction to Fe(II) were determined for 1.06×10^{-4} M $\leq C_{Fe(III)} \leq 2.04 \times 10^{-4}$ M. A plot of $i_{D,L}$ vs. concentration was linear with a slope of 0.167 ± 0.003 μA/μM.

At low concentrations of Fe(III) ($C_{Fe(III)} < 10^{-5}$ M), $i_{D,L}$ is obscured by charging currents and surface processes occurring at the disk electrode. However, the i_R–E_D curve shows a definite shielding wave due to the reduction of Fe(III) at the disk (Figure 8).

A small stripping peak in the anodic i_R–E_D scan with an area of about 0.2 μC is observed at about 0.5 V. This peak is probably due to the impurities that contribute to the residual shielding of 25 nA. This residual current was fairly constant from day to day despite thorough cleaning of the cell and limited the determination of Fe(III) to concentration levels of $C_{Fe(III)} \geq 5 \times 10^{-7}$ M.

A plot of Δi_R vs. concentration of Fe(III) is shown in Figure 4. For 5.30×10^{-7} M $\leq C_{Fe(III)} \leq 4.24 \times 10^{-6}$ M, a slope of 0.062 ± 0.002 μA/μM was obtained, yielding an experimental value of $N = 0.371$. This value compares well with the theoretical value of 0.374 for Electrode II.

Simultaneous Determination of Ag(I) and Cu(II). The shielding method is also applicable to the simultaneous determination of mixtures of metal ions, provided their half-wave potentials are sufficiently separated.

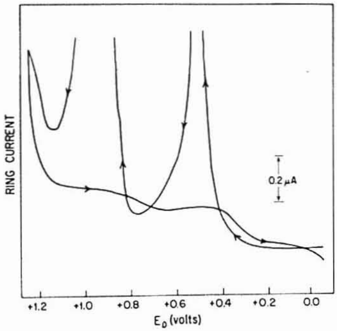

Figure 9. Ring current–disk potential curve for $C_{Cu(II)} = 7.62 \times 10^{-7}$ M, $C_{Ag(I)} = 6.86 \times 10^{-7}$ M. Electrode II, potential scan rate 200 mV/s. $E_R = -0.25$ V

Tindall and Bruckenstein previously performed simultaneous determinations of Ag(I) and Cu(II) by stripping voltammetry from the Pt disk of a RRDE and collection at the ring electrode (*16*). Solutions 10^{-5} M to 10^{-8} M in Ag(I) and Cu(II) in 0.2 M H_2SO_4 were determined by this method with 10–15% reproducibility. Therefore, this system seemed well suited for determination of Ag(I) and Cu(II) by the ring shielding technique.

Initially, studies were performed in 0.2 M H_2SO_4 using Electrode II. Tindall and Bruckenstein (*15*) have studied Cu(II) reduction in sulfuric acid at a Pt RRDE. They used an $E_R = -0.22$ V, and found poor agreement between the value of N as calculated from electrode geometry and that observed from experiment. They concluded that a potential of −0.22 V was not sufficient to attain the limiting convective diffusion-controlled current for Cu(II) reduction. We, too, found this to be the case. Also, at this potential pseudo-collection effects due to uncompensated ohmic interactions were a problem (*17*).

A gold ring–platinum disk RRDE (Electrode III) allowed using a more cathodic ring potential ($E_R = -0.25$ V) than was possible at platinum. Even though this E_R was not sufficient to reach the limiting convective diffusion-controlled current on gold, the results were superior to using a platinum ring at a less cathodic E_R. At more cathodic gold ring potentials, reproducible ring currents could not be obtained.

Disk limiting currents for Ag(I) reduction were obtained as described above for the determination of Ag(I) in the absence of Cu(II). Attempts to measure limiting currents for Cu(II) reduction were unsuccessful at both the Pt and Au RDEs. However, a well-defined wave for Cu(II) reduction was found using a carbon RDE with an area of 0.281 cm². Steady-state currents for Cu(II) reduction to Cu(0) were obtained at $E_D = -0.50$ V and a plot of $i_{D,L}$ vs. concentration gave a slope of 0.427 ± 0.004 μA/μM for 2.02×10^{-5} M $\leq C_{Cu(II)} \leq 9.33 \times 10^{-5}$ M. The calculated disk limiting current for Cu(II) reduction to Cu(0) at Electrode III is 0.691 μA/μM.

Shielding studies were performed for series of solutions 1×10^{-7} M to 5×10^{-6} M Ag(I) and Cu(II) in 0.2 M H_2SO_4. Initially, the concentration of one ion was held constant while the other ion's concentration was changed to determine whether the observed ring shielding currents for Ag(I) and Cu(II) were independent of one another.

A typical i_R-E_D curve for a mixture of Ag(I) and Cu(II) is shown in Figure 9. The ring is initially shielded in the region $+1.1 \text{ V} \leq E_D \geq +0.6$ V because of underpotential deposition of Ag(0). The ring is then further shielded for $E_D \leq +0.5$ V

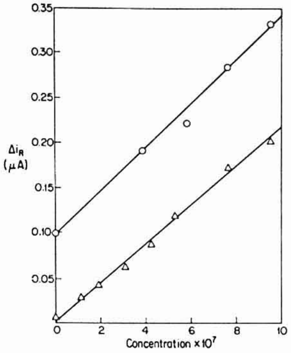

Figure 10. Plot of Δi_R vs. concentration of Ag(I) and Cu(II) for simultaneous determinations. (O) Cu(II), slope = 0.257 ± 0.015 μA/μM; intercept = 0.086 ± 0.011 μA. (Δ) Ag(I), slope = 0.218 ± 0.008 μA/μM; intercept = −0.001 ± 0.004 μA

because of underpotential deposition of Cu(0). Two ring current peaks are present in the anodic scan due to Cu and Ag oxidation at the disk. If the total metal deposition exceeds one monolayer, an additional ring current peak is found (*16*). We observed this peak only at higher concentrations in mixtures of Ag(I) and Cu(II).

Results for simultaneous determination of Ag(I) and Cu(II) (approximately equal concentrations) gave good results for 1.17×10^{-7} M $\leq C_{\mathrm{Ag(I)}} \leq 6.86 \times 10^{-7}$ M. A plot of Δi_R vs. $C_{\mathrm{Ag(I)}}$ yielded a straight line of slope 0.218 ± 0.008 μA/μM (Figure 10). The experimental collection efficiency of 0.419 compares well with the theoretical value of $N = 0.409$ for Electrode III.

Plots of Δi_R vs. $C_{\mathrm{Cu(II)}}$ for $C_{\mathrm{Cu(II)}} \geq 5 \times 10^{-7}$ M were linear and had a slope of 0.257 ± 0.015 μA/μM for 3.88×10^{-7} M $\leq C_{\mathrm{Cu(II)}} \leq 1.15 \times 10^{-6}$ M (Figure 10). This slope yields a value of $N = 0.372$. The rather poor agreement with the theoretical collection efficiency ($N = 0.409$) arises because an $E_R = -0.25$ V on gold is not sufficiently cathodic to produce a convective diffusion-controlled ring current for Cu(II) reduction. Satisfactory results at $C_{\mathrm{Cu(II)}} \leq 5 \times 10^{-7}$ M could not be obtained.

For $C_{\mathrm{Cu(II)}} \geq 5 \times 10^{-6}$ M, a plot of Δi_R vs. $C_{\mathrm{Cu(II)}}$ had a downward curvature because appreciable amounts of copper deposit at the ring during the experiment. As was noted by Tindall and Bruckenstein (*16*), after more than about 10 atom layers of copper deposit on the ring, reduction of copper became very irreversible, and there is a decrease in the observed collection efficiency. This decrease is not encountered at lower copper concentrations since the duration of the experiment is too short to deposit significant amounts of copper at the ring electrode.

Table II. Comparison of Analytical Sensitivities

	sensitivity in ng/mL			
element	DPP (*18*)	NFAAS (*18*)	ICPAES (*18*)	ring shielding^a
Ag		0.001	4	4.3
Bi	0.2		5.0	10.5
Cu	13.7		1	9.5
Fe	1000.		5	22.

^{a} Detection limit taken as amount required to double background response.

CONCLUSION

The use of the ring shielding mode of a rotating ring-disk electrode affords a simple, fast method for the determination of micromolar and submicromolar levels of electroactive species in solution. The ability of the ring electrode to monitor species consumed at the disk provides a significant analytical advantage over direct electrode voltammetry at low solution concentrations. The technique provides good accuracy for concentration levels of $\geq 5 \times 10^{-7}$ M.

Table II presents a comparison of the sensitivity obtained by us for the ring shielding technique with that previously given (*18*) using differential pulse polarography (DPP), nonflame atomic absorption spectroscopy (NFAAS) and inductively coupled plasma sources for atomic emission spectroscopy (ICPAES). As can be seen, the ring shielding technique is quite competitive.

LITERATURE CITED

(1) S. Bruckenstein, *Elektrokhimiya*, **2**, 1085 (1966).
(2) W. J. Albery, S. Bruckenstein, and D. T. Napp, *Trans. Faraday Soc.*, **62**, 1932 (1966).
(3) D. T. Napp, D. C. Johnson, and S. Bruckenstein, *Anal. Chem.*, **39**, 481 (1967).
(4) S. Bruckenstein and B. Miller, *Acc. Chem. Res.*, **10**, 54 (1977).
(5) V. G. Levich, "Physicochemical Hydrodynamics", Prentice-Hall, Englewood Cliffs, N.J. 1962, p 60.
(6) Ref. 5, p 107.
(7) A. N. Frumkin, L. N. Nekrasov, V. G. Levich, and Yu. B. Ivanov, *J. Electroanal. Chem.*, **1**, 84 (1959).
(8) W. J. Albery and S. Bruckenstein, *Trans. Faraday Soc.*, **62**, 1920 (1966).
(9) W. J. Albery and M. L. Hitchman, "Ring-Disc Electrodes", Oxford University Press, Ely House, London W.1. 1971.
(10) D. Untereker, W. Sherwood, G. Martinchek, T. Reidhammer, and S. Bruckenstein, *Chem. Instrum.*, **6**, 259 (1975).
(11) D. F. Untereker, Ph.D. Thesis, SUNY at Buffalo, Buffalo, N.Y., 1973.
(12) G. W. Tindall and S. Bruckenstein, *Electrochem. Acta.*, **16**, 245 (1971).
(13) S. H. Cadle and S. Bruckenstein, *Anal. Chem.*, **43**, 932 (1971).
(14) S. H. Cadle and S. Bruckenstein, *J. Electrochem. Soc.*, **119**, 1966 (1972).
(15) G. W. Tindall and S. Bruckenstein, *Anal. Chem.*, **40**, 1051 (1968).
(16) G. W. Tindall and S. Bruckenstein, *J. Electroanal. Chem.*, **22**, 367 (1969).
(17) M. Shabrang and S. Bruckenstein, *J. Electrochem. Soc.*, **122**, 1305 (1975).
(18) J. J. Dulka and T. H. Risbey, *Anal. Chem.*, **48**, 640A (1976).

RECEIVED for review September 18, 1978. Accepted November 20, 1978. This work has been supported by the Air Force Office of Scientific Research under Grants AFOSR 783621 and 742572.

Optimization of Precision in Dual Wavelength Spectrophotometric Measurement

Kenneth L. Ratzlaff* and Hamzah bin Darus[1]

Department of Chemistry, The Michael Faraday Laboratories, Northern Illinois University, DeKalb, Illinois 60115

The theory describing the precision of dual wavelength spectrophotometric (DWS) measurement is extended and validated using a DWS instrument fully under computer control. DWS measurement is shown to be effective in combatting uncertainty due to optical artifacts produced by samples and cells under non-ideal conditions. A method of controlling the light level makes possible measurement of analyte absorbance in the presence of several units of interferent absorbance.

Recently, a treatment (*1*) of the precision of Dual Wavelength Spectrophotometric (DWS) measurement produced several new conclusions concerning the conditions under which optimum precision could be obtained and made several comparisons with Single Wavelength Spectrophotometric (SWS) measurement. Among these are the following.

(1) In the absence of interferents and sample presentation variations, SWS measurement will generally provide better precision than DWS measurement.

(2) Employment of DWS measurement may reduce sample presentation variations; this may lead to better precision for DWS measurement than for SWS when the sample creates distortions in the beam.

(3) Although the absorbance of an interferent may be cancelled in DWS measurement (the primary advantage of DWS), the interferent seriously degrades the precision so that measurement is nearly prohibited in the presence of greater than two to three units of interferent absorbance.

In the investigation described herein, the theoretical treatment is expanded to cover more carefully sample presentation variations and to present a new mode of light intensity programming. With regard to the latter, the output signal of a spectrophotometer may be scaled in a variety of ways to suit the measurement and the signal processing system. Commercially significant techniques for SWS instruments include programming the slit, which may degrade resolution, and programming the gain of the photomultiplier tube, which yields no improvement if the uncertainty in the measurement is signal shot-noise limited. Neither method is suitable for DWS measurement in the presence of serious optical interference. Consequently, new programming techniques must be investigated.

The theoretical investigations must be validated by experimental studies. To that end, the development of a highly flexible DWS spectrophotometer is described which is fully under computer control. The extent of that control makes possible both the self-optimization of a wide variety of experimental parameters and the control and adjustment of those parameters where required to test their effect.

THEORETICAL

As previously described (*1*), the measured DWS value, ΔA, is the difference in the absorbances at λ_1 and λ_2:

$$\Delta A = A_1 - A_2 = (\epsilon_1 - \epsilon_2)bc = (1 - \beta)\epsilon_1 bc \qquad (1)$$

where ϵ_1 and ϵ_2 are the molar absorptivities at λ_1 and λ_2, and b, c, and β are length, concentration, and the ratio, ϵ_2/ϵ_1, respectively. Expressed in terms of the detected radiant powers,

$$\Delta A = -\log (\Phi_1/\Phi_2) + \log K \qquad (2)$$

where Φ_1 and Φ_2 are the transmitted radiant powers and K is the ratio of the incident intensities, Φ_{01}, Φ_{02}, at wavelengths λ_1 and λ_2, respectively.

Where D is the absorbance or scattering of an interferent and is equal at both wavelengths, the relative standard deviation in the measurement of ΔA was written as

$$\%\sigma_{\Delta A} = (2.3(1 - \beta)A_1)^{-1}\left[\left[\frac{\sigma_1}{10^{-D}10^{-A_1}E_{01}}\right]^2 + \left[\frac{\sigma_2}{10^{-D}10^{-\beta A_1}E_{01}}\right]^2\right]^{1/2} \times 100\% \qquad (3)$$

where E_{01} is the photosignal resulting from the incident intensity at λ_1; $\sigma_1{}^2$ and $\sigma_2{}^2$ are the variances in the photosignal resulting from the measurements of Φ_1 and Φ_2. When $\beta = 0$ and $K = 1$, this equation describes SWS precision as well.

The uncertainties in the photosignals, σ_1 and σ_2, are related to those photosignals in three possible ways: independent of, proportional to the square root of, and proportional to that signal.

The relative standard deviation in the value of ΔA for independent uncertainty is

$$(\%\sigma_{\Delta A})_I = \frac{\sigma_I 10^D}{2.3E_{01}(1 - \beta)A_1}\,[10^{2A_1} + K^{-1}\,10^{2\beta A_1}]^{1/2} \times 100\% \qquad (4)$$

where $\sigma_I = \sigma_1 = \sigma_2$ and σ_I/E_{01} is the uncertainty in any photosignal measurement relative to the reference signal. Equation 4 is plotted for various values of β as the dotted lines in Figure 1 where $\sigma_I/E_{01} = 0.5 \times 10^{-3}$.

For square root uncertainty

$$(\%\sigma_{\Delta A})_P = \frac{10^{D/2}}{2.3(1 - \beta)A_1}\left[\frac{1}{PE_{01}}\,[10^{A_1} + K^{-1}10^{\beta A_1}]\right]^{1/2} \times 100\% \qquad (5)$$

where the product PE_{01} may be considered to be the number of photoevents in the measurement interval for E_{01}. The value of P may be calculated from operational parameters since $P^{-1} = 2\,meR_f\Delta f$ where m, e, R_f, and Δf are PMT gain, electronic charge, feedback resistance of the OA current-to-voltage converter, and noise equivalent bandwidth. The proportionality factors involved in P are discussed in references 1 and 2. Equation 5 is plotted in various values of β in Figure 2 for $PE_{01} = 10^6$.

Finally for proportional uncertainty

$$(\%\sigma_{\Delta A})_P = \frac{\sqrt{2}\xi}{2.3(1 - \beta)A_1} \times 100\% \qquad (6)$$

where ξ is the "flicker factor", a proportionality factor between

---

[1] Present address, Department of Chemistry, Kansas State University, Manhattan, Kansas.

0003-2700/79/0351-0256$01.00/0 © 1979 American Chemical Society

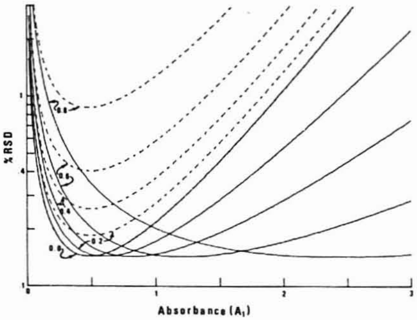

Figure 1. Percent relative standard deviation (% RSD) as a function of absorbance for various values of β under conditions of independent uncertainty. The dashed lines and solid lines represent measurement without and with programmable attenuation, respectively. The lines are calculated from Equations 4 and 10, respectively, where $\sigma_I/E_{01} = 5 \times 10^{-4}$

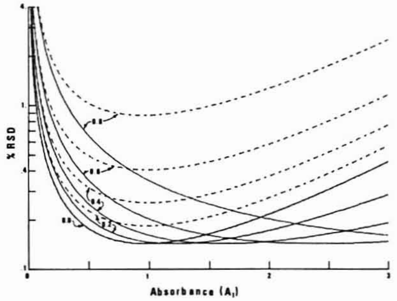

Figure 2. Percent relative standard deviation (% RSD) as a function of absorbance for various values of β under conditions of square root uncertainty. The dashed lines and solid lines represent measurement without and with programmable attenuation, respectively. The lines are calculated from Equations 5 and 11, respectively, where $PE_{01} = 10^6$

the signal and the uncertainty in that signal; ξ is considered here to be approximately equal for both wavelengths. Obviously, $(\%\sigma_{\Delta A})_P$ monotonically decreases with A_1 so that it will seldom be limiting except at low A_1.

In all the above cases, $\%\sigma_{\Delta A}$ is proportional to $(1 - \beta)^{-1}$ so that the expected precision is poorer for DWS measurement than for SWS since a SWS measurement may be represented by setting $\beta = 0$. In Equations 4 and 5, the dependence of $\%\sigma_{\Delta A}$ on D is very strong, drastically degrading precision when interferences are present.

Correlated Sample Presentation Variations. In discussing the various contributions to proportional uncertainty in SWS measurement, Ingle and co-workers (*2, 3*) have pointed out that the most significant might be that due to variations in the optical qualities of the sample and cell, even in high quality cells. Where flow cells or cells of lower quality must be used, the problem is accentuated. In DWS, these variations are partially correlated however, and the suggestion has been made (*1*) that their effect could be reduced.

This may be shown somewhat more rigorously by adding to Equation 3 the covariance term of propagation of error mathematics (*4*). This step is necessary since the two beams, whose radiant powers are ratioed in Equation 2, follow a nearly identical path; consequently, the optical variations are largely correlated. Equation 3 now becomes

$$(\%\sigma_{\Delta A})_V = (2.3(1-\beta)A_1)^{-1}\left[\left[\frac{\sigma_1}{10^{-D}10^{-A_1}E_{01}}\right]^2 + \left[\frac{\sigma_2}{K10^{-D}10^{-\beta A_1}E_{01}}\right]^2 - 2\left[\frac{\sigma_1}{10^{-D}10^{-A_1}E_{01}}\,\frac{\sigma_2}{K10^{-D}10^{-\beta A_1}E_{01}}\right]\right]^{1/2} \quad (7)$$

Substituting for σ_1 and σ_2, ξ is specified separately at λ_1 and λ_2 as ξ_1 and ξ_2.

$$\sigma_1 = \xi_1 E_{01} 10^{-(D + A_1)}$$

$$\sigma_2 = \xi_2 K E_{01} 10^{-(\mathrm{D} + \beta A_1)}$$

$$(\%\sigma_{\Delta A})_V = (2.3(1-\beta)A_1)^{-1}|\xi_1 - \xi_2| \times 100\% \quad (8)$$

Although the term $\xi_1 - \xi_2$ may approach null, the wavelength dependences of the phenomena which produce the variance will generally make it non-zero; these phenomena probably include light scattering by surfaces and suspended materials and refraction by oblique surfaces and gradients in the sample. In any case, by comparing Equation 8 (adapted to SWS by setting β to 0) with Equation 6, it is apparent that the uncertainty due to sample presentation will be less for DWS than for SWS if $(\xi_1 - \xi_2)/(1 - \beta) < 2\xi$.

Precision with Programmable Attenuation. Where the magnitude of the reference incident power, Φ_{01} or Φ_{02}, is not limited by source intensity or the throughput of the optical system, an effective upper limit is determined by the detector and data acquisition system; a photomultiplier will fatigue if operated at excessive photocurrent levels while multichannel detectors such as vidicons, photodiode arrays, and charge-coupled device photoarrays will saturate. Amplifiers and analog-to-digital converters also have an upper limit past which they no longer provide meaningful values. On the other hand, for each unit of absorbance by analyte or interferent, the signal is reduced by an order of magnitude resulting in decreased precision. Examination of Equations 4 and 5 suggests that for optimum precision the photosignal should be kept as close to E_{01} as possible.

When making a DWS measurement, the values of both Φ_{01} and Φ_{02} are less than the incident radiant powers. Therefore, if the incident power could be increased at both wavelengths by precisely the same factor so that the photosignal at λ_1 or λ_2 approaches the limit, the precision could be improved without loss of accuracy. That factor would be the inverse of the transmittance at the wavelength producing the larger signal; in this treatment, that wavelength has been considered to be λ_2. In such a case both measurements could be made at a higher signal level.

The factor by which E_{01} can be increased is $10^D 10^{\beta A_1}$ so that Equation 3 becomes

$$\%\sigma_{\Delta A}' = \{2.3(1-\beta)A_1\}^{-1}\left[\left[\frac{\sigma_1}{10^{-(1-\beta)A_1}E_{01}}\right]^2 + \left[\frac{\sigma^2}{KE_{01}}\right]^2\right]^{1/2} \times 100\% \quad (9)$$

The prime indicates that the intensity is programmed.

Where the uncertainty is constant, $\sigma_I = \sigma_1 = \sigma_2$.

$$(\%\sigma_{\Delta A}')_I = \frac{\sigma_I}{2.3(1-\beta)A_1E_{01}}\,[10^{2(1-\beta)A_1} + K^{-2}]^{1/2} \times 100\% \quad (10)$$

Equation 10 is plotted for various values of β as the solid lines in Figure 1.

As it was for Equation 5, square root uncertainty is treated by making σ_1 and σ_2 proportional to the square root of the signal.

$$\sigma_1 = \{(10^{-(1-\beta)A_1})E_{01}/P\}^{1/2}$$

$$\sigma_2 = (KE_{01}/P)^{1/2}$$

$$(\%\sigma_{\Delta A})_S = (2.3(1-\beta)A_1)^{-1}\,[10^{(1-\beta)A_1}/E_{01}P + (KE_{01}P)^{-1}]^{1/2} \times 100\% \quad (11)$$

Equation 11 is plotted for various values of β as the solid lines in Figure 2.

In the case of proportional uncertainty, the precision is independent of the magnitude of the photosignal. Consequently, controlling the intensity will have no effect. However, since the total variance of the measurement is the sum of the individual variances, measurements are usually limited by the independent or square root uncertainties which are usually higher than the proportional uncertainty.

In comparing Equations 4 and 5 with 10 and 11, two significant differences stand out. First, the dependence of the precision on A_1 is weaker where $\beta > 0$ in Equations 10 and 11; this is easily observed in Figures 1 and 2. Secondly, and more significantly, the very strong dependence of the precision on D in Equations 4 and 5 is eliminated.

It should be noted that the required capacity to increase radiant power by the factor of $10^{(D+\beta A_1)}$ is not readily obtained since, if increased radiant power was available, it might appear reasonable to use it at all times. However, since the detection system will have an upper limit, the radiant power must be reduced from its maximum to a level compatible with the detection system. The radiant power can then be increased as D and βA_1 increase. Alternatively, if an integrating detector or a voltage-to-frequency converter and counter is used, the integrated radiant power can be programmed by simply changing the integration period.

EXPERIMENTAL

Instrumental. The system developed to test the principles developed above is based on a GCA McPherson EU-721 spectrophotometer system and a microcomputer-based minicomputer system. The computer system is built around an 8080 and/or Z-80 microprocessor on the S-100 bus. Peripherals include floppy disk, CRT, and printer. Programs were written in BASIC with assembler subroutines. The computer system was described in detail elsewhere (*5*).

The original light source module was replaced with a high intensity light source module to obtain the requisite wide dynamic range in intensity necessary for the application of Equations 10 and 11. The module contains a 30-V, 375-W tungsten halide lamp (Sylvania DWZ) with a linear filament. A concave mirror collects and collimates the light, and the infrared radiation is removed by a heat-absorbing filter. A Kepco Ks36-30M regulated dc power supply is operated in the current-regulated mode, and current level may be controlled by the computer via an 8-bit digital-to-analog converter.

A second mode of programming the intensity is accomplished by use of linear variable transmission wedges which are positioned in the beam by driving a precision rack (Berg No. RI-8) with a dc gear motor (Hughes C-54). Unregulated ±6-V power to drive the motor is switched with mechanical relays. Micro switches at the limit positions limit the travel; these switches also signal the computer of limit condition. Using short pulses (about 100 ms) to the motor and reading the photocurrent between each, the light intensity can be adjusted under program control to within 10% of a present level in 1 s or less.

An absolute shaft encoder (Norden ADC-13-BNRY-A), which generates 128 counts per revolution, is used to monitor the position of the attenuator. The value is read via parallel I/O ports. A 48-tooth, 64-pitch spur gear couples the encoder to the rack providing resolution of 0.47 mm per count.

Several linear optical attenuators were tried in hope of finding one which attenuates equally over a wide wavelength region. The first was a linear neutral density wedge (Edmund Scientific). A second wedge was produced by imaging a pattern in gold on quartz; the pattern consists of a 40-tooth comb, each tooth being a triangle approximately 0.64 mm by 330 mm. The 1:1 photographic negative for the comb was also tested.

A third mode of programming was the use of an iris, adjustable under program control. A geared pulley was mounted on the iris and coupled by a plastic belt to a pulley on a small stepping motor (HSI 36740-63) so that it may be closed in 180 steps. The fully open position is indexed via a micro switch, and a given aperture can be reproduced by counting a preset number of steps.

The signal level but not the intensity could also be programmed via the gain on the photomultiplier tube or by a programmable gain amplifier; the former was used. A 0- to 10-V digital-to-analog converter controls the voltage on the photomultiplier tube in the EU-701-30 detector module. It should be noted, however, that programming the photomultiplier gain has no effect on the photon flux, and consequently it has no effect on square root uncertainty. However, it does provide a convenient method for initially adjusting the output current level to the input of the data acquisition system.

The photomultiplier current is converted to a voltage using an operational amplifier (RCA 3140) with a 10-MΩ resistor in parallel with a 100-pf capacitor in the feedback loop. The relatively long time-constant eliminates the need for a sample-and-hold amplifier preceding the analog-to-digital converter.

The analog-to-digital converter is a 10-bit successive approximation converter whose effective resolution was increased according to the technique suggested by Horlick (*6*); a sine wave generator was connected to the amplifier's summing point through a 10^8-Ω resistor, thereby adding pseudo-random noise to the signal. The generator was adjusted at 1 kHz for approximately 1 V peak-to-peak output with 0.5 V offset. By summing 255 conversions for each measurement, the effective resolution is approximately 12 binary bits.

The monochromator (EU-700) is a Czerny-Turner mount grating monochromator. The wavelength control may be driven by either stepper motor or dc slew motor; each of these was interfaced to the computer so that it may be activated under program control. An encoder, coupled to the drive, produces pulses which were directed to an up/down counter in the computer interface so that the current wavelength is continuously available to the program.

DWS wavelength modulation is performed by rotating the mirror which focuses the light from the grating onto the exit slit. The mount for the parabolic mirror was replaced by a precision mirror mount (Oriel, Model 1450); a precision spur gear was mounted on the horizontal rotation micrometer and coupled to a gear on a stepping motor (Superior Electric, Type SS25-1140) mounted outside the monochromator. Absolute indexing of the drive is possible by stepping to a limit switch. The motor is driven by pulses produced by a computer output port. The excursion of the wavelength modulation was limited by loss in intensity at $\Delta\lambda$ more than about −20 nm, where K drops to about 0.3.

A split beam module based on the design of Defreese and Malmstadt (*7*) was also used for some preliminary work to obtain simultaneous dual wavelength output. The exit folding mirror was replaced by a beam splitter so that radiation appears both at the original exit slit and on the front focal plane. A carriage containing an adjustable slit and photomultiplier tube housing is positioned laterally along the focal plane by a stepping motor. Except where noted, this module was not used for the investigations described herein.

A Programmable Sample Chamber (EU-721-11) was used. This module contains an oscillating cell holder which may be halted in either sample or reference position upon receipt of a TTL signal. Internal reed relay closures signal the computer when the holder has reached one position or the other.

Reagents. A stock solution of $K_2Cr_2O_7$ dissolved in 0.1 M KOH was used to prepare a series of solutions of varying absorbances. These were used for studies of precision as a function of absorbance at the analytical wavelength pair 395 and 407 nm. At these wavelengths $\beta = 0.292$.

For the studies of precision as a function of interferent concentration, a series of solutions were prepared in which varying amounts of *p*-nitrophenol were added to a constant amount of potassium chromate. At the analytical wavelength pair employed for potassium chromate, β for *p*-nitrophenol is 1.00, and ΔA = 0.

Study of the Programmable Attenuator. It was first necessary to determine whether or not the intensity could be precisely programmed; this was done by measuring the wavelength dependence of each of the programming techniques.

For each technique, the value of K was determined as a function of attenuation at the 395/407 nm wavelength pair. This was performed by programing the light source power supply, by varying the position of the attenuator with each type of optical wedge, or by varying the aperture of the iris. K could also be determined as a function of encoder or stepper position for future use.

Study of Sample Presentation Variations. To determine the extent to which DWS measurement can correlate the sample presentation variations, it is useful to increase those variations by using a flow cell with nonhomogeneous contents or a poor quality conventional cell; a plastic cell was used. With the cell position fixed in the cell holder, both A_1 and ΔA were measured by making a set of 20 measurements, averaging, and computing the standard deviation. This procedure was repeated 20 times with the cell removed and replaced between each set.

The 20 averages were then averaged, and the standard deviation of that population was determined and compared with the average standard deviation of the 20 sets. The standard deviation of the averages would, in the absence of positioning variations, be expected to be equal to the average standard deviation of the 20 sets divided by $\sqrt{20}$. The extent to which those values are different is then a measure of the effect of sample presentation uncertainty on both SWS and DWS measurement.

Study of DWS Uncertainties. DWS measurements were made both as a function of A_1 and of D in order to compare Equations 4 and 5 with 10 and 11. Each datum consists of the standard deviation of 20 measurements with the cell in a fixed position.

The programmed sequence for DWS operation will be briefly described. Upon initialization, the computer closes the attenuator to a minimum light level, zeroes the dual wavelength stepper drive, and queries the operator for the current monochromator wavelength, λ_1, the desired λ_1 and $\Delta\lambda$, and LMODE. If LMODE = ' YES ', the computer will later optimize λ_1 for the particular interferent.

If it is necessary to search for λ_1, the slew motor is activated in the appropriate direction and stopped when the encoder value indicates that the monochromator is close to λ_1. The number of steps required to reach λ_1 is then computed and the monochromator is stepped to $\lambda_1 \pm 0.01$ nm.

The photomultiplier voltage is then optimized under program control so that the larger signal of those corresponding to the incident intensities at λ_1 and λ_2 will produce a current such that the A/D converter will approach full-scale.

If LMODE = ' YES ', the operator is requested to place a sample of pure interferent in the sample chamber. The computer adjusts λ_1 (and consequently λ_2) by determining K, moving the interferent sample into position, determining ΔA, and changing λ_1 if the absolute value of ΔA exceeds the uncertainty of the measurement.

The reference is again positioned in the beam and K is determined. The operator is then requested to place the sample in the chamber, and that sample is moved into the beam. At this point, the computer positions the attenuator until one beam, I_1 or I_2, produces a near full-scale analog-to-digital converter reading. Then the rack encoder position must be read or the stepper position must be noted so that the value of K may be corrected by the value of the relative transmission computer from the data which was stored. At that point, 20 values of ΔA may be determined, and the average, standard deviation, and relative standard deviation are determined. A new sample is then requested.

If an SWS measurement is to be made, the attenuator must be kept at a constant position since the reference intensity is constant.

Table I. Sample Presentation Uncertainty

SWS	DWS ($\Delta\lambda$ = 12 nm)
A_1 = 0.8207	ΔA = 0.5809
20 measurements without changing cell	
%σ = 0.12%	%σ = 0.15%
20 repetitions of above, replacing cell between each	
%σ = 0.15%	%σ = 0.05%

The measurement can be forced into conditions whereby it is limited by independent, square root, or proportional uncertainty by control of slit width and signal processing parameters.

For study under conditions of independent uncertainty, the limiting uncertainty in this system lies within the data acquisition system, possibly a somewhat artificial though not atypical situation. Square root uncertainty is reduced by opening the slit somewhat so that the feedback loop reduces PMT gain voltage to about 350 V while maintaining full-scale photocurrent; this ensures a high photon flux and low square root uncertainty. The independent uncertainty is primarily due to the 10-bit analog-to-digital converter. The technique for expanding its resolution as described earlier is defeated primarily by reducing the number of conversions to 16 and by reducing the sine wave frequency so that it may not approximate random noise as well.

For study under conditions of square root uncertainty, the slit width is closed to about 160 μm. The consequent reduction in photosignal with the attenuator closed causes the computer to increase the detector voltage to about 1000 V. This corresponds to a photoelectron rate of roughly 10^8 photons-s^{-1} producing a full-scale analog-to-digital conversion (*8*).

The time required for 255 conversions is 38 ms, and since the current-to-voltage amplifier time constant is about 1 ms, the measurement interval can be taken as roughly 38 ms. Consequently, a measurement represents the detection, at full scale, of roughly 3×10^6 photons. This estimate is of sufficient accuracy only to provide confidence that the measurement precision under these conditions must be limited by square root uncertainty.

For study of proportional uncertainty, other sources must be greatly reduced so that they are not limiting; this is accomplished by opening the slit to 900 μm and performing the signal processing in the normal mode. However, since this relative standard deviation monotonically decreases while the relative standard deviation due to other uncertainties increases with absorbance, it is difficult to create conditions in which the photoelectron rate is so high and independent uncertainty is so low that proportional uncertainty is limiting over a wide range; no attempt to do so was successful.

RESULTS AND DISCUSSION

Programmable Attenuation. Three modes of attenuation were attempted. In no case was K constant with intensity. The technique of programming the light source current was rejected because of the slow response. Because of the thermal inertia of the tungsten–halide lamp, up to 40 s were required for the intensity to be constant within the uncertainty of the measurement; this created a problem in the critical function of reducing the radiant power in order to remain within the range of the electronics inputs.

The dynamic range of the remaining modes was limited since the intensity could not be continuously reduced to near zero; the various linear attenuators and the iris had intensity ranges of 100 to 200. The iris proved to be the method of choice since it is not vulnerable to dirt on an optical surface. A look-up table of K values for each discrete stepping motor position can readily be produced for the analytical wavelength pair.

Sample Presentation Variations. In this study the results, summarized in Table I, indicate that sample presentation variations are significant in SWS measurement, but less significant in DWS measurement. For the measurements made without moving the cell, Equation 3 predicts that the

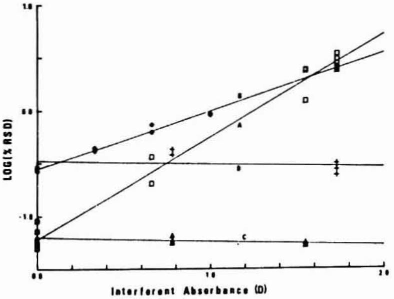

Figure 3. Experimental study of precision as a function of interferent absorbance (*D*). (A) Independent uncertainty conditions (□) with no attenuator, (B) square root uncertainty conditions (♦) with no attenuator, (C) independent uncertainty conditions (▲) with attenuator, (D) square root uncertainty conditions (+) with attenuator

relative standard deviation for DWS measurement should be greater than that for SWS by a factor of $(1 - \beta)^{-1}$. Since $\beta = 0.29$, the increase should be by a factor of 1.4; this is approximately the case.

When the values for each of the 20 sets are averaged, the relative standard deviation, exclusive of sample presentation uncertainty, should be decreased by a factor of $20^{-1/2}$. For the DWS case, the resultant relative standard deviation is only slightly larger than the predicted 0.034% indicating that the sample presentation uncertainty is less than $\{(0.05)^2 - (0.034)^2\}^{1/2}$ or 0.036%. For the SWS case, the predicted relative standard deviation of the averages should be 0.027% indicating that the sample presentation uncertainty is about 0.13%. These results indicate that where sample presentation uncertainty is significant, it can be largely correlated in the DWS measurement.

This experiment was also attempted using the split beam module; however, the results were less positive indicating that the deflections of the beam by the sample had different effects on the two detectors; this result should have been expected since the beams for the two wavelengths travel a much less identical path than they do when the wavelength is modulated by the mirror.

DWS Precision as a Function of *D*. As Equations 4 and 5 suggest, the precision of DWS measurement in the absence of a programmable attenuator is a strong function of *D*; for independent and square root uncertainties, the relative standard deviations are proportional to 10^D and $10^{D/2}$, respectively. However, with the attenuator, the dependence on *D* is eliminated (Equations 10 and 11).

The experimental dependence on *D* is shown in Figure 3. For these data, $\beta = 0.29$, and $A_1 = 0.22$. A linear regression analysis shows that curve A, corresponding to Equation 4, has a slope of $10^{0.94D}$ which is quite close to the theoretical value of $10^{1.0D}$. Similarily, curve B, corresponding to Equation 5, has a slope of $10^{0.55D}$ compared with the theoretical $10^{0.5D}$. However, when the programmable attenuator is utilized, the slope is nearly zero for both independent uncertainty (curve C) and square root uncertainty (curve D).

The programmable attenuation technique is limited by the dynamic range of the attenuator; in this case, a range of 105:1 in incident intensity was used limiting the sum of $\beta A + D$ to a maximum of about $\log_{10}(105)$ or 2.07.

DWS Precision as a Function of A_1. In the examples shown for both independent and square root uncertainty, employment of the programmable attenuator yields marked improvement in precision at higher absorbance for measurements limited either by independent uncertainty or by square root uncertainty. In Figures 4 and 5, the curves drawn through the experimental points are theoretical curves for $K = 1.0$ and $\beta = 0.29$, and the fit is sufficiently good to substantiate the predictions generated by the theory. It should be noted that *K* is not constant as a function of A_1 when the programmable attenuator is used. The consequent changes in the curves are, however, less than the uncertainty in determining the precision; therefore, they are ignored.

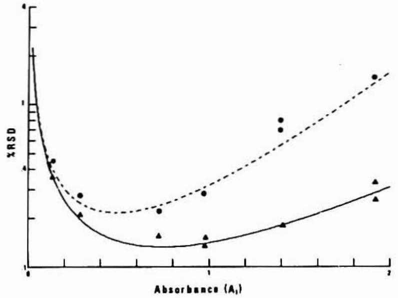

Figure 4. Experimental study of precision under conditions of independent uncertainty as a function of absorbance. (●) No programmable attenuator. (▲) With attenuator. The dashed and solid lines are calculated for $\beta = 0.29$, $K = 1.0$ from Equations 4 and 10

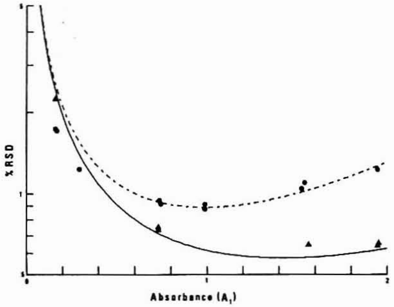

Figure 5. Experimental study of precision under conditions of square root uncertainty as a function of absorbance. (●) No programmable attenuator. (▲) With attenuator. The dashed and solid lines are calculated for $\beta = 0.29$, $K = 1.0$ from Equations 5 and 11

CONCLUSIONS

Two important conclusions can be drawn from this investigation.

(1) Where sample presentation variations are a serious problem, they may be significantly reduced by DWS measurement since the variations producing these uncertainties are largely correlated. The need for cells of high optical quality has recently been emphasized (2). However, except where pathlength variations might occur, this requirement might be relaxed for DWS measurement. Furthermore, in cases where the sample itself degrades optical quality, the DWS measurement might also be advantageous; such cases would include analyses of samples in flow cells where turbulence and density gradients can induce flicker. These data also support the assertion (2) that sample variations are not due to changes in pathlength since such changes would not be cancelled by DWS measurement.

(2) The range of molecular interferent concentration over which the value of ΔA may be precisely measured is greatly increased. In principle, if there was unlimited control over

incident radiant power, measurements could be made in the presence of several units of interferent absorbance without loss in precision.

Here the results may at first appear artificial; radiant power was attenuated at low β and D rather than being increased at high D or $\beta > 0.0$. However, it must be remembered that PMT fatigue at excessive light level and electronic over-range at high input current present real limits to the dynamic range. Furthermore, the detector signal can be integrated over longer periods of time by using integrating detectors or by using an analog-to-frequency converter and counter.

Although the range of allowable molecular interferent may be very great, when the interferent is a scattering substance, one must be much more cautious. As has been discussed previously (*9*), the effect of a scattering interferent cannot ever be completely suppressed by application of Equation 1. This is due to the fact that scattering of radiation monotonically decreases with wavelength so that no wavelength pair exists where the scattering would exactly cancel.

The instrumental work in this investigation illustrates the types of adaptations and corrections which may be made when an instrument is under complete computer control. For example, the addition of attenuator and encoder was a relatively simple task entailing the construction of only very simple additional circuits and the addition of a few statements in BASIC. However, although the methods of programming the attenuator and of modulating wavelength were imminently suitable for an investigation as this, they might not be preferred for routine work. A servo motor could probably be used to bring the attenuator to balance more rapidly, and other techniques for obtaining dual wavelength modulation have been discussed previously (*10*) and may be preferred for particular applications.

We should point out that in addition to extending the range of the DWS technique, a significant application of the work described herein should be the weighting of points used for a calibration curve. It is now clear that the precision of a measurement may vary widely with A_1, β, and possibly D, and low precision data points should not be valued as strongly in a calibration curve. Consequently, when executing a linear or polynomial regression analysis of calibration curve data, the data should be weighted according to their reliability (*4*). This could be readily written into a program which would either store both absorbance and precision as a function of concentration or use relative weighting factors computed from equations presented here.

LITERATURE CITED

(1) K. L. Ratzlaff and D. F. S. Natusch, *Anal. Chem.*, **49**, 2170 (1977).
(2) L. D. Rothman, S. R. Crouch, and J. D. Ingle, Jr., *Anal. Chem.*, **47**, 1226 (1975).
(3) J. D. Ingle, *Anal. Chim. Acta*, **88**, 131 (1977).
(4) Philip R. Bevington, "Data Reduction and Error Analysis for the Physical Sciences", McGraw-Hill, New York, 1969.
(5) Kenneth L. Ratzlaff, *Am. Lab.*, **10**, (2), 17 (1978).
(6) Gary Horlick, *Anal. Chem.*, **47**, 352 (1975).
(7) J. D. Defreese, K. M. Walczak, and H. V. Malmstadt, *Anal. Chem.*, **50**, 2042 (1978).
(8) RCA Photomultiplier Manual, RCA Electronic Components, Harrison, N.J., 1970.
(9) K. L. Ratzlaff and D. F. S. Natusch, "Theoretical Assessment of Accuracy in Dual Wavelength Spectrophotometric Measurement", submitted to *Anal. Chem.*
(10) K. L. Ratzlaff, F. S. Chuang, D. F. S. Natusch, and K. R. O'Keefe, *Anal. Chem.*, **50**, 1799 (1978).

RECEIVED for review August 14, 1978. Accepted November 20, 1978. Paper presented in part at the Great Lakes Regional American Chemical Society Meeting, Stevens Point, Wis., 1977. Partial financial support provided by the Research Corporation.

Reduction of Matrix Interferences for Lead Determination with the L'vov Platform and the Graphite Furnace

Walter Slavin* and D. C. Manning

The Perkin-Elmer Corporation, Main Avenue, Norwalk, Connecticut 06856

The addition to the graphite furnace of a thin pyrolytic graphite plate (L'vov Platform) on which the sample is deposited, makes it possible to atomize the sample at more nearly constant temperature conditions. This reduces analytical interferences that arise from a variation in the appearance temperature for Pb when it is present in different matrices. In addition, this platform makes it possible to volatilize the sample into a gas that is hotter than the surface from which the sample is volatilized. This reduces the interference resulting from the volatility of Pb halides. Using the platform, we can determine Pb in matrices which contain chloride, sulfate, and phosphate without resorting to matrix modifications. It remains necessary to carbide-coat the platform surface to reduce its reactivity with Pb.

We have studied (*1*) the potential interference effects that occur in atomic absorption graphite furnace analyses. Our initial work used Pb as a test element because it appears to be the most widely determined in the furnace. We used a chloride matrix because the literature indicated that the chloride matrix introduced the greatest problems in the determination of Pb. We showed that Pb can be determined in a chloride matrix using NH_4NO_3 as a matrix modifier additive to permit removal of a large proportion of the chloride in the charring step prior to atomization of the Pb. In addition, it was necessary to control the surface of the graphite tubes (we used molybdenum coating on pyrolytic tubes), to use signal integration to avoid errors due to changes in peak shape, and to use an atomization ramp which separated in time the residual background signal from the Pb signal. With these precautions, we were able to detect less than 20 pg of Pb in solutions containing 1% NaCl or $MgCl_2$.

While the method of additions has been widely used to quantitate analyses where interferences are present, this procedure involves extrapolation from the observed results. It would be distinctly preferable to use simple standards with

0003-2700/79/0351-0261$01.00/0 © 1979 American Chemical Society

a minimum of matrix matching to interpolate the analysis of unknown samples from conventional analytical curves. It would also be preferable to reduce or omit the matrix modifiers previously required because materials added in large quantity to samples or standards carry the risk of contamination.

L'vov's original furnace design (*2*) used an electrically heated tube into which the sample was volatilized from a graphite electrode that was independently heated. Thus the sample was introduced into the furnace which had already reached constant thermal conditions. The Massmann (*3*) design (on which most of the commercial furnaces are based) was simplified by depositing the sample directly on the wall of the furnace tube. Thus the sample is volatilized into the furnace tube as the wall passes through a temperature appropriate for the particular sample.

An important criterion for using the signal integration method of quantitating furnace analyses is that the residence times of all analyte atoms in the furnace are equal during the measurement period (*4*). However the residence time depends strongly upon the temperature of the furnace, because both the diffusion coefficient and the vapor density are temperature dependent. Since the metal is volatilized while the furnace temperature is changing, changes in the matrix which alter the time when the metal vapor is atomized will cause the metal to be atomized at a different temperature. This in turn will alter the residence time and thus the analytical results even when signal integration is used for quantitation. It would clearly be advantageous to volatilize the sample into an environment that is not changing in temperature.

It is also important to reduce to a minimum the time taken to establish constant temperature conditions. Previous Massmann-type furnace power supplies achieve the final temperature by applying a specific voltage across the graphite furnace so that at equilibrium the desired temperature will be produced. In this situation, the rate of temperature increase depends upon the difference between the starting and final temperature for the atomization step. In the Model HGA-2200 (and HGA-76B and HGA-500), a silicon diode detector is used (*5*) to determine when the temperature has reached the desired value. This permits the final temperature to be selected independently of the heating rate. When the diode detector observes that the final desired temperature has been reached, the electrical conditions of the furnaces are automatically reset to the conditions required to maintain that temperature. In this study, we use the maximum heating rate to heat the furnace as rapidly as possible to its final temperature.

L'vov et al. (*6*) have recently described the use of a thin pyrolytic graphite plate (L'vov Platform, trademark of the Perkin-Elmer Corporation) added inside the furnace tube. The sample is deposited upon this platform which rests on the inner wall of the furnace. The platform is largely heated by radiation from the furnace tube. This arrangement provides two theoretical advantages.

First, the time when the platform reaches the appearance temperatures for a particular metal will be delayed relative to the time–temperature relationship of the furnace wall. Thus the metal will be atomized when the furnace has more nearly reached constant temperature conditions.

The second advantage concerns the volatilization of molecular halides. Segar and Gonzalez (*7*) reported that copper was co-volatilized with sodium salts in the graphite furnace producing an attenuated signal for copper in the presence of NaCl. L'vov (*8*) and others have shown that such interferences arise for many metals in a halide matrix because the metal halide is volatilized as a molecule at a temperature lower than required to decompose the compound on the graphite surface. Since the gas temperature follows the wall temperature quite closely (*9*), the L'vov Platform makes it possible to volatilize the sample into the inert gas which is at a higher temperature than the sample itself. Thus there is more likelihood that the metal halide will be decomposed at the higher temperature.

Table I. Experimental Conditions for Pb with L'vov Platform

λ 283 nm, slit 5 (2.0 nm)
Pb EDL
D_2 background correction used
Furnace: step 1 (dry), 270 °C for 30 s
step 2 (char), ramp 15 s, 550 °C for 15 s
step 3 (atomize), max power, 2000 °C for 16 s
step 4 (auto max temp)
argon flow 12 mL/min
15-s integration

In their publication, L'vov and his colleagues (*6*) reported gains in peak amplitude sensitivity using the platform for the highly volatile elements (Cd and Pb) and moderately volatile elements (Cu and Ni), and no improvement for relatively involatile metals like Mo. More importantly, they found a significant reduction of interference effects for reasons that L'vov defends on theoretical grounds (*8*).

In addition, the platform extends the life of the furnace tube. The platform can be made of solid pyrolytic graphite, a material which is less chemically active than ordinary graphite tubes. It should make the furnace more easily adapted to corrosive materials such as perchloric acid.

Gregoire and Chakrabarti (*10*) investigated the platform with an aim to increasing the sensitivity of furnace methods, but they were not successful. In this paper, we will show that the interference effects of chloride, sulfate, and phosphate upon the Pb determination are greatly reduced using the L'vov Platform.

EXPERIMENTAL

The Perkin-Elmer Model 603 atomic absorption spectrophotometer was used with the Model HGA-2200 graphite furnace and the Temperature Ramp Accessory. Pyrolytically coated graphite tubes were used in the furnace. The Model AS-1 Auto Sampler was used to improve the precision. In all cases, 20-μL aliquots were used. We used disposable polystyrene cups in the AS-1, throwing them away after a single usage. The cups were rinsed with deionized water and dried prior to use. Eppendorf Micro Pipets with polyethylene tips were used for all the dilutions reported. Throughout this study, the background signal was recorded simultaneously with the analytical signal on a Perkin-Elmer Model 56 two-pen recorder using the deuterium arc as the light source. To correct automatically for absorption base-line drift, we used a circuit described by Epstein (*11*). Most measurements were repeated in triplicate. Integrated absorbance readings were printed using the Model PRS-10 Printer Sequencer. The experimental conditions are summarized in Table I. It should be noted that the Platform does not reach the wall temperature, which explains the 270 °C wall temperature for drying.

The fourth step on the temperature program of the HGA-2200 is an automatic 5-s interval at the maximum temperature. To be sure that the tube is purged, we lengthened that step to 8 s. This was accomplished by changing a resistor in the Temperature Ramp Accessory. We also lengthened the cool-down interval prior to the start of the next cycle to permit the platform to cool sufficiently. This was done by taking the trigger signal for the next cycle from the circuit that indicates that cool down is complete. These capabilities are routinely available on the new HGA-500 graphite furnaces.

Choice of Analytical Wavelength. Our early experimental work on the furnace wall had utilized the 217.0-nm line, the most sensitive absorbance line for Pb. Since the highest matrix concentration that can be used experimentally was limited by the amount of background that could be corrected, we tested the several matrices for background absorption at the 217.0-nm and the 283.3-nm Pb lines. These background signals may be due to scattering by solid particles or to molecular absorption. We did

Table II. Peak Background Absorbance of Several Salts

	peak absorbance	
	217.0 nm	283.3 nm
0.1% NaCl	0.26	0.36
0.2% NaCl	0.49	0.60
0.5% NaCl	0.74	1.10
0.1% NaH_2PO_4	0.57	0.07
0.2% NaH_2PO_4	1.16	0.17
0.5% NaH_2PO_4	--	0.40
0.1% Na_2SO_4	0.66	0.08
0.2% Na_2SO_4	1.05	0.17
0.5% Na_2SO_4	--	0.30
0.9% Na_2SO_4	--	0.46
2.0% Na_2SO_4	--	0.70

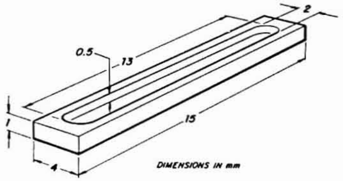

Figure 1. Design of the L'vov Platform used in these studies, not to scale

not attempt to distinguish between the two effects in this study. The data are summarized in Table II for solutions of sodium phosphate, chloride, and sulfate. The background for phosphate and sulfate materials was much smaller at 283.3 nm so we used this wavelength. If solutions contain mostly chloride, the 217.0-nm line may be preferable.

Platform Design. L'vov used a rectangular plate of pyrolytic graphite, 4 × 5 mm and 1 mm thick. However, in our hands that platform would hold no more than about 10 μL of sample and even in that case there was a tendency for sample to spill over the sides. We have therefore designed a larger platform (Figure 1) of somewhat greater mass, about 90 mg. It is considerably easier to use. With this design we can use as much as 50 μL of sample, although in all of the work reported here we have used 20-μL samples, dispensed from the Model AS-1 Auto Sampler. We have observed no problems due to dispensing. In the particular Model 603 we used, the platform vignetted about 10% of the beam from the lead electrodeless discharge lamp.

The platform is made of solid pyrolytic graphite with the lamellae oriented parallel to the plane of the plate. Thus the thermal conductivity in the plane of the plate is very high, tending to maintain the temperature constant over the surface.

We have experimented with platforms of different materials and different designs. Solid pyrolytic graphite was preferable to ordinary graphite, although the observed phenomena were not very different. When the contact edge between the platform and the tube was reduced to three points, the reduced thermal transfer did not materially alter the performance. We saw very little difference in performance between the smaller, lighter platforms as used by L'vov and the larger ones used in most of this work.

Heating Rate. In this work and in our earlier work (*1*), we have consistently observed that the Pb absorption signal decreases as the heating rate increases. This is true whether peak area or peak height measurements are used to quantitate the Pb signal. We studied the effect systematically with data summarized in Figure 2. The heating rate was determined by timing the period between a charring temperature and a temperature about 70% of the final selected atomization temperature. The furnace tube temperature was determined either with an optical pyrometer (Leads & Northrup Model 8632-C) or with an automatic pyrometer (Ircon Model 2000) at temperatures above 1500 °C. In all cases the sample was deposited on the L'vov Platform, although it is the heating rates of the tube that are recorded in Figure 2. An experiment with solutions containing 1% NaCl as well as 0.05 μg/mL Pb produced a curve with the same slope as shown in Figure 2. The reduction of sensitivity as the heating rate increases can be explained by a reduction of the residence time.

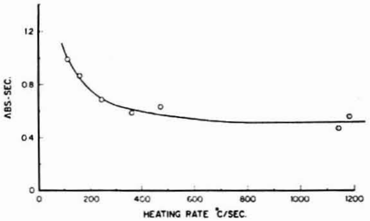

Figure 2. Heating rate versus integrated absorbance for a solution containing 0.05 μg/mL Pb (1 ng). The points represent different initial and final temperatures. The spread of the data about the best fit curve reflects the difficulty of measuring the heating rate accurately

Consistent with this explanation is the observation that the Pb absorbance signal found is not directly dependent upon the final steady-state temperature. Despite some loss in sensitivity, we used the maximum heating rate for this work because, in conjunction with the platform, this condition mimimized interferences.

Optimum Thermal Conditions. Almost all experimental conditions that we have used with the platform remove the interference experienced with a chloride matrix upon the absorption of Pb. When the platform was used with the same experimental conditions that we have used in our previous work (*1*) for the determination of Pb in a chloride matrix on the wall of the furnace, no interference from the chloride was found up to concentrations in excess of 4% NaCl, even though the peak NaCl background absorption was very large. However, these experimental conditions did not remove Pb interferences previously reported for a sulfate matrix (*12*) nor for a phosphate matrix. Probably this is because the phosphate and sulfate interferences result from a shift of the appearance temperature for Pb, as documented below.

Theoretically preferable experimental conditions require fast heating of the furnace to the selected steady-state temperature. We compared the recovery of Pb from solutions containing chloride, phosphate, and sulfate at different final temperatures from 1500 to 2500 °C, using the maximum rate of heating to achieve these final temperatures. The test solutions contained 0.05 μg/mL Pb added to solutions containing 1% NaCl, 1% NaH_2PO_4, and 1% Na_2SO_4. While the recovery of Pb in the presence of NaCl was reasonably independent of the experimental conditions, we obtained better recovery of Pb in the presence of sulfate and phosphate using lower final temperatures.

Observation of the recorder tracings indicated that the Pb peak at higher final temperatures extended for a longer time and often resulted in a second smaller peak following the initial peak. Previous experience in our laboratory and in L'vov's (*6*) indicates that this effect results from condensation of Pb and the matrix on the cooler outer ends of the furnace tube and the subsequent revolatilization of the Pb as the heat reaches the ends. At lower final temperatures, the portion of the tube above the atomization temperature for Pb reaches equilibrium more rapidly. The condensed metal and matrix are then removed in the final high temperature clean-up cycle.

One limitation of the method we describe here is that the background and the element absorption signals are not separated in time as was the case in our previous method for Pb in a chloride matrix atomized from the wall of the furnace tube (*1*). Thus the present procedure does not tolerate so large an amount of NaCl. However it accommodates other potential interferences by providing more theoretically optimum thermal conditions.

RESULTS

The object of these experiments was to reduce the interference of various matrices upon the absorbance of Pb. We believe that some of these interference effects result from a shift of the Pb appearance temperature in different matrices. We confirmed this using samples containing 0.1 μg/mL Pb and appropriate concentrations of chloride, phosphate, sulfate,

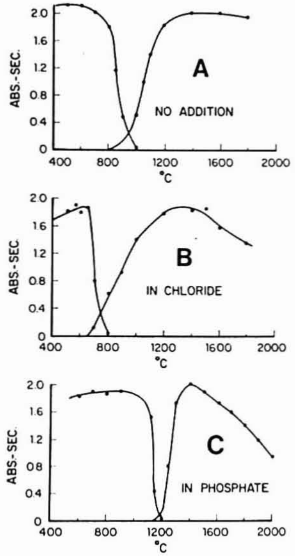

Figure 3. Char and atomization curves for samples deposited on the furnace wall containing 0.1 μg/mL Pb and: (A) no additions, the Pb being added as nitrate; (B) in 0.04% NaCl; and (C) in 0.01% NaH_2PO_4. For the char cycles, the atomization temperatures was always 1400 °C. For the atomization cycle of A and B, the char temperature was 600 °C, for C it was 1000 °C

and nitrate matrices that were charred and atomized on the furnace wall at different temperatures (*13*). Some of the resulting curves are shown in Figure 3. The lefthand portion of each curve indicates the absorbance signal found for Pb using the charring temperatures indicated. Atomization was performed at about 1400 °C in each case. In the right hand portion of the curve, charring is performed at the levels specified in the figure caption, close to the maximum found before loss of Pb in the charring cycle. Curves for 0.07% $NaNO_3$ and 0.06% Na_2SO_4 are omitted but both were at about 80 °C higher temperatures than the chloride curve.

For each matrix the Pb signal begins to appear in the atomization curve at about the same temperature that the Pb signal has begun to decrease in the charring curve. However, it is clear that this temperature is different for the several matrices studied. Obviously, for Pb determination with samples atomized from the furnace wall, these variations in appearance temperature will cause the Pb to be volatilized into the gas atmosphere at a temperature which will depend upon the matrix, thus producing different signals for different matrices.

Deposition of the sample onto the platform should cause these variations to be smaller since for each matrix the gas temperature should be more nearly constant when the Pb appearance temperature is reached. Within the limits that we could measure, this was true.

Extensive experiments were run with graphite furnace tubes, some of which were pyrolytically coated and some that were not. In some cases the graphite platform was molybdenum coated by our procedure (*1*) and in some cases it was not. There were variations in the experimental data as a result of the somewhat different environments. Since Fuller (*14*) and we (*1*) have shown that the degree of interference of chloride in the Pb determination depends upon the surface history of the graphite tube, the observations were adequately consistent. These comparison experiments involved the removal of the chloride interferences which are discussed in a later section of this paper. Some indications of the consistency of the data is indicated in Table III. "A" and "B" are platforms of somewhat different design in that the contact edge of the "B" platforms was reduced. Three different furnace tubes are represented from two manufacturers.

Table III. Pb Platform Studies

% NaCl added	signal (abs-sec) mfg 1 "A"	mfg 1 "B"	mfg 1 "A"	mfg 1 "B"	mfg 2 "A"	mfg 2 "B"
0	0.77	0.78	0.77	0.80	0.74	0.80
0.001	0.76	0.78	0.76	0.81	0.72	0.79
0.005	0.81	0.82	0.79	0.85	0.77	0.79
0.01	0.81	0.82	0.81	0.87	0.77	0.80
0.02	0.83	0.85	0.84	0.88	0.78	0.80
0.05	0.82	0.84	0.85	0.87	0.78	0.80
0.1	0.78	0.81	0.82	0.87	0.75	0.73
0.2	0.79	0.86	0.86	0.87	0.78	0.78
0.4	0.84	0.87	0.87	0.84	0.80	0.80
1.	0.76	0.84	0.84	0.87	0.81	0.82
2.	0.80	0.84	0.83	0.74	0.85	0.83
3.	0.83	0.84	0.84	0.77	0.87	0.83
4.	0.80	0 84	0.85	0.76	0.87	0.82
mean	0.80	0.83	0.83	0.83	0.79	0.80
S.D.	0.025	0.029	0.034	0.049	0.048	0.027

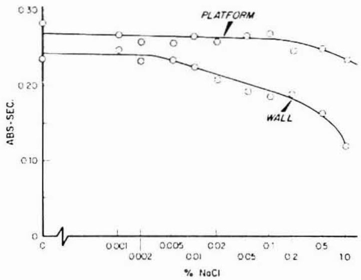

Figure 4. Interference of NaCl upon the absorbance of 0.05 μg/mL Pb atomized from the platform and from the tube wall. The wall conditions are the same as those used for the platform in Table I except that drying was done at 110 °C and max power was not used for atomization

Using the experimental conditions of Table I, the effect of chloride, phosphate, and sulfate matrices on the absorbance of Pb was determined on the L'vov Platform. These results were compared with measurments made by atomizing samples from the wall of the furnace tube using conditions that differed from Table I in that drying was accomplished at 110 °C and normal power was used in the atomization cycle. The results are shown in Figures 4–6. In the case of chloride and sulfate, the interferences on the platform are small until about 1% of the interfering material, where the amount of background absorption is already limiting. For particular experimental purposes, the addition of appropriate amounts of ammonium nitrate will reduce the background absorption for the chloride in situations where higher concentrations of chloride are encountered. In the case of the phosphate, the interference even on the platform begins to be significant at about 0.1%. However, the interference is considerably smaller on the platform than it is when the sample is determined by atomization from the wall of the furnace tube.

Some experiments were run with mixtures of the several interfering species with results that were similar to the results

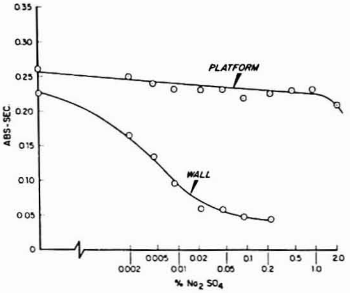

Figure 5. Interferences of sulfate on the determination of Pb. Varying amounts of Na_2SO_4 were added to 0.05 μg/mL Pb and these solutions were atomized both from the platform and from the tube wall. The conditions are as in Figure 4

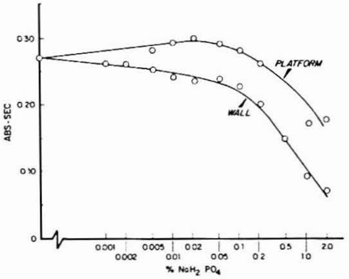

Figure 6. Interference of phosphate on the determination of Pb. Varying concentrations of NaH_2PO_4 were added to 0.05 μg/mL Pb and the solutions were atomized both from the platform and from the wall. Conditions are as in Figure 4

obtained when these matrix materials were studied separately.

The object of all the previous experiments was to find conditions which would make it possible to analyze real samples with complex matrices using standards that are as simple as possible. A recent paper by Regan and Warren (*15*) described the determination of Pb in drinking water samples using the graphite furnace. In most of the samples that they tested, they could not obtain quantitative recovery of Pb that they added to the drinking water samples using aqueous standards. They were able to greatly relieve this poor recovery by adding 1% ascorbic acid to the samples and to the standards.

We performed recovery experiments on a group of environmental water samples by adding Pb to each sample. Using environmental water samples containing from 200 to 800 μg/mL of Ca and Mg, up to 0.5% SO_4 and 0.01% Cl, we could recover from about 40 to 60% of the Pb added. Since this result is inconsistent with the previous interference studies, we looked for a problem found in our earlier work (*1*) that depended upon the surface of graphite upon which the sample was deposited. Some of these experiments are summarized in Figure 7. We added Pb to successive dilutions of one of the environmental water samples and plotted the recovery against the dilution. Using ordinary and pyrolytic graphite platforms we found variations in recovery with the history of the platform as Fuller (*14*) and we (*1*) have previously reported. From many experiments, two typical curves are shown in the lower part of Figure 7.

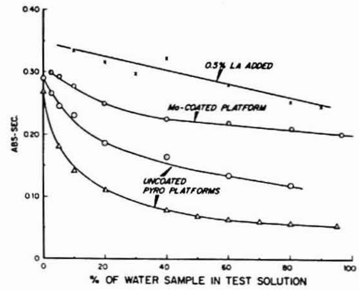

Figure 7. Recovery experiments from an environmental water sample. The sample was diluted and 0.05 μg/mL Pb was added to each solution and plotted against the absorbance signal. The abscissa indicates the fraction of the original environmental water sample (in percent) remaining after dilution. The conditions for this analysis were as shown in Table I

We Mo treated the Platform by our previous procedure (*1*), presumably producing a Mo carbide surface. The variation in recovery was much smaller and there was little variation with condition of the platform surface. Similar results were obtained by treating the platform with solutions of a Ta salt as shown in Figure 7. However, in our hands, the Ta carbide tended to flake off after about ten firings, returning the platform to its performance prior to Ta coating. Additions of 0.5% La (as the sulfate) to each solution produced results that were very similar to those of the Mo coated platform.

The similarity of the results for the several carbide-forming metals suggest that it remains necessary to carbide-coat both the platform and the furnace tube to obtain useful analytical results for Pb in complex matrices.

Combining the advantages of the determination of Pb in complicated matrices with the L'vov Platform with a matrix modifier technique using ammonium nitrate (*1*), ascorbic acid (*15*), or lanthanum additions (*12*) may provide procedures that will produce satisfactory results on real samples with complicated matrices.

ACKNOWLEDGMENT

We thank Sabina Slavin, R. D. Ediger, F. J. Fernandez and W. B. Barnett for their suggestions and criticisms.

LITERATURE CITED

(1) D. C. Manning and W. Slavin, *Anal. Chem.*, **50**, 1234 (1978).
(2) B. V. L'vov, *Spectrochim. Acta*, **17**, 761 (1961).
(3) H. Massmann, *Spectrochim. Acta, Part B*, **23**, 215 (1968).
(4) B. V. L'vov "Atomic Absorption Spectrochemical Analysis", Adam Hilger, Ltd., 31 Camden Rd., London NW1, 1970 (Distributed in the United States by American Elsevier Publishing Co., New York).
(5) F. J. Fernandez and J. Iannarone, *At. Absorpt. Newsl.*, **17**, 117 (1978).
(6) B. V. L'vov, L. A. Pelieva, and A. I. Sharnopolskii, *Zh. Prikl. Spectrosk.*, **27**, 395 (1977).
(7) D. A. Segar and J. G. Gonzalez, *Anal. Chim. Acta*, **58**, 7 (1972).
(8) B. V. L'vov, *Spectrochim. Acta, Part B*, **33**, 153 (1978).
(9) W. M. G. T. van den Broek and L. de Galan, *Anal. Chem.*, **49**, 2176 (1977).
(10) D. C. Gregoire and C. L. Chakrabarti, *Anal. Chem.*, **49**, 2018 (1977).
(11) M. S. Epstein, *At. Absorp. Newsl.*, **16**, 75 (1977).
(12) A. Andersson, *At. Absorp. Newsl.*, **15**, 71 (1976).
(13) B. Welz, Paper presented at the XX Colloqium Spectroscopicum Internationale, Aug. 1977, Chlum, Czechoslovakia.
(14) C. W. Fuller, *At. Absorp. Newsl.*, **16**, 106 (1977).
(15) J. G. T. Regan and J. Warren, *Analyst (London)*, **103**, 447 (1978).

RECEIVED for review September 28, 1978. Accepted November 13, 1978.

Molecular Absorption Spectra of Complex Matrices in Premixed Flames

R. C. Fry[1] and M. B. Denton*

Department of Chemistry, University of Arizona, Tucson, Arizona 85721

The question of molecular spectral interferences by undissociated inorganic matrix salts is inevitably raised when the direct atomic absorption analysis of digested or untreated complex materials is considered. Data presented in these studies indicate that the problem is not nearly as serious for premixed flame systems as has been reported for electrothermal and total consumption burner atomization.

Nonatomic absorption by matrix species represents one of the most severe and troublesome interferences encountered in direct trace level atomic absorption analysis of complex materials. This interference is correctable by techniques reviewed recently by Zander (*1*) if it does not exceed reasonable limits. However, Fernandez (*2*) and Culver (*3, 4*) have indicated that the ability of correction schemes to handle this problem in flameless atomizers is exceeded during the attempted analysis of some samples if the matrix is not first oxidized by digestion.

Data concerning the molecular band nature of nonatomic absorbance encountered in flame systems was presented by Koirtyohann and Pickett (*5, 6*). A Beckman total consumption burner was used to spray sample and support an O_2–H_2 flame contained horizontally by a long path absorption tube. A 1% solution of sodium chloride was reported to give a spurious signal as high as 0.6 absorbance unit.

Culver (*4*) has more recently discussed the relative contribution to nonatomic absorbance of "smoke signals" caused by solid carbon scattering centers present early in the time variant atomization process when volatile elements such as arsenic and mercury are determined directly by carbon rod atomization of untreated biological samples. Culver and Surles (*3*) have also studied a pronounced molecular component of nonatomic absorption in carbon rod atomization due to undissociated matrix species such as diatomic and triatomic alkali and alkaline earth halides. These inorganic molecular spectra persist during later stages of transient electrothermal atomization (*7*) to interfere with the atomic spectra of many less volatile elements that would normally appear resolved in time from the earlier organic "smoke peak". This molecular spectral component of nonatomic absorption was demonstrated by Culver and Surles (*3*) to be as high as 0.6 absorbance unit in a carbon rod analyzer for as little as 5 μL of 0.1% sodium chloride matrix. More complex matrices can easily drive the spurious absorbance much higher to a point where correction schemes no longer function properly (*2*), especially if the readout scale is expanded for maximum analyte sensitivity.

A recent review by Zander (*1*) again presented the above mentioned data of Culver (*3*) along with the earlier data of Koirtyohann and Pickett (*5*) as a comparison of the relative amount of nonatomic absorbance encountered in flame (long path total consumption) and nonflame (electrothermal) atomization techniques. Although the article presented a correct and thorough review of nonatomic absorption effects and correction techniques, no data were included for premixed slot burner flame systems.

To clarify the relative magnitude of nonatomic absorbance encountered in atomization systems, the present investigation deals with the characterization of molecular absorption spectra in conventional premixed slot burner flame systems. Recent development of a new high solids nebulizer has provided a means of considerably increasing the sample handling ability of atomic absorption spectrometry (*8*). Untreated samples as complex as whole blood, tomato sauce, etc. may now be directly atomized in the newly reported system (*8*). A further purpose of the present paper is to outline the type and degree of nonatomic absorption interference that results when such complex samples are directly introduced into premixed flames. Molecular spectra produced by a variety of untreated clinical, environmental, and food matrices are presented in addition to the spectra of individual undissociated inorganic salts.

EXPERIMENTAL

Apparatus. Studies with samples below 5% salt content were carried out utilizing a Varian-Techtron Springvale, Vic., Australia) AA-5 single beam atomic absorption spectrometer including the standard Varian nebulizer with an added small volume sampling cone similar to that of Manning (*9*). A 10-cm Varian air–acetylene slot burner and Hewlett-Packard (Palo Alto, Calif.) model 17501A strip chart recorder were used.

Studies on samples between 5% and 50% salt and solids content were carried out utilizing a second single beam atomic absorption spectrometer fitted with the flow through, high solids nebulizer recently developed for spectrochemical analysis by Fry and Denton (*8*). This system included an Instrumentation Laboratories (Lexington, Mass) "High Solids" 0.81 mm × 5 cm single slot nitrous oxide–acetylene burner head and a high solids 10-cm single slot air–acetylene burner head similar in design (except for the wider 0.81 mm × 10 cm "high solids" slot) to the 0.51 mm × 10 cm slot air–acetylene Varian-Techtron burner head. Varian-Techtron and Jarrell-Ash (Waltham, Mass.) H_2 continuum and Cd (neon filled) hollow cathode lamps were utilized for all measurements.

Procedure. The hollow cathode lamps were operated at 15 and 5 mA, respectively, for H_2 and Cd. "Zero" and "100 %*T*" were reset at each wavelength utilized in the H_2 continuum for point by point assessments of the molecular absorption spectrum of each matrix studied. Spectral bandwidths of 0.6 nm were used.

To avoid burner slot clogging and gumming by the more complex clinical, environmental, and food matrices, measurements on these samples were made by the small volume cone method of nebulizer sampling discussed by Sebastiani et al. (*10*), Berndt and Jackwerth (*11*), and Manning (*9*). Sample volumes of 0.2 and 1 mL were utilized for the standard premix nebulizer and the new "high solids" systems, respectively. This procedure yields transient recorder signals of concentration sensitivity and precision similiar to that of the steady-state response normally encountered with larger sampling volumes. All other less complex samples were aspirated until a normal steady-state response was perceived at the readout.

RESULTS AND DISCUSSION

Premixed Molecular Flame Spectra of Polyatomic Inorganic Species. Figure 1 presents the earlier reported (*1*) review data (redrawn) of the molecular NaCl spectrum for

---

[1] Present address: Department of Chemistry, Kansas State University, Manhattan, Kansas 66506

0003-2700/79/0351-0266$01.00/0 © 1979 American Chemical Society

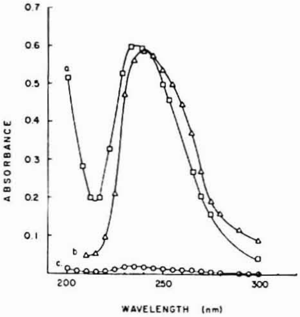

Figure 1. NaCl spectra. (a) 0.1% NaCl, carbon rod; (b) 1% NaCl, long path total consumption; (c) 5% NaCl, *premixed* flame

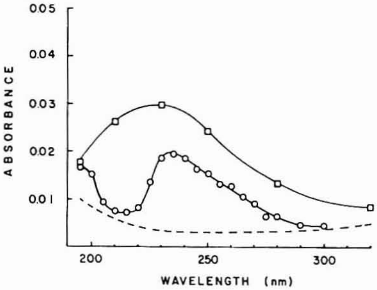

Figure 2. Expanded scale (10×) molecular spectra in premixed air–acetylene. 20% $MgSO_4$ below noise limit at all wavelengths. (□) 5% $CaCl_2$; (O) 5% NaCl; (--)noise limit

carbon rod analyzer (curve a) and flame (curve b) atomization (redrawn) along with the flame (curve c) data observed in the present studies. The large discrepancy in the two flame curves arises from gross differences in the method of sample introduction. Curve b was generated on the "total consumption" tubular system of Koirtyohann and Pickett (*5*). The median aerosol droplet diameter introduced for such systems is reported to be 28 μm (*12*) whereas the median aerosol droplet diameter introduced into *premixed* systems (Figure 1, curve c) is reported to be 8.6 μm (*13*). From a qualitative point of view, it should be apparent that desolvation will be greatly delayed (*14*) for the total consumption burner (considering the larger starting droplet diameter and droplet volume) and the tube temperature lower in comparison to the premixed system. The entire atomization sequence including droplet desolvation, salt crystal vaporization, and dissociation of molecular matrix species in the gas phase cannot be expected to be nearly as complete in the analytical viewing zone. Additional droplets much larger (but normally rejected in a premixed system) than the median would enhance the presence of undissociated salt species even further when viewed horizontally in a total consumption system. The tubular total consumption system should therefore be expected to result in more pronounced molecular spectra. This (as well as the 4× path length difference) appears to account for the differences observed for the molecular spectra in the two flame systems. Figure 2 gives expanded scale molecular spectra of $CaCl_2$, NaCl, and $MgSO_4$ in the *premixed* air–acetylene flame for the purpose of wavelength identification. $MgSO_4$ decomposes above 1124 °C which accounts for the absence of any measurable molecular spectrum (even at 20% salt content) in the ~2250 °C air–acetylene flame. $CaCl_2$ (mp 772 °C, bp >1600 °C) and NaCl (mp 801 °C, bp 1413 °C) produce wavelength maxima at 225 and 234 nm, respectively, which are in general agreement with the carbon rod analyzer data of Culver and Surles (*3*) and the calculations (NaCl) of Herzberg (*15*). Molecular band absorbance by undissociated matrix species therefore appears to predominate over scattering in premixed flame systems (as well as in total consumption systems and carbon rod analyzers) as the major cause of nonatomic absorbance when inorganic salts are present in large amounts. The magnitude of observed spurious absorbance in premixed flames is, however, actually ~150× less (Figure 1) than the "flame" spectra given in the earlier review (*1*).

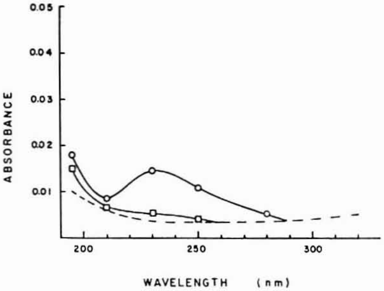

Figure 3. Expanded scale spectra of untreated complex materials in premixed air–acetylene using high solids system. Whole blood, evaporated milk concentrate, and tomato sauce *all below noise limit!* (O) Seawater; (□) urine; (--)noise limit

Premixed Molecular Flame Spectra of Complex Materials. Figure 3 gives the expanded scale molecular band spectra of untreated seawater, urine, whole blood, evaporated milk concentrate, and tomato sauce introduced directly (high solids system) as aerosols into a 10-cm premixed air–acetylene flame. It can be seen that samples (milk, blood, etc.) approaching 50% *organic* solids content give no measurable spectrum above the noise level. In sharp contrast to the electrothermal atomization case (*4*), organic species appear readily degraded in the flame producing no measurable scattering or molecular spectra.

Only those samples with appreciable *inorganic* salt content such as seawater and urine produced measurable spectra in premixed flames (although greatly reduced in comparison to other atomizers). The spectra of urine and seawater of Figure 3 compare well with the NaCl spectrum of Figure 2. This is as expected since NaCl is the principal dissolved salt (~1% in seawater and ~0.6% in urine) in these matrices. The spectrum of KCl (*3*) is very similar to that of NaCl. The presence of KCl in addition to NaCl in seawater accounts for the slightly more pronounced absorbance seen in Figure 3 than would normally occur if NaCl alone were present.

Concentration Dependence. Figure 4 demonstrates the effect of species concentration on the molecular spectrum of triatomic $CaCl_2$ in premixed air–acetylene flames. A Beer's law relationship between absorbance and concentration appears to govern the system below a solution concentration of 15% $CaCl_2$. Nonlinearities observed at higher salt content are most likely due to a shift in the droplet size produced by the nebulizer accompanied by a change in transport efficiency resulting in fewer droplets successfully emerging from the premix chamber. This droplet size–salt content phenomena has been discussed by Skogerboe (*16, 17*).

The high temperature environment and small sample droplets encountered in premixed flame systems seem to

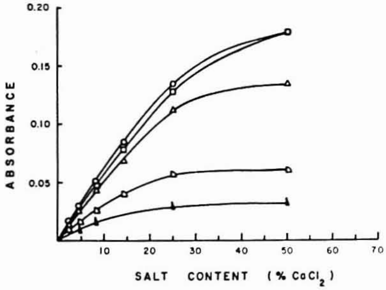

Figure 4. Concentration dependence of triatomic $CaCl_2$ absorbance in premixed air-acetylene using high solids system. (□) 210 nm; (O) 230 nm; (△) 250 nm; (◻) 280 nm; (Å) 320 nm

Table I. Line: Background Ratio in Several Atomizers

atomizer	path, cm	Cd line (L), atomic absorbance/ppm	NaCl background (B), absorbance/% NaCl	(L/B) ratio
premixed N_2O-C_2H_2	5	0.06	0.00042	143.0
premixed air-C_2H_2	10	0.30	0.0035	84.7
carbon rod (*4*)	1	147.	6.0	24.4
total consumption system (*6*)	40	3.5	0.6	5.8

induce dissociation of those species that would otherwise give rise to molecular spectra to a greater extent than cooler flames and electrothermal atomizers. This must however, ultimately be judged in terms of the predominance of atomic spectra as well. Table I therefore lists data pertaining to the ratio (line-to-background) of the atomic analyte (Cd) spectrum at 228.8 nm to the molecular matrix spectrum of sodium chloride.

The table demonstrates that, although electrothermal atomization is analytically far more sensitive (owing to its rapid rate of atomization, reduced internal volume, and reduced gas dilution of atomic vapor) as a sample introduction technique than aerosol generation, it yields a lower line-to-background *ratio* than the premixed flame. It was also found that all untreated naturally occurring samples (seawater, urine, whole blood, milk, etc.) tested produced no measurable molecular spectra whatsoever in the "high solids" premixed N_2O-C_2H_2 flame system, thereby minimizing the need for correction schemes in those analyses of complex materials for which the atomic absorption analyte sensitivity in this flame is adequate.

CONCLUSIONS

Premixed flames exhibit molecular band spectra due to undissociated inorganic polyatomic species; however, the predominance of such spectra is approximately 150 times less than the long path total consumption burner flame data reported in a recent review (*1*). In sharp contrast to electrothermal atomization, no scattering or molecular spectra due to untreated *organic* solids (even up to 50% solids content) was detectable in new, high solids, premixed flame systems (*8*). The spectra due to inorganic species are also greatly reduced compared to those reported in long path total consumption systems and electrothermal atomization.

The fact that abnormally high salt concentrations had to be employed with a "high solids" premixed system in these studies in order to produce a molecular spectrum sufficiently pronounced (above the noise limit) to study, indicates that this interference is not nearly as serious for premixed flames as it is for other atomization techniques. Actual samples (even though complex) are generally of lower salt content and can be directly analyzed by premixed flame atomic absorption spectrometry with small or negligible levels of spectral interference that (even if pronounced enough to require correction) do not overwhelm the readout as would frequently be the case with electrothermal techniques. These studies have demonstrated that molecular spectral interferences are small, or only moderate in magnitude ($\leq 0.2\ A$) for premixed flame systems. This holds true even when the sample complexity is pushed to extremes, such as the direct atomization of whole blood, tomato sauce, evaporated milk concentrate, 50% $CaCl_2$, etc. in the new high solids system developed by Fry and Denton (*8*).

LITERATURE CITED

(1) A. T. Zander, *Am. Lab.*, **8** (11), 11 (1976).
(2) F. J. Fernandez, *At. Absorpt. Newsl.*, **12**, 70 (1973).
(3) B. R. Culver and T. Surles, *Anal. Chem.*, **47**, 920 (1975).
(4) B. R. Culver, Analytical Methods for Carbon Rod Analyzers", Varian Techtron Pty. Ltd., Springvale, Victoria, Australia, 1975.
(5) S. R. Koirtyohann and E. C. Pickett, *Anal. Chem.*, **37**, 601 (1965).
(6) S. R. Koirtyohann and E. C. Pickett, *Anal. Chem.*, **38**, 585 (1966).
(7) H. Koizumi and K. Yasuda, *Anal. Chem.*, **48**, 1178 (1976).
(8) R. C. Fry and M. B. Denton, *Anal. Chem.*, **49**, 1413 (1977).
(9) D. C. Manning, *At. Absorpt. Newsl.*, **14**, 99 (1975).
(10) E. Sebastiani, K. Ohls, and G. Riemer, *Fresenius Z. Anal. Chem.*, **264**, 105 (1973).
(11) H. Berndt and E. Jackwerth, *Spectrochim. Acta, Part B*, **30**, 169 (1975).
(12) J. A. Dean and W. J. Carnes, *Anal. Chem.*, **34**, 192 (1962).
(13) S. R. Koirtyohann and E. C. Pickett, *Anal. Chem.*, **38**, 1087 (1966).
(14) C. T. J. Alkemade, in "Analytical Flame Spectroscopy", R. Mavrodineaunu, Ed., Macmillan, London, 1970.
(15) G. Herzberg, "Molecular Spectra and Molecular Structure I. Spectra of Diatomic Molecules", 2nd ed., Van Nostrand, Princeton, N.J. 1950, p 501.
(16) R. K. Skogerboe and K. W. Olson, 1976 Pacific Conference (#76), Phoenix, Ariz., Nov. 9, 1976.
(17) R. K. Skogerboe and K. W. Olson, *Appl. Spectrosc.*, **32**, 181 (1978).

RECEIVED for review October 3, 1977. Resubmitted November 6, 1978. Accepted November 6, 1978.

Gas Chromatographic–Mass Spectrometric Determination of Etorphine with Stable Isotope Labeled Internal Standard

Satya P. Jindal,* Theresa Lutz, and Per Vestergaard

Rockland Research Institute, Orangeburg, New York, 10962

A quantitative gas chromatographic–mass spectrometric assay was developed for the determination of etorphine in urine. Etorphine, on treatment with *N,O*-bis(trimethylsilyl)trifluoroacetamide forms two etorphine trimethylsilyl derivatives—etorphine-TMS and etorphine(TMS)$_2$. Experimental conditions were developed for selective and quantitative conversion of etorphine to etorphine-TMS. The assay utilizes selected ion focusing to monitor in a GLC effluent the molecular ion generated by electron impact ionization (EI) of etorphine-TMS. Etorphine-d_3 was synthesized and used as an internal standard. The assay can measure 2 ng/mL of the drug with about 5% precision. The methodology is used for the urinary assay of etorphine of a rabbit given a single subcutaneous dose (1 μg/kg) of the drug.

Etorphine, a 6,14-endoetheno-tetrahydrothebaine derivative is an analgesic of unprecedented high potency (*1–3*). When given subcutaneously, etorphine is 1000 to 80 000 times as potent as morphine (*4*) and is characterized by its rapid onset and short duration of action. Its ability to cause catatonia at very low dose levels has resulted in its use for the immobilization of game animals (*5*). The fact that it works sublingually and has abuse potential (*6*) raises the possibility that it may become a future threat in the drug abuse field.

The low dose levels at which etorphine is used (1 μg/kg) demands a sensitive measurement technique for its determinations in biological fluids. Etorphine could not be detected in urine with commonly available methodology including gas–liquid chromatography after the administration of highly euphoronigenic doses in man (*7*). Recently, in a preliminary communication (*8*) we reported a mass spectrometric assay of etorphine in urine using commercially available tritiated etorphine as an internal standard. The internal standard was a complex mixture of nontritiated, monotritiated, and ditritiated etorphine; consequently, the assay precision, particularly at low levels of etorphine, was unsatisfactory. This paper reports a mass fragmentographic assay of etorphine in urine using stable isotope-labeled etorphine as an internal standard. Selective ion monitoring, the technique built on combined gas chromatography–mass spectrometry (*9, 10*) was used to develop a very sensitive and specific assay of etorphine in urine utilizing site specific deuterium-labeled etorphine as an internal standard. The methodology was used to study the urinary excretion of free etorphine in rabbits after a single subcutaneous dose.

EXPERIMENTAL

Materials. Analytical grade etorphine, *N*-desmethyl etorphine (Reckitt and Colman Pharmaceutical Division, Hull, U.K.); methyl iodide-d_3, isotopic purity 99%, (International Chemical and Nuclear Corp., Irvine, Calif.); *N,O*-bis(dimethylsilyl)acetamide (BDSA), Applied Science Laboratories, State College, Pa.); *N,O*-bis(trimethylsilyl)trifluoroacetamide (BSTFA, Pierce Chemical Co., Rockford, Ill.) were used without further purification. All solvents used were of ACS analytical grade (Pfaltz and Bauer, Flushing, N.Y.), silanized tubes with screw caps lined with Teflon (Kimble, Owens, Chicago, Ill.) were used for extraction. Urine samples were processed as soon as obtained.

Synthesis of Etorphine-d_3 (*N*-Methyl-d_3). Etorphine-d_3 was synthesized by treatment of *N*-desmethyl etorphine with methyl iodide-d_3 using an established procedure for alkylation of secondary amines (*11*). The labeled compound gave satisfactory mass spectral (electron impact ionization, EI) characteristics. A selected ion detection analysis of etorphine-d_3 showed the presence of an ion equivalent to 98.7% ± 0.15% ($n = 6$) etorphine-d_3 and an ion equivalent to 1.1% ± 0.15% ($n = 6$) etorphine.

Animals. All animals used in this work were male, New Zealand white rabbits.

Extraction of Etorphine from Urine. To 1 mL of urine was added an appropriate amount of etorphine-d_3 (typically 28 ng/mL) as an internal standard. The urine was adjusted to pH 9 with 1 N NH_4OH and extracted twice with 6 mL protions of *N*-butylchloride. The organic fractions were combined, 1 mL 0.1 N HCl was added to it, and the solution was shaken for 15 min and centrifuged. The organic layer was discarded, the aqueous phase was adjusted to pH 9 with 1 N NH_4OH and extracted twice with 3 mL portions of *N*-butylchloride. The organic fractions were combined, dried with sodium sulfate, filtered, and the solvent was evaporated at 50 °C under a gentle stream of nitrogen. Recovery of etorphine, added to control urine, was studied at the 5 ng/mL level.

Formation of Derivatives. Etorphine has two hydroxyl functions; either both of these or at least one of these must be selectively and quantitatively derivatized for the molecule to have good GLC characteristics. Similar compounds (*12*), on treatment with BSTFA, are known to give a complex mixture of derivatives. Multiderivatization in the area of biopharmaceutical analyses is a serious problem, which could adversely affect the sensitivity and possibly specificity of the mass spectrometric assay. Consequently experimental conditions were worked out for the quantitative preparation of etorphine-TMS-1 and etorphine-(TMS)$_2$-2 from etorphine.

Etorphine-TMS-1. Etorphine (100 ng) was taken in a Reacti-Vial, to this was added 150 μL of BSTFA. The mixture was heated at 60 °C for 1 h. After this period, the solution was cooled to room temperature, excess reagent was removed at 40 °C under a gentle stream of N_2, the residue was reconstituted in 10 μL of benzene; an aliquot of this solution was injected into the GLC-mass spectrometer. The total ion current trace showed the material to be homogenous on two different columns (1.5% OV-1 and 1% OV-17) and its mass spectrum (Figure 1) is in agreement with the structure.

Etorphine-(TMS)$_2$-2. Etorphine (100 ng) was taken in a Reacti-Vial, to this was added 50 μL of pyridine and 150 μL of BSTFA. The material was heated at 120 °C for 2 h. After this period, the reagents were removed at 40 °C under a gentle stream of N_2; the residue was reconstituted in 10 μL of benzene. An aliquot of this solution was injected into the GLC-mass spectrometer. Again the material was found to be homogenous on two different columns and its mass spectrum (Figure 2) confirms the structure.

Instrumentation. Mass spectrometry was done using an LKB 9000 GC-MS system (*9, 10*) equipped with the multiple ion detector/peak matcher accessory (MID/PM). Gas chromatography was performed on a 1.8-m glass column (2-mm i.d.) packed with 1.5% OV-1 on gas chrom Q 100–200 mesh. The column temperature was maintained at 225 °C, flash heater at 235 °C, separator at 240 °C and the ion source at 250 °C. The accelerating voltage was 3.5 kV in the scan mode and 3.0 kV in the MID mode, the ionization potential was 70 eV, and the trap current was set

0003-2700/79/0351-0269$01.00/0 © 1979 American Chemical Society

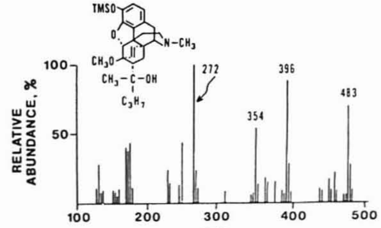

Figure 1. Mass spectrum of etorphine-TMS

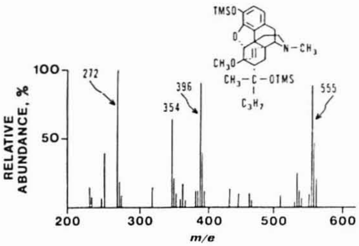

Figure 2. Mass spectrum of etorphine-(TMS)$_2$

at 60 μA. The magnetic field was kept constant by focusing the background ion (column bleed) at m/e 429 and the additional voltages were 108 V and 89 V for measuring the ion intensities at m/e 483 and 486, respectively.

RESULTS AND DISCUSSION

The mass spectrum of etorphine-TMS-1 (Figure 1) shows a molecular ion at m/e 483, a base peak at m/e 272 and other major peaks at m/e 354 and 396, respectively. A priori, one would expect some localization of charge on nitrogen atom in the molecular ion, to be followed by cleavage at the three carbon–carbon bonds β to the nitrogen atom (*13, 14*) leading to radical ions a, b, and c shown in Scheme I. The ions b and c with radical sites at bridge head and at primary C-13, respectively, are rather unstable; consequently they are expected to be of minor importance. The ion a, resulting from the cleavage of the C_9–C_{10} bond, is a benzylic radical and must be of major importance in the electron impact fragmentation of the molecule. The ion a, probably, is in equilibrium with ion d, an isomeric benzylic radical ion, arising by H-transfer from C-16 to C-10 followed by C_{13}–C_{15} bond cleavage. This kind of H-atom migration is stereochemically feasible and has been well documented in electron impact ionization of morphine and similar compounds (*14–16*). The intense molecular ion peak at m/e 483 must be attributed to the great stability of these benzylic radical ions. Reasonable mechanism for the fragmentation pattern (*16, 17*) is proposed in Scheme I. To assist in the interpretation of the spectrum, fragmentation of several analogous etorphine derivatives was examined. The peak at m/e 396 in the spectrum of etorphine-TMS, resulting from the loss of stable tertiary radical (CH_3-$\dot{C}$(OH)–C_3H_7), as expected, is shifted to higher mass by 3 amu in the spectrum of etorphine-d_3-TMS (Figure 3); to lower mass by 14 amu in the spectrum of etorphine-dimethylsilyl ether (not shown here) and appears at the same m/e value in the spectrum of etorphine-(TMS)$_2$ (Figure 2). Again, in agreement, with the proposed fragmentation, the ions at m/e 354, 272 in the spectrum of etorphine-TMS are shifted to higher mass by 4 amu in the spectrum of ditritiated etorphine-TMS((15,16-^{3}H)8) and to lower mass by 14 amu in the spectrum of etorphine-dimethylsilyl ether.

Scheme I. Proposed Fragmentation Mechanism for Electron Impact Ionization of Etorphine-TMS

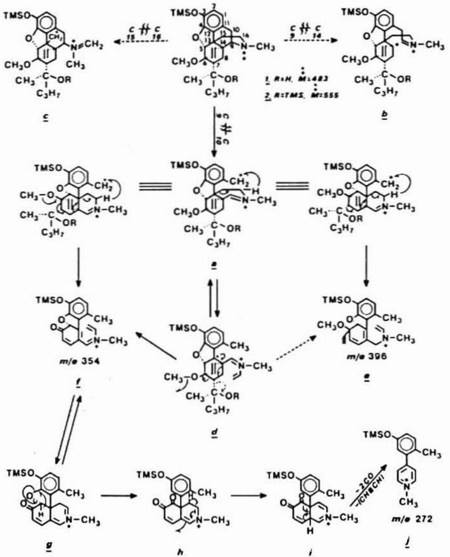

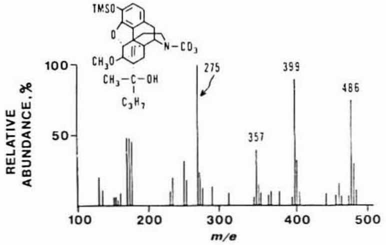

Figure 3. Mass spectrum of etorphine-d_3-TMS

GC-MS-SIM Quantitation. The ion at m/e 483 is specific for etrophine-TMS (m/e 486 for etorphine-d_3-TMS), is a convenient working mass for SIM assay and is not observed in the electron impact ionization spectra of other opiates (*18, 19*) and known metabolites of etorphine (*20*). Consequently, urinary etorphine extract along with the labeled etorphine-d_3 was treated with BSTFA at 60 °C, excess reagents were evaporated, an aliquot of the reconstituted solution was injected into the GLC-mass spectrometer; etorphine was quantitated by measuring the ion intensities at m/e 483 and 486, respectively. Control urine samples subjected to the described procedure for etorphine analysis showed no significant background ions at m/e 483 and 486. Known amounts of etorphine along with their isotopic analogue in "fixed" amount were added to control urine and processed as described above. A plot of ion intensity ratio (m/e 483/486) vs. the amount of etorphine per fixed amount of etorphine-d_3, was linear with a slope of 0.98 ± 0.02 and an intercept of 0.04 ± 0.02 ng. These data affirm a simple linear relationship between the appropriate ion intensity ratios and the concentration of etorphine and exclude any isotopic exchange or any significant kinetic isotope effect in the fragmentation

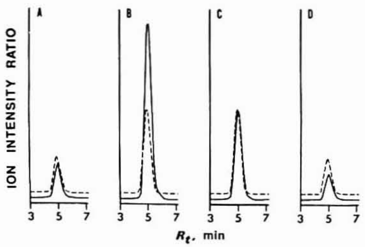

Figure 4. Selective ion chromatograms for etorphine-TMS ((–) *m/e* 483 and etorphine-d_3-TMS (---) *m/e* 486) obtained from 4-mL aliquots of selected samples of rabbit urine and processed as described above. Part A, Urine at 1.25 h after the dose, 5 ng of etorphine-d_3 (---) was added as internal standard. Etorphine found was 5.3 ng. Part B, Urine at 3 h after the dose, 20 ng of etorphine-d_3 (---) was added as internal standard and etorphine found was 42 ng. Part C, Urine at 5 h after the dose, 20 ng of etorphine-d_3 (---) was added as internal standard and etorphine found was 21.6 ng. Part D, Urine at 52 h after the dose, 5 ng of etorphine-d_3 (---) was added as internal standard and etorphine found was 2.96 ng

process. Six control urine samples containing 5 ng/mL of etorphine were analyzed by the above method using 5 ng/mL of etorphine-d_3 as internal standards. The results for these samples were 4.8 ± 0.25 ng/mL of etorphine. Another set of six control urine samples containing 5 ng/mL of etorphine were processed as above, this time the internal standard etorphine-d_3, 5 ng/mL was added in each sample after the extraction. The recoveries for these samples, based on comparison of the ion intensity ratios of the two sets were 68 ± 12%. The wide range of recoveries observed is expected in the field of trace analysis and is attributed to variable glassware and GLC column adsorption. The assay of etorphine, presented here, is sensitive, specific, and, with minor changes, is applicable to other body fluids and tissues. The sensitivity of the assay, being a function of extraction efficiencies, GLC column conditions, and the ion source, cannot be quoted in absolute terms. With near-zero leak current in the ion source, clean and freshly silanized GLC column, glassware, and better than 60% recoveries, an assay sensitivity of approximately 2 ng/mL is possible.

A number of experiments were performed on rabbits to determine urinary excretion after the subcutaneous administration of varying doses of etorphine. In a typical experiment, a 6-kg rabbit was given a single subcutaneous dose of 5 μg of etorphine hydrochloride in water. Urine was collected by catheterization periodically at 2-h intervals for 7 h after the dose was given. The last sample was collected 52 h after the administration. Appropriate amounts of urine samples were taken and processed as described. Selected ion chromatograms (Figure 4) obtained from urine samples are clean symmetrical peaks and the amounts of endogenous etorphine were calculated from the ratio of ion intensities at *m/e* 483 and 486, respectively. The cumulative urinary excretion of intact drug, indicating the half-life of excretion to be approximately 5 h, corroborates its reported pharmacological activity of short duration. Furthermore, the animal excretes less than 20% of the drug in its native form, evidently pointing to its extensive metabolism and or conjugation to biologically inactive conjugates.

LITERATURE CITED

(1) K. W. Bentley and D. G. Hardy, *J. Am. Chem. Soc.*, **89**, 3267 (1967).
(2) K. W. Bentley, D. G. Hardy, and B. Meek, *J. Am. Chem. Soc.*, **89**, 3273 (1967).
(3) K. W. Bentley and D. G. Hardy, *J. Am. Chem. Soc.*, **89**, 3281 (1967).
(4) J. D. Robinson, B. A. Morris, and V. Marks, *Res. Commun. Chem. Pathol. Pharmacol.*, **10**, 1 (1975).
(5) J. M. King and B. H. Carter, *East Afr. Wildl. J.*, **3**, 19 (1965).
(6) D. R. Jasinski, J. D. Griffith, and C. B. Carter, *Clin. Pharmacol. Ther.*, **17**, 267 (1975).
(7) C. W. Gordetzky and M. P. Kullberg, *Clin. Pharmacol. Ther.*, **17**, 273 (1975).
(8) S. P. Jindal and P. Vestergaard, *J. Pharm. Sci.*, **67**, 260 (1978).
(9) C.-G. Hammar, B. Holmstedt, and R. Ryhage, *Anal. Biochem.*, **25**, 53 (1968).
(10) B. Holmstedt and L. Palmer, *Adv. Biochem. Psychopharmacol.*, **7**, 1 (1973).
(11) R. E. McMahon and F. J. Marshall, *Adv. Tracer Methodol.*, **4**, 29 (1968).
(12) K. Verebey, M. A. Chedekel, S. J. Mulé, and D. Rosenthal, *Res. Commun. Chem. Pathol. Pharmacol.*, **12**, 67 (1975).
(13) R. S. Gohlke and R. W. McLafferty, *Anal. Chem.*, **34**, 1281 (1962).
(14) D. M. S. Wheeler, T. H. Kinstle, and K. L. Rinehart, Jr., *J. Am. Chem. Soc.*, **89**, 4494 (1967).
(15) H. Audier, M. Fetizon, D. Ginsburg, A. Mandelbaum, and T. Rull, *Tetrahedron Lett.*, 13 (1965).
(16) H. Nakata, Y. Hirata, A. Tatematsu, H. Tada, and Y. K. Sawar, *Tetrahedron Lett.*, 829 (1965).
(17) G. R. Waller, "Biochemical Applications of Mass Spectrometry", John Wiley and Sons, New York, 1972, p 655.
(18) W. O. R. Ebbighausen, J. H. Mowat, H. Stearns, and P. Vestergaard, *Biomed. Mass Spectrom.*, **1**, 305 (1974).
(19) J. Chao, R. Saferstein, and J. Manura, *Anal. Chem.*, **46**, 296 (1974).
(20) M. Gordon and J. A. Vida, *Annu. Rep. Med. Chem.*, **12**, 20 (1977).

RECEIVED for review July 21, 1978. Accepted November 20, 1978. Supported by the Office of Research of the Department of Mental Hygiene of the State of New York.

Hydroxyl Ion Negative Chemical Ionization Mass Spectra of Steroids

T. A. Roy and F. H. Field*

The Rockefeller University, New York, New York 10021

Yong Yeng Lin and Leland L. Smith

The University of Texas Medical Branch, Galveston, Texas 77550

The OH^- negative chemical ionization spectra of 35 steroids have been investigated. Spectra are dependent upon the nature, number, and proximity of the functional groups in the several compounds. The predominant reaction observed is proton abstraction, and $(M - 1)^-$ is found for all but two compounds. Other reactions involve nucleophilic attack by OH^- on the sample molecule and nucleophilic attack by $(M - 1)^-$ on N_2O. These processes are frequently accompanied by loss of H_2 and H_2O, which sometimes aids in determining the nature and environment of substituents in the compounds. The amount of the fragmentation of the molecules is relatively small. The overall sensitivity of the method is somewhat greater than that for CH_4 positive chemical ionization with the group of steroids investigated.

In this paper we report on the mass spectral behavior of 35 steroids under OH^- negative chemical ionization (NCI) conditions. Smit and Field (*1*) have described the formation of OH^- by the electron bombardment of a mixture of N_2O and CH_4 and the use of OH^- as a reactant ion in NCI. Their study showed that reaction of OH^- with a variety of organic compounds was quite mild, and, in most cases, abundant $(M - 1)^-$ ions were formed. We refer the reader to their report (*1*) for a detailed discussion on the formation of OH^- and a brief review of negative ion publications.

The present investigation has attempted to provide information on OH^- negative ion spectra which might serve as the basis of an analytical method for an important group of biomolecules. The ammonia, methane, and isobutane positive chemical ionization (PCI) spectra of a similar group of steroids have been determined by Lin and Smith (*2*).

EXPERIMENTAL

The steroids examined were commercial samples from Steraloids Inc., Wilton, N.H., or Research Plus Steroid Laboratories, Inc., Denville, N.J., or were prepared in our laboratories. All samples were analyzed by thin-layer and gas chromatography and, in some instances, by high pressure liquid chromatography.

Mass spectra were obtained with a Biospect mass spectrometer manufactured by Scientific Research Instrument Corp., Baltimore, Md. The instrument was modified for negative ion detection using the negative ion detection system developed by Smit, Rosseto, and Field (*3*). All samples (1–2 μg) were introduced by means of the direct insertion probe. The spectra were recorded on an Infotronics Corp. (Houston, Tex.) CRS 160 mass spectrometer digital readout system. Ionization of the reaction mixture was effected by electrons emitted from a rhenium filament. The electron accelerating voltage was adjusted to give maximum ion intensity, generally about 450 V in the OH^- NCI experiments and about 250 V in some CH_4 PCI experiments. The source pressure was maintained at 3.0 Torr (2/1 mixture of CH_4/N_2O) in the OH^- NCI experiments and 1.0 Torr in the CH_4 PCI experiments. The source temperature was maintained at 200 °C in all experiments. The reader is referred to the study of Smit and Field (*1*) for a detailed description of the effects of temperature, pressure, and reactant gas ratio on the reactant ion spectrum.

RESULTS

General Reactions. We will first discuss the general characteristics of the spectra and later turn our attention to a more detailed discussion of individual spectra. Table I lists the spectra obtained for 30 of the steroids investigated. The spectra of the five cholesteryl esters studied are given in Table II. As is well known, the nature of the tuning of a quadrupole mass spectrometer markedly affects the discrimination properties of the instrument. As best we could determine, the spectra of the compounds in Table I were obtained under non-mass discriminating conditions, which are relatively easy to achieve because the spectra do not span a wide mass range. The spectra of the compounds in Table II do span a large mass range, and for these the instrument was tuned so as not to discriminate against the high mass ions and perhaps to emphasize them somewhat.

The predominant reaction for all these compounds is proton abstraction to form the $(M - 1)^-$ ion. We assume this abstraction involves hydrogens attached to or adjacent to groups or atoms which lend some degree of stability to the resulting anion, e.g., oxygen, carbon–carbon double bonds, etc. The relative intensity of the $(M - 1)^-$ ion varies from 100% in the spectrum of the saturated ketone, 5α-cholestan-3-one (4) to 0% in the spectra of cholesteryl benzoate (32) and 5α-cholestane (1). The numbers in parentheses following the names of the steroids refer to the numbers identifying the compounds in Tables I and II. Following the initial reference to a compound, we will normally refer to it by its assigned number only.

An $(M - 3)^-$ ion is observed in the spectra of a number of the compounds, particularly those containing the hydroxyl group or the carbon–carbon double bond. We postulate that the formation of this ion involves loss of H_2 following initial proton abstraction. In the case of alcohols, this can produce a resonance stabilized enolate ion. Thus, in 5α-cholestan-3β-ol (12), for example,

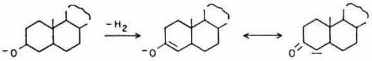

(1)

Obviously, loss of H_2 can occur across the 2,3 C–C bond also. The presence of the $(M - 3)^-$ ion in alkenes, dienes, etc., also probably involves loss of H_2 from an initially formed $(M - 1)^-$ ion. Abstraction of an allylic hydrogen can generate an allylic carbanion as $(M - 1)^-$, and subsequent loss of H_2 serves to lower the energy of the ion by extending the conjugated system and further delocalizing the negative change. Thus, in cholest-5-ene (2), for example,

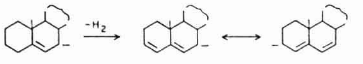

(2)

An $(M - 5)^-$ ion is also sometimes observed with these types

0003-2700/79/0351-0272$01.00/0 © 1979 American Chemical Society

Table I. OH⁻ NCI Spectra[a] of Steroids

			mass and relative intensities[b] m/e (RI)									
no.	compound	mol wt.	$(M-1)^-$	$(M-3)^-$	$(M-5)^-$	$(M-19)^-$	$(M-21)^-$	$(M-37)^-$	$(M+43)^-$	$(M+25)^-$	$(M+15)^-$	other ions
1	5α-cholestane	372		369(65)	367(25)				413(10)			
2	cholest-5-ene	370	369(5)	367(30)	365(20)				413(40)			383(5)[c]
3	cholesta-3,5-diene	368	367(70)	365(27)								381(3)[c]
4	5α-cholestan-3-one	386	385(100)									
5	cholest-4-en-3-one	384	383(93)	381(7)								
6	cholest-7-en-3-one	384	383(71)	381(17)								397(12)[c]
7	cholesta-3,5-dien-7-one	382	381(86)	379(6)	377(5)						397(3)	
8	cholest-4-ene-3,6-dione	398	397(90)	395(5)	393(5)							
9	3β-hydroxycholest-5-en-7-one	400	399(24)			381(76)						
10	3β-hydroxy-5α-cholestan-6-one	402	401(90)			383(10)						
11	3β-hydroxycholest-5-en-24-one	400	399(87)			381(13)						
12	5α-cholestan-3β-ol	388	387(52)	385(18)		369(8)	367(3)		431(19)			
13	5β-cholestan-3α-ol	388	387(48)	385(16)		369(11)	367(3)		431(22)			
14	cholest-5-en-3β-ol	386	385(72)			367(10)	365(12)		429(6)			
15	cholest-4-en-3β-ol	386	385(7)	383(49)	381(8)	367(14)	365(22)					
16	cholest-4,6-dien-3β-ol	384	383(5)	381(10)		365(77)	363(8)					
17	5α-cholestane-3β,5-diol	404	403(65)			385(18)	383(3)	367(14)				
18	5β-cholestane-3β,5-diol	404	403(64)			385(18)		367(18)				
19	5α-cholestane-3β,6β-diol	404	403(59)			385(23)		367(18)				
20	cholest-5-ene-3β,4β-diol	402	401(5)	399(5)	397(5)	383(73)	381(12)					
21	cholest-5-ene-3β,7α-diol	402	401(18)	399(4)		383(26)	381(8)	365(44)				
22	cholest-5-ene-3β,7β-diol	402	401(22)			383(31)	381(8)	365(39)				
23	(20S)-cholest-5-ene-3β,20-diol	402	401(32)	399(3)		383(40)	381(12)	365(9)		427(4)		
24	(24S)-cholest-5-ene-3β,24-diol	402	401(64)	399(12)	397(3)	383(12)	381(4)	365(5)				
25	cholest-5-ene-3β,25-diol	402	401(46)	399(4)	397(4)	383(26)	381(11)	365(9)				
26	5,6α-epoxy-5α-cholestan-3β-ol	402	401(70)			383(25)		367(5)				
27	5,6β-epoxy-5β-cholestan-3β-ol	402	401(53)			383(40)		367(7)				
28	3β-hydroxy-5α-cholest-6-ene-5-hydroperoxide	418	417(6)	415(10)		399(12)	397(10)	381(45)				365(10)[d], 401(7)[e]
29	(20R)-cholest-5-ene-3β,20,21-triol	418	417(26)			399(54)	397(5)	381(15)				
30	5α-cholestane-3β,5,6β-triol	420	419(28)	417(20)		401(14)	399(12)	383(13)				365(10)[f], 381(3)[g]

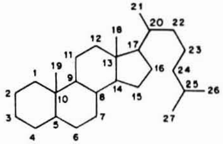

[a] P_{N_2O} = 1 Torr; P_{CH_4} = 2 Torr. The source temperature was 200 °C. [b] Relative intensity as percentage of total ionization attributed to sample. ^{13}C isotope ion intensities included in the tabulated intensities. Relative intensities above 3% tabulated. [c] $(M-H+N_2O-N_2-H_2)^-$. [d] $(M-H-H_2O-H_2O_2)^-$. [e] $(M-OH+e)^-$. [f] $(M-H-3H_2O)^-$. [g] $(M-H-2H_2O-H_2)^-$.

Table II. OH⁻ NCI Spectra[a] of Several Cholesteryl Esters (XOOCR)[b]

			mass and relative intensities m/e (RI)					
no.	compound	mol. wt.	$(M-1)^-$	$(RCOO)^-$	$(RCOO-H_2O)^-$	$(XO-H_2O)^-$	$(XO-H_2O-H_2)^-$	$(XO-H_2O-2H_2)^-$
31	cholesteryl acetate	428	427(53)	59(37)		367(5)	365(5)	
32	cholesteryl benzoate	490		121(100)				
33	cholesteryl palmitate	624	623(39)	255(47)			365(4)	363(3)
34	cholesteryl oleate	650	649(63)	281(28)	263(4)	367(5)		
35	cholesteryl stearate	652	651(53)	283(39)	265(3)	367(5)		

[a] Same conditions as in Table I. [b] X = cholesteryl group ($C_{27}H_{45}$).

of compounds, and the ion is almost surely formed by the same kind of H_2 loss process as is involved in $(M-3)^-$ ion formation.

An $(M-19)^-$ ion is observed, to some degree, for all 22 steroids in Table I which contain at least one hydroxyl group. We believe that this ion is formed by the elimination of the elements of water following the initial proton abstraction. In those cases where the $(M-1)^-$ is the alkoxide, a resonance stabilized allylic anion can be formed, and we suggest as an illustrative possibility

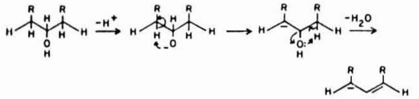

(3)

An $(M-21)^-$ ion is often observed in the spectra of the alcohols as well, and we presume that this represents the loss of both H_2 and H_2O from the $(M-1)^-$ ion in such a way as to lower the energy of the system. The $(M-37)^-$ ion observed in the spectra of all the diols and two triols in Table I doubtless results from the loss of a second water molecule. The energy and intensity of this ion may be related to the position of the hydroxyl groups in the molecule. Generally, where elimination of a second molecule of water will serve to lower the energy of an ion by increasing resonance (electron delocalization) we observe relatively large $(M-37)^-$ ions. Specific examples of these observations will be discussed later.

Another general type of reaction observed between the OH⁻ ion and the cholesteryl esters, specifically, appears to involve nucleophilic attack by OH⁻. The major pathway for nucleophilic attack by OH⁻ involves cholesteryl–oxygen bond cleavage. This results in the formation of the conjugated base of the acid moiety

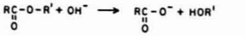

$$\underset{\overset{\|}{O}}{RC}{-}O{-}R' + OH^- \longrightarrow \underset{\overset{\|}{O}}{RC}{-}O^- + HOR' \quad (4)$$

This is a departure from condensed phase chemistry where nucleophilic attack by OH⁻ occurs at the carbonyl carbon of the ester, which results in acyl–oxygen bond cleavage.

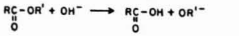

$$\underset{\overset{\|}{O}}{RC}{-}OR' + OH^- \longrightarrow \underset{\overset{\|}{O}}{RC}{-}OH + OR'^- \quad (5)$$

Small ions (rel int ≅ 5%) are observed in the spectra of the cholesteryl esters at m/e 367 and 365 and are presumably derived via water loss from the cholest-5-enoxide ion which would be the result of conventional OH⁻ attack at the carbonyl carbon of the ester. These observations with the cholesteryl esters are in accord with the findings on esters in Smit and Field's study (*1*).

Still another reaction type observed is that involved in the formation of the ions $(M+43)^-$, $(M+25)^-$, and $(M+15)^-$. This reaction appears to be a nucleophilic attack of an $(M-1)^-$ ion, produced from the sample, on the N_2O reactant gas. The $(M+43)^-$ ion is found in the spectra of the saturated monoalcohols and some of the carbon–carbon unsaturated steroids. The $(M+25)^-$ and $(M+15)^-$ ions are only found in the spectra of the compounds containing carbon–carbon unsaturation. The $(M-1)^-$ nucleophile is presumably the alkoxide ion in the case of the saturated monoalcohols and the allylic carbanion in the case of the carbon–carbon double bond containing compounds. The $(M+43)^-$ and $(M+25)^-$ ions have been reported by Smit and Field (*1*), who proposed that the ions represented the species $(M-H+N_2O)^-$ and $(M-H+N_2O-H_2O)^-$, respectively. A recent study (*4*) has indicated that reaction of N_2O with various organic ions in a flowing afterglow system may be characterized as addition of N_2O followed by loss of H_2O, N_2, or CH_2O. We suggest that the $(M+15)^-$ observed in the present study represents the species $(M-H+N_2O-N_2)^-$. The mechanism proposed (*1*) to explain the loss of H_2O from the $(M+43)^-$ ion was based on initial nucleophilic attack of the $(M-1)^-$ ion at the central atom of N_2O. Both of the principal resonance structures of N_2O assign a positive charge to the central atom, and this would seem a logical point of attachment. However, work by Dawson and Nibbering (*5*) using labeled N_2O indicates that attachment actually takes place at the terminal nitrogen, at least when $CH_2{=}C^-\cdot$ is the nucleophile. Revising the mechanism for elimination of H_2O from $(M-H+N_2O)^-$ is not complicated when this point of attachment is used. The $(M+43)^-$ ion formed with a simple alkene can lose water and cyclize to form a pyrazole anion

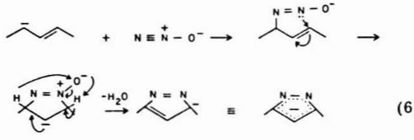

(6)

Assuming the same initial point of attachment of N_2O, we tentatively suggest the following mechanism for the elimination of N_2 from the $(M+43)^-$ ion

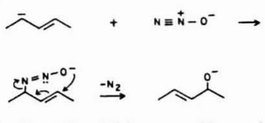

(7)

The relative intensity of this group of ions, which we shall generally refer to as the $(M+n)^-$ ions, is believed (*1*) to be related to the energy of the $(M-1)^-$ ions. We observe that the introduction of additional functional groups or elements into compounds containing carbon–carbon unsaturation greatly reduces the intensity of the $(M+n)^-$ ions. We attribute this to a lowering of the energies of the $(M-1)^-$ ions by the presence of the substituents.

OH^- NCI Spectra of Individual Steroids. 5α-Cholestane (1) is the only saturated hydrocarbon steroid included in this study, and it was not expected to show much reactivity since it was previously found (*1*) that alkanes did not react with OH^-. A comparison of the total ion current attributed to the sample for 5α-cholestane and for several monofunctional compounds (the monoketone (4), the monoalcohol (13) and the alkene (2)) revealed that 5α-cholestane was some $^1/_{20}$–$^1/_{50}$ as reactive as the functionalized compounds. The ions in the spectrum of (1) present a pattern similar to that observed in the spectrum of cholest-5-ene (2), and they may result from thermal dehydrogenation of (1) in the source followed by ionization as described below for (2).

Cholest-5-ene (2) and cholesta-3,5-diene (3) are the only unsaturated hydrocarbons included in Table I. The $(M - 1)^-$ in the monoolefin (2) is quite weak; most of the ionization observed involves loss of hydrogen from $(M - 1)^-$ or reaction of $(M - 1)^-$ with N_2O. As discussed in the previous section, we infer that the initial $(M - 1)^-$ in monoolefins like (2) is of high energy and reacts further to form a lower energy ion. By contrast, the introduction of a second double bond in conjugation with the first as in the diene (3) apparently allows for the formation of a low energy $(M - 1)^-$ ion, which does not appreciably react further (rel int = 70%). A significant amount of hydrogen loss is observed in both (2) and (3), but the relative intensity of the $(M + n)^-$ ions in (3) is just 3% as compared to a value of nearly 50% in (2). The higher total reactivity in (2) reflects the higher energy of the $(M - 1)^-$ ion in (2).

$(M + n)^-$ ions are also found in the spectrum of 5α-cholest-7-en-3-one (6) but not in the spectrum of a positional isomer, cholest-4-en-3-one (5). The two functional groups in the enone (6) are not in conjugation, and the spectrum contains ions that can be associated with each of the groups. Thus the spectrum displays an intense $(M - 1)^-$ ion (rel int ≃ 71%) typical of a saturated monoketone (e.g., 5α-cholestan-3-one (4)) and $(M + n)^-$ ions (rel int ≃ 12%) such as those observed with the alkene (2). On the other hand, the carbonyl and carbon–carbon double bond in the enone (5) are conjugated and the spectrum is dominated by the $(M - 1)^-$ ion (rel int ≃ 90%) and completely devoid of $(M + n)^-$ ions. Here again we suggest that the lack of $(M + n)^-$ ions in (5) is related to the relatively low energy of the $(M - 1)^-$ in that the removal of an allylic hydrogen produces a highly conjugated anion. Thus,

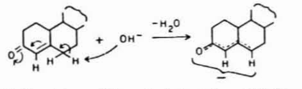

(8)

Cholest-3,5-dien-7-one (7) and cholest-4-en-3,6-dione (8) are both highly conjugated, and the spectra display intense $(M - 1)^-$ ions and small or zero intensities of $(M + n)^-$ ions. The spectra are analogous to those of the α,β-unsaturated ketone (5).

The spectra of several of the steroids are of interest since they may provide information on the relative acidity of the hydrogens associated with the carbonyl and the hydroxyl group. We noted above that the spectrum of the saturated ketone (4) displays only one ion, the $(M - 1)^-$. On the other hand, spectra of the saturated alcohols, 5α-cholestan-3β-ol (12) and 5β-cholestan-3α-ol (13) show $(M - 1)^-$ ions of only about 50% relative intensity, with ions representing loss of H_2 and H_2O and association with N_2O accounting for the remainder of the ionization. These results suggest that the $(M - 1)^-$ ion associated with the ketone is of lower energy than the $(M - 1)^-$ ion in the alcohols. 3β-Hydroxy-5α-cholestan-6-one (10) is a compound containing both the carbonyl and hydroxyl group. The two groups are sufficiently isolated so as to minimize interaction between the two. Thus, we might expect the spectrum of (10) to reflect the influence of both groups on the ionization of the molecule. Here, the $(M - 1)^-$ ion is dominant (rel int 90%); the $(M - 19)^-$ ion accounts for the remaining ionization observed. The complete absence of H_2 loss or N_2O association and the small amount of H_2O loss implies that only a small fraction of the $(M - 1)^-$ ion can be attributed to proton abstraction from oxygen. Such results suggest that, in the gas phase, the hydrogens α to the carbonyl group are more acidic than the hydroxyl hydrogen in alcohols. This would represent a departure from condensed phase chemistry where the acidity of secondary alcohols such as (12) and (13) is generally found to be 10–100 times greater than the acidity of aliphatic ketones (*6*).

We note here that the general features of the spectra of alcohols (12) and (13) are characteristic of the alcohols in Table I. These two particular alcohols are configurational isomers, and the differences in their spectra are too subtle to allow a clear distinction between the two. This is also the case for two other pairs of configurational isomers ((17 and 18) and (21 and 22)) in Table I. A fourth pair of configurational isomers, the epoxides (26) and (27), display significantly different spectra and will be discussed later.

Cholest-5-en-3β-ol (14) (cholesterol) and cholest-4-en-3β-ol (15) are positional isomers. The spectrum of (14) displays a sizable $(M - 1)^-$ ion (rel int ≃ 70%) and also ions associated with loss of H_2O and reaction with N_2O. The isomer (15) displays very little $(M - 1)^-$, an intense $(M - 3)^-$ (rel int ≃ 50%), and ions associated with the loss of H_2O amounting to 35% of the total ionization. No measurable $(M + n)^-$ intensity is observed in the spectrum of (15). The $(M - 1)^-$ ion in (14) is somewhat greater in intensity than the $(M - 1)^-$ (rel int ≃ 50%) ion in the saturated alcohols (12 and 13). This difference may be experimentally significant, and we make the tentative hypothesis that a substantial amount of the $(M - 1)^-$ ion in the spectrum of (14) may in fact be an allylic anion and not the alkoxide ion, i.e.,

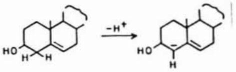

(9)

The hydrogens at the C_4 position will be activated by both functional groups, and the anion resulting from the removal of a proton from this position may well be of lower energy than the $(M - 1)^-$ ion in saturated alcohols. The intense $(M - 3)^-$ ion in the spectrum of the alcohol (15) may represent loss of H_2 from the alkoxide ion to produce a resonance stabilized enolate ion analogous to that in reaction 1. Of course, the H_2 loss will not occur across the 3–4 bond in (15), but loss across the 2–3 bond is possible and would serve the function of lowering the energy of the ion. However, it is difficult to envision loss of H_2O from this species to give the observed $(M - 21)^-$ ion (rel int 22%). Neither is it easy to envision the production of $(M - 21)^-$ ion by loss of H_2O followed by loss of H_2 or for these entities to be lost simultaneously. Here also we suggest that a substantial amount of the $(M - 1)^-$ ion formed may be the allylic carbanion and not the alkoxide ion. With this hypothesis we can easily account for the observed ions, e.g.,

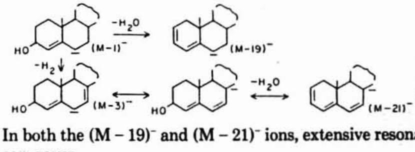

(10)

In both the $(M - 19)^-$ and $(M - 21)^-$ ions, extensive resonance can occur.

Cholest-4,6-dien-3β-ol (16) is similar to (15), having an additional carbon–carbon double bond in conjugation with the 4-ene-3-ol system. The spectrum of (16) displays an intense $(M - 19)^-$ (rel int 77%). As was seen for (15), it is difficult to envision loss of H_2O from the alkoxide ion or enolate ion (alkoxide-H_2) produced from this type of allylic alcohol. On the other hand, the $(M - 19)^-$ ion can be formed directly from the allylic carbanion by loss of H_2O.

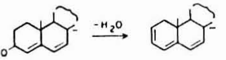

(11)

It is interesting to note that this ion is identical to the $(M - 3)^-$ ion in the diene (3) discussed earlier. The $(M - 3)^-$ ion in the diene (3) is presumably formed by loss of H_2 from $(M - 1)^-$, whereas the $(M - 19)^-$ ion in the diene-ol (16) apparently results from loss of H_2O from the $(M - 1)^-$ ion. A comparison of their relative intensities, 27% and 77%, respectively, may be indicative of the relative ease of removal of H_2 and H_2O under these experimental conditions.

The spectra of 5α-cholestane-3β,5-diol (17), 5β-cholestane-3β,5-diol (18), and 5α-cholestane-3β,6β-diol (19) all display prominent $(M - 1)^-$ ions (rel int 60%). Essentially all the remaining ionization can be attributed to the $(M - 19)^-$ and $(M - 37)^-$ ions, which are of about equal intensity. It was suggested earlier that the intensity of the $(M - 37)^-$ ion may be related to the position of the hydroxyl groups in diols such as (17)–(19). These three are saturated diols, and it may be assumed that the $(M - 1)^-$ ion is the alkoxide. It can be seen that elimination of the second molecule of water will serve to increase the resonance in the ion and further delocalize the charge

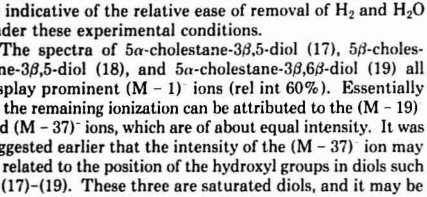

(12)

We observe fairly intense $(M - 37)^-$ ions with these three alcohols, which we attribute to the stability of the conjugated systems in the ions.

This view is reinforced when one observes the spectra of the six ene-diols (20)–(25). Cholest-5-ene-3β,4β-diol (20) is a vicinal diol and its spectrum displays an intense $(M - 19)^-$ (rel int 73%) ion and no measurable $(M - 37)^-$ ion. We suggest the following scheme for the formation of $(M - 19)^-$ ions

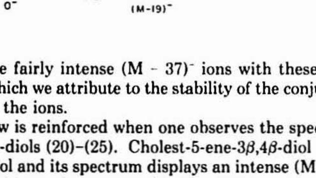

(13)

The position of the hydroxyl groups in (20) make it difficult to envision a mechanism for the loss of a second H_2O molecule. It is gratifying, therefore, that no $(M - 37)^-$ ions are observed. On the other hand, the configuration isomers, cholest-5-ene-3β,7α-diol (21) and cholest-5-ene-3β,7β-diol (22) display intense $(M - 37)^-$ ions, but in these molecules loss of the second water molecule yields a resonance stabilized system

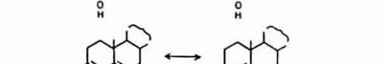

(14)

The ene-diols, (20*S*)-cholest-5-ene-3β,20-diol (23), (24*S*)-cholest-5-ene-3β,24-diol (24), and cholest-5-ene-3β,25-diol (25), have the two hydroxyl groups in the molecule far removed from one another. Loss of a second molecule of water from these compounds would not be expected to lower the energy of the ion particularly, and thus we observe relatively weak $(M - 37)^-$ ions in their spectra (~10% rel int).

The two epoxides, 5,6α-epoxy-5α-cholestan-3β-ol (26) and 5,6β-epoxy-5β-cholestan-3β-ol (27) are the only pair of configurational isomers studied whose spectra reveal any significant difference. The trans-fused epoxide (26) displays an $(M - 1)^-$ ion which is of significantly greater intensity than the $(M - 1)^-$ ion observed in the cis-fused isomer (27). We offer no rationale for this apparent difference, which was consistent over many replicate measurements. One might expect that OH^- would attack the epoxide ring as a nucleophile and open the ring; however, no $(M + 17)^-$ ion, which would result from such an attack, is observed in the spectrum of either epoxide. However, the spectra of the epoxides show significantly higher $(M - 19)^-$ intensities than those of the alcohols (12) and (13), which differ in structure from the epoxides only by the lack of the epoxide group, and we think that the epoxide ring is involved, to some extent, in the ionization of the molecule. We suggest the following mechanism whereby an $(M - 1)^-$ ion could be formed by a bimolecular elimination process involving OH^- attack on the C_6 hydrogen

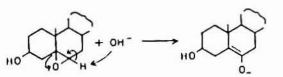

(15)

Loss of H_2O from this ion would extend the conjugation and account for the prominent $(M - 19)^-$ ions observed for both epoxides.

Two triols were included in the study, and their spectra show quite different patterns. (20*R*)-Cholest-5-ene-3β,-20,21-triol (29) is structurally analogous to cholesterol (14) differing only by the addition of vicinal hydroxyl groups in the C_{17} side-chain. It is apparent from a comparison of the spectra of these two compounds that these exocyclic hydroxyls have a substantial effect on the ionization of the triol. Compound (29) shows a lower $(M - 1)^-$ intensity and a higher $(M - 19)^-$ intensity than (14). It seems clear that a significant fraction of the $(M - 1)^-$ ions in (29) are exocyclic alkoxide ions, and some of these lose water to produce allylic alkoxide ions. We point out that the intense $(M - 19)^-$ ion (rel int >50%) in the spectrum of (29) is reminiscent of the $(M - 19)^-$ ion (rel int >70%) in the vicinal diol (20) (see reaction 14). 5α-Cholestane-3β,5,6β-triol (30) is structurally analogous to 5α-cholestan-3β-ol (12) and 5α-cholestan-3β,5-diol (17), and its spectrum contains ions found in both these analogues. A sizable $(M - 3)^-$ ion (rel int $\simeq$ 20%) is observed in the spectrum of (30), which is comparable to that observed for the monoalcohol (12). This ion presumably represents the loss of H_2 from an alkoxide (see reaction 1). In addition, the spectrum of (30) contains ions at $(M - 19)^-$ and $(M - 37)^-$ comparable to those seen in the spectrum of the 3,5-diol (17). In both instances, loss of water could be expected to stabilize the ion by resonance. The loss of a third hydroxyl from the triol (30) could produce a highly conjugated system, and we observe a small $(M - 55)^-$ ion (rel int $\simeq$ 10%) in the spectrum. This ion is not found in the spectrum of the triol (29); formation of such an ion in (29) would require an allene structure and would offer no stabilization due to resonance.

The spectrum of 3β-hydroxy-5α-cholest-6-ene-5-hydroperoxide (28) is rather complex and not readily interpreted. Although an $(M - 1)^-$ ion is observed, its intensity is quite weak. The ion may originate from proton abstraction at the alcohol or the hydroperoxide function, the latter being the more acidic in the condensed phase. Ions at $(M - 19)^-$ and $(M - 37)^-$ are the most intense in the spectrum, and these may represent loss of H_2O, and H_2 and H_2O_2, respectively, from an alkoxide $(M - 1)^-$. Cholesta-4,6-dien-3-one, which can be formed by elimination of H_2O_2 and H_2 from (28) is a known thermal degradation product from the hydroperoxide (*7*). Thus,

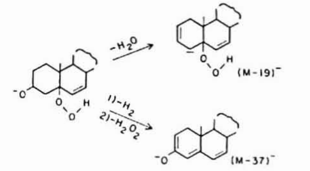

(16)

The presence of a very weak ion at $(M - 17)^-$ suggests that some free radical mechanisms may be occurring here. The source temperature of 200 °C might well produce some degree of thermal homolysis of the peroxide bond since D(RO-OH) = 43–44 kcal/mol for R = Me, Et, *i*-Pr and *t*-Bu (*8*). The resultant radical could then be converted to a molecular anion by resonance capture of a low energy electron in the source. Thus,

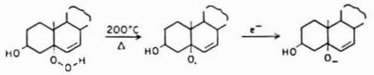

(17)

The ions resulting from nucleophilic attack by OH^- on the esters were discussed in the section on general reactions. The other major ion observed for these compounds is $(M - 1)^-$, which accounts for a significant amount of the ionization in the spectra of cholesteryl acetate (31) and the three fatty acid esters, cholesteryl palmitate (33), cholesteryl oleate (34), and cholesteryl stearate (35). This ion may result from abstraction of one of the allylic protons adjacent to the C-5 double bond in the steroid nucleus; however, the complete absence of $(M + n)^-$ ions in these spectra would tend to discount this possibility. A more appealing mechanism (*1*) involves abstraction of a proton α to the carbonyl group of the ester. Thus, for cholesteryl stearate

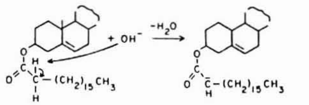

(18)

We note that there is no $(M - 1)^-$ ion in the spectrum of the benzoate ester (32), which has no hydrogens in the α-position. The relative intensities of the major ions in the spectra of the four esters studied may be dependent on the availabilities of these hydrogens. In addition, these ion intensities may also be dependent upon the relative stabilities of the carboxylate and alkoxide ions.

Sensitivity. A few experiments were carried out to obtain information on the relative sensitivities of OH^- NCI and CH_4 PCI for these steroidal compounds. The compounds chosen for investigation were 5α-cholestan-3-one (4), cholestan-3-ols (12 and 13), and cholesteryl stearate (35). These are monofunctional steroids containing the important functional groups (carbonyl, hydroxyl, and ester) found in the total body of steroids here investigated. The experimental technique used involved completely evaporating from the mass spectrometer probe equal amounts of a compound (in the range 1–3 μg) using first the positive and then the negative mode of ionization. The intensities of the ions produced were measured continuously during the course of the evaporation, and the sum of the intensities of all the ions for all of the scans during a given evaporation was used as a measure of the ionization sensitivity. Prior to data collection, the instrumental parameters were adjusted to achieve unit resolution using perfluorotributyl amine for CH_4 PCI and perfluoromethyloctanoate for OH^- NCI. Instrumental adjustments were kept at an absolute minimum in changing from the positive to negative mode of operation and were generally limited to slight changes in lens voltages.

Table III. Relative Sensitivities $\Sigma I(\mathrm{NCI})/\Sigma I(\mathrm{PCI})$

compound	relative sensitivities
5α-cholestan-3-one(4)	4.7
cholestan-3-ols(12&13)	3.8
cholesteryl stearate(34)	7.1

The relative sensitivities may be defined as the ratios of the total ionizations obtained as described above for OH^- NCI to those obtained for CH_4 PCI. The sensitivities obtained (averages of 10–15 reasonably concordant replicates) for the three compounds investigated are given in Table III. The sensitivities in the negative mode are somewhat greater than those in the positive mode, but not enough to constitute a marked analytical advantage. In our opinion the approximate equivalence of the sensitivities is to be expected for processes involving ion–molecule reactions which are rather similar in terms of the masses of the reacting ions, the exothermicities of the reactions, and the compositions and properties of the reaction mixtures. The differences which do exist between the sensitivities are probably the consequence of small effects which we do not presently understand.

We have compared the OH^- NCI sensitivities with CH_4 PCI sensitivities because the latter is among the highest to be found for positive chemical ionization systems. We have long recognized from qualitative observations that a relationship exists between the sensitivity of chemical ionization reactions and the exothermicities of the reactions, and we have recently make quantitative measurements of this phenomenon (*9*). Milder reagent gases such as isobutane and ammonia are in widespread use in positive chemical ionization, and the exothermicities of the reactions of $t\text{-}C_4H_9^+$ and NH_4^+ from these gases with the steroids of this study will be appreciably lower than the exothermicities of the reactions of CH_5^+ and $C_2H_5^+$ from methane with the steroids. Thus it is quite possible that the OH^- NCI sensitivity with these steroids will be significantly higher than the isobutane and, especially, ammonia sensitivities.

Divers Comments. The ammonia, methane, and isobutane positive chemical ionization spectra of many of these steroids have been measured by Lin and Smith (*2*). It is not feasible nor particularly profitable here to make a compound by compound comparison of the four kinds of chemical ionization spectra. Speaking therefore only in general terms, all four methods are soft ionization methods which produce no fragmentation of the steroid carbon skeleton. The amount of fragmentation involving carbon–oxygen bonds is least for NH_3 PCI, OH^- NCI $\simeq$ $i\text{-}C_4H_{10}$ PCI, and most for CH_4 PCI. No markedly different structural properties are delineated by the positive and negative methods. We have found that the sensitivity for OH^- NCI is somewhat higher than that for CH_4 PCI, and we pointed out that it may be significantly higher than those for $i\text{-}C_4H_{10}$ and NH_3 PCI. We are of the opinion that the combination of low fragmentation and high sensitivity (high reaction exothermicity) is more favorable in OH^- NCI than in the three PCI methods. In all of this it must be kept in mind that the PCI measurements were made at an ion source temperature of 100 °C and a source pressure of about 0.4 Torr. The OH^- NCI measurements were made at a source temperature of 200 °C and a source pressure of 3 Torr. More fragmentation and less ionization (sensitivity) will be encountered in the PCI methods at a higher source temperature.

The OH^- NCI spectra of virtually all of the compounds studied here could be put to good analytical use. The $(M - 1)^-$ ion is the most intense ion in the spectra of 22 of the steroids, and it is of sufficient intensity to allow facile identification of molecular weights for all save two of them. While some association ions are observed (referred to above as $(M + n)^-$ ions), the amount is small in total, and absent for most of the compounds. By contrast, the $(M + NH_4)^+$ ion is found extensively in the NH_3 PCI spectra, and this ion will be markedly lower in abundance or perhaps absent at higher source temperature.

The OH^- NCI results with OH containing steroids are particularly valuable, for such compounds generally show an $(M - 1)^-$ ion of useful intensity and ions produced by the loss of 18 additional mass unit for each OH in the molecule. In some cases the relative intensities of these ions give information about the positions of the OH groups relative to each other and to other groups in the molecule. As an example, such information allows one to distinguish between the diols (20) and (21), which are positional isomers.

The OH^- NCI spectra of cholesteryl esters of fatty acids such as cholesteryl stearate are particularly attractive, for they contain peaks giving information about the molecular weight of the component ($(M - 1)^-$), the identity of the acid present ($RCOO^-$), and the presence of the cholesterol carbon skeleton ($(XO\text{-}H_2O)^-$). In CH_4 and $i\text{-}C_4H_{10}$ PCI the fragmentation of these molecules is so extensive that no molecular weight information is available.

LITERATURE CITED

(1) A. L. C. Smit and F. H. Field, *J. Am. Chem. Soc.*, **99**, 6471 (1977).
(2) Y. Y. Lin and L. L. Smith, *Biomed. Mass Spectrom.*, in press.
(3) A. L. C. Smit, M. A. J. Rosseto, and F. H. Field, *Anal. Chem.*, **48**, 2042 (1976).
(4) V. M. Bierbaum, C. H. DePuy, and R. H. Shapiro, *J. Am. Chem. Soc.*, **99**, 5800 (1977).
(5) J. H. J. Dawson and N. M. M. Nibbering, *J. Am. Chem. Soc.*, **100**, 1929 (1978).
(6) D. J. Cram, "Fundamentals of Carbanion Chemistry", Academic Press, New York, 1965.
(7) L. L. Smith, M. J. Kulig, and J. I. Teng, *Steroids*, **22**, 627 (1973).
(8) R. Hiatt, "Hydroperoxides", in "Organic Peroxides", D. Swern, Ed., Wiley Interscience, New York, 1971, p 46.
(9) M. Meot-Ner (Mautner) and F. H. Field, *J. Am. Chem. Soc.*, **100**, 1356 (1978).

RECEIVED for review August 4, 1978. Accepted November 6, 1978. The Rockefeller University portion of this work was supported in part by a grant from the Division of Research Resources, National Institutes of Health, and that of the University of Texas Medical Branch of National Institutes of Health Grant #HL-10160.

High Sensitivity, Continuous Flow Thermochemical Analyzer

Richard S. Schifreen,[1] Carolyn Sue Miller,[2] and Peter W. Carr*

Department of Chemistry, University of Minnesota, Minneapolis, Minnesota 55455

A flow enthalpimeter for use with two fluid streams has been designed. It is based on a related device for use with one fluid stream and a bed of catalyst. Satisfactory results were obtained only when the two thermistors, which comprise part of a differential temperature measurement system, are subjected to the same net flow. In addition, any volume located between the point of reagent mixing and the adiabatic column must be minimized. Assays for mineral acid, calcium ion, and nitrite based upon their reaction with tris(hydroxymethyl)aminomethane, ethylene bis(oxyethylenenitrilo)tetraacetic acid, and sulfamic acid, respectively, have been developed. Detection limits ranged from 10 μM to 1 mM, depending upon the heat of reaction and achievable base-line stability. Sample volumes of 120 μL and a flow rate of 2.5 mL/min allow for a throughput of nearly 60 samples/h. In general, sample volume, concentration, and flow rate affected the signal height and width in a fashion similar to that observed with an immobilized enzyme analyzer based on a related flow system. The chief differences in behavior occur at low sample concentration.

In principle, thermochemical methods of analysis are applicable to any reaction which either generates or absorbs heat. These techniques, however, require a controlled environment and are often more tedious than other methods which provide the same information. Consequently, thermochemical analysis is often not considered for routine work when some alternative technique is available.

Various attempts have been made to circumvent these limitations. In 1965, Priestly et al. introduced continuous flow enthalpimetry (*1*). This approach was based upon mixing a reagent and sample stream in a plastic cylinder. Three thermistors monitored the temperatures of the sample, reagent, and product streams providing a differential measurement system. They recognized the need for a reaction chamber possessing high mixing efficiency and low thermal capacity and conductivity. This was accomplished by fitting the inlets to the small reaction cylinder with narrow inlets to give two opposed mixing jets.

An isothermal instrument has been developed by Christensen et al. (*2*). Their reaction vessel is immersed in a controlled temperature bath and maintained at a constant temperature by a Peltier cooler and digitally controlled heater. Reaction heats are measured at steady-state by the rate of heat addition required to maintain the pre-set temperature. This instrument is capable of measuring heats of reaction at various pressures and quantitating large volume samples. Its primary advantage lies in that it is independent of the heat capacity of the solution and of the characteristics of the calorimetric vessel as a result of the isothermal mode of operation.

A third device has been developed by Peuschel and Hagedorn (*3-5*) and is being manufactured by Technicon

---

[1] Present address, Clinical Chemistry Laboratory, Hartford Hospital, Hartford, Conn. 06115.

[2] Present address, Technical Services, Schilling Division, McCormick and Co., Inc., Salinas, Calif. 93901.

0003-2700/79/0351-0278$01.00/0 © 1979 American Chemical Society

Corp. (*6*). The sample and reagent streams are introduced into a 1-mL plastic and stainless steel cell agitated by a Teflon encased magnetic stirrer. A single thermistor continuously monitors the cell temperature. The entire apparatus is immersed in a controlled temperature bath which is necessary since only the cell temperature is monitored. The system is sensitive to temperature changes of 5 m°C with a precision of less than 1%. A wide variety of reactions, including precipitation, have been adapted to this instrument. Because of limitations in the cell design, however, only sample volumes of 1 mL or greater and high concentration can be analyzed at a rate of 20–40 samples per hr.

Censullo and Jordan described a method they term "peak enthalpimetry" (*7*). This system is similar to the one described here in that a packed bed was used to provide mixing. Detection limits with this device were at best a decade worse than those available with the present apparatus, and sample throughput at comparable flow rates was lower.

The flow enthalpimeter developed in our laboratory for use with immobilized enzymes meets the requirements of accuracy, precision, and throughput necessary for routine analysis without the need for an electronic temperature controller. In this study the instrument was modified to mix a soluble reagent and sample stream while retaining the desirable operating characteristics of the immobilized enzyme reactor system.

The reactions chosen for study in this work are all well characterized thermochemical systems. They are: the neutralization of Tham (tris(hydroxymethyl)aminomethane) with hydrochloric acid (*8*), the complexation of calcium with EGTA ((ethylene bis(oxyethylenenitrilo)tetraacetic acid) (*9,10*) and the oxidation of nitrite by sulfamic acid (*11*). At this time a precipitation reaction cannot be used in the flow system.

The reactions involved in the various assays are:

HCl-THAM

$$\mathrm{H^+ + THAM \rightleftharpoons HTHAM^+};\ \Delta H_{25\,^\circ\mathrm{C}} = -11.3\ \mathrm{kcal/mol} \tag{1}$$

Ca-EGTA (pH = 8.0)

$$\mathrm{Ca^{2+} + H_2EGTA^{2-} + 2THAM \rightleftharpoons CaEGTA^{2-} + 2HTHAM^+};\ \Delta H_{25\,^\circ\mathrm{C}} \cong -30.6\ \mathrm{kcal/mol} \tag{2}$$

Nitrite-Sulfamic Acid

$$\mathrm{NH_2SO_3H + HNO_2 \rightleftharpoons N_2 + HSO_4^- + H_2O + H^+};\ \Delta H_{25\,^\circ\mathrm{C}} = -95.6\ \mathrm{kcal/mol} \tag{3}$$

The heat of the calcium-EGTA reaction is approximate since the EGTA exists in several forms at pH 8.0.

The purpose of the present work was to present details of the design of a new thermochemical flow reactor system and evaluate the analytical characteristics of the device in terms of its linear dynamic range, precision, and throughput.

EXPERIMENTAL

Reagents. The acid–base neutralization system employed a reagent buffer of 0.5 M tris(hydroxymethyl)aminomethane (Tham, buffer grade, Sigma Chemical Co., St. Louis, Mo. 63178), 100 mM reagent grade sodium chloride, and 1 mM ethylenediaminetetraacetic acid–disodium salt (EDTA, "Baker Analyzed", J. T. Baker Chemical Co., Phillipsburg, N.J. 08865) adjusted to a pH of 8.5 with hydrochloric acid. The sample buffer was 100 mM sodium chloride. Samples were prepared by serial dilution of a hydrochloric acid solution calibrated against primary standard grade Tham (Sigma Chemical Co.). All samples contained 100 mM sodium chloride.

The compleximetric reagent was 0.25 M ethylene bis(oxyethylenenitrilo)tetraacetic acid (EGTA, Sigma Chemical Co.) dissolved in a 0.5 M Tham (Sigma Chemical Co.) buffer adjusted to pH 8.0 with hydrochloric acid. Sample buffer was a 0.5 M Tham solution at pH 8.0. Samples were prepared by dissolving the appropriate amount of reagent grade calcium chloride dihydrate in the sample buffer. An interference study was performed by adding reagent grade magnesium chloride to the sample.

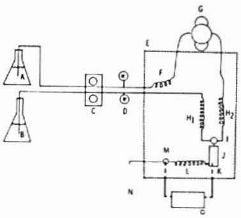

Figure 1. Schematic drawing of the flow enthalpimeter modified for mixing soluble reagents. (A) Sample buffer, (B) reagent buffer, (C) peristaltic pump, (D) pressure gage-pulse suppressor, (E) insulated water bath, (F) pre-equilibration coil, (G) injection valve, (H_1, H_2) matched equilibration coils, (I) mixing Tee connector, (J) reactor column, (K) sensing thermistor, (L) equilibration coil matched to H_1 and H_2, (M) reference thermistor, (O) ac phase-lock bridge

The redox reaction reagent buffer contained 50 mM sulfamic acid (certified, Fisher Scientific Co., Fairlawn, N.J. 07410) dissolved in 0.1 M hydrochloric acid. The sample buffer was 0.1 M hydrochloric acid. Nitrite samples were prepared by weighing out the appropriate mass of reagent grade sodium nitrite into the sample buffer. No attempt was made to exclude oxygen since all reagents were discarded after 24 h. Deionized water was used for the preparation of all reagents.

Instrumentation. The construction of a flow enthalpimeter using an immobilized enzyme reactor was described in detail earlier (*12*). The components used for the soluble reagent system were the same as described previously, although the system is configured very differently. Figure 1 shows a schematic of the modified flow system.

The sample (A) and reagent (B) buffer streams are pumped by a two-channel Masterflex peristaltic pump (C) (Model 7545 pump and controller, Model 7013 and 7013-20 heads, Model 6408041 tubing, Cole-Parmer Instrument Co., Chicago, Ill. 60648) through a pulse suppressor and pressure gage assembly (D) into the stirred, insulated water bath (E). The sample stream passes through the stainless steel pre-equilibration coil (F) and into the injection valve (G). Both streams then pass through matched equilibration coils (H_1) and (H_2) constructed of stainless steel needle tubing (95 cm, 21 gage, 0.02-inch i.d., Precision Sampling Corp., Baton Rouge, La. 70815) and enter opposing channels of a Tee connector (I) (0.07-cm i.d. channels, Altex Scientific, Berkeley, Calif. 94710) where they are mixed. The flow then passes through a 1-cm Teflon fitting into the reactor column (J). It is important that this fitting be drilled with a channel no wider than 0.07-cm i.d., giving a total pre-column mixing volume of 30 μL. A second fitting having a 0.128-cm i.d. channel yielding a pre-column mixing volume of 75 μL was also evaluated. For all experiments, an "adiabatic" column 3.3 cm long with an internal diameter of 3 mm and an approximate volume of 0.42 mL was used and was packed with acid-washed 80–120 mesh solid glass beads (A. H. Thomas Co., Philadelphia, Pa. 19105). In some experiments the glass was treated with dimethyldichlorosilane (DMDCS) by the method of Robinson (*13*). For this work, the glass was dried at 150 °C, rather than the recommended 500 °C, in order to remove bound water without disturbing the surface silanol groups. After passing through the reactor column, the solution passes the sensing thermistor (K) and through a third stainless steel equilibration coil (L). Finally, the buffer passes a reference thermistor mounted in a Tee fitting (M) and out to waste (N). The temperature difference measured by the thermistors is converted to a disbalance voltage by a differential ac phase-lock Wheatstone bridge (O).

Procedure. The instrument is operated in exactly the same manner as the immobilized enzyme reactor system. Five minutes before the first analysis, the stirring motor and pump are started to ensure full thermal equilibration as indicated by a flat base line. Flow rate is measured at the system outlet as the time

Table I. Calibration Curve—Hydrochloric Acid–Tham Reaction[a]

sample concentration, mM	peak height,[b] m°C	CV,[c] %	$w_{1/2}$, mL
blank	0.00	-	-
0.1	0.00	-	-
0.5	0.40	19	0.72
1	1.13	16	0.68
5	8.87	5.0	0.59
10	20.4	1.1	0.51
20	45.7	1.1	0.49
50	116	0.68	0.49
100	225	3.1	0.49
500	860	0.23	0.59
1000	1025	0.38	0.69

[a] Conditions: 120-μL samples; flow rate = 2.5 mL/min; pH = 8.5, 0.5 M Tham buffer. [b] Linear least squares analysis (0.5–100 mM): slope = 2.28 ± 0.02 (m°C/mM); y intercept = 1.13 ± 1.06 (m°C). [c] Correlation coefficient = 1.000; Student's t = 99.5.

required to fill a vessel of known volume. In this case, no sample dilution was necessary and the sample was merely drawn into the sampling valve and injected. Apparent temperature changes were calculated as the product of the measured resistive disbalance of the thermistors and their approximate thermal coefficient of -400 Ω/°C. Peak width at half maximum height ($w_{1/2}$) was converted to volume units via the measured flow rate.

RESULTS AND DISCUSSION

Preliminary Experiments. A number of preliminary designs were tried. There are several important design factors which were discovered. First, both the signal and reference thermistors must be placed *in series* with respect to the total fluid flow. If this is not done, the base line wanders because of slight changes in flow rate since self-heated thermistors are quite flow sensitive (*14*). The alternative to this is to use very stable pumps or decrease the voltage applied to the thermistors (which was approximately 0.5 V peak to peak in this work) at the expense of some loss in sensitivity and temperature resolution (*15–17*). Second, placement of the reference thermistor in an "X" connector at the point of mixing of the two fluid streams results in a negative pre-peak due to observation of the reaction which takes place around the thermistor. Third, attempts to design a reactor where one flow tube was joined to the column along its axis and the other tube joined to the column through a radial aperture gave very irreproducible peaks. This design was an attempt to avoid reaction outside an "adiabatic" column. We believe that this irreproducibility is a result of very *inefficient* radial dispersion and incomplete mixing.

The system described above is a compromise (vide infra) design which avoids the above problems. It is interesting to note that placement of both the signal and reference thermistors after the packed column introduces some thermal smoothing. Second, no double peaks were observed, indicating that all heat produced in the column was completely discharged to the heat sink.

Linear Dynamic Range. All three chemical systems were evaluated with respect to their linear dynamic range. In general, the upper limit was determined by the concentration of the reagent in the reactant stream and the lower limit by the base-line noise and drift of the instrument. For all systems the linear range extended over at least two orders of magnitude.

The appropriate calibration curves and supporting data appear in Tables I–III. Figure 2 shows a representative recorder tracing for the analysis of hydrochloric acid. Sample carry-over, as can be seen, is negligible.

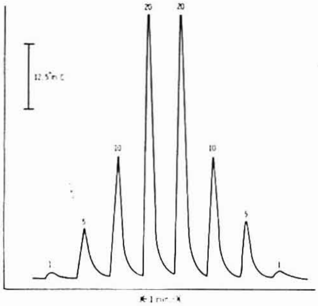

Figure 2. Representative recorder tracing for the determination of hydrochloric acid. Conditions: 120-μL samples, flow rate = 2.5 mL/min, pH = 8.5. Concentrations (mM): 1, 5, 10, 20, 20, 10, 5, 1

Table II. Calibration Curve–Calcium–EGTA Reaction[a]

sample concentration, mM	peak height,[b] m°C	CV,[c] %	$w_{1/2}$, mL
blank	0.00	-	-
0.1	0.37	14.2	0.61
0.5	1.05	16.7	0.61
1	2.36	4.0	0.62
5	13.6	3.5	0.61
10	28.2	2.2	0.59
20	58.2	1.2	0.59
50	150	2.4	0.59
100	301	1.9	0.59
10 mM Ca^{2+}			
1 mM Mg^{2+}	28.2	2.4	0.59
10 mM Hg^{2+}	32.1	1.3	0.59

[a] Conditions: 120-μL samples; flow rate = 2.5 mL/min; pH = 8.0, 0.25 M EGTA, 0.5 M Tham. [b] Linear least squares analysis: slope = 3.02 ± 0.01 (m°C/mM); y intercept = −1.04 ± 0.35 (m°C). [c] Correlation coefficient = 1.000; Student's t = 340.

Table III. Calibration Curve—Nitrite–Sulfamic Acid Reaction[a]

sample concentration, mM	peak height,[b] m°C	CV,[c] %	$w_{1/2}$, mL
blank	0.00	-	-
0.01	0.21	9.4	0.70
0.05	0.77	3.5	0.59
0.1	1.59	1.5	0.59
0.5	7.33	1.3	0.59
1.0	12.2	2.3	0.59
2	24.2	2.1	0.59
5[d]	70.8	2.4	0.59
10	125	6.1	0.59

[a] Conditions: 120-μL samples; flow rate = 2.5 mL/min; 50 mM sulfamic acid, 0.1 M hydrochloric acid. [b] Linear least squares analysis: slope = 12.48 ± 0.07 (m°C/mM); y intercept = 0.13 ± 0.27 (m°C). [c] Correlation coefficient = 1.000; Student's t = 176. [d] These data rejected as an outlier.

Sensitivity, as expected, was proportional to the heat of reaction. This accounts for both the high sensitivity and low limit of detection observed for the nitrite analysis.

Precision is a function of the base-line stability. The high concentrations of Tham used in several of the buffers increased flow noise and consequently increased both the noise and drift over the optimum levels of 50 μ°C peak to peak and

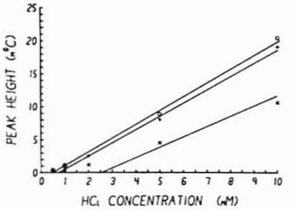

Figure 3. Calibration curve for hydrochloric acid at low concentration showing the intercept effect. Solid line represents the least squares line for the entire calibration curve in Table I. Conditions: (o) Pre-column mixing volume = 30 μL, flow rate = 2.5 mL/min, pH = 8.5. (+) Pre-column mixing volume = 75 μL, flow rate = 2.5 mL/min, pH = 8.5. (x) Pre-column mixing volume = 75 μL, flow rate = 1.1 mL/min, pH = 8.5

7 μ°C/min, respectively, when water was present in both flow channels. As expected, the nitrite analysis, which did not utilize Tham in either channel, had the best precision. This effect is probably due to the significantly greater viscosity of the 0.5 M Tham solutions over that of pure water. In addition, inexpensive, buffer grade Tham contains particles of an insoluble impurity having a diameter between 0.5 and 5 μm. These particles produce and deposit a yellow-brown color at the column inlet and gradually increase the system pressure drop. The column must be repacked when the pressure drop exceeds 20 psi in either channel at a flow rate of 2.5 mL/min. The problem may be eliminated by using primary standard grade Tham or by passing the Tham solutions through a 0.45-μm Millipore filter.

Examination of Table II shows that the determination of calcium with EGTA is much less susceptible to interference by magnesium than the corresponding EDTA based assay would be. Equimolar magnesium, in fact, only contributes a 14% interference in peak height over that obtained with a pure calcium sample despite the large excess of EGTA present. We have shown previously that calcium may be titrated thermometrically with this reagent without interference (*18*).

Effect of Concentration and System Variables on Peak Width. Examination of Tables I–III shows that only the hydrochloric acid studies show significant variations in peak width as a function of concentration. Increased spreading at high concentrations due to incomplete conversion has been observed previously with the immobilized enzyme reactor system (*12*). This was, however, thought to be related to a slow zero-order kinetic process which could not occur in this system, even at the 500 mM or 1000 mM concentrations where complete reaction is stoichiometrically impossible. The similarity of the effect to that seen with the immobilized enzyme reactor, however, bears further study. It is clear that our understanding of microreactors is quite incomplete.

The increase of peak width at low concentrations has not been observed with any other system. This increased peak spreading correlated with the presence of an intercept in the calibration curve which is a result of nonlinearity in the calibration curve at low sample concentrations. Figure 3 compares this effect for several different configurations of the system. It appears that reducing the pre-column mixing residence time, either by decreasing dead volume or increasing the flow rate, reduces the intercept. This may correspond to thermal interactions with the plastic fittings which have been observed previously (*12*) or to the amount of mixing and reaction which occurs before entering the adiabatic region. The direction of the intercept corresponds to a loss of sample or of heat.

The area under a thermal peak should be independent of variations in peak width or asymmetry which result from sample dispersion or slow heat transfer (assuming no heat losses) between components or between solid and liquid phases. We can estimate peak area as the product of peak height and peak half-width. As shown in Figure 4, the same data given in Figure 3 become linear and have a smaller intercept when this correction is applied. The continued existence of the intercept may be due to very severe peak tailing which makes the peaks non-Gaussian and limits the validity of estimating peak areas in this manner. Even under ideal conditions, calibration by peak area does not completely correct for differences in slope because these are due to the heat loss characteristics of the different fittings as well as to changes in peak shape.

It is interesting that only the acid–base system shows thermal spreading at low concentrations. In addition, hydrochloric acid peaks falling in the linear range were narrower than the corresponding peaks obtained with the other two reactions. This suggests a mechanistic difference, since simple adsorption, dilution due to dead volume, or other common sources of tailing should produce wider peaks regardless of sample concentration. Peaks obtained with a column whose packing had been silanized with DMDCS were identical to peaks obtained with an untreated column. This eliminated adsorption of protons or other ionic species to the glass packing material as a cause of the tailing phenomenon. The origin of this phenomenon is not understood. Clearly, a better limit of detection could be obtained if the process could be eliminated.

Effect of Flow Rate on Peak Height and Width. A flow rate study was carried out with the acid–base reaction system at a concentration in the optimum range of the calibration curve (10 mM). The curve obtained is shown in Figure 5 and is qualitatively similar to that of our immobilized enzyme reactor system, i.e., an optimum flow rate exists. In this work the optimum occurs at about 2.5 mL/min which is nearly twice that for the immobilized enzyme reaction. This increased

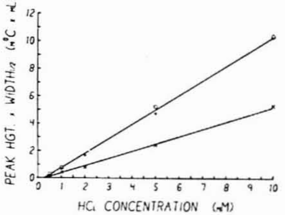

Figure 4. Hydrochloric acid calibration curve by estimated peak area. Solid line represents the least squares line of the data shown. Conditions: (o) Pre-column mixing volume = 30 μL, flow rate = 2.5 mL/min, pH = 8.5. (+) Pre-column mixing volume = 75 μL, flow rate = 2.5 mL/min, pH = 8.5. (x) Pre-column mixing volume = 75 μL, flow rate = 1.1 mL/min, pH = 8.5

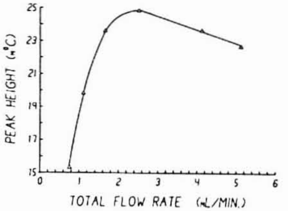

Figure 5. Effect of flow rate on peak height. Conditions: 120-μL samples of 10 mM HCl, pH = 8.5, 0.5 M Tham buffer, column silanized with DCDMS

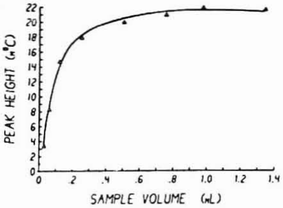

Figure 6. Effect of sample volume on peak height. Conditions: 10 mM HCl, flow rate = 2.5 mL/min, pH = 8.5, 0.5 M Tham buffer

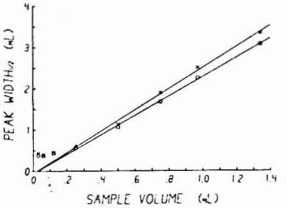

Figure 7. Mixing factors—hydrochloric acid–Tham reaction. Solid line represents the least squares line for sample volumes 0.25–1.40 mL. Conditions: (o) Pre-column mixing volume = 30 μL, flow rate = 1.1 mL/min, pH = 8.5, mixing factor = 2.35 ± 0.05. (x) Pre-column mixing volume = 75 μL, flow rate = 1.2 mL/min, pH = 8.5, mixing factor = 2.56 ± 0.09

optimum flow rate is probably a result of the considerably increased extent of heat loss from the pre-column mixing "Tee". Although the data is not given here, peak width (in volume units) increases with flow rate from 2.5 mL/min and higher. Previous studies showed that this was not a thermal effect since it was also observed with a refractive index detector (*12*). We attributed the phenomena to slow interphase mass transfer. This cannot be the whole explanation since in this work the solid phase is nonporous and the reaction takes place in the bulk liquid phase, not on the surface of a catalyst. There are several significant differences between the packings in this work and the previous report (*12*). As mentioned above, 80–120 mesh nonporous particles were used here in contrast to the previously small (200–400 mesh) porous material. Both of these changes could lead to increased resistance to interphase heat transfer. The coupling theory of Giddings (*19*) would predict very significant thermal wall effects since heat diffusion is quite fast relative to mass diffusion. It is also possible that the increase in peak half-width is due to the length of column needed to provide complete mixing of the reagents. It is extremely difficult to pinpoint the source of this phenomenon. We believe that further detailed studies are needed which might also be very relevant to gaining greater insight into trans-column broadening processes.

Effect of Sample Volume on Peak Height and Width. Sample volume had the same effect on peak height as in previous studies (*12*). Results obtained with the acid–base reaction are shown in Figure 6. Analysis of the steady-state peak heights indicates a retention, at a flow rate of 1.1 mL/min, of only 45% of the total heat generated by the reaction. This is significantly less than the 66% retention of heat measured for the immobilized enzyme system at the same flow rate with the same column. The greater extent of heat loss in the mixing system is due to the passage of the reacting sample through the mixing chamber and plastic fittings before reaching the adiabatic column. The rate of heat loss for routine applications of the mixing system was decreased by increasing the flow rate to the optimum of 2.5 mL/min indicated by the flow rate study (see Figure 5).

Careful matching of the flow rates in both the sample and reagent streams should result in the sample being diluted by *exactly a factor of two*. According to the concepts developed previously for the immobilized enzyme reactor (*12*), the slope of a plot of the peak width of the high volume samples versus sample volume should be exactly two. Any deviation from a value of two would reflect either mismatching of the flow rates between the two channels or non-ideal mixing. A slope less than two indicates inadequate mixing of the sample with reagent, while a value greater than two is characteristic of over-mixing or tailing resulting from either pre-column mixing dead volume or thermal interactions.

Mixing efficiency, at the flow rates studied, should be related only to the physical configuration of the mixing chamber and reaction column. This was verified by measuring the mixing factor or slope of a plot of peak width versus sample volume at high sample volumes for a variety of physical configurations and chemical conditions using the hydrochloric acid–Tham reaction. Only a change in the pre-column mixing volume appeared to affect the mixing factor as shown in Figure 7. The mixing factor, as expected, indicated more *efficient* mixing, i.e., slope closer to the ideal, as the pre-column mixing volume was decreased by decreasing the diameter of the channels.

Analytically, the same trade-off between sensitivity and throughput is present as in the immobilized enzyme reactor system. Increasing sample volume beyond the appearance of a flat-topped steady-state peak does not improve sensitivity, but degrades throughput. Similarly, decreasing sample volume below the limit set by the column dispersion does not improve throughput, but decreases sensitivity.

CONCLUSIONS

The utility of a flow enthalpimeter for the determination of a wide variety of materials by acid–base, complexation, and redox chemistry has been demonstrated. In the case of nitrite determination, we were able to match the detection limit of a state-of-the-art commercial calorimeter with substantially improved throughput. The assays have a precision of approximately 1–3% over much of the linear range. At this time, use of packed-bed columns prevents the use of precipitation processes in conjunction with this flow calorimeter. We can estimate the limit of detection for any material via assumption of peak to peak base-line noise of 50 μ°C (i.e., if the viscosity effects and column clogging described above can be eliminated), retention of at least 40% of the heat generated (which is a conservative assumption), use of a 100-μL sample (which provides 50% of the maximum possible signal), and a heat capacity of 1 cal/°C·cm^3. Based upon the model developed previously (*12*), we find that correcting for heat loss and dispersion of the small sample:

$$\Delta T(°\mathrm{C}) = \frac{0.2\Delta H(\mathrm{cal/mol}) \times C(\mathrm{mol/cm^3})}{1\ \mathrm{cal/°C{\cdot}cm^3}} \tag{4}$$

For a typical reaction of 10 000 cal/mol and thermal detectability of 50 μ°C we see that detection limits of 25 μM are realizable. In view of a total of 100-μL sample volume, this is a relatively small amount of material.

It is impossible to avoid comparison with the commercially available Technicon Thermometric Analyzer. For a given reaction, the flow enthalpimeter is capable of quantitating a sample of one-tenth the volume and one-tenth the concentration of that practical for the Technicon system. The precision of the flow enthalpimeter is, however, poorer by a factor of two or more. The Technicon Thermometric Analyzer, with its single thermistor sensor, requires an electronic temperature controller which is avoided in the flow enthalpimeter by using a differential measurement system. As with other Technicon instrumentation, the Thermometric Analyzer utilizes a segmented flow system. Finally, the reaction cell of the Thermometric Analyzer allows for the use of precipitation reactions at the expense of requiring a larger sample volume than needed for comparable analyses with the flow enthalpimeter. The throughput of the automated Technicon Analyzer and the manually operated flow enthalpimeter are about the same; however, automating the injection process of the flow enthalpimeter would increase its throughout by a factor of two to three while still retaining base-line resolution of the samples.

The practical utilization of either instrument depends on the ability to either eliminate or correct for interfering heats of dilution or reaction resulting from chemical mismatch between the sample and sample buffer. This is, however, a problem intrinsic to all forms of thermochemical analysis and one which must be addressed uniquely for each analyte under consideration.

The placement of the reference thermistor after the sensing thermistor is critical to the operation of the flow enthalpimeter. Optimum performance is obtained by minimizing the mixing volume prior to the column. The best arrangement would be bringing the two reagent tubes concentrically into the entrance of the reactor. This configuration is, however, very difficult to construct with commercial plastic fittings.

The "peak" enthalpimeter described by Censullo and Jordan did contain a mixing chamber formed by joining two concentric reagent tubes (*7*). Their peaks, however, showed considerable tailing and were much wider than those reported here for equivalent sample volumes. This apparent discrepancy is due to both increased dispersion in the peak enthalpimeter's two-meter thermal equilibration coil and thermal tailing in the plastic reaction chamber. The contribution of these factors to peak shape and width has been documented previously (*12*).

Sensitivity and the lower limit of detection are determined by the chemistry involved in a particular analysis. For dilute samples, extraneous heats of mixing can be subtracted as part of the blank. Selectivity can be enhanced by using only the necessary concentration of reagent to complete the reaction of interest and through the use of masking agents.

Our studies of the mass transfer and dispersion relationships in analytical reactor systems indicate that we do not fully understand these processes. It is of great interest that peak widths are sometimes a function of sample concentration. Current models (*12*) do not predict this effect for reactions having first-order kinetic mechanisms. Further study will be required before a general explanation for this phenomenon can be proposed.

LITERATURE CITED

(1) P. T. Priestly, W. S. Sebborn, and R. F. W. Selman, *Analyst (London)*, **90**, 589 (1965).
(2) J. J. Christensen, L. D. Hansen, D. J. Eatough, R. M. Izatt, and R. M. Hart, *Rev. Sci. Instrum.*, **47**, 730 (1976).
(3) G. Peuschel and F. Hagedorn, *Fresenius Z. Anal. Chem.*, **277**, 177 (1975).
(4) F. Hagedorn, G. Peuschel, and R. Weber, *Analyst (London)*, **100**, 810 (1975).
(5) R. Weber, G. Blanc, G. Peuschel, and F. Hagedorn, *Anal. Chim. Acta*, **86**, 79 (1976).
(6) Technicon Corporation, "Thermometric Analyzer", Product Bulletin, Tarrytown, N.Y. 10591.
(7) A. C. Censullo, J. A. Lynch, D. H. Waugh, and J. Jordan in "Analytical Calorimetry", Vol. 3, Plenum Press, New York, 1974, p 217.
(8) C. D. McGlothlin and J. Jordan, *Anal. Lett.*, **9**, 245 (1976).
(9) R. H. Calicott, Ph.D. Dissertation, The University of Georgia, Athens, Ga., 1975.
(10) J. J. Christensen and R. M. Izatt, "Handbook of Metal Ligand Heats and Related Thermodynamic Quantities", Marcel Dekker, New York, 1970.
(11) L. D. Hansen, B. E. Pichter, and D. J. Eatough, *Anal. Chem.*, **49**, 1779 (1977).
(12) R. S. Schifreen, D. A. Hanna, L. D. Bowers, and P. W. Carr, *Anal. Chem.*, **49**, 1929 (1977).
(13) P. J. Robinson, P. Dunnill, and M. D. Lilly, *Biochim. Biophys. Acta*, **242**, 659 (1971).
(14) W. D. Bostick and P. W. Carr, *Anal. Chem.*, **46**, 1095 (1974).
(15) L. D. Bowers and P. W. Carr, *Thermochim. Acta*, **10**, 129 (1974).
(16) L. D. Bowers and P. W. Carr, *Thermochim. Acta*, **11**, 225 (1975).
(17) A. E. von Til and D. C. Johnson, *Thermochim. Acta*, **14**, 1 (1978).
(18) R. Callicott and P. W. Carr, *Clin. Chem. (Winston-Salem, N.C.)*, **22**, 1084 (1976).
(19) J. C. Giddings, "Dynamics of Chromatography", Marcel Dekker, New York, 1965.

RECEIVED for review July 31, 1978. Accepted November 13, 1978. This work was supported by National Science Foundation Grant CHE 75-19412.

Liquid Chromatographic–Fluorometric System for the Determination of Indoles in Physiological Samples

George M. Anderson*[1] **and William C. Purdy**

Department of Chemistry, McGill University, Montreal, Quebec, Canada

A liquid chromatographic–fluorometric system has been used to determine a variety of indolic metabolites of tryptophan in cerebrospinal fluid, brain, plasma, and urine. Detection limits of 5–22 pg were obtained for the compounds of interest by measuring their native fluorescence after excitation at 254 nm. The sensitivity and selectivity of the system enabled new or greatly simplified methods to be developed.

The measurement of a variety of indolic metabolites of tryptophan (TRP) in various physiological samples is required for the elucidation of TRP metabolism. Because TRP serves as the precursor of the neurotransmitter serotonin and of the behaviorly-active trace-amine tryptamine, its metabolism is of special interest in neurochemistry (*1–6*).

Fluorometric methods have been widely employed for the determination of indolic compounds in physiological samples (*7, 8*). Recently methods involving liquid chromatography with on-line fluorometric detection have been developed, allowing some of the measurements to be made more easily, and with greater specificity and sensitivity (*9–18*).

Here we show that a liquid chromatographic–fluorometric system, which we have used for measuring indoles in cerebrospinal fluid (CSF) (*15, 16*), can be used to determine indolic compounds in CSF, brain, plasma, and urine, with a minimum of sample preparation.

EXPERIMENTAL

Apparatus. Liquid chromatography was performed with a Waters 6000A pump, U6K injector, and 30 cm × 3.9 mm (i.d.) reverse-phase column of 10 μm "micro-Bondapak C_{18}" (Waters

---

[1] Present address: Child Study Center, Yale University, 333 Cedar St., New Haven, Conn. 06510.

© 1979 American Chemical Society

Table I. Chromatographic and Detectability Data for Compounds Studied

compound	retention time, min	chromatographic conditions[a]	detection limit, pg[b]
tryptophan	3.5	1	18
5-hydroxyindoleacetic acid	4.6	1	22
indoleacetic acid	3.9	2	5
indolepropionic acid	6.0	2	7
5-hydroxytryptophan	7.8	3	12

[a] Conditions: (1) 2.0 mL/min, 90%, pH 4.3, 0.01 M sodium acetate, 10% acetonitrile. (2) 2.0 mL/min, 70% pH 4.0, 0.01 M sodium acetate, 30% acetonitrile. (3) 1.5 mL/min, 97%, pH 4.1, 0.01 M sodium acetate, 3% methanol. [b] Injected quantity giving a signal/peak-to-peak noise ratio of 2.

Associates, Milford, Mass. 01757). An Aminco Fluoromonitor (American Instrument Co., Silver Spring, Md. 20910) was modified so that a mercury penlamp (Model 11SC-1, U.V. Products, San Gabriel, Calif. 91778) could be employed as the excitation source. The penlamp was positioned parallel to the flow-cell, at a distance of 2.5 cm. A 9.0-mm diameter, 254-nm interference filter (Waters Associates) with a transmittance of 0.41 was employed as the excitation filter. A Corning 7-51 glass filter was used as the emission filter. A Supersil ~70-μL, 26 mm × 2 mm (i.d.) flow-cell was used with a holder having 1.25-mm slits (cell and holder from Aminco). The excitation filter was centrally positioned giving an effective (illuminated and collected) cell volume of ~14 μL. An RCA 931-B photomultiplier (S-4 response) was used with a supply voltage of -700 V. Usually an RC low-pass filter with a time constant (τ) of 1.5 s was employed in addition to a built-in damping circuit (τ = 0.1 s at 0.3 sensitivity).

Reagents. Standards were purchased from the Sigma Chemical Co., St. Louis, Mo. 63178. The acetonitrile used was "glass-distilled U.V. grade" from Burdick and Jackson Laboratories, Muskegon, Mich. 49442. The methanol was spectrograde from American Chemicals Ltd., Montreal, Quebec. All other chemicals were reagent grade. Solvent systems were prepared by adjusting 0.01 M sodium acetate to the proper pH with glacial acetic acid. The proper proportion of organic modifier (v/v) was then added and the solution stirred for ~30 min before use.

Methods. *Determination of TRP and 5-HIAA in Human and Rat CSF.* Human CSF was obtained via lumbar puncture from patients undergoing diagnostic pneumoencephalography (PEG). Rat CSF was obtained from the cisterna magna by cisternal puncture through the atlanto-occipital membrane. CSF samples were stored at -70 °C in acid-washed glass test tubes or polypropylene tubes. Chromatographic analysis was performed by direct injection of 1-20 μL of human or rat CSF. The chromatographic conditions are given in Table I.

Determination of IAA and IPA in Human and Rat CSF. Sampling and storage procedures were as above. Analysis was by the direct injection of 25-50 μL of human or rat CSF. Chromatographic conditions are given in Table I.

Determination of IAA and IPA in Rat Brain. Rat brains were removed intact, rinsed with 0.9% saline, blotted dry, and stored in Parafilm at -70 °C until analyzed. Whole rat brains (~2 g) were thawed at ~5 °C for 10 min in polycarbonate centrifuge tubes and then homogenized for 40 s in 2.5 volumes of 0.1 M $ZnSO_4$ containing 0.02% ascorbic acid. After the addition of 2.5 volumes of 0.1 M $Ba(OH)_2$, the samples were stirred on a vortex mixer for 3 s and then centrifuged at 18000 *g* for 15 min. Solutions were kept at, and operations performed at, 0-5 °C. Approximately 1.0 mL of the supernatant was removed and stored at -70 °C in a polypropylene tube. Chromatographic analysis was by the direct injection of 50 μL of the supernatant (see Table I for chromatographic conditions).

Determination of 5-HTP in Human Plasma. A 0.2-mL plasma sample was deproteinized by adding 0.2 mL of 10% trichloroacetic acid (TCA) solution. The mixture was stirred on a vortex mixer for 3 s at 0, 2, and 4 min after the addition of the TCA. The sample was then centrifuged and ~0.2 mL of the supernatant carefully removed. The sample was kept at 0-5 °C during the procedure and stored at -20 °C until chromatographic analysis (see Table I). An injection volume of 50 μL was usually employed.

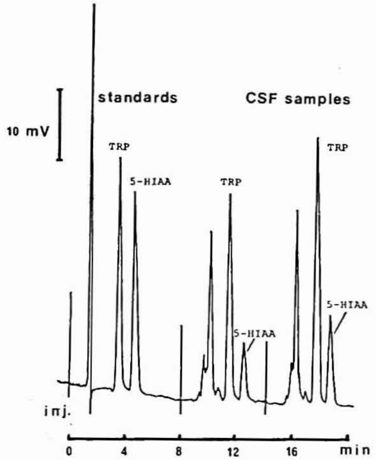

Figure 1. Determination of TRP and 5-HIAA in 10 μL rat CSF samples. Standards (1.0 ng each) at 0.3 sensitivity, samples at 1.0 sens. (less sensitive). Samples contain ~300 ng TRP/mL and ~100 ng 5-HIAA/mL. Chromatographic conditions 1, Table I

Determination of IAA and IPA in Rat Plasma. A 0.20-mL plasma sample was deproteinized by the addition of 0.60 mL of absolute ethanol. The sample was stirred for 3 s on a vortex mixer, allowed to sit for 5 min at ~0 °C then centrifuged. Approximately 0.2 mL of the supernatant was transferred to an acid-washed tube. For chromatographic analysis (Table I), 5-20 μL of the supernatant was injected.

Determination of TRP, IAA, and Indoxylsulfate (ISO_4) in Human Urine. Urine which had been acidified and frozen immediately upon collection was thawed and centrifuged to remove any trace of precipitate. A small portion (e.g. 0.2 mL) of the centrifuged urine was diluted 5- or 10-fold with distilled water and 2-10 μL directly injected. A solvent system of 93% pH 5.1, 0.01 M sodium acetate/7% acetonitrile was used, with a flow rate of 2.0 mL/min.

RESULTS AND DISCUSSION

The retention times and detection limits observed for the compounds of interest are given in Table I. The chromatographic conditions are those used for their analysis in physiological samples.

The determination of TRP and 5-HIAA in two different rat CSF samples is shown in Figure 1. Single point standards are used when quantitating the compounds (by peak height). The recovery of added TRP and 5-HIAA was greater than 95% for samples spiked with 25 to 1000 ng of the compounds. No extraction is required as in another chromatographic-fluorometric procedure for 5-HIAA (*17*), and although an amperometric method (*19*) has a comparable sensitivity for 5-HIAA, its application is limited to the determination of phenolic metabolites.

In Figure 2, the determination of IAA and IPA in 50 μL rat CSF samples is shown. Added IAA and IPA were both completely recovered (>95% for the 1- to 10-ng range) from pooled rat CSF and human CSF samples. The method is an improvement on that previously reported by us (*15*), in that no extraction or internal standard is necessary. A detection

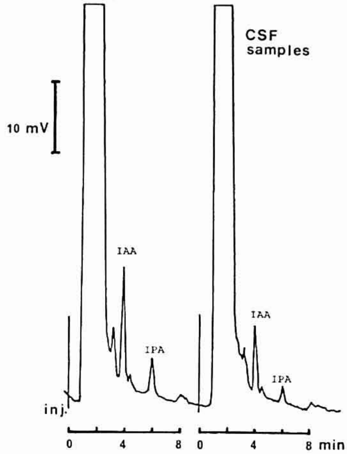

Figure 2. Determination of IAA and IPA in two rat CSF samples by the direct injection of 50 μL of untreated CSF, 0.3 sens. Chromatographic conditions 2, Table I

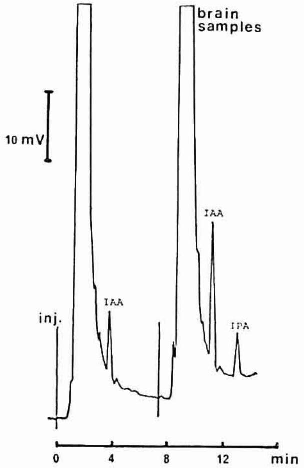

Figure 3. Determination of IAA and IPA in rat brain by the injection of 50 μL of a 5/1 v/w homogenate. The spiked sample has 10 ng/g IAA and IPA added, 0.3 sens. Chromatographic conditions 2, Table I

limit of 0.12 ng IAA/mL of CSF is obtained when a 50-μL sample is injected. An average value of ~5 ng IAA/mL has been observed in rat CSF.

The determination of IAA and IPA in rat brain is shown in Figure 3. A detection limit of 0.5 ng IAA/g brain is obtained with this direct injection method. The recovery of added IAA was 98 ± 2%, while 49 ± 7% (means ± standard error [SEM]) of the added IPA was recovered. The recoveries are for seven rat brains; 10 ng of IAA and IPA were added. The method is much simpler, and slightly more sensitive, than the present gas chromatographic–mass spectroscopic (GC-MS) method (*20*). A value of 8.3 ± 0.8 (mean ± SEM) ng IAA/g was observed for seven whole rat brains. The method is sensitive enough to allow the determination of IAA in single rat brain-area samples. Any IPA observed can be attributed to IPA in blood (see below), the brain containing ~3% blood by weight. A small amount (~1 ng/g) of the brain IAA also arises from this source.

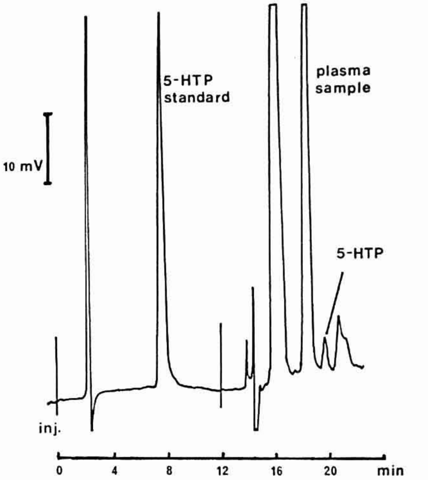

Figure 4. Chromatogram showing the determination of 5-HTP in deproteinized human plasma, along with a 1.0-ng 5-HTP standard. The equivalent of 25 μL of plasma was injected, sens. 0.3. The sample contains 3.3 ng/mL of 5-HTP. Chromatographic conditions 3, Table I

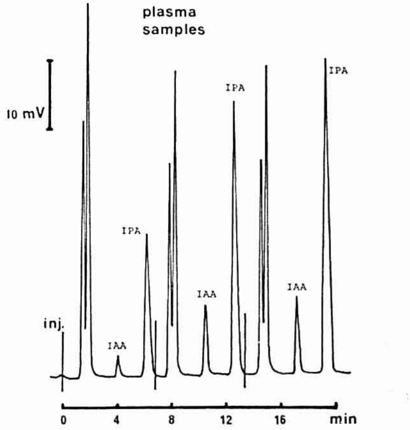

Figure 5. Determination of IAA and IPA in three 5-μL samples of deproteinized rat plasma, sens. 3.0. Chromatographic conditions 2, Table I

A chromatogram showing the determination of 5-HTP in a plasma sample from a patient receiving TRP and benserazide (a decarboxylase inhibitor) is shown in Figure 4. The identification of the peak is based on its retention time in several solvent systems, its behavior in extraction systems, and its behavior when a 280-nm excitation source and/or 300-nm cut-off emission filter were used. Added 5-HTP was completely recovered; when a 50-μL injection volume is used, a detection limit of 0.5 ng 5-HTP/mL plasma is obtained. The

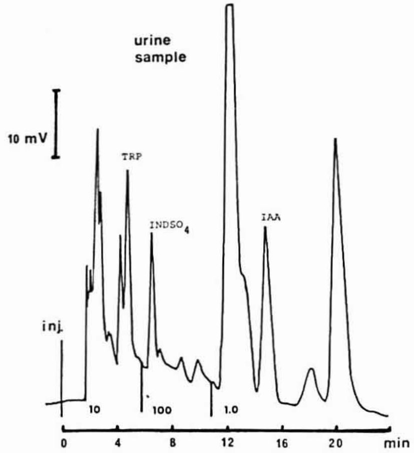

Figure 6. Chromatogram of 1 μL of untreated urine. Numbers immediately beneath chromatogram are sensitivities (change indicated by downward spike). Concentrations for the sample shown are: TRP 32 ng/μL, INDSO$_4$ 120 ng/μL, and IAA 1.8 ng/μL (multiply by 1.2 for mg/24 h). See text for experimental details

detection limit is significantly lower than the ~10 ng/mL limit obtained with the best previous method (*18*); also a simpler sample preparation is employed here.

In Figure 5, the determination of IAA and IPA in three different rat plasma samples is shown. The recoveries of added IAA and IPA were 80 ± 2% and 77 ± 2% (means ± SEM) respectively. Because the recoveries were consistent for the 12 spiked samples examined, no internal standard was used. A detection limit of 2 ng/mL was obtained using a 20-μL injection; typical values of 100 ng IAA/mL and 1 μg IPA/mL were observed. The identities and amounts of IAA and IPA observed were confirmed by thin-layer chromatography (TLC) of acidified plasma extracts. The method is much simpler and quicker than previous methods, the increased sensitivity (detection limits of ~2 ng/mL vs. 100 ng/mL (*21*)) is important as the average value observed for IAA in rat plasma has been ~75–100 ng/mL.

A chromatogram showing the determination of TRP, IAA, and ISO$_4$ in 1.0 μL of human urine is shown in Figure 6. The identities and approximate amounts of the compounds observed were checked by TLC of urine (or urine extracts). TRP and ISO$_4$, which apparently interfered with one another in a previous chromatographic–fluorometric method (*11*), are here easily separated and quantitated. Preliminary results for TRP, IAA, and ISO$_4$ levels in normal human urines have been within previously determined ranges (*22–24*).

The sensitivity and selectivity of the system, and the fact that the native fluorescence of the compounds is being measured, allow new or greatly simplified determinations to be developed. The detection limits obtained are ≳ 10-fold lower than the best previous chromatograph–fluorometric methods, (*12–14, 17, 18*) reported for several of the indoles. The limiting noise has been shown to be photon shot-noise (*16*); because of the square-root dependence of photon shot-noise on background light levels, further decreases in detection limits will be difficult. At present, the system is comparable in detectability to recently developed laser–fluorometric systems (*25, 26*) and to GC–MS methods. The system would appear to be applicable to the determination of many indolic species in various complex matrices.

ACKNOWLEDGMENT

We thank Simon N. Young of the Department of Psychiatry, McGill University, for supplying the rat CSF and plasma samples and for his helpful suggestions. Thanks also to Serge G. Gauthier, of the same department, for supplying the human CSF and plasma samples.

LITERATURE CITED

(1) Cooper, J. R.; Bloom, F. E.; Roth, R. H. "The Biochemical Basis of Neuropharmacology"; 3rd ed.; Oxford University Press: New York, 1978.
(2) Siegel, G. J.; Albers, R. W.; Katzman, R.; Agranoff, B. W., Ed.; "Basic Neurochemistry"; 2nd ed.; Little, Brown and Co.: Boston, Mass., 1976.
(3) Cohen, D. J.; Young, J. G. *J. Am. Acad. Child Psychiat.* **1977**, *16*, 353.
(4) Wolstenholm, G. E. W.; Fitzsimmons, D. W., Ed.; "Aromatic Amino Acids in the Brain; Ciba Foundation Symposium *22*, Associated Scientific Publishers: New York, 1974.
(5) Costa, E.; Gessa, G. C.; Sandler, M., Ed.; "Advances in Biochemistry and Psychopharmacology"; Raven Press: New York, 1974; Vols. 10 and 11.
(6) Young, S. N.; Sourkes, T. L. in "Advances in Neurochemistry"; Agranoff, B. W.; Aprison, M. H., Ed.; Plenum Press: New York, 1977, Vol. 2.
(7) Udenfriend, S. "Fluorescence Assay in Biology and Medicine", Academic Press: New York, 1969, Vol. 2.
(8) Lovenberg, S. W.; Engelman, K. "Methods of Biochemical Analysis", Suppl. Vol., Glick, D., Ed.; Interscience: New York, 1971.
(9) Brown, H. H.; Rhindress, M. C.; Grisevold, R. E. *Clin. Chem.* (*Winston-Salem, N.C.*) **1971**, *17*, 92.
(10) Chilcote, D. D. *Clin. Chem.* (*Winston-Salem, N.C.*) **1974**, *20*, 421.
(11) Karger, B. L.; Graffeo, A. P. *Clin. Chem.* (*Winston-Salem, N.C.*) **1976** *22*, 184.
(12) Meek, J. L. *Anal. Chem.* **1976**, *48*, 375.
(13) Neckers, L. M.; Meek, J. L. *Life Sci.* **1976**, *19*, 1579.
(14) Meek, J. L.; Neckers, L. M. *Brain Res.* **1975**, *91*, 336.
(15) Anderson, G. M.; Purdy, W. C. *Anal. Letts.* **1977**, *10*, 493.
(16) Anderson, G. M.; Young, S. N.; Purdy, W. C., in "Trace Organic Analysis: A New Frontier in Analytical Chemistry", *Natl. Bur. Stand.* (*U.S.*) *Spec. Publ.* **1979**, No. 519.
(17) Beck, O.; Palmskog, G.; Hultman, E. *Clin. Chim. Acta* **1977**, *79*, 149.
(18) Engbaek, F.; Magussen, I. *Clin. Chem.* **1978**, *24*, 376.
(19) Wightman, R. M.; Plotsky, P. M.; Scope, E.; Delcore, R.; Adams, R. N. *Brain Res.* **1977**, *131*, 345.
(20) Warsh, J. J.; Chan, P. W.; Godse, D. D.; Corcina, D. V.; Stancer, H. C. *J. Neurochem.* **1977**, *29*, 955.
(21) Trefz, F. K.; Byrd, D. J.; Kochen, W. *J. Clin. Chem. Clin. Biochem.* **1976**, *14*, 65.
(22) Jepson, J. B. In "Chromatographic and Electrophoretic Techniques", 3rd ed.; Smith, I, Ed.; Heineman: London, 1969, Vol. I.
(23) Byrde, D. J.; Kochen, W.; Idzko, D.; Knorr, E. *J. Chromatogr.* **1974**, *94*, 85.
(24) Hoskins, J. A.; Pollitt, R. J. *J. Chromatogr.* **1975**, *109*, 436.
(25) Bradley, A. B.; Zare, R. N. *J. Am. Chem. Soc.* **1976**, *98*, 620.
(26) Ando, M. E.; Richardson, J. H. *Anal. Chem.* **1977**, *49*, 955.

RECEIVED for review August 28, 1978. Accepted November 22, 1978. The authors acknowledge the National Research Council of Canada for partial support of this work. Portions of this work were presented at the 2nd ISTRY Conference, Madison, Wis., August 10–12, 1977, and at the 9th Materials Research Symposium, National Bureau of Standards, Gaithersburg, Md., April 10–13, 1978.

Dual Wavelength Spectrophotometric Detector for High Performance Liquid Chromatography

Kuang-Pang Li* and John Arrington

Department of Chemistry, University of Florida, Gainesville, Florida 32611

Peak overlapping is very common in multicomponent elution even with optimized high performance liquid chromatography. Quantitization of the seriously interfered components is not feasible with conventional detection methods. We report here the utilization of dual wavelength spectrophotometry (DWS) as a high resolution, high precision, and high selectivity detector for the remedy of this problem. The basic principles of the novel detection method are illustrated and demonstrated with examples of polycyclic aromatic hydrocarbon analysis.

Multiple component determination with high pressure liquid chromatography (HPLC) depends mainly upon the separation efficiency of the chromatographic system. By properly selecting the mobile and stationary phases and operational conditions, such as recycling, solvent programming, temperature or flow programming, multicolumn technique, etc., very high efficiency may be obtained. However, even under the most optimal conditions, peak-overlapping is still very common in the chromatography of structural related compounds. It takes a lot of patience and great care to reveal the analytical information about these hard-to-resolve components. In these cases, if the detector itself also provides means of differentiation for the components in the eluent, it will add a new dimension of resolution to the chromatographic system.

When properly designed, the means of differentiation may arise from the slight difference in any physical or chemical properties of the components. Here we report the utilization of the small spectral difference for the differentiation of structurally closely related compounds. This is accomplished by coupling the HPLC to a spectrometer operating in the dual wavelength mode. Careful selection of the two wavelengths enables us to flip the elution peak of either component in a highly overlapping profile. As a result, not only is the resolution increased but also the identity of the components may be revealed. Methods of quantitation for the individual components are also discussed.

PRINCIPLES

In normal operation of an analytical chromatographic system using an absorption detector, the Beer–Lambert law may be strictly applied for solute detection. Since absorbance is an additive parameter, the instantaneous signal of an eluting profile containing n components is the sum of the absorbance of the individual components, that is,

$$A_\lambda = b\sum_{i=1}^{n} (a_i)_\lambda C_i \qquad (1)$$

where $(a_i)_\lambda$ is the molar absorptivity of the ith component at a wavelength λ, b is the cell length of the detector, and A_λ is the transient absorbance observed during elution. If the dimension used for b is cm and that for C_i is molarity, M, $(a_i)_\lambda$ will have a unit cm^{-1} M^{-1}.

Conventionally, absorption is measured against a reference which is usually an air cell. Absorption of the mobile phase is compensated with proper zero adjustment. Variation due to light scattering by both solvent and solute molecules and that due to flow and lamp current fluctuation are not compensated for. Moreover, components which do not absorb at the wavelength, usually a spectral line from a mercury lamp, e.g., 254 nm or 280 nm, will not be detected and components which absorb at that wavelength will be indifferently registered as predicted in Equation 1. Therefore, if the resolution is much less than unity, precise quantitation of the individual components is almost impossible from the resulting chromatogram.

Differing from the conventional double-beam arrangement, the dual wavelength spectrometry developed by Chance (*1–3*) employs two different wavelengths, λ_1 and λ_2, which are sent through the sample cell along the same light path in a time-sharing manner. The difference in absorbances at these wavelengths is amplified and measured. As a result, fluctuations due to light scattering, source, and flow variations can be minimized. Components which do not absorb at one wavelength but absorb at the other can also be registered. The elution signal observed can thus be expressed as,

$$\Delta A = A_{\lambda 1} - A_{\lambda 2} = b\sum_{i=1}^{n}\beta_i C_i \qquad (2)$$

where $\beta_i = (a_i)_{\lambda 1} - (a_i)_{\lambda 2}$ is the compound absorptivity of the ith component and can be either positive or negative depending on the values of $(a_i)_{\lambda 1}$ and $(a_i)_{\lambda 2}$. When β_i is positive, the elution peak of the ith component will appear on one side of the base line. It will show up on the other side if β_i is negative. Therefore, by proper selection of the two wavelengths, one can make the elution peaks of some components above and the others below the base line. Such alternating coding of the signal provides not only higher resolution than the chromatographic system alone can possibly attain but also additional information about the identity of the components. This is often possible because two different molecules having similar retention times could not possibly have an identical spectrum over the entire UV-visible region.

With the present chromatographic technology, the number of components in an overlapping peak is seldom greater than 3, i.e., $n \le 3$. We will concentrate on the cases where $n = 2$ and $n = 3$.

Assuming in both cases the elution of each component is Gaussian in shape, that is,

$$C_i(t) = \frac{vC_i^0}{f\sigma_i\sqrt{2\pi}} \exp\left[-\frac{(t - t_{Ri})^2}{2\sigma_i^2}\right] \qquad (3)$$

where $i = 1, 2,$ or 3. C_i^0 is the initial concentration of the ith component in the sample, and v and f are the volume of sample injected and the flow rate, respectively. The retention time of the ith component is represented by the symbol t_{Ri} and the corresponding standard deviation by σ_i.

Substitution of Equation 3 into Equation 2 gives, for $n = 2$,

0003-2700/79/0351-0287$01.00/0 © 1979 American Chemical Society

$$\Delta A = \frac{v}{f}[b\gamma_1 C_1{}^0 + b\gamma_2 C_2{}^0] \quad (4)$$

where

$$\gamma_i = \frac{\beta_i}{\sigma_i\sqrt{2\pi}} \exp\left[-\frac{(t - t_{Ri})^2}{2\sigma_i{}^2}\right]$$

where $i = 1, 2$. The parameters γ_1 and γ_2 can be either positive or negative depending on the values of β_1 and β_2, so can ΔA.

Assuming that the selection of wavelengths gives positive β_1 and negative β_2 values, and that t_{R1} is slightly smaller than t_{R2}, the second term on the right hand side of Equation 4 is therefore negative. In a certain range of t, e.g., $t < t_{R1}$, the absolute value of this term is smaller than that of the first term, because of the rapid decrease of the exponential with the increase of the argument, ΔA is positive. It stays positive until $b\gamma_1 C_1{}^0$ is just compensated for by $b\gamma_2 C_2{}^0$. After that ΔA goes negative, passes through a minimum, and approaches zero from the negative side as t increases. This results in a wave-like elution curve with the peak and valley related to the relative amounts of the two components, respectively.

To reveal the concentrations of the components in the original sample, the area under the elution profile is needed. Since the Gaussian function is a normalized function, integration of Equation 4 yields,

$$\Delta A_{\mathrm{T}} = \frac{v}{f}[b\beta_1 C_1{}^0 + b\beta_2 C_2{}^0] \quad (5)$$

Combining Equations 4 and 5, one obtains,

$$C_1{}^0 = \frac{f(\beta_2 \Delta A - \gamma_2 \Delta A_{\mathrm{T}})}{bv(\gamma_1\beta_2 - \gamma_1\beta_2)} \quad (6)$$

$$C_2{}^0 = \frac{f(\gamma_1 \Delta A_{\mathrm{T}} - \beta_1 \Delta A)}{bv(\gamma_1\beta_2 - \gamma_2\beta_1)} \quad (7)$$

Since the β's and γ's can be obtained from calibration, both $C_1{}^0$ and $C_2{}^0$ can be obtained from the measurable values of ΔA and ΔA_{T}.

In the case where three components are overlapping, one can choose two wavelengths which makes β_2 negative while β_1 and β_3 are positive. The concentration of all three components can be measured by measuring ΔA_{T} and two ΔA values, e.g., a peak and a valley or two peaks.

EXPERIMENTAL

Reagent grade methyl alcohol was obtained from Mallinckrodt Inc., Paris, Kentucky. Polycyclic aromatic hydrocarbons (PAH) were purchased from the following sources and were used without further purification: triphenylene, phenanthrene, and anthracene from Aldrich Chemical Company, Inc., Milwaukee, Wis.; benzo[*e*]pyrene from Columbia Organic Chemicals Co. Inc., Columbia, S. C.; chrysene from City Chemical Corporation, New York, N.Y.; pyrene from Eastman Kodak Co., Rochester, N.Y.; 1,2-benzanthracene from Research Organic/Inorganic Chemical Corp., Belleville, N.J.; and benzo[*a*]pyrene from Switzerland.

Stock solutions of the PAH were prepared in methanol and were kept refrigerated no longer than two weeks. Synthetic samples were prepared daily by mixing the stock solutions in proper proportion and diluted to volume with methanol.

An ALC/GPC 203 (from Waters Associates, Inc., Milford, Mass.) high pressure liquid chromatograph equipped with a μBondpak C_{18} column (P/N27324) and a loop injector was used. The HPLC is coupled to an Aminco DW-2 UV-visible spectrophotometer by direct connection of the outlet of the HPLC detector to the inlet of a flow cell (Precision Cells, Inc. 8495, 0.25 mL) in the spectrophotometer. The HPLC was operated isocratically in the reversed phase mode with 74% methanol in distilled water. The column temperature was maintained at 37 °C by circulating constant temperature water through a jacket around the column. The signal output from the HPLC detector was recorded with a strip chart recorder (OmniScribe series B-5000, Houston Instrument, Austin, Texas) at a chart speed of 1 cm/min. The chart speed of the DW-2 was set at 1 in./100 s.

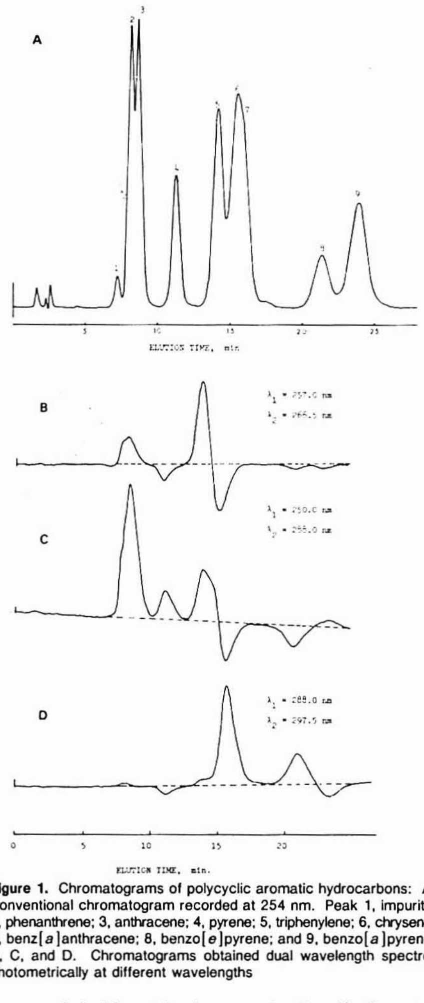

Figure 1. Chromatograms of polycyclic aromatic hydrocarbons: A. Conventional chromatogram recorded at 254 nm. Peak 1, impurity; 2, phenanthrene; 3, anthracene; 4, pyrene; 5, triphenylene; 6, chrysene; 7, benz[*a*]anthracene; 8, benzo[*e*]pyrene; and 9, benzo[*a*]pyrene. B, C, and D. Chromatograms obtained dual wavelength spectrophotometrically at different wavelengths

RESULTS AND DISCUSSION

A typical chromatogram of a mixture containing 8 PAH was reproduced in Figure 1A. It is seen that the separation of pyrene, benzo[*e*]pyrene and benzo[*a*]pyrene is satisfactory. The microparticulate column, however, fails to resolve either phenanthrene from anthracene, or triphenelene, chrysene, and benz[*a*]anthracene from each other. The overlapping of chrysene with benz[*a*]anthracene is particularly serious. Similar observations have been reported with different stationary and mobile phases (*4–6*). None of these investigations using the C_{18} reverse phase column has succeeded in a complete resolution of the PAH. Quantitation of these seriously overlapping species is not feasible with the conventional absorbance measurement method.

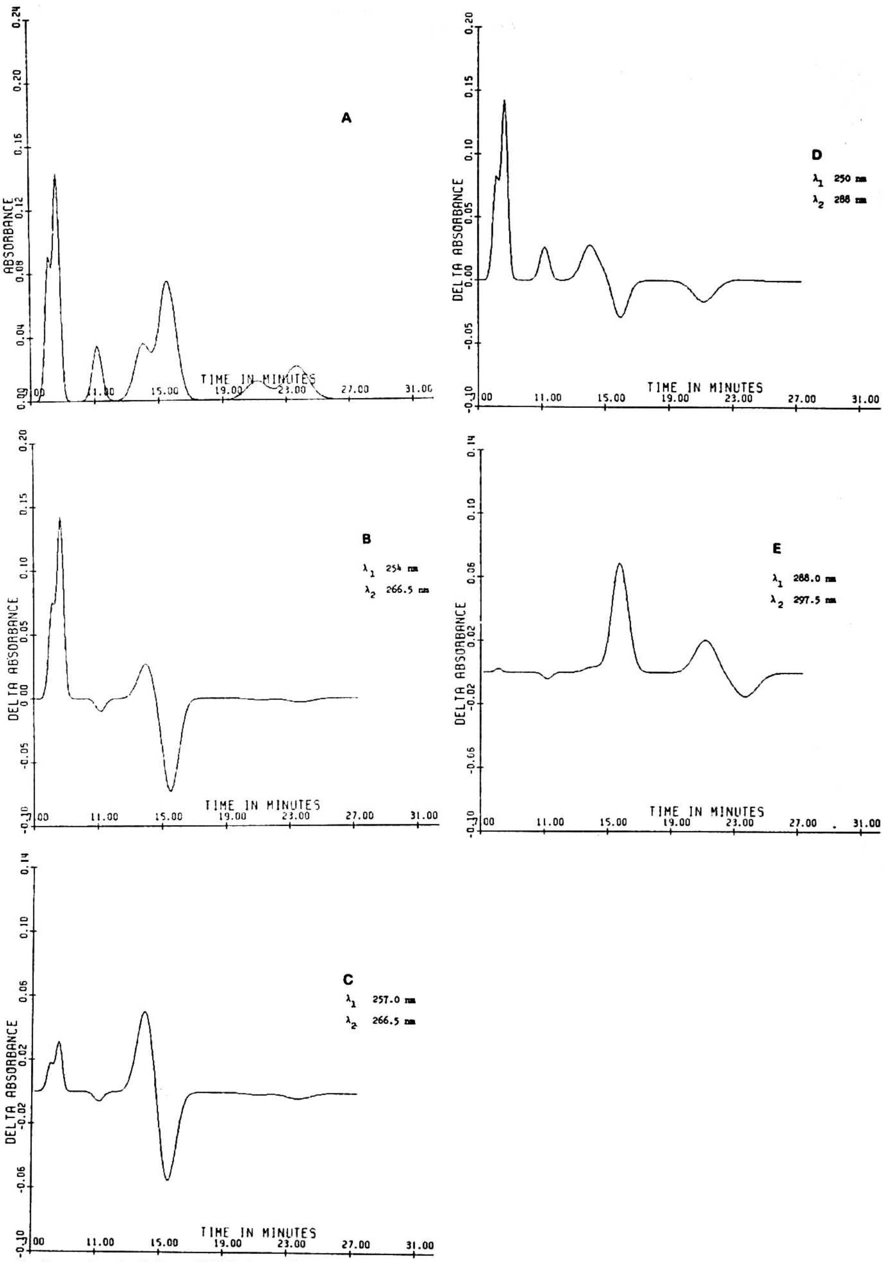

Figure 2. Computer simulations of PAH chromatograms

A fluorescence detector may provide quantitative information about either or both components in an overlapping peak only if they fluoresce strongly and differently. But there are far less fluorescent than nonfluorescent compounds and fluorescence is a spectral property which depends heavily on the environment the molecules are in and on the presence of

Table I. Parameters Used for Chromatogram Simulation

components	concentration, M × 10^4	retention times,[b] min	peak width,[b] min	molar absorptivities,[a] $(M\ cm)^{-1}$ 250 nm	254 nm	257 nm	266.5 nm	288 nm	297.5 nm
phenanthrene	1.03×10^{-4}	8.15	0.25	64 600	64 231	24 086	11 562	6 423	4 817
anthracene	0.53_6	8.70	0.25	200 000	200 520	44 560	534	356	531
pyrene	3.26	11.20	0.29	11 800	11 800	13 146	15 169	2 831	4 247
triphenylene	0.83_2	14.05	0.50	73 053	79 902	132 995	15 980	9 816	2 169
chrysene	1.33	15.5	0.50	43 375	68 487	91 316	164 000	9 360	9 132
benz[*a*]anthracene	1.57	15.8	0.50	33 102	36 525	38 809	45 656	90 170	7 419
benz[*e*]pyrene	1.24	21.2	0.67	20 816	23 970	24 601	27 124	54 249	11 985
benz[*a*]pyrene	1.37	23.7	0.75	38 689	43 736	42 894	50 464	36 166	66 865

[a] Calculated from Sadtler UV spectra. [b] Obtained from the following chromatographic conditions: Temp = 37 °C, flow rate = 1.21 mL/min, mobile phase = 35 mL H_2O/100 mL CH_3OH, solvent = CH_3OH (Mallinckrodt), column packing = μ Bondapak C_{18}, pressure = 2300 psi.

quenching or sensitizing species. These facts make the fluorometer a very selective but less versatile detector in liquid chromatography.

The HPLC-DWS system reported here has the selectivity the fluorescence detector has and the versatility it does not have. In addition, its ability to determine simultaneously both components in a highly overlapping peak is very unique.

Because of the additional dead volume of the flow cell, post column mixing in the DWS is believed to be much worse than that in the HPLC detector. Even under such an adverse condition, the resolution of this novel differentiating detection technique is seen to be much better than the conventional method. Resolution can be even better if the analytical column is directly coupled to the DWS.

Since the chart speed of the DWS is different from that used for the HPLC, it is not easy to line them up for comparison. So we extract the chromatographic information from the chromatogram and spectral information from Sadtler spectra (see Table I) and substitute them into Equations 1 and 2. By means of a computer we can simulate chromatograms under different conditions (Figure 2). These simulations help a lot in confirming the identity of the PAH.

It is seen from Table I that phenanthrene, anthracene, and triphenylene have greater molar absorptivities at 254 nm than at 266.5 nm but the rest of the PAH absorb more strongly at 266.5 nm. If one chooses λ_1 = 254 nm and λ_2 = 266.5 nm, the elution profile of phenanthrene, anthracene, and triphenylene will be on the positive side while the others will be on the negative side. Providing that all PAH concentrations are comparable, the largest negative peak in the resulting chromatogram will be chrysene because it has the greatest difference in absorptivity (Figure 2B).

When the wavelength λ_1 is changed from 254 nm to 257 nm, the absorptivities of phenanthrene and anthracene decrease drastically, as do their elution peaks (Figure 2C), whereas the triphenylene peak is enlarged significantly.

Now, if the two chosen wavelengths are 250 and 288 nm, benz[*a*]anthracene will be flipped negative and pyrene positive as shown in Figure 2D. However, the best wavelengths for determination of benzanthracene, benzo[*e*]pyrene, and benzo[*a*]pyrene in the multiple component mixture are 288 and 297.5 nm. At these wavelengths (Figure 2E) the interference from triphenylene and chrysene is negligibly small and the elution signals are of considerable size. All these simulations match with the real chromatograms (Figure 1, B–D) with fantastic resemblance in both peak shape and relative peak sizes. This implies that such simulation may be very useful in real sample determination. With a computer-interfaced system, such matching may be reached in real time. Even though a complete analysis may not be feasible in this manner, the identity and quantity of the concerned components may be revealed.

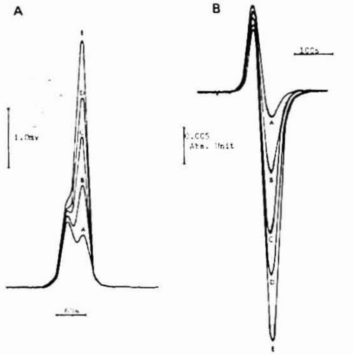

Figure 3. Chromatograms of triphenylene and chrysene. Wavelength used: λ_1 = 257 nm and λ_2 = 266.5 nm. Amount of triphenylene injected: 38.1 ng; amount of chrysene introduced: A, 69.7 ng; B, 139.4 ng; C, 209.1 ng; D, 278.8 ng; and E, 348.5 ng

Figure 3 shows chromatograms of a series of binary mixtures of triphenylene and chrysene. The amount of triphenylene is kept constant and that of chrysene is varied. The elution profiles recorded conventionally at 254 nm were reproduced in Figure 3A, whereas those displayed in Figure 3B are chromatograms obtained dual wavelenth spectrophotometrically at 257 and 266.5 nm. At these two wavelengths, the compound absorptivities of triphenylene and chrysene are of opposite signs. As a result, the elution of chrysene appears in a valley. The depth of the valley is seen to be proportional to the concentration of chrysene. If this amplitude is plotted against the amount of chrysene injected onto the column, a straight line is obtained. The line does not pass through the origin because of the interference of triphenylene. Referring back to Equation 4, it is seen that the intercept of this line with the ordinates is corresponding to the quantity of $bv\gamma_1 C_1^0/f$. Dividing this quantity by the concentration of triphenylene one obtains the value of $bv\gamma_1/f$. In the actual calculation, we used the absolute amount, in nanograms, instead of concentration. A conversion factor must be included. But this factor is later eliminated automatically. As long as we keep the units consistent, there is no need to worry about the conversion.

The area of the elution profile is measured with a compensating polar planimeter (Keuffel & Esser Co., New York). It is also proportional to the concentration as indicated in Equation 4. The intercept yields $bv\beta_1/f$ in the same manner as γ_1. Once these parameters are found, a reduced parameter corresponding to the quantity $(bv/f)[\gamma_1 \Delta A_T - \beta_1 \Delta A]$ can be

Table II. Calibration of Chrysene in the Presence of Triphenylene[a]

amount introduced ng,		$\Delta A \times 100$	ΔA_T	(bv/f)-$[\gamma_1 \Delta A_T - \beta_1 \Delta A] \times 10^5$
69.7		−0.40	+0.031	1.13
139.4		−1.15	−0.021	2.22
209.1		−1.95	−0.074	3.42
278.1		−2.60	−0.115	4.40
348.5		−3.45	−0.172	5.67
	slope	-1.084×10^{-4}	-7.182×10^{-4}	1.617×10^{-3}
	intercept	3.56×10^{-3}	7.99×10^{-2}	-1.44×10^{-7}
	correlation	0.9990	0.9983	0.9991

[a] Amount of triphenylene introduced is 38.1 ng.

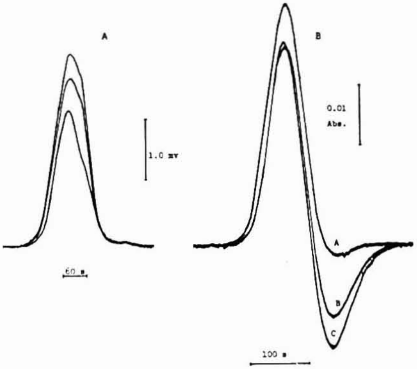

Figure 4. Chromatograms of chrysene and benz[*a*]anthracene. Wavelengths used: 266.5 and 288 nm. Curve A: chrysene, 306 ng, benz[*a*]anthracene, 190 ng; Curve B, chrysene, 306 ng; benz[*a*]-anthracene, 379 ng; and Curve C, chrysene, 306 ng; benz[*a*]-anthracene, 474 ng

evaluated and tabulated in Table II. If this parameter is plotted against the concentration of chrysene, a straight line is again constructed. This line will pass through the origin with a slope equal to $(bv/f)^2\,[\gamma_1\beta_2 - \gamma_2\beta_1]$ as predicted from Equation 7. This line may serve as the calibration curve for the quantitization of chrysene in an unknown sample.

The same calibration procedure can be applied to triphenylene in the presence of chrysene or to other binary mixtures such as chrysene and benzanthracene even though the components are nonresolvable in the conventional manner (Figure 4, A and B). Computer simulations demonstrate that this flip-over is often possible unless the two components have identical elution profiles.

It is most convenient to measure a peak height or valley depth when the peak and valley are of comparable size. However, in most times, particularly in real sample analysis, the interfering component may be much more concentrated than the component of interest. To overcome this problem, one can either use a standard addition method to enlarge the peak size of that component or choose wavelengths such that the ΔA of the interfering component is partially, if not completely, diminished without giving up too much sensitivity for the component of interest.

The Aminco DW2 spectrophotometer has the highest sensitivity range of 0.005 absorbance unit. We have been using the full-scale range of 0.1 and 0.05 throughout this work. With these ranges, we can easily quantitize triphenylene, chrysene, and benzanthracen at the 50-ng level or less. We expect that 1–5 ng of these PAH can be determined in the presence of their mutual interferences with the present setup. The limit of detection can be lowered if the absorption light path is increased. This is advantageous because post-column mixing is not as critical in this method as in the other detection techniques. The volume of the flow cell can be enlarged without seriously affecting the quality of the chromatogram.

Although the basic principles of this method were developed based on Gaussian profiles, components with non-Gaussian elution can be determined as well.

LITERATURE CITED

(1) B. Chance, *Rev. Sci, Instr.*, *13*, 158 (1942).
(2) B. Chance, *Rev. Sci. Instr.*, *22*, 634 (1951).
(3) B. Chance, *Science*, *120*, 767 (1954).
(4) B. S. Das and G. H. Thomas, *Anal. Chem.*, *50*, 967 (1978).
(5) M. Dong, D. C. Locke and E. Ferrand, *Anal. Chem.*, *48*, 368 (1976).
(6) M. A. Fox and S. W. Staley, *Anal. Chem.*, *48*, 992 (1976).

RECEIVED for review August 16, 1978. Accepted November 10, 1978. The authors gratefully acknowledge the National Science Foundation (Grant No. MP 575-02520) for partial support of this work.

Analysis of Gasoline for Antiknock Agents with a Hydrogen Atmosphere Flame Ionization Detector

M. D. DuPuis and H. H. Hill, Jr.*

Department of Chemistry, Washington State University, Pullman, Washington 99164

A hydrogen atmosphere flame ionization detector (HAFID), modified from a commercial FID, is demonstrated as a selective gas chromatographic detector for the determination of antiknock agents in gasoline. By a simple one to ten dilution of a leaded gasoline, alkyllead compounds were detected with no interference from overlapping chromatographic peaks of hydrocarbons. The two samples analyzed in this study contained 1.22 and 0.38 g/gal Pb as tetraethyllead (TEL). Similarly, methylcyclopentadienylmanganese tricarbonyl (MMT), corresponding to 6 mg/gal of Mn, could be easily detected in an unleaded gasoline sample. Detection limits were calculated to be 7.2×10^{-12} g/s of Pb and 1.7×10^{-14} g/s of Mn. Optimal operating conditions are discussed.

The hydrogen atmosphere flame ionization detector (HAFID) introduced in 1972 (*1*) and subsequently developed through 1976 (*2–5*) is a sensitive and selective gas chromatographic detector for organometallic compounds. Minimum detectable amounts for certain metal containing compounds extend to the low picogram and sub-picogram range with selectivities of 10^4 and 10^5 when compared to *n*-hydrocarbon responses.

Its basic design can be compared to a standard flame ionization detector modified so that oxygen enriched air is premixed with the column effluents and introduced through the jet tip while hydrogen doped with small amounts of silane is introduced directly into the detector housing so that the flame burns in a hydrogen atmosphere. For optimal response, the collecting electrode is positioned 5 to 7 cm from the flame compared to only 0.5 cm for the FID collector. Response mechanisms remain unclear but it is believed that the enhancement of organometallic response rests with a charge transfer process between the ions responsible for the flame background current and the organometallics or their combustion products to form a stable ionic species that is capable of being efficiently collected several centimeters from the flame (*4*).

Because of the HAFID's simple design and the high sensitivity and selectivity to organometallic compounds, it appears ideal for routine determination of volatile antiknock agents in gasolines by gas chromatography.

Alkylleads and MMT are the most common antiknock agents. TEL has been used commercially since 1920 but in recent years lead concentration in gasolines has been restricted because of environmental concerns. Since the passage of the Clean Air Act in 1970, maximum allowable lead concentrations in gasolines have dropped continually from 2.5 g/gal in 1970, to 2 g/gal in 1974, to 1.25 g/gal in 1977, 0.8 g/gal in 1978 with a new goal of 0.5 g/gal by October 1979 (*6*). As the use of lead was restricted, other organometallics were substituted. The most successful of these substitutes is MMT (*7*). One gram of Mn as MMT is as effective in improving octane rating as 3.22 grams of Pb as TEL. MMT has been used as the antiknock agent in many unleaded gasolines but since low levels of manganese in the atmosphere may lead to chronic manganese poisoning and since buildup of Mn_3O_4 deposits may decrease efficiency of catalytic converters, it has recently been banned. It is still added to some leaded gasolines and is also used as a fuel oil additive. Wherever this antiknock agent is allowed, sensitive analytical methods will be necessary to routinely monitor and ensure compliance with legal concentration limits.

One common method for the determination of antiknock agents has been to couple various spectroscopic units with a gas chromatograph. Coker (*8*) reported a gas chromatography/atomic absorption spectrometry technique for alkylleads in which he could analyze a sample in 5 min with a detection limit of 0.2 ppm lead, a value, he points out, suitable for determining trace lead in unleaded gasoline. Uden et al. (*9*) recently reported a technique for MMT with a detection limit of 3 ng of Mn utilizing a direct GC interface to an argon plasma emission detector. Alkyllead has recently been determined in the atmosphere with a GC-microwave plasma detector by Reamer et al. (*10*).

Other GC detection methods that have been investigated for alkyllead analysis include several electron capture procedures (*11–13*), a flame ionization method which requires a complicated separation and derivation step (*14*), and a dithiozone spectrophotometric technique (*15, 16*).

Potential of the HAFID for use as an antiknock detector has been pointed out by Hill and Aue. Their detector had a selectivity for tetraethyllead over dodecane of 10^4 with an MDA of 51 pg TEL injected (*4*). They showed a chromatogram where a peak for TEL could be easily detected in an injection of gasoline diluted 1 to 100 in hexane (*5*). MMT response has never been characterized in the HAFID.

The purpose of this study is to construct an optimized HAFID from a FID design different from any previously reported, to compare detection limits, response selectivity, and calibration curves for tetraethyllead with those obtained in earlier work, to report response characteristics of MMT, and to demonstrate the HAFID as a selective detector for antiknock agents in gasoline.

EXPERIMENTAL

HAFID Design. The HAFID constructed for this work was a modification, similar in design to the HAFID reported in ref. 4, of one of the FID units from a Hewlett-Packard dual FID system (Model 18812A). In this design, illustrated in Figure 1, the base of the original FID was unmodified but the FID electrode and mounting were substituted with a stainless steel cap containing a collecting electrode and an ignitor. The collector, the terminal pin of a coaxial bulkhead fitting, screwed into the stainless steel cap so that the pin was 53 mm above the jet tip. The original jet tip (0.5-mm i.d.) was bored to an internal diameter of 1.5 mm. Two 1.5-V Ray-O-Vac 900 Hobby batteries provided the current to a KB-15 glow plug for detector ignition. Ions were collected with a −90 V potential supplied from an Eveready no. 490 battery placed between the pin electrode and a Keithley Model 417 picoammeter. After amplification, the signal could be recorded directly with a Sargent-Welch Model XKR strip chart recorder or channeled via a Hewlett-Packard Model 18871A A/D converter for print out and peak integration with a Hewlett-Packard 18850A terminal. The final modification was to interchange the air and hydrogen lines from normal FID operation.

Detector Conditions. *HAFID.* Detector temperature was maintained at 250 °C. The total hydrogen gas flow was held constant at 1600 mL/min and for optimal response was doped

0003-2700/79/0351-0292$01.00/0 © 1979 American Chemical Society

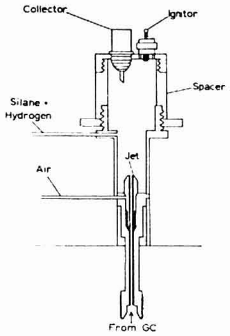

Figure 1. HAFID modified from a Hewlett-Packard FID. Air enriched with O_2 is passed down the outside of the jet through an orifice not pictured above and mixes with the GC effluent at the column exit

with 34 ppm of silane by mixing proper proportions of pure hydrogen (Airco Specialty Gases, Santa Cruz, Calif.) and hydrogen doped with 100 ppm silane (Airco Specialty Gases, Santa Cruz, Calif.). Air, 120 mL/min, was enriched with 150 mL/min of oxygen before entering the jet tip.

FID. Detector temperature was maintained at the same temperature as the HAFID. Flow rates used were those recommended by the manufacturer: Hydrogen, 30 mL/min and air, 240 mL/min.

Standards and Samples. TEL (ICN Pharmaceuticals, Inc., Plainview, N.Y.) was diluted in hexane to produce standard solutions at concentrations of 10 μg/μL, 1 μg/μL, 100 ng/μL, 10 ng/μL, and 1 ng/μL. Each concentration was sealed in a 25-mL screw cap glass sample tube with an aluminum foil liner and stored at 5 °C. They were warmed to room temperature before use. TEL was the only alkyllead standard available for use in this study. Peaks for tetramethyllead (Me_4Pb), trimethylethyllead (Me_3EtPb), dimethyldiethyllead (Me_2Et_2Pb), and triethylmethyllead (Et_3MePb) were identified from retention patterns reported in earlier work (*8*, *11*, *16*).

MMT (Alfa Division, Ventron Corp., Danvers, Mass.) standards were diluted in iso-octane to concentrations decreasing by a factor of 10. The concentrations ranged from 10 μg/μL to 10 pg/μL. Because MMT undergoes light induced decomposition, standards were kept in brown bottles and were prepared fresh each day. Dodecane was used to characterize the HAFID response to hydrocarbons for determination of detector selectivity. A solution of 500 ng/μL was prepared in hexane.

Gasoline samples were collected in brown glass bottles from local service stations, transferred to the laboratory, and analyzed as soon as possible.

Chromatographic Conditions. *General.* A Hewlett-Packard 5830A gas chromatograph with dual FID detection (one modified to HAFID) was used throughout this study. The column, 6 ft × $^1/_4$ in. o.d. (2-mm i.d.) borosilicate packed with 80/100 mesh Ultra-Bond 20 M (RFR Corp., Hope, R.I.), was interchanged between detectors. The injection port temperature of 225 °C and the carrier gas flow of 20 mL/min of helium remained the same throughout the study.

Silane Optimization. Injection of 1 ng MMT and 5 ng TEL was repeated as the silane mixing ratio with hydrogen was varied from 5 to 60 ppm. The total hydrogen flow was held constant at 1600 mL/min. Column temperature for MMT was 140 °C and for TEL was 90 °C.

Calibration Curves. Under optimal silane doping conditions of 34 ppm, calibration curves were obtained from TEL and MMT standards with the same isothermal column conditions used for silane optimization. Selectivities of these compounds were calculated by comparing the 5 ng TEL response and the 25 pg MMT response to that response obtained for 500 ng of dodecane.

Sample Analysis. Gasoline samples analyzed for alkylleads were diluted 1 to 10 with hexane in order not to saturate the detector with lead. The analysis was accomplished by injecting 0.5 μL of the diluted sample and temperature programming the column from 30 °C held for 5 min to 120 °C held for 5 min at a rate of 20 °C/min. MMT analysis was accomplished by injecting 0.25 μL of the gasoline directly into the column held isothermally at 140 °C. Both FID and HAFID detection methods were used for each sample under identical chromatographic conditions.

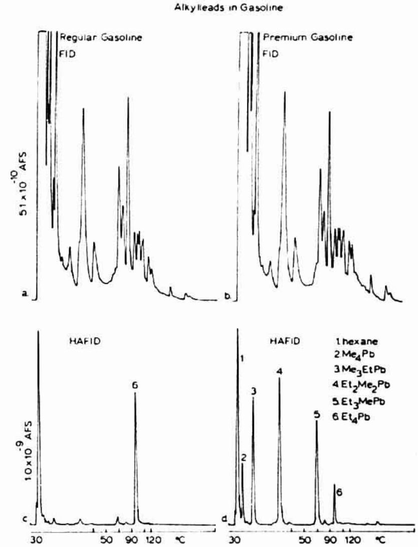

Figure 2. HAFID and FID analysis of alkylleads in gasoline. (a) FID tracing of a regular grade gasoline. (b) FID tracing of a premium grade gasoline. (c) HAFID tracing of a regular grade gasoline. (d) HAFID tracing of a premium grade gasoline. Chromatographic conditions: He (carrier gas) = 20 mL/min, injection temperature = 225 °C, temperature program: 30 °C for 5 min, 20 °C/min, 120 °C for 5 min. Column = 6 ft × $^1/_4$ in. o.d. (2-mm i.d.) borosilicate packed with 80/100 mesh Ultra-bond 20 M. Detector conditions: HAFID-H_2 = 1600 mL/min, SiH_4 = 34 ppm, O_2 = 150 mL/min, air = 120 mL/min, temp. = 250 °C. FID-H_2 = 30 mL/min, air = 240 mL/min, temp = 250 °C

RESULTS AND DISCUSSION

Figure 2 demonstrates the effectiveness of the HAFID for analysis of gasolines for alkylleads with several illustrative chromatograms. Chromatograms a and b are respective FID tracings of a regular grade and a premium grade gasoline. The complexity of these chromatograms caused by the FID's sensitive response to numerous hydrocarbon components, masks the alkyllead peaks and makes analysis impossible. Chromatograms c and d are HAFID tracings of the same samples under identical chromatographic conditions juxtaposed with the appropriate FID tracings. Alkyllead peaks contain little or no interference from hydrocarbons making them easily identified and quantified from standards.

Results for MMT were similar to those for alkylleads. Figure 3a shows MMT detection in a sample of unleaded gasoline while Figure 3b illustrates the difficulty of a FID analysis for the same sample and under the same chromatographic conditions. Figure 3c is a chromatogram obtained with the HAFID for a gasoline sample not containing MMT while Figure 3d is of a 25-pg MMT standard. Note that the retention time for the standard does not correspond with a detectable peak in the FID tracing.

The minimum detectable amount (MDA) of 30 pg obtained for tetraethyllead compares favorably with that of 51 pg reported earlier (*4*). The detector's minimum detectable limit

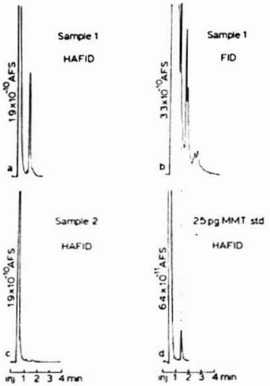

Figure 3. HAFID and FID analysis of MMT in gasoline. (a) HAFID tracing of a nonleaded gasoline containing MMT. (b) FID tracing of gasoline sample used in a. (c) HAFID tracing of nonleaded gasoline not containing MMT and (d) HAFID tracing of a 25-pg standard of MMT. Conditions are the same as in Figure 2 except column temperature was held constant at 140 °C

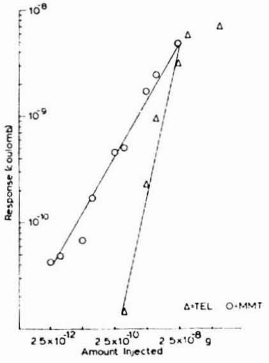

Figure 4. Calibration curves for MMT and TEL

(MDL) for TEL was calculated to be 1.1×10^{-11} g/s or a MDL for Pb of 7.2×10^{-12} g/s. MMT produced a more sensitive response than TEL with a minimum detectable amount of 200 fg and a detection limit of 6.6×10^{-14} g/s for MMT or 1.7×10^{-14} g/s when calculated for Mn. Detection limits for Mn-containing compounds have not previously been reported for the HAFID. Selectivities, calculated for dodecane, were comparable to those reported for the earlier models (*4*).

Quantitative data could be interpolated easily from the calibration curves shown in Figure 4. All points, except one, fell within 10% of the standard curves. TEL was determined to be present at a concentration of 1.90 g/gal (1.22 g of Pb/gal) in the regular gasoline and at 0.60 g/gal (0.38 g of Pb/gal) in the premium sample. As expected, the amount of MMT found in the unleaded gasoline was considerably lower than TEL concentrations found in the leaded gasolines with a value of 24 mg/gal for MMT (6 mg/gal for Mn). These concentrations are about 10 times less than the maximum allowed (62.5 mg of Mn/gal). Since MMT decomposes readily, the Mn value obtained with this method accurately reflects the level of active antiknock agent but does not necessarily represent the total Mn concentration in the sample.

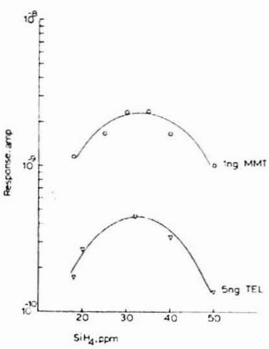

Figure 5. Optimization of silane in hydrogen

Although calibration curves were linear on a log–log scale, their slope exceeded 1.0 indicating that the response was not a linear function of concentration. Specific geometrical design characteristics or thermal decomposition in the injection port may be a cause of nonlinear response, but further investigations are required before definite explanations can be proposed.

Construction of the HAFID on the H.P. 5830A was carefully patterned after an earlier model built on a Bendix 2500 (*4*), but three design characteristics were noticeably different. First, since both HAFIDs were constructed by modifying FIDs, internal diameters differed as dictated by original FID designs. The i.d. in the reaction zone of the HAFID on the H.P. instrument was 10 mm compared with 32 mm for the Bendix instrument. No experiments have been performed comparing internal diameter variations, and it is not clear what effects these changes have on response. Second, the platinum loop electrode was substituted with the terminal pin of an Amphenol, coaxial connector. Cursory comparisons of the pin head electrode and a platinum loop electrode indicate that electrode shape does not affect response.

The location at which hydrogen was introduced into the detector is the third and a most important design variation. In the model of this study (see Figure 1), hydrogen enters the detector 21 mm above the jet tip as a stream perpendicular to the exiting gases from the flame. In the detector on the Bendix unit, hydrogen was introduced beneath the jet through diffusers so that a laminar hydrogen flow passed by the flame. This difference is believed to be the primary reason the optimal silane doping concentration was significantly higher than in the earlier model. Figure 5 shows the response of 1 ng of MMT and 5 ng TEL as a function of the mixing ratio of silane in the hydrogen gas with an optimal value for both compounds of 34 ppm. The optimum in the earlier detector was 5 ppm and compares favorably with 7 ppm obtained for a newly constructed detector (not discussed in this paper) in which hydrogen is also introduced beneath the flame jet. When hydrogen is introduced below the flame, silane is transferred to the flame with the hydrogen flow; but when silane is introduced above the flame, it first contacts combustion products from the flame. The higher requirement for silane could then be attributed to reactions with H_2O, O_2, and other gases in the exhaust, reducing its effective concentration in the atmosphere.

As is obvious from this discussion, many questions are still unanswered concerning the mechanism of this enhanced metal ionization response. How is the doping gas transferred to the reaction zone? Why is the doping gas necessary? Do other doping agents exhibit similar effects? What is the ionic species that is collected 53 mm from the flame? Is detector geometry of paramount importance? Yet, for practical analytical purposes, it is simple and inexpensive to modify virtually any commercial flame ionization detector to a dependable selective organometallic detector. Hydrogen doped with the appropriate amount of silane can be purchased from many of the gas supply houses. For routine operation, the only major disadvantage is the large volume of unburned hydrogen which requires an efficient hood system for venting the exiting gases. Hydrogen, however, is used in chromatography as a carrier gas and in the flame photometric detector as a detector gas. When compared to atomic absorption spectrometers and microwave emission detectors with their associated expense and respective flame flashback and high voltage hazards, the HAFID appears to be an attractive alternative for GC detection of organometallics and especially for the determination of antiknock agents in gasolines.

LITERATURE CITED

(1) W. A. Aue and H. H. Hill, Jr., *J. Chromatogr.*, **74**, 319 (1972).
(2) W. A. Aue and H. H. Hill, Jr., *Anal. Chem.*, **45**, 729 (1973).
(3) H. H. Hill, Jr. and W. A. Aue, *J. Chromatogr. Sci.*, **12**, 541 (1974).
(4) H. H. Hill, Jr. and W. A. Aue, *J. Chromatogr.*, **122**, 515 (1976).
(5) H. H. Hill, Jr., Ph.D. Thesis, Dalhousie University, Halifax, N.S., Canada, 1975.
(6) E. V. Anderson, *Chem. Eng. News*, **56** (6), 12 (1978).
(7) R. M. Whitcomb, "Non-Lead Antiknock Agents for Motor Fuels", Noyes Data Corporation, London, England, 1975.
(8) D. T. Coker, *Anal. Chem.*, **47**, 386 (1975).
(9) P. C. Uden, R. M. Barnes, and F. P. Disanzo, *Anal. Chem.*, **50**, 852 (1978).
(10) D. C. Reamer, W. H. Zoller, and T. C. O'Haver, *Anal. Chem.*, **50**, 1449 (1978).
(11) H. J. Dawson, Jr., *Anal. Chem.*, **35**, 542 (1963).
(12) E. J. Bonelli and H. Hartmann, *Anal. Chem.*, **35**, 1980 (1963).
(13) E. A. Boettner and F. C. Dallos, *J. Gas Chromatogr.*, **3** (6), 190 (1965).
(14) N. L. Soulages, *Anal. Chem.*, **38**, 28 (1966).
(15) W. N. Parker, G. Z. Smith, and R. L. Hudson, *Anal. Chem.*, **33**, 1170 (1961).
(16) W. N. Parker and R. L. Hudson, *Anal. Chem.*, **35**, 1334 (1963).

RECEIVED for review September 5, 1978. Accepted October 19, 1978. Acknowledgment is made to the donors of the Petroleum Research Fund, administered by the American Chemical Society, to the National Science Foundation (Grant No. CHE 77-25743), to the Washington State University Research and Arts Committee (Project No. 1136), and to the Environmental Research Center, Washington State University, for partial support of this research.

Simultaneous Determination of Americium and Curium in Soil

Michael H. Hiatt* and Paul B. Hahn

U.S. Environmental Protection Agency, Office of Research and Development, Environmental Monitoring and Support Laboratory, P.O. Box 15027, Las Vegas, Nevada 89114

A method is presented for the routine determination of americium and curium in 10 g of soil. The soil is dissolved with a mixture of nitric acid and hydrofluoric acid. Insoluble sulfates and phosphates are metathesized with boiling sodium hydroxide solutions. Plutonium and iron are sorbed on anion-exchange resin from 9 M hydrochloric acid after which the plutonium can be eluted and further purified for electrodeposition. Americium and curium are purified by cation-exchange and liquid–liquid chromatography. Mean recoveries of americium and curium were 58% and 56%, respectively, for prepared soil samples. The minimum detectable activity for the individual nuclides is 0.002 pCi/g. For americium and curium activities of 0.1 to 1.0 pCi/g, the relative standard deviations for replicate analysis ranged from 3% to 8%. The deviations of the means from their known values were generally within ±3%.

The increasing demand to monitor α-emitting nuclides near nuclear facilities has led to the development of different methodology for analysis of environmental soil samples (*1–8*). In this study it was desired to develop a method to determine americium and curium in 10-g soil samples which could be combined with existing methodology to determine plutonium. Although solvent extraction techniques have been extensively used for the isolation and purification of the actinide elements (*3, 5, 6*), this method employs ion-exchange techniques as this laboratory's experience has shown that far less manpower is required to routinely process large quantities of samples by column chromatography. An additional consideration was a reluctance to use large quantities of volatile organic solvents whose use may be deemed potentially hazardous.

The 10-g soil samples are dissolved with nitric and hydrofluoric acids (*8*). The sodium hydroxide metathesis and ammonium hydroxide precipitations render the sample soluble in strong hydrochloric acid where plutonium can then be isolated by anion-exchange chromatography (*7*).

Cation-exchange chromatography is used to separate the alkaline earths from the americium–curium fraction by using dilute hydrochloric acid eluents. Remaining trace contaminants are dramatically removed by using strong perchloric acid washes.

Americium-243 was used to trace both curium and americium in soil samples which were spiked with americium-241 and curium-243, -244. As fractionation between the americium-243 tracer and the curium spike was not observed, a curium nuclide is not necessary to trace in-situ curium when using this method. For environmental concentrations, interference from other transplutonium actinides is not considered to be a problem.

EXPERIMENTAL

Test Samples. The soils analyzed were prepared by adding spikes of americium-241 and a mixture of curium nuclides, curium-243 and curium-244, to 10-g aliquots of standard plutonium soils. The nuclides added were previously calibrated by evaporation and 2π counting (*9*).

The standard soil samples contained plutonium in a refractory form and were also analyzed for plutonium to demonstrate that the dissolution procedure would solubilize and equilibrate refractory actinides with soluble tracer. The standard plutonium

This article not subject to U.S. Copyright. Published 1979 by the American Chemical Society

soils were prepared by adding a known amount of plutonium-239 to 200-mesh soil, muffling at 700 °C for several hours, pulverizing, and blending with blank soil (*10*, *11*).

The analyses were traced with americium-243 and plutonium-236 tracers, also calibrated by evaporation and 2π counting.

Soil Dissolution. Add americium-243 tracer to 10 g of soil in a 250-mL TFE Teflon beaker. Add 60 mL 16 M nitric acid and 30 mL 29 M hydrofluoric acid and digest on a hot plate with occasional stirring for 1 h. Remove beaker from hot plate and add 30 mL each of 16 M nitric acid and 29 M hydrofluoric acid and continue digesting on a hot plate for 1 h. Remove the beaker from the hot plate and allow to cool. Cautiously add 20 mL of 12 M hydrochloric acid and continue digesting on a hot plate for 45 min. Add 5 g of boric acid and continue digesting for 15 min. Add 200 mg sodium bisulfate and evaporate the solution to an approximate volume of 10 mL (*8*). Neutralize the solution with the addition of 33% sodium hydroxide. Add 15 g of sodium hydroxide pellets, cover the Teflon beaker, and boil for 1 h to metathesize insoluble sulfates and phosphates. Cool the solution and transfer to a 500-mL pyrex centrifuge bottle and centrifuge. Discard the supernate and swirl the precipitate with 50 mL of distilled water and 1 g of boric acid. Acidify the slurry with 30 mL of 16 M nitric acid and allow to reflux on a hot plate for 0.5 h. Cool and adjust the pH to 9 with 14 M ammonium hydroxide. Centrifuge and again discard the supernate. Dissolve the resulting precipitate with 12 M hydrochloric acid and repeat both sodium and ammonium hydroxide precipitations using just enough 12 M hydrochloric acid to redissolve the precipitates (omit the addition of boric acid). Adjust the final solution to 6 M hydrochloric acid by adding an equal volume of 12 M hydrochloric acid and evaporating the solution to a volume of 40 to 50 mL. Cool and again add 12 M hydrochloric acid equal to the solution volume to adjust to 9 M in hydrochloric acid for the subsequent anion-exchange separation.

Anion-Exchange Separation. Pass the 9 M hydrochloric acid sample solution obtained from the dissolution through an anion-exchange column as described by Talvitie (*7*). Save the 9 M hydrochloric acid eluates (sample and three washes) for further americium and curium purifications. Talvitie's method can be continued for a plutonium determination.

Cation-Exchange Separation. Evaporate the 9 M hydrochloric acid eluates from the anion-exchange separation to 50 mL. Cool and transfer to a 250-mL centrifuge bottle. Adjust the pH to 9 with 14 M ammonium hydroxide. Centrifuge and discard the supernate. Dissolve the precipitate with 8 mL of 12 M hydrochloric acid, add 5 drops of 30% hydrogen peroxide and heat for 15 min. Allow to cool and dilute to a volume of 200 mL with distilled water.

Prepare a 1.4-cm i.d. column containing 24 mL of Bio-Rad 50W-X4, 50- to 100-mesh cation-exchange resin and condition with 100 mL of 0.5 M hydrochloric acid at a flow rate of 6 mL/min. Pass the 200-mL dilute hydrochloric acid sample through the column at a rate of 3 mL/min and discard the effluent. Rinse the centrifuge bottle with an additional 25 mL of 0.5 M hydrochloric acid, pass the rinse through the column, and discard the effluent. Elute alkaline earths and titanium with 200 mL of 1.0 M hydrochloric acid containing 2 drops 30% hydrogen peroxide and discard. Elute the americium and curium with 80 mL of 9 M hydrochloric acid and collect the eluate in a 100-mL beaker. Evaporate the solution to dryness, and dissolve the residue with 3 mL of 6 M hydrochloric acid; heat on a hot plate and allow to cool.

Prepare a 0.7-cm i.d. column containing 2.7 mL of Bio-Rad AG 50W-X4, 100- to 200-mesh resin in 0.5 M hydrochloric acid. Condition the column with 20 mL of 0.5 M hydrochloric acid. Dilute the americium and curium solution to 40 mL with distilled water and pass the solution through the freshly prepared cation ion-exchange column at the maximum flow rate. Discard the effluent. Rinse the beaker with consecutive 10- and 5-mL portions of 0.5 M hydrochloric acid and pass the rinses through the column. Discard the effluents. Elute any remaining iron with two successive 5-mL portions of 1.0 M ammonium thiocyanate followed by two successive 10-mL portions of 1.0 M hydrochloric acid. Remove the remaining non-rare earth impurities with successive 15- and 20-mL, 8.0 M perchloric acid washes. Elute americium, curium, and rare earth metals with one 10-mL and one 5-mL portion of 6 M hydrochloric acid and collect the effluents in a 50-mL beaker.

Table I. Americium-241 Results

known activity,[a] pCi/g		results,[b] pCi/g
0.144		0.134 ± 0.008
		0.168 ± 0.008
		0.156 ± 0.010
		0.147 ± 0.008
		0.143 ± 0.008
		0.155 ± 0.010
		0.144 ± 0.008
		0.147 ± 0.008
		0.127 ± 0.007
	average	0.147 ± 0.012[c]
0.288		0.292 ± 0.012
		0.286 ± 0.012
		0.277 ± 0.014
		0.286 ± 0.012
		0.308 ± 0.014
		0.305 ± 0.014
	average	0.292 ± 0.012[c]
0.576		0.583 ± 0.019
		0.609 ± 0.026
		0.570 ± 0.020
	average	0.587 ± 0.020[c]
0.720		0.646 ± 0.021
		0.678 ± 0.021
		0.714 ± 0.026
	average	0.679 ± 0.034[c]

[a] Prepared by spiking 10 g of blank soil with americium-241 calibrated by evaporation and 2π counting. [b] 1σ counting uncertainty. [c] Standard deviation of replicate determinations.

Rare Earth Separation. Remove the rare earths by the extraction chromatography method of Filer (*12*) using diethylenetriaminepentaacetic acid (DTPA) eluents with a column of bis(2-ethylhexyl)phosphoric acid (HDEHP) supported on Tee Six powder (Analabs, Inc., Hamden, Conn.). Add 20 mL 16 M nitric acid, 10 mL of 12 M perchloric acid and 1 mL of 18 M sulfuric acid to the DTPA eluents containing the americium and curium and evaporate the solution to sulfuric acid fumes and proceed with the electrodeposition.

Electrodeposition. Add 3 mL of distilled water to the fumed solution and heat gently on a hot plate. Transfer the solution to an electrodeposition cell and rinse the beaker with two 3-mL aliquots of 1:99 sulfuric acid. Adjust the resultant solution to the straw colored end point of thymol blue (pH 2–2.3) using ammonia vapors from an adapted wash bottle (inside stem removed) containing ammonium hydroxide. Electrodeposit at 1.1 A for 60 min (*13*).

RESULTS AND DISCUSSION

Results of the analyses performed on 10-g soil samples containing known quantities of americium-241 and curium-243, -244 are presented in Tables I and II. The results of the multiple analyses agreed with the established values and no systematic errors were evident. Yields ranged from 42% to 67% for the americium-243 tracer. Relative standard deviations ranged from 3% to 8% for replicate americium and 4% to 7% for replicate curium determinations. Deviations of the means from the known values ranged from −6% to +2% for americium and −7% to −0.1% for curium. As there was no evidence of fractionation between americium and curium, americium-243 is a viable tracer for curium using this method for soils.

The equilibration of the soluble plutonium-236 tracer and the refractory plutonium-239 in the soils is shown by the

Table II. Curium-243 and Curium-244 Composite Results

known activity,[a] pCi/g		results,[b] pCi/g
0.219		0.192 ± 0.010
		0.231 ± 0.010
		0.232 ± 0.012
		0.219 ± 0.011
		0.216 ± 0.010
		0.207 ± 0.010
	average	0.216 ± 0.015[c]
0.438		0.387 ± 0.017
		0.389 ± 0.018
		0.395 ± 0.016
		0.409 ± 0.015
		0.432 ± 0.018
		0.427 ± 0.018
	average	0.406 ± 0.019[c]
1.09		1.035 ± 0.030
		1.156 ± 0.043
		1.076 ± 0.033
	average	1.089 ± 0.062[c]

[a] Prepared by spiking 10 g of blank soil with a mixture of ^{243}Cm + ^{244}Cm calibrated by evaporation and 2π counting. [b] 1σ counting uncertainty. [c] Standard deviation of replicate determinations.

Table III. Refractory Plutonium-239 Results

	known activity, pCi/g	results[a]	runs
^{239}Pu	0.0509	0.0489 ± 0.0046	6
^{239}Pu	0.464	0.445 ± 0.031	9
^{239}Pu	2.60	2.50 ± 0.16	6

[a] Standard deviation of replicate determination.

determinations of plutonium-239 reported in Table III. These results demonstrate the solubility of the refractory actinides using the nitric acid and hydrofluoric acid soil dissolution.

Ten grams of soil has been chosen as an adequate sample size for the desired sensitivity and to minimize discrepancies due to the particulate nature of actinides in some soils (*10*, *14*). The hydrofluoric acid–nitric acid dissolution of 10 g of soil results in a cumbersome salt burden. An actinide-concentrating precipitation, such as ferric hydroxide, is necessary to remove salts enabling ion-exchange chromatography in a moderate size column.

The hydroxide precipitations were found to be necessary to aid the dissolution of insoluble actinides and to remove large quantities of interfering cations and salts. Additional investigation showed that without use of the sodium hydroxide precipitations, americium-241 (0.06 MeV γ) was found in undissolved residues from the original dissolution by Ge(Li) α counting. Further analysis of such residues by X-ray diffraction detected sulfur at significant levels suggesting the presence of insoluble sulfates which would carry the actinides. The addition of the sodium hydroxide metathesis step resulted in the complete dissolution of americium prior to the anion-exchange separation.

The ammonium hydroxide precipitations are necessary to remove significant portions of calcium generally found in soil samples. If significant quantities remain, calcium may precipitate as a chloride in the 9 M hydrochloric acid solution and inhibit the anion-exchange separation. In 10-g soil samples, the concentration of alkaline earths still remaining after the ammonium hydroxide precipitations is still great enough that cation-exchange separations are necessary to eliminate alkaline earth contamination in the final americium–curium electrodeposition. The alkaline earth removal is accomplished by the 1.0 M hydrochloric acid washes in the cation-exchange separations (*15*).

The efficiency of the hydroxide precipitations for concentrating americium and other actinides of interest was determined by spiking 10 g of background soil, dissolving the soil as described, and analyzing the decanted supernates from the various precipitations. Values reported in Table IV are percentages lost to the supernates. Initial spikes were approximately 10 nCi. Attempts were not made to prevent absorption of carbon dioxide in the sodium hydroxide solutions and absorbed carbonate anions could account for the high uranium losses observed. The losses for the other nuclides were found to be minimal.

Sorption characteristics of the elements on cation-exchange resin in perchloric acid (*15*) suggested the use of 8 M perchloric acid washes to remove any remaining interferences since only a few elements besides the rare earths and actinides are sorbed from such a solution. The use of these washes was found to increase recoveries and dramatically increase α spectral resolution.

The concentrations of rare earths encountered in 10-g soil samples can also cause spectral resolution to diminish. In previous analyses, the rare earth concentrations were so great in many samples as to deposit a 1-mm thick layer of rare earth oxides on the planchet. For this reason, the removal of rare earths by liquid–liquid extraction chromatography using HDEHP-treated Teflon columns is considered necessary for soils (*12*).

Preliminary evidence has demonstrated that the method may be useful for the analysis of other types of environmental samples. Biological samples can be prepared for this method by ashing, dissolution in hydrofluoric acid–nitric acid, and precipitating the actinides with ammonium hydroxide. The sample can then be dissolved in 9 M hydrochloric acid and processed by continuing with the anion-exchange separation. Water samples can be analyzed by this method with an initial ammonium hydroxide coprecipitation utilizing an iron carrier. When the volume of the precipitate is large, the sample can be treated like the 10-g soil sample. When the amount of precipitate is small, the hydrofluoric acid–nitric acid dissolution can be abbreviated and subsequent hydroxide precipitations eliminated. Glass fiber air filter samples can be treated identically to the soils without appreciable differences in the yields. Non-soil samples do not require the rare earth separation.

Table IV. Analysis of Hydroxide Supernates

	sodium hydroxide supernates, %			ammonium hydroxide supernates, %			combined supernates, %
	1st	2nd	total	1st	2nd	total	
^{208}Po	0.4	1.0	1.4	0.5	0.9	1.4	2.8
^{238}Pu	0.4	0.2	0.3	0.0	0.0	0.0	0.3
^{243}Am	0.1	0.2	0.3	0.1	0.1	0.2	0.5
^{230}Th	0.5	0.3	0.8	0.0	0.0	0.0	0.8
^{237}Np	0.1	0.4	.05	0.8	0.3	1.1	1.6
^{238}U	8.3	27.3	35.6	0.1	0.2	0.3	35.9

The minimum detectable activity for an α peak region with a 0.003 cpm background and a detector with 22% counting efficiency is 0.01 pCi for a 1000-min counting time. A 10-g sample with a 50% chemical yield would then give a 0.002 pCi/g minimum detectable limit for an americium or curium determination.

LITERATURE CITED

(1) R. Bojanowski, H. D. Livingston, D. L. Scheider, and D. R. Mann, "A Procedure for the Analysis of Americium in Marine Environmental Samples", Reference Methods for Marine Radioactivity Studies II, International Atomic Energy Agency, Vienna, Technical Report Series No. 169 (1973).
(2) M. C. de Bortoli, *Anal. Chem.*, **39**, 375 (1967).
(3) B. L. Hampson and D. Tennant, *Analyst (London)*, **98**, 873 (1973).
(4) S. A. Reynolds and T. G. Scott, *Radiochem. Radioanal. Lett.*, **23** (4), 269 (1975).
(5) T. G. Scott and S. A. Reynolds, *Radiochem. Radioanal. Lett.*, **23** (4), 275 (1975).
(6) C. W. Sill, K. W. Puphal, and F. D. Hindman, *Anal. Chem.*, **46**, 1725 (1974).
(7) N. A. Talvitie, *Anal. Chem.*, **43**, 1827 (1971).
(8) U.S. Atomic Energy Commission, "Measurement of Radionuclides in the Environment—Sampling and Analysis of Plutonium in Soil", U.S. AEC Regulatory Guide 4.5 (1974).
(9) C. W. Sill, *Anal. Chem.* **46**, 1426 (1974).
(10) P. B. Hahn, E. W. Bretthauer, P. B. Altringer, and N. F. Mathews, "Fusion Method for the Measurement of Plutonium in Soil: Single-Laboratory Evaluation and Interlaboratory Collaborative Test", Office of Research and Development, U.S. Environmental Protection Agency, EPA-600/7-77-078 (1977).
(11) C. W. Sill and R. D. Hindman, *Anal. Chem.*, **46**, 113 (1974).
(12) T. D. Filer, *Anal. Chem.*, **46**, 608 (1974).
(13) N. A. Talvitie, *Anal. Chem.* **44**, 280 (1972).
(14) C. W. Sill, *Health Phys.*, **29**, 619 (1975).
(15) F. Nelson, T. Murase, and K. A. Krause, *J. Chromatogr.*, **13**, 503 (1964).

RECEIVED for review September 14, 1978. Accepted November 21, 1978.

CORRESPONDENCE

Regression Line That Starts at the Origin

Sir: When analytical results for experimental measurements of a dependent variable, y, are theoretically obtained with an independent variable, x, it is customary to calculate the "best straight line" using the equation

$$y = a + bx \tag{1}$$

through the region of experimental points by the method of least squares, where a is the intercept on the y axis (*1*). However, theoretical, graphical representation of some analytical measurements, especially Beer's law, consists of a straight line that begins at the origin. In spectrophotometry, this would be expected to occur if corrections have been carefully made for blank absorptions and cell differences.

In view of this contradiction, it would seem appropriate, for a system that has been well tested, to determine instead the best straight line through the experimental points, *commencing at the origin*:

$$y = bx \tag{2}$$

This will unavoidably reduce the precision slightly, but could increase the accuracy. If forced to choose, most analytical chemists would place accuracy above precision.

The derivation of the method for calculating such a best straight line is considerably simpler than that for the determination of a and b. Following the same procedure as for the more general case, the sum of the squares of the deviations of each value

$$y_i' = bx_i \tag{3}$$

from y_i will be

$$S = \Sigma(y_i - bx_i)^2 \tag{4}$$

$$= \Sigma(y_i^2 - 2bx_iy_i + b^2x_i^2) \tag{5}$$

Taking the derivative of S with respect to b, setting it equal to zero for a minimum, and solving for b,

$$\partial S/\partial b = \Sigma(-2x_iy_i + 2bx_i^2) = 0 \tag{6}$$

$$b\Sigma x_i^2 = \Sigma x_iy_i \tag{7}$$

$$b = \Sigma x_iy_i/\Sigma x_i^2 \tag{8}$$

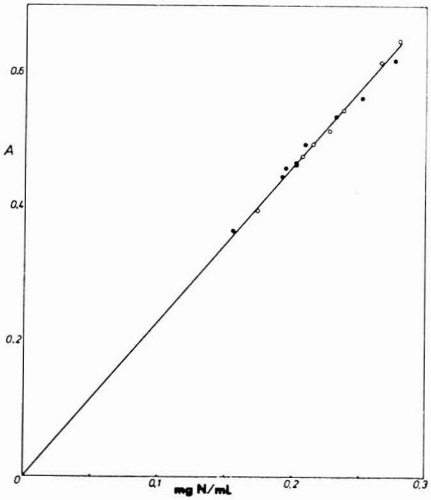

Figure 1. Distribution of absorbances for two sets of rice and the best straight line through the origin common to both sets. (O) Brown rice. (●) Milled rice

Though S is a measure of the total deviation of points from the best line, it is more common to use the *standard error of estimate*

$$s_e = \sqrt{S/(n - 2)} \tag{9}$$

which puts it on an individual basis like standard deviation.

A practical application of the proposed procedure is given by some analyses that are part of a paper being submitted to another journal for publication (2). Each of eight samples of brown rice was divided into two parts; one part was milled, the other left unmilled. The sixteen samples were then

© 1979 American Chemical Society

Table I. Comparison of Absorptivities of Two Sets of Solutions Calculated from the Best Straight Lines and from the Best Straight Lines through the Origin[a]

rice	equation	s_e	equation	s_e
brown	$A = 2.35c - 0.011$	0.003	$A = 2.30c$	0.003
milled[b]	$A = 2.06c + 0.051$	0.008	$A = 2.30c$	0.012

[a] Cell thickness 1.000 cm. [b] Another publication of protein determination in brown and milled rice by the Kjeldahl reaction also shows a larger standard error of estimate for milled rice (*3*).

analyzed for total nitrogen by the Kjeldahl method (1.170 to 1.886% N and 1.051 to 1.864% N for the two sets, respectively) and used to test a procedure developed by the authors for determining protein nitrogen by the biuret reaction. The absorbances of the solutions of the copper–nitrogen complex for the two sets of samples are shown plotted vs. the nitrogen concentration in Figure 1.

Introducing symbols for spectrophotometry into Equations 1 and 2 gives, respectively,

$$A = a_0 + abc \tag{10}$$

and

$$A = abc \tag{11}$$

The results calculated from the two equations are shown in Table I, the most striking being the different absorptivities using Equation 10 (2.35 and 2.06) and identical ones (2.30) using Equation 11. A slight difference in the two absorptivities might be expected, since the layer removed by milling contains a small amount of protein that might be different in nature. However, there should then also be a difference when using Equation 11, but there is not. Hence, the identity of absorptivities from best straight lines through the origin demonstrates the desirability of the proposed method.

LITERATURE CITED

(1) "Official Methods of Analysis of the A.O.A.C.", William Horwitz, Ed., 12th ed., Association of Official Analytical Chemists, Washington, D.C., 1975, xvi–xvii.
(2) "A Moderately Rapid, Accurate, Room-Temperature Method for the Spectrophotometric Determination of Protein in Rice by the Biuret Reaction", F. C. Strong III and P. Theis-Maimone, submitted for publication.
(3) L. C. Parial, L. W. Rooney, and B. C. Webb, *Cer. Chem.*, **47**, 38–43 (1970).

Frederick C. Strong III

Faculdade de Engenharia de
Alimentos e Agrícola
Universidade Estadual de Campinas
Caixa Postal No. 1170
13100 Campinas, S.P., Brasil

RECEIVED for review May 24, 1978. Accepted October 30, 1978.

Exchange of Comments: Analytical Methods of Bis(chloromethyl) Ether in Air

Sir: Since the carcinogenicity of bis(chloromethyl) ether (BCME) was established, its potential presence in the industrial environment became a grave concern (*1–4*).

To ascertain its actual existence and level in suspected industries and to protect the workers from this occupational hazard, air monitoring is essential. Thus, various quantitative analytical procedures for BCME have been reported. Among them are:

(A) Direct gas chromatography (GC)

(B) On-Column Concentration–GC. The BCME, together with some of the other contaminants, is first allowed to adsorb on the front section of the column at room temperature and then analyzed at a programmed higher temperature (*5*).

(C) Adsorber–GC combination. The BCME, together with some of the other contaminants, is first allowed to adsorb on the packing in a trapping tube and then thermally flashed onto a GC analytical column or a set of analytical columns (*6, 7*).

(D) Adsorber–mass spectrometry (MS) combination. The BCME, together with some of the other contaminants, is first allowed to adsorb on the packing in a trapping tube, and then is thermally eluted into the reservior of a high-resolution mass spectrometer (*8*).

(E) Adsorber–GC–MS combination. The BCME, together with some of the other contaminants, is first allowed to adsorb on the packing in a trapping tube, then thermally flashed onto a GC analytical column, and finally the BCME fraction is gated into a mass spectrometer (*9, 10*).

The preceding methods are all technically sound and straightforward in application. They differ in sensitivity, selectivity, cost of equipment, and requirement for trained personnel.

In addition to the above methods, there is a unique derivatization method which first appeared in this journal (*Analytical Chemistry*) in 1975, followed by a modified version a year later (*11, 12*).

This derivatization method involves the conversion of BCME, by means of trichlorophenol and methoxide in methanol, into a derivative which is then to be assayed by GC. The stock reagent consists of 25 g of sodium methoxide and 5 g of trichlorophenol in 1 L of methanol. In other words, methoxide is more than 18-fold in molar excess. The derivative was identified, as stated in the article, as $Cl_3C_6H_2OCH_2OCH_2OCH_3$, but no spectral or other evidence was given to substantiate its identity. An 86 to 115% recovery was reported according to the data in Table II of the original article. (Data in Table III of the same article show an 84 to 160% variation.) No reason was offered for an 18-fold molar excess of sodium methoxide, in spite of the fact that BCME undergoes extensive decomposition in the presence of methoxide, and that it has been used in scrubbers to destroy BCME. At the end of the original article, a statement was made to the effect that the sensitivity could be increased 6- or 8-fold by using stoichiometric quantities of sodium methoxide and trichlorophenol, with recoveries varying from 82 to 100%. This realization of the basic principle of chemical stoichiometry did not, however, prompt a re-examination of the experiments, nor promote a critical evaluation of the chemistry involved.

The derivatization apparently involves the following equilibrium:

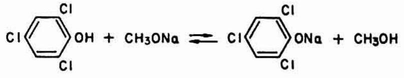

Both the methoxide and the trichlorophenoxide then react with BCME and can give one unsymmetric derivative and two symmetrical derivatives as follows:

0003-2700/79/0351-0299$01.00/0 © 1979 American Chemical Society

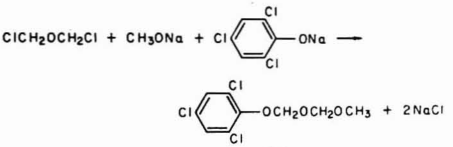

(A)

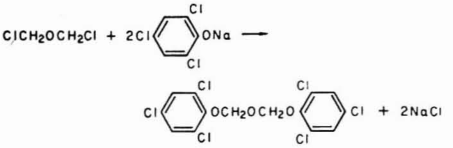

(B)

$$ClCH_2OCH_2Cl + 2CH_3ONa \longrightarrow CH_3OCH_2OCH_2OCH_3 + 2NaCl$$

(C)

The product distribution naturally depends on the relative reactivities and relative concentrations of the methoxide and trichlorophenoxide species. In addition, the decomposition of BCME in the presence of methoxide is known to be extensive. The formation of derivative C from BCME and methoxide is possible but this species is also invisible to an electron capture detector. The formation of derivative B from BCME and trichlorophenoxide is expected but is unmentioned and unidentified in the derivatization mixture in spite of the fact that it is twice as visible to an electron capture detector in comparison with derivative A. Furthermore the degree of decomposition of BCME and the relative extents of formation of the derivatives, A, B, and C, may be different for different samples under the crudely controlled conditions. In view of all these uncertainties, the yield of derivative A alone can hardly be taken as a measurement of the BCME existing in the air. Nevertheless, an accuracy of 86–115% recovery was reported. Claims of absence of BCME were positively stated when the tests by this method gave negative responses.

A year later, an improved version of the method by the same author (*12*) appeared in this journal. This improved version involves no change in the derivatization procedure, just a change in chromatographic conditions. One of the possible symmetrical derivatives, $Cl_3C_6H_2OCH_2OCH_2OC_6H_2Cl_3$ (derivative B), was now identified from the same derivatization medium of a known sample in addition to the previously identified unsymmetrical derivative (derivative A). What promoted their effort to look for the new product in the same derivatization mixture were the positive responses of BCME in three of their experiments by the original technique, a fact they could not accept. Since negative responses were found for the new symmetrical derivative in their three experiments in question, the quantification of BCME is now to be determined in terms of this newly found symmetrical derivative which, as was reported in the article, again gives high recoveries. The original unsymmetrical derivative which has been established at 86–115% recovery from known amounts of BCME samples is now attributed to the unproved and unexplained existence of chloromethylal (D) in the following reaction (*12*):

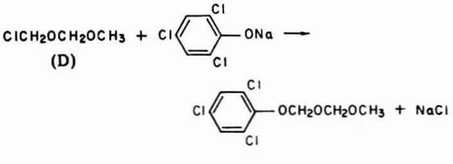

(D)

Chloromethylal can conceivable originate from three sources. One is the reaction of BCME and methoxide. It happens to be the product of the intermediate step in the formation of either derivative A, or derivative C, or the decomposition of BCME, all of which originate from the actual presence of BCME, and therefore it is not a false signal. Another possible source is from the reaction of formaldehyde, hydrogen chloride, methanol, and the unisolable chloromethanol. But it certainly cannot take place in the basic derivatization mixture inside an impinger. Putting it in general terms, while hemiacetal formation is catalyzed by either acids or bases, the subsequent acetal formation is catalyzed by acids only. Mechanistically speaking, bases can do nothing to hemiacetals except attack their hydroxyl functions, which is exactly the reverse of hemiacetal formation.

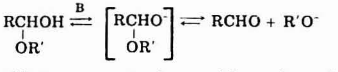

$$\begin{array}{c}\mathrm{RCHOH}\\|\\\mathrm{OR'}\end{array} \overset{B}{\rightleftharpoons} \left[\begin{array}{c}\mathrm{RCHO^-}\\|\\\mathrm{OR'}\end{array}\right] \rightleftharpoons \mathrm{RCHO} + \mathrm{R'O^-}$$

Only acids can consumate the acetal formation as follows.

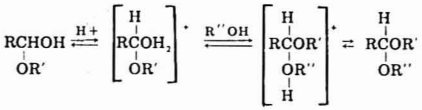

$$\begin{array}{c}\mathrm{RCHOH}\\|\\\mathrm{OR'}\end{array} \overset{H+}{\rightleftharpoons} \left[\begin{array}{c}\mathrm{H}\\|\\\mathrm{RCOH_2}\\|\\\mathrm{OR'}\end{array}\right]^+ \overset{R''OH}{\rightleftharpoons} \left[\begin{array}{c}\mathrm{H}\\|\\\mathrm{RCOR'}\\|\\\mathrm{OR''}\\|\\\mathrm{H}\end{array}\right]^+ \rightleftharpoons \begin{array}{c}\mathrm{H}\\|\\\mathrm{RCOR'}\\|\\\mathrm{OR''}\end{array}$$

A third source of chloromethylal is its pre-existence in air. Appropriate control experiments should be run to determine its presence or absence. In addition, the detection of the new symmetric derivative (B) in a known sample has not always yielded the expected response as experienced by its originator (*13*).

Therefore, the reasoning for this derivatization method for determination of BCME in air is confusing and chemically unsound.

LITERATURE CITED

(1) B. L. VanDuuren et al., *Arch. Environ. Health*, **16**, 472–476 (1968).
(2) J. L. Gargus, W. H. Reese, Jr., and H. A. Rutter, *Toxic Appl. Pharmacol.*, **15**, 92–96 (1969).
(3) B. K. J. Leong, H. N. Macfarland, and W. H. Reese, Jr., *Arch. Environ. Health*, **22**, 663–666 (1971).
(4) S. Laskin et al., *Arch. Environ. Health*, **23**, 135–136 (1971)
(5) F. W. Williams and M. E. Umstead, *Anal. Chem.*, **40**, 2232–2234 (1968).
(6) D. G. Parkes et al., *Am. Ind. Hyg. Assoc. J.*, **37**, 165–173 (1976).
(7) R. L. Wilkins and L. S. Frankel, U.S. Patent 3,807,217.
(8) L. Collier, *Environ. Sci. Technol.*, **6**, 930–932 (1972).
(9) L. A. Shadoff, G. J. Kallos, and J. S. Woods, *Anal. Chem*, **45**, 2341–2344 (1973).
(10) K. P. Evans et al., *Anal. Chem.*, **47**, 821–824 (1975).
(11) R. A. Solomon and G. J. Kallos, *Anal. Chem.*, **47**, 955–957 (1975).
(12) J. C. Tou and G. J. Kallos, *Anal. Chem.*, **48**, 958–963 (1976).
(13) Final Report, "Research Study on Bis(cloromethyl) Ether Formation and Detection in Selected Work Environments," Sept. 17, 1976, Sec. XVII D, Contract No. 210-75-0056, The Bendix Corporation.

Charles C. Yao*

Poly-Tech Laboratories, Inc.
P.O. Box 15623
Orlando, Florida 32858

Heinrich Zollinger

Technisch-chemisches Laboratorium
Eidgenössische Technische Hochschule (ETH)
8092 Zurich, Switzerland

RECEIVED for review January 26, 1978. Resubmitted June 6, 1978. Accepted July 31, 1978.

Sir: Yao and Zollinger express their concern about the derivatization methods for the determination of bis(chloromethyl) ether (BCME) in air, the methods in question were published in *Analytical Chemistry* (*1, 2*). We have carefully reviewed their comments, specifically with respect to the issues of concern they have raised.

Because of the carcinogenicity of BCME (*3, 4*) and its impact on the environment, extensive research has been conducted in many laboratories throughout the world. The development of analytical methods, the study on the stability of BCME and its possible formation from many sources has been thoroughly researched in our laboratory over the past few years (*1, 2, 5–12*). Yao and Zollinger have reviewed many analytical techniques that have been developed in the scientific community to monitor BCME at parts per billion levels in air for environmental control. However, most of these techniques require expensive and sophisticated instrumentation that would not be accessible to a small laboratory or convenient for on-site plant analysis. The derivatization procedure (*1, 2*) developed in our laboratory has adequately met our objectives for a rapid, practical, and reliable analytical technique.

It is well established that the reaction of BCME with sodium methoxide and the sodium salt of 2,4,6-trichlorophenol will produce three main derivatives, 2,4,6-trichlorophenoxymethyl methoxymethyl ether (A), bis(2,4,6-trichlorophenoxymethyl) ether (B) (*1, 2*), and bis(methoxymethyl) ether (C). All these products were confirmed by both mass spectrometry and nuclear magnetic resonance (*13*).

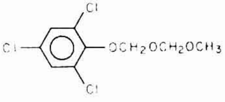

(A)

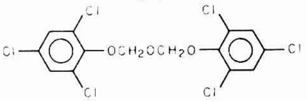

(B)

$CH_3OCH_2OCH_2OCH_3$

(C)

The distribution of these products in this reaction depends on the relative reactivity of BCME and concentration of phenoxide and methoxide species. We also realize from the chemistry of this reaction that 100% conversion of BCME to any single product is impossible. However, for a reliable analytical procedure, the reaction products need not be stoichiometric, but the percent conversion must be constant and reproducible relative to the amount of the particular product being determined. In respect to derivative A, reference 1 clearly shows the linearity of the procedure relative to the concentration of BCME (Table I) for derivative A. Even though the absolute conversion of BCME to this derivative is unknown, it is very reproducible. BCME recoveries of 86–115% were obtained utilizing derivative A by comparing the response from standards of BCME in air to the response for similar amounts of BCME added to the derivatizing solution directly. It is not a measure of the percent conversion of BCME to derivative A. The procedure was further verified and validated by analysis of prepared vapor standards by the GC derivative procedure and GC-Mass Spectrometric technique (5) (Table III, reference 1) of the underivatized sample.

Since the first GC procedure was designed for derivative A, there was no attempt at this point to determine derivative B. Later when the above procedure (*1*) was used on certain samples, possible interferences were encountered. It was realized, as previously stated, that derivative B was also present from the chemistry involved but did not elute from the GC column under the conditions employed. A different GC procedure was developed for detecting derivative B. The linearity of response was determined for derivative B (*2*) and a recovery study was carried out as described previously for derivative A. Again it is not necessary to know the conversion efficiency of BCME to the products as long as the conversion is reproducible. It has been demonstrated that sensitivity could be increased by changing the amounts of sodium methoxide and 2,4,6-trichlorophenol, thus increasing the conversion efficiency for derivatives A and B relative to the previous conditions (*1*). The excess sodium methoxide was added to form the sodium salt of 2,4,6-trichlorophenol so that the trichlorophenol would not be extracted into the hexane. In the improved procedure, the BCME is allowed to react before addition of NaOH to eliminate any free trichlorophenol.

The derivatizing reagents are used in fixed proportion and at concentrations many orders of magnitude higher than that of the BCME present in the sample, and thus a constant reagent environment is maintained for all samples, and hence the same product mixture is always produced.

Yao and Zollinger have clearly misinterpreted the role of the possible interference, chloromethylal, reported in our study (*2*). It was pointed out (*2*) that *if* chloromethylal were present, it would be expected to yield the same derivative A as BCME and thus would constitute an interference. It is common in trace analytical work to encounter interferences that may be difficult to identify and whose source is not readily identified. In fact, the use of the later procedure (*2*) measures the derivative B for which chloromethylal is not an interference, if present, and thus provides a more specific determination of BCME. Chloromethylal is not a main issue.

Yao and Zollinger question the validity of the derivative method. Factual data that would support their comments or data that would refute that of the published methods, however, are not presented. The derivative method for the determination of BCME has been used successfully by many analytical chemists in our laboratory and others in the scientific community (*14, 15*). This method has also been recommended (*16*) for use by subcommittee 5 of the APHA Intersociety Committee. Yao himself has evaluated and used the derivative method quantitatively during an extensive field survey with many tables of data presented in his final report (*17*).

The derivatization method is specifically designed to detect and measure parts per billion BCME in environmental air, and it has been repeatedly shown to be technically and chemically sound. We are not aware of any data which do not support the analytical integrity of the published derivative methods.

LITERATURE CITED

(1) R. A. Solomon and G. J. Kallos, *Anal. Chem.*, **47**, 955 (1975).
(2) J. C. Tou and G. J. Kallos, *Anal. Chem.*, **48**, 958 (1976).
(3) B. L. VanDuuren, B. M. Goldschmidt, C. Katz, L. Langseth, G. Mercado, and A. Sivak, *Arch. Environ. Health*, **16**, 472 (1968).
(4) R. T. Drew, S. Laskin, M. Kuschner, and N. Nelson, *Arch. Environ. Health*, **30**, 61 (1075), and references therein.
(5) L. A. Shadoff, G. J. Kallos, and J. S. Woods, *Anal. Chem.*, **45**, 2341 (1973).
(6) G. J. Kallos and R. A. Solomon, *Am. Ind. Hyg. Assoc. J.*, **34**, 469 (1973).
(7) J. C. Tou, L. B. Westover, and L. F. Sonnabend, *J. Phys. Chem.*, **78**, 1096 (1974).
(8) J. C. Tou and G. J. Kallos, *Am. Ind. Hyg. Assoc. J.*, **35**, 419 (1974).

0003-2700/79/0351-0301$01.00/0 © 1979 American Chemical Society

(9) J. C. Tou, L. B. Westover, and L. F. Sonnabend, *Am. Ind. Hyg. Assoc. J.*, **36**, 374 (1974).
(10) J. C. Tou and G. J. Kallos, *Anal. Chem.*, **46**, 1866 (1974).
(11) G. J. Kallos and J. C. Tou, *Environ. Sci. Technol.*, **11**, 1101 (1977).
(12) G. J. Kallos, U.S. Patent 4 042 326 (1977).
(13) G. J. Kallos and R. A. Solomon, unpublished data.
(14) G. M. Rusch, A. R. Sellekumar, S. L. LeMendola, G. V. Katz, S. Laskin, and R. E. Albert, *Am. Ind. Hyg. Assoc., Abstr.* 176, May 1978, Los Angeles, Calif.
(15) K. S. McCallum, Rohm and Haas Co., private communication.
(16) E. Sawicki, T. Belsky, R. A. Friedel, D. L. Hyde, J. L. Monkman, R. A. Rasmussen, L. A. Ripperton, and L. D. White, "Methods of Air Sampling and Analysis", American Public Health Association, 1977, pp 874–877.
(17) C. C. Yao and G. C. Miller, Final Report "Research Study on Bis-(chloromethyl) Ether Formation and Detection in Selected Work Environments", Sept. 17, 1976, Contract No. 210-75-0056, The Bendix Corporation.

G. J. Kallos*
R. A. Solomon
J. C. Tou

Analytical Laboratories
Dow Chemical U.S.A.
Midland, Michigan 48640

RECEIVED for review October 16, 1978. Accepted October 17, 1978.

Thin Carbon Foils for the Elimination of Charging Effects in Proton Induced X-Ray Emission Spectrometry

Sir: The advantages of ion excitation, particularly proton excitation in X-ray emission analysis (*1*) have been debated at length in the literature (*2*). The most important advantages of ion excitation over electron or X-ray excitation are the high cross sections for X-ray emission and the low background contribution from bremsstrahlung. If the target consists of a thin uniform sample, the continuous background radiation is low, but if the target thickness is increased to such an extent that the proton beam is stopped completely, a considerable increase in the background continuum occurs, especially if the sample is a good insulator. The acceleration of electrons toward the sample targets that have acquired a positive charge from the proton beam results in an increase in the background bremsstrahlung in the 0–20 keV region. The effects of this increase in the bremsstrahlung on the X-ray emission spectra are twofold: many subtle features in the emission spectra are obscured and the accurate measurement of peak heights or peak areas for purposes of quantitation is almost impossible.

Several experimental modifications for minimizing the charge buildup on the sample target and reducing the bremsstrahlung have been proposed. The evaporation of a conductor onto the sample (*3, 4*) or mixing the sample with a conducting compound (*5*) are unsatisfactory because the sample can be readily contaminated. An increase in the pressure of the sample chamber has also been shown to be effective (*6*), but this also increases the probability of contaminating the sample. The most satisfactory device that has been used is a hot filament that is positioned close to the sample target. Electrons emitted from the hot filament prevent the accumulation of positive charge on the target. Commercially available tungsten filaments, however, were found to be a severe source of contamination (*6, 7*). In a successful modification of this approach, a commercial carbon filament was clamped between two carbon rods, to form an "electron gun" and the electrons from the carbon filament effectively neutralized the charge on the sample target. A perforated aluminum cap that was maintained at +100 V was placed over the carbon filament to prevent contamination of the sample with impurities in the carbon filament (*6*).

A simple and effective alternative to the "electron gun" is

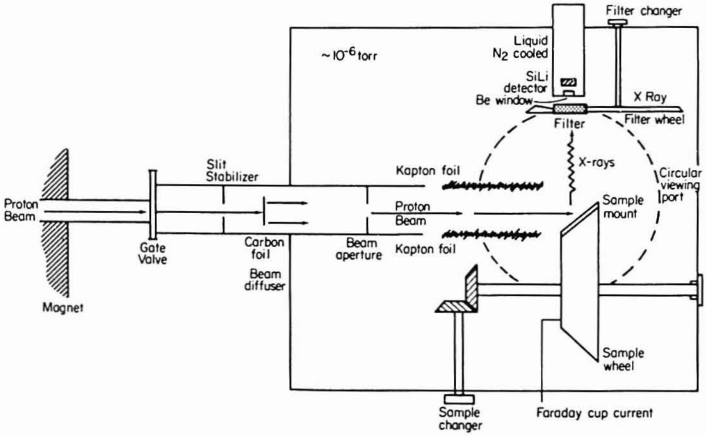

Figure 1. Sample chamber showing the position of the carbon foil in the proton beam. (The figure is not drawn to scale)

0003-2700/79/0351-0302$01.00/0 © 1979 American Chemical Society

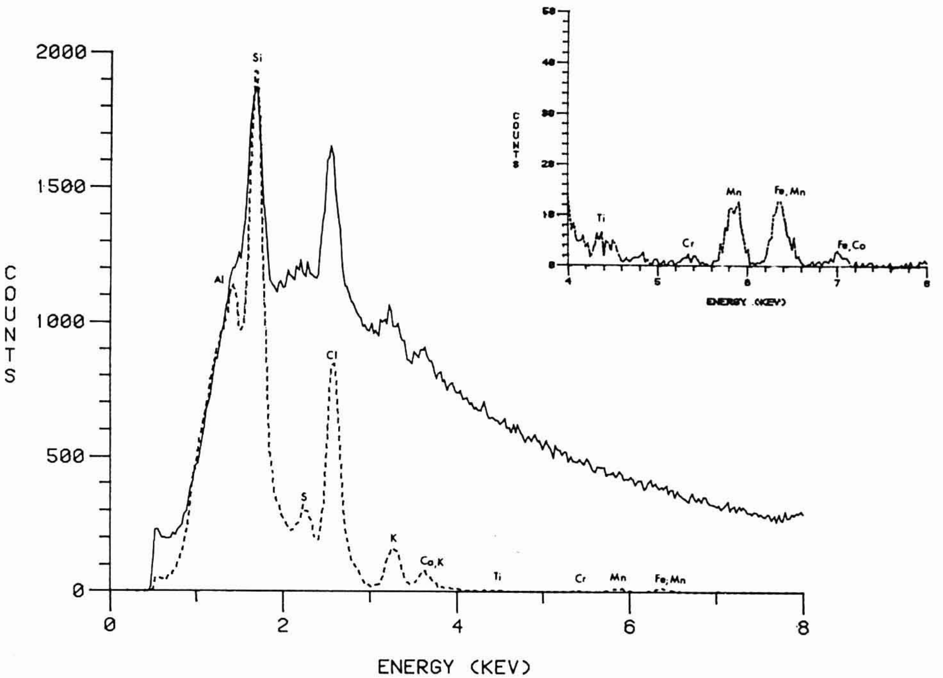

Figure 2. Proton induced X-ray emission spectra of polyethylene with the carbon foil in the proton beam (---) and without the carbon foil (—). The spectrum in the upper right hand corner is the broken line spectrum between 4 and 8 keV with an expanded vertical axis

the use of thin carbon foils (5–10 μg/cm^2). The carbon foil is placed in the proton beam path approximately 8–10 cm in front of the sample (Figure 1). The carbon foil acts not only as a source of electrons but also as a beam diffuser. The effectiveness of the carbon foil in reducing the background radiation is shown in Figure 2. The sample target consisted of a piece of linear polyethylene that was cut from a polyethylene bottle which was used to store an aqueous solution that contained several cations and anions. Each spectrum in Figure 2 was obtained after a 5-min irradiation of the polyethylene target at 1 MeV. The spectrum (drawn in a solid line) was obtained in the absence of the carbon foil and shows the consequences of the charge accumulation on the target. The spectral resolution is poor and none of the transition metal ions could be detected. With the carbon foil in place, the sensitivity and resolution increased dramatically as shown in Figure 2 (broken line). This technique for the reduction of background radiation has been used extensively with samples mounted on Kapton (DuPont trademark, $(C_{22}H_{10}N_2O_4)n$) foil. Kapton is essentially free of impurities and has a high thermal stability. It is also an excellent insulator and is therefore subject to charging effects.

High quality carbon foils are commercially available in a variety of thicknesses. In no instance did the use of the carbon foil result in any observable sample contamination. The foils are extremely stable and can be used continuously for several months.

LITERATURE CITED

(1) T. B. Johansson, R. Akselsson, and S. A. E. Johnansson, *Nucl. Instrum. Methods*, **84**, 141 (1970).
(2) G. L. Macdonald, *Anal. Chem.*, **50**, 135R (1978).
(3) F. Folkmann, C. Gaarde, T. Huus, and K. Kemp, *Nucl. Instrum. Method*, **116**, 487 (1974).
(4) J. W. Mandler, R. B. Moler, E. Raisen, and K. S. Rajan, *Thin Solid Films*, **19**, 165 (1973).
(5) R. C. Jopson, H. Mark, and C. D. Swidt, *Phys. Rev.*, **127**, 1613 (1963).
(6) M. Ahlberg, G. Johansson, and K. Malmqvist, *Nucl. Instrum. Methods*, **131**, 377 (1975).
(7) H. Oona, unpublished results.

H. Oona
Stephen J. Kirchner
Peter L. Kresan
Quintus Fernando*

Department of Chemistry
University of Arizona
Tucson, Arizona 85721

Harry Zeitlin

Department of Chemistry
University of Hawaii
Honolulu, Hawaii 96822

RECEIVED for review September 21, 1978. Accepted October 30, 1978. This effort was sponsored in part by NOAA, Office of Sea Grant under grant No. 04-7-158-44129 with added support provided by the Department of Planning and Economic Development, State of Hawaii.

Exchange of Comments: Particle Size Effects in the Determination of Respirable α-Quartz by X-ray Diffraction

Sir: Edmonds, Henslee, and Guerra (*1*) appear to have misinterpreted their experimental results relating to orientation. The authors appear to assume (Discussion, Orientation) that the relative intensity of diffraction lines of a randomly oriented phase will be the same for both bulk and thin-layer preparations. This is not a valid assumption, I feel. Whereas the intensity of a diffraction line for an "infinitely" thick sample is independent of θ_{iJ} and directly proportional to the quantitation constant of the diffraction line k_{iJ}, the intensity/weight of a thin-layer sample (relatively free of absorption effects) is proportional to k_{iJ}cosec θ_{iJ} (*2, 3*). For a diffractometer with a θ compensating slit, both statements would need to include another θ_{iJ} term but, considering bulk sample relative to thin-layer, the previous sentence would remain valid. Thus, from the authors' Table III, if the determined relative intensities of a bulk sample of randomly oriented Minusil 15 was 100:101:110:112 = 15:100:9:17, then the expected relative intensities for the same randomly oriented sample as a thin-layer would be 19:100:7:9. This is reasonably close to what the authors found in their Table III for air filtered Minusil 15 as a thin-layer.

My laboratory is active in the field of quantitative thin-layer X-ray powder diffractometry. In such work, diffraction intensity is assessed by integrated peak area, a constant divergence slit is used, and standards are prepared by filtration of respirable dust (<7 μm) from an airborne suspension and weighing. Results of such work do not support conclusions 1, 2, and 5 of the Edmonds, Henslee, and Guerra paper.

Conclusion 1. My laboratory has not found any evidence to support a contention that respirable α-quartz exhibits significant preferred orientation when prepared by filtration from airborne suspension on either silver or Nuclepore-polycarbonate membrane filters. Standards for <200 μg/cm^2 of respirable α-quartz on silver and Nuclepore filters prepared for previous studies (*3, 4*) were read for the four most intense α-quartz lines. The results are given in Table I and are consistent with random orientation, in that the relative k_{iJ} values found for the four lines match that predicted by calculated data for a randomly oriented α-quartz (*5, 6*).

Conclusion 2. My laboratory uses a pure natural α-quartz crystal as its α-quartz standard. The crystal is disc-milled for 60 s, and the resulting powder used directly in a simple dust chamber. The volume fraction of respirable dust in such a preparation lies in the range 30–60%. The exact detail of the particle size range is irrelevant, at least in theory, since respirable dust is selected from an airborne suspension by the use of the Higgins cyclone (*7*) [Casella (London) catalog no. A7650/1], the mass effect of the amorphous layer is relatively small even in such a respirable fraction, and the total respirable dust collected is determined by weighing. Both silver (*3*) and Nuclepore (*4*) filters gave similar experimental k_{iJ} values for respirable α-quartz 101. These values have proved to be only slightly lower than the k_{iJ} value predicted by theoretical calculation (*6*), as summarized in Table II.

Table I. Relative k_{iJ} Values of Diffraction Lines of Respirable α-Quartz Deposited at <200 μg/cm^2 on Membrane Filters

filter	filter loading, μg/cm^2	α-quartz relative k_{iJ}[a] 100	101	112	211
theory (*6*)		18.0	100	14.5	10.9
silver (*3*)	23	18.7 ± 1.7	100 ± 2.2	14.4 ± 2.0	15.1 ± 2.2
	40	20.0 ± 1.3	100 ± 1.3	16.8 ± 1.3	11.2 ± 1.3
	84	17.2 ± 0.5	100 ± 0.7	14.6 ± 0.7	12.4 ± 0.7
	192	19.9 ± 0.3	100 ± 0.5	15.2 ± 0.3	13.0 ± 0.3
	212	17.5 ± 0.2	100 ± 0.5	14.8 ± 0.2	11.7 ± 0.2
Nuclepore (*4*)	59	17.0 ± 1.1	100 ± 1.1	13.6 ± 0.9	11.7 ± 0.9
	66	17.1 ± 0.9	100 ± 1.1	14.7 ± 0.9	9.4 ± 0.9
	70	17.7 ± 0.8	100 ± 1.0	13.8 ± 0.8	11.7 ± 0.8
	155	17.3 ± 0.4	100 ± 0.5	14.9 ± 0.4	10.9 ± 0.4
	176	17.7 ± 0.4	100 ± 0.4	14.4 ± 0.4	11.6 ± 0.4
	179	18.6 ± 0.4	100 ± 0.4	14.6 ± 0.4	12.2 ± 0.4

[a] The range shown represents the effect on the relative k_{iJ} value of ± one standard deviation of the counter measurement (*8*).

Table II. k_{iJ} Values for Respirable α-Quartz 101 Deposited on Membrane Filters

filter	k_{iJ}, net counts cm^2 μg^{-1} light loaded filter <200 μg/cm^2	heavy loaded filter[a]	ref.
silver, 3.0-μm pore size, matte side	42	44.0 ± 1.3	(*3*)
Nuclepore, 0.8-μm pore size, gloss side	44.5	45.3 ± 0.94	(*4*)
theory	46.3	46.3	(*6*)

[a] Mean ± standard deviation of experimental measurements using Ag 111 for absorption correction.

Conclusion 5. Calibration curves from this laboratory have shown no obvious change in slope at ~100 μg/cm^2 for the 101 reflection of respirable α-quartz deposited by air filtration onto silver (*3*) or Nuclepore (*4*) filters. Certainly, if such a change of slope was observed for 100 μg/cm^2 of α-quartz it would be unlikely that absorption was the cause since absorption theory (*3*) would predict less than a 2% effect on diffraction intensity at this loading of α-quartz.

An inherent assumption in the liquid suspension filtration technique as applied to thin-layer XRD work is that all suspended particles are captured and held at the filter surface. Theoretically, filtration efficiencies from water are significantly

0003-2700/79/0351-0304$01.00/0 © 1979 American Chemical Society

less than from air. I wonder whether the results of Edmonds, Henslee, and Guerra relating to particle size effects indicate true particle size-XRD effects or rather indicate (at least in part) relative filter efficiencies for the different particle sizes coupled with a particle size effect on diffraction peak height. Regardless of the validity or otherwise of such speculation, I feel it is poor analytical chemistry practice for standards to be prepared by water filtration when field samples are collected by airborne filtration.

LITERATURE CITED

(1) J. W. Edmonds, W. W. Henslee, and R. E. Guerra, *Anal. Chem.*, **49**, 2196–2203 (1977).
(2) G. Heidermanns, *Staub-Reinhalt. Luft* (*Eng. ed.*), **34**, 207–211 (1974).
(3) S. Altree-Williams, *Anal. Chem.*, **49**, 429–432 (1977).
(4) S. Altree-Williams, J. Lee, and N. V. Mezin, *Ann. Occup. Hyg.*, **20**, 109–126 (1977).
(5) D. K. Smith, *Norelco Rep.*, **15**, 57–65, 76 (1968).
(6) S. Altree-Williams, *Anal. Chem.*, **50**, 1272–1275 (1978).
(7) R. I. Higgins and P. Dewell, in "Inhaled Particles and Vapours, II", C. N. Davies, Ed., Pergamon Press, Oxford, 1967, pp 575–586.
(8) H. P. Klug and L. E. Alexander, "X-ray Diffraction Procedures", 2nd ed., John Wiley and Sons, New York, 1974, pp 360–364.

Stephen Altree-Williams
Division of Occupational Health & Radiation Control
Health Commission of New South Wales
P.O. Box 163,
Lidcombe, Australia 2141

RECEIVED for review June 2, 1978. Accepted November 6, 1978.

Sir: Altree-Williams (*1*) has ignored the primary data supporting α-quartz preferred orientation on sampling membranes and casually applied the relationship between intensity and volume of sample irradiated for a normal (fixed divergence slit) diffractometer to data obtained on a diffractometer fitted with a variable divergence (θ-compensating) slit. His failure to use the equations as they apply to the latter instrument compounds his misinterpretation and disguises some interesting facts which subsequently reinforce the original conclusions (*2*).

The intensity of a given (*hkl*) for a flat sample whose surface is at a parafocusing diffractometer center is as follows (*3*)

$$I_{hkl} = 4 \int_0^d \int_0^{l/2} \int_0^{w/2} f_{(hkl)} e^{-2\,\mu^* x \text{ cosec } \theta_{hkl}} \, \mathrm{d}z\mathrm{d}y\mathrm{d}x \qquad (1)$$

where d = sample thickness; l = extent of sample irradiation tangent to the focusing circle; w = extent of sample irradiation normal to the focusing circle (assumed constant); μ^* = mass absorption coefficient, cm^{-1}; θ_{hkl} = Bragg angle for lattice plane (*hkl*); and $f_{(hkl)}$ = scattering factor for lattice plane (*hkl*) including form, Lorentz, and polarization factors.

For an instrument with fixed divergence slit, the beam cross-section (b) is constant and l varies with θ as

$$l = b/\sin \theta_{hkl} \qquad (2)$$

Evaluation of Equation 1 yields

$$I_{hkl} = k_{hkl} \frac{1}{\mu^*} \left(1 - e^{-2\mu^* d \text{ cosec } \theta_{hkl}}\right) \qquad (3)$$

where k_{hkl} includes terms which are constant at θ_{hkl}. For limiting values of d, one obtains

$$d \rightarrow \infty;\ I_{hkl} \propto k_{\text{hkl}}/\mu^* \qquad (4)$$

and

$$d \rightarrow 0;\ I_{hkl} \propto 2dk_{\text{hkl}} \text{ cosec } \theta_{hkl} \qquad (5)$$

in agreement with Altree-Williams (*1*).

For an instrument with a variable divergence slit (θ-compensating slit), however, the relationships *do not* simply include another θ_{hkl} term, but change drastically. Since the slit size is chosen to always irradiate the same sample surface area, l becomes a constant and Equation 1 leads to

$$I'_{hkl} = \frac{k'_{hkl}}{2\,\mu^* \text{ cosec } \theta_{hkl}} \left(1 - e^{-2\mu^* d \text{ cosec } \theta_{hkl}}\right) \qquad (6)$$

For limiting values of d, one obtains

$$d \rightarrow \infty;\ I'_{hkl} = \frac{k'_{hkl}}{2\mu^*} \sin \theta_{hkl} \qquad (7)$$

and

$$d \rightarrow 0;\ I'_{hkl} = k'_{hkl} d \qquad (8)$$

indicating that for thin samples a constant volume is irradiated. Therefore, the *the relative intensities for a thin sample* ($d \ll 1/\mu^*$) *measured on a diffractometer fitted with an aligned θ-compensating slit are directly comparable to relative intensities measured for a bulk sample on a conventional diffractometer* (*i.e., JCPDS data*). Since the data for thin deposits of α-quartz in Table III (*2*) indicate substantially lower I/I_0 values than literature data, the conclusion of preferred orientation is supported. As Altree-Williams properly indicates, the I/I_0 for thin samples should be corrected by cosec θ_{hkl} to yield acceptable agreement with I/I_0 for bulk samples measured on the compensating slit instrument. However, this indicates only that both the bulk and thin samples as prepared exhibit nearly the same degree of (preferred) orientation.

Conclusion 2 should cause no difficulties to persons who have read the entire paper. In particular Table I, which is the primary data supporting variation of orientation with particle size, and Table V, which indicates *equivalent* X-ray diffraction response (k_{hkl}) for air and filtered liquid suspensions of Min-u-sil 5. Perhaps it was remiss not to state conclusion 0, made clear in the body of the paper, *that standard filters prepared by air and filtered liquid suspension are equivalent if deposition area and particle size distribution are identical for the α-quartz used.* Conclusion 2 then refers to the preparation of standard filters by *liquid* filtration. In this case, failure to use a standard with size distribution equivalent to field samples will permit particles larger than the respirable fraction to be more efficiently filtered than sub-respirable particles, which then contribute significantly to increasing k_{hkl} due to preferred orientation (Reference 2, Table I). Since Altree-Williams is preparing standards by air suspended dust collection through a size selecting cyclone, obviously the particle size distribution of the starting material is irrelevant. He has size selected a standard equivalent to the distribution obtained in field sampling. It must be pointed out, however, that with few exceptions, the literature on α-quartz X-ray diffraction methods is replete with "pure α-quartz was used", but without reference to the means of deposition on the filter paper.

The suggestion that loss of preferred orientation may

© 1979 American Chemical Society

contribute to a change in calibration curve slope at ~100 $\mu g/cm^2$ α-quartz was based in part upon the observed changes in I/I_0 (reference 2, Table III). Having established that some degree of similar preferred orientation is present at all thicknesses of the α-quartz used in these studies, the apparent change in slope then is not attributable to this cause. It is most likely an artifact present in wt/cm^2 data which extends beyond the range of our normal samples.

Although theoretical efficiencies are lower for liquid suspension filtration than for air, the observed data (reference 2, Table V) do not in fact show this, and indeed indicate the better standards were prepared from liquid suspension filtration. While purist notions may lead one to adhere to air filtration for the preparation of standards, practical considerations lead one to select less time consuming procedures *where shown to be experimentally equivalent* (*2*). In light of the magnitude of effect that particle orientation has upon the calibration curves for standards prepared from *liquid filtered suspensions*, use of calibration curves obtained in this manner with a properly sized standard contribute less error to the analyses than does *sample* orientation (particle shape), over which the analyst has no control.

The final point of the paper (2) is the necessity for inter-laboratory verification of methods developed to analyze for a common problem of this complexity. In a given laboratory, unknown variables have a habit of becoming constants.

ACKNOWLEDGMENT

The author thanks Ludo K. Frevel for reviewing the manuscript.

LITERATURE CITED

(1) S. Altree-Williams, *Anal. Chem.*, preceding comment in this issue.
(2) J. W. Edmonds, W. W. Henslee, and R. E. Guerra, *Anal. Chem.*, **49**, 2196–2203 (1977).
(3) A. J. C. Wilson, *J. Sci. Instrum.*, **27**, 321–325 (1950).

J. W. Edmonds

Analytical Laboratories, Bldg. 574
Dow Chemical Co.
Midland, Michigan 48640

RECEIVED for review October 6, 1978. Accepted November 6, 1978.

AIDS FOR ANALYTICAL CHEMISTS

Determination of the Natural Abundance of Iron-58 by Neutron Activation Analysis

P. F. Schmidt*

Bell Telephone Laboratories, Incorporated, Allentown, Pennsylvania 18103

J. E. Riley, Jr.

Bell Telephone Laboratories, Incorporated, Murray Hill, New Jersey 07974

The natural abundance of iron-58 is very low and has been reported by various investigators in the range from 0.29 to 0.33%. With Fe_2O_3 samples highly enriched in ^{58}Fe being available from Oak Ridge National Laboratory (ORNL), a straightforward determination of the natural abundance of ^{58}Fe is possible by co-irradiation of the enriched and natural material, and comparison of the ^{59}Fe photopeak intensities.

This experiment was performed with an Fe_2O_3 sample 82.48% enriched in ^{58}Fe, and a natural iron foil, the iron content of which had been determined to be 99.63% by mass spectroscopic examination. The relevant data and an outline of the calculations are given in the Appendix. The natural abundance of ^{58}Fe was found to be 0.283% ± 0.010%, in good agreement with a recent recommendation by Holden (*1*) based on older mass spectroscopic data (2). The presently accepted thermal cross section for ^{58}Fe is 1.14 b; in establishing this cross section, the natural abundance of ^{58}Fe was assumed to be 0.33% (*3*). Since the natural abundance enters the calculation of necessity, the thermal cross section of ^{58}Fe should be higher by the ratio

$$\frac{0.33 \times 1.14}{0.283} = 1.33 \text{ b}$$

APPENDIX

Description of the Measurements and Calculations to Determine the Natural Abundance of ^{58}Fe from the Co-Irradiation of a 99.63% Pure Natural Iron Foil with an Fe_2O_3 Sample 82.48% Enriched in ^{58}Fe

None of the trace impurities in the iron foil have large resonance integrals which could produce a measurable self-shielding effect. The purities of both the iron foil and of the Fe_2O_3 sample were established by mass spectrometry, for the iron sample by the Analytical Chemistry Department at Murray Hill, for the Fe_2O_3 sample by ORNL (no impurities were detected in the latter case).

Materials Used. $Fe_2{}^*O_3$, 2.46 mg, 82.48% enriched in ^{58}Fe, obtained from ORNL. The isotopic analysis of this material is given as follows:

	at.%	precision
^{54}Fe	0.46	±0.05
^{56}Fe	15.57	±0.10
^{57}Fe	1.48	±0.05
^{58}Fe	82.48	±0.10

The symbol Fe* is used hereafter to refer to iron of the above isotopic composition.

21.93 mg Fe foil, 99.63% pure = 21.85 mg pure iron

Both the $Fe_2{}^*O_3$ and the Fe foil were co-irradiated for 60 s in the "front row position" of the University of Missouri

0003-2700/79/0351-0306$01.00/0 © 1979 American Chemical Society

Research Facility at Columbia, Mo. The nominal flux in this position is stated to be 8×10^{13} n cm^{-2} s^{-1}.

After irradiation, the samples were each dissolved in 5.00 cm^3 reagent grade HCl and were then counted in the same (rigidly fixed) position at a distance of about 4.6 cm from the front surface of a co-axial Ge-Li detector; dead times were in the 3–5% range. The areas of the ^{59}Fe photopeaks at 1099 keV were evaluated by hand, the background on both sides of the peak being smooth and low.

End of 60-s irradiation: 6/28/77 at 1400 EDT

Start of 10 000-s acquisition on the 2.46 mg $Fe_2{*}O_3$: 7/8/77 at 1030 EDT

total net count: 134945

Start of 65 000-s acquisition on the 21.93 mg Fe: 7/7/77 at 0815 EDT

total net count: 39542

All decay factors were calculated according to the equation:

$$D = e^{-\lambda t_d} \times \frac{(1 - e^{-\lambda t_{acq}})}{\lambda t_{acq}}$$

where t_d = time elapsed between the starts of acquisition on the two samples, t_{acq} = duration of acquisition, and λ = decay constant (= $0.69315/T_{1/2}$).

Calculation of the Natural Abundance of ^{58}Fe. The molecular weight of the $Fe_2{*}O_3$, and the atomic weight of the Fe* of the given sample can be calculated from the atomic masses. We used the data by Mattauch, Thiele, and Wapstra in "1964 Atomic Mass Table", *Nucl. Phys.*, **67**, 1–31 (1965) in our calculation.

The molecular weight of $Fe_2{*}O_3$ for our sample was calculated as 163.160.

The molecular weight of Fe* for our sample was calculated as 57.58322.

163.160 g $Fe_2{*}O_3$ = 6.022×10^{23} molecules $Fe_2{*}O_3$ =
1.2044×10^{24} atoms Fe*, containing $1.2044 \times 10^{24} \times$
$0.8248 = 9.93389 \times 10^{23}$ atoms of ^{58}Fe

2.46 mg $Fe_2{*}O_3$ = 1.497755×10^{19} atoms ^{58}Fe

21.850 mg pure Fe = 2.356×10^{20} atoms iron (MW = 55.847)

21.850 mg pure Fe, start counting 7/7/77 at 0815 for 65 000 s

uncorrected count rate: 0.608 338 counts/s

count rate corrected for decay while counting: 0.611 869 7 counts/s

2.46 mg $Fe_2{*}O_3$, start counting 7/8/77 at 1030 for 10 000 s uncorrected count rate: 13.494 5 counts/s

count rate corrected for decay while counting: 13.506 53 counts/s

count rate corrected for 26.25-h decay (from 7/7 at 0815 to 7/8 at 1030): 13.7360 counts/s

$2.356 \times 10^{20} \times$ % abundance ^{58}Fe: 0.611 869 7 counts/s

1.497755×10^{19} atoms ^{58}Fe: 13.736 counts/s

Natural Abundance of ^{58}Fe: 0.2832%.

LITERATURE CITED

(1) N. E. Holden, BNL-NCS 50605, March 1977.
(2) G. E. Valley and H. H. Anderson, *J. Am. Chem. Soc.*, **69**, 1971 (1947).
(3) N. E. Holden, Brookhaven National Laboratory, personal communication.

RECEIVED for review May 17, 1978. Accepted October 16, 1978.

Errors in the Atomic Absorption Determination of Calcium by the Standard Addition Method

J. W. Hosking,* K. R. Oliver, and B. T. Sturman

Department of Chemistry, Western Australian Institute of Technology, Bentley, W.A. 6102, Australia

As part of an investigation into the use of lithium metaborate fusions as a general technique for the dissolution of materials containing silicates, the technique was applied to a variety of standard analyzed samples. The resulting solutions were analyzed for silicon, aluminum, calcium, and several other elements by atomic absorption spectrometry. Silicon and aluminum have been shown to cause serious interferences in the determination of calcium in the air–acetylene flame (*1*).

The method of standard additions is often recommended as a means of correcting for interferences in atomic absorption spectrometry (*2–4*). The variation in the effect of matrix components on the absorbance at different analyte concentrations has, in general, been neglected although it has been mentioned by several authors (*1, 2, 5–8*). In an attempt to overcome this problem, Magill and Svehla (*1*) have suggested the use of a releasing agent in calcium determinations by standard additions with the air–acetylene flame. They also recommended the use of the nitrous oxide–acetylene flame, with potassium as an ionization buffer, for the determination of calcium in the presence of other ions. When the method of standard additions was used to determine calcium in a standard analyzed sample of portland cement after lithium metaborate fusion, the results differed significantly from the known calcium content of the sample.

The fact that the results were inaccurate led us to evaluate various techniques for the atomic absorption determination of calcium in the presence of dissolved silicon and aluminum, and to investigate the evident shortcomings of the method of standard additions.

EXPERIMENTAL

Samples. The analyzed cement samples were portland cement 24b (62.9% CaO, 20.8% SiO_2, 6.22% Al_2O_3) and British Chemical Standard No. 372 (65.8% CaO, 21.3% SiO_2, 5.35% Al_2O_3). Both of these samples were from the Bureau of Analysed Samples Ltd, Middlesbrough, England. Synthetic samples with the same calcium, aluminum, and silicon concentration as portland cement 24b were prepared from calcium carbonate, alumina, and silica.

Reagents. The high purity silica was British Chemical Standard No. 313 (99.6% SiO_2, 0.02% CaO). Lithium metaborate was prepared from lithium carbonate (<0.03% Ca) and boric acid (<0.005% Ca) and was recrystallized from hot aqueous solution (*9*). Lanthanum chloride solution was prepared by dissolving lanthanum oxide in AR hydrochloric acid. The calcium content of different batches of lanthanum oxide from the same supplier was sometimes unacceptably high. Only material of very low calcium content (<0.0002%) was used in this work. The calcium standards were prepared from Titrisol ampules (E. Merck) and from AR calcium carbonate (dried at 200 °C) dissolved in AR

0003-2700/79/0351-0307$01.00/0 © 1979 American Chemical Society

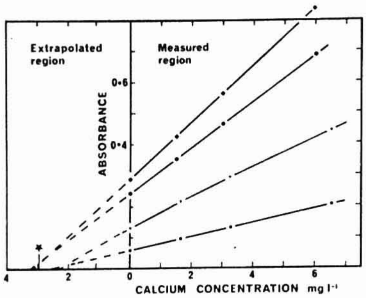

Figure 1. Determination of calcium in portland cement by extrapolation of multiple standard addition curves. (■) Observation height high in fuel lean air-acetylene flame, (▼) observation height low in fuel lean air-acetylene flame, (●) observation height for optimum sensitivity in fuel rich air-acetylene flame, 0.2% La (as $LaCl_3$) present as a releasing agent, (▼) nitrous oxide-acetylene flame at conditions of optimum sensitivity, (★) correct concentration

hydrochloric acid. Other reagents were AR grade.

Fusions and Dissolution. Cement, 0.2 g, (or appropriate amounts of calcium carbonate, alumina, or silica) were fused with 1.0 g of lithium metaborate in a platinum crucible at 970 °C for 30 min. The crucible with the cooled melt was placed in 180 mL of 5% v/v concentrated hydrochloric acid and magnetically stirred. After dissolution of the melt, the solution was made up to 250 mL. This solution was diluted 1:124 in 2% v/v hydrochloric acid so that the calcium concentration was close to 3 mg L^{-1}.

Synthetic Matrix Standards. These were prepared by fusing alumina and silica with lithium metaborate as described above. The aluminum and silicon concentrations in the final solutions were the same as those from portland cement 24b.

Atomic Absorption Spectrometry. Calcium was determined by atomic absorption spectrometry using a Varian Techtron AA5. Except where otherwise stated, measurements were made in the air-acetylene flame at conditions of optimum sensitivity. The nitrous oxide-acetylene flame was also used at conditions of optimum sensitivity. Appropriate reagent blanks were prepared in each case and found to give an absorbance of less than 0.002.

Standard Additions. In the multiple additions method, accurately measured amounts of standard calcium solutions were added to each of four equal aliquots of the unknown solution as described, for example, in Ref. 2 to 4. No calcium was added to one aliquot and amounts equivalent to approximately 50%, 100%, and 200% of the calcium in the unknown solution were added to the others. After the solutions were diluted to the same volume, the absorbances were measured and the absorbance–concentration curve extrapolated graphically to zero absorbance. For some determinations, the absorbance-concentration plot was slightly curved. The extrapolations were also made using a computer program which fitted the data to a straight line and to an appropriate second-order polynomial equation.

In the single addition method (*10*), only the solution to which no calcium had been added and that with approximately 100% additional calcium were used. The unknown calcium concentration was calculated from the relative increase in the absorbance.

Suppression and Enhancement. The percentage suppression (or enhancement) caused by an interfering species was determined from the relative absorbances of a pair of solutions of equal calcium concentration, of which only one contained the interferent. Scale expansion and a chart recorder were used, and multiple readings were made on duplicate solutions to achieve more precise results at low calcium concentrations.

RESULTS AND DISCUSSION

Some typical standard additions graphs are shown in Figure 1, and errors in the calcium concentration as determined by standard additions are shown in Table I. These results are clearly unsatisfactory, as it should be possible to determine calcium at these levels by atomic absorption spectrometry with an error not exceeding ±1 or 2% of the true value.

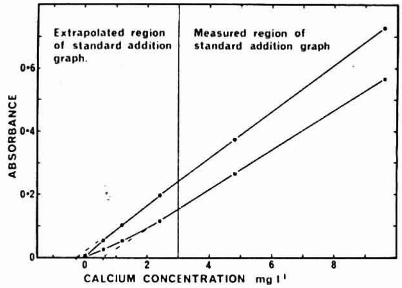

Figure 2. Calibration curves for calcium showing the deviation in the extrapolated region caused by the combined silicon and aluminum interference in lithium metaborate and hydrochloric acid solutions (concentrations as in the analysis of portland cement 24b). (■) No releasing agent, (●) 0.2% lanthanum releasing agent

The linear or near-linear curves as illustrated in Figure 1 and the general agreement between the graphical and computer extrapolated values in Table I suggest that the errors were not the result of inaccurate extrapolation. As shown in Table I, the errors were reduced in a lean air–acetylene flame and further reduced in the nitrous oxide–acetylene flame. The addition of 0.2% lanthanum as a releasing agent improved the result in the air–acetylene flame but unacceptably large errors were obtained in many determinations. The reduction in error correlates with the reduction in chemical interference, as suggested by Magill and Svehla (*5*).

To identify the principal source of the error, it was necessary to determine the shape of the analytical curve in the extrapolated region. Standard calcium solutions (0 to 10 mg L^{-1}) were prepared with the major matrix components present in the same concentrations as in the cement solutions. Analytical curves obtained with these solutions are shown in Figure 2. The known calcium concentration of the portland cement 24b solution was 2.96 mg L^{-1}. The analytical curve below this concentration corresponds to the extrapolated region of the standard addition graph. Figure 2 shows that it is not possible to predict the shape of the extrapolated region of these curves from the data obtained in the measured region. It is significant that each of the analytical curves in Figure 2 is linear in the "measured region", as this is the only portion that would be observed in a standards addition determination. This clearly demonstrated that a linear standard addition graph does not necessarily produce the correct result.

The variation in the shape of the analytical curve at low calcium concentration led to further investigations. The effect of chemical interference at different analyte concentrations was studied by measuring the percentage suppression or enhancement produced by a constant concentration of interfering species. The significant variations in the percentage suppression or enhancement at low calcium concentrations are shown in Figure 3.

The multiple standard addition technique will give the correct result only (i) when there is no chemical interference and the entire analytical curve can be defined accurately by the data from the "measured region", OR (ii) when interfering species are present and the percentage suppression or enhancement is constant over the entire analytical curve. In this case, the standard addition graph will have the same shape as that observed in the absence of interfering species. The suppression or enhancement will alter the sensitivity and, hence, change only the slope of the graph.

If the percentage suppression or enhancement is directly proportional to the analyte concentration, the absorbance–

Table I. Errors in Calcium Analysis by Standard Addition Techniques

			error, %[a]			
			multiple addition method			
				computer		
				polynomial equation		
sample	releasing agent	flame conditions	graphical	2nd order	1st order	single addition method
portland cement 24b	none	fuel rich air-acetylene	−27	−28	−19	−18
portland cement 24b	none	fuel lean air-acetylene (base of flame)	−18	−20	−6	−11
portland cement 24b	none	fuel lean air-acetylene (high in flame)	−9	−5	−9	−9
portland cement 24b	1% La	fuel rich air-acetylene	+5	+2	+17	+9
portland cement 24b	none	nitrous oxide-acetylene	+6	+2	+5	+9
$CaCO_3$, Al_2O_3, SiO_2	none	fuel rich air-acetylene	−20	−28	−23	−11
$CaCO_3$, Al_2O_3, SiO_2	none	fuel lean air-acetylene (base of flame)	−23	−17	−22	−21
$CaCO_3$, Al_2O_3, SiO_2	none	fuel lean air-acetylene (high in flame)	−5	+7	−3	−2
$CaCO_3$, Al_2O_3, SiO_2	0.2% La	air-acetylene[b]	+3	+5	+1	+3
			+3	+7	+3	+3
			+1	+11	0	+6
			+7	+1	+8	+2
$CaCO_3$, Al_2O_3, SiO_2	none	nitrous oxide-acetylene	+8	+7	+11	+8
Al_2O_3, SiO_2 + standard $CaCl_2$	0.2% La	air-acetylene[c]	+4	+12	+3	+4
			+5	+11	+6	+5
			+10	+7	+11	+10
			+10	+12	+10	+10
Al_2O_3, SiO_2 + standard $CaCl_2$	1% La	fuel rich air-acetylene	+10	+10	+12	+10
Al_2O_3, SiO_2 + standard $CaCl_2$	none	nitrous oxide-acetylene	+8	+8	+8	+8
$CaCl_2$ in 2% hydrochloric acid and 1000 mg L^{-1} phosphate as phosphoric acid	none	fuel rich air-acetylene	+1	+3	+38	+17

[a] % error = ((measured calcium content − known calcium content)/known calcium content) × 100. [b] Replicate determinations using various flame conditions, slit widths, lamp currents, and aspirator rates. [c] Determinations of solutions prepared from different fusions, flame conditions varied.

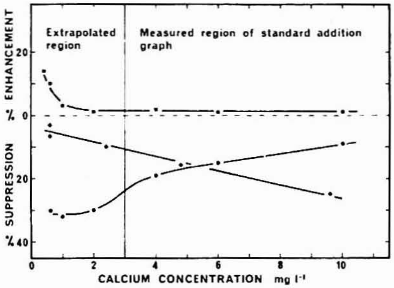

Figure 3. Percentage suppression or enhancement of the calcium absorbance due to the presence of interfering species. (●) Lithium metaborate, hydrochloric acid, silicon, and calcium; (■) lithium metaborate, hydrochloric acid, silicon, aluminum, and 0.2% lanthanum (concentrations ● and ■ as in the analysis of portland cement 24b); (♦) 1000 mg L^{-1} phosphate as phosphoric acid

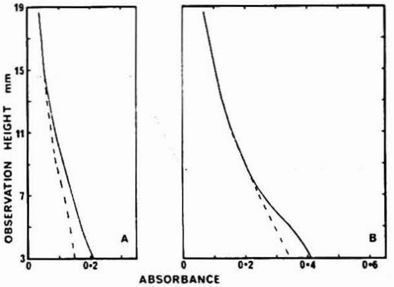

Figure 4. Flame profiles for (A) 3.0 mg L^{-1} calcium and (B) 6.0 mg L^{-1} calcium in a fuel lean air–acetylene flame in 2% hydrochloric acid (–) and in 2% hydrochloric acid solution of lithium metaborate, silicon, and aluminum as in the cement analysis (---)

concentration graph will be a smooth curve. However, in this case, the extrapolated region can in principle be predicted from the measured region and the method of multiple standard additions may still be applicable.

The single additions method is necessarily restricted to those cases where the percentage enhancement or suppression is constant.

Figure 3 shows that the percentage suppression or enhancement due to silicon and aluminum is neither constant nor directly proportional to the calcium concentration even in the presence of lanthanum. This explains the inaccuracy of the method of standard addition for the determination of calcium in portland cement even in the presence of a releasing agent.

The effects of observation height and flame conditions were also investigated. Chemical interferences in calcium determinations in the air–acetylene flame are generally less severe in the fuel lean flame (*11*). The flame profiles in Figure 4 show regions where there was less than 1% interference. As is shown in Figure 4, the observation height required for less than 1% interference varied with changes in the calcium concentration. This indicates that at a constant observation height the percentage suppression or enhancement will be different for solutions of different calcium concentrations,

Table II. Calcium Determination by the Calibration Curve Technique

sample	releasing agent	matrix components matched in standards	flame conditions	error, %[a]
portland cement 24b	nil	HCl, Si, Al, $LiBO_2$	fuel rich air-acetylene	−2
portland cement 24b	0.2% La	HCl only	fuel rich air-acetylene	−1
portland cement 24b	nil	HCl, $LiBO_2$	nitrous oxide-acetylene	−1
$CaCO_3$, Al_2O_3, SiO_2	nil	HCl, Si, Al, $LiBO_2$	fuel rich air-acetylene	<1
$CaCO_3$, Al_2O_3, SiO_2	0.2% La	HCl only	fuel rich air-acetylene	<1
$CaCO_3$, Al_2O_3, SiO_2	nil	HCl, $LiBO_2$	nitrous oxide-acetylene	<1
portland cement B.C.S. 372	nil	HCl, Si, Al, $LiBO_2$	fuel rich air-acetylene	<1
portland cement B.C.S. 372	0.2% La	HCl only	fuel rich air-acetylene	<1

[a] % error = ((measured calcium content − known calcium content)/known calcium content) × 100.

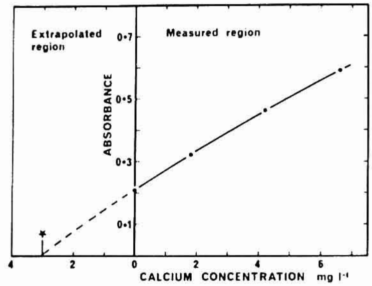

Figure 5. Determination of calcium in the presence of excess phosphate (1000 mg L^{-1}, as phosphoric acid) by extrapolation of a multiple standard addition curve. (★) Correct concentration

which explains the inaccurate results obtained even when the measurements were made high in the fuel lean flame (Table I).

In the above examples, the stoichiometric ratios of calcium to silicon and to aluminum were in the order of 1:1. To investigate the effect of a large excess of interferent, the exercise was repeated with a calcium to phosphate ratio of the order 1:250. It was not practical to have such a large excess of silicon or aluminum. Figure 3 shows that, with the large excess of phosphate, the percentage suppression was very close to being directly proportional to the calcium concentration and the absorbance concentration plot was a smooth curve. When these data were plotted as a standard addition graph (Figure 5) the "measured region" could be used to predict the "extrapolated region", limited only by the difficulty of extrapolating a curve. As indicated in Table I, a relatively small error was obtained for the standard addition determination of calcium (at 3 mg L^{-1}) in a large excess of phosphate (1000 mg L^{-1}).

It was evident from this work that the method of standard additions is not a reliable solution to the problem of chemical interference in the determination of calcium by atomic absorption spectrometry. Results obtained when the conventional calibration curve technique was used for the determination of calcium in cements and in the synthetic mixture are shown in Table II.

These results are all more accurate than those obtained by the standard additions method under comparable experimental conditions (Table I). The calibration curve technique gave very satisfactory results when the fuel-rich air-acetylene flame was used and calcium standards were prepared with aluminum, silicon, lithium metaborate, and hydrochloric acid to match the matrix of the sample solution. Matrix matching is rather inconvenient and may not be possible with an unknown sample, but it was found that equally accurate results were obtained without matrix matching, provided that 0.2% lanthanum was added to the standards and to the sample solutions as a releasing agent. As an alternative, use of the nitrous oxide-acetylene flame was found to give accurate results when the standard solutions were prepared with lithium metaborate and hydrochloric acid to match the sample solutions.

LITERATURE CITED

(1) W. A. Magill and G. Svehla, *Fresenius' Z. Anal. Chem.*, **268**, 177 (1974).
(2) J. Ramirez-Munoz, "Atomic-Absorption Spectroscopy and Analysis by Atomic-Absorption Flame Photometry", Elsevier, Amsterdam, 1968, p 328.
(3) "Analytical Methods for Flame Spectroscopy", Varian Techtron, Melbourne, Australia, 1972, p 14.
(4) "Analytical Methods for Atomic Absorption Spectrophotometry", Perkin-Elmer, Norwalk, Conn., 1976, pp 1–5.
(5) W. A. Magill and G. Svehla, *Fresenius' Z. Anal. Chem.*, **270**, 177 (1974).
(6) W. A. Magill and G. Svehla, *Fresenius' Z. Anal. Chem.*, **269**, 337 (1974).
(7) R. Cioni, A. Mazzucotelli, and G. Ottonello, *Analyst (London)*, **101**, 956 (1976).
(8) J. B. Willis, "Analytical Flame Spectroscopy: Selected Topics", R. Mavrodineanu, Ed., Springer-Verlag, New York, 1970, p 565.
(9) C. O. Ingamells, *Anal. Chim. Acta*, **52**, 323 (1970).
(10) O. Menis and T. C. Rains, "Analytical Flame Spectroscopy: Selected Topics", R. Mavrodineanu, Ed., Springer-Verlag, New York, 1970, p 74.
(11) "Analytical Methods for Atomic Absorption Spectrophotometry", Perkin-Elmer, Norwalk, Conn., 1976, "Calcium Standard Conditions", p 2.

RECEIVED for review January 23, 1978. Accepted October 24, 1978.

Analysis of Bis(trimethylsilyl)acetamide for Purity by Proton Magnetic Resonance Spectrometry

Gordon Munro,* John H. Hunt, and Leonard R. Rowe

Glaxo-Allenburys Research Ltd., Ware, Herts., England

Michael B. Evans

The Hatfield Polytechnic, Hatfield, Herts., England

Bis(trimethylsilyl)acetamide (BSA) (I) is widely used to prepare trimethylsilyl (TMS) derivatives for gas-liquid chromatography (GLC) (*1-3*).

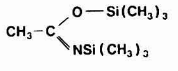

(I)

During recent attempts to prepare TMS ethers of phenylalkanolamines containing more than one hydroxyl group (*4*), evidence of incomplete conversion was obtained under conditions recommended for the exhaustive silylation of the hydroxyls (*5*). To eliminate one possible reason for this discrepancy, the reagent used was analyzed by gas chromatography using Smith's method (*6*). Although all the recommended precautions were precisely followed, nonreproducible results were obtained which questioned the validity of the method. In contrast, we have found that proton magnetic resonance spectrometry affords a simple and reliable method for the analysis of commericially available BSA.

EXPERIMENTAL

Reagents. With the exception of pyridine which was dried over molecular sieve 4A and redistilled, all reagents were used as obtained from commercial sources.

Measurement. Proton magnetic resonance (PMR) spectra were obtained using either a Perkin-Elmer R-12-B or a Varian A-60-A 60-MHz spectrometer. All chemical shift values were measured relative to 1,4-dioxan (downfield shifts are positive). Samples (50 mg) were weighed into 2-mL glass vials and 0.50 mL of pyridine containing 3% w/v of 1,4-dioxan was added. These solutions were transferred to PMR spectrometer tubes for analysis.

Gas chromatograms were obtained using Perkin-Elmer F-17 and F-30 gas chromatographs equipped with glass columns and flame ionization detectors. The columns used (1-m length, 2.0-mm i.d.) were packed with mixtures of liquid phase (liquid paraffin or silicone OV-101) and 60-80 mesh support (Gas Chrom Q) prepared by the procedure described by Smith (*6*). To recover components from the column effluent, a Perkin-Elmer F-17 gas chromatograph fitted with a post-column splitter and double surface trap (*7*) was used. GLC/MS was performed using an A.E.I (Associated Electrical Industries, Manchester, England) M.S. - 30 D.S. - 50 mass spectrometer and data system coupled to a Pye 104 gas chromatograph.

Calculation of Results. Quantitative GLC results were obtained by internal normalization from peak areas determined using an Infotronics C.R.S. 204 integrator. No corrections were made for differences in molar response at the flame ionization detector since Smith (*6*) has shown these to be practically identical for the compounds included in this study. Quantitative PMR results were obtained from peak areas determined by triangulation. Conversion of peak areas into molar or weight ratios was performed as follows.

(i) Molar ratio of BSA:hexamethyldisiloxane (HMDS) (II): monosilylacetamide (MSA) (III) =

$$\frac{\text{area of BSA peak}}{N_{\text{BSA}}} : \frac{\text{area of MSA peak}}{N_{\text{MSA}}} : \frac{\text{area of HMDS peak}}{N_{\text{HMDS}}}$$

(ii) Weight ratio of BSA:HMDS:MSA =

$$\frac{\text{area of BSA peak}}{N_{\text{BSA}} \times \text{MW}_{\text{BSA}}} : \frac{\text{area of MSA peak}}{N_{\text{MSA}} \times \text{MW}_{\text{MSA}}} : \frac{\text{area of HMDS peak}}{N_{\text{HMDS}} \times \text{MW}_{\text{HMDS}}}$$

where N_{BSA}, N_{MSA}, and N_{HMDS} are the number of absorbing nuclei in BSA, MSA, and HMDS contributing to the resonance signal being measured and MW_{BSA}, MW_{MSA}, and MW_{HMDS} are the molecular weights of BSA, MSA, and HMDS, respectively.

Table I. Analysis of BSA Maintained at Elevated Temperatures for Half an Hour

temperature	% w/w BSA	% w/w MSA	% w/w HMDS
probe (ca. 37 °C)	82.6	10.5	6.9
60 °C	82.6	10.5	6.9
90 °C	83.1	10.6	6.2

During hydrolysis experiments and when making standard additions of HMDS and MSA to BSA, 1,4-dioxan was used as an internal standard. Calculations were then performed as described by Kasler (*8*) or the mole ratios of either HMDS or MSA to 1,4-dioxan were determined as previously described.

$(CH_3)_3{-}Si{-}O{-}Si{-}(CH_3)_3$

(II)

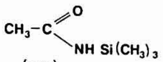

(III)

RESULTS AND DISCUSSION

BSA would be expected to react vigorously with active hydrogen present in the liquid and support phases. To remove these active sites, Smith (*6*) recommended the prolonged pre-treatment of apolar columns with dry nitrogen and repeated injections of BSA. However, we have found that this treatment does not necessarily yield reproducible analyses for the purity of BSA. During the early stages of conditioning, trapping experiments reveal that virtually no BSA is eluted and that the amount of BSA eluted increases gradually with time over a period of two days. Subsequently reproducible results could be obtained, provided the flow of carrier gas was maintained at the analysis temperature; but when columns were stored between analyses, considerable reconditioning was required before reproducible results could again be obtained. Furthermore traces of acetonitrile were frequently detected, consistent with thermal degradation (*6*) either during vaporization or elution and asymmetric (tailing) peaks were frequently observed. Chromatograms which gave rise to nonreproducible analyses displayed base-line shifts as illustrated in Figure 1.

Such chromatograms are generally associated with on-column decomposition (*9*, *10*). In view of the results shown in Table I, this decomposition of BSA is almost certainly hydrolytic rather than thermal. Consistent with a plug flow reactor (*9*), the decomposition was found to be more significant at slower flow rates (i.e., at increased column residence times). GLC/MS analysis of the asymmetric peaks gave inconclusive evidence, presumably due to decomposition of BSA in either the GLC/MS interface or ion source. In each case the spectra revealed the presence of BSA with HMDS and MSA.

Proton Magnetic Resonance. The synthesis, infrared (IR), and PMR spectroscopic characteristics of BSA have been reported (*10*, *11*). Consistent PMR spectra were readily obtained using a wide range of solvents, including carbon

0003-2700/79/0351-0311$01.00/0 © 1979 American Chemical Society

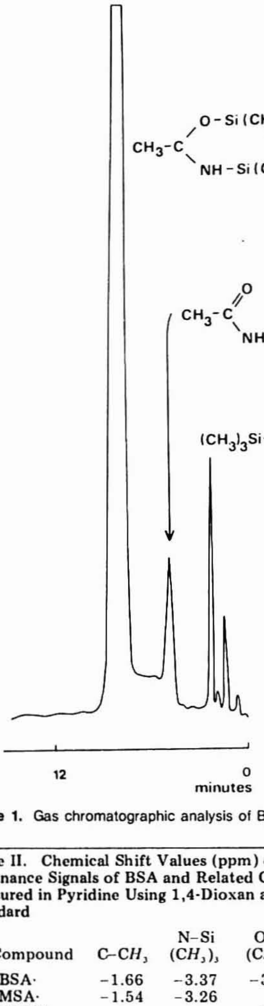

Figure 1. Gas chromatographic analysis of BSA

Table II. Chemical Shift Values (ppm) of the Resonance Signals of BSA and Related Compounds Measured in Pyridine Using 1,4-Dioxan as Internal Standard

Compound	C-CH_3	N-Si $(CH_3)_3$	O-Si $(CH_3)_3$	$(CH_3)_3$ -Si-Cl
BSA	-1.66	-3.37	-3.37	
MSA	-1.54	-3.26		
HMDS			-3.47	
acetamide	-1.53			
trimethylchlorosilane				-3.22
acetonitrile	-1.74			

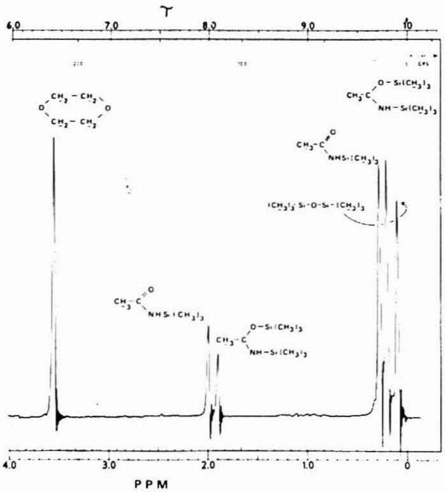

Figure 2. Proton magnetic resonance spectrum at 60 MHz of a mixture of BSA, HMDS, and MSA scanned at 2 Hz s^{-1} with 1,4-dioxan as reference

Table III. Repetitive Analyses of BSA Samples (from the Same Batch)

	% w/w of BSA	% w/w of MSA	% w/w of HMDS
	74.9	13.5	11.7
	76.9	14.4	8.69
	79.0	11.9	9.19
	78.5	13.3	8.32
	79.4	12.4	8.22
	76.5	16.1	7.49
	80.1	11.6	8.4
	73.6	15.3	11.2
	77.7	14.2	8.2
	79.7	11.1	8.58
mean	77.6	13.4	9.0
std. dev.	2.15	1.65	1.36
95% confidence limits, 2 analyses)	77.6 ± 3.4	13.4 ± 3.8	9.0 ± 2.6

tetrachloride, 1,4-dioxan, benzonitrile, benzene, and pyridine. Discrete resonances assignable to BSA, HMDS, and MSA were observed in most of these solvents. Table II shows the chemical shift values assigned to BSA, MSA, and HMDS in pyridine which was found to be the most appropriate solvent. Acetamide and trimethylchlorosilane both of which might be present from the route of synthesis of BSA (*10*) and acetonitrile, a thermal degradation product, are also included in the table to demonstrate that they could be detected in the presence of BSA. Figure 2 shows the PMR spectrum of a mixture of BSA, HMDS, and MSA.

To evaluate PMR as a quantitative analytical method, several samples of BSA from the same batch were analyzed. Peak heights, peak areas (triangulation), and integrated peak areas were measured for all the resonance signals observed on both 5- and 10-ppm scales under optimized instumental conditions. The method giving the most reproducible results which was used for all subsequent determinations consisted of measurement of the peak areas (triangulation) of the C-CH_3 signal of BSA and MSA and the $(CH_3)_3$-Si signal of HMDS on the 10-ppm scale. Results of the reptitive analyses are shown in Table III.

Limits of detection for HMDS and MSA were determined and found to be 0.5% and 1.0% w/w, respectively, taking a signal to noise ratio of 2:1 as the lower limit of detection. The lack of a pure sample of BSA greatly inhibited attempts to check the accuracy of our proposed analytical method. However, when solutions of BSA in pyridine were prepared and consecutive additions of either HMDS (0.02-mL aliquots) or MSA (0.02-mL aliquots of a 20% w/v solution in pyridine) were made, the peak areas of the HMDS and MSA signals increased linearly with the amount of HMDS or MSA added. Furthermore, the concentrations of HMDS and MSA obtained by this standard addition technique were in good agreement with the initial analysis.

The BSA solutions used in analyses were found to be unchanged after two days at probe temperature. Other samples were prepared and analyzed after being heated at 60 and 90 °C, respectively, for 30 min in the variable temperature probe. No significant decomposition was detected.

As expected the addition of water to solutions under test produced rapid hydrolysis of BSA to HMDS and MSA.

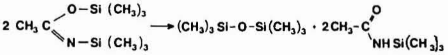

$$2\,CH_3C(=N\text{-}Si(CH_3)_3)(O\text{-}Si(CH_3)_3) \rightarrow (CH_3)_3Si\text{-}O\text{-}Si(CH_3)_3 \cdot 2\,CH_3\text{-}C(=O)NHSi(CH_3)_3$$

Subsequently, measured amounts of water (0.02-mL aliquots of a 4% w/v solution of water in pyridine) were added and the production of HMDS and MSA was monitored. Results after regression analysis confirmed that each mole of BSA yielded 0.5 mol of HMDS and 1.0 mol of MSA as expected. This confirms the accuracy of our method. No significant decomposition occurred when solutions were treated with dry oxygen, and sparging with nitrogen produced no notable improvement in the spectra. Therefore it seems that degassing is not necessary.

LITERATURE CITED

(1) R. H. Horrocks, E. J. Hindle, A. P. Lawson, D. H. Orrell, and A. J. Poole, *Clin. Chim. Acta*, **69**, 93 (1976).
(2) A. J. Poole, D. I. Slater, and D. H. Orrell, *Clin. Chim. Acta*, **73**, 527 (1976).
(3) M. Lauwerys and A. Veroruyssa, *Chromatographia*, **9**, 520 (1976).
(4) G. Munro, J. H. Hunt, L. R. Rowe, and M. B. Evans, *J. Pharm. Pharmacol.*, **28**, Suppl. 27P (1976).
(5) P. R. King, Glaxo-Allenburys Research (Greenford) Ltd., Greenford, Middlesex, England, Private Communication.
(6) E. D. Smith, *J. Chromatogr. Sci.*, **10**, 34 (1972).
(7) R. K. Stevens and J. P. Mold, *J. Chromatogr.*, **10**, 398 (1963).
(8) F. Kasler, "Quantitative Analysis by N.M.R. Spectroscopy", Academic Press, New York, 1973.
(9) O. Levenspiel, "Chemical Reaction Engineering", 2nd ed. John Willey, New York, 1972, p 107.
(10) M. B. Evans, *Chromatographia*, **3**, 337 (1970).
(11) L. Birkofer, A. Ritter, and W. Giessler, *Angew, Chem.*, **75**, 93 (1963).
(12) J. F. Klebe, H. Finkbeiner, and D. M. White, *J. Am. Chem. Soc.*, **88**, 3390 (1966).

RECEIVED for review June 21, 1978. Accepted October 11, 1978.

Pressure-Volume Technique for the Calibration of Ozone Analyzers

Ikuo Watanabe[1] **and Edgar R. Stephens***

Statewide Air Pollution Research Center, University of California, Riverside, California 92521

The calibration of instruments for monitoring ozone or oxidant in polluted air has always presented a special problem because ozone is an unstable gas not readily handled in pure form. Historically, analysts have made use of the oxidation of the iodide ion in buffer solution with the assumption that iodine is formed in stoichiometric yield. Attempts to verify this assumption have sometimes given positive (*1*, *2*) and sometimes negative results (*3*, *4*). The situation was complicated by the fact that many variations of the iodide method were in use. It is unlikely that any two laboratories ever used iodide methods which were identical in every detail. The most recent version uses a boric acid buffer (*5*, *6*).

Direct comparisons finally produced such discordant results that regulatory agencies began to explore alternatives not dependent on the stoichiometry of iodide oxidation. The two most popular alternatives are gas phase titration (GPT) (*1*) and ultraviolet absorption spectrophotometry (UV) (*7*). The GPT method depends on the stoichiometric fast reaction of ozone with nitric oxide and requires accurate measurement of flow rates. In addition, the user must either prepare a known mixture of nitric oxide in an inert gas (which has its own pitfalls) or trust such a primary standard provided by some third party. This may not be readily available in some parts of the world. The ultraviolet method is more direct but does require a special long path cell (1–5 m) since 1 ppm of ozone absorbs only about 3% of an ultraviolet beam per meter. The error in measurement of either light intensity (with and without O_3) is magnified about thirty-fold by the necessary Beer–Lambert law calculations of ozone for these parameters.

The method described in this paper depends on the measurement of ozone by the pressure change which accompanies the conversion of a small portion of oxygen to ozone in a closed system:

$$3O_2 \rightarrow 2O_3 \qquad (1)$$

A very brief discharge of 12000 V through a trapped volume of pure oxygen at atmospheric pressure produces about 1% ozone. The decrease in total moles causes a decrease in either volume or pressure or both depending on the apparatus. This change can be used to calculate the amount of ozone formed. In this study, the ozone formed had a volume of only a few hundredths of a cubic centimeter so pressure change at constant volume was used. After equilibration and measurement, this ozone is swept into a dilution vessel of large, known volume to achieve a known concentration in the sub-ppm range. This method had previously been used to determine the infrared absorptivity of ozone (*8*, *9*) and to calibrate an older model ozone photometer as well as to validate a potassium iodide procedure (*10*). In all four studies the P/V "absolute" ozonizer gave consistent, reliable results.

In this study, a coulometric (Mast Development Co. Model 724.2) potassium iodide analyzer and two ultraviolet photometers (Dasibi Model 1003AH) were tested. Each of these could, in principle, be an "absolute" analyzer (i.e., not requiring calibration). The ultraviolet absorptivity of ozone is accurately known and this instrument measures fractional light absorption by digital techniques which can be used directly to compute concentration. The coulometric analyzer is "internally calibrated" if a stoichiometric yield and measurement of electrons is assumed. But no instrument is foolproof, so independent calibrations are required at least for verification. Ozone analysis is especially vulnerable because decomposition to oxygen is thermodynamically favored and, if it occurs in air, it would likely go undetected because of the excess of oxygen, and traces of catalyst could easily cause such decomposition. The present method permits the monitoring of such ozone loss for all steps except the transfer from ozonizer to dilution bottle.

EXPERIMENTAL

Apparatus. The major elements of the calibration system (shown in Figure 1) are the P/V ozonizer, the dilution bottle (46.6 L), and the instrument to be calibrated. The dilution flask should

---

[1] Present address: Institute of Public Health 4-6-1 Shirokanedai, Minato-Ku, Tokyo 108, Japan.

0003-2700/79/0351-0313$01.00/0 © 1979 American Chemical Society

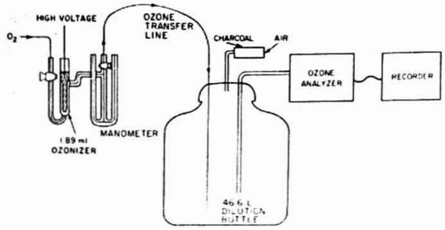

Figure 1. Ozone generated in the 1.89-mL volume by electrical discharge is measured by pressure change on the oil manometer and diluted into the large bottle

be large so that the instrument being calibrated will reach a steady reading without excessive dilution of the calibration mixture and so that the amount of ozone generated in the ozonizer will be as large as possible. For $^1/_2$ ppm of ozone in 46.6 L, 23.3 μL of pure ozone is required. If the discharge converts 1% of the trapped oxygen to ozone, the volume of the ozonizer should be 2.33 mL. This is much smaller than the ozonizers used in previous studies which ranged from 11.0 to 205 mL. The ozonizer volume was measured by weighing with and without water before sealing the 3-legged manometer to the ozonizer body. The volume of the connecting capillary was estimated to be 0.27 mL from its dimensions. This was added to give a total volume of 1.89 mL. This is probably the minimum practical since the connecting volume is an appreciable fraction of the total, and the accuracy of the method depends directly on the accuracy of measurement of this volume. The volume of the dilution bottle was also measured by water filling, one of the simplest and most reliable of all physical measurements. It is important that the temperature of the ozonizer be the same after ozonization as before. This was kept to ±0.02 °C for 1 h, in spite of a 2 °C change in room temperature, by immersing the ozonizer in a water bath in a vacuum jar to provide a large heat sink and by covering the water with silicone oil. Minimizing the time of ozonization (3–15 s) is also advantageous. Provided uniform, constant temperature is maintained, the volume of ozone can be calculated by applying conservation of mass and the perfect gas law:

$$v_{O_3} = 2V\Delta p/P \tag{2}$$

where v_{O_3} and V are the volumes of ozone and of the ozonizer (1.89 mL), respectively, and $\Delta p/P$ is the fractional change in pressure which accompanies ozone formation. Silicone oil of 0.963 g/mL density was used in the 3-legged manometer so formation of 1% ozone causes a pressure decrease of 5.37 cm at constant volume and 1 atm pressure. The third leg of the manometer was capped with a small syringe and a screw to manipulate the manometric fluid so that the trapped volume would be constant. The viscous silicone oil required some time to drain from the walls of the 2-mm i.d. manometer. Complete drainage is not necessary, however, so long as pressure equilibration is attained. In addition, a few minutes were required to establish thermal equilibrium. Keeping the discharge time short also minimized the time necessary for this. It should be noted that ozone decomposition which occurred in the ozonizer during the equilibration period would not cause any error since the pressure at any instant truly reflects the amount of ozone present. Nor is there any error caused by lack of ozone generation in the connecting capillaries. Again the pressure reflects the total number of moles without any assumption of uniformity of concentration. Any ozone which dissolved in the manometric fluid would of course be lost but the contact here is minimal.

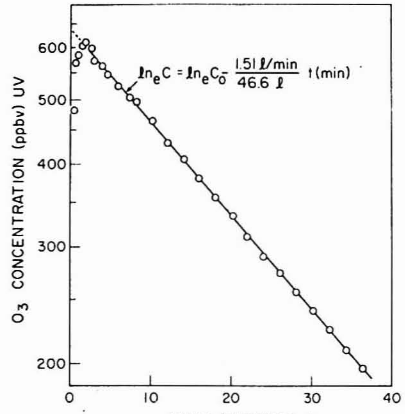

Figure 2. Sampling at 1.51 L/min dilutes the standard at the rate calculated for perfect mixing (UV photometer)

Procedure. After measurement of the pressure difference, the ozone was swept immediately into the dilution bottle with a small volume of oxygen and allowed to mix. Since the P/V ozonizer has a volume of only 1.89 mL, 20 mL of oxygen is more than adequate to transfer the ozone with little loss in the bottle due to dilution. Contact time in this transfer is minimized. Then the analyzer was connected to the bottle and the concentration was recorded vs. time. Sampling from a limited volume of course causes dilution of the ozone at a measurable rate as shown in Figure 2. Charcoal filtered room air was allowed to enter the dilution bottle through the tube shown. For perfect mixing the concentration should decrease at an exponential rate

$$C = C_0 e^{-(F/V)t};\ \ln C = \ln C_0 - \frac{F}{V}t \tag{3}$$

with F = 1.51 L/min as sampled by one of the UV photometers (Dasibi 15) and V = 46.6 L; the halftime for dilution is (46.6/1.51) × ln 2 = 21.4 min. The flow rate through another photometer (Dasibi 06) was 0.6 L/min giving a halftime of 53.8 min. (These photometers have built-in flowmeters.) The solid line in Figure 2 shows this theoretical dilution rate superimposed on the concentrations from the recorder trace. The agreement shows two things.

(1) The assumption of good mixing is valid (otherwise the plot would not be linear).

(2) No significant decomposition of ozone occurred during the sampling period (otherwise the rate of decrease would exceed that caused by dilution). Since ozone decomposition in the ozonizer is also monitored by the pressure measurement, only the transfer step itself (a few seconds) is unvalidated. A loss here would not be the same from test to test.

The calibration point was taken to be the concentration extrapolated to zero time. In routine use, it would not be necessary to measure the sample flow rate since it does not enter into any calculation. This is an important advantage of the P/V method. To verify the stability of the ozone in the bottle, sampling by the UV photometer was interrupted for various time intervals and the concentration (back extrapolated to time of reconnection) was compared with the final value of the preceding sample period. Figure 3 demonstrates the good agreement which was obtained. In this figure, the number of minutes of interruption is shown adjacent to each point.

RESULTS AND DISCUSSION

Having demonstrated that the bottle did not destroy ozone appreciably, comparisons were made between the ozone calculated from the pressure change and that indicated by the two photometers. Each of these instruments had been calibrated by comparison with the standard photometer of the California Air Resources Board prior to these tests. Combining data from the two photometers yielded a least squares equation of $[O_3(UV)] = 0.97[O_3(\Delta P)] - 1$ (in ppb) with a correlation coefficient R of 0.998. In these tests, the slopes of the logarithmic concentration vs. time plots (of which Figure 2 is an example) gave calculated dilution flow rates within 10% of the measured flow rates.

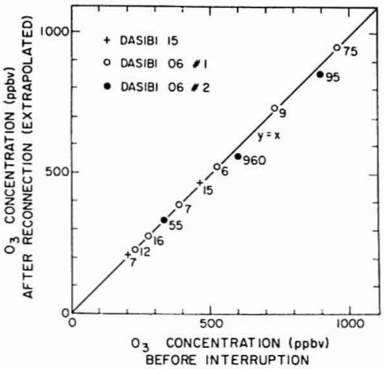

Figure 3. No significant loss of ozone occurred during time intervals comparable to those needed to calibrate the UV analyzer

The P/V ozonizer was also used to evaluate a coulometric KI analyzer (Mast Development Corp.). Although the contact time between the air sample and the reagent in this analyzer is of the order of seconds, the time for nearly full response is greater than 20 min. This long lag increases the potential error in the back extrapolation so the equilibration time was reduced by pre-equilibrating the analyzer with a second ozone stream of similar concentration generated by an ultraviolet lamp. This procedure reduced the equilibration time by one half.

Trials with charcoal-filtered room air as a diluent gas gave very low results, so most of the experiments were done with cylinder nitrogen. The current (in microamperes) produced by the analyzer was compared with that calculated from the ozone concentration according to the formula

$$i = 0.0392CFP/T \qquad (4)$$

where i is current (μA), C = concn of O_3 in ppb, F = sample flow rate mL/min, P is barometric pressure (atm), and T is absolute temperature (K). Linear regression yielded the best fit equation $i_{\text{measd}} = 1.04i_{\text{calcd}} - 0.03$ with $R = 0.999$.

Again, it would not be necessary to measure flow rate in a routine calibration of this analyzer. These results indicate that the P/V ozonizer can be depended on to produce accurately known quantities of ozone for the preparation of primary standards for the calibration of ozone analyzers in the range below 1 ppm. It offers a viable alternative to the UV and GPT methods.

LITERATURE CITED

(1) J. A. Hodgeson, R. E. Baumgardner, R. E. Martin, and K. E. Rehme, *Anal. Chem.*, **43**, 1123 (1971).
(2) S. L. Kopcynski and J. J. Bufalini, *Anal. Chem.*, **43**, 1126 (1971).
(3) A. W. Boyd, C. Willis, and R. Cyr, *Anal. Chem.*, **42**, 670 (1970).
(4) J. N. Pitts, Jr., J. M. McAfee, W. D. Long and A. M. Winer, *Environ. Sci. Technol.*, **10**, 787–793 (1976).
(5) D. L. Flamm, *Environ. Sci. Technol.*, **11**, 978 (1977).
(6) R. J. Paur, R. K. Stevens, and D. L. Flamm, **EPA-600/3-771a**, Jan. 1977, International Conference on Photochemical Oxidant Pollution and Its Control, Proceedings, Vol. I, "Status of Calibration Methods for Ozone Monitors".
(7) W. B. DeMore and M. Patapoff, *Environ. Sci. Technol.*, **10**, 897 (1976).
(8) P. L. Hanst, E. R. Stephens, W. E. Scott, and R. C. Doerr, *Anal. Chem.*, **33**, 1113–1115 (1961).
(9) J. M. McAfee, E. R. Stephens, D. R. Fitz, and J. N. Pitts, Jr., *J. Quant. Spectrosc. Radiat. Transfer*, **16**, 829 (1976).
(10) F. R. Burleson and E. R. Stephens, "*Chemical Methods* in Air Pollution", California Department of Health, "Volumetric Calibrations of the Kruger Ozone Photometer", 1960.
(11) F. R. Burleson and E. R. Stephens, California Department of Health, Conference Workshop 1959, "The Formation and Recovery of Absolute Quantities of Ozone".

RECEIVED for review June 22, 1978. Accepted October 20, 1978.

Wet Digestion Method for the Determination of Mercury in Biological and Environmental Samples

J. Ross Knechtel* and **J. L. Fraser**

Wastewater Technology Centre, Environmental Protection Service, Environment Canada, Burlington, Ontario L7R 4A6, Canada

Cold vapor atomic absorption spectrophotometry has proved very effective for the determination of mercury in a wide range of sample types. The original procedure described by Hatch and Ott (*1*) and modifications such as those suggested by Uthe et al. (*2*), Bishop et al. (*3*), and Hendzel et al. (*4*) depend on wet oxidation by a combination of concentrated nitric and sulfuric acids, some heat, and usually an oxidizing agent such as potassium permanganate.

When measuring the mercury content in botanical samples and sewage sludges, the main consideration is the high carbon content (vegetation samples: 40–50%; dried sewage sludges, 15–30% C). Carbon acts as a strong reducing agent on mercury during sample digestions. This commonly leads to volatilization losses of mercury. Because of this difficulty, usually only small amounts of sample (about 0.1 g) are taken for analysis when evaluating plant tissue or sewage sludges for mercury content by cold vapor atomic absorption (*2–4*). As the mercury content in vegetation samples is usually very low (10–50 ng/g), the 0.1-g sample weight would be insufficient for a reliable and accurate mercury determination. Thus a need for a method capable of handling larger sample weights exists.

Malaiyandi and Barrette (*5*) published a wet oxidation procedure for total mercury analysis capable of the digestion of up to 5 g of sample. The method, however, required special glassware, at least a 1-h digestion, and constant attention. These aspects made it impractical for the routine determination of mercury.

Deitz et al. (*6*) described a variation in the Malaiyandi et al. (*5*) method. The Deitz method appeared to be more practical than the Malaiyandi method as the special glassware was eliminated and constant attention was no longer necessary. However difficulty was experienced in obtaining accurate results using the Deitz et al. (*6*) method and the use of long neck volumetric flasks presented some practical difficulties.

The proposed method is a modification of the Deitz (*6*) procedure. An aluminum hot block with digestion tubes is utilized for sample preparation. The new method has proved to be sensitive, fast, accurate, and reproducible. It has been used successfully on grass tissue, fish tissue, sewage sludges,

0003-2700/79/0351-0315$01.00/0 © 1979 American Chemical Society

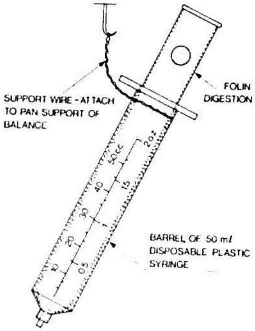
SUPPORT WIRE - ATTACH TO PAN SUPPORT OF BALANCE
FOLIN DIGESTION TUBE
BARREL OF 50 ml DISPOSABLE PLASTIC SYRINGE
2oz
50cc
40
30
20
10
15
1
0.5

Figure 1. Weighing device used on analytical balance

and soil samples. The detection limit is 0.01 µg/g Hg.

EXPERIMENTAL

All glassware used should be rinsed with concentrated nitric acid and distilled water.

All digestions were carried out in a fume hood. Samples were saturated with nitric acid before heat was applied (see Digestion). Foaming sometimes occurred upon the addition of nitric acid. Heat was not applied until this condition subsided.

The mercury-laden vapor was dried using a drying trap of concentrated sulfuric acid as described by Kothandaraman et al. (*7*). The sulfuric acid in this trap was changed daily. At the outlet of the absorption cell, an activated carbon filter and a saturated acidic potassium permanganate solution were used to remove the mercury vapor.

Apparatus. Samples were digested in Folin digestion tubes calibrated at 25 and 50 mL. The tubes were heated in an aluminum hot-block (26.5 cm × 19.0 cm × 7.5 cm) with 24 holes 2.54 cm in diameter and 5.6 cm deep. The block was heated on a small hot-plate capable of generating and maintaining a temperature of 160 °C.

Mercury measurements were made using a Fisher Scientific Hg-3 mercury meter equipped with a Hewlett-Packard recorder (model 7101B-24).

A 250-mL bottle fitted with an aspirator was used to generate mercury vapor for measurement.

Reagents. Stannous chloride (10%) was prepared by diluting a 40% stannous chloride solution (in concentrated hydrochloric acid) with distilled water. Both solutions should be stored in dark bottles.

Mercury standard solution (1000 ppm) was prepared by dissolving 1.353 g of reagent grade $HgCl_2$ in 1 L of distilled deionized water. A working standard solution (10 ppm) was prepared from the stock by diluting 10 mL of the stock standard solution to 1 L, to which 10 mL concentrated nitric acid and 13 mL of 0.25 N $K_2Cr_2O_7$ solution had been added. This solution was stable for at least 3 months. Nitric acid and potassium dichromate may contain some mercury and the working standard solution should be checked against a similar dilution of the stock solution which does not contain any preservatives in order to obtain its true concentration.

Recommended Procedure. *Digestion.* An appropriate amount of sample (0.50 g for vegetation, soil, fish, and sludge samples) was weighed into a Folin digestion tube using a device such as the one shown in Figure 1. Reagent grade V_2O_5, 80 to 100 mg, were added followed by 10.0 mL of concentrated nitric acid. After the foaming subsided, the tube and contents were heated in the hot-block (at 160 °C) for 5 min. The tube was removed, and cooled before 15.0 mL of concentrated sulfuric acid were added. The tube was then replaced in the hot-block for 15 min, then removed and allowed to cool. A "blank" digestion containing all the reagents was also done along with samples.

Determination of Mercury. The digested sample was transferred cautiously to a graduated cylinder and made up to a total volume of 100 mL with deionized water. The whole sample or suitable aliquot diluted to 100 mL was transferred to the mercury reduction flask. After addition of 10 mL of stannous chloride (10%), the aspirator was placed into the mercury reduction flask as rapidly as possible, and the mercury was purged into the absorption cell using compressed air (1800 mL/min).

Table I. Accuracy and Precision of Proposed Method

material	certified value, µg/g	present method, µg/g	precision, %
NBS Orchard Leaf	0.155 ± 0.015	0.152 ± 0.005	3.3
NBS Bovine Liver	0.016 ± 0.002	0.017 ± 0.004	23.5
sludge B (*8*)	26.5^c	25.7 ± 1.1	4.3
ocean perch	N/D^a	0.049 ± 0.006	12.2
SO-1^d	0.022 ± 0.003 (*9*)	0.022 ± 0.003	11.4
SO-2^d	0.082 ± 0.009 (*9*)	0.100 ± 0.007	6.5
SO-3^d	0.017 ± 0.006 (*9*)	0.014 ± 0.004	31.4
SO-4	N/A^b (*9*)	0.033 ± 0.003	10.0

[a] N/D = not determined. [b] N/A = not available. [c] Proposed value. [d] Reference soil samples.

Table II. Comparison of Results Obtained on Fish Samples Using the Proposed Method and Other Methods

sample	measured result, µg/g Hg, (proposed method)	result (other)	method used
1	0.16	0.15	(*10*)^b
2	0.17	0.15	(*10*)^b
3	0.18	0.15	(*10*)^b
4	0.18	0.15	(*10*)^b
5	2.1	1.5	NAA^a
6	0.12	0.18	NAA
7	4.80	4.6	NAA

[a] NAA = neutron activation analysis. [b] Cold vapor atomic absorption following cool (60 °C) digestion using H_2SO_4 and H_2O_2.

The amount of mercury in the sample was calculated by comparing the recorder response for samples vs. that for known standards which were determined daily.

RESULTS AND DISCUSSION

Accuracy and Precision. The accuracy and precision of the present method were evaluated using reference materials with certified or accepted concentrations of mercury. The results are shown in Table I. The accuracy and precision demonstrated by the analysis of reference materials are quite acceptable.

To obtain further precision data on mercury in fish tissue, a bulk sample of ocean perch was prepared and analyzed. The data are presented in Table I.

Additional fish samples were also analyzed for mercury by the method described. Portions of these same samples were analyzed by other laboratories recognized for their expertise in mercury analysis. The comparative results show satisfactory agreement (Table II).

Information on the application of the proposed method to soil sample analysis was also obtained. Mercury analyses were performed on four soil samples (SO-1 to SO-4) which constitute part of the Canadian Certified Reference Materials Project (*9*). A summary of the results obtained is presented in Table I.

Detection Limit. With the system and method as described using a sample weight of 0.5 g, the detection limit is 0.01 µg/g Hg (fish samples, sewage sludges, vegetation samples, and soil samples).

Applicability of Method. The method is particularly suitable for routine work where a simple, rapid, and accurate approach is required. It is appealing to the small laboratory since it allows for the digestion of a large number of samples in a small working area (in this case 24 samples in an area of 26.5 × 19.0 cm). The digestion process is simple in comparison to Hatch et al. (*1*) and Uthe et al. (*2*). Chemicals such as potassium permanganate and hydroxylamine hydrochloride are no longer required. The use of vanadium pentoxide as the catalyst is a decided advantage. This chemical may be rendered mercury-free by incineration. The use of digestion tubes reduces the space requirement for digestion.

ACKNOWLEDGMENT

The authors thank Y. K. Chau, National Water Research Institute, Canada Centre for Inland Waters for reviewing the manuscript. We also thank B. Teifenbach, Department of Chemical Engineering, University of Toronto, and D. P. Sturtevant, Water Quality Branch, Canada Centre for Inland Waters, for providing mercury analyses on fish tissue used in the study.

LITERATURE CITED

(1) W. R. Hatch and W. L. Ott, *Anal. Chem.*, **40**, 2085–2087 (1968).
(2) J. F. Uthe, F. A. J. Armstrong, and M. P. Stainton, *J. Fish. Res. Bd. Can.*, **27**, 805–811 (1970).
(3) J. N. Bishop, L. A. Taylor, and P. L. Diosady, "High Temperature Acid Digestion for the Determination of Mercury in Environmental Samples", Ontario Ministry of the Environment, March 1975.
(4) M. R. Hendzel and D. M. Jamieson, *Anal. Chem.*, **48**, 926–928 (1976).
(5) M. Malaiyandi and J. P. Barrette, *J. Assoc. Off. Agric. Chem.*, **55**, 951–959 (1972).
(6) F. D. Deitz, J. L. Sell, and D. Bristol, *J. Assoc. Off. Anal. Chem.*, **56**, 378–382 (1973).
(7) P. Kothandaraman and J. F. Dallmeyer, *At. Absorpt. Newsl.*, **15**, 120–121 (1976).
(8) R. Knechtel, K. Conn, and J. Fraser, "The Analysis of Chemical Digester Sludges for Metals by Several Laboratory Groups", Environmental Protection Service report (Canada) EPS 4-WP-78-1 (January 1978).
(9) G. H. Faye, Coordinator CCRMP, Ottawa, Canada K1A OG1, personal communication, 1978.
(10) H. Agemian and V. Cheam, *Anal. Chim. Acta*, **101**, 193–197 (1978).

RECEIVED for review August 2, 1978. Accepted November 13, 1978.

Probe for Direct Exposure of Solid Samples to the Reagent Gas in a Chemical Ionization Mass Spectrometer

Robert J. Cotter

Johns Hopkins University School of Medicine, Department of Pharmacology and Experimental Therapeutics, Baltimore, Maryland 21205

Mass spectroscopists have for a long time been interested in obtaining spectra of nonvolatile and thermally labile compounds. In the past, it has usually been necessary to derivatize such samples to produce a more volatile or thermally stable compound for introduction into the ion source via a direct probe or gas chromatograph. Chemical ionization is often used to enhance the abundance of the molecular ion and to reduce fragmentation. More recently, field desorption has been used to produce intense molecular ion species from nonvolatile compounds without the need for derivatization. However, this technique is not readily available to many.

Recently, there has been increased interest in methods which involve exposing the sample directly to the electron beam or the reagent gas plasma (*1–4*). One attraction of this approach is that it requires only simple modifications to enable its use in conventional mass spectrometers having EI or CI sources.

To date, several critical operational parameters have been identified for these direct exposure methods. Ohashi et al. (*2*) and Hansen and Munson (*4*) have made systematic studies of the effect of the sample position relative to the electron beam. Baldwin and McLafferty (*1*), Hunt (*3*), and Hansen and Munson (*4*) have all suggested the importance of a nonmetallic surface, such as glass or Teflon. Finally, the effects of temperature and heating rate have been investigated by a number of authors (*3–6*).

In our laboratory we have designed a number of probes for our DuPont 21-491 mass spectrometer, which allow for direct exposure of the sample to the reagent gas inside the source. Because of our own preference for leaving the ion source intact for other work, these designs have focused on modifications of the direct probe itself. It is the purpose of this paper to present a simple design for a probe which we have found produces good spectra in many cases for compounds which we previously needed to derivatize.

EXPERIMENTAL

Experiments were conducted on a DuPont 24-491 double focusing mass spectrometer, interfaced to an INCOS data system and having a combination CI/EI source. Isobutane was used as the reagent gas at a source pressure of approximately 0.5 Torr. Source temperatures ranged between 200 to 380 °C.

The direct exposure probe tip was designed as a replacement for the recessed quartz sample holder which is ordinarily mounted on the 21-491 direct probe. It is made from a single piece of $^1/_4$-inch Vespel rod, available from E. I. DuPont de Nemours, Wilmington, Del. The design is shown in Figure 1. When in position in the ion source, the tip is approximately 2 mm from the center of the electron beam. The tip makes an angle of approximately 45° with the electron beam, but is perpendicular to the path of the ions leaving the source. A diagram of the entire probe and ion source which illustrates this geometry is shown in Figure 2.

Samples were deposited on the probe tip by dusting the solid on the tip, or by applying the sample to the tip in solution and allowing the solvent to evaporate.

RESULTS AND DISCUSSION

Using the Vespel probe we have obtained good spectra for representative samples of a number of classes of thermally labile compounds. For example, an MH^+ peak was obtained from arginine (hydrochloride) at m/e 175 with 5% relative intensity. The spectrum is shown as Figure 3. MH^+ ions of mass 132 were observed from creatine with 11% relative abundance. The enhancement of abundance of these two molecular ion species is comparable to that observed by Hunt (*3*) using a field desorption emitter and by Munson (*4*) using a Teflon extension as direct exposure probes. Neither arginine nor creatine produce MH^+ peaks using the normal direct probe.

Sucrose, introduced on the Vespel probe, produces a protonated molcular ion species of mass 343 with 1.2% relative abundance. This is considerably higher than the abundance

0003-2700/79/0351-0317$01.00/0 © 1979 American Chemical Society

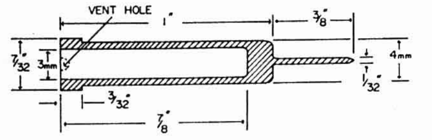

Figure 1. Cross section of direct exposure probe tip

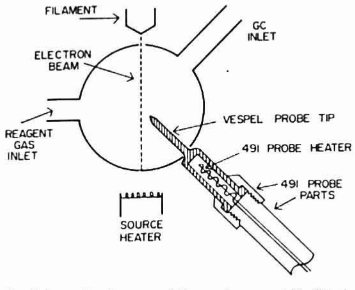

Figure 2. Schematic diagram of the probe assembly fitted with the direct exposure probe tip and inserted into the 21-491 source

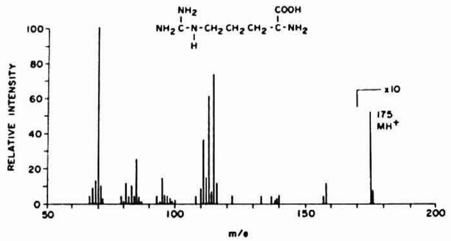

Figure 3. Chemical ionization mass spectrum of arginine hydrochloride. Source temperature was 310 °C

obtained recently using rapid heating and photoplate detection (7). The spectrum of sucrose is shown as Figure 4.

In our laboratory we have been interested in obtaining mass spectra of a number of glucuronides. In the past we have always formed derivatives of these compounds in order to produce a spectrum with a clearly recognizable molecular ion species. Figure 5 shows a mass spectrum of *p*-nitrophenyl-β-D-glucuronide obtained using the direct exposure probe. The MH^+ ion at mass 316 is easily identified.

In a number of cases we have used the extended Vespel probe tip simply to enhance the abundance of molecular ion species where it is either weak or difficult to obtain reproducibly using the conventional quartz sample holder. Bilirubin is such an example. Using the Vespel probe we easily detected the MH^+ ion of bilirubin at mass 585 as the base peak in the chemical ionization spectrum. The probe also provided an improved spectrum in the EI mode, producing a molecular ion of mass 584 of 40% relative abundance.

Vespel was chosen for fabrication of the modified probe tip reported here for a variety of reasons. It is easily machined. The Vespel probe tip serves both as a relatively inert surface for sample support and as a good electrical insulator between the ion source voltage and ground. Its thermal conductivity is somewhat higher than that of Teflon, and allows the sample to be heated. As an important advantage over Teflon, Vespel retains its rigid shape after repeated heatings (up to 380 °C in our source). We have also found that the Vespel surface does not require cleaning between sample loadings, other than exposure to the elevated temperatures of the ion source. In addition, because the sample surface area is slightly porous, samples deposited from solution or by dusting generally adhere better than they do on a glass probe.

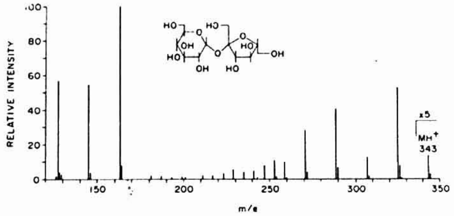

Figure 4. Chemical ionization mass spectrum of sucrose. Source temperature was 230 °C

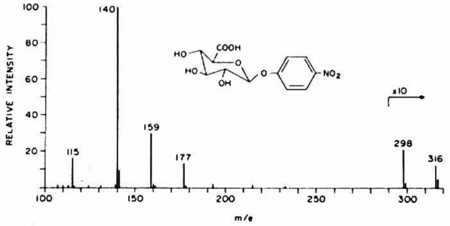

Figure 5. Chemical ionization mass spectrum of *p*-nitrophenyl-β-D-glucuronide. Source temperature was 220 °C

Like all direct probe spectra, the quality of spectra obtainable from the direct exposure probe is sensitive to sample temperature and heating rate (*3–6*). In addition, the spectrum with the largest relative abundance of molecular ion species is often recorded only a few seconds after insertion of the Vespel probe. Thus, an instrumental system which provides rapid repetitive scanning is advantageous. Peaks having *m/e* values higher than the MH^+ ion are sometimes observed, but can generally be reduced or eliminated by decreasing sample size. With some samples, we have as yet failed to produce any meaningful spectra.

In conclusion, however, the probe design described here for the DuPont 21-491 will produce spectra of good analytical quality for many compounds not susceptible to analysis with conventional direct probes. In addition, the probe composition and geometry suggested in this paper can undoubtedly be adapted to other mass spectrometers having a chemical ionization source.

ACKNOWLEDGMENT

The author is grateful to Catherine Fenselau, in whose laboratory this work was performed.

LITERATURE CITED

(1) M. A. Baldwin and F. W. McLafferty, *Org. Mass Spectrom.*, **7**, 1353 (1973).
(2) M. Ohashi, K. Tsujimoto, and A. Yasuda, *Chem. Lett.*, 439 (1976).
(3) D. F. Hunt, J. Shabanowitz, F. K. Botz, and D. A. Brent, *Anal. Chem.*, **49**, 1160 (1977).
(4) G. Hansen and B. Munson, *Anal. Chem.*, **50**, 1130 (1978).
(5) R. J. Beuhler, E. Flanigan, J. Greene, and L. Friedman, *J. Am. Chem. Soc.*, **96**, 3990 (1974).
(6) R. J. Cotter and C. C. Fenselau, American Society of Mass Spectrometry Annual Meeting, St. Louis, Mo., 1978.
(7) W. R. Anderson, Jr., W. Frick, and G. D. Daves, Jr., *J. Am. Chem. Soc.*, **100**, 1974 (1978).

RECEIVED for review August 3, 1978. Accepted October 27, 1978. This work was supported in part by a grant from the U.S. National Institutes of Health, GM-21248, and was presented at the 1978 ASMS meeting in St. Louis, Mo.

Spectrophotometric Determination of Secondary Amines

Dale H. Karweik* and **Carl H. Meyers**[1]

Department of Chemistry, Wayne State University, Detroit, Michigan 48202

A rapid, selective method for the trace analysis of secondary alkyl amines has been sought since the early 1930's. Primary interest in these years was directed toward the determination of secondary amines in pharmaceutical mixtures (*1–3*). Recently it has been noted that nitrates found in food, either added as a preservative or from nitrate rich soils, can be reduced by bacteria to nitrite (*4*). The nitrite anion in the presence of ppm amounts of dimethylamine in foods such as spinach or fresh fish can react to form dimethyl nitrosamine (*5*). Similar reactions can take place with the secondary amines found in tobacco smoke (*6–7*). Because of the carcenogenic properties of nitrosamines, it would be desirable to be able to determine not only trace amounts of nitrosamines but also the unconverted secondary amines.

The reaction of carbon disulfide with dimethylamine was first investigated by Dowden (*8*) as a possible method for the detection of small amounts of secondary amines in biological fluids. The reaction results in the formation of a dialkyl dithiocarbamate complex which forms a stable complex with metal ions. The reaction illustrated in Equation 1 requires the presence of a base (ammonia or pyridine) to force the reaction to completion. The copper bis(dithiocarbamate) complex ($Cu(DTC)_2$) can then be extracted into a suitable organic solvent such as chloroform or benzene and the concentration of the amine determined directly from the $Cu(DTC)_2$ complex or indirectly from the amount of copper remaining in the aqueous phase.

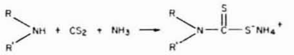

(1)

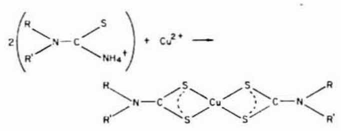

(2)

The direct determination has been used in principle by several authors for the determination of dimethylamine (*2, 3, 8*) and more recently for several alkyl and aryl amines (*1*). Improvements in the direct determination and the development of an indirect determination are reported in this paper for a variety of symmetric secondary amines.

EXPERIMENTAL

Apparatus. Spectrophotometric measurements were made using 1.00-cm matched cells on a Cary 14 spectrophotometer. A Perkin-Elmer 137 infrared spectrophotometer was used to assay the *n*-methylaniline. Atomic absorption measurements were made using a Model 1301 Beckman Atomic Absorption system with a DB-G spectrophotometer and recorder. A Model WL-22603A Westinghouse copper hollow cathode lamp was used for all measurements. Excess organic solvents were removed from the aqueous layer prior to AA analysis using a simple vacuum method.

Reagents. Stock solutions of the secondary amines were prepared from freshly opened bottles of diethylamine (Fisher), dibutylamine (Kodak), morpholine (MCB), *n*-butylaniline (Aldrich), and dibenzylamine (Kodak). The stock solutions are prepared by dissolving 1.00 mL of the secondary amine in 400.0 mL of saturated ether/water or 400 mL of (7:1) water:ethanol solution for dibenzylamine. Following neutralization with 2 N hydrochloric acid, the solutions are diluted to 1.00 L with saturated ether/water solution or water for dibenzylamine.

Table I. Beer's Law Behavior of Copper Bis(dithiocarbamate) Complexes

amine	concn range, ppm	ϵ	slope[a]
diethylamine	0–3	1.14×10^4	0.076
dibutylamine	0–12	1.18×10^4	0.043
dibenzylamine	0–4	1.09×10^4	0.025
morpholine	0–7	1.26×10^4	0.064

[a] Slope is equal to absorbance divided by ppm concentration.

Table II. Summary of Results of the Direct Determination of Secondary Amines

secondary amines	no. of samples	ppm	abs., 434 nm	abs. SD	detection limit, ppm
diethylamine	6	2.46	0.187	±0.003	0.02
dibutylamine	7	6.14	0.276	±0.003	0.07
dibenzylamine	6	3.69	0.097	±0.003	0.04
morpholine	6	8.00	0.516	±0.011	0.01

Stock solutions to deliver approximately 100 μg of copper can be prepared by dissolving copper shot (99.99%) in nitric acid or by dissolving $CuCl_2 \cdot 2H_2O$ in water. Solutions of 97.0 μg/mL and 105.8 μg/5.0 mL were prepared by the respective methods.

Analyzed spectral grade chloroform (Baker) and reagent grade carbon disulfide (Fisher) were used without further purification.

Recommended Procedure. Transfer 10.0 mL of the secondary amine sample to a 125-mL separatory funnel; followed by 5.0 mL of 1.2 M, pH 9.4 ammonia–ammonium chloride buffer; and 100 μg of copper(II) stock solution. Add 0.5 mL of carbon disulfide, followed by 10.0 mL chloroform, shake for 60 s, and allow the layers to separate. Add 1.0 mL of 25% (v/v) acetic acid, shake for 60 s, and allow the two layers to completely separate.

For the direct method, transfer the chloroform extract to a 25-mL volumetric flask and wash the aqueous layer with a second 10-mL portion of chloroform, combining the two extracts before dilution to volume. A reference blank is prepared by substituting an equivalent amount of water for the secondary amine solution. The absorbance of the copper complex in chloroform is measured at 434 nm vs. the reference blank.

For the indirect method, the aqueous layer, following extraction and removal of the organic solvent traces (*9*), is diluted to 25.0 mL with distilled water. The excess copper can be analyzed using AA and a standard curve or spectrophotometrically using Gahler's neocuproine method (*10*).

RESULTS AND DISCUSSION

The visible absorption spectra of various concentrations of copper(II) bis(dibutyldithiocarbamate) in chloroform are shown in Figure 1. These spectra are typical for all the complexes reported. In all cases the copper:amine ratio was found to be 1:2. Beer's law plots of all the solutions produced linear plots with zero intercepts. The concentration range studied, the molar absorbtivity at 434 nm, and the slope of the Beer's law plot are given in Table I for the four amines studied.

---

[1] Permanent address: Pall Corporation, 30 Sea Cliff Avenue, Glen Cove, N.Y. 11542.

0003-2700/79/0351-0319$01.00/0 © 1979 American Chemical Society

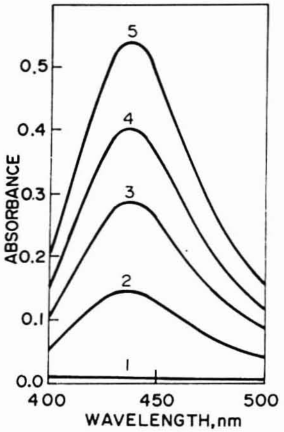

Figure 1. Absorption spectra of Cu-bis(dibutyldithiocarbamate). Concentrations of $Cu(DBDTC)_2$ in $CHCl_3$: (1) blank, (2) 3.00 ppm, (3) 6.1 ppm, (4) 9.2 ppm, (5) 12.3 ppm

The slope of the plot is given by the absorbance divided by the concentration in ppm. The precision of the direct determination was determined via replicate determinations on a known "unknown". The results of the precision study are summarized in Table II. The detection limit is defined as the concentration which produces an absorbance equal to three times the standard deviation of the blank. The indirect method for analysis of the secondary amines is based on the determination of the copper(II) ions remaining in the aqueous solution. The neocuproine spectrophotometric method (*10*) was used for all the amines except dibutylamine which was determined indirectly by atomic absorption spectrometry. The precision of the method was studied in two ways. First, multiple samples of "known unknowns" were analyzed and the percent recovery was determined. Second, the amines were analyzed by both the direct and indirect methods. The results of these studies are summarized in Table III. The concentrations listed in Tables II and III are the concentrations expected in the extract, based on the known concentrations of the corresponding secondary amines.

In all cases the slope of the plot of the amine concentration determined by the direct method vs. the concentration found by the indirect method was found to be equal to the previously determined percent recovery. Additionally the standard deviation of the slope was found to be nearly equal to the absolute standard deviation determined in the recovery experiments. The slopes and standard deviations were calculated using a standard linear curve fitting method (*11*). The calculated intercept in all cases was equal to or less than the probably error calculated for the indirect method. Using either method of analysis, 6 samples plus blank can be completed within 1 h. The solutions of copper(II) dithiocarbamates show no change in absorbance over a period of several days. Therefore the spectrophotometric procedure need not be performed immediately.

Table III. Summary of Results of the Indirect Determination of Secondary Amines

secondary amine	no. of samples	ppm	% recovery	absolute SD
diethylamine[a]	6	2.46	97.6	0.08
dibutylamine[b]	7	6.14	94.7	±1.8
dibenzylamine[a]	6	3.70	95.5	±2.8
morpholine[a]	6	8.0	89.5	±2.2
n-methylaniline[a]	6	- - -	0.0	- - - -
n-butylaniline[a]	6	- - -	0.0	- - - -

[a] Visible spectrophotometry. [b] Atomic absorption spectrometry.

The method reported here offers several advantages over previously reported determinations (*1, 8*) which result from changes in the solvent system. The basic changes result from the substitution of ammonia for pyridine as the required base and from the substitution of chloroform for the mixture of isopropanol and benzene as the extraction solvent. In addition to the replacement of toxic solvents, these changes result in a decrease in the color development time. Umbreit reports that color development required 20 min for *N*-methylaniline and 180 min for diethylamine (*1*). By replacing pyridine with ammonia, this was reduced to less than 15 min for all the amines reported in this paper. However, it should be noted that with this solvent system the *N*-alkyl anilines do not produce complexes which are extractable in chloroform. No absorbances were detected for Cu(II) bis(dithiocarbamate) complexes formed from *N*-methyl-, *N*-ethyl-, or *N*-butylaniline. This may result from the substitution of ammonia for pyridine (*12, 13*).

A further advantage is derived from the development of the indirect determination. The indirect method can be used to either corroborate the results of the direct determination or as the primary method for samples which contain spectral interferences. This would include interferences caused by scattering and other overlapping absorbance bands.

ACKNOWLEDGMENT

The authors acknowledge the late David F. Boltz for the initial suggestion of the project and for early direction of one of the authors (C.H.M.).

LITERATURE CITED

(1) G. R. Umbreit, *Anal. Chem.*, **33**, 1572 (1961).
(2) L. Nebbia and F. Guerrieri, *Chim. Ind.* (*Milan*), **35**, 896 (1953).
(3) E. L. Stanley, H. Baum, and J. L. Gove, *Anal. Chem.*, **23**, 1779–82 (1951).
(4) J. Weisburger and R. Raineri, *Toxicol. Appl. Pharmacol.*, **31**, 369 (1975).
(5) S. Hypta, *Nafta*, **28**, 31 (1972).
(6) M. Pailer, W. J. Hübsch, and H. Kuhn, *Fachliche Mitt. Osterr. Tabakregie*, **7**, 109 (1967).
(7) M. Pailer, J. Völlmen, C. Karmencic, and H. Kuhn, *Fachliche Mitt. Osterr. Tabakregie*, **10**, 165 (1970).
(8) H. C. Dowden, *Biochem. J.*, **32**, 455 (1938).
(9) J. A. Bowman and J. B. Willis, *Anal. Chem.*, **39**, 1210 (1967).
(10) A. R. Gahler, *Anal. Chem.*, **26**, 577 (1954).
(11) P. R. Bevington, "Data Reduction and Error Analysis for the Physical Sciences", McGraw Hill, New York, 1969, pp 92–118.
(12) S. J. Snedker, *J. Soc. Chem. Ind.*, **44**, 74T (1925).
(13) H. S. Fry and B. S. Farguhar, *Recl. Trav. Chim. Pays-Bas*, **57**, 1223 (1930).

RECEIVED for review August 8, 1978. Accepted October 27, 1978.

Author Index

Altree-Williams, S. 304
Anderson, G. M. 283
Arrington, J. 287

Bengert, G. A. 186
Blotcky, A. J. 178
Bruckenstein, S. 250
Bruno, S. F. 196

Cantwell, F. F. 218
Carr, P. W. 278
Chau, Y. K. 186
Cohen, N. 207
Cotter, R. J. 317

Darland, E. J. 240, 245
Darus, Hamzah bin 256
Denton, M. B. 266
Dromey, R. G. 229
DuBois, H. R. 196
DuPuis, M. D. 292

Edmonds, J. W. 304
Enke, C. G. 240, 245
Evans, M. B. 311

Falcone, C. 178
Fernando, Q. 302
Field, F. H. 272
Fraser, J. L. 315
Fry, R. C. 266

Ghose, A. K. 199
Gifford, P. R. 250
Gobby, P. L. 223
Grimsrud, E. P. 223

Hahn, P. B. 295
Hansen, E. H. 199
Henry, F. T. 215
Hiatt, M. H. 295
Hill, H. H., Jr. 292
Hobson, D. W. 178
Hornshuh, J. E. 245
Hosking, J. W. 307
Howard, C. C. 210
Hunt, J. H. 311

Ianniello, R. M. 204
Ibrahim, S. A. 207

Jespersen, N. D. 204
Jindal, S. P. 269

Kallos, G. J. 299
Kan, N-S. 182
Karweik, D. H. 319
Kim, S. H. 223
Kirch, T. O. 215
Kirchner, S. J. 302
Knechtel, J. R. 315
Kramar, O. 186
Kresan, P. L. 302

Leroi, G. E. 240, 245
Li, K-P. 287
Li, N. C. 182
Lin, Y. Y. 272
Lutz, T. 269

McMillan, D. J. 189
Manning, D. C. 261
Medina, V. A. 178
Meyers, C. H. 319
Miller, C. S. 278
Mohammed, H. Y. 218
Mottola, H. A. 199
Munro, G. 311
Murray, R. W. 236

Oliver, K. R. 307
Oona, H. 302

Pastore, A. T. 196
Purdy, W. C. 283

Rack, E. P. 178
Ratzlaff, K. L. 232, 256
Rich, S. 204
Riggin, R. M. 210
Riley, J. E., Jr. 189, 306
Rowe, L. R. 311
Roy, T. A. 272
Ruzicka, J. 199

Schifreen, R. S. 278
Schmidt, P. F. 189, 306
Sharma, G. M. 196
Singh, N. P. 207
Slavin, W. 261
Smith, L. L. 272
Solomon, R. A. 299
Stephens, E. R. 313
Strong, F. C., III 298
Sturman, B. T. 307
Susco, D. M. 182

Tewari, K. C. 182
Thorpe, T. M. 215
Tou, J. C. 299

Vestergaard, P. 269

Watanabe, I. 313
White, H. S. 236
Wong, P. T. S. 186
Wrenn, M. E. 207

Yao, C. C. 299

Zeitlin, H. 302
Zollinger, H. 299

Future Articles

Determination of Quinidine and Dihydroquinidine in Plasma by High Performance Liquid Chromatography
B. J. Kline, W. A. Turner, and W. H. Barr

Parameters for the Radio Method by X-Ray Microanalysis
A. G. S. Janossy, K. Kovacs, and I. Toth

Application of Microporous Membranes to Chemiluminescence Analysis
V. Nau and T. A. Nieman

Optimization of the Analytical Oxidation of Dihydronicotinamide Adenine Dinucleotide at Carbon and Platinum Electrodes
J. Moiroux and P. J. Elving

Reticulated Vitreous Carbon Flow-Through Electrodes
A. N. Strohl and D. J. Curran

Determination of Trace Elements in Light Element Matrices by X-Ray Fluorescence Spectrometry Using Incoherent Scattered Radiation as an Internal Standard
R. D. Giauque, R. B. Garrett, and L. Y. Goda

Correction for Background Current in Differential Pulse, Alternating Current, and Related Polarographic Techniques in the Determination of Low Concentrations with Computerized Instrumentation
A. M. Bond and B. S. Grabaric

Development and Characterization of a Miniature Inductively Coupled Plasma Source for Atomic Emission Spectrometry
R. N. Savage and G. M. Hieftje

Determination of Organic Methylmercury in Fish by Graphite Furnace Atomic Absorption Spectrophotometry
G. T. C. Shum, H. C. Freeman, and J. F. Uthe

Influence of Errors and Matching Criteria upon the Retrieval of Binary Coded Low Resolution Mass Spectra
G. Van Marlen, A. Dijkstra, and H. A. van't Klooster

Fiber Optic Waveguides for Time-of-Flight Optical Spectrometry
W. B. Whitten and H. H. Ross

Chronopotentiometry with Programmed Current
L. H. Chow and G. W. Ewing

Fluidic Logic Element Sample Switch for Correlation Chromatography
R. Annino, M.-F. Gonnord, and G. Guichon

Now you can weigh with analytical precision (0.1mg) on a fully automatic electronic top-loader or on a fully automatic electronic suspended-pan balance, as the weighing situation or your personal preference dictates.

The new top-loader that weighs with analytical precision is our Model 1201MP. Compact and very affordable, this addition to our popular 1200 Series has a capacity of 30g and weighs to 0.1mg at the touch of a button. Its many advanced features include a built-in microprocessor, instant electronic taring, memory and weight recall, BCD output for printer connection, and a large, bright digital display with reading stability indicator. Pan access is provided from the top and both sides of the glass enclosed weighing chamber.

For 0.1mg precision in an electronic analytical balance, we offer our new Model 2003MP. Fully automatic push-button operation and other features are similar to our electronic top-loaders. In addition, a door-activated switch blocks display of the last digit except when both chamber doors are closed, thereby preventing air current-induced instability of the readout. With a capacity of 166g, larger pan and larger weighing chamber, the 2003MP is more versatile and somewhat more costly.

For literature write: Sartorius Balances, Division of Brinkmann Instruments, Inc., Cantiague Road, Westbury, N.Y. 11590.

Sartorius introduces an electronic top-loader with the same precision (0.1mg) as our new electronic analytical balance.

sartorius
sartorius
2003MP
0.9756 g
45892 g

FULLY AUTOMATIC ELECTRONIC ANALYTICAL BALANCE WITH 0.1mg PRECISION, MODEL 2003MP

FULLY AUTOMATIC ELECTRONIC TOP-LOADING BALANCE WITH 0.1mg PRECISION, MODEL 1201MP

sartorius

CIRCLE 16 ON READER SERVICE CARD